



IMPERIAL AGRICULTURAL  
RESEARCH INSTITUTE, NEW DELHI

MOIPC-94 III 191-22842-5000







# JOURNAL OF COLLOID SCIENCE

*Editor-in-Chief*

VICTOR K. LAMER, Columbia University, New York

*Editors:*

F. E. BARTELL  
T. R. BOLAM  
E. F. BURTON  
R. M. FUOSS  
H. R. KRUYT

J. W. MCBAIN  
E. K. RIDEAL  
WILLIAM SEIFRIZ  
A. W. THOMAS  
ARNE TISELIUS

ROBERT D. VOLD

*Consulting Committee:*

W. T. ASTBURY  
J. J. BIKERMAN  
W. CLAYTON  
P. DEBYE  
W. FEITKNECHT  
ALEXANDER FRUMKIN  
WILLIAM D. HARKINS

ERNST A. HAUSER  
WILFRIED HELLER  
HANS JENNY  
S. S. KISTLER  
HERMAN MARK  
J. N. MUKHERJEE  
F. F. NORD

THE SVEDBERG

23209



IARI



1946

ACADEMIC PRESS INC. PUBLISHERS  
NEW YORK, N. Y.

Copyright 1946, by Academic Press, Inc.  
Made in United States of America

## CONTENTS OF VOLUME 1

No. 1, JANUARY, 1946

A. SZENT-GYÖRGYI. Contraction and the Chemical Structure of the Muscle Fibril.....	1
M. SPIEGEL-ADOLF AND E. A. SPIEGEL. Polarization and Permeability (Quantitative Measurements).....	21
WILLIAM SEIFRIZ. Torsion in Protoplasm.....	27
H. JENNY. Adsorbed Nitrate Ions in Relation to Plant Growth...	33
D. J. CRISP. Surface Films of Polymers. Part I. Films of the Fluid Type.....	49
VICTOR K. LAMER AND MARION D. BARNES. Monodispersed Hydrophobic Colloidal Dispersions and Light Scattering Properties. I. Preparation and Light Scattering Properties of Monodispersed Colloidal Sulfur.....	71
MARION D. BARNES AND VICTOR K. LAMER. Monodispersed Hydrophobic Colloidal Dispersions and Light Scattering Properties. II. Total Scattering from Transmittance as a Basis for the Calculation of Particle Size and Concentration.....	79
PAUL STAMBERGER. The Method of Purifying and Concentrating Colloidal Dispersions by Electrodecantation.....	93
WILLIAM D. HARKINS, RICHARD W. MATTOON AND MYRON L. CORRIN. Structure of Soap Micelles as Indicated by X-Rays and Interpreted by the Theory of Molecular Orientation. II. The Solubilization of Hydrocarbons and Other Oils in Aqueous Soap Solutions.....	105

No. 2, MARCH, 1946

EMANUEL GONICK AND JAMES W. MCBAIN. Physical-Chemical Properties of Solutions of the Colloidal Electrolyte Hexanamine Oleate.....	127
GEORGE JURA AND WILLIAM D. HARKINS. The Contact Angle Between Water and a Monolayer of Egg Albumin on Glass as a Function of Film Pressure.....	137
J. N. MUKHERJEE AND R. P. MITRA. Some Aspects of the Electrochemistry of Clays.....	141
D. J. CRISP. Surface Films of Polymers. Part II. Films of the Coherent and Semi-Crystalline Type.....	161
P. H. HERMANS AND A. WEIDINGER. The Hydrates of Cellulose..	185
M. MOONEY. A Viscometer for Measurements during Thixotropic Recovery; Results with a Compounded Latex.....	195
Book Reviews.....	209

No. 3, MAY, 1946

S. E. SHEPPARD, A. S. O'BRIEN AND G. L. BEYER. Studies in Amphipathic Adsorption. I. The Adsorption of Polyvinyl Alcohol on Silver Bromide.....	213
---	-----

STEPHEN P. MARION AND ARTHUR W. THOMAS. Effect of Diverse Anions on the pH of Maximum Precipitation of "Aluminum Hydroxide".....	221
J. J. HERMANS. The Behavior of Rubberlike Materials when Stretched.....	235
P. H. HERMANS, J. J. HERMANS AND D. VERMAAS. Optical Properties of the System Cellulose-Water.....	251
L. H. CRAGG. The Terminology of Intrinsic Viscosity and Related Functions.....	261
ROBERT J. HARTMAN, RAYMOND A. KERN AND EDWARD G. BOBALEK. Adsorption Isotherms of Some Substituted Benzoic Acids.....	271
A. FRUMKIN. New Electrocapillary Phenomena.....	277
Book Reviews.....	293

## No. 4, JULY, 1946

TODD M. DOSCHER AND ROBERT D. VOLD. Phase Relations in the System: Sodium Stearate-Cetane.....	299
HARRY S. OWENS AND W. DAYTON MACLAY. Effect of Methoxyl Content of Pectin on the Properties of High-Solids Gels.....	313
OTTO TREITEL. Elasticity, Plasticity and Fine Structure of Plant Cell Walls.....	327
S. M. NEALE. Fundamentals of Dye Absorption.....	371
Book Reviews.....	381

## No. 5, OCTOBER, 1946

H. F. WALTON, E. N. HIEBERT AND E. H. SHOLTES. Quaternary Ammonium Salts as Colloidal Electrolytes.....	385
EMANUEL GONICK. Micellar Association of Ionic and Non-Ionic Detergents in Non-Ionizing Solvents.....	393
K. H. GUSTAVSON. Investigation of the Formation of Chromium Salt Complexes by Means of Organolites.....	397
H. J. WOODS. The Contribution of Entropy to the Elastic Properties of Keratin, Myosin and Some Other High Polymers.....	407
JOHN RUNNSTRÖM, LUDWIK MONNÉ AND ELSA WICKLUND. Studies on the Surface Layers and the Formation of the Fertilization Membrane in Sea Urchin Eggs.....	421
NILS GRALÉN. The Molecular Weight of Lignin.....	453
Letters to the Editor.....	467
Book Reviews.....	473

## No. 6, DECEMBER, 1946

R. H. HARRIS AND ETHEL JESPERSON. A Study of the Effect of Various Factors on the Swelling of Certain Cereal Starches...	479
P. H. HERMANS AND A. WEIDINGER. On the Transformation of Cellulose II into Cellulose IV.....	495
I. E. PUDDINGTON. A Simple Surface Pressure Balance.....	505
W. C. BIGELOW, D. L. PICKETT AND W. A. ZISMAN. Oleophobic Monolayers. I. Films Adsorbed from Solution in Non-polar Liquids.....	513
B. JIRGENSONS. The Coagulation of Lyophilic Colloids by Organic Substances and Salts. IX.....	539
INDEX.....	549

# CONTRACTION AND THE CHEMICAL STRUCTURE OF THE MUSCLE FIBRIL

A. Szent-Györgyi

*From the Physiological-Chemical Institute of the University Medical School,  
Budapest, Hungary*

*Received December 3, 1945*

It is evident that muscle function must be explained by its structure. The elementary process of contraction and relaxation takes place in molecular or micellar dimensions and, hence, the chemist or colloid-chemist has the best chance to explain its mechanism.

Histology has taught us that the rapidly moving body muscles consist of fibers of about 0.1 mm. diameter which are, in essence, but a bundle of several thousand very thin fibrils enclosed by a common sheath. The fibrils, about 0.001 mm. in diameter, show a cross-striation: they look as if they were built of small discs. Discs of higher (Q) and lower (I) double refraction alternate. The latter exhibit even a finer structure, being divided in two halves by the "Z-line." The slowly moving muscle cells of internal organs are different. They are spindle-shaped and their fibrils show no cross-striation. Accordingly, we call them "smooth muscle cells" to distinguish them from the "cross-striated" body muscles. I will limit myself to the latter and will come back to the smooth muscle only at the end of this paper.

The contractile elements of the muscle are the fibrils. These occupied the attention of leading biochemists, such as Danilewsky (1), Halliburton (4) and v. Fürth (2, 3) as early as the eighties of the last century. It was found that the bulk of the fibrillary mass could be dissolved by strong salt solutions and was precipitated on dilution. The precipitate had the character of a protein, and was termed "myosin" (v. Fürth). Full attention was given myosin in this century by H. H. Weber (5) who devised an ingenious method for its study: he squirted the salt solution of myosin into water. Here, the salt being eluted, the myosin gelatinized in the form of threads, which are a fascinating experimental material. Later, v. Muralt and Edsall (6, 7) took up the study of myosin and showed that its solution had a high and anomalous viscosity and a strong double refraction of flow (DRF).

Lately, attention was turned toward myosin by the discovery of Engelhardt, Ljubimova and Meitina (8) who found that the elasticity

of myosin threads was increased in a specific way by adenosine-tri-phosphate (ATP), a substance which is known to supply the energy of muscular contraction by splitting off its phosphate groups. Engelhardt (9) and Ljubimova later showed that it was myosin itself which splits off the first phosphate of ATP. Needham and his collaborators (10) showed that ATP, in small doses, decreased the DRF and viscosity of myosin solution.

The chief result in this field from my laboratory<sup>1</sup> was to show that the fibril is constructed of two proteins, neither of which is contractile in itself. If brought together, they form a complex protein which has the remarkable property of reversible contractility; it can be contracted or relaxed by constituents of muscle, salts and ATP. One of these proteins was obtained in crystalline condition (Fig. 1) so that the entire investi-



FIG. 1

Myosin Crystals. Magnification, 1 : 90

gation could be conducted with recrystallized material. The name "myosin" was retained for this protein, although its properties differed widely from those of v. Fürth's myosin. The other protein was discovered and obtained in analytically pure condition by F. B. Straub (11), who termed it "actin." The complex of the two proteins we called "actomyosin." The old "myosin" was actomyosin of indefinite composition.

### MYOSIN

Myosin is a hydrophilic colloid. It is soluble in water; its isoelectric point (IP) is at pH 5.3. It has a fairly high but normal viscosity, which indicates that its particles are slightly elongated. They have a strong tendency toward association as expressed by the splendid DRF in

<sup>1</sup> The experiments have been published in the three consecutive volumes of "Studies from the Institute of Medical Chemistry, University of Szeged" (S. Karger, Basel, 1942-43), and have been summed up in supplement No. XXV, Vol. 9 *Acta Physiologica Scandinavica* 1945, where the bibliography may be found. Future work will be published in the *Hungarica Physiologica Acta*.

aqueous solution. This DRF readily disappears if the pH is raised or salt is added in higher concentration. Myosin, in many respects, resembles soaps.

Myosin has a striking and unique property: though a hydrophilic colloid, it is precipitated by very small concentrations of neutral salts. 0.025 *M* KCl, for instance, suffices for its quantitative precipitation. If the KCl concentration is raised to 0.1 *M*, the precipitate dissolves with a strong DRF. This DRF disappears if the KCl concentration is raised above 0.3 *M*. This action of KCl is not specific and is duplicated by NaCl or other neutral salts. In the experiments to be reported here KCl has been used throughout as neutral salt.

The explanation of these reactions has been given by the analysis of I. Banga (12) who showed that myosin binds cations, leaving the anion unbound. In the presence of 0.025 *M* KCl myosin is maximally precipitated and binds 5  $K^+$  ions per unit weight of 17,600 g. This maximal precipitation is evidently the expression of the isoelectric state. If the KCl concentration is increased, more  $K^+$  is bound and the protein dissolves. At pH 5.3, the IP of myosin, no  $K^+$  is bound at all; the  $K^+$ -binding capacity increases with the pH. These results can also be summed up by saying that the IP of free myosin is 5.3, different K-myosinates have different IPs and the IP shifts further toward the alkaline side the richer the proteinate in K. The myosin with one  $K^+$  per unit weight has a great tendency for crystallization at its IP of 6.5. It is in this form that myosin has been obtained as crystals (Fig. 1). The IP of myosin- $K_5$  is about pH 7 (meaning by "myosin" the unit weight of 17,600 g.) while the IP of myosin containing more than 5  $K^+$  will be on the alkaline side and at pH 7 this myosin will be cationic.

Another way of describing these phenomena would be by saying that the IP of myosin is extended by KCl toward the alkaline side. The extension, or shift, of the IP of proteins by salts is a common phenomenon and was described many years ago by Michaelis and the author. These reactions, which are due to the unequal adsorption of ions and are the core of the problem of muscular contraction, are thus common to all proteins. They are specific for myosin only in so far as the extent of the reaction is concerned: no other protein is known to give an equally strong adsorption and shift of IP as myosin.

The results of Banga's measurements are summed up in Fig. 2. The metal adsorption is characterized by a straight line with a break corresponding to the maximum of precipitation. What is most unexpected in this curve is that it becomes steeper, *i.e.*, the  $K^+$ -binding becomes more intense as we pass this point of maximum precipitation; myosin acquires a greater affinity for metals by its discharge. The curves obtained with  $Ca^{++}$  and  $Mg^{++}$  are similar in their structure. They show that the



affinity of myosin for these bivalent ions is higher than for  $K^+$ . It is noteworthy that the break in the curve of  $Ca^{++}$  and  $Mg^{++}$  coincides with the concentration of these metals in muscle, which means that none of these ions will be capable of charging myosin positively. This can be done only by the  $K^+$ , the concentration of which, in muscle, is about

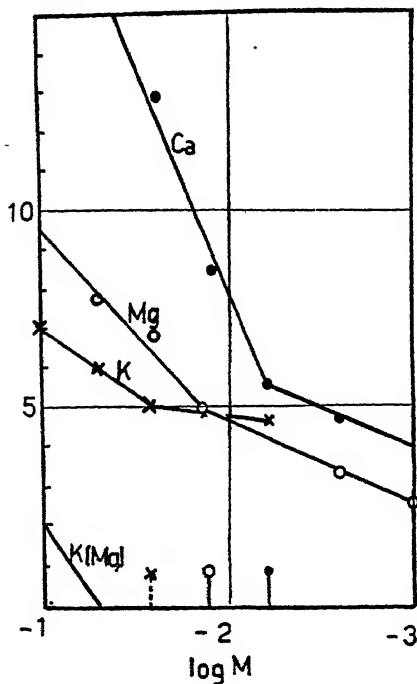


FIG. 2

## Metal-Binding of Myosin

Abcissa:  $\log M$  concentration of KCl. Ordinate: equivalents of metal bound by 17,600 g. of myosin. Curve on the left: the  $K^+$  binding of Mg-myosinate containing 5 equivalents of  $Mg^{++}$ . The vertical lines correspond to the concentration of the corresponding metal in muscle (in 77% of water according to Dubuisson).

0.1  $M$  while the maximum of precipitation, corresponding to the isoelectric condition, lies at 0.025  $M$ .

Adsorption, in mixtures, depends on relative concentrations. If  $K^+$  is present in 0.025  $M$ , and  $Mg^{++}$  in 0.012  $M$  concentration, both of which correspond, in themselves, to the isoelectric state of myosin at neutral reaction, only  $Mg^{++}$  will be bound, this ion having a higher affinity for myosin. If the  $Mg^{++}$  concentration is kept at 0.012  $M$  and the  $K^+$  concentration is increased,  $K^+$  will be adsorbed. The steepness of this

K<sup>+</sup>-adsorption curve of Mg-myosinate (see Fig. 2) explains why Mg<sup>++</sup> sensitizes myosin toward K<sup>+</sup> (see below).

The colloidal state of myosin thus depends on the nature and concentration of the cations present. It is possible to coordinate the colloidal reactions with the metal binding. So, for instance, the observation that myosin is precipitated by KCl at concentrations higher than 0.001 *M* and is redissolved by 0.1 *M* KCl means, according to the curve in Fig. 2, that myosin, containing less than 4 K<sup>+</sup> or more than 7 K<sup>+</sup> per unit weight, is soluble in water while myosin-K<sub>4-7</sub> is insoluble and isoelectric. Myosin, with less than 4 K<sup>+</sup> equivalents of other metals is negatively, with more than 7 probably positively charged.

These metal adsorption curves afford a quantitative basis for muscle physiology. The high K<sup>+</sup>-binding capacity of the "myosin" was noted some time ago by Montigel in Verzář's laboratory.

ATP, if present, inhibits to some extent the precipitation of myosin by KCl. This can be expected from a pentavalent anion, the trivalent PO<sub>4</sub><sup>=</sup> anion having a slight inhibitory effect already. As shown by the analysis of Banga, this inhibition is due to the binding of ATP by myosin. If the quantity of ATP bound by the unit weight of myosin is plotted against the ATP concentration, a straight line is obtained, which suggests that it is some sort of a "chemical" link which joins the two substances. The first experiments suggest that in presence of 0.4% ATP (total ATP-concentration of muscle is 35%) about 1 molecule of ATP is bound by every unit weight of myosin.

The K<sup>+</sup>-adsorption curve of myosin is not materially changed by the ATP present. If, however, this ATP-myosinate complex is precipitated by alcohol, not only the ATP will be taken down into the myosin precipitate but also the K<sup>+</sup> ions which have served to balance this bound pentavalent anion.

### ACTIN

Actin is a hydrophilic colloid with its IP at pH 4.7. Similarly to myosin, actin too has a unique property: it is capable of existing in globular as well as in fibrous form. These forms can be transformed reversibly into each other. If extracted by Straub's method, actin is obtained in globular form; if a small amount of KCl (or any other neutral salt) is added, the actin is transformed into a somewhat thixotropic fibrous colloid with a splendid and permanent DRF. Though the particles of this fibrous form cannot be very long—as indicated by the relatively low viscosity—actin has, in this state, many properties typical of a fibrous colloid. By raising the pH and dialyzing the salt out, the fibrous actin can be transformed into the globular form again. If the fibrous form is termed F and the globular G, the change may be called the G-F

or F-G transformation. The G-F transformation may be explained in two ways: either by an uncoiling of globular particles, or by a linear association of the latter to something like a string of beads. Special experiments must decide between these two possibilities. The rising light diffraction rather suggests the latter possibility, so I will employ this mode of explanation.

What lends special interest to these transformations is the fact that they occur in contraction. If actomyosin contracts, its F actin is broken up into G actin. G actin does not form a contractile system with myosin and has to polymerize to F actin before a new contraction can occur. The rate of the G-F transformation depends on various factors, for instance, on the concentration of actin and the presence of myosin which greatly catalyzes the reaction. Under conditions prevailing in the muscle fibril, the rate must be very high.

The G-F transformation depends on the presence of ions in a remarkable manner (Straub).  $K^+$  in concentrations comparable to those in muscle, readily effects the transformation but only if  $Mg^{++}$  is present. Traces of  $Mg^{++}$  such as 0.0001 *M*, although entirely inactive themselves, greatly sensitize the actin toward the action of  $K^+$ . In complete absence of  $Mg^{++}$  actin is unable to associate at all.  $Ca^{++}$  has the opposite effect. In equally small concentrations it completely inhibits association. The three ions balance each other, which may explain the known physiological equilibration. The antagonistic action can also be observed in precipitation. Actin is precipitated by small concentrations of  $Ca^{++}$  and again brought into solution by  $K^+$ .

This effect of ions is not limited to the association of G-actin particles but also holds for the reaction of actin with myosin for actomyosin formation. It has been noted that in entire absence of  $Mg^{++}$  actomyosin becomes very labile and dissociates. Traces of  $Mg^{++}$  stabilize the system so that we can say that the presence of  $Mg^{++}$  is equally necessary for the development of the link between particles of actin and myosin. On the other hand  $Ca^{++}$ , in very small concentration, makes actomyosin react as if it consisted of free actin and myosin.<sup>2</sup>

#### ACTOMYOSIN

If a solution of myosin and F-actin are mixed, the sudden rise of viscosity indicates that a new substance has been formed. The viscosity becomes not only high but also anomalous (Fig. 3), indicating that the new substance consists of very long particles. The actomyosin has all typical properties of a highly polymerized fibrous colloid. At higher concentrations it forms a rather solid, thixotropic gel.

<sup>2</sup>  $Mg^{++}$  and  $Ca^{++}$  in very high concentrations catalyze the  $G \rightleftharpoons F$  transformation.

Actomyosin is very hydrophilic and swells; in the absence of salts, exceedingly. If an actomyosin-thread is suspended in water and the salts are washed out, the thread swells to a very loose glassy mass. This swelling is prevented by 0.001 *M* KCl or other neutral salts. If the salt is added to a swollen gel, this becomes turbid and shrinks. If salts are added to a salt-free actomyosin suspension, it precipitates.

Evidently, this precipitation of actomyosin by salts is a reaction of the myosin moiety. Banga has found that the metal-binding capacity of myosin is not changed materially by the actomyosin formation. Like myosin, actomyosin also is precipitated by very small concentrations of

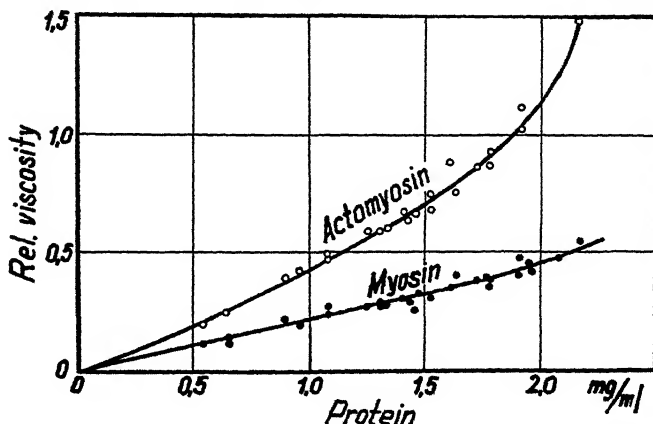


FIG. 3

Viscosity of Actomyosin, Extracted from Muscle

Upper curve: actomyosin. Lower curve: the same in presence of ATP. The latter curve is marked "myosin" since it is governed by the viscosity of this protein and is approximately identical with the curve for pure myosin. The actomyosin, in this case, contained 1 part of actin to 5 parts of myosin.

neutral salts. The maximum of precipitation is slightly shifted toward the higher salt concentrations. While the maximum of precipitation of myosin is at 0.025 *M* KCl, in the case of actomyosin the maximum is at 0.05 *M*, where the myosin has a positive charge and the actomyosin is a complex consisting of a positive and a negative colloid.

It is important, however, that even at the maximum of its precipitation, actomyosin is still rather hydrophilic. The precipitates, obtained from suspensions, are flocculent, rather loose and voluminous. I never succeeded in obtaining a precipitate containing less than 95% of water. Similarly, the actomyosin gels, at the maximum of shrinking, contain very great amounts of water. Thus, for instance, the actomyosin threads used in our work, which were prepared in 0.05 *M* KCl, consisted of

maximally salt-precipitated actomyosin, and usually contained 2% of actomyosin and 98% of water.

If the concentration of KCl is raised above 0.05 *M*, the solidity decreases until above 0.4 *M* it liquefies. On further increase, the viscosity gradually drops and reaches a minimum at 2 *M*, corresponding to the additive value of the viscosity of myosin and actin, indicating that the actomyosin had completely dissociated into its components (Fig. 4).

The actomyosin formed from G-actin and myosin is quite different. Its viscosity is low, it forms no gel, although it is also precipitated by neutral salts. If not state otherwise, "actomyosin" means the F-form.

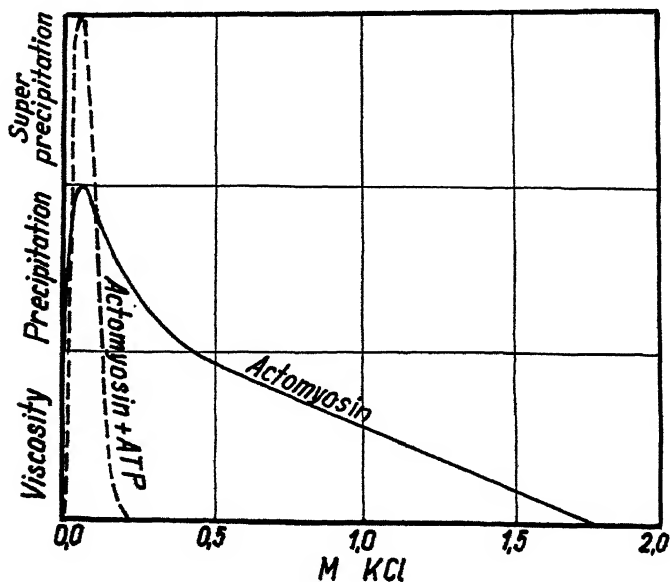


FIG. 4

Semiquantitative Curve Showing the Behavior of Actomyosin in Presence and Absence of ATP at Various KCl Concentrations

All these reactions of actomyosin are profoundly changed by the addition of small amounts of ATP, as shown by Fig. 4. One could sum up the effect of ATP by saying that it makes all the reactions much more abrupt, greatly exaggerates them, and acts, so to say, as a lubricant. As previously shown in the complete absence of salt, actomyosin swells greatly; on addition of ATP the gel not only swells, it dissolves and the low viscosity indicates that it has not only dissolved but has also dissociated. In absence of ATP, actomyosin suspension is precipitated by neutral salts, forming a rather loose, hydrophilic precipitate. In presence of ATP a very coarse, granular precipitate is obtained, rapidly settling

to a rather small volume, which will be called "*superprecipitation*" to distinguish it from the simple salt precipitation. A salt-free actomyosin gel shrinks and dehydrates to some extent on addition of salt. In the presence of ATP this shrinkage becomes so rapid, and excessive that it gives the impression of active contraction (Figs. 5 and 6). Superprecipitation of suspensions is thus identical with the contraction of gels. The



FIG. 5

a: Actomyosin Thread; b: Same Thread Contracted. Magnification 1 : 30



FIG. 6

Contraction of an Actomyosin Gel on Addition of ATP  
The gel filling the test tube, contracted to a small plug

gel, while shrinking to a small volume, presses out all water. The low water content (50%) shows that the actomyosin has given up practically all water and consists of wet, but anhydrous, matter. This excessive shrinking can be studied with advantage on actomyosin-threads into which, owing to the relatively large surface, the ATP diffuses rather rapidly. If an actomyosin thread is prepared in a 0.05 *M* KCl solution, this thread consists of actomyosin which has shrunk and dehydrated under the influence of the salts present. If ATP is now added to this system, the thread contracts within a few seconds to about  $\frac{1}{3}$  of its original length and becomes proportionately thinner (Fig. 5).

As described above an actomyosin gel can be dissolved by higher salt concentrations (0.4 *M*), and can be brought to dissociation by 2 *M* KCl. In the presence of ATP, the gel is dissolved and completely dissociated by 0.2 *M* KCl. Superprecipitation and contraction are thus

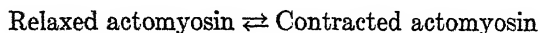
limited to a very small range of KCl concentrations, outside of which the actomyosin dissolves and dissociates, and within which it superprecipitates and contracts.

Since Banga has shown that the  $K^+$  adsorption curves of myosin and actomyosin are not changed by the presence of ATP, we can correlate these observations with the curves of Fig. 2. In terms of K adsorption we can express our results by saying that, in the presence of ATP, actomyosin is stable only if it contains 4-7  $K^+$  per unit weight of myosin. K-myosinate, containing less or more  $K^+$  than 4-7, forms, in the presence of ATP, no compound with actin at all. The actin compound formed is hydrophobic.

$Mg^{++}$ , if added to the system in very small concentration, narrows the stability range of actomyosin still further. In the presence of  $Mg^{++}$  and ATP actomyosin in suspension dissolves and dissociates in 0.1 M KCl.

As shown previously, ATP forms a compound with myosin; in the presence of ATP we are thus not dealing with free myosin, but with myosin-ATP. We can also sum up our observations by saying that while actomyosin- $K_{0-11}$  is stable and fairly hydrophilic (with a maximum and minimum of hydrophilic activity at  $K_6$ ) actomyosin-K-ATP complexes are only stable between  $K_{4-8}$  and are hydrophobic. Naturally, the range of stability also depends on the ATP-concentrations, *i.e.*, the ATP saturation of the myosin. The higher the ATP concentration, the smaller this stability range. At the physiological 0.4% ATP concentration the range is rather narrow.

Actomyosin-ATP is thus unstable at room temperature in the relaxed condition. According to the nature and concentration of the salts present, it either dissociates or contracts. Actomyosin-ATP, in the relaxed state, is only stable at low temperature, *e.g.*, at 0°C. where there is no contraction. When dissociated actomyosin is caused to contract, the reaction taking place in two distinct steps, the first step being the union of actin with myosin, and the second the contraction of the actomyosin formed. The reaction



seems to be an equilibrium reaction with the equilibrium shifted to the left at low temperature, and to the right at room temperature. At room or body temperature the intermediary "relaxed-actomyosin" being unstable, dissociated actomyosin appears to pass directly into the contracted actomyosin. All these reactions are perfectly reversible and dissociated (relaxed) actomyosin can be brought to association (contraction) at a constant ATP, by varying the salt concentration or at a constant salt concentration by varying the ATP-concentration. Very slight variations (15%) suffice to produce these changes. To be more exact, it is not the

double protein which contracts and relaxes but its nucleotide compound. The ATP-saturation of the protein depends on the ATP concentration present. It requires high ATP saturation and, consequently, high ATP-concentration to have a strongly reacting system. It seems that, *in vivo*, the whole high physiological ATP-concentration is needed to make a well-reacting system. If the ATP-concentration is decreased it is the relaxation which suffers first and parallel with the decreased ATP-concentration the system begins to contract (*Erdős*). It seems that pathological conditions characterized by a decreased ability of certain muscle cells to relax (angina pectoris, dysmenorrhea, vasospastic gangrene) are due to such a decrease of the physiological ATP-level and can be relieved by restoration of this level through the administration of the nucleotide. This is the case when the concentration of ATP is decreased in an excitable muscle. The result will be different if the ATP is decomposed in an unexcitable system, as is the case *post mortem*, where there is simply left the stiff, slightly salt-precipitated, and thus slightly contracted, ATP-free actomyosin. This condition called *rigor mortis*, can also be relieved by the introduction of ATP.

The reaction of actomyosin, naturally, depends not only on the concentration of salts and ATP, but also on the relative concentration of the actin and myosin which make up the actomyosin. The two proteins can react in all proportions. As shown by Balenovic and Straub, the most reactive system is obtained by uniting 1 part of actin with 2.5 parts of myosin. The analysis of the muscle by the same authors has shown that muscle contains the two proteins in this 1:2.5 relationship. Muscle thus contains maximally active actomyosin. The data in this paper relate, if not stated otherwise, to such actomyosin prepared from 2.5 parts of crystalline myosin and 1 part of actin.

A few words may be said about G-actin and its actomyosin. Similarly to F-actin, G-actin also readily forms a compound with myosin which is precipitated by salts. The viscosity of this compound, however, is about the same as that of free myosin. There is also a great difference in the behavior of the G-actomyosin and F-actomyosin in the presence of ATP. It has been shown that at certain salt concentrations F-actomyosin-ATP is stable and contracts. No contraction of G-actomyosin has been observed and, in the presence of ATP, the compound dissociates at any salt concentration into G-actin and myosin or respectively, actin and myosin-ATP. The G-actin thus forms no compound at all with the myosin-ATP.

#### A THEORY OF CONTRACTION

Contraction, which is only an extreme degree of colloidal shrinkage, can be advantageously studied in actomyosin threads. These threads



resemble in their appearance muscle fibers. There is, however one very essential difference between the contraction of threads and muscles. While the former is isodimensional, the latter is anisodimensional. In other words: while, on contraction, the thread becomes shorter and thinner, muscle becomes shorter and thicker. While the thread shrinks in three dimensions, muscle shrinks only in one. There is also, however, a corresponding difference in the structure of both formations. While, in muscle, the micelles are stretched out coaxially to the fiber, in threads the micelles are distributed at random.

It is possible, however, as shown by Gerendás, to arrange the micelles of the thread to some extent similarly to muscle and this is by stretching. In such stretched thread the contraction is anisodimensional and the thread, on contraction, becomes shorter and thicker. This is very important because it gives some information about the mechanism of contraction.

The extensive shrinking of colloids is always due to the loss of intermicellar water. In our stretched threads the micelles are stretched out coaxially to the thread and thus, correspondingly, the intermicellar splits are also running parallel to the fiber axis. If the water is pressed out of such a split, this could never make the thread shorter, it could only make it thinner. Hence, if the thread becomes shorter and thicker on contraction, this cannot be explained by the loss of intermicellar water but only by the shortening of the micelles. If, during contraction, water is lost, this is not the cause but the result of the contraction, the intermicellar water being pressed out by the contracting micelles which must shorten at least to  $\frac{1}{3}$  of their original lengths since the threads contract by  $\frac{2}{3}$ .

But, how can a micelle shorten to such an extent, a micelle composed of two colloids, one of which (myosin) is capable only of dehydration, while the other, actin, is quite inert and is not precipitated or dehydrated by neutral salt at all?

To find the answer let us try to picture an actomyosin micelle. As has been shown, F-actin consists of short rods. If myosin is attached to this actin rod on one side then we will have a double rod, consisting of two sticks, one of which is inert and the other capable of very limited shrinkage due to loss of its hydrate water. The problem is thus: what will happen with a double rod, if one of the rods shrinks to a small extent, while the other remains unchanged? This is a very simple geometrical problem, which can be answered not only by geometry but also by our experience in every day life. The warping of wooden boards is due to the fact that the two sides of the board do not expand or contract equally under the influence of changes in humidity and thus behave as double rods. If one of the components of the double rods becomes shorter,

the system has to bend and has to bend very extensively. If the system is, say, 100 units long and 1 wide and one of the sticks shortens by 3 units, the whole system must curl into a circle and be shortened by  $\frac{2}{3}$  of its total length, or 66 units.

This is illustrated by the model in Fig. 7a. The wooden stick represents actin. To make it look more like actin, the stick has been cut into



FIG. 7

Model of the Actomyosin Micelle; a: Distended; b: Contracted

cubes (the actin thread being composed of smaller, globular particles). The myosin is represented by a rubber tube which has been stretched to some extent before its ends were fixed to the actin rod. If the system is released then the rubber will shorten somewhat, imitating the dehydration of the myosin. What happens is shown in Fig. 7b: the stick curls up. This model also explains why the actin fibers have to be built

of globular particles. If the actin stick, in the model, could not break up into smaller particles, it would resist bending.

This model of muscular contraction is capable of explaining an old puzzle of muscle physiology. Since the muscle is formed of colloids, muscular contraction can be looked upon as a one-dimensional, very extensive colloidal shrinking. The shrinking of colloids takes place in two stages: the loss of intermicellar water and the loss of hydrate water. The quantity of intermicellar water may be very large, the corresponding shrinkage thus very extensive; the quantity of hydrate water is always very small, the corresponding shrinkage thus very limited. Still, only this latter shrinkage is connected with the greater thermodynamic changes and correspondingly only this latter is capable of doing work. The loss of intermicellar water, though very extensive, is thermodynamically neutral and is thus useless as a source of work. Muscular contraction is extensive but still capable of doing work throughout its whole range. A simple explanation is given by our model in which the very slight dehydration of myosin (contraction of rubber) is magnified into a very extensive shortening. The whole mechanism is a most ingenious device in which the very small shrinkage of a colloid, due to the loss of hydrate water, is magnified to an extensive motion.

#### STERIC RELATIONS

If we imagine the muscle fibril as being built of actin-myosin double rods, we may ask how these single actin and myosin rods are actually placed side by side. In model experiments we can try different ways of putting sticks together; all but one will lead us into difficulties. The only arrangement which will be found acceptable is a spiral one. On first approach we may imagine, for instance, the actin forming long threads and the myosin winding round this actin thread. This system will resemble a screw. If the myosin dehydrates it will bend and shorten to something like a cork screw.

There is only one difficulty experienced with such a model, a difficulty caused by the analytical data of muscle. Muscle contains about 8% of myosin and about 3% of actin, which makes 11% of actomyosin. All this actomyosin is contained in the fibril which occupies about  $\frac{1}{3}$  of the total volume of muscle. The fibril thus contains no less than 33% of actomyosin, which is strongly hydrated. "Strongly hydrated" means that a relatively great part of the water present is bound to the protein, further increasing its volume and decreasing the volume of free water. We may suppose, by approximation, that actomyosin binds roughly an amount of water equal to its dry weight. This would thus leave us with 66% of hydrated actomyosin and 34% of free water. Thus,  $\frac{2}{3}$  of the

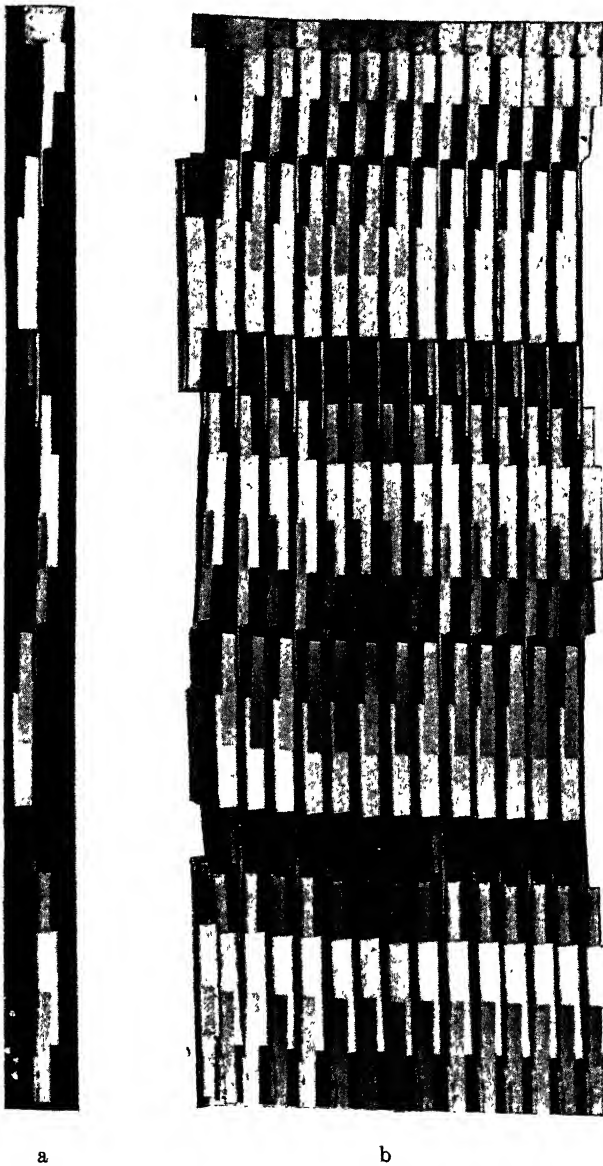


FIG. 8

a. Model of One Spiral. The Actin Thread is Represented by a Glass Rod, the Myosin by Celluloid Plates Stuck to the Rod in a Spiral. b. 14 Spirals Placed Side by Side

volume is occupied by the hydrated protein and  $\frac{1}{3}$  by free water. Free water means free space,  $\frac{1}{3}$  free space means exceedingly close packing. It is impossible to pack sand closer, though its grains fit fairly well together. How could it be possible to bring the particles of such an irregular formation, like a screw, into such close proximity? This is possible only if the single screws are put side by side in such a way that the screw threads of the one fit into the grooves of its neighbors. If we do this, then all the screw threads must run parallel to each other and in any cross-section of the system all the screw threads must be found in the same phase, that is, lying on the same side of their actin axis.

Such a regular arrangement, however, will have a remarkable effect on the optical properties of the system. If we were to pick out one single screw and look at it from the side, we would find that its optical properties change periodically as the myosin screw thread winds around the actin. The system will have certain optical properties when the myosin is to the right or left of the actin and different ones when it bends away, or is just before or behind the actin. If, at any level, all the screws are in the same phase, then this periodic change of the optical properties of the single screws must sum up to a cross-striation. This is illustrated by Fig. 8.

Now muscle *has* a cross-striation which shows even the finer structure postulated for a system of spirals. This cross-striation has always been explained by a segmental structure of the muscle fibril. The above considerations, however, make it probable that this cross-striation is only an optical appearance. To decide between the two possibilities, muscle fibrils have been rotated under the microscope. If the cross-striation is due to a spiral arrangement, on rotation the cross-striation must shift along the axis, and must shift by two periods on turning through  $360^\circ$ . Naturally, if the cross-striation is due to segmental structure, no such shift could be observed. The experiment showed that, on rotating the fibril through  $360^\circ$ , the cross-striation shifted by two periods.

All this, naturally, only holds for the muscle with 33% of actomyosin in the fibril and the consequent close packing. Body muscle moves rapidly, has to develop great force within short periods of time, must have a great deal of contractile substance crowded into a small space. This does not hold for the slowly moving muscle cells of our inner organs. There is no need here for such close packing and consequently the single spirals will not be in the same phase and the optical periodicity of the single spirals will not sum up to a cross-striation.

This gives a rather satisfactory explanation of the existence of the two kinds of muscle, smooth and striated. It also explains why the embryonic heart muscle begins to contract before developing its cross-

striation, and how such an apparently complicated structure, as cross-striated muscle, can appear suddenly in the phylogenetic scale.

The actual structure of the single spirals is unknown. The only dimension known at present is the length of a full turn of the screw, which is 0.002 mm. for mammals (diameter of one Q and I stripe). The model in Fig. 8a supposes that the actin thread is formed by one row of micelles (black pearls). It is in agreement with the quantitative

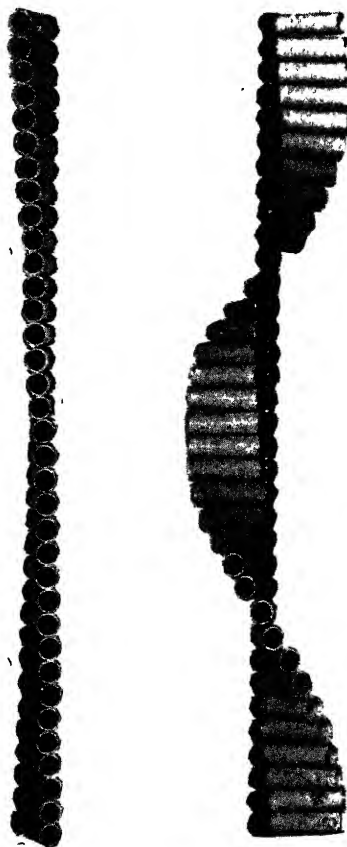


FIG. 9

Model of a Single Actomyosin Spiral

relations of actin and myosin in muscle and in agreement with the rather probable assumption that the elongated myosin particles (celluloid tubes in the model) are attached to the actin at one end. If the diameter of the myosin micelle is 50 Å, as H. H. Weber supposes, then 400 micelles would make one full turn and the spiral would be rather flat, as shown in Fig. 8b. The model is not in agreement with the dimensions of the myosin micelle as given by Weber and Stöver, according to whom the micelle is 50 Å wide and 500 Å long, with the axial ratio of 1/10. To bring the model into agreement with this ratio the single celluloid tubes would have to be split into about ten thinner rods. In this case the pitch of the screw would be between that of Fig. 8a and b.

## PHOSPHATASE ACTIVITY

Physiology teaches that resting muscle is enzymatically inactive. Contracting muscle splits ATP and there is a certain relation between the quantity of ATP split and the tension developed. This means that it is finally the splitting of the ATP which pays the energy bill of contraction. We may thus ask what it is which causes the ATP-splitting when the muscle contracts and what stops it when the muscle relaxes, and how does the muscle know exactly how much ATP to split?

The observations of Banga offer an easy explanation. She has shown that the ATP-splitting by myosin is greatly inhibited while that of actomyosin is greatly enhanced by  $Mg^{++}$ . Actomyosin, in presence of ATP, is always contracted at ordinary temperatures. Thus, Banga's results may be formulated by saying that the phosphatase activity of relaxed dissociated actomyosin is inhibited, that of contracted actomyosin is greatly accelerated by  $Mg^{++}$ . Muscle contains a rather high concentration of  $Mg^{++}$ . Thus; we can understand that in rest, with the actomyosin system relaxed, it will not split ATP and will start doing so as soon as it is contracted and will split only as long as it is in this state and will stop doing so as soon as it is relaxed and there is no need of further liberation of energy.

These observations suggest a satisfactory answer to another old problem of muscle physiology: Is energy needed for contraction or relaxation? In the picture developed in this paper, resting muscle contains its actin-myosin system in the relaxed, dissociated condition. Excitation brings about the association to actomyosin. The actomyosin passes spontaneously into the more stable contracted state which is poorer in energy. External work may be done because of this difference. Then the splitting of ATP sets in supplying the energy needed for relaxation.

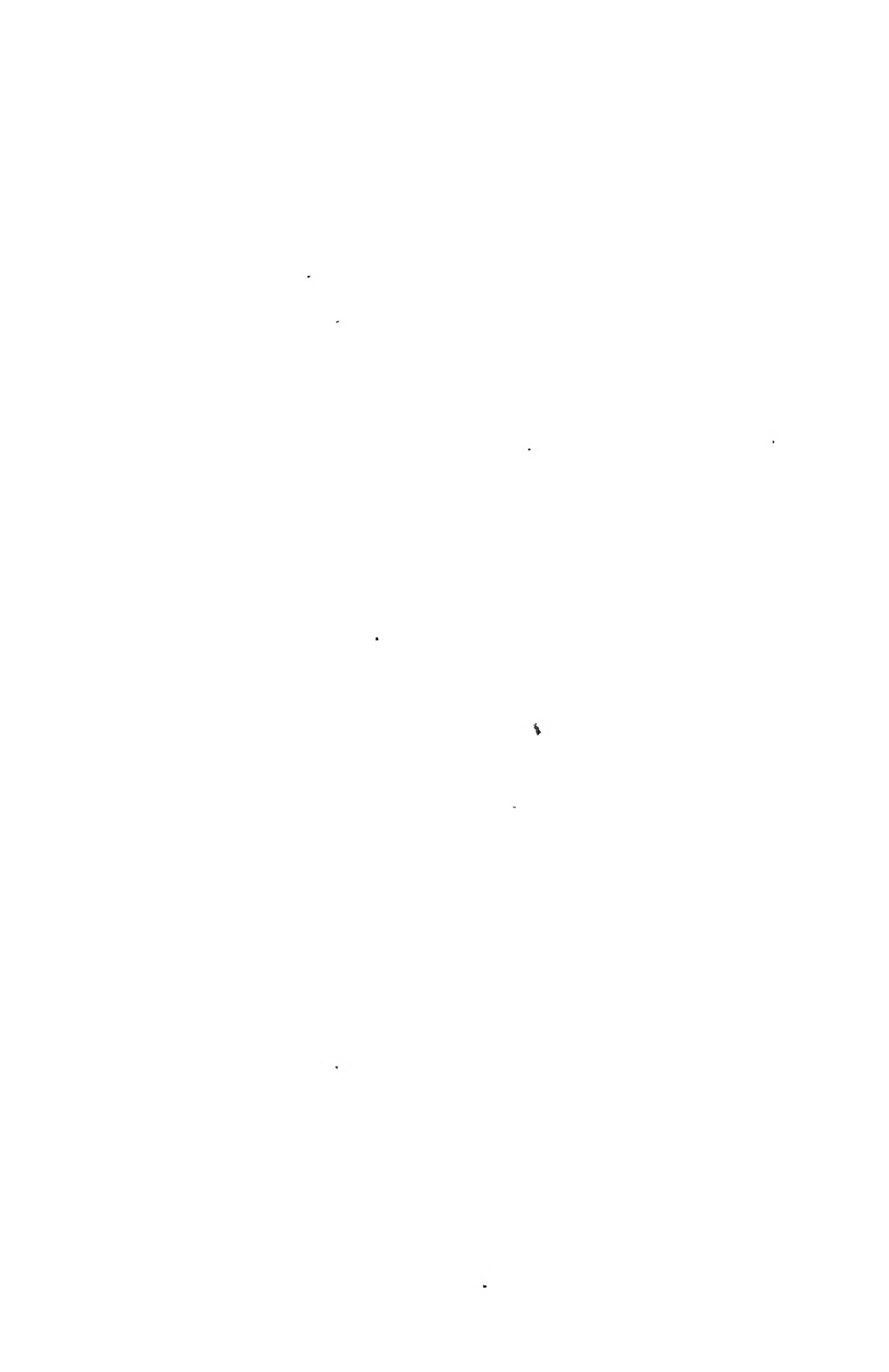
Whether the splitting of ATP is immediately involved in the mechanism of this process we do not know. But there are many other things we do not know, and it is hoped that the observations presented in this paper will facilitate their approach.

## REFERENCES

1. DANILEWSKY, A., *Z. physiol. Chem.* **5**, 158 (1881).
2. VON FÜRTH, O., *Arch. exp. Path. u. Pharmacol.* **36**, 231 (1895).
3. VON FÜRTH, O., *Ergeb. Physiol.* **17**, 363 (1919).
4. HALLIBURTON, W. D., *J. Physiol.* **8**, 133 (1887).
5. WEBER, H. H., *Ergeb. Physiol.* **36**, 109 (1934).
6. EDSALL, J. T., *J. Biol. Chem.* **89**, 289 (1930).
7. VON MURALT, A. L., AND EDSALL, J. T., *J. Biol. Chem.* **89**, 315, 351 (1930).

8. ENGELHARDT, W. A., LJUBIMOVA, M. N., AND MEITINA, R. A., *Compt. Rend. Acad. Sci. U.R.S.S.* **30**, 644 (1941).
9. ENGELHARDT, W. A., *Yale, J. Biol. Med.* **15**, 21 (1942).
10. DAINTY, M., KLEINZELLER, A., LAWRENCE, A. S. C., MIALI, M., NEEDHAM, J., NEEDHAM, D. M., AND SHEN, S. C., *J. Gen. Physiol.* **27**, 355-99 (1944).
11. STRAUB, F. B., Studies from the Institute of Medical Chemistry, University of Szeged, Basel-New York **2**, 3 (1942).
12. BANGA, I., AND SZENT-GYÖRGYI, A., Studies from the Institute of Medical Chemistry, University of Szeged, Basel-New York, **5**, 25 (1942).





## POLARIZATION AND PERMEABILITY (QUANTITATIVE MEASUREMENTS)<sup>1</sup>

M. Spiegel-Adolf and E. A. Spiegel

*From the Departments of Colloid Chemistry and Exp. Neurology,  
Temple University School of Medicine, Philadelphia, Pa.*

*Received November 7, 1945*

### INTRODUCTION

The measurement of the permeability of membranes is of interest to colloid chemists as well as biologists. If one wishes to ascertain the permeability of cellular membranes within the organs of animals, the usual chemical methods as a rule can hardly be applied, particularly when rapid changes of permeability are to be recorded. Due to their semipermeability to electrolytes, the cell membranes are the seat of electrical double layers. They show polarization phenomena, *i.e.*, an electromotive force in opposite direction develops, when a direct current flows through the organ. If an alternating current passes through the organ this counterforce, and consequently the impedance measured, is smaller the higher the frequency of the A. C. Gildemeister (1) has pointed out that determination of the capacitance may serve as an indicator of the polarizability and thus indirectly of the permeability. The measurement of the polarization capacity requires complete balancing of the Wheatstone bridge, so that its zero arm is practically free of current. This is sometimes rather inconvenient, particularly when one deals with rapid changes due to experimental procedures.

Therefore, we developed a method based upon another manifestation of polarization; *viz.*, the fact that the difference between the conductivity at a certain high frequency ( $C_h$ ) and that at a certain low frequency ( $C_l$ ) is larger the more polarizable the membrane under study (2). From the measurements of  $C_h$  and  $C_l$  the polarization index  $\Delta = \frac{100(C_h - C_l)}{C_l}$  is calculated (2). Applying such measurements to the brain, it was found that some epileptogenous agents diminish the density of the cell membranes, while hypnotics and anesthetics act in the opposite direction (3, 4).

To analyze the basic chemical and colloid chemical conditions, experiments on artificial membranes have been performed (2, 5). In

<sup>1</sup> Aided by a grant from the John and Mary R. Markle Foundation.

artificial membranes containing body constituents it could be shown that proteins may be substituted by other colloids, while the presence of lipids seems to be necessary for achieving polarizability. By perforating polarizable collodion or lecithin-collodion membranes repeatedly, a progressive reduction of  $\Delta$  was produced (5). These findings pointed to a relationship between permeability and polarizability. However it seemed desirable to present a more direct evidence of such a relationship by a quantitative study. In the experiments to be reported here, frog's skins were used in order to obtain data from a natural membrane.

*Method:* The experiments were performed on the skin of the trunk of winter frogs. On such isolated preparations, a series of alternating measurements of  $\Delta$  and of the permeability for an electrolyte (NaCl) or for a non-electrolyte (urea) were made during the first stages of *post mortem* deterioration of the specimen. The skin was inserted flat between the ground flanges of the central and one external compartment of a Pauli electro dialysis apparatus, the original wire mesh Pt electrodes of which had been coated electrolytically with platinum black. The surface inserted measured 452 mm.<sup>2</sup>. Between the central and the other external compartment no membrane was inserted, so that the apparatus was changed into a system consisting of 2 cells only.

For the determination of  $\Delta$ , the apparatus was filled with 0.1 *N* NaCl solution on either side of the skin. The bridge arrangement was the same as previously described (3, 4). Frequencies of 547 and 5120 cycles respectively were used. The measurements were made at room temperature.

For the dialysis experiments the 0.1 *N* NaCl solution in the apparatus was replaced in the compartment facing the inner side of the skin by a 5.4% dextrose solution, and in the compartment facing the external surface of the skin, by a *N* NaCl solution. Each dialysis lasted 50 minutes and was performed at room temperature. This time interval was chosen because it permitted one to make from 5-6 dialysis experiments on one specimen within 1-2 days. After each dialysis experiment both the NaCl and the dextrose solution were replaced by fresh solutions. Since the maximum amount dialyzed did not exceed 1.2% of the initial concentration, the gradient was practically constant during a single experiment. NaCl entering the dextrose solution was determined, following each dialysis experiment, by measuring the conductivity of samples of the dialysate (dextrose-NaCl mixture) at 30°C. To convert the conductivity values to NaCl concentration, a standardization graph which had previously been obtained from NaCl-dextrose mixtures of known concentrations was used.

In a second series of experiments, the permeability of the skin preparations for urea was tested, a solution containing 16.2% urea and 5.4% dextrose solution being on the outer surface and a 5.4% dextrose solution on the inner side of the skin. With this group also each dialysis lasted 50 minutes. The urea content of the dialysate was determined by means of a Zeiss interferometer, a 5.4% dextrose solution serving for comparison. The conversion of the interferometric readings into urea concentrations was made by means of a standardization curve obtained by interferometry of 5.4% dextrose solutions containing urea in various concentrations. Before and after each dialysis experiment the  $\Delta$  of the membrane was determined by double measurements.

## RESULTS

If an isolated preparation of frog's skin is kept in a 0.1 *N* NaCl solution, the polarizability of the specimen, as determined by the polar-

ization index  $\Delta$ , increases in the first 1-4 hours, and then gradually declines reaching values close to zero about 5-50 hours *post mortem* (Fig. 1). The dialysis experiments were, as a rule, performed during the decrease of the  $\Delta$  values. In order to compare polarizability and permeability, the average of  $\Delta$  for each dialysis period was computed from the values before and after dialysis, and the mean  $\Delta$  was plotted against the amount of NaCl or urea which had passed through the membrane in the corresponding interval of 50 minutes.

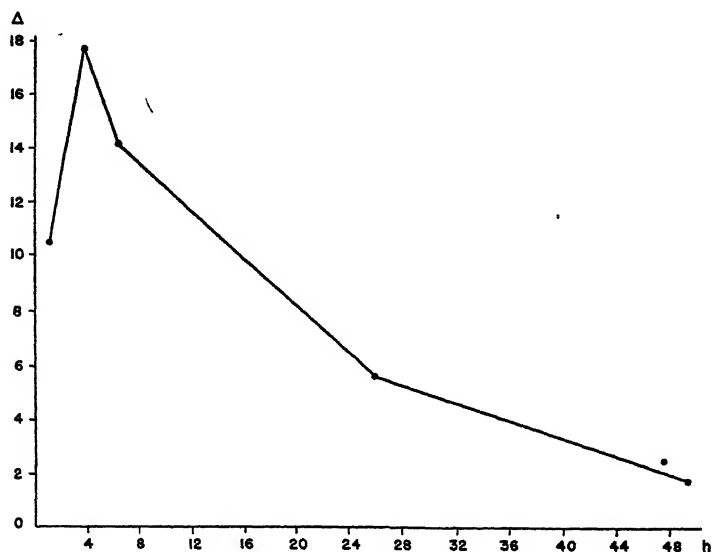


FIG. 1

Post Mortem Changes of  $\Delta$  (Frog Skin)  
Abscissa: Time after death

Fig. 2 shows the result of such a typical experiment, in which NaCl permeated into the dextrose solution. A linear relationship between the changes of  $\Delta$  and of the permeability for NaCl is demonstrable. It is evident that the intersection of the graph and the  $x$ -axis indicates the value of  $\Delta$  for which the membrane is completely impermeable to NaCl. The intersection of the graph and the  $y$ -axis shows the amount of NaCl that penetrates the membrane after a complete loss of  $\Delta$ . This value is finite, and it may be inferred that the membrane has some semi-permeability left after the loss of polarizability. The first derivative of the above graph can be used as characteristic of the membrane. Changes of  $\Delta$  are a function of time. If time is substituted for  $\Delta$  in the above graph, the resultant first derivative at a specified time indicates the rate at which salt is dialyzed at this time, and this corresponds to the permeability.

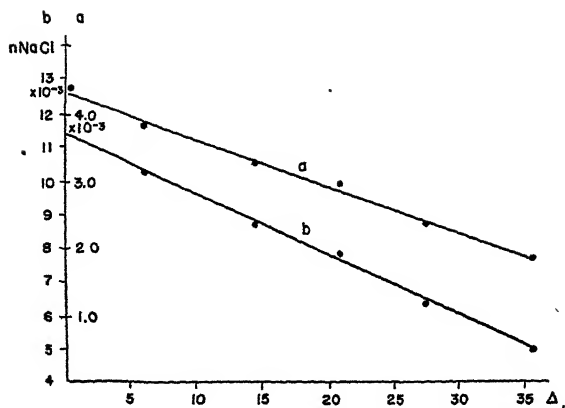


FIG. 2

Relationship Between  $\Delta$  and Permeability for NaCl (Frog Skin)

Ordinate of curve a is conductivity of dialysate.

Ordinate of curve b is NaCl concentration of dialysate.

The relationship between polarizability and permeability for a non-electrolyte, such as urea, is illustrated in Fig. 3. The amount of urea passing through the frog's skin in 50 minute intervals is plotted against the average value of the  $\Delta$  measurements performed before and after each dialysis. Contrary to the results obtained with NaCl, the resulting graph is non-linear. It shows, however, that with decreasing  $\Delta$  the amount of urea passing through the membrane increases. Thus it seems warrantable to infer that changes of  $\Delta$  indicate changes of permeability for an electrolyte, such as NaCl, as well as for non-electrolytes, such as urea.

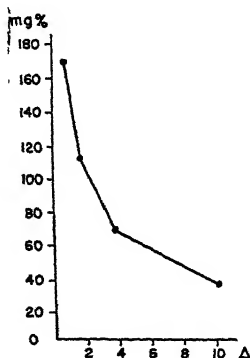


FIG. 3

Relationship Between  $\Delta$  and Permeability for Urea (Frog Skin)

Ordinate: Urea concentration of dialysate

Another characteristic of the urea experiments requiring comment is the fact that the permeability for urea rises very steeply with decreasing  $\Delta$  values. If an extrapolation of the graph in Fig. 3 is permissible, it seems to indicate that after a complete disappearance of  $\Delta$  the membrane probably would hold back only little, if any, urea while only a rather limited amount of NaCl can permeate the membrane at a zero value of  $\Delta$ . The differences are obvious on comparison of the NaCl- $\Delta$  and the urea- $\Delta$  graphs. Differences in the behavior of semipermeable membranes toward ionized and non-dissociated substances have been observed by Weatherby (6), who refers them to the electrical status of both the membrane and the permeating substance. One of us (Spiegel-Adolf (7)) has been able to show that neutral NaCl solutions give a positive charge to globulins within the concentration range used in these experiments. No such changes can be produced by urea. This may account, at least partly, for the differences in the shape of the NaCl and of the urea curves. Changes in the degree of hydration of the membrane proteins produced by the urea (Heim (8), Spiegel-Adolf (9)) may also play a role.

#### SUMMARY

The relationship between polarizability and permeability was studied on isolated frog skins during the initial stages of *post mortem* deterioration. The polarizability was determined by measuring the conductivity at a high ( $C_h$ ) and at a low frequency ( $C_l$ ) of A. C. and calculating the difference of these measurements expressed in percentage of  $C_l$  (polarization index  $\Delta$ ). In one series of experiments the permeability for NaCl was determined, and in a second series that for urea. Both groups of experiments indicated that decrease of polarizability is associated with increase of permeability.

#### REFERENCES

1. GILDEMEISTER, M., *Handbuch der normalen und pathologischen Physiologie*. Edited by A. Bethe *et al.* 8, II, 657 (1928).
2. SPIEGEL-ADOLF, M., AND SPIEGEL, E. A., *Proc. Soc. Exptl. Biol. Med.* 32, 139 (1934).
3. SPIEGEL, E. A., AND SPIEGEL-ADOLF, M., *Am. J. Psychiatry* 92, 1145 (1936).
4. SPIEGEL, E. A., AND SPIEGEL-ADOLF, M., *J. Nervous Mental Disease* 90, 188 (1939).
5. SPIEGEL-ADOLF, M., *J. Gen. Physiol.* 20, 695 (1937).
6. WEATHERBY, J. H., *J. Cellular Comp. Physiol.* 21, 1 (1943).
7. SPIEGEL-ADOLF, M., *Globuline*. Th. Steinkopff. Dresden-Leipzig, 1930.
8. HEIM, F., *Biochem. Z.* 291, 88 (1937).
9. SPIEGEL-ADOLF, M., *Federation Proc.* 3, 63 (1944).



# TORSION IN PROTOPLASM

William Seifriz

*From the Botanical Laboratory, University of Pennsylvania, Philadelphia, Pa.*

*Received August 8, 1945*

## INTRODUCTION

Several years ago, in a discussion on the spiral paths followed by organisms in movement and growth, I expressed the belief that a state of torsion is established in protoplasm when it is in motion, provided certain simple conditions are met. These conditions exist in a freely suspended strand of protoplasm in which flow is only in one direction at any given moment. A thread of the plasmodium of a myxomycete satisfies the foregoing requirements.

Experimental verification of the assumption that a state of torsion exists in protoplasm under specified conditions was accomplished by the following method. One end of a freely hanging strand of the myxomycete *Physarum polycephalum* was affixed, by adhesion, to the under side of a cover slip. To the lower end of the strand a delicate glass needle was attached and adjusted to a horizontal position. The needle served as a pointer to indicate the direction and extent of twist and, therefore, of torsion in the thread. With the freely hanging protoplasmic thread and its horizontal needle thus suspended from a cover slip, the slip was placed in position over a small moist chamber, the protoplasmic thread hanging within the chamber. The swing of the needle and the flow of the protoplasm were observed through the microscope.

There would be no evident reason for the swing of the needle, first in one direction and then in another, were there not an alternating twist in the protoplasmic thread, and there would be no reason for the twist were not some force bringing it about. This force is the flow of protoplasm. Obviously, movement alone is not sufficient. The flow of a liquid in a plastic tube will bring about a twisting of the tube only if the wall is spirally wrapped or fluted as in the case of the rifling of a gun barrel.

The protoplasm of the slime mold *Physarum* is in a constant state of flow; the movement is first in one direction and then in the opposite direction. This rhythmic motion of protoplasm has been the subject of much investigation (9), and is now recognized as a fundamental form of movement in living matter. The average time of flow in one direction in *Physarum* was established by Kamiya (3) at 47.5 seconds.



When a horizontal needle, which is attached to a freely hanging thread of protoplasm, is observed through the microscope after a lapse of time sufficient to permit the dismembered protoplasm to resume normal streaming, the needle will be seen to swing rhythmically to the right and to the left. Many irregular movements occur. These are due to disturbances caused by severance of the strand, support of a needle, and readjustment necessary when so small an amount of protoplasm is subjected to such extreme conditions. But even more significant than experimental factors in causing irregular movements are the disturbances frequently occurring in healthy plasmodia. The 45 to 50 second rhythm in protoplasmic flow is maintained only when the slime mold is progressing continuously in one direction. Change in direction of locomotion, or change in the internal physiological state of the plasmodium is sufficient to cause an upset in the normal rhythm of progression. There are also interference phenomena so well analyzed in terms of harmonics by Kamiya (3). In spite of these disturbances there is a surprising regularity in protoplasmic flow and, therefore, in twist and torsion of the protoplasmic strand, as revealed by the swing of the needle. This rhythm is shown in Fig. 1.

The experimental work here reported progressed in two stages. There was first the direct observation that what had been predicted on the basis of theory was in fact true. A state of torsion is set up in protoplasm when that protoplasm is in a state of flow. This fact was then placed on a quantitative basis.

Quantitative observations necessitated somewhat more intricate technique. Means were needed by which the precise degree of swing of the needle could be measured at stated intervals. To accomplish this, the moist chamber containing the hanging thread of protoplasm with its attached needle was placed on a revolving microscope stage. The needle was kept in one position by rotating the stage, first to the right and then to the left, as the needle swung left and right. The vernier readings were noted at convenient intervals of time, including always the moment of reversal in direction of swing. The latter readings are important because they establish the points of return, the peaks and troughs of the curve. Intermediate readings determine the shape of the curve and reveal unexpected irregularities.

The curve in Fig. 1 presents five significant facts: (1) that there is a rhythmic twist in the protoplasmic thread; (2) that the amplitude of the arc over which the needle travels attains a maximum of  $60^\circ$ ; (3) that the swing is always slightly greater in one direction than in the other; (4) that there are irregularities in movement which come in groups between periods of perfect rhythm; and (5) that the beat is 25 seconds, exactly half of the expected 50 seconds. Of the foregoing facts, the first,

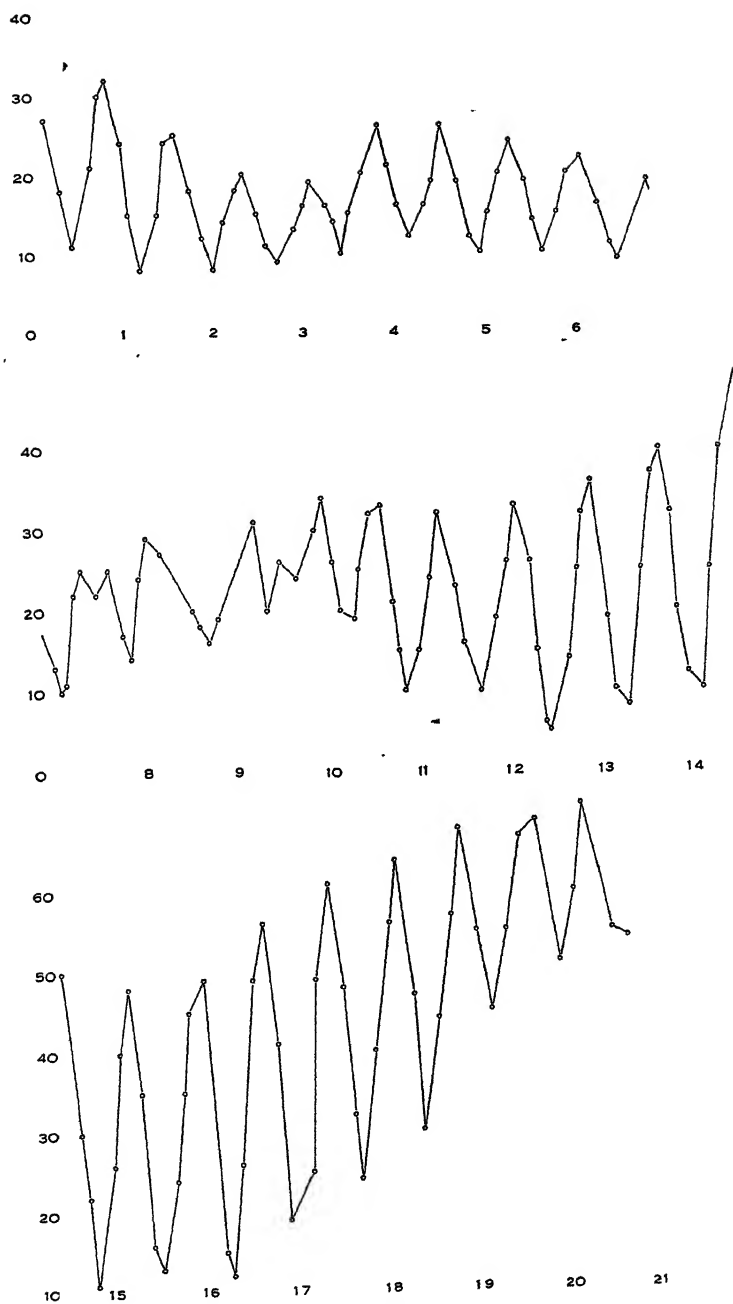


FIG. 1

Graph of the Torsion Rhythm in Protoplasm.  
The amplitude in degrees, and the direction in twist of the protoplasmic thread,  
are plotted as ordinates against time as abscissae.

that a state of torsion is set up in moving protoplasm, was my primary interest. Once this prediction was experimentally verified, interest then centered in the greater swing in one direction, and the relation between 50 second periods of flow and 25 second periods of twist.

That there is a progressive increase in the amplitude of swing as the protoplasm flows first in one direction and then in the other in its shuttle movement, is shown by the gradual incline and decline in the peaks of the curve (Fig. 1). The protoplasm, therefore, increasingly tightens, then loosens, its spiral twist. The first portion of Fig. 1 shows a downward trend of the curve peaks; the right half of the central portion and the last third of the curve show the same effect in the opposite direction. They indicate a greater swing in one direction at each pulsation.

The left half of the central portion of the curve is a period during which irregularities in movement occur due either to physical or physiological readjustments, or to interference in the several rhythms known to occur in a plasmodium (3). It is these perfectly normal disturbances, as well as abnormal experimental ones, which frequently upset the rhythm.

During the preliminary experiments attempts were made to establish a correlation between the rhythm in swing of the needle and the time of protoplasmic flow but without success, for there were too many conflicting observations. Swing of the needle to the right *and* to the left while the protoplasm continued to flow in the *same* direction was frequently observed but only later understood. That twist and torsion are due to protoplasmic movement seemed inevitable, and it also appeared likely that a swing to the right would occur when flow is in one, up or down, direction, with a swing to the left when flow is in the opposite direction. The difficulty was a matter of technique. There is also a disturbing lag in the swing of the needle. The lags were frequently recorded, thus confusing the synchronism between flow and twist. These difficulties were later mastered and the cause of the apparent lack of synchronism understood.

The tidal flow of protoplasm is a shuttle movement. If such a movement is the energy source of a mechanism, then the force which it can exert is greatest midway between the two terminals, for the speed is greatest there. A tidal flow will, consequently, exert an ever increasing force until its maximum speed is reached at the mid point, and from there on, though the protoplasm is still flowing in the same direction, the available force decreases until it reaches zero at the expiration of the period of flow. The protoplasmic strand will therefore attain maximum torsion at the mid point. To twist the thread further will require greater force, but the available energy is now falling off. From the mid point on, the protoplasm is still moving in the same direction but at an ever decreasing speed; as a result, the strand will unwrap, the torsion which

was set up now operating against the decreasing force of protoplasmic flow.

The following two groups of observations indicate what takes place.

Direction of	
protoplasmic flow:	swing of needle
down	left
up	right
up	left
down	right
down	left
down	right
up	left
up	right

It will be noticed that at each reversal in direction of flow, there is a corresponding reversal in direction of swing of the needle, but there is also a reversal in swing of the needle while flow continues in one direction.

### THEORY

The thought which led directly to the foregoing experimental proof of a state of torsion in protoplasm was based on the knowledge that there are many spiral tendencies in animate nature, revealed in the shape, growth, and locomotion of a great variety of organisms and tissues (7). Asymmetry in form and movement occurs in men, trees (8), protozoa (6) and chromosomes (3). From the work of Astbury (1), Mark (4), Meyer (5) and others on the molecular structure of elastic systems, it is possible to interpret the spiral tendencies of living matter in terms of molecular configuration. Obviously, not all the constituents of living matter need have a spiral or asymmetric orientation, but only the fibrous, the structural proteins (2); nor need all macro-spirals in nature be correlated with micro-spirals or molecular asymmetry. However, every attempt to explain the twist in tree trunks in terms of external forces rather than inner molecular structure proved to be wholly unsuccessful (8). A molecular interpretation of the spiral form and movement of organisms is in keeping with modern chemical interpretations of the structure of organic matter, particularly elastic material. Outward spiral form and movement are due either to asymmetric molecules or to a spiral orientation of molecules.

A molecular interpretation, though convincing, in no way affects the experimental fact that a state of torsion is established in flowing protoplasm.

## SUMMARY

1. A delicate glass needle suspended in a horizontal position on the end of a freely hanging strand of myxomycete protoplasm swings alternately to the right and to the left through an arc of about  $40^\circ$  when the protoplasm is in a state of flow.

2. The swing of the needle is the result of a twisting of the living thread, brought about by streaming of the protoplasm.

3. As a result of the spiral twist produced by streaming, a state of torsion is set up in the protoplasm.

4. The period of swing of the needle is half the period of rhythmic flow in one direction.

5. That the period of swing is but one-half the period of flow is due to a gradually increasing force brought about by increase in rate of flow up to the mid point of movement in one direction, after which there is a gradual lessening in the force applied and a consequent unwrapping of the protoplasmic thread.

6. A molecular interpretation of the structural basis of spiral form and movement in protoplasm is given, based on the known asymmetry of molecules.

## REFERENCES

1. ASTBURY, W. T., *Ann. Rev. Biochem.* **8**, 113 (1939); *Proc. Roy. Soc. (London)* **B129**, 307 (1940).
2. BANGA, I., AND SZENT-GYÖRGYI, A., *Science* **92**, 514 (1940).
3. KAMIYA, N., *The Structure of Protoplasm* (edited by W. Seifriz), p. 199, Ames, Iowa (1942).
4. MARK, H., *Chem. Rev.* **23**, 121 (1939).
5. MEYER, K. H., *Die hochpolymeren Verbindungen*, Leipzig (1940).
6. SCHAEFFER, A. A., *Anat. Record* **34**, 115 (1927).
7. SEIFRIZ, W., *Science* **77**, 50 (1933).
8. SEIFRIZ, W., *Science* **78**, 361 (1933).
9. SEIFRIZ, W., *Botan. Rev.* **9**, 49 (1943).

# ADSORBED NITRATE IONS IN RELATION TO PLANT GROWTH

H. Jenny <sup>1</sup>

*From the University of California, Berkeley, Calif.*

*Received November 13, 1945*

## INTRODUCTION

Nutrition of plants in soils is a domain of colloid science *par excellence*, for it involves the interaction of two complicated colloidal systems: the soil and the plant. In its practical aspects it constitutes the basis of food production and, in turn, of animal and human nutrition.

In soils, a large portion of the nutrient ions exists in the adsorbed state. To account for the availability of adsorbed *cations* to plants two fundamentally different theories have been proposed. First, the soil solution theory, which, in its latest form, takes into account the excretion of carbon dioxide by plant roots. Hydrogen ions of carbonic acid replace adsorbed nutrient cations according to the principles of cation exchange. The ions thus liberated become an integral part of the soil solution which is considered equivalent to the nutrient solution of the plant physiologist. The second theory, known as contact exchange (Jenny and Overstreet, 1938), postulates a direct transfer of cations from soil to plant by means of intermingling of the electric double layers of the clay and root surfaces. In any given soil both mechanisms may operate singly or in combination.

As to the utilization of adsorbed *anions* such as  $\text{NO}_3^-$ ,  $\text{SO}_4^-$ , and  $\text{Cl}^-$  by plants, very little systematic work has been done. In 1935, E. M. Brown (University of Missouri) and the author grew bluegrass (*Poa pratensis*) on mixtures of colloidal clay and iron hydroxide gels containing both exchangeable anions and cations. Because of the difficulty of preparing suitable kinds and amounts of satisfactory exchange compounds, the work was discontinued. Schlenker (1940, 1942) grew corn plants, soybeans and other crops in mixtures of permutite, a cation adsorbent, and De-Acidite or aniline black, an anion adsorbent. His results indicated that for a given combination of nutrients the ions in the adsorbed state produced better plant growth than the ions in solution. Converse *et al.* (1943) confirmed the suitability of commercial cation and

<sup>1</sup> Division of Soils, Berkeley, California. A. Nelson, J. G. Johnson, and C. Willard assisted in greenhouse and laboratory work.

anion exchangers as media for plant growth. These authors offered no suggestions as to the mechanism of release of adsorbed anions to roots.

Fortunately, recent advances in the development of synthetic anion exchange resins offer unique opportunities for studying the behavior of adsorbed nutrient anions in soil-plant systems. In the present paper investigations on nitrate ions adsorbed on amberlites are reported. These were begun in 1939 but had to be interrupted. Meanwhile Graham and Albrecht (1943) have published an interesting report on this same subject.

#### ADSORPTIVE PROPERTIES OF ANION EXCHANGE AMBERLITE

Amberlite IR-4 was purchased from the Resinous Products and Chemical Company, Philadelphia, Pennsylvania. According to the manufacturers, this resin is a polymerization product of formaldehyde

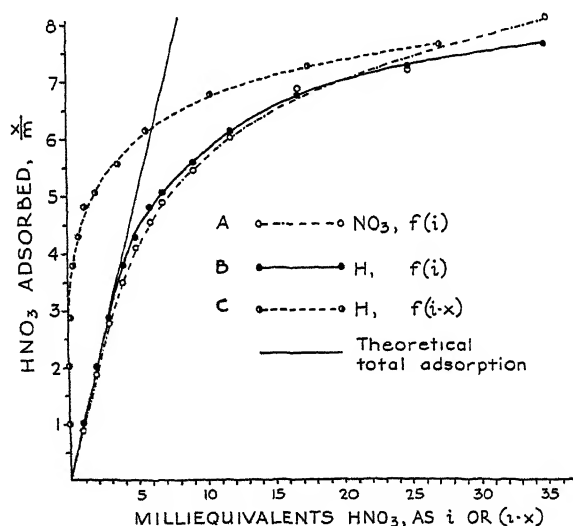


FIG. 1

Adsorption of  $\text{HNO}_3$  by Untreated, but Washed, Anion Exchange Amberlite (IR-4)

and polyamines. The brown, gel-like material varied in particle size from 0.5 to 2 mm. in diameter. The density of air dry amberlite, as determined with a pycnometer, was 1.26, and the total nitrogen content was 14.65%.

In water, amberlite is slightly soluble, yielding a yellowish solution whose intensity, as measured colorimetrically, increased approximately in proportion to the ratio of amberlite to water. At a concentration of 100 g. amberlite in 1000 cc. water, 0.60% solid was found in solution. The yellow supernatant liquid had a distinct Tyndall beam but no particles could be seen in the ultramicroscope.

Amberlites are known to bind acids in relatively large amounts. One g. portions of dry amberlite were placed in 500 cc. volumetric flasks and  $\text{HNO}_3$  was added in various concentrations. The systems were brought to volume with distilled water and permitted to react for several days. The supernatant liquids were then decanted and their contents of nitric acid determined by titration and by Devarda's reduction method. The results are shown in Fig. 1. Curves A and B indicate the amounts of  $\text{NO}_3^-$  (Devarda's method) and of titratable  $\text{H}^+$  adsorbed as a function of the initial concentration ( $i$ ) of free  $\text{HNO}_3$ . The difference between the two curves probably reflects the solubility or dispersion of  $\text{NO}_3^-$ -amberlite. The third curve, C, portrays the adsorption of titratable acid ( $x$ ) as a function of the equilibrium concentration ( $i - x$ ) of free  $\text{HNO}_3$ . At low concentrations of acid added ( $i$ ) nearly all is adsorbed. Bhatnagar *et al.* (1936) and Myers (1942) report that the adsorption of acids by resins follows Freundlich's adsorption isotherm

$$\log \frac{x}{m} = \log k + \frac{1}{p} \log (i - x) \quad (1)$$

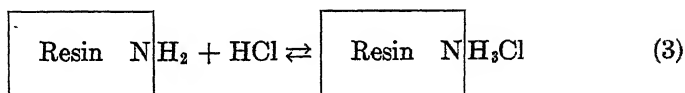
$x$  denotes the amount of acid taken up by  $m$  grams adsorbent and  $i$  the initial amount of acid added. The experimental data of Fig. 1 very definitely do not obey Freundlich's equation. Plotting of  $\log x/m$  against  $\log (i - x)$  gives a curve that deviates widely from the expected straight line.

#### THE CONCEPT OF AMBERLITE-OH

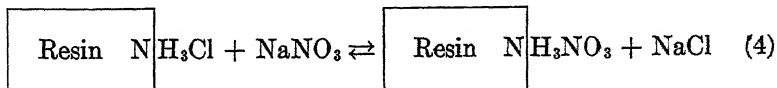
The fixation of acids by resins (R) is commonly considered a molecular adsorption according to the equation



Since the active adsorption spots are presumably  $\text{NH}_2$  groups, we may write, using rectangles as symbols of resin, instead of R,



If a neutral salt is added to resin-Cl, anion exchange takes place according to the equation

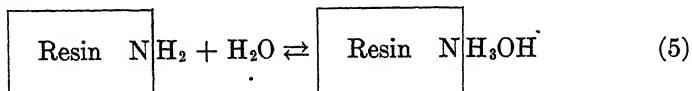


In contrast to the molecular adsorption process (equation 3), the exchange reaction involves replacements of anions only. The cations do not participate in the exchange reaction.

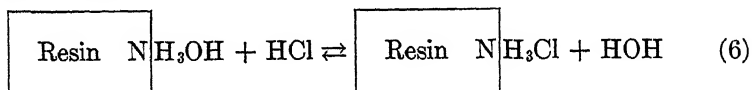


The whole picture of electrolyte adsorption by resins would be simplified and unified if one were able to demonstrate that the uptake of free acids is an ionic exchange reaction rather than an adsorption of total molecules.

Dry amberlite immersed in water produces a significant evolution of heat. It is plausible that some of the water molecules attach themselves to the  $\text{NH}_2$ -groups as follows:



The hydrated resin may react with acids as follows:



In this formulation the fixation of acid is represented as an anion exchange reaction in accordance with equation (4).

The hydrated amberlite may be designated as amberlite-OH. There are various lines of evidence that indicate the presence of  $\text{OH}^-$  ions on amberlite.

*Alkalinity of Dissolved Amberlite.* Suspensions of amberlite in water have pH values ranging from 7 to 9. Yellow-colored supernatant liquid containing 0.0632 g. solid in 100 cc. had a pH of 8.93. To bring 250 cc. of this solution to pH 7 required 6.40 cc. of 0.1 N HCl or 4.05 milliequivalents HCl per 1 g. of solid. We may conclude that dissolved amberlite acts as a base.

*Suspension Effect.* One gram of finely-powdered amberlite, suspended in 50 cc. water, gave a pH reading of 8.4 (glass electrode). After the particles had settled out, the supernatant liquid had a pH of only 7.8. Repetition of this experiment always showed that the suspension had a slightly higher pH than the clear supernatant liquid. This so-called suspension effect (Wiegner, 1931; Overstreet, 1945) demonstrates the presence of adsorbed  $\text{OH}^-$  ions which affect the electrode.

*Electric Charge.* In an electrodialysis cell, finely-ground amberlite accumulates on the membrane facing the cathode. Consequently, untreated amberlite particles have positive electric charges which must be balanced by negative counter-ions, presumably  $\text{OH}^-$  ions.

*Mutarotation.* Glucose exhibits pronounced mutarotation which is catalyzed by  $\text{OH}^-$  ions. Hydrogen ions, within the range of pH 2 to 7, have no influence on the constant of velocity of rotation. A number of experiments were conducted for detecting adsorbed, catalyzing  $\text{OH}^-$  ions on amberlite. Twenty g. of washed amberlite (IR-4), having a volume

of 15.84 cc., were placed in a measuring flask and water was added to the 515.84 cc. mark. After thorough shaking and after all of the particles had settled to the bottom of the flask, some of the clear supernatant liquid was removed and placed in a 50 cc. flask containing 2.5000 g. of glucose. Rotation was determined with a polarimeter according to standard procedures (Bates *et al.*, 1942). To the remaining amberlite suspension were added 25.0000 g. of glucose, and the flask was again filled to the mark. At 10 minute intervals, portions of the clear supernatant liquid were removed and examined in the polarimeter. All rotation curves followed the characteristic monomolecular reaction type of equation. The velocity constants of mutarotation at 26°C. were as follows:

Sugar in supernatant liquid  $k = 0.025$

Sugar in contact with amberlite  $k = 0.036$ .

These experiments were repeated with various modifications and, in all instances, it was found that sugar in the supernatant liquid rotates more slowly than sugar in contact with amberlite-OH. Amberlite-nitrate was examined in the same manner. Within experimental error, the velocity constants for distilled water, supernatant liquid and suspension were identical. These results indicate that solid amberlite particles have a definite, though low,  $\text{OH}^-$  ion activity.

In view of the presence of  $\text{OH}^-$  ions on amberlite, the adsorption of acids may be considered a neutralization reaction. An attempt was made to express the experimental concentration relationships (Fig. 1) by equations based on the law of mass action. Owing to lack of information on activities of adsorbed ions, the equations had but semiempirical significance. The agreements were neither better nor worse than those of the Freundlich equation.

#### COMPARISON OF AMBERLITE- $\text{NO}_3$ AND $\text{NaNO}_3$ AS NUTRIENT SUPPLIES FOR PLANT GROWTH

Several pounds of untreated amberlite were leached with dilute nitric acid solution. The material was dried at 60–80°C. The adsorbed nitrate was replaced on 1 g. portions by 2 liters of 1 *N*  $\text{NaCl}$  or  $\text{Na}_2\text{SO}_4$  and determined in the leachate by the Devarda reduction method. This nitrate amberlite contained 4.22 milliequivalents  $\text{NO}_3^-$  per g. air-dry resin.

Seeds of Romaine lettuce were germinated in flats and, at the age of four weeks, transplanted to earthenware flower pots whose walls had been coated with asphalt paint. These pots contained 1600 g. of Oakley sand and either amberlite- $\text{NO}_3$  or  $\text{NaNO}_3$  varying in amounts from 1.50 to 60.00 m.e.  $\text{NO}_3^-$ . Since Oakley sand is deficient in phosphorus, as well

as in nitrogen, all pots were given 164 mg.  $P_2O_5$  as monocalcium phosphate.

The pots, having one lettuce plant each, were watered about once a day. Percolating solution was returned to the surface of the pot. After six weeks the plants were harvested and the oven-dry weights ( $60^\circ C.$ ) recorded (Table I and Fig. 2).

TABLE I

*Growth of Lettuce (Tops) as a Function of  $NO_3^-$  Concentration in Soil*  
(Amberlite- $NO_3^-$  versus  $NaNO_3$ )

Milliequivalents $NO_3^-$ added per plant	0	1.50	5.00	10.00	15.00	20.00	25.00	40.00	60.00
Number of replicates	4	6	6	4	4	4	4	3	3
Average weight of 1 plant: grams									
$NaNO_3$	0.32	1.71	3.58	5.35	4.53	2.93	2.28	1.39	0.05
Standard error of mean	$\pm 0.055$	$\pm 0.085$	$\pm 0.189$	$\pm 0.467$	$\pm 0.118$	$\pm 0.623$	$\pm 0.390$	$\pm 1.153$	$\pm 0.020$
Amberlite- $NO_3^-$	0.32	1.65	2.93	3.93	4.63	5.33	5.08	4.50	4.50
Standard error of mean	$\pm 0.055$	$\pm 0.084$	$\pm 0.133$	$\pm 0.103$	$\pm 0.361$	$\pm 0.085$	$\pm 0.138$	$\pm 0.520$	$\pm 0.153$

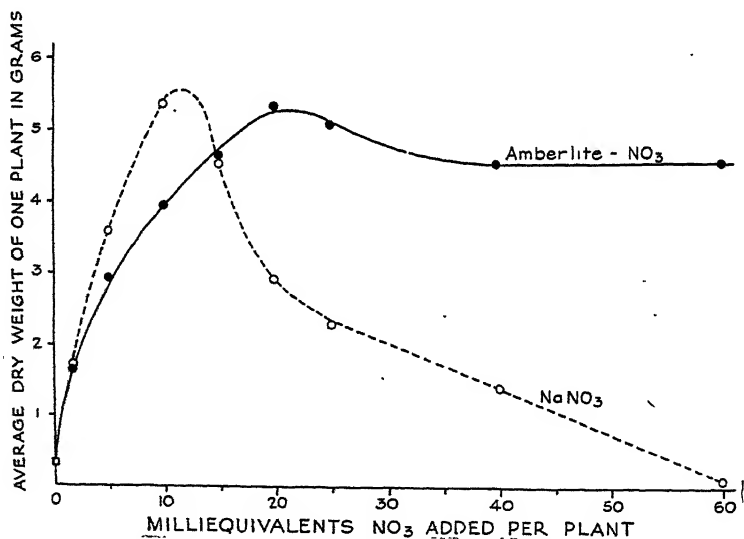


FIG. 2

Comparison of Adsorbed  $NO_3^-$  and  $NaNO_3$  as Nutrient Media for Lettuce Plants

Fig. 2 portrays several noteworthy features. At high salt concentrations sodium nitrate produced profound yield depressions. Probably these were the result of high osmotic pressures and sodium toxicity. The moisture equivalent of Oakley sand is only 4% so that a pot would contain, at field capacity, only 64 g. of water. Sixty milliequivalents  $NaNO_3$  dissolved in this amount of water gives a concentration of 0.9  $N$  which is known to be toxic to plants.

Unlike  $\text{NaNO}_3$ , the amberlite- $\text{NO}_3$  produced no statistically significant yield depressions and no toxic effects were noticeable. Apparently amberlite- $\text{NO}_3$  acts as a reservoir of readily available nitrates.

At intermediate concentrations (10 m.e.  $\text{NO}_3^-$ ) the sodium salt was more readily utilized than amberlite. At very low  $\text{NO}_3^-$  concentrations the two acted alike. Graham and Albrecht, who grew corn plants at correspondingly low nitrate levels, also observed that amberlite- $\text{NO}_3$  and  $\text{Ca}(\text{NO}_3)_2$  are equally efficient.

It is of interest to compare the magnitudes of the standard errors of the means (Table I). To facilitate comparison, the errors or variabilities are plotted in Fig. 3 as percentages of their respective means. In the

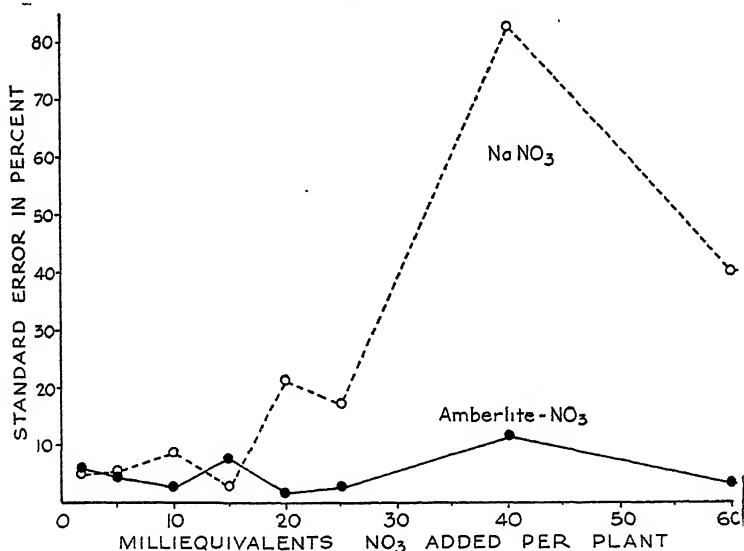


FIG. 3

Standard Errors of Means of Lettuce Yields as Affected by Adsorbed and Free  $\text{NO}_3^-$

amberlites the errors are low and bear a relatively constant proportion to the mean yields. In the  $\text{NaNO}_3$  systems they become larger as the salt concentration increases, undoubtedly reflecting the erratic toxic effects of the higher salt concentrations.

#### PLANT GROWTH IN RELATION TO DEGREE OF $\text{NO}_3^-$ SATURATION

In colloid chemical literature the degree of saturation of a specific adsorbed ion is defined as equivalents of the adsorbed ions divided by the total adsorption capacity (in equivalents) of the adsorbent. Since the adsorption capacity of amberlite has not yet been defined, the degree of saturation (D. S.) is arbitrarily expressed as milliequivalents  $\text{NO}_3^-$

per 100 g. of amberlite. Of particular interest are experiments in which the amount of adsorbed  $\text{NO}_3^-$  is held constant while the degree of saturation is made to vary.

One month old lettuce plants were grown for seven weeks in pots containing Bodega dune sand, to which had been added some phosphate and 12 milliequivalents of  $\text{NO}_3^-$  adsorbed on various amounts of amberlite. At high degrees of saturation the 12 milliequivalents were adsorbed on 2.58 g. of amberlite, at low degrees on 237 g. The yields are shown in Table II and also in Fig. 5. At low degrees of saturation the yields

TABLE II

*Average Lettuce Yields Per Pot and Plant Composition in Relation to Degree of Saturation (12 milliequivalents  $\text{NO}_3^-$  per plant and pot)*

	1	2	3	4	5	6	7	8	9	10	$\text{NH}_4\text{NO}_3$	Check
Degree of saturation, *M.E. $\text{NO}_3^-$ per 100 g. of amberlite	5.06	8.32	26.6	52.0	100	161	199	246	298	464	12.0 M.E. N	no nitrogen
G. of amberlite associated with 12 M.E. $\text{NO}_3^-$	237	144	45.1	23.1	8.34	7.45	6.03	4.87	4.03	2.58		
Replicates	6	5	6	6	6	6	6	6	6	6	6	5
Average dry weight of lettuce	0	0.68	2.18	4.23	4.73	5.65	6.10	6.48	6.10	7.06	8.12	0.11
Standard error	—	$\pm 0.15$	$\pm 0.20$	$\pm 0.26$	$\pm 0.43$	$\pm 0.43$	$\pm 0.48$	$\pm 0.16$	$\pm 0.16$	$\pm 0.26$	$\pm 0.13$	$\pm 0.01$
Total N, per cent	—	2.28	2.65	2.22	2.13	2.01	1.65	1.60	1.87	1.45	1.31	0.56
Total P as $\text{PO}_4^{3-}$ , per cent	—	0.41	0.72	0.70	0.80	0.78	0.78	0.63	0.74	0.62	0.62	0.54
Total $\text{Ca}^{++}$ , per cent	—	1.05	1.50	1.50	1.53	1.46	1.52	1.30	1.52	1.20	1.15	—
Total $\text{K}^+$ , per cent	—	1.23	1.39	1.39	0.92	0.92	0.78	0.68	0.72	0.67	0.69	—

\* M.E. = milliequivalents.

were small, even zero, whereas at high degrees they were large. Clearly, the presence of increasing proportions of amberlite-OH greatly depressed the yield.

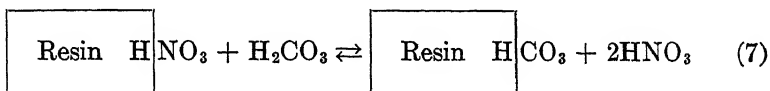
In the light of similar relationships observed with clays and cations one might be inclined to interpret the growth function of lettuce as a consequence of ion competition. According to the complementary ion principle (Jenny and Ayers, 1939; Marshall, 1944) the adsorbed  $\text{NO}_3^-$  would become less available as the degree of saturation decreases.

The appearance of the lettuce plants did not favor such an explanation. All plants exhibited a lush green color and no signs of yellowing, characteristic of nitrogen starvation, could be detected. Likewise, Kjeldahl analysis of the dried plants revealed a consistently high nitrogen content. Conceivably, the amberlite might have fixed the phosphate added to the sand, but plant analysis did not lend support to this idea. All plants were high in total and soluble phosphate, except possibly No. 2. Likewise, the contents of  $\text{Ca}^{++}$  and  $\text{K}^+$  of the tops were not limiting. Except for the set of plants (No. 1) that died soon after transplanting,

all specimens looked normal, save for variations in size. The possibility of unfavorable pH effects will be discussed later in the paper.

#### NATURE OF RELEASE OF NITRATE IONS ADSORBED ON AMBERLITE

To explain the utilization of adsorbed nitrates by plants, Graham and Albrecht (1943) proposed an anion exchange process based on the carbon dioxide excretion of roots:



The equation is not balanced, and no experimental proof of this reaction was furnished by these investigators. In the present study numerous exchange reactions were examined, and special attention was paid to the role of the degree of saturation.

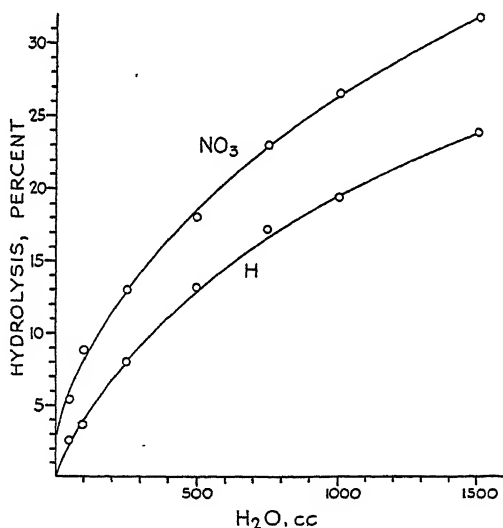


FIG. 4

Hydrolysis of Amberlite-NO<sub>3</sub>

*Hydrolysis.* One g. samples of amberlite-OH were placed in volumetric flasks ranging in size from 50 to 2000 cc. To each was added 4.165 milliequivalents of HNO<sub>3</sub>, and the flasks were then filled with carbon dioxide free water. After five days the clear supernatant liquids were decanted and their contents in titratable acid and NO<sub>3</sub><sup>-</sup> determined. Fig. 4 shows the amounts of nitric acid in *per cent* remaining in solution. The acidity curve lies below the nitrate curve, a feature which reflects, presumably, the dispersion of amberlite-NO<sub>3</sub>. Hydrolysis is appreciable, especially

at high dilutions. From the viewpoint of nutrient availability, sufficient  $\text{NO}_3^-$  may be released by hydrolysis to permit satisfactory initial plant growth.

*Influence of Degree of Saturation.* The aforementioned partially saturated amberlites-OH (Table II) were placed in volumetric flasks in amounts corresponding to 5 milliequivalents  $\text{NO}_3^-$  in 500 cc. The volume of amberlite was taken into account by adding 0.793 cc.  $\text{H}_2\text{O}$  for each g. of amberlite. The following systems were investigated:

- $\text{H}_2\text{O}$ , free of  $\text{CO}_2$ ,
- $\text{H}_2\text{O}$ , saturated with  $\text{CO}_2$ ,
- KCl, 5 milliequivalents in 500 cc.,
- $\text{CaCO}_3$ , 5 grams in 500 cc.,
- Saturated solution of  $\text{Ca}(\text{HCO}_3)_2$ , at atmospheric pressure of  $\text{CO}_2$ .

Following a reaction period of 10 days, the solutions were filtered and  $\text{NO}_3^-$  was determined according to Devarda's method. The results are graphically presented in Fig. 5.

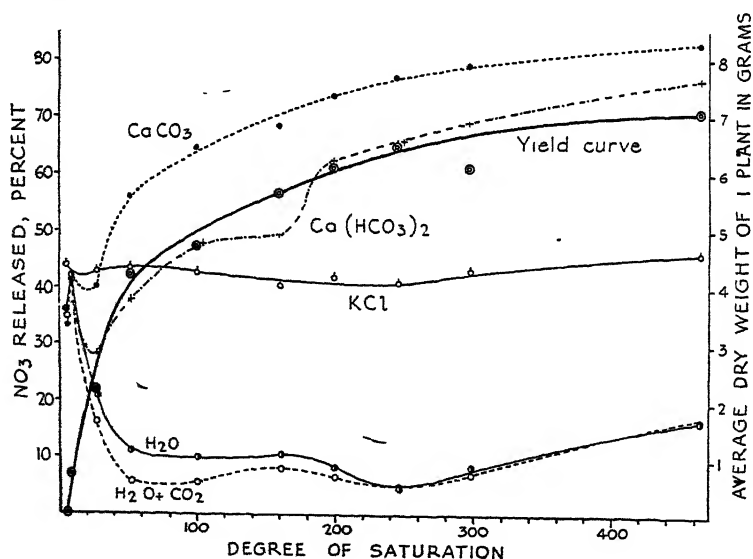


FIG. 5

Plant Yields and Release of Adsorbed Nitrates by Various Electrolytes  
in Relation to Degree of Saturation

Water, and water saturated with  $\text{CO}_2$ , produced identical replacements of  $\text{NO}_3^-$  at high degrees of saturation. At low degrees carbon dioxide repressed the outgo of  $\text{NO}_3^-$ . These results are unexpected, and they do not support the replacement theory of Graham and Albrecht.

Potassium chloride liberated from 40–45% of the adsorbed  $\text{NO}_3^-$ , irrespective of the degree of saturation. The largest release of  $\text{NO}_3^-$  was brought about by  $\text{CaCO}_3$ . Calcium bicarbonate occupied an intermediate position.

The exchange values at the two lowest degrees of saturation are accurate only within 10%. There was appreciable coloring of the solution and only an approximate correction factor for the decomposition of the dissolved amberlite by the Devarda process could be applied.

In view of the observed plant responses, the pH values of the amberlite systems (Table III) are of special interest. At high degrees of saturation

TABLE III  
*pH in Relation to Degree of Saturation (D. S.)*

No.	D. S. M.E. $\text{NO}_3^-$ 100 g. amberlite	$\text{H}_2\text{O}$	$\text{H}_2\text{O}$ + $\text{CO}_2$	KCl	$\text{CaCO}_3$	$\text{Ca}(\text{HCO}_3)_2$	Soil at end of experiment
1	5.06	9.0	8.9	9.1	9.1	9.0	8.1
2	8.32	8.5	8.4	8.7	8.7	8.5	8.0
3	26.6	7.5	7.3	8.0	8.1	7.6	7.5
4	52.0	6.7	6.6	7.2	7.6	6.9	7.5
5	100	6.2	6.7	6.9	7.5	7.3	7.6
6	161	5.7	5.4	6.6	7.7	—	7.6
7	199	5.2	5.1	6.3	7.4	7.1	7.1
8	246	4.6	4.3	6.3	7.4	7.4	7.1
9	298	4.1	3.8	5.2	7.4	7.3	7.4
10	464	2.8	—	3.0	7.2	6.5	7.7
<i>x</i>	no amberlite	—	—	—	—	—	6.9
<i>y</i>	$\text{NH}_4\text{NO}_3$	—	—	—	—	—	7.9

tion the solutions not containing carbonates were strongly acid (pH 3); at low degrees of saturation all supernatant liquids were distinctly alkaline (pH 9). Arnon (1942) observed that lettuce raised in culture solutions made relatively poor growth at pH 9. However, the pH values of the soil-amberlite mixtures, measured at the end of the experiment, lend but meager support to the possibility that growth reduction was caused by unfavorable soil reactions.

#### INTERACTION BETWEEN AMBERLITE AND SOIL

Granting a coexistence of cation and anion exchange, the addition of  $\text{CaCl}_2$  to a mixture of H-resin and resin-OH should result in an adsorption of  $\text{Ca}^{++}$  and  $\text{Cl}^-$ . Two g. each of air-dry commercial H-amberlite (IR-100) and amberlite-OH (IR-4) were mixed and 1.94 milliequivalents of dissolved  $\text{CaCl}_2$  were added. The system was brought to a volume of



250 cc. with distilled water. Analysis of the clear supernatant liquid revealed a removal of 89.9%  $\text{Ca}^{++}$  but, surprisingly, no change in  $\text{Cl}^-$  concentration. Subsequent analysis disclosed the presence of considerable amounts of  $\text{Na}^+$  in the IR-100 product. The adsorption of  $\text{Ca}^{++}$  could be accounted for by cation interchange with  $\text{Na}^+$ .

The experiment was repeated with cation exchanger (IR-100) that had been leached with  $\text{HCl}$  and washed with  $\text{H}_2\text{O}$  to eliminate  $\text{Na}^+$ . Now, the expected effect could be observed. The amberlite mixture removed from  $\text{CaCl}_2$  solution 60.9% of  $\text{Ca}^{++}$  and 71.5%  $\text{Cl}^-$ .

As a corollary to these observations, one might anticipate that an anion exchanger will release adsorbed anions upon the addition of a cation exchanger such as Ca-amberlite, Ca-clay or soil. Experiments

TABLE IV

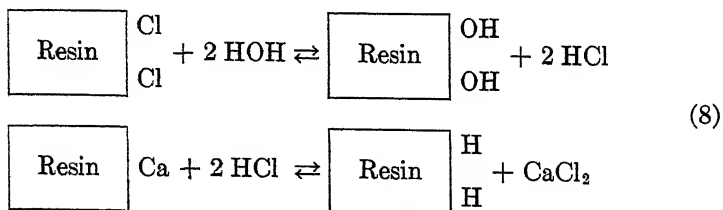
*Release of  $\text{Ca}^{++}$  and  $\text{Cl}^-$  from Mixtures of Ca-amberlite (Na-free, 1.495 M.E.  $\text{Ca}^{++}$  per g.) and Amberlite-Cl (8.17 M.E.  $\text{Cl}^-$  per g.), Volume 500 cc.*

Data not corrected for hydrolysis of amberlites

Ca-amberlite	Amberlite-Cl	$\text{Ca}^{++}$ released		$\text{Cl}^-$ released	
M.E.	M.E.	M.E.	per cent	M.E.	per cent
0	5.000			0.275*	5.5*
1.000	5.000	0.46	46.0	0.609	12.2
2.500	5.000	0.810	32.4	0.867	17.3
10.000	5.000	1.578	15.8	1.597	31.9
15.000	5.000	1.87	12.5	1.855	37.1
5.000	0	0.184*	3.6*	—	—
5.000	1.000	0.610	12.2	0.599	59.9
5.000	2.500	0.850	17.0	0.867	34.6
5.000	5.000	1.100	22.0	1.169	23.4
5.000	10.000	1.373	27.5	1.500	15.0

\* Hydrolysis.

with mixtures of Ca-amberlite and amberlite-Cl confirmed this belief (Table IV). Calcium and chloride were released in approximately equal amounts. The exchange may be presented as a two-step process as follows:



As an alternative, it is, of course, permissible to write first the reaction between Ca-resin and HOH, followed by the interaction of resin-Cl and  $\text{Ca}(\text{OH})_2$ . If the two types of colloid are in mutual contact, one might expect the reaction to take place between penetrating ion swarms:

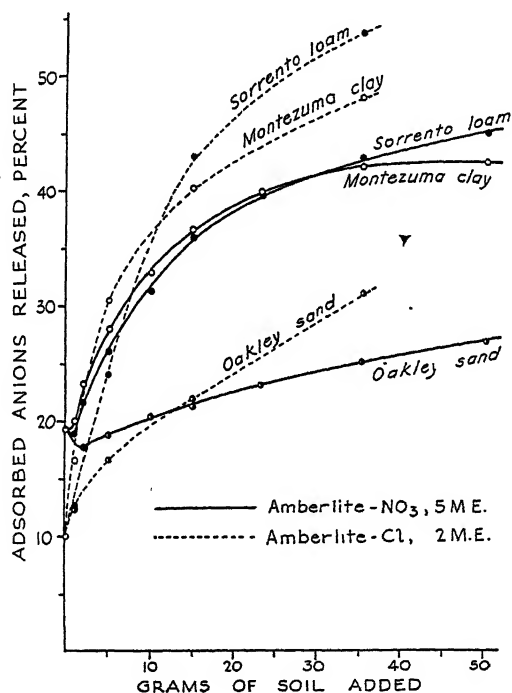
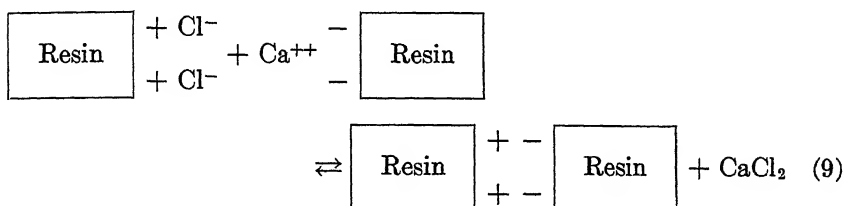


FIG. 6

Release of Adsorbed Nitrates and Chlorides by Interaction of Amberlites and Various Soils

The two resin particles would attract each other and possibly remain in mutual contact. Indeed, if yellow colored, supernatant liquid of an amberlite-OH suspension is passed through a column of coarse H-amberlite the percolating liquid is colorless, which indicates an attraction between the two resins.

Corresponding exchange experiments with mixtures of amberlite- $\text{NO}_3$  and various kinds and amounts of soil are presented in Fig. 6. The replacements reach considerable magnitudes. They depend on the nature of the soil and the ratio of amberlite to soil. Interaction of soil and resin probably constitutes the most important mechanism of liberation of adsorbed anions in soil amberlite mixtures.

## DISCUSSION

If amberlite- $\text{NO}_3$  is added to a nutrient solution, substantial amounts of  $\text{NO}_3^-$  are liberated by hydrolysis and anion exchange. Thus, amberlite-nitrate, especially at high degrees of saturation, acts as a reservoir of readily available nitrate ions to plants. At high concentrations of amberlite contact effects between resin and plant roots may enter into play. Plant root surfaces are predominantly electronegative, having cationic ion swarms, whereas those of acid resins are electropositive, having anionic ion swarms. Ion exchange, or intermingling of the two oppositely-charged electric double layers, according to equations 8 and 9, may bring about disturbances in the behavior of the root surfaces. It appears possible, though no proof exists, that the decrease in lettuce growth observed at high concentrations of amberlite (Fig. 5) are the results of unfavorable contact effects.

Cation and anion exchange resins mixed with sand or gravel have been suggested as growth media for large scale hydroponics and water culture installations. According to the present study, sufficient amounts of nutrients will be set free to make possible vigorous plant growth. Moreover, the equilibrium tendencies between adsorption and desorption of ions by the resins should exert a favorable regulatory or buffering effect on ion fluctuations and concentrations in the nutrient medium.

Exchange materials, especially resins- $\text{NO}_3$ , may serve as fertilizer carriers in coarse textured, sandy soils. In arid regions certain crops have to be irrigated often, sometimes every other day, and large amounts of soil nitrates are leached out. Use of nitrates in adsorbed form would tend to reduce these losses materially. Application of phosphated resins to soils high in kaolinitic and ferruginous colloids might be promising as sources of available phosphates to crops. Unfortunately, the present high cost of anion exchange resins precludes their agricultural use.

## SUMMARY

1. Anion exchanger or acid amberlite (IR-4) contains  $\text{OH}^-$  ions of low activity. The adsorption of free acids may be considered a neutralization reaction.

2. Amberlite- $\text{NO}_3$  incorporated in soil acts as a reservoir of readily available nitrates. At high concentrations, it is superior to  $\text{NaNO}_3$ .

3. The degree of saturation of amberlite- $\text{NO}_3$  has a marked effect on plant growth. At very low degrees of saturation plant growth is nil. The exchangeability of adsorbed nitrate bears a complicated and unexplainable relationship to the degree of saturation. Carbon dioxide does not enhance the outgo of adsorbed nitrate.

4. Mixing of Ca-amberlite and amberlite-Cl produces  $\text{CaCl}_2$ . Likewise, the addition of soil to amberlite- $\text{NO}_3$  releases substantial amounts of  $\text{NO}_3^-$ .

#### REFERENCES

1. ARNON, D. I., AND JOHNSON, C. M., *Plant Physiol.* **17**, 525-539 (1942).
2. BATES, F. J., *et al.*, *Natl. Bur. Stand. (U. S.) Circ.* **C-440** (1942).
3. BHATNAGAR, *et al.*, *J. Indian Chem. Soc.* **13**, 679-688 (1936).
4. CONVERSE, C. D., *et al.*, *Plant Physiol.* **18**, 114-121 (1943).
5. GRAHAM, E. R., AND ALBRECHT, W. A., *Am. J. Botany* **30**, 195-198 (1943).
6. JENNY, H., AND OVERSTREET, R., *Proc. Natl. Acad. Sci. (U. S.)* **24**, 384-392 (1938).
7. JENNY, H., AND AYERS, A. D., *Soil Sci.* **48**, 443-459 (1939).
8. MARSHALL, C. E., *Agr. Exp. Sta. Missouri, Bull.* **385** (1944).
9. MYERS, R. J., *Adv. Colloid Sci.* **1**, 317-351 (1942), New York.
10. OVERSTREET, R., *Soil Sci.* **59**, 265-270 (1945).
11. SCHLENKER, F. S., *Am. J. Botany* **27**, 525-529 (1940).
12. SCHLENKER, F. S., *Soil Sci.* **54**, 247-251 (1942).
13. WIEGNER, G., *J. Soc. Chem. Ind.* **50**, 103-112 (1931).



# **SURFACE FILMS OF POLYMERS.**

## **PART I. FILMS OF THE FLUID TYPE**

**D. J. Crisp**

*From the Department of Colloid Science, The University, Cambridge, England*

*Received August 3, 1945*

### **INTRODUCTION**

Surface films of high polymeric substances have been studied only to a limited extent. Films prepared by allowing soluble proteins to spread at an air-water interface present certain difficulties and have led to rather variable results. Carbohydrate derivatives have been spread from organic solvents by Katz and Samwel (1929), Adam (1933) and Harding and Adam (1933). Although the results show reasonable agreement, Adam has expressed doubt whether these compounds all give uniformly spread films, since in some, such as triacetylcellulose, unspread patches may be seen under dark-field illumination. He reports a similar effect with poly-methyl and -ethyl methacrylates (Adam, 1930). Katz, however, claims that identical specific areas were found with various samples of acetyl cellulose, although in some cases the films were optically clear while in others heterogeneous patches were visible. Hence, the amount of unspread material appears to be insignificant.

The data available on surface films of synthetic polymers are even more scanty. Katz and Samwel (1928) have prepared monolayers of polyvinyl acetate, polymethyl acrylate and polyanethole, the specific areas indicating complete spreading and no cross-linkage in the original plastic. Moss (1934) studied force-area curves of polyethylene succinates at low surface pressures, but, owing to the character and low molecular weight of the material, solubility effects are apparent in the results. More satisfactory data were later obtained by Harkins, Carman and Ries (1935) using highly polymerized  $\omega$ -hydroxydecanoic acid.

There is no doubt that some polymers give only partially spread films, nitrocellulose for instance, where the specific area varies with experimental conditions (Davey and de Vore, 1931). Cellulose itself yields only a surface precipitate from cuprammonium hydroxide solution. On the other hand, both Adam and Katz agree that the etherified celluloses form perfectly spread monolayers.

It appeared necessary, therefore, to investigate conditions under which polymers could be spread to give monomolecular layers. These conditions fulfilled, the use of a wide range of products would be possible from which the behavior of such monolayers might be related to molecular structure. A study of simpler systems is likely to be of value in interpreting the data derived from the spreading of proteins.

### CONDITIONS FOR SPREADING

The polymer must possess water-attracting groups, yet be not too freely soluble in water. Thus, at one extreme, polymers of hydrocarbons and halogen derivatives of hydrocarbons do not spread but leave flakes or smears on the surface while, at the other extreme, certain polycarboxylic acids are so soluble in neutral aqueous substrates that no film can be obtained. Between these limits polymers may be arranged according to their spreading properties into four groups which, although not sharply distinguished, serve to illustrate the two main factors influencing spreading. Ability to spread is increased by hydrophilic groups, notably by carboxyl and hydroxyl residues, while cohesive forces in the molecule reduce spreading. The latter may be judged qualitatively by the degree of crystallinity, the softening temperature or the molar cohesion. Thus the poor spreading of cellulose acetate compared with cellulose ethers is due to the greater internal cohesion as demonstrated by their softening temperatures, *e.g.*, cellulose triacetate 240° (Baker, Fuller and Pape, 1942), ethyl cellulose 99–130° (Meyer, K. H., 1942). Both cellulose and "Nylon" have powerful lattice forces, as indicated by their crystalline structure. Hence, in spite of having polar groups, their capacity to form monolayers is very small. Or again, the introduction of  $\alpha$ -methyl groups into polyacrylates, which stiffens the main valence chain and renders the plastic harder, decreases spreading very markedly.

*Group I.* Amorphous, usually soft polymers giving stable fluid films gelating\* at high surface pressures (20–30 dynes/cm.), *e.g.*, polyvinyl acetate, polyacrylates, cellulose ethers, aliphatic aldehyde compounds of polyvinyl alcohol.

*Group II.* Amorphous, usually tough or brittle polymers which give coherent films gelating at low surface pressures (0–10 dynes/cm.), *e.g.*, polymethacrylates.

*Group III.* Semi-crystalline polymers with weakly hydrophilic groups, spreading with difficulty to give unstable solid films, *e.g.*, "Nylon" on neutral substrate, cellulose nitrate and acetate, benzaldehyde compound of polyvinyl alcohol.

\* "Gelate" means here "acquire elasticity of shear."

*Group IV.* Semi-crystalline polymers with strongly hydrophilic groups which spread spontaneously from the solid, giving fluid films collapsing at low surface pressures (0–5 dynes), *e.g.*, polyvinyl alcohol, polyacrylic and methacrylic acid on acid substrates.

#### EFFICIENCY OF SPREADING

Experiments were carried out on films of typical plastics to assess how far spreading was complete and uniform.

The most direct means of detecting heterogeneities or unspread material is by observation under dark field illumination. Unfortunately, the method is so sensitive that results may be rather difficult to interpret. For instance Zocher and Stiebel (1930) noticed granular appearances, or "point structure," in all fatty acid films from lauric to carotenic acid, yet, in spite of the presence of microcrystals, the specific areas agree with each other and with X-ray data.

In the present work polyvinyl acetate and polymethyl acrylate were optically clear from zero pressures up to areas considerably less than those at which the film gellates and collapses. When the area was very small, folds and cracks appeared as bright streaks at right angles to the direction of compression; on re-expanding the film flattens out but its uniform appearance is not regained. Polyethyl acrylate and polyvinyl alcohol were also uniform, the former showing no heterogeneity at very small areas where it must have been much more than a monolayer in thickness. These films are evidently well spread, and remain uniform even when thickened by compression into a multi-molecular layer, which eventually collapses into folds. Films of polymethyl methacrylate appear to collapse irreversibly. When first spread at an area of 2 m<sup>2</sup>/mg. the optical appearance was uniform. At about 1.2–1.3 m<sup>2</sup>/mg. separate micelles (or islands) could be seen by their boundaries becoming visible. At about 1.0 m<sup>2</sup>/mg. the boundaries seemed to close up on each other and subsequent reduction in area gave rise to greyish patches of collapsed polymer. These grew rapidly between 0.8–0.7 m<sup>2</sup>/mg. when the surface pressure on the film was rising steeply, while at 0.6–0.5 m<sup>2</sup>/mg. cracks and lines indicated complete collapse. The re-expansion of these crumples was very weak.

Other evidence was found to support these conclusions. No increase in the specific area was observed in any of the films on standing at zero surface pressure, films left for periods up to one hour remaining within 1% of their initial area. Again, if islands of unspread material were left by the spreading solution, a lower concentration would probably give a more uniform film. No change in specific area was obtained when solutions of polymers of Group I were diluted, nor for polymethyl methacrylate



over a range of dilution from 0.005–0.2%. Similarly, none of the amorphous polymers gave any change in area or phase boundary potential when spread from different solvents (*e.g.*, for polyvinyl acetate: water-propyl alcohol 1:1, acetone, benzene; for polymethyl acrylate: acetone, benzene, toluene; polymethyl methacrylate: acetone, benzene, toluene, benzene-xylene 1:1).

The surface potentials were uniform over the whole film as soon as it was subjected to measurable surface pressures. Group I polymer films could be compressed and re-expanded several times without change in area or hysteresis effects. There was no change in specific area when the initial area over which they were spread was increased. Quantitative spreading could even be achieved against their own surface pressure by continuous addition of solution from a syringe.

Only with methyl methacrylate was the evidence not quite as definite as would be desired. But it is very hard to explain the consistent results for specific areas under such variable conditions if randomly distributed patches of abnormal thickness exist in the film. Non-uniform spreading would be due either to

- (i) too rapid evaporation or solution of solvent giving the polymer molecules insufficient time to orientate into a monolayer, or
- (ii) some degree of coalescence of the polymer chains occurring after spreading.

By using solvents of different volatility and solutions of different strengths the period for orientation varies considerably, yet specific areas have been found to be the same. A very similar test was made by spreading various amounts (0–65% by weight) of plasticizer (butyl-phthalylbutyl glycolate) with the film. The plasticizer molecules insinuate themselves between the methacrylate chains, but can gradually be squeezed out under pressure. When the area is sufficiently reduced, the

TABLE I

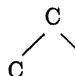
Condition (isoelastic)	Per cent plasticizer by weight				
	0%	6.7%	22%	65%	Mean
Resistant	1.44 m <sup>2</sup> /mg.	1.45 m <sup>2</sup> /mg.	1.36 m <sup>2</sup> /mg.	1.40 m <sup>2</sup> /mg.	1.41 m <sup>2</sup> /mg.
Elastic	1.20	1.34	1.31	1.10	1.24
Weak gel	0.97	1.05	1.15	0.94	1.03
Strong gel	0.89	0.92	0.83	0.82	0.87

pressure-area curve becomes identical with that for non-plasticized film; apparently only polymethyl methacrylate remains in the surface, and the film becomes resistant, elastic and, finally, a solid gel-like layer.

Points of comparable elasticity determined roughly by blowing talcum powder dusted on the surface occurred at approximately the same specific areas irrespective of the amount of plasticizer originally spread with the film (Table I). Since the area at which gelation sets in must represent some definite molecular configuration, the effect of increasing the dispersion of the methacrylate chains by plasticizer molecules would be to increase the observed gelation area if unspread material were originally present.

If the film is not a monomolecular layer this must be due to the molecules cohering together after spreading. This might take place as a uniformly distributed "heterophase" (see below), thus accounting for the uniform appearance under the ultramicroscope. If the molecules are strongly coherent in this way, the separation of nonhomogeneous masses on compression and the weak re-expansion of the film typical of Group II polymers is accounted for.

The low value of the specific area has been adduced as an argument against the view that highly coherent polymers, such as ethyl and methyl methacrylate, are well spread (Adam, 1930). However, main chains lying in the surface can pack into a small area since the carbon atoms joining two polymer units are separated only by the



C interatomic distance of 2.5 Å in the direction of the main chain, instead of the diameter of the methylene chain (4–5 Å). Thus for a polyvinyl derivative with an inter-residue distance of 2.5 Å and closest approach of 4–5 Å between chains, the area will be only about 11 Å<sup>2</sup>, ignoring the size of the polar group. Reference to subsequent graphs will show that polymethyl acrylate, which is certainly well spread, compresses down to the same area as polymethyl methacrylate at 16 dynes/cm. The low areas observed do not, therefore, invalidate uniform spreading.

Polymers of Group III are probably all badly spread. Their appearance under a dark field illuminator is heterogeneous, and their specific areas vary considerably with the strength of the spreading solution and the initial area available.

Polymers belonging to Group IV are remarkable in being water-soluble, yet spreading quantitatively from aqueous and alcoholic solutions. Unfortunately, the films are so exceedingly compressible that accurate comparisons of specific areas are not possible. The results indicate that dilution of the aqueous spreading solutions below 0.05% has no effect on the specific area, while the addition of 50% ethyl or, better, propyl alcohol improved spreading very slightly. However, since these differences were more pronounced at the lowest surface pressures, and were reduced when the films were allowed to stand, it is possible that these small differences were due to a transient complex between, say, polyvinyl alcohol and propyl alcohol. Similar phenomena have been noticed when gliadin is spread from a solution containing propyl alcohol. By far the most important factor in obtaining quantitative spreading is to ensure that negligible diffusion into the substrate occurs. Lowering

the specific gravity and increasing the rate of spreading by means of an alcohol solvent is important, but it is equally important that the syringe needle be placed in the surface, bevelled edge uppermost, and the solution delivered slowly and evenly. If the needle is dipped below, or discrete droplets be allowed to fall, errors of 20–50% may be caused by solution into the substrate. The time allowed for the readings is also an important factor owing to collapse of the film above 2 or 3 dynes/cm. compression.

### SPREADING AT THE OIL-WATER INTERFACE

Force-area curves for a number of polymers were recorded at the oil-water interface, by measuring the interfacial tension by means of a ring, as recommended by Alexander and Teorell (1939). The results are given in Part II. In order to obtain efficient spreading the following precautions are necessary to prevent loss of polymer into one of the bulk phases.

(I) The syringe needle should be broad with an obliquely bevelled tip as is usual with hypodermic syringes (B.W. No. 215 was suitable). This shape enables the tip to be placed at the interface causing a slight depression. If it lies above the interface the polymer solution diffuses into the oil; if below it rises as droplets which burst and much diffuses away again.

(II) The solvent must be carefully chosen so that it carries the polymer away from the phase in which it is soluble. Thus the solvent should have as high a solubility as possible in the non-solvent phase, so as to carry the polymer toward it by diffusion, and a suitable specific gravity to assist in carrying it to the interface. Other precautions, though not pertinent to the subject of spreading, should be mentioned.

(III) The area of the interface must be corrected for the rise at the sides of the glass vessel and the increase in area due to the contours round the ring. Even in vessels of area 300 sq. cms., this correction is sometimes greater than 10%.

(IV) The ring may become coated by a hydrophobic interfacial film changing its contact angle from zero. This is particularly apt to occur when the ring is drawn right through the interface, subsequent readings of the pull being low. As few readings as possible should be taken in the upper limit of the force-area curve, and the ring cleaned between runs by immersion in chrome-sulphuric acid after flaming.

### THE EFFECT OF MOLECULAR WEIGHT

Previous work by Moss (1934) and by Harkins, Carman and Ries (1935) indicates that the area occupied per unit of polymer is independent of its molecular weight. Our measurements, made with a series of fractions of polyvinyl acetate whose molecular weight varied more than tenfold, gave the same result although the lowest fraction occupied significantly smaller areas above 10 dynes/cm. pressure ( $F$ ), probably as a result of pressure-soluble fractions of very short chain length (Table II). On the other hand the molecular weight has a small but definite effect on the mechanical properties of the film, the higher fractions gelating at slightly larger areas and lower surface pressures.

It follows that the surface pressure, like the swelling pressure of a bulk gel, is a property of the polymer segment rather than of the molecule (Boissonnas and Wolff, 1940; Schulz, 1937). Surface films of polymers are therefore to be regarded rather as two-dimensional sols or gels in which the osmotic or imbibition pressure of the water is balanced by the surface pressure applied to the film, than as molecularly dispersed layers. The latter will occur only at surface pressures below those normally measured.

TABLE II  
*Polyvinyl Acetate Films*

Mean degree of polymerization*	Surface pressure	Area/Unit	Area where film shows viscosity	Pressure	Gelation area	Gelation pressure
10-20	10 dynes/cm.	18.0 Å <sup>2</sup>	—	—	—	—
35	10 dynes/cm.	18.7 Å <sup>2</sup>	—	—	—	—
65	10 dynes/cm.	18.9 Å <sup>2</sup>	5 Å <sup>2</sup>	25.8 dynes/cm.	3 Å <sup>2</sup>	26.2 dynes/cm.
200	10 dynes/cm.	18.9 Å <sup>2</sup>	8.5 Å <sup>2</sup>	24.7 dynes/cm.	7 Å <sup>2</sup>	25.3 dynes/cm.
280	10 dynes/cm.	18.8 Å <sup>2</sup>	11 Å <sup>2</sup>	22.5 dynes/cm.	9 Å <sup>2</sup>	24.5 dynes/cm.
330	10 dynes/cm.	18.2 Å <sup>2</sup>	12 Å <sup>2</sup>	21.0 dynes/cm.	9 Å <sup>2</sup>	24.5 dynes/cm.

\* There is a wide spread of molecular weight about this mean (Blease and Tuckett, 1941).

If, for instance, the co-area per segment of polyvinyl acetate is assumed to be 50 Å<sup>2</sup> when under zero surface pressure, a polymer of molecular weight 4000 will occupy 2500 Å<sup>2</sup>. It is unlikely that such molecules would exist as a vapor film unless widely separated in space; assuming this to be only ten times the co-area, each molecule will occupy 25,000 Å<sup>2</sup>, and therefore exert a surface pressure of the order of less than 0.02 dynes/cm.

The effect of the molecular weight on the gelation point can be explained as a result of the displacement of polymer segments above the level of the original monolayer. These displaced segments constitute an "overfilm" in which the bulk mechanical properties of the material emerge. These properties are known to depend upon the molecular weight of the specimen.

#### FLUID TYPE OF FILM (GROUP I)

All polymers which spread to give a fluid expanded type of film having a relatively high collapse pressure are amorphous, and the majority are soft or semi-fluid in texture. This indicates low cohesion between the chains which allows the polymer to give finite surface pressures when expanded to large areas (e.g., 100 Å<sup>2</sup> per residue with polyvinyl derivatives) and also gives freedom to the polar group to orientate in the interfacial field.

When spread at the air-water interface these substances yield fluid films which, if they gelate, do so at high pressures (above 15 dynes/cm.) and at areas well below that at which the film is unimolecular. When the films gelate the  $F-A$  curve is sigmoid showing a collapse region at higher pressures, but the softest materials (*e.g.*, ethyl and *n*-butyl acrylate) have a definite collapse pressure and behave as "piston oils." It is possible to compress these films to a very small fraction of their expanded area ( $\frac{1}{10} - \frac{1}{20}$ ) without irreversible change or hysteresis effects. When the films are compressed into a very thick polylayer, elastic fibers can be spun off the surface. Multilayers can be built up on chromium strips at high surface pressure ( $> 15$  dynes/cm.) provided the films are not too viscous.

#### STATE OF FLUID TYPE OF FILM

Force area ( $F-A$ ) curves for a series of polyacrylic esters are shown in Fig. 1. Secondary and tertiary butyl acrylates have also been studied, the curves for these not differing widely from that of normal butyl acrylate. All give measurable pressures with the apparatus used at areas of 60–100 Å<sup>2</sup> per monomer residue, and all remain fluid at the collapse point except for methyl and tertiary butyl acrylate which show gelation at 19–20 and 25–26 dynes/cm. respectively. Normal aliphatic side chains exercise an internal lubricating effect (plasticizing) which is absent from short or branched chain derivatives; thus, primary polybutyl acrylate is soft and sticky; secondary, rubbery; and tertiary, hard and brittle. It is these properties which determine the "gelation" of the film by formation of an overfilm; up to surface concentrations equivalent to a monolayer all three remain fluid.

TABLE III

Esters	Spreading pressure	Poly esters	Collapse pressure
Ethyl isovalerate	29 dynes/cm.	Methyl acrylate	20.5 dynes/cm.
Ethyl caproate	25.4 dynes/cm.	Ethyl acrylate	23.2 dynes/cm.
Ethyl nonylate	19.0 dynes/cm.	Iso propyl acrylate	25.0 dynes/cm.
		<i>n</i> -Butyl acrylate	22.5 dynes/cm.
Isoamyl butyrate	22.8 dynes/cm.	Polyvinyl acetate	26.4 dynes/cm.

The formation of a three-dimensional amorphous overfilm is indicated by the collapse pressures. If a polymer collapses into an amorphous layer the energy required to take a unit from the interface into the overfilm will be of the same order as that required to transfer similarly a molecule of a liquid of the same character (*i.e.*, same polar group and comparable hydrocarbon chain). Table III gives the spreading pressures of simple esters and collapse pressures of typical fluid poly-ester films.

Electron diffraction pictures of multilayers of these plastics show broad halos, again indicating an amorphous state of aggregation (Coudouros, 1943).

Reference to the areas occupied per polymer unit indicates that the films cannot be classed as "liquid expanded" in the ordinary sense (Adam, 1930). Methyl acrylate for instance can be reduced to an area of 12–15 Å<sup>2</sup> per unit before the curve becomes inflected, while the linear portions, if extrapolated, cut the area axis between 20–30 Å<sup>2</sup>. These areas are considerably less than those occupied by the polar groups in expanded films of long chain esters, and resemble more the areas of condensed films. Moreover, it is not possible to fit the curves to a hyperbolic formula of the type  $(F + F_0)(A - A_0) = kT$ . But the films cannot be classed as condensed either, since they show no "point structure" or irreversible collapse, and their compressibility is much greater than that of closely packed hydrocarbon chains in a condensed film of, say, a

TABLE IV

Film	Area elasticity $-A \frac{dF}{dA}$ of linear region	Thickness (approx.)	Force on molecules per sq. cm.
Methyl acrylate	24 dynes	8 Å	$3 \times 10^8$ dynes
<i>n</i> -Butyl acrylate	72 dynes	10 Å	$7 \times 10^8$ dynes
Stearic acid	2500 dynes	26 Å	$960 \times 10^8$ dynes

fatty acid. Even if allowance is made for the thickness of the polymer monolayer being less, the value of the area elasticity (reciprocal compressibility) is of quite a different order (Table IV). Two features of the force-area curves must therefore be accounted for:

1. An expanded region of low pressure at areas of 30–100 Å<sup>2</sup> per residue.
2. An approximately linear region at areas corresponding to close packed chains, but with high compressibility.

1. The set of curves shown in Fig. 1 is probably typical of a series of polymer films in which the side chain length is varied. Very similar results will be noted for aldehyde compounds of polyvinyl alcohol (Fig. 6) and for cellulose derivatives. The lower members of the series (methyl to propyl acrylate, Formvar) give significant surface pressures in the expanded region where the higher members (*e.g.*, butyl acrylate, Octvar) give none. It is probable that N. K. Adam's suggestion (1933) that the expanded region is due to kinetic agitation of the main chains is correct although dipole-dipole interaction may give a surface pressure supplementary to the thermal energy. When the side chains contain more than 4 or 5 carbon atoms an attraction exists in the surface reducing the

kinetic movements, the low pressure region, therefore, becoming more condensed. This is analogous to the effect noted by Schofield and Rideal (1926) in films of fatty acids where attractions were noted when the molecule contained more than 5 or 6 carbon atoms. The surface pressure in this expanded region is independent of molecular weight since the chief factor determining its magnitude is the entropy term of the chain segments, the two dimensional Van't Hoff term being negligible. The three dimensional analogy has already been treated by several workers (Haller, 1937; Meyer, 1942).

2. From the high compressibility of polymer films at high surface pressures we are forced to conclude that some process other than straightforward compression of the chains is taking place. This process, involving much higher compressibility and enabling the units to pack into very small areas, is probably a reversible collapse of the segments, which pass out of the surface plane gradually building up the overfilm. The electrical properties of the film confirm this. Fig. 2 gives the pressure,  $F$ , and surface potential,  $\Delta V$ , of a typical fluid poly ester, polyethyl acrylate. The derived values of apparent surface moment are also plotted, giving direct evidence of the state of the polar groups. Along  $AB$  the surface pressure is negligible, the potential fluctuating, but at  $B$  the surface pressure is appreciable and in the low pressure region  $BC$  the moment remains almost constant. Thus, the molecules have been forced into contact but there is free space between the individual chains which can be reduced without altering the orientation of the polar groups. In the region  $CD$  the moment falls more rapidly, finally decreasing steadily to zero when  $\Delta V$  reaches a maximum ( $DE$ ). It is not possible to decide with certainty whether the fall in moment along  $CD$  is due to reorientation of the polar groups at the surface to give a decreased moment, or to partial collapse in which there is equilibrium between segments at the interface giving the normal moment and randomly orientated segments in the partially formed overfilm whose moments will not contribute to the surface potential. But in view of the relatively small areas occupied per segment and the similarity in form of  $\Delta V-A$  curves of all such polymers, the latter seems much more likely. Thus, along  $CD$  the energy expended in compressing the film is used, partly in forcing some of the residues away from the surface, and partly in overcoming repulsions between the molecules. As the pressure rises, more and more energy is expended in forcing groups into the overfilm until, at the maximum surface pressure (collapse or piston pressure), the whole energy of compression is used up in this way, the packing at the interface being constant.

It will be noted from the curves in Figs. 1 and 7, that at higher surface pressures the members with longer side chains occupy a greater area and are less compressible, the curves tending to intersect each other. This

may be due, in part, to the larger size of the unit, but another factor is probably more important: when the side chain is large, the main chains are thereby separated, but when only short side chains are present the cohesive forces between the main chains are greater (Baker, Fuller and Pape, 1942). This reduces the energy to withdraw segments from the water surface and so facilitates the formation of a partial overfilm in the

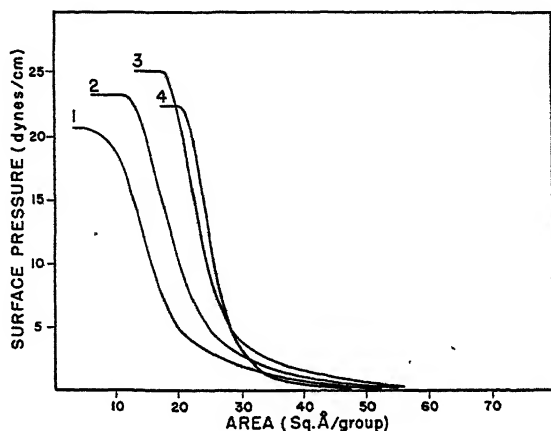


FIG. 1

## Force-Area Curves for Polyacrylates

1. Polymethyl Acrylate; 2. Polyethyl Acrylate; 3. Polyisopropyl Acrylate;
4. Poly-*n*-butyl Acrylate

lower members (see below), thus decreasing their specific areas. One might inquire why films having long hydrocarbon chains show much greater resistance to collapse than polymer films. The answer is that fields of force between interlocking  $-\text{CH}_2-$  groups provide a high energy barrier to be overcome before the molecules can escape from the film into a crystal state. These forces are revealed by the rigidity of solid films and the very high viscosity (relative to bulk viscosities) of liquid condensed films (Joly, 1938). For this reason condensed films, though unstable and containing incipient crystal nuclei, are remarkably permanent. We may attribute the increased area elasticity of higher acrylates (Table IV) in part also to the buttressing effect of methylene groups on the orientated side chains.

## ESTIMATION OF LIMITING AREAS

By making certain assumptions it is possible to obtain an approximate value of the area occupied by the close-packed chains. If it is assumed that



- (1) the linear region of the  $F$ - $A$  curve represents an essentially close-packed interfacial layer,
- (2) at zero pressure all the residues lie in the surface,
- (3) and the removal of groups from the interface to the overfilm is a linear function of  $F$ ,

then, by extrapolation to zero pressure, the surface area per unit may be found.

Alternatively the  $\Delta V$ - $A$  curve may be employed if the following assumptions are made in addition to (1) and (2) above:

- (4) There is negligible reorientation of the polar groups on compression of the film so that the moment of those remaining at the interface is constant.
- (5) Polar groups forced into the overfilm do not contribute to the surface potential.

The limiting area will then be

$$A_0 = \frac{4\pi\mu_m}{\Delta V_0}$$

where  $\mu_m$  = Maximum moment observed in low pressure region,

$\Delta V_0$  = Maximum surface potential.

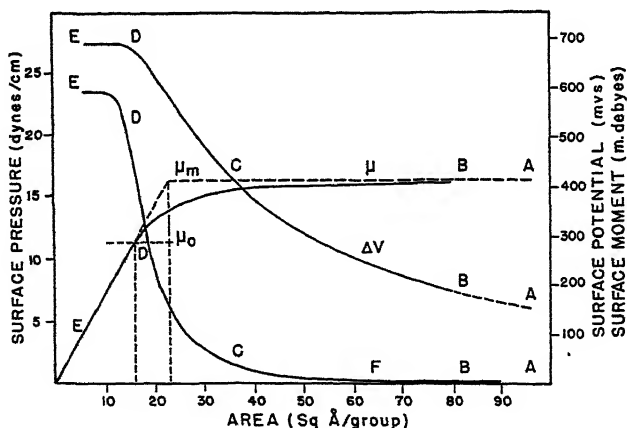


FIG. 2

Surface Pressure Potential ( $\Delta V$ ) and Moment ( $\mu$ ) Data for Ethyl Acrylate Polymer, 18°C. (M.W. 12,000)

The value of  $\mu$  in the compressed state is not likely to be greater than that in the expanded region where the dipoles are free to orientate in the field normal to the surface. The moment in the compressed state cannot be less than the value  $\mu_0$  at the point  $D$  (Fig. 2). Thus, by assuming

the fall in  $\mu$  to be entirely due to collapse (assumption 3) or, alternatively, to be entirely due to re-orientation, it is possible to measure extreme values for the limiting area. This is conveniently done by dropping perpendiculars from the extrapolated  $\mu$ - $A$  curve at the values  $\mu_0$  and  $\mu_m$  to the area axis (Fig. 2).

### POLYACRYLATE MONOLAYERS

The assumptions adopted above may now be applied to the data found experimentally. The table below summarizes the results for the homologous series.

TABLE V

Substance	Surface moment at zero pressure $\mu_m$	Area extrapolated to zero pressure $A, F \rightarrow 0$	Maximum area in condensed state $A_\mu \rightarrow \mu_m$	Minimum area in condensed state $A_\mu \rightarrow \mu_0$	Minimum moment in condensed state $\mu_0$
Polymethyl acrylate	340 milli-debyes	21.5 Å <sup>2</sup>	22.0 Å <sup>2</sup>	12.5 Å <sup>2</sup>	190 milli-debyes
Polyethyl acrylate	410 milli-debyes	25.0 Å <sup>2</sup>	23.0 Å <sup>2</sup>	16.0 Å <sup>2</sup>	280 milli-debyes
Polyisopropyl acrylate	500 milli-debyes	29.0 Å <sup>2</sup>	25.5 Å <sup>2</sup>	19.0 Å <sup>2</sup>	360 milli-debyes
Poly <i>n</i> -butyl acrylate	455 milli-debyes	29.3 Å <sup>2</sup>	25.0 Å <sup>2</sup>	22.0 Å <sup>2</sup>	390 milli-debyes
Poly secondary butyl acrylate	500 milli-debyes	29.5 Å <sup>2</sup>	26.0 Å <sup>2</sup>	22.0 Å <sup>2</sup>	420 milli-debyes
Poly tertiary butyl acrylate	525 milli-debyes	29.6 Å <sup>2</sup>	28.5 Å <sup>2</sup>	22.5 Å <sup>2</sup>	420 milli-debyes

It is clear from the values of the dipole moments of the higher members that, in these at least, the  $\vec{C} = 0$  and  $\text{OCH}_2$  dipoles must both contribute to the vertical component and, therefore, the *cis* configuration of the ester group prevails (Alexander and Schulman, 1937). If molecular models of polyacrylic esters are constructed, it will be observed that only the *trans* orientation is compatible with a really close-packed condition of the main chains, but the moment would be very small. If the residues are forced into the *cis* position the main chain must be distorted while the area increases considerably. From the fact that all three butyl derivatives occupy about the same area and give the same order of electric moment, the orientation of the polar groups must allow plenty of space for the alcoholic side chain. Only one position will allow this (Fig. 3a and 3b), the main chain being somewhat below the side chains, and, in the case of secondary and tertiary derivatives, covered by them (Fig. 3c). The calculated values of limiting area and moment were found to be 26.5 Å<sup>2</sup> and 500 millidebyes respectively. The area is calculated from the usual interatomic distances and van der Waals radii, the closest approach of two chains being assumed to be 2.4 Å, and the moment taken from data by Alexander and Schulman (1937).

Comparison with observed results shows good agreement in the higher members both for moments and limiting areas, the area obtained by zero pressure extrapolation

being rather larger than that from the electrical data at high surface pressure. The values given in column five are too small, indicating that collapse rather than re-orientation accounts for the decrease in moment.

Polymethyl and -ethyl acrylates do not agree well with calculations, the moments and areas being too small. The moment for an expanded long chain methyl ester is not available, but expanded ethyl esters, *e.g.*, ethyl myristate, give normal moments of 500 m.d. It is unlikely therefore that any difference exists in the surface moment of the methyl or ethyl ester residue. The low moment must therefore be due either to

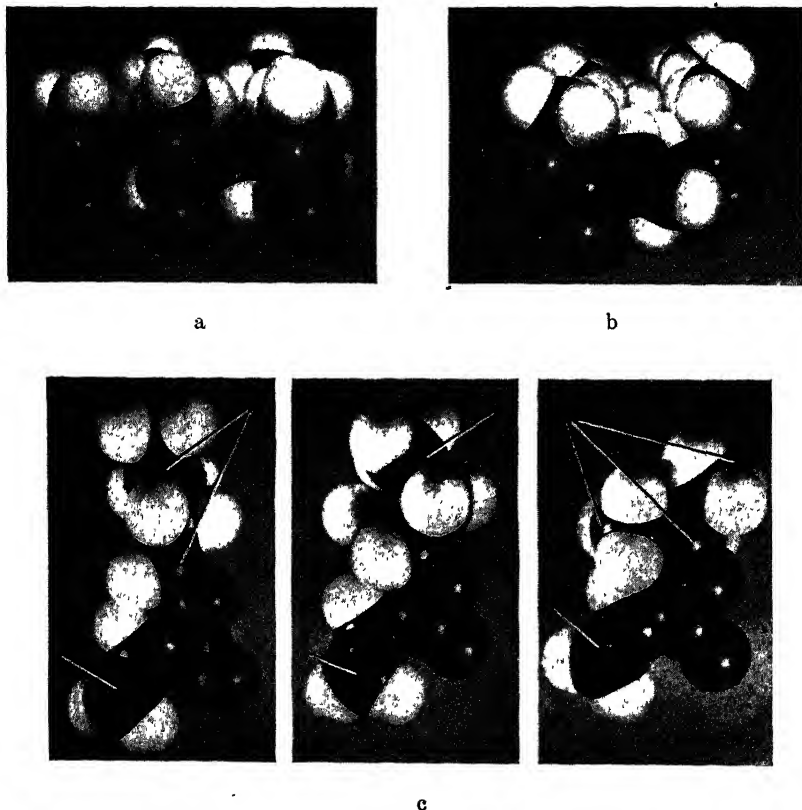


FIG. 3

#### Orientation of Acrylate Polymers at the Air-Water Interface

(a) Polymethyl acrylate, side view of chain; (b) Polymethyl acrylate, viewed along the chain; (c) Units of polybutyl acrylate viewed along the chain, *a*, normal, *b*, secondary, *c*, tertiary. [Main chain is marked 1. Side chain 2.]

(1) orientation toward the *trans* position in methyl and ethyl acrylate, or (2) some of the residues not contributing to the moment even at zero pressure. The former explanation seems unlikely.

If re-orientation toward the *trans* position took place the moment would be reduced without a very marked difference in the limiting area. Measurements on molecular

models indicate that the moment should fall sharply as shown in Fig. 4. Experimental data show, however, that the moments are reduced only in the same ratio as the areas with the result that, in the close-packed condition near the collapse point, all the members approximate to the same  $\mu - A$  curve (Fig. 4). This is to be expected if some of the segments in the lower members are effectively absent from the interface even at zero surface pressure, while the true surface areas and moments remain the same throughout the series.

Moreover, polar groups situated at an air-water interface are subjected to a strong electrostatic field. This has been calculated to be as much as  $H = 1.5 \times 10^8$  volts/cm. at a clean water surface (Mitchell, 1936) but it is not possible to use this figure to

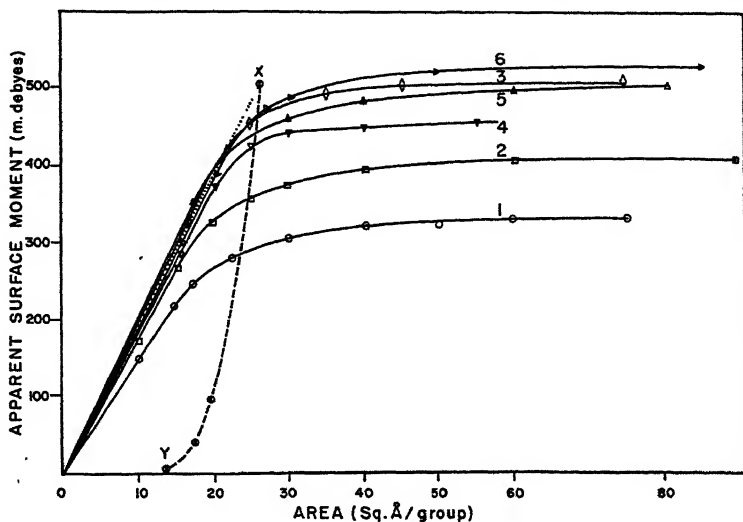


FIG. 4

#### Apparent Surface Moments of Polyacrylates

1. Methyl; 2. Ethyl; 3. *iso*-Propyl; 4. *n*-Butyl; 5. *sec*-Butyl; 6. *tert*-Butyl
- OX. Expected fall in moment if groups are progressively removed from the interface;
- XY. Expected fall in moment if re-orientation occurs. (Calculated)

calculate dipole energies in different orientations because the field may be considerably influenced by the presence of adsorbed molecules. The field will, however, exercise an influence tending to orientate ester groups into the *cis* configuration, which will prevail in the absence of internal or applied lateral forces. Since the lateral attractions of at least 18 methylene groups are required to achieve such re-orientation (Alexander, 1942) it is unlikely that the single layer of methylene groups in the polyvinyl "backbone" would be sufficient to bring this about against the electrical energy  $H\Delta\mu$ . This electrostatic energy could only be overcome by dipole association outside the interfacial field. It is, therefore, unlikely that any significant proportion of the residues would occupy the *trans* position unless constrained by applied surface compression.

It follows, therefore, that in the lowest members, even at zero surface pressure, some of the segments are absent from the surface, presumably associated together in a partially formed overfilm. Assumption (2) made in estimating limiting areas is therefore not necessarily true; it cannot be taken for granted that the films lie perfectly flat on the surface.

If spontaneous association of certain of the residues does occur, the energy state in the surface and in the overfilm cannot be very different. The free energy of a simple molecule resembling the polymer unit can be measured relative to solution in the aqueous phase both at the surface and in the pure state. The free energy change when removed from water to the pure state will be

$$\Delta G_1 = -RT \log_e \frac{p}{p_0 N}$$

$p$  = vapor pressure (fugacity) in solution at concentration  $N$  = mol. fraction

$p_0$  = vapor pressure (fugacity) of the pure solute

The free energy change, when removed from a very dilute solution to a dilute surface, will be identical on pressure or concentration scale

$$\Delta G_2 = -RT \log_e \left( \frac{C_s}{C} \right)_{C \rightarrow 0}$$

$C_s$  = concentration in surface phase derived from the surface concentration  $\sigma_s$  and an assumed surface thickness  $\tau$

$C$  = concentration in solution

Table VI shows these to be of the same order, which indicates that a polymer film of such units should readily pass into a molecular configuration similar to that of the bulk, and an equilibrium within the film of

TABLE VI

(T = 298°K.)

Substance	$p/N$	$p_0$	$p/p_0 N$	$\Delta G_1$	$\Delta G_2$
Methyl acetate	3830 mm.	214 mm.	17.9	-1715 cal./mol.	-2390 cal./mol.
Ethyl acetate	5580 mm.	94.5 mm.	59.1	-2425 cal./mol.	-3000 cal./mol.
Propyl acetate	8380 mm.	31.6 mm.	265	-3320 cal./mol.	-3650 cal./mol.

Data, Column I from Butler (1937).

II International Critical Tables.

V Langmuir, (1917).

segments attracted to the water molecules and segments attracted to each other is therefore possible.

It is likely that the lower members will associate more strongly since the short range forces bringing the ester groups into dipole doublets will be greater when the side chain is short, and the forces between the main chains will also be greater.

The co-existence in equilibrium of spread and unspread "heterophases" (Frenkel, 1939) within the film is worthy of comment. Such

conditions can only arise with large molecules where the same molecule partakes in the structure of both heterophases. It is analogous to the fringed micelle model of crystalline-amorphous phases in plastics which has been treated thermodynamically by Tuckett and Frith (1944).

It has hitherto been assumed that a sharp phase distinction exists between spread and unspread regions in a film. This is valid for long chain fatty molecules to which a strict phase rule can be applied, uniformity of the monolayer thickness (apart from two-dimensional phase changes) being synonymous with completeness of spreading. In polymer

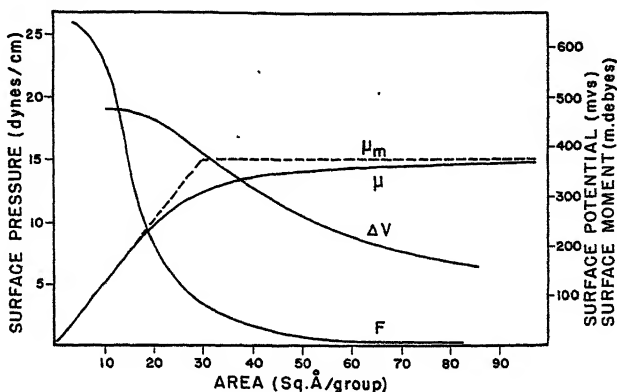


FIG. 5

Surface Pressure, Potential and Moment of Polyvinyl Acetate. (18°C.)

films however uniform spreading may be compatible with a layer which is not strictly two-dimensional in form but contains a proportion of three-dimensional phase of submolecular size. As indicated above, the proportion of material in the third dimension above the monolayer increases as the film is constrained into a smaller area, and finally, when the maximum surface pressure is reached, a true bulk phase separates out above as a thin sheet of gel. There follows the important conclusion that polar groups which do not lie exactly in the plane of the surface but have been forced slightly above it, can nevertheless contribute to the two-dimensional pressure of the film.

#### POLYVINYL ACETATE (FIG. 5)

Polyvinyl acetate differs from polymethyl acrylate only in the reversed position of the ester group. The film is similar but has a greater expansion at low surface pressures, a higher limiting area and dipole moment. These differences parallel those of long chain condensed films of acetates and, say, ethyl esters.

The moment of polyvinyl acetate is 365 m.d. indicating a structure

nearer to the *cis* than the *trans* state. The *cis* orientation of the ester group is also borne out by the ready hydrolysis of polyvinyl acetate at a rate comparable with that of ethyl acetate (Lee and Sakurada, 1939). The limiting area by extrapolation of the  $F$ - $A$  curve is  $24 \text{ \AA}^2$ , and from the  $\mu$ - $A$  curve  $29 \text{ \AA}^2$ . The high value obtained from the  $\mu$ - $A$  curve and the steady fall in  $\mu$  over the expanded region suggest that some re-orientation of the polar group may be taking place.

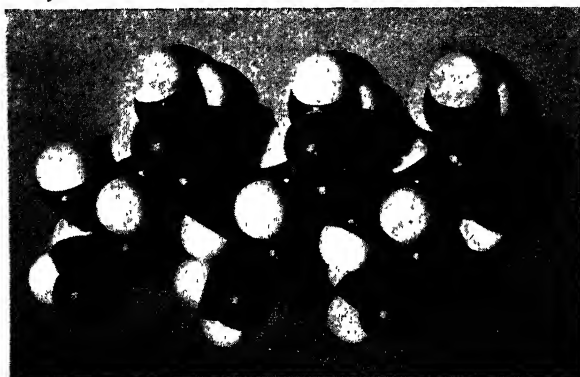


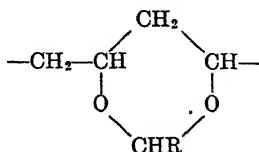
FIG. 6

Orientation of Polyvinyl Acetate Viewed from Below

In polyvinyl acetate all the acetyl residues are probably arranged on one side of the main-chain when this is set in a linear zig-zag form. This conclusion follows from measurements of the X-ray spacing of polyvinyl alcohol (Fuller, 1940) which is prepared by direct hydrolysis of the acetate. Molecular models reveal that steric hindrance will prevent all the acetyl groups arranging themselves simultaneously into the *cis* form with the resultant moment vertical. An arrangement in which the component dipoles deviate somewhat to give a moment of 360–400 m.d. and occupy an area of  $25 \text{ \AA}^2$  is shown in Fig. 6. Since the electric force on the dipoles is balanced by repulsion between the methyl groups and the main chain, external compression of the film might cause further re-orientation towards the *trans* position as suggested above.

#### ALDEHYDE COMPOUNDS OF POLYVINYL ALCOHOL

These substances are prepared by condensation of polyvinyl alcohol with the appropriate aldehyde, the units being six membered rings,



Commercially they are known as Formvar, Alvar, *etc.*, the prefix signifying the aldehyde used in their preparation.

The aliphatic members are amorphous and give a very typical set of  $F$ - $A$  curves (Fig. 7), showing the effect of side-chain length which has already been commented upon. Calculation of the area of the ring structure lying flat gives  $5.0 \times 7.65 \text{ \AA}^2 = 38 \text{ \AA}^2$  which is in reasonable

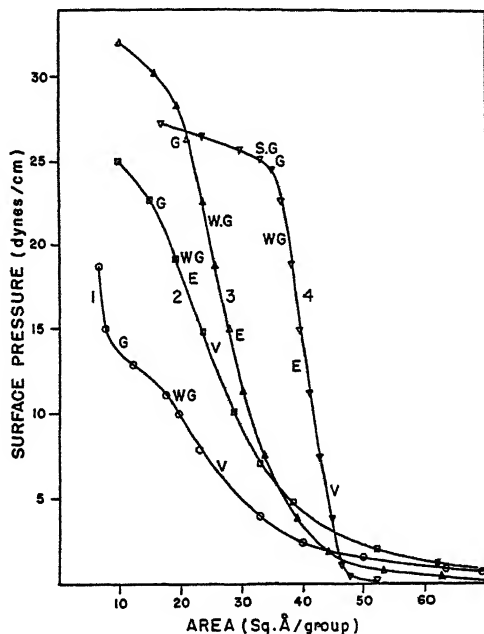


FIG. 7

Force-Area Curves of Aldehyde Compounds Derived from Polyvinyl Alcohol

1. Formvar (from Formaldehyde); 2. Alvar (from Acetaldehyde); 3. Butvar (from Butyraldehyde); 4. Octvar (from Octaldehyde)

agreement with the extrapolated values of the  $F$ - $A$  curves. The value from the  $\mu$ - $A$  curve for Formvar is rather low, and it is possible that some tilting of the ring structure occurs, though this will be opposed by the electrical forces acting on the dipoles (Table VII). The high area of Octvar is due to the branched side chain.

TABLE VII

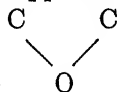
Substance	Area by extrapolation $A(F \rightarrow 0)$	Area by extrapolation $A(\mu \rightarrow \mu_m)$
Formvar	$36 \text{ \AA}^2$	$29 \text{ \AA}^2$
Alvar	$38.5 \text{ \AA}^2$	$35.5 \text{ \AA}^2$
Butvar	$36.5 \text{ \AA}^2$	—
2° Octvar	$45 \text{ \AA}^2$	—



It is interesting to note that the linking of the polar groups in pairs does not affect the flexibility of the chains. As long as the side chains are not too coherent (as with Benvar and Octvar) kinetic agitation is still sufficient to contribute a pressure at areas where there is considerable free surface between the chains.

The polar group gives a maximum surface moment of 300 m.d. in the case of Formvar and 340 m.d. for Alvar; those of higher members were not determined. If the aldehyde-alcohol condensation group is treated as containing two etheric oxygen atoms, the moment may be calculated by vector addition, using the observed value of 230 m.d. of the long-chain ether as a basis. We may first calculate the apparent

moment of the C—O bond. If this has moment  $\mu$ , and  $\alpha$  is the valence angle:—



$$\mu_e = \sqrt{2\mu^2 + 2\mu^2 \cos \alpha}$$

Putting  $\alpha = 110^\circ$ ,  $\mu_e = 230$  m.d.; then  $\mu = 200$  m.d.

The orientation of the ether groups relative to each other must next be determined. This will depend on the position of the free valences on the original polyvinyl alcohol backbone. If, as is indicated by X-ray analysis (Fuller, 1940), they lie on the same side of the backbone when this is placed in the "straight zig-zag" form the valencies will be co-planar and 2.5 Å apart. The distance between the C—O bonds of the aldehyde alcohol group is 2.4 Å when co-planar so that the fitting of these bonds will involve little distortion. There is no steric hindrance to prevent all polar groups along the chain orientating simultaneously in the interfacial field, so that the moment required is the resultant of their moments. Calculation, assuming the normal valence angles, gives a value  $1.62\mu = 324$  m.d. in good agreement with observed values.

If it is assumed that the polyvinyl alcohol residues do not lie on the same side of the backbone, a lower value of dipole moment would be expected. It is necessary either to distort the backbone to allow the aldehyde-alcohol group to fit, thus the polar groups cannot orientate simultaneously, or alternatively, one of the ether groups must be rotated through about  $45^\circ$  in the direction causing a reduction in the resultant moment to about 230 m.d. It follows, therefore, that the observed values accord only with the structure proposed on the basis of X-ray analysis of polyvinyl alcohol.

Benvar forms a very coherent film and occupies a rather small area ( $32 \text{ Å}^2$ ). It collapses spontaneously, and its surface moment is also small (240 m.d.) suggesting that the film may be badly spread. If  $\mu$  is extrapolated to the theoretical value of 320 m.d. the area occupied is  $42 \text{ Å}^2$ ,

a more reasonable value. The benzene rings impart a very strong cohesion to the film, as noted by Adam with benzyl cellulose, a fact which also accounts for the rigidity of the polymer in bulk.

### SUMMARY

Many linear polymers containing water-attracting groups, such as polyesters, polyethers, polyalcohols and polyacids, may be spread uniformly at the air-water and oil-water interface. Polymers with the least internal cohesion spread most easily, those with high internal cohesion do not spread well.

The character of the resulting film depends on the balance between the lateral attractions at the surface and the water-attracting properties of the polar groups. The specific area occupied per monomer unit is independent of the molecular weight in high polymers.

Fluid films gelating only at high surface pressure are termed "fluid amorphous type." They exhibit a low pressure region in which there is free space between the chains, a high pressure region where an increasing proportion of the groups are formed into an "overfilm," and a collapse pressure or pressure range where the "overfilm" is complete and has properties of the bulk polymer. Segments in the overfilm are in equilibrium with segments in the monolayer, the process being reversible.

Certain films appear to have a small proportion of residues distributed into an "over-film" at zero pressure.

Estimations of the limiting area from the  $F$ - $A$  and  $\Delta V$ - $A$  curves are in reasonable agreement with known intermolecular dimensions and probable molecular configurations. The values of apparent surface moments are comparable to those in long chain films, and the dipoles are, in the majority of vinyl derivatives, free to orientate fully.

### REFERENCES

- ADAM, N. K., *The Physics and Chemistry of Surfaces*. Clarendon Press (1930).  
ADAM, N. K., *Trans. Faraday Soc.* **29**, 108 (1933).  
ALEXANDER, A. E., AND SCHULMAN, J. H., *Proc. Roy. Soc. (London)* **A161**, 115 (1937).  
ALEXANDER, A. E., AND TEORELL, T., *Trans. Faraday Soc.* **35**, 727 (1939).  
ALEXANDER, A. E., *Proc. Roy. Soc. (London)* **A179**, 486 (1942).  
BAKER, W. O., FULLER, C. S., AND PAPE, N. R., *J. Am. Chem. Soc.* **64**, 776 (1942).  
BLEASE, R. A., AND TUCKETT, R. F., *Trans. Faraday Soc.* **37**, 571 (1941).  
BOISSONASS, G. G., AND WOLFF, E., *Helv. Chim. Acta* **23**, 430 (1940).  
BUTLER, J. A. V., *Trans. Faraday Soc.* **33**, 229 (1937).  
COUMOULOS, G., *Proc. Roy. Soc. (London)* **A182**, 166 (1943).  
DE VORE, H. B., AND DAVEY, W. P., *J. Phys. Chem.* **35**, 2129 (1931).  
FRENKEL, J., *J. Chem. Phys.* **7**, 538 (1939).  
FULLER, C. S., *Chem. Revs.* **26**, 143 (1940).  
HALLER, W., *Kolloid-Z.* **78**, 341 (1937).

- HARDING, J. B., AND ADAM, N. K., *Trans. Faraday Soc.* **29**, 108 (1933).  
HARKINS, W. D., CARMAN, E. F., AND RIES, H. E., *J. Chem. Phys.* **3**, 692 (1935).  
KATZ, J. R., AND SAMWEL, P. J. P., *Naturwissenschaften* **16**, 592 (1928).  
KATZ, J. R., AND SAMWEL, P. J. P., *Ann.* **474**, 296 (1929).  
JOLY, M., *J. phys. radium* **11**, 471 (1937).  
LANGMUIR, I., *J. Am. Chem. Soc.* **39**, 1883 (1917).  
LEE, S., AND SAKURADA, I., *Z. physik. Chem.* **A184**, 268 (1939).  
MEYER, K. H., *Natural and Synthetic High Polymers*, New York (1942).  
MITCHELL, J. S., *Proc. Roy. Soc. (London)* **A155**, 696 (1936).  
MOSS, S. A., *J. Am. Chem. Soc.* **56**, 41 (1934).  
SCHULZ, G. V., *Naturwissenschaften* **25**, 346 (1937).  
SCHOFIELD, R. K., AND RIDEAL, E. K., *Proc. Roy. Soc. (London)* **A110**, 167 (1926).  
TUCKETT, R. F., AND FRITH, E. M., *Trans. Faraday Soc.* **40**, 251 (1944).  
ZOCHER, H., AND STIEBEL, F., *Z. physik. Chem.* **A147**, 401 (1930).

# MONODISPERSED HYDROPHOBIC COLLOIDAL DISPERSIONS AND LIGHT SCATTERING PROPERTIES.

## I. PREPARATION AND LIGHT SCATTERING PROPERTIES OF MONODISPERSED COLLOIDAL SULFUR

Victor K. LaMer and Marion D. Barnes

*From the Department of Chemistry, Columbia University, New York, N. Y.*

*Received October 17, 1945*

### INTRODUCTION

One of the important problems of Colloid Chemistry is the rapid and facile determination of particle size distribution in the preparations encountered in nature and in the laboratory. For particles so large that settling under gravity or with the ultracentrifuge proceeds with sufficient rapidity, sedimentation methods have proven feasible though tedious. As the size decreases sedimentation procedures become progressively more difficult to execute. Likewise, in this range the limits of resolution of the light microscope make direct observations difficult and unreliable. Although the electron-microscope is competent to deal with this problem, the instrument is not always readily available and the difficulties of preparing a representative sample for examination have not been fully surmounted.

Optical methods based upon the scattering of light have long been recognized (1, 2, 3) as furnishing a means of determining particle size in these ranges where sedimentation and direct observation under the light microscope were impractical.

The chief difficulty has been the preparation of sols with a sufficiently high degree of uniformity of particle size upon which to base the fundamental measurements; in other words, to adequately check theory and to calibrate the method. Although the electromagnetic theory of the scattering of light of transparent spheres has been well worked out by Rayleigh (4), Love (5), Mie (6), Debye (7) and others, no satisfactory experimental confirmations of the general theory exist except perhaps in the region of very small particles, *i.e.*, for radii much less than the wave length of the incident light. It is only in this region that the more familiar limiting form of the theory, as developed originally by Rayleigh (10) is valid. Above this region it is necessary to use the more general

forms as developed by Love and by Mie and for which preliminary numerical calculations have been made by Blumer (11) and others (12).

Undoubtedly, the tedium of these mathematical calculations, when one proceeds beyond the Rayleigh region, constitutes one reason why more conclusive experimental checks have not been attempted, but the lack of suitable mono-dispersed preparations for experimental verification appears to have been the most important impediment. In fact, it will be shown that considerable progress can be achieved by a purely empirical approach to the problem without recourse to the complex mathematical analysis when mono-dispersed preparations are at hand.

The early investigators of the Tyndall beam were motivated as well as restricted by Rayleigh's now relatively simple first approximation treatment, which involved only the greater scattering of blue light as compared to red and his well known simple polarization scattering by a dielectric sphere. Only recently have investigators had any theoretical reasons for expecting higher order effects. Blumer (1925-6) apparently was the first to emphasize on theoretical grounds that a dispersion of wave length was to be expected in the scattered light of larger particles. Our experimental observations could have been predicted from his calculations.

It is interesting to note that, although Faraday (8), then Tyndall (9) and later Rayleigh (10) mixed acid and thiosulfate solutions to generate sulfur sols to produce the Tyndall effect and these sols have since become the standard medium by which physicists demonstrate the beam, apparently no one has reported any of the beautiful spectral orders first noted qualitatively by Ray (13) and now produced in greater variety, stabilized and investigated quantitatively by us.

The literature abounds with references to blue scattering, reddish hue of transmitted light and opalescence—a mark of polydispersity—but we have found no references (except that of Ray) to the angular scattering of red, blue, yellow, etc., bands. These scattering spectral orders should not of course be confused with the corona and the rainbow since these effects result respectively from refraction and internal reflection in much larger particles.

The earlier investigators may have missed observing these spectral scattering orders because they used too concentrated solutions, or perhaps discarded their dilute solutions before sufficient growth occurred. Our success in producing stable mono-disperse systems resides principally in the choice of properly diluted solutions which, of course, eliminates secondary coagulation and consequent polydispersity. The exercise of the well known techniques of thorough mixing and cleanliness of solutions and glassware also play a part in reproducing the preparations. Our solutions apparently contain a sufficient number of nuclei to produce a

mono-disperse system if the concentrations are not too great. Equally good mono-dispersity is obtained at still greater dilutions but the rate of growth is slow and the particle number is too low for precise optical measurements. After the kinetics of the sol growth have been investigated more thoroughly, the necessary conditions, precautions and concentration limits will be described more confidently and precisely.

In this series of papers, we shall describe first a simple and direct method of preparing sulphur dispersions which are highly homogeneous in respect to particle size and describe qualitatively their interesting and beautiful optical properties as regards the angular distribution of the various colors of the Tyndall beam as a means of characterizing the particle size.

In the second paper, the optical transmittance will be compared with theory and the form of the transmittance curve employed as a means of characterizing both the particle size and concentration of the sol.

In later papers we propose to report the observed scattering phenomena in more quantitative fashion in terms of the polarizations, angles and wave lengths of the scattered light. An investigation of the laws of thermal migration of these particles under specified temperature gradients is projected.

Sulfur is an ideal substance for such investigations because it possesses a high index of refraction, is almost transparent to visible light and is free from the theoretical complication of electrical conductivity of the dispersed phase. Sulfur was tried first primarily for these and reasons of convenience, but other materials, certainly selenium and other polymers, will undoubtedly prove to be of equal interest.

### PREPARATION

The preparation of monodispersed colloidal sulfur has been attempted previously by several investigators with varying degrees of success. Oden (14) prepared a dispersion consisting of a variety of particle sizes of sulfur by acidifying a thiosulfate solution with concentrated  $\text{H}_2\text{SO}_4$ , and attempted to isolate monodispersed sols from the mixture by a fractionation method involving selective coagulation with an electrolyte solution and peptization of the resulting coagulum with water. The method is tedious and only partially successful. More recently Janek (16) has prepared a similar sol employing solutions of sodium sulfide, sodium sulfite and sulfuric acid. After precipitation, filtration and re-dispersion a fairly stable sol transmitting red light was obtained.

In the present experiments one (1.00) ml. of 1.50 N  $\text{H}_2\text{SO}_4$  was added to 995 ml. of distilled water in a liter volumetric flask and thermostated at 25°C. One (1.00) ml. of 1.5 N  $\text{Na}_2\text{S}_2\text{O}_3$  was added rapidly from a 2 ml.

hypodermic syringe, the volume quickly made up to 1 liter, mixed thoroughly and returned to the thermostat. After about an hour the appearance of a colloidal dispersion was detected with a Tyndall beam. The particles of the sol continued to grow over a period of 24 to 30 hours, after which they became large enough to settle out very rapidly.

Practically monodispersed sols were prepared in this way by stopping the growth after various time intervals by titrating the unreacted thiosulfate with a solution of iodine, leaving a slight excess of thiosulfate to help stabilize the dispersion.

### HOMOGENEITY OF THE PARTICLES

The evidence of the uniformity of the particle size follows:

(a) Ultra-microscopic examination indicated spheres of the same brightness and size. There was no twinkling of the particles in Brownian movement, indicating the absence of irregular shapes.

(b) In the case of large particles the precipitate on a glass slide shows uniform spheres under the ordinary light microscope.

(c) When oil droplets of the proper size are observed in the classical Millikan apparatus, those drops which fall at the same rate exhibit the same colors, whereas droplets which fall at different rates exhibit different colors. Under an ultramicroscope all the particles of our specially prepared sols showed the same colors.

The sulfur is dispersed as a liquid. This is shown by the observation of the coalescing of spherical particles in the ultramicroscope and the solidification of large amounts of freshly precipitated sulfur when rubbed between the fingers.

### GROWTH AND OPTICAL EFFECTS

Interesting optical effects accompanied the growth of these highly homogeneous dispersions. These were observed by employing a practically parallel beam of plane polarized white light with its electrical vector in a vertical direction. The beam was viewed from various angles with the eye in a plane perpendicular to the electric vector. The color of the Tyndall spectrum produced and viewed in this way was first observed to be pale blue in all directions with the scattered light practically 100% polarized at right angles to the direction of propagation of the beam as predicted by Rayleigh's simple theory. This color gradually changed as the particles grew larger. The intensity of scattered light became greatest in the direction of the propagation of the beam and the percentages of depolarized light increased for all angles. A wide red band developed in the spectral region of greatest intensity.

With continued growth of particle size, a second order spectrum was produced in which the red band was broadest and most intense. The Tyndall spectrum showed an increasing number of orders in which red and green predominated until an apparent maximum of 9 orders was attained. For still larger particle sizes the orders became practically indistinguishable and settling occurred relatively rapidly. On long standing, or addition of excess electrolyte, partial coagulation of the sols resulted in destruction of all orders shown in the Tyndall spectrum regardless of the number originally present. This coagulation caused first a loss in sharpness of the orders, *i.e.*, a sort of blend of the various orders, and finally their complete disappearance. Since the partial

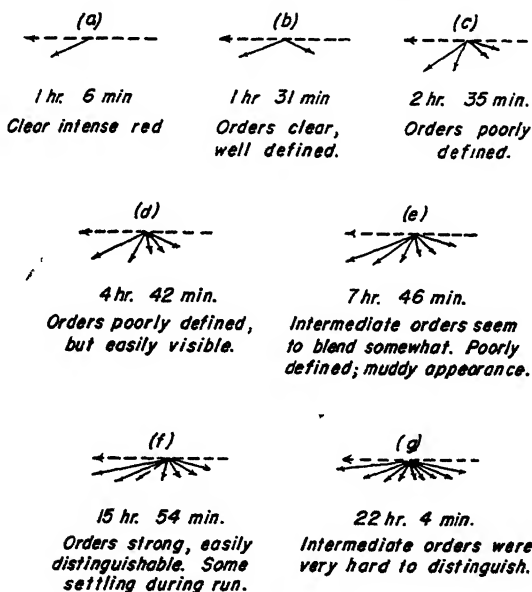


FIG. 1

coagulation results also in a loss of homogeneity, one may associate the existence of orders in the Tyndall spectrum with the homogeneity of the system. Ray (13) observed the production of this same color effect in acidified solutions of thiosulfate. However, his observations seem to show only about 2 or 3 orders and no indication was made that the phenomenon was dependent on the homogeneity of the particle size.

#### THE SOLS PREPARED

Fig. 1 shows a summary of the properties of the series of sols whose transmittance is reported in the following paper. The initial concentration of the thiosulfate and acid in the solution is the same in all cases



(0.0015  $N$ ). The horizontal arrows show the direction of propagation of light through a dispersion, the other arrows show intensity, number and position of the red band.

When two monodisperse sols of different particle size are mixed the originally sharply defined orders disappear or become very diffuse except in the extreme forward or backward directions of the scattered light. From this it is obvious that whenever a distribution of particle size exists one would observe only an opalescent effect.

The reaction of thiosulfate with acid has been studied by Bassett and Durrant (15), and by Prakke and Stiasny (17), who demonstrated that a variety of products may be produced on decomposition of thiosulfate. The product obtained seems to depend greatly on the concentrations of acid and thiosulfate employed. Both papers are in agreement in that sulfur and sulfite are produced in dilute solutions. A study of the factors governing the formation and growth of the sulfur particles is needed and will be considered in a later paper.

#### SUMMARY

1. A simple, direct method for the preparation of colloidal dispersions of very uniform particle size has been described.

2. A series of monodispersed sols of different particle sizes has been prepared and stabilized.

3. Monodispersed sols of small particle size exhibit the optical properties predicted by the Rayleigh equation, but in the case of sols of larger particles we have observed the higher order effects that can be predicted from the general electromagnetic theory of light scattering.

4. These higher order effects are characterized by the dispersion of the scattered light resulting in bands (or spectra) of different colors whose intensity, polarization and angular distribution depend upon the particle size.

#### REFERENCES

1. FREUNDLICH, H., *Kapillarchemie*, 2nd Ed. (1923), p. 518-529, Akademische Verlagsgesellschaft, Leipzig (1923).
2. KRAEMER, E. O., *Treatise on Physical Chemistry*, 2nd Ed. (Taylor, Editor), p. 1600-1605, Van Nostrand (1931).
3. THOMAS, A. W., *Colloids*, Chap. 3 and 6, McGraw-Hill (1934).
4. LORD RAYLEIGH (J. W. Strutt), *Phil. Mag.* **12**, 81 (1881); *Proc. Roy. Soc. (London)* **A84**, 25 (1910); see *Collected Scientific Papers* **1**, 518.
5. LOVE, A. E. H., *Proc. London Math. Soc.* **30**, 308 (1899); **31**, 489 (1899).
6. MIE, G., *Ann. Physik* **25**, 377 (1908).
7. DEBYE, P., *Ibid.* **30**, 57 (1909).
8. FARADAY, M., *Trans. Roy. Soc. (London)* **147**, 154 (1856).

9. TYNDALL, J., *Phil. Mag.* **37**, 384 (1869).
10. LORD RAYLEIGH, *loc. ref.* 4 (1881).
11. BLUMER, H., *Z. Physik* **32**, 119 (1925); **38**, 304, 920 (1926); **39**, 195 (1926).
12. ENGELHARD, H., AND FRIESS, H., *Kolloid-Z.* **81**, 129 (1937).
13. RAY, B., *Proc. Indian Assoc. Cultivation Sci.* **7**, 1 (1921).
14. ODEN, S., *Kolloid-Z.* **8**, 186 (1911).
15. BASSETT, H., AND DURRANT, R. G., *J. Chem. Soc.* **1931**, 2929.
16. JANEK, A., *Kolloid-Z.* **64**, 31 (1933).
17. PRAKKE, F., AND STIASNY, E., *Rec. trav. chim.* **52**, 615 (1933).



# MONODISPERSED HYDROPHOBIC COLLOIDAL DISPERSIONS AND LIGHT SCATTERING PROPERTIES.

## II. TOTAL SCATTERING FROM TRANSMITTANCE AS A BASIS FOR THE CALCULATION OF PARTICLE SIZE AND CONCENTRATION

Marion D. Barnes and Victor K. La Mer

*From the Chemistry Department, Columbia University, New York, N. Y.*

*Received November 27, 1945*

### INTRODUCTION

The desirability of the rapid and accurate determination of particle sizes of polymers by an optical method, the effect of particle size and number on transmittance of light through smokes and fogs, the production and explanation of colors in colloidal dispersions and many related phenomena have all served to focus interest on the fundamental theory of the scattering of light by material particles. Many efforts have been made to confirm experimentally the prevailing theory, but in general these efforts have been inadequate. Previous attempts have failed in the case of liquid media primarily because the systems examined were poly-dispersed, *i.e.*, inhomogeneous in respect to particle size, also the previous measurements were lacking in the precision obtainable with modern optical apparatus.

It was the purpose of this investigation to obtain an experimental proof of the theory of scattering of light by transparent particles and to calculate from the measured total scattering curves the radius of the particles and the number of particles per unit volume.

### THEORY

A periodic wave striking a material body of any kind causes an oscillation of surface charges synchronous with the incident wave. A secondary field inside and outside the material body arises as a result of this movement of charge. The resultant field is the vector sum of the primary and secondary fields. This interaction of light and matter has been thoroughly treated mathematically by Debye (1) and Mie (2).

The electromagnetic condition of any point outside the material particle struck by a plane electromagnetic wave was calculated by Mie

employing the classical equations of Maxwell. He assumed the particles to be spherical, and for a system of particles the spheres were considered to be so far apart that secondary scattering is negligible. His treatment gave equations for calculating the intensity and condition of polarization of total and angular scattered light as a function of the ratio of the refractive index of the particles to that of the medium and the ratio of the diameter of the particles to the wave length of light. For details of the development of the theory, one is referred to the original article of Mie or to various summaries published in connection with attempted experimental proofs of the theory (3, 4) or to modified treatments (5, 6, 7, 8).

The equations obtained by Mie are of a general nature and, therefore, applicable to many different systems provided the optical constants for the constituents thereof are known. The optical constants of the dispersed phase and dispersion medium are taken into account by employing in the equations the complex index of refraction:

$$(1) \quad m = \nu(1 - i\kappa)$$

where  $\nu$  = ordinary refractive index

$\kappa$  = absorption coefficient.

In transparent sols, which are to be considered in this paper,  $\kappa = 0$  and  $m$  becomes the ordinary refractive index.

The limiting equations of Mie which describe the energy loss due to absorption of light and to scattering are respectively:

$$(2) \quad K = \frac{6\pi}{\lambda'} Im(-A_1 - A_2 + P_1)$$

$$(3) \quad K' = \frac{4\pi}{\lambda'} \alpha^3 \left( |A_1|^2 + |P_1|^2 + \frac{3}{5} |A_2|^2 \right)$$

where  $K$  = extinction coefficient

$K'$  = scattering coefficient

$\lambda'$  = wave length in water

$Im$  = imaginary part of the expression

$\alpha = 2\pi r/\lambda'$

$r$  = radius of particles

$$A_1 = u_1 \left( \frac{m'^2 - v_1}{m'^2 + 2w_1} \right); \quad A_2 = u_2 \left( \frac{m'^2 - v_2}{m'^2 + 1.5w_2} \right)$$

$$P_1 = u_1 \left( \frac{v_1 - 1}{1 + 2w_2} \right)$$

$$m' = \frac{m}{m_0}$$

$m_0$  = complex refractive index of medium

$m$  = complex refractive index of particle

$||$  = the real values of ---

$u$ ,  $v$  and  $w$  are complex functions of  $m'$  and  $\alpha$ , and for very small particles become numerically equal to 1.

$A_1$  and  $P_1$  describe respectively the energy carried by the first electric partial wave and the first magnetic partial wave.

The above limiting equations require modification to describe the energy loss due to particles whose diameter is very large compared to the wave length of light. The modification consists in the inclusion of sufficient terms to account for the energy loss due to increasing number of electrical and magnetic partial waves with increasing particle diameter. For particles very small compared to the wave length of light, practically all of the energy is carried by the first electrical partial wave and the scattering Equation (3) becomes

$$F_1 = \frac{24\pi^3 V}{\lambda'^4} |A_1|^2$$

where  $V$  = volume of the particle.

This is identical with the familiar equation of Rayleigh (9):

$$(4) \quad F_1 = \frac{24\pi^3}{\lambda'^4} V \left( \frac{m'^2 - 1}{m'^2 + 2} \right)^2$$

Mie has employed this theory in calculating the scattering of colloidal gold particles, a case in which the absorption coefficient  $\kappa$  is important in the complex index of refraction  $m$ .

Equation (3) has been used by Casperson (3) in calculating the scattering of the transparent sols of sulfur and gum mastic. Gribnau (4) has used Equations (3) and (2) in calculating the scattering and absorption of selenium sols. Their calculations cover a range in  $m$  of 1.3 to 2.2 and were used for particles whose diameter is approximately the same as the wave length of visible light. They obtained a series of *smooth* curves which show a marked dependence on particle size.

In order to describe the scattering by particles having a value of  $\alpha$  approximating unity, many terms  $A_1, A_2, A_3, \dots A_n; P_1, P_2, P_3, \dots P_{(n-1)}$  must be included in Equations (2) and (3). The calculation of the numerical values of these terms is exceedingly laborious. Tables for certain values of  $m$  and  $\alpha$  have been developed by Blumer (10), and a smooth curve for  $K$  as a function of  $\alpha$  is given by Stratton and Houghton (5) for  $m = 1.33$  and valid for water fogs. Recently, more accurate and extensive computations employing large numbers of terms  $A_n, P_{(n-1)}$  have been made by Lowan (11) and collaborators, and verified in part by Langmuir (12). Of particular interest in this investigation is Lowan's

theoretical curve in Fig. 1. This curve is for a refractive index ratio of 1.5. It will be seen that there are two principal maxima, and on the greater of these there are several secondary maxima in the region where calculated points are numerous. These primary and secondary maxima have not been found experimentally in previous attempts to confirm

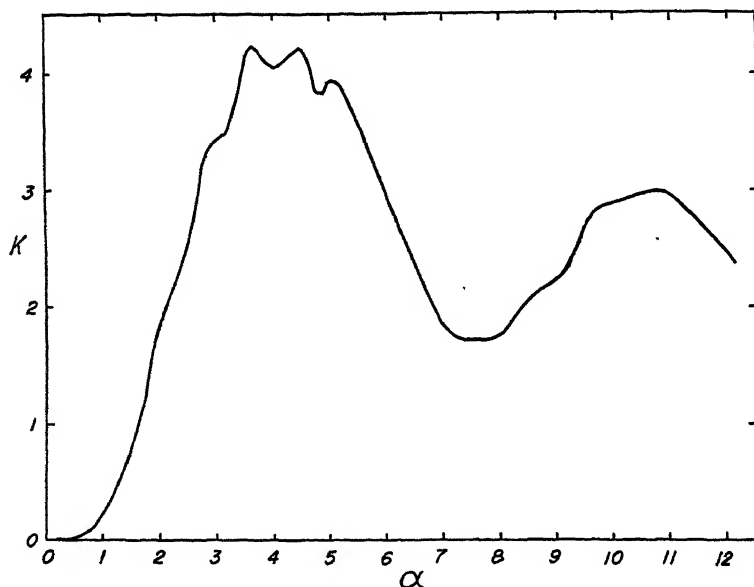


FIG. 1

Theoretical Curve Showing the Scattering Coefficient  $K$  vs.  $\alpha$  ( $\alpha = 2\pi r$ )

the Mie theory. This is probably due to the inhomogeneity of sols investigated.

#### EXPERIMENTAL

The properties and method of preparation of monodispersed colloidal sulfur are discussed in detail in the previous paper (13). The measurements of transmitted light were made on a photoelectric spectrophotometer constructed by one of us (M.D.B.). Monochromatic light for transmittance measurements was obtained from a Coleman Double Monochromator Spectrophotometer, Model 10-S, by placing a right-angle prism in the path of the light between the collimating lens and the slit. The light emerging from the prism was focused on a  $15\text{ m}\mu$  slit, passed through a condensing lens, a long absorption tube and finally focused on the cathode of a photo tube.

The absorption tubes were  $44.40 \pm 0.05$  cm. in length. They were constructed from 45 mm. pyrex tubing and were carefully ground so

that they were optically interchangeable. These tubes were conveniently mounted on a metal carriage permitting rapid and reproducible replacement or shifting of position.

The optical arrangement was completely enclosed. Partitions separated the absorption tubes from the monochromator and from the photo tube. Scattered light was thus effectively eliminated before reaching the photo tube which was approximately 25 cm. from the proximal end of the absorption tubes.

The electrical circuit used was essentially that of Eglin (14, 15). The photo tube was an RCA No. 922, operated at 45 volts with a load resistance of 20 megohms. As a slide-back potentiometer, a Leeds & Northrup Type K-2 was used. The sensitivity of this instrument was sufficient to permit a precision of 0.1% in transmittance over the range 400  $m\mu$  to 800  $m\mu$ . Beyond these limits the precision fell off considerably.

In a typical run on a 5-order sol, one absorption tube was filled with the dispersion, the other with a sample of the same distilled water used in preparing the sol. The transmission of the solvent and the transmission of the dispersion were measured at various wave lengths in rapid succession. The two measurements required about one minute, during which time there was no change in light intensity, photo-tube dark current or other instrumental variables.

Approximately two hours were required to complete the series of readings over the range 370  $m\mu$  to 850  $m\mu$ . During this time a notable change occurred in the transmittance readings. This change (apparently due to settling or redissolving of particles) was corrected for by making readings at the reference points 370, 450, 650 and 800  $m\mu$  in rapid succession. The curve was then adjusted to fit these points.

## RESULTS

*A Typical Run:* Table I shows values for the run described in detail in the previous paragraph. These values are plotted in Fig. 2. A dashed

TABLE I

$\lambda$ ( $m\mu$ )	$\lambda'$ ( $m\mu$ )	$I_0$ (volts)	$I$ (volts)	$\log \frac{I_0}{I}$ (measured)	$\log \frac{I_0}{I}$ (corrected)
370	275	.0248	.0105	.375	.375
450	336	.1190	.0663	.255	.255
650	488	.3567	.1026	.542	.542
800	603	.0753	.0215	.544	.544
370	275	.0249	.0108	.364	.375
380	283	.0365	.0161	.356	.366
390	290	.0555	.0256	.337	.347
400	298	.0759	.0372	.310	.320
410	306	.0845	.0445	.279	.289



TABLE I (Continued)

$\lambda$	$\lambda'$	$I_0$	$I$	$\log \frac{I_0}{I}$	$\log \frac{I_0}{I}$
( $m\mu$ )	( $m\mu$ )	(volts)	(volts)	(measured)	(corrected)
420	313	.0892	.0494	.258	.268
430	321	.0970	.0543	.253	.263
440	329	.1066	.0604	.248	.258
450	336	.1198	.0682	.246	.256
460	344	.1346	.0749	.255	.266
470	351	.1496	.0800	.272	.283
480	359	.1616	.0831	.290	.301
490	367	.1768	.0883	.301	.312
500	374	.1913	.0928	.314	.326
510	382	.2079	.0957	.337	.348
520	390	.2259	.0980	.364	.376
530	397	.2484	.1016	.389	.402
540	405	.2684	.1055	.405	.418
550	412	.2881	.1103	.417	.430
560	420	.3119	.1165	.428	.442
570	428	.3292	.1188	.443	.456
580	435	.3390	.1170	.462	.477
590	443	.3567	.1169	.484	.477
600	450	.3590	.1136	.500	.515
610	458	.3627	.1125	.508	.523
620	466	.3701	.1129	.516	.532
630	473	.3752	.1138	.519	.534
640	481	.3724	.1125	.520	.536
650	488	.3736	.1114	.525	.542
660	496	.3629	.1066	.532	.547
670	504	.3589	.1031	.542	.557
680	511	.3518	.0989	.551	.566
690	519	.3333	.0923	.558	.572
700	526	.3103	.0857	.559	.572
710	534	.2722	.0745	.562	.575
720	542	.2212	.0512	.559	.571
730	549	.1598	.0447	.553	.564
740	557	.1064	.0302	.547	.557
750	565	.0863	.0246	.545	.555
760	572	.0808	.0228	.549	.550
770	580	.0766	.0217	.548	.550
780	587	.0744	.0212	.545	.548
790	595	.0748	.0214	.543	.547
800	603	.0747	.0215	.542	.546
810	610	.0716	.0207	.539	.545
820	618	.0614	.0177	.540	.548
830	626	.0137	.0127	.537	.545
840	633	.0285	.0084	.548	.552
850	641	.0211	.0063	.524	.534

$\lambda$  = wave length in air;  $\lambda'$  = wave length in water

$I_0$  = transmission of solvent;  $I$  = transmission of dispersion

line indicates the uncorrected curve, and a solid line indicates the curve corrected for change in sol while readings were being made. For sols of larger particle size the correction was greater than that of Fig. 2, while for smaller sols it was of lesser consequence.

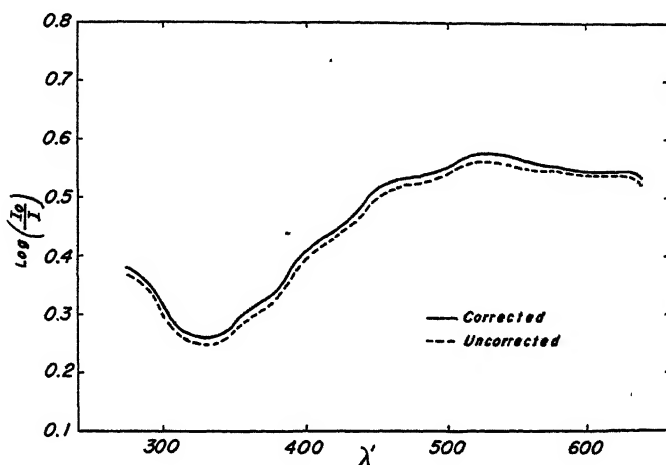


FIG. 2

Total Scattering vs. Wave Length for a Typical Run

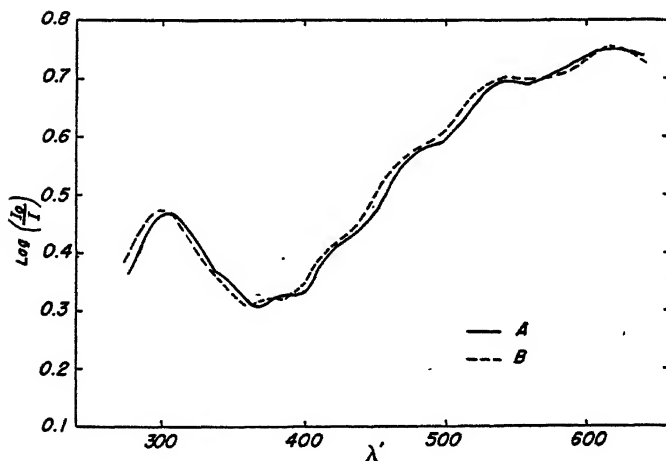


FIG. 3

Total Scattering vs. Wave Length for Duplicate Runs

*Reproducibility* of sols and measurements is indicated for a 6-order sol in Fig. 3. The two sols were prepared in exactly the same way and measured after the same length of time. However, a slight difference in particle size is indicated by the displacement of A compared to B.

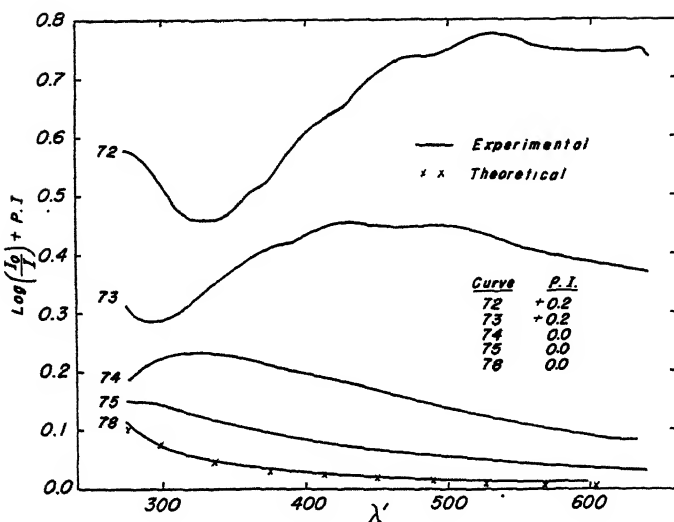


FIG. 4

Total Scattering Curves for Sols of Smaller Particle Sizes

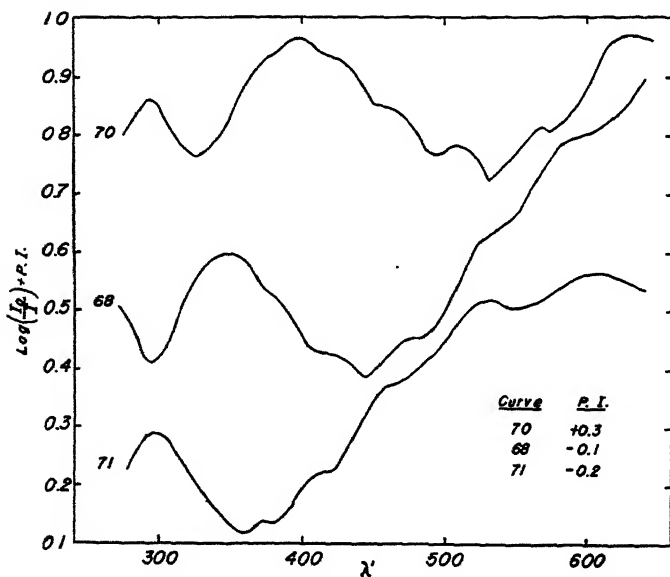


FIG. 5

Total Scattering Curves for Sols of Larger Particle Sizes

Difficulty in reproducing the size and number of particles in a given sol was finally overcome by using aliquot portions from a large volume of distilled water for the runs and by adopting a strict routine in cleaning the flask after each run. This consisted in washing the flasks successively with warm cleaning solution, distilled water, ethyl alcohol and finally with several portions of distilled water.

*Scattering curves* with sol numbers are shown in Figs. 4 and 5. Fig. 4 shows the curve for smallest particle sizes measured. No orders were present in the Tyndall spectrum, but highly polarized grayish blue light was scattered in all directions. The cross line shows Rayleigh's theoretical scattering curve for very small particles.

The sols whose curves are shown in Figs. 4 and 5 are described qualitatively in the first paper of this series (13). Tabulated on the figures are the plotting increments (P. I.) used to displace the curves conveniently in a  $Y$  direction on the plot. All these curves have been corrected for changes occurring during measurement.

### DISCUSSION

*The Requirements of the Theory:* The sols investigated meet the conditions of spherical shape and homogeneity required by the Mie theory. Ultra-microscopic examination showed the distance between particles to be 50 to 100 times their diameter. The particles were likewise shown to be spherical and of a fairly homogeneous size. There was no scintillating or twinkling as the particles underwent Brownian motion.

The equations employed by Casperson and others assume perfectly transparent particles. That sulfur is not perfectly transparent in liquid form is evident from the color of sulfur just above its melting point. The pale yellow color, however, indicates weak absorption in the violet and a complete transparency over the rest of the visible range. That this very slight absorption contributes little is shown by the fact that the curve for small particles (No. 78, Fig. 4) corresponds almost exactly to the theoretical curve (cross line) for small transparent particles.

*The Total Scattering Curves:* The curves shown in Fig. 4 correspond in a general way to those calculated by Casperson. However, the former extend the range of wave lengths covered by the latter from 420  $m\mu$  to 275  $m\mu$ . This is made readily possible experimentally because we are dealing with a liquid system in which the wave length of light in the liquid is related to its wave length in air by the equation

$$\lambda'_{(\text{water})} = \frac{\lambda_{(\text{air})}}{m_{0(\text{air})}}$$

where  $m_{0(\text{air})}$  is the refractive index of water related to dry air at 25°C. and 760 mm. (16).

In this critical range the nature of the curve is changing most rapidly with increasing particle diameter and we have found in this region an interesting scattering minimum which moves gradually to longer wave lengths for larger particle sizes. This minimum is first evident in curve No. 73 at 275  $m\mu$ , and in the curve for largest diameters measured it is located at 515  $m\mu$ . This minimum is not shown by the calculations of Gribnau and Casperson.

Another interesting feature shown by our curves which has not been shown by previous experimental investigations of dispersed sulfur is the superposition of secondary maxima on the general form of the scattering curve. The phenomenon is first observed in the curve for a 3 order sol

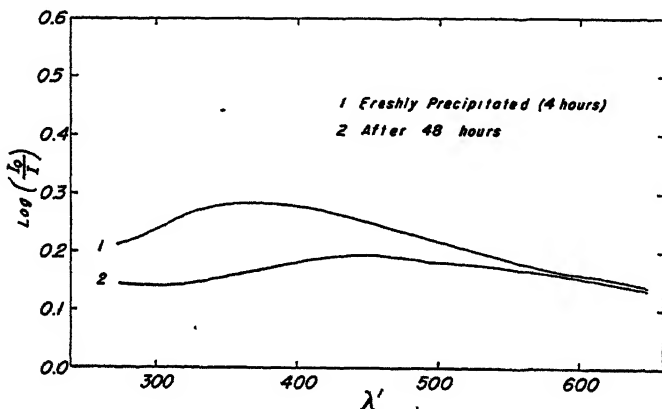


FIG. 6

Total Scattering Curves for Poly-disperse Sols

(No. 79) and becomes more obvious in sols of larger particle sizes. The secondary maxima are sharper and more pronounced the more homogeneous the particle size, and are practically lacking in heterogeneous sols. Fig. 6 shows curves for such sols prepared by adding a solution of sulfur in acetone to water. Ultramicroscopic examination of these sols showed particles of many sizes present. Inspection of the curve shows a complete lack of secondary maxima and minima.

The presence of a few secondary maxima on the total scattering curve has been shown theoretically. See Fig. 1. These maxima are to be associated with the increasing number of electrical partial and magnetic partial waves arising from the scattering of light by the larger particles. The calculation of theoretical scattering curves for larger values of  $\alpha$  is exceedingly laborious. As a result, the theoretical curves do not show nearly as many secondary maxima as are shown by our experimental curves. In addition, our results show for the largest particle sizes a third

primary maximum (at 300 m $\mu$ ) not indicated in the calculations of any previous investigators. See Fig. 5.

*Calculation of Radius and Concentration of Particles:* The scattering coefficient  $K$  is a function of  $m$  and  $\alpha$ . Fig. 7 shows the variation of  $\log K$  with  $\log \alpha$  where  $m = 1.5$ . The scattering coefficient describing the

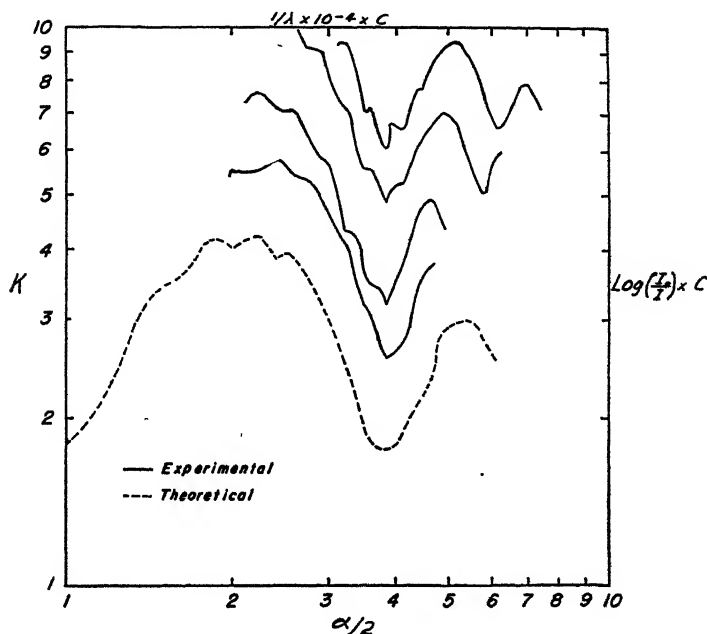


FIG. 7

Log-Log Plot. Dotted Line:  $\log K$  vs.  $\log \alpha/2$ . Solid Lines  $\log [I_0/I]$  vs.  $1/\lambda$   
scattering per particle is related to the conventional extinction coefficient by

$$\log \frac{I_0}{I} = \frac{K 2\pi r^2 n l}{2.3}$$

where  $n$  = number of particles per cubic centimeter  
 $l$  = length of path traversed by the light.

Taking logarithms of both sides of this equation and transposing gives

$$\log K - \log \left[ \log \frac{I_0}{I} \right] = - \log \frac{2\pi r^2 n l}{2.3}$$

In a given experiment,  $n$ ,  $l$ , and  $r$  are constant and  $K$  and  $\log I_0/I$  vary in the same way with  $1/\lambda'$ . Therefore, if one plots  $\log [I_0/I]$  against  $\log 1/\lambda'$  and  $\log K$  against  $\log \alpha$  on the same graph, the displace-

ment along the ordinate necessary to superpose a maximum in the experimental curve on a maximum in the theoretical curve is numerically equal to

$$-\log \frac{2\pi r^2 n l}{2.3}$$

Since  $\alpha = 2\pi r/\lambda'$  and  $\log \alpha - \log 1/\lambda' = \log 2\pi r$ , the displacement along the abscissa necessary to superpose a maximum in the experimental curve on a maximum in the theoretical curve is numerically equal to  $\log 2\pi r$ . Thus one can obtain  $r$  from a calculation based on this measurement. Using this value of  $r$ , the known value of  $l$  and the measured vertical displacement, a value for  $n$  can be calculated.

Fig. 7 shows the plot of  $\log [\log I_0/I]$  against  $\log 1/\lambda'$  and  $\log K$  against  $\log \alpha$ . The dotted line represents the theoretical curve and solid lines indicate various experimental curves which have been displaced laterally so that the scattering minima are superposed.

Calculated values of  $r$  and  $n$  are shown in Table II.

TABLE II

Sol No.	Age	Tyndall spectrum (orders)	$n \times 10^{-7}$ (particles/cc.)	$r$ ( $\mu$ )
72	4 hrs. 42 min.	5	3.43	0.40
71	7 hrs. 46 min.	6	2.42	0.42
68	15 hrs. 54 min.	7	1.07	0.53
70	22 hrs. 41 min.	9	0.81	0.64

It will be observed from the above table that the number of particles decreases as the radius increases. This decrease is apparently due to the settling out of particles rather than to their coagulation since the older sols are much more homogeneous (the orders observed are clearer and the scattering curve shows the secondary maxima to be sharper) than the sols of smaller particle size which required a much shorter time for growth.

#### ACKNOWLEDGMENT

Our best thanks are extended to Drs. David Sinclair and Seymore Hochberg for many helpful discussions and suggestions on both the theory and measurements involved.

The interest of Dr. Lowan and his collaborators in computing the extensive functions involved in plotting Fig. 1 is appreciated.

#### SUMMARY AND CONCLUSIONS

1. Accurate determinations of the total scattering curves for various particle sizes have been made over the range of wave length from  $275 \text{ m}\mu$  to  $600 \text{ m}\mu$  for a system of monodispersed sulfur particles in water.

2. The form of the transmittance curve as predicted by the Mie theory of the scattering of light by colloidal particles has been experimentally verified in minute detail.

3. The diameter and number of particles per unit volume have been calculated from the transmittance as a function of wave length with the aid of this theory.

4. The nature of the total scattering curve has been experimentally determined in a range of  $\alpha$  values ( $\alpha = 2\pi r/\lambda'$ ) wherein it has been too difficult to calculate it.

#### REFERENCES

1. DEBYE, P., *Ann. physik.* (4), **30**, 57 (1909).
2. MIE, G., *Ann. physik.* (4), **25**, 377 (1908).
3. CASPERSON, T., *Kolloid-Z.* **60**, 151 (1932); **65**, 162 (1933).
4. GRIBNAU, FR. B., *Kolloid-Z.* **77**, 289 (1936); **82**, 15 (1938).
5. STRATTON, J. A., AND HOUGHTON, H. G., *Phys. Rev.* **38**, 159 (1931).
6. STRATTON, J. A., *Electromagnetic Theory*, McGraw-Hill Book Co., New York, 1941, p. 563.
7. JOBST, G., *Ann. physik.* **76**, 863 (1925).
8. GANS, R., *Ann. physik* (4), **62**, 331 (1920).
9. RAYLEIGH, J. W. STRUTT, *Phil. Mag.* (5), **47**, 377 (1899).
10. BLUMER, H., *Z. Physik* **32**, 119 (1925); **38**, 304, 920 (1926).
11. LOWAN, A., unpublished calculation.
12. LANGMUIR, I., unpublished calculation.
13. LA MER, V. K., AND BARNES, M. D., *J. Colloid Sci.* **1**, 71 (1946).
14. REICH, H. J., *Theory and Application of Electron Tubes*, McGraw-Hill Book Co., New York, 1944, p. 546.
15. EGLIN, J. M., *J. Optical Soc. Am.* **18**, 393 (1929).
16. TILTON, L. W., AND TAYLOR, J. K., *J. Research Natl. Bur. Standards* **13**, 207 (1934).





# THE METHOD OF PURIFYING AND CONCENTRATING COLLOIDAL DISPERSIONS BY ELECTRODECANTATION

Paul Stamberger \*

*Received August 3, 1945*

## INTRODUCTION

Electrodecantation has been used for several decades as a laboratory tool in the study of structure and concentration of colloidal dispersions. It is a simple and elegant method based on the electrophoretic migration of colloids. In recent years successful effort was made to adapt the process for commercial use. In the course of this development new experience in the technic and adaptability of the process was gained. In this paper, after a brief historical survey, recent improvement in the technic of electrodecantation will be described.

## HISTORICAL

Electrodecantation is based on stratification phenomena in the electric field observed during undisturbed electro dialysis by Wo. Pauli. It has been used by Pauli and his collaborators for concentrating, separating and purifying a great variety of colloidal dispersions. The process based on this stratification phenomena has been termed "Electrodecantation" by Pauli. This name is now adopted.

Electrodecantation in its final effect is a separative as well as a concentrative process. It is based substantially on cataphoretic phenomena. The electrical field is necessary and the colloidal particles must migrate toward a vertical membrane. In addition, however, separation in superimposed horizontal layers also takes place. These layers contain the components of the sol in various concentrations. One of the layers contain nearly all the dispersed particles while the other one is practically free of these.

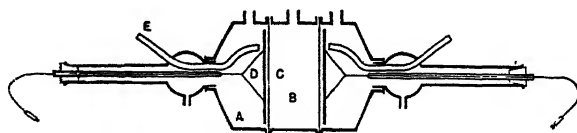
The simplest way of carrying out the process is in a conventional horizontal electro dialysis cell.

Shortly after the dispersion is subjected to an electric field the formation of superimposed layers above and below the original dispersion can be observed, all the dispersion being replaced finally by such growing

\* Present address: The Stamford Rubber Supply Company, Stamford, Conn.

layers. The thickness of these layers depends on the concentration of the original colloidal dispersion as well as on the working conditions, such as potential difference applied.

Electrostratification has been used for investigating the *composition* of sols by concentrating and purifying them, and furthermore for separating colloidal components from solutes as well as separating mixtures of colloids.



A = Electrode compartment;                      B = Working compartment;  
C = Membranes;                                  D = Electrodes;  
E = Leveling tube

FIG. 1

Electrodialysis Apparatus Used also for Electrodecantation

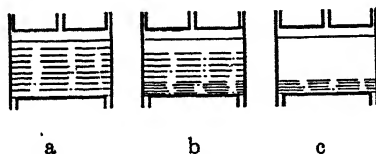


FIG. 2

Progress of Separation During Electrodecantation

Some of the more important investigations are the following. Pauli (1) investigated the origin of the charge of chlorosols of platinum, the sols being purified by electrodecantation. Pauli and Neurath (2) prepared neutral ferric oxide sols of high purity. The positive charge of this highly purified sol could be reversed easily by addition of multivalent anions from  $K_4Fe(CN)_6$  and  $Na_4P_2O_7$ . Gold sols investigated by Pauli, Szper and Szper (3), were concentrated until they ultimately contained 60–70 g. of Au per 1000 ml. of sol. Coagulation could only be avoided in this case by using special precautions (4). Highly concentrated silver iodide sols were prepared by Verwey and Kruyt (5) and the density of the charge determined. The various colloidal constituents of starch sols were separated by Samec and Haertl (6) and by Samec and Mayer (7).

Electrodecantation can frequently be applied when dialysis is difficult, for example, with dispersions containing ions having a slow diffusion rate through a membrane mixed with monovalent ions which have a high diffusion rate. The slowly diffusing multivalent ions remain in the

cell during the progress of dialysis and may gradually change the pH of the dispersion, as in dispersions containing  $\text{SO}_4^{=}$  and  $\text{P}_2\text{O}_7^{=}$  anions and  $\text{K}^+$  or  $\text{Na}^+$  cations.

In addition to application for structural investigation of sols, electrodecantation is frequently used as a straight concentration process on a laboratory or commercial scale in preference to gravity separation by centrifuging or evaporation.

#### THE NATURE OF THE STRATIFICATION PHENOMENA AND ITS APPLICATION

Our knowledge of all the factors influencing the process are still somewhat limited, although the fundamental phenomenon on which the process is based has been established. Blank and Valko (8) were the first to analyze the manner in which the stratified layers form. They concluded that this stratification is the result of the combined influence of electrical and gravitational forces. The migrating colloidal particles are retained by a membrane, with consequent concentration on its surface, on which a very thin concentrated layer is formed. This layer is now subjected to the influence of gravitational forces and tends to move up or down along the surface of the membrane, in accordance with the relative density with respect to that of the surrounding liquid. There is also a corresponding reduction in the concentration of the dispersion at the opposite membrane surface, resulting in a flow of extremely dilute dispersions in the opposite direction. In this manner dispersions of different concentrations spread out above and below the original cell liquid and the horizontal layers can be removed by decantation.

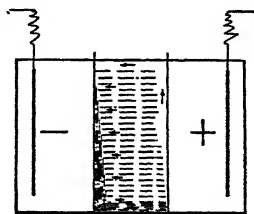


FIG. 3

The Illustration of Electrostratification by Blank and Valko

A proof of the correctness of this analysis, in which the function of the membranes is clarified, is furnished by the experiments of Verwey and Kruyt (9).

Convincing information on the formation of these layers and their behavior on the membranes can be obtained by visual observation of an

illuminated membrane surface under carefully selected conditions, which may be specified as follows.

The dispersion used was prepared from a heavy mineral oil (Bayol XX of the Standard Oil Company) which has been colored black by dissolving Sudan BTN (General Dyestuff Corporation) in the oil. The water dispersion was obtained with 2% ammonia solution using 4% ammonium oleate as emulsifying agent. The dispersion was diluted to a volume fraction of 0.1, and placed in the apparatus shown in Fig. 4. The electrode cells were filled with a 2% ammonia solution. Considerable distance is left between the electrodes and membranes. Hence, all changes on the membranes can be easily seen when the membranes are well illuminated.

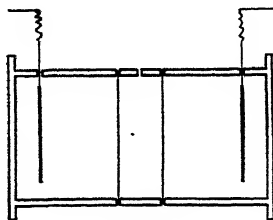


FIG. 4

Cell for Visual Observation of the Membranes

When the membrane toward which the particles migrate was observed it appeared gray. When an electrical field of 0.3 volt/cm. was applied, the gray shade became somewhat deeper but remained unchanged during the experiment. The separation into two superimposed layers which collected at the bottom and top of the cell could be observed in 10–20 minutes. However, when the intensity of the field was increased to 2 volt/cm., the same membrane within two minutes appeared black, indicating deposition on the membrane, and the black color gradually deepened.

This behavior may be explained thus: When 0.3 volt/cm. was applied the concentrated layer which formed moved upward continuously in accordance with Blank and Valko's view. A deposit formed however, when a field strength of 2 volt/cm. was applied, which demonstrates the fact that the separation process takes place undisturbed only under certain conditions.

To remove or refloat such a deposited layer from the membrane, reversal of the current flow had to be instituted. Shortly after such a reversal in the above experiment, the black color on the membrane fades and the movement of the boundary layer of the concentrated layer behind the membrane is visible, a picture similar to the raising of a curtain. The commercial application of the process, in the majority of

cases, requires such a periodic reversal of the current as suggested by Pauli and Stamberger (10).

Observing the other membrane from which the particles move away, the following unexpected picture could be seen. Shortly after the electrical field was established formation of drops of the aqueous phase began to appear on the membrane. These drops move slowly downward, flowing together and forming wavelike images similar to those produced by rain drops hitting the window. The intensity of this flow diminishes and after some time again increases. If the unit is tapped with the hand, the intensity of the flow increases. The same picture could be observed when the field strength was 2 volt/cm., except that the flow took place continuously and with greater intensity. It is worth while noting that, instead of a continuous uniform layer sliding down, drops form on the membrane. It is not easily understood how these drops can form in a readily miscible water solution, such as the colloidal dispersion used.

Since both the electrical attraction and gravitational forces are acting the final influence must be considered, *e.g.*, the *migration velocity* of the particles in the electrical field,  $V_e$ , and the *rate of movement* of the layer in the field of gravity,  $V_g$ .

In the first experiment with a weaker electrical field the migration velocity,  $V_e$ , of the particles toward the electrode was lower than the velocity of movement,  $V_g$ , of the layer accumulated on the membrane. In the second experiment  $V_e > V_g$ . While moving in the field of gravity new particles migrate toward, and continue to accumulate on, the membrane. Hence, the thickness of the layer will increase continuously. Furthermore, as long as the particles in this layer are under the influence of the electrical field, they will move closer and closer to each other and, if they are not removed from the membrane, they will coagulate after a certain period. The method for removal of deposited particles from the membranes at will was found to consist in reversal of polarity of the electrodes, when the whole layer will move undisturbed from the membrane and spread out horizontally.

Even with a slight difference in density the velocity of movement of such a concentrated layer in the field of gravity is much higher than the rate of migration toward the electrical pole and, instead of moving and depositing again on the other membrane, a few seconds after inversion of the current it will spread out in a horizontal layer the thickness of which increases rapidly with time.

In considering the motion in the field of gravity, it is evident, that the velocity of the movement  $V_g$  on the membrane will be directly proportional to the hydrostatic lift and inversely proportional to the frictional resistance on the membrane. The hydrostatic lift is determined by the difference between the density of the concentrated layer and that

of the original dispersion. It can be calculated easily from the density of the suspended particles in the dispersion and from the volume fraction of these in the original dispersion and in the concentrated layer. Assuming that the dispersion medium is water with a density of 1:

$$D_2 - D_1 = (F_2 - F_1)d + (F_1 - F_2)$$

where  $F_2$  and  $F_1$  are the volume ratios of the dispersed particles in the concentrated and original dispersion and  $d$  the density of the dispersed particles.  $D_2$  is the density of the layer formed on the membrane and  $D_1$  that of the original dispersion. The frictional resistance will depend on the viscosity of the concentrated layer on the membrane.

The density and hydrostatic lift relationship is linear. The limit for  $F_2$  will vary from dispersion to dispersion, but will seldom be higher than 0.6 to 0.7. Because of the linear increase of hydrostatic lift with concentration a nonadhering layer which will move freely on the surface of the membrane in the field of gravity can only exist as long as the

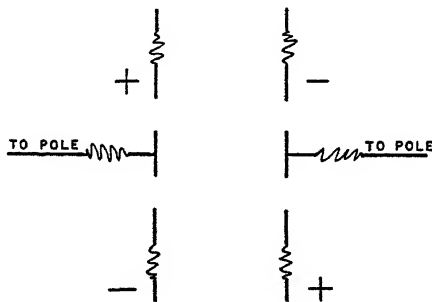


FIG. 5

Diagrammatic Arrangement for Reversing the Current

viscosity-concentration curve of the dispersion does not show great deviation from the linear. However, this condition will be found only with dilute hydrophobic dispersions. In most cases, the working conditions are such that the relationship between viscosity and concentration is exponential. Therefore, in the majority of cases, periodic reversal of the current is essential.

By considering the influence of the concentration on the hydrostatic lift, as well as on the viscosity, the optimum potential difference, as well as the length of the period for reversing the current, can be estimated. Thus, when the density of the particles is high and the viscosity of the dispersion at relatively high concentrations is low, electrical fields of greater strength can be applied and frequently no periodic reversal of electrode polarity is necessary. However, the density of most organic substances is slightly over or under 1 and good results can only be

obtained under carefully selected conditions. The periods selected must be long enough to build up the concentration on the membrane and can vary from a few minutes to half an hour. The rate of movement of such a layer in the field of gravity after reversal of the current will be faster than in the electrical field and stratification is finished before it can move to any distance toward the opposite electrode. For this reason stratified separation will take place, although under similar conditions no separation could be effected by electrophoresis alone. Accumulation of slowly diffusing ions on the membrane, is also prevented under these conditions.

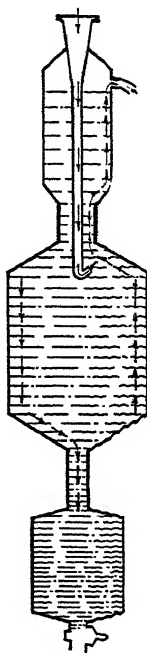


FIG. 6

New Type of Electrodecantation Cell Recommended by Wo. Pauli

Periodic reversal of the current can easily be accomplished mechanically by the use of a timing device or by use of a double-throw double-pole knife switch which can be operated by hand. The arrangement for the circuit for such a simple device is given in Fig. 5.

The conditions under which electrodecantation can be carried out successfully also depend on the concentration of the sol and, frequently, formation of a permanent deposit on the membrane and subsequent coagulation, is observed if the concentrated stratified layer remains in contact with the membrane for a prolonged period of time. Apart from the fact that the concentration of the sol cannot be built up under these



conditions, the surface area of the membrane on which the deposit is formed loses its effectiveness. The same is true for the surface area in contact with the colloid-free layer. Removal of the two layers and continuous replacement of the volume removed with new dispersion is advisable (11). A modification of the working cell for this purpose is recommended by Wo. Pauli (4) and is given in Fig. 6.

The narrower the working cells are, the less time is required for the dispersed particle to reach the membrane. Furthermore, the larger the surface area of the membranes in contact with the dispersion, the greater will be the rate of separation. A practical way to enlarge the surface area of the membranes was proposed by Stamberger and Schmidt (11), who introduced additional diaphragms between the two electrode cells. Thus the separation or stratification takes place in each additional cell and not only in those next to the electrodes. The current consumption, of course, remains unchanged and the economy of the process is much improved. A diagrammatic view of such an arrangement is given in Fig. 7 and a reproduction of a laboratory unit in Fig. 8.\* Both units consist of two electrode cells and a number of working cells.

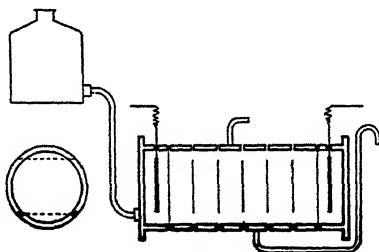


FIG. 7

Unit with Plurality of Membranes for Continuous Work

Such units can be built from two end plates and a number of rings of about 15 mm. width. A convenient material for the construction is a transparent plastic, for example Lucite. Such a unit can be used for continuous operation and can be fed simply by gravity through the walls of the rings, which are assembled in such a manner that a connecting channel is formed from the perforations of the individual rings. The dispersion is evenly distributed into each cell through openings in the rings leading from the perforation to the inside of the cells. The rings for assembling the electrode cells have no such openings and their content does not communicate with the other cells. The cells holding the colloidal dispersion can be interconnected simply by using membranes, the upper and lower segments of which have been cut off. This arrangement makes

\* Courtesy Brosites Machine Company, New York.

it possible to remove the stratified top and bottom layer through central openings. Furthermore, it will prevent the layers remaining in contact with the membranes after stratification.

Suitable material for the membranes are thin sheets of cellulose hydrate (cellophane). The electrodes must be built of noncorrosive material such as platinum or stainless steel.

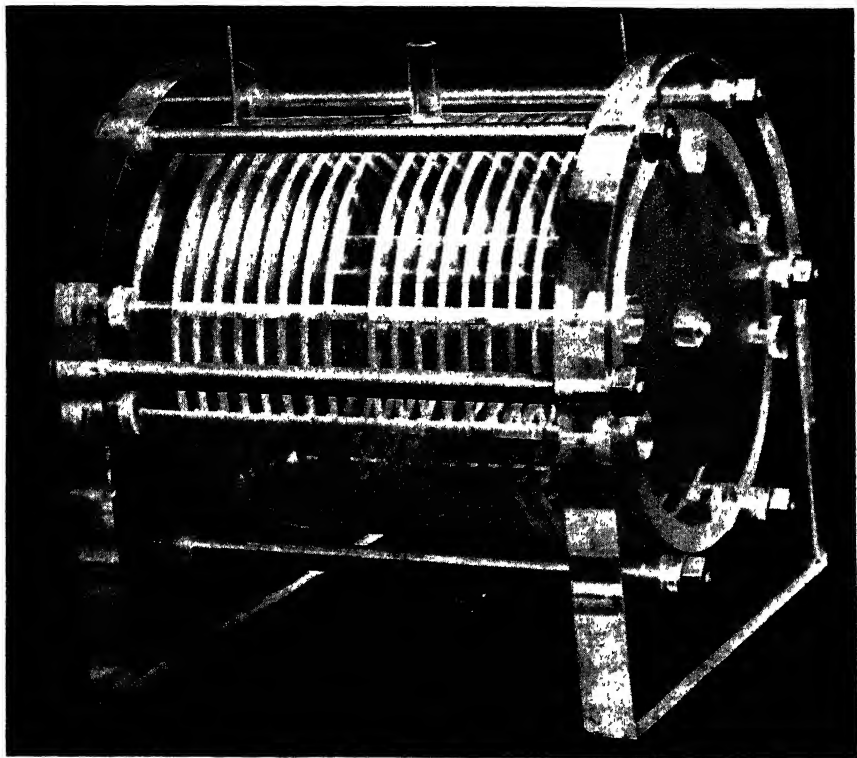


FIG. 8

Laboratory Unit from Lucite

The rate of flow into and from the cells can be regulated by capillaries.

Units for commercial operation are also built using these same principles. A practical commercial unit contains as many as 150 to 200 membranes. To economize further, the membranes must be placed close to each other, the distance being limited only by structural considerations. A unit with 20,000 cm.<sup>2</sup> of membrane surface will produce at a potential gradient of 0.8 volt/cm., 6000 ml. 60% concentrate from a dispersion originally of 30% concentration having a migration velocity of  $3 \times 10^{-6}$  cm./sec. The current consumption is independent of the number of

membranes and is determined only by the cross section of the unit, the electrical resistance of the liquid column between the electrodes and the potential applied. A lower potential will be always more economical. The principles of such units have also been described by Stamberger and Schmidt (11). Commercial experiences obtained with rubber latex have been commented upon by Murphy (12) in a recent publication.

As the process is based on formation and removal of freely flowing liquid layers, the highest concentration obtainable is limited. All substances which have any effect on the flow properties of the dispersion will greatly influence the properties of the concentrated layer. Addition of substances which decrease the viscosity of the concentrated colloidal dispersion is advantageous.

On concentrating to a high solid content it is found that the layer formed on the membrane has a tendency to adhere to it and ultimately form a permanent deposit. The addition of colloidal electrolytes or similar substances is recommended by Stamberger (13) to overcome the tendency for such deposition on the membrane. Membranes covered with a deposited, even, uncoagulated layer lose their effectiveness and must be cleaned. Colloidal electrolytes accumulate on the surface of the membranes, and these large ions form an ionic atmosphere increasing the charge on the surface, and its repulsion of the colloid having the same charge, thus preventing permanent adhesion.

The energy consumption of a commercial unit is relatively low. For example, to concentrate a natural rubber latex of 35% to 60% only 20 to 60 watt hours are needed (depending on the unit) to yield 1 lb. of rubber in a 60% concentrate. Therefore, it compares favorably even with evaporation.

### CONCLUSIONS

The electrodecantation process has advantages but naturally it also has limitations. Dispersions containing small particles can be efficiently handled, since the separation is independent of the particle size (depending only on the hydrostatic lift of the concentrated layer). No foaming or other irreversible changes take place, such as frequently occur during evaporation.

The limitations are partly in the stability of the dispersion since those of low stability show a tendency to coagulate on the membranes. A further limitation is the conductance of the system. Dispersions of high conductance will not only cause large consumption of electrical current but will also produce unwanted secondary effects, such as heating and electrolytic decomposition at the electrodes. In this latter case, previous dialysis of the dispersion can be recommended.

Our knowledge of the phenomena of electrostratification is still very limited. No investigation on the processes which take place on the membranes has been carried out so far. The membranes are in contact on each side with solutions of evidently different ionic concentration. Thus a potential difference must exist which has an effect on the process. No determination of the potential on the membranes has been carried out. It is not known to what distance the particles can approach the surface of the membranes without adhering to them. The properties of the dispersion which will influence the ultimate concentration of the stratified layers are not yet clear. It appears probable that forces similar to those acting to influence the sedimentation volume on simple gravity sedimentation and centrifuging are of importance. Calculations, such as have been made by Kirkwood (14) on fractionation of proteins by electrophoresis, can also be used for electrodecantation.

#### SUMMARY

The presentation of information on the electrostratification phenomenon and examples of its application have been given. It is hoped that further basic information will increase our knowledge of colloidal phenomena as well as extend the applicability of the process.

#### REFERENCES

1. PAULI, W., *Trans. Faraday Soc.* Discussion of Colloidal Electrolytes, p. 19 (1935).
2. PAULI, W., AND NEURATH, H., *Kolloid-Z.* **70**, 125 (1935).
3. PAULI, W., SZPER, J., AND SZPER, S., *Trans. Faraday Soc.* **35**, 1178 (1939).
4. PAULI, W., *Helv. Chim. Acta* **25**, 155 (1942).
5. VERWEY, E. J. W., AND KRUYT, H. R., *Z. phys. Chem.* **167 A**, 149 (1933).
6. SAMEC, M., AND HAERTL, H., *Kolloid-Beihfte* **12**, 281 (1920).
7. SAMEC, M., AND MAYER, A., *Kolloid-Beihfte* **13**, 272 (1921).
8. BLANK, F., AND VALKO, E., *Biochem. Z.* **195**, 220 (1923).
9. VERWEY, E. J. W., AND KRUYT, H. R., *loc. cit.*
10. PAULI, W., AND STAMBERGER, P., U. S. Pat. 2,247,065 (June 24, 1941).
11. STAMBERGER, P., AND SCHMIDT, E., Austrian Pat. 5677/1936, 5678/1936; Brit. Pat. 505,752 and 505,753.
12. MURPHY, E. I., *Trans. Inst. Rubber Ind.* **18**, 173 (1942).
13. STAMBERGER, P., U. S. Pat. 2,375,957 (May 15, 1945).
14. KIRKWOOD, J. G., *J. Chem. Phys.* **9**, 796 (1942).



# STRUCTURE OF SOAP MICELLES AS INDICATED BY X-RAYS AND INTERPRETED BY THE THEORY OF MOLECULAR ORIENTATION

## II. The Solubilization of Hydrocarbons and Other Oils in Aqueous Soap Solutions\*

William D. Harkins, Richard W. Mattoon  
and Myron L. Corrin

*From the Department of Chemistry, University of Chicago, Chicago, Illinois*

*Received October 26, 1945*

### INTRODUCTION

#### *General Structure of Soap Micelles*

In the first paper of this series (1) a soap micelle was pictured as a pile of four, or probably more, double layers of oriented soap molecules, as represented in Fig. 1. These double layers are separated by layers of water and are presumably kept apart by the mutual repulsion of the positive ions (negative with a cationic soap) produced by the ionization of the molecules. Evidently there is an equilibrium between this "bound water" in the micelles and the free water outside, since the water layers thicken as the percentage of water with respect to soap increases. The long or *layer* spacing obtained from the X-ray diffraction has a magnitude  $d_l$  given by the relation:

$$d_l = d_0 + k_1 \log (1/c) \quad (1)$$

in which  $c$  is the fraction of soap present,  $d_0$  in simple cases is close to twice the length of the soap molecule, and  $k_1$  is another constant. A linear equation

$$d_l = b - ac \quad (2)$$

is also valid between 10% and 30% soap.

If an oil is dissolved in the soap solution, the value of  $d_l$  is increased and the new relation for any soap may be written

$$d_l = d_0 + k_1 \log (1/c) + k_0 f_0 \varphi_0 \quad (3)$$

\* The work reported in this paper was done in connection with the Government Research Program on Synthetic Rubber under contract with the Office of Rubber Reserve, Reconstruction Finance Corporation.

in which  $f_o$  is the fugacity of the oil and  $\varphi_o$  varies with its nature. Thus, from the X-ray work alone it is natural to assume that the oil has dissolved between the hydrocarbon layers, *i.e.*, between the hydrocarbon ends of the soap molecules, as shown in Fig. 1. These oil layers are

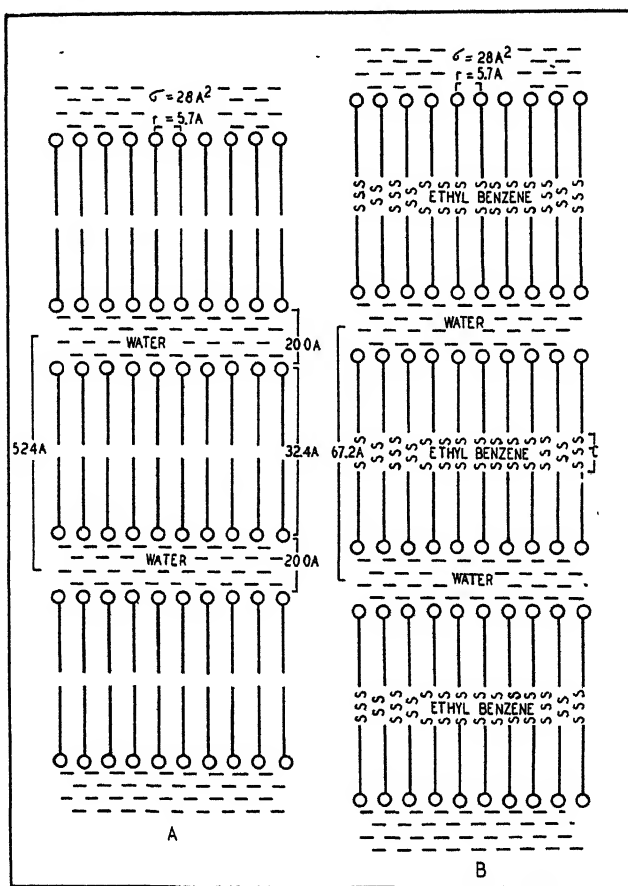


FIG. 1

Idealized Diagrammatic Cross-section of Soap Micelles in  
15% Aqueous Potassium Laurate

- A. Without additive oil. B. Saturated with ethyl benzene. The actual structures are undoubtedly far less ordered. The only spacings actually measured are the long and short spacings

usually produced by the diffusion of molecules from an oil-water interface, covered with a monolayer of soap molecules, into the adjacent micelles.

Now, in Paper I it was shown that over the concentration range from 7.5 to 30% soap in which X-ray measurements were made, the area per

soap molecule is almost constant at 26 to 28  $\text{\AA}^2$  for close packing. Since, however, the layers of soap molecules exhibit a liquid structure in the plane of the layer, a somewhat larger area, 30  $\text{\AA}^2$ , has been assumed as a *mean* value for the calculations given later. At the lowest soap concentrations, 5%, the area (26  $\text{\AA}^2$ ) decreases slightly beyond this with decrease of concentration. It is possible that when the critical concentration is reached this area has become so large that the micelle is no longer stable.

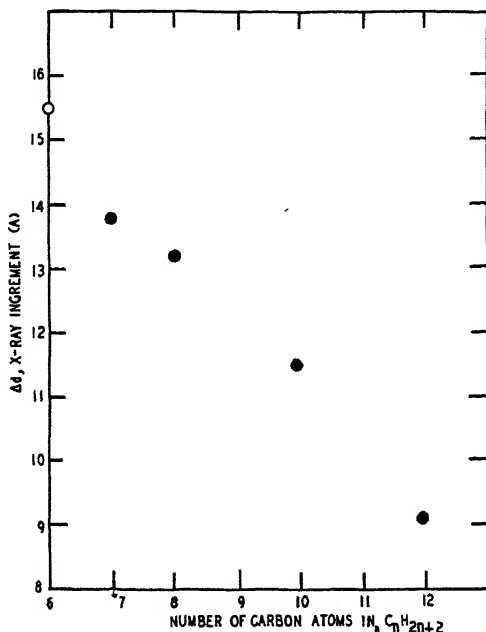


FIG. 2

The Variation in the X-Ray Increment,  $\Delta d$ , in 20% Potassium Laurate Solutions Saturated with Normal Paraffins at Room Temperature with Chain Length of the Paraffin

Each point (with the exception of that for hexane, regarded as preliminary) represents check experiments in which saturation was approached from both sides

In earlier work Kiessig and Philippoff (1) obtained an increase ( $\Delta d$ ) in the layer spacing of 36  $\text{\AA}$  when a potassium oleate solution was saturated with benzene, while in the present work the value found is very much less (15.4  $\text{\AA}$ ) in a solution of potassium laurate.

Although, in the present paper,  $\Delta d$  may in some instances be indicated as the thickness of the oil layer, it should be kept in mind that actually it is merely the increment  $\Delta d$  in the layer spacing produced by the presence of the oil. It is possible that the oil may have an effect on the activity



relations of such a nature that the water spacing is affected, or the oil may have other effects. Thus, the value of  $\Delta d$  may include effects, positive or negative, on the water layer, on the structure of the soap layers, or on the amount of soap in micellar form. Also,  $\Delta d$  is so close to the magnitude of the dimensions of the molecules of the oil that it is at present difficult to see by just what mechanism it is determined. Light on this problem may appear when the effects of molecules of many sizes and shapes have been determined.

The increment ( $\Delta d$ ) in the X-ray layer spacing ( $d_i$ ) due to solution of the oil is one type of "oil spacing" but, in addition, there is another spacing which may be calculated. This, designated by  $\tau$ , is the volume of oil in the micelles divided by the calculated area of the double layers of soap in the micelles. Thus  $\tau$  may be designated as the mean thickness of the oil layer.

Unfortunately, the X-ray layer spacing of the micelles cannot be determined for dilute soap solutions. Thus, all soap solutions for which  $\Delta d$  can be obtained are highly concentrated. The question arises: is the value of  $\tau$  the same as that of  $\Delta d$ ? Now,  $\Delta d$  is directly an experimental, though not a very accurately determined, quantity. However, in order to calculate a mean thickness ( $\tau$ ) of the oil layer from experimental quantities, it is necessary to introduce certain specific assumptions. To what extent these are justified may be learned when a more extensive knowledge of the relations of soap micelles is attained.

The first assumption introduced is that the area of the oil layer (Fig. 1) in the micelles is equal to the area of the double layers of soap in the micelles. For close packing of the soap molecules the area occupied by a soap molecule is from 26 to 28 Å<sup>2</sup>. However, since the structure in the plane of the layer is that of a liquid, the mean area must be slightly larger, and is here assumed to be 30 Å<sup>2</sup>. The second assumption is that all of the micellar soap is in the form of double lamellar layers. This would be inaccurate if other types of micelles also exist.

Since, for the high soap concentrations considered here, almost all of the soap seems to exist in the micellar form, the area ( $\Sigma$ ) of the double soap layers and also of the oil layers should be given approximately by:

$$\Sigma = 30(N/2) \times 10^{-16} \text{ sq. cm.}$$

where  $N$  is the number of soap molecules in the volume or the mass of soap solution considered. Then,

$$\tau = V/\Sigma$$

in which  $V$  is the volume of the oil in the micellar layers (see section VII).

Now, if  $\tau$  and  $\Delta d$  are found to be very different, this might be due to the incorrectness of the assumptions used in the calculation of  $\tau$ , but it

might also be true that the expansion of the micelle with respect to the layer spacing may not be produced wholly by the mean thickness of the oil layer.

## II. Increment ( $\Delta d$ ) in the X-Ray Spacing ( $d$ ) in Saturated Solutions of Normal Paraffins in 20% Potassium Laurate

Fresh 20% solutions of potassium laurate were sealed in glass tubes, together with a slight excess of hydrocarbon under investigation. The hydrocarbons used were normal octane, decane and dodecane. One sample of each oil was shaken for 20 days at 25°C., while another was shaken for 5 days at 50°C., 1 day at 75°C. and then 3 days at 25°C.

TABLE I

*Apparent Layer Thickness of  $n$ -Paraffins Saturated in 20.0% Aqueous Potassium Laurate*

$n$ -Paraffin added in slight excess	Shaken 21 days at 25°C.	Shaken 5 days at 50°C. 1 day at 70°C. 3 days at 25°C.	Centrifuged	Micelle layer spacing $\pm 1$ Å	$\Delta d$ Apparent layer thickness $\pm 1.6$ Å	Mean
0	—	—	—	49.6 $\pm$ 0.6	0	
C <sub>8</sub> H <sub>18</sub>	Yes	No	No	62.3	12.7	13.2
C <sub>8</sub> H <sub>18</sub>	No	Yes	Yes	63.2	13.6	
C <sub>10</sub> H <sub>22</sub>	Yes	No	No	61.5	11.9	11.5
C <sub>10</sub> H <sub>22</sub>	No	Yes	No	60.7	11.1	
C <sub>12</sub> H <sub>26</sub>	Yes	No	No	59.2	9.6	9.1
C <sub>12</sub> H <sub>26</sub>	No	Yes	No	58.5	8.9	
C <sub>12</sub> H <sub>26</sub>	No	Yes	Yes	58.5	8.9	

On the whole, as shown in Table I, there is good agreement between the samples treated according to these two different procedures, *i.e.*, whether equilibrium is approached from below or above saturation. In preliminary work by R. S. Stearns,  $\Delta d$  was found to have the value 13.0 Å for *n*-heptane and 15.5 Å for *n*-hexane. It is apparent that there is, at saturation, a general increase of spacing with decrease in the number of carbon atoms present in the molecule. A rather large experimental error is involved in  $\Delta d$ , since it is obtained by the subtraction of one large number from another of almost the same magnitude.

It is interesting to point out that the addition of 3 g. of potassium laurate to 100 g. of a 25.0% aqueous potassium laurate solution *reduces* the micelle layer spacing from 47.1 to 46.2 Å, or only 0.9 Å; whereas, the addition of 3 g. of *n*-heptane, for instance, *increases* the micelle layer spacing from 47.1 to 58.6 Å, or 11.5 Å.

*III. The Apparent Density and Specific Volume of Heptane Solubilized in Soap Solutions and a Method for the Determination of the Solubility of an Oil in a Soap Solution*

Results of considerable interest have been obtained from measurements of both the apparent density and the X-ray oil spacing ( $\Delta d$ ) of *n*-heptane when solubilized in 25% aqueous solutions of potassium laurate. The soap was prepared by the addition of an excess of alcoholic solution of potassium hydroxide to an alcoholic solution of Eastman lauric acid at about 40°C. The solution was cooled, the potassium laurate filtered off and washed with alcohol. The soap was then recrystallized from alcohol and again from acetone and dried in high vacuum. The heptane was a specially pure sample supplied by the Bureau of Standards. It had been stored over sodium. The density of the heptane as determined by the procedure described below was 0.67981<sub>6</sub> g./cc. at 25°C. compared to 0.67963 as reported in the literature (3). Solutions of potassium laurate were prepared by weight from the dry soap and conductivity water. The samples were prepared by weight on a balance sensitive to better than 0.01 mg. (actually to 0.003 mg. under the best conditions) with weights which had previously been calibrated. All weights were reduced to *vacuo*. The samples were shaken for 18 hours at room temperature with the exception of the sample which contained the highest amount of heptane, for which a period of 40 hours was used.

The densities of both the soap solutions and the systems containing solubilized heptane were determined in pycnometers of about 26 cc. capacity fitted with capillary necks 2 mm. in diameter. The height of the liquid was read to 0.01 mm. with reference to a fixed mark by means of a Geneva cathetometer with the pycnometer immersed in a water bath held at  $25 \pm .005^\circ\text{C}$ . The balance and weights described above were employed. The pycnometer was calibrated with boiled-out conductivity water. The variation in volume was 0.0067757 cc. per 1.00 mm. on the neck.

The volumes of final solutions and those of the soap solutions were calculated from their weight and density. The soap solutions were freshly prepared (less than 8 hours old) for each sample, and the density of each solution was determined. The average density of the soap solutions was  $1.019270 \pm 0.000049$  g./cc. The weight of heptane divided by the difference in volume of the final solution and soap solution is equal to the apparent density.

The increase in volume of a 25% solution of potassium laurate when heptane is dissolved (solubilized) in it is found to be less than the volume of the heptane added except at saturation, where the total volume is equal to that of the soap solution plus the volume of the heptane. This fact

is of interest in its relation to the usual theory of solubilization of oils in soap micelles, according to which the oil is dissolved as a layer between the hydrocarbon ends or "tails" of the soap molecules.

The density of the 25% potassium laurate solution at 25°C. was found to be  $1.019270 \pm 0.000049$  g. per cc., but when 3.56519<sub>4</sub> g. of heptane was dissolved in 100 g. of the soap solution the density decreased to 1.002008<sub>9</sub> (Fig. 3).

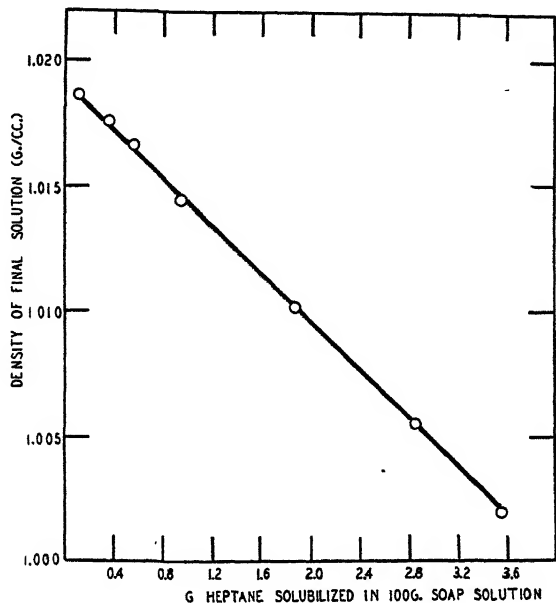


FIG. 3

The Relationship Between the Density at 25.00° C. of 25% Potassium Laurate Solutions Containing Varying Amounts of Solubilized Heptane and the Amount of Solubilized Heptane per Unit Weight of Soap Solution

TABLE II

*Density of Solutions of n-Heptane in 25% Potassium Laurate Solutions at  $25 \pm 0.005^\circ \text{C.}$ , and the Apparent Density of Heptane in the Oil Layers of Soap Micelle*

G. heptane solubilized in 100 g. of 25% $\text{KC}_{12}$	Density of final solution, g./cc.	Apparent density of heptane, g./cc.	Apparent specific volume
0.08449 <sub>7</sub>	1.018832 <sub>7</sub>	0.6944 <sub>4</sub>	1.4400 <sub>1</sub>
0.36108 <sub>9</sub>	1.017569 <sub>3</sub>	0.68843 <sub>4</sub>	1.4525 <sub>7</sub>
0.55460 <sub>1</sub>	1.016626 <sub>8</sub>	0.68798 <sub>3</sub>	1.4535 <sub>2</sub>
0.93761 <sub>0</sub>	1.014432 <sub>4</sub>	0.68595 <sub>8</sub>	1.4578 <sub>2</sub>
1.8632 <sub>8</sub>	1.010160 <sub>6</sub>	0.68402 <sub>0</sub>	1.46194 <sub>5</sub>
2.84955 <sub>2</sub>	1.005487 <sub>3</sub>	0.68180 <sub>2</sub>	1.46670
3.56519 <sub>4</sub>	1.002008 <sub>9</sub>	0.67985 <sub>1</sub>	1.47091
Density of bulk heptane = 0.67981 <sub>8</sub>			1.470986

The apparent densities and specific volumes in the soap solutions of the heptane, presumably almost entirely in the soap micelles, are shown in Table II and in Fig. 4. If it were to be assumed that all of the heptane is present in the oil layers of the soap micelles, then the indication would be that the fitting between the hydrocarbon ends of the soap molecules and the hexane molecules is tighter at all the lower concentrations of

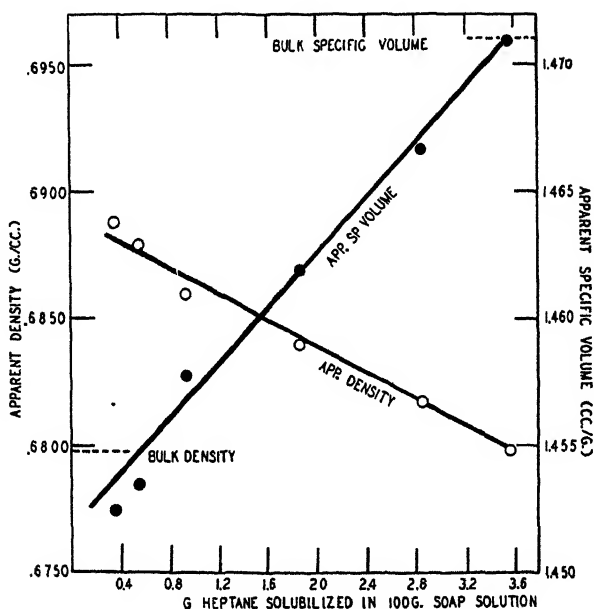


FIG. 4

The Variation of the Apparent Density and Apparent Specific Volume of Solubilized Heptane as a Function of the Amount of Solubilized Heptane per Unit Weight of Soap Solution

These quantities are calculated from experimental volume relationships

hexane but that at saturation the mean fitting gives the same values as if both the soap solution and the heptane preserve exactly their volumes when separate.

Fig. 4 shows that the apparent specific volume of the heptane increases linearly with the amount of heptane solubilized. Whether the function is linear when the amount of oil is extremely small might be determined by the use of a float.

The fact that the apparent density (or the specific volume) of the solubilized oil becomes equal to that of the oil itself at saturation seems to give, whenever this relation holds, the most accurate method as yet found for the determination of the solubility of an oil in a soap solution.

It possesses three great advantages: (1) no analysis for the amount of oil is needed, (2) no determination need be made at saturation, and (3) density measurements are extremely accurate.

The method consists in a determination of the densities of several aqueous solutions of the soap, unsaturated with oil, in which known weights of oil have been dissolved. A plot is then made of the density of these solutions as a function of the amount of oil dissolved (this plot is linear). The solubility is given by extrapolation of the line thus obtained to the value of the density calculated for a solution in which the volumes of soap solution and oil are additive. The concentration at which this is attained is the solubility. It is obvious that some of the concentrations used should correspond to nearly saturated solutions.

The density ( $\rho$ ) of the solutions, water, soap and *n*-heptane, is plotted in Fig. 3 as a function of  $C$ , the weight of heptane solubilized in 100 g. of soap solution. The relation (Fig. 3) is linear as follows:

$$\rho = -0.0048257 C + 1.019192$$

When  $D_A = 0.679816$  (the density of hexane in bulk),  $C = 3.6226$  g. heptane per 100 g. soap solution, which may be taken as the maximum solubilization (solubility). By 40 hours of vigorous shaking a sample of 3.5662 g. was completely dissolved, which is only 0.0564 g. less than the amount calculated. No excess above this was used, and no higher amount was tried. It should be remembered that in direct determinations a large excess of oil is used if it is desired to obtain saturation in any reasonable period.

#### IV. Solubilization of Triptane, 2,2,3-Trimethylbutane

The relation between the apparent density of solubilized triptane and the weight of triptane solubilized per unit weight of 25% potassium laurate solution is completely different from that displayed by heptane. The data, obtained by the same procedure described above for heptane, are given in Table V and plotted in Fig. 5. As with heptane all the samples were shaken for 18 hours with the exception of the final sample (3.7320<sub>99</sub>) g./100 g. soap solution) which was shaken for 40 hours.

A linear relation, obtained by least squares without weighting, holds between  $C$ , the g. of triptane solubilized per 100 g. of soap solution, and  $D_A$ , the apparent density of the solubilized triptane. This relation is

$$D_A = 0.0040522_5 C + 0.6865_4$$

If the density values are weighted, employing a weighting factor proportional to  $C$ , the equation becomes

$$D_A = 0.0041568_9 C + 0.6862_8$$

With the first equation the average deviation is  $\pm .000236$  in the apparent densities with a maximum variation of .000500. With the second equation the average deviation is .000258 with a maximum deviation of .000709.

The maximum possible error, assuming a possible error of 0.02 mg. in each weighing and an error of 0.05 mm. in each cathetometer reading and so combining the resulting errors as to produce a maximum, is

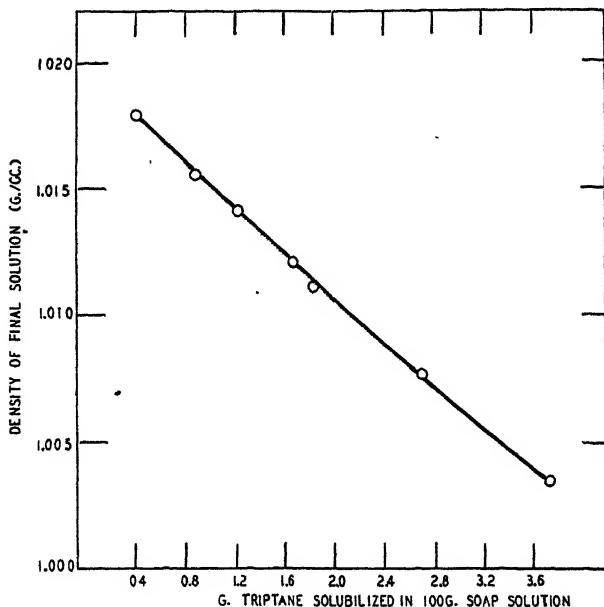


FIG. 5

The Relationship Between the Density at 25.00° C. of 25% Potassium Laurate Solutions Containing Various Amounts of Solubilized Triptane and the Amount of Solubilized Triptane per Unit Weight of Soap Solution

0.30% for the solution containing the least triptane ( $C = 0.40082_9$ ) or  $D_A = .6886_6 \pm .0020_7$ ; 0.038% for the solution containing the most triptane ( $C = 3.7320_{99}$ ) or  $D_A = .7019_8 \pm .0002_7$ .

The extrapolated value of the apparent density for an infinitely dilute solution of triptane in 25% potassium laurate (.6862<sub>8</sub> by the weighted equation) is within experimental error (0.064%) of the bulk density of triptane (.68584<sub>2</sub>). The method employed for the determination of the solubility of heptane in the soap solution cannot be employed with triptane since the apparent density, instead of approaching the bulk value with increasing concentration, actually increases to some unknown value.

When the apparent specific volume of the solubilized triptane is plotted against the weight of triptane solubilized in 100 g. of soap solu-

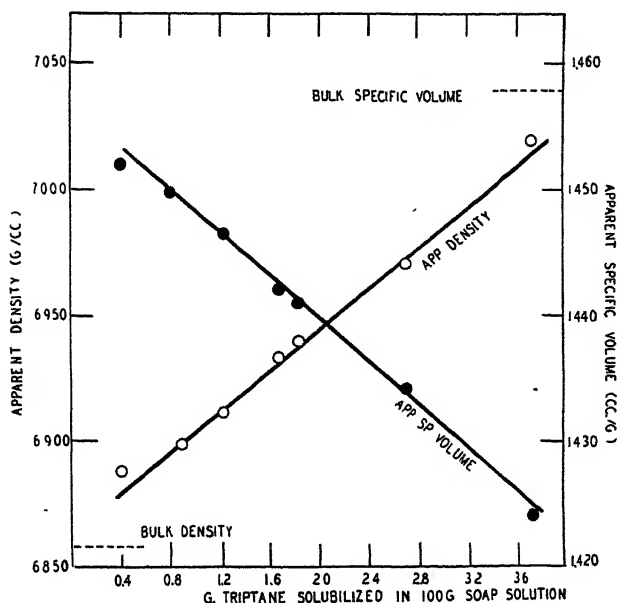


FIG. 6

The Variation of the Apparent Density and Apparent Specific Volume of Solubilized Triptane as a Function of the Amount of Solubilized Triptane per Unit Weight of Soap Solution

These quantities are calculated from experimental volume relationships

TABLE III

The Apparent Density and Apparent Specific Volume of Triptane (2,2,3-Trimethylbutane) Solubilized in 25% Potassium Laurate at 25° C.

C	D	D <sub>A</sub>	V <sub>A</sub>
G. triptane solubilized in 100 g. soap soln.	Density of final solution (g./cc.)	Apparent density of solubilized triptane (g./cc.)	Apparent specific volume of solubilized triptane (cc./g.)
0.40082 <sub>9</sub>	1.01785 <sub>30</sub>	0.6886 <sub>59</sub>	1.452 <sub>10</sub>
0.88658 <sub>5</sub>	1.01554 <sub>35</sub>	0.6898 <sub>70</sub>	1.449 <sub>55</sub>
1.2169 <sub>01</sub>	1.01407 <sub>94</sub>	0.6911 <sub>62</sub>	1.446 <sub>84</sub>
1.6657 <sub>51</sub>	1.01206 <sub>04</sub>	0.6933 <sub>47</sub>	1.442 <sub>28</sub>
1.8262 <sub>89</sub>	1.01126 <sub>38</sub>	0.6939 <sub>76</sub>	1.440 <sub>97</sub>
2.7024 <sub>83</sub>	1.00765 <sub>94</sub>	0.6971 <sub>21</sub>	1.434 <sub>47</sub>
3.7320 <sub>99</sub>	1.00345 <sub>26</sub>	0.7019 <sub>81</sub>	1.424 <sub>54</sub>

Density of triptane at 25°C = 0.68584<sub>2</sub> g./cc.

The maximum possible error in the apparent density of the first solution ( $C = 0.40082_9$ ) is  $\pm 0.3\%$ , i.e.,  $D_A = .6886_{59} \pm .0020_{65}$ .

The maximum possible error in the apparent density of the final solution ( $C = 3.7320_{99}$ ) is  $\pm 0.038\%$ , i.e.,  $D_A = .7019_{81} \pm .0002_{67}$ .



tion (Fig. 6) another apparently linear relation results, described by the following equation (by least squares and weighted with respect to  $C$ ):

$$V_A = -0.0085735_8 C + 1.456877_1$$

with an average deviation of .000526 and a maximum deviation of .00134. The relations between  $C$  and  $D_A$  and  $V_A$  cannot both be linear, but it is impossible to decide on the basis of the available data which is linear, if either one is actually linear. The extrapolated value of the specific volume at infinite dilution, 1.456877<sub>1</sub> cc./g., agrees well with the bulk value, 1.45806<sub>2</sub>.

*V. X-Ray Increments ( $\Delta d$ ) for Undersaturated Solutions of  
n-Heptane in 25% Potassium Laurate*

It is found that the value of the X-ray increment ( $\Delta d$ ) of microlayers of *n*-heptane in micelles of potassium laurate is, below saturation, a linear function of the amount of oil added and increases to 13.85 Å at a concentration of 3.6226% of heptane at saturation in the 25% solution of potassium laurate used. The values of  $\Delta d$  are given in Table IV and Fig. 7. The value of  $\Delta d$  is given by the relation:

$$\Delta d = 3.82 C$$

if  $\Delta d$  is in Å and  $C$  in g. heptane per 100 g. soap plus water.

TABLE IV

*X-Ray Increments ( $\Delta d$ ) of Undersaturated and Saturated Solutions of n-Heptane in 25%  
Aqueous Solution of Potassium Laurate at Room Temperature*

G. <i>n</i> -heptane solubilized in 100 g. of 25.00% aqueous potassium laurate	$d$ , micelle layer spacing, Å	$\Delta d$ , in Å
0	47.1*	0
0.08449 <sub>7</sub>	47.6	0.5
0.36108 <sub>9</sub>	48.1	1.0
0.55460 <sub>1</sub>	49.1	2.0
0.93761 <sub>0</sub>	50.7	3.6
1.27 <sub>5</sub>	52.5	5.4
1.8632 <sub>8</sub>	54.4	7.3
2.84955 <sub>2</sub>	57.7	10.6
3.56519 <sub>4</sub> †	60.8	13.7
3.6226†	—	13.85§

\* Three separate exposures each gave  $47.1 \pm 0.5$  Å.

† All solutions were water-clear except this one which was very slightly turbid.

‡ Saturation, calculated from density equation.

§ Saturation thickness, calculated from  $\Delta d = 3.82 C$  (Fig. 7).

VI. *The Increase in Layer Spacing of Soap Due to Triptane*  
*(2,2,3-Trimethylbutane)*

Work similar to that on *n*-heptane was carried out using a very pure sample of triptane, an isomer of *n*-heptane. The values of the increment,  $\Delta d$  in the layer spacing, for various weights,  $C$ , in g. of triptane solubilized in 100 g. of 25.00% aqueous potassium laurate solution are given in

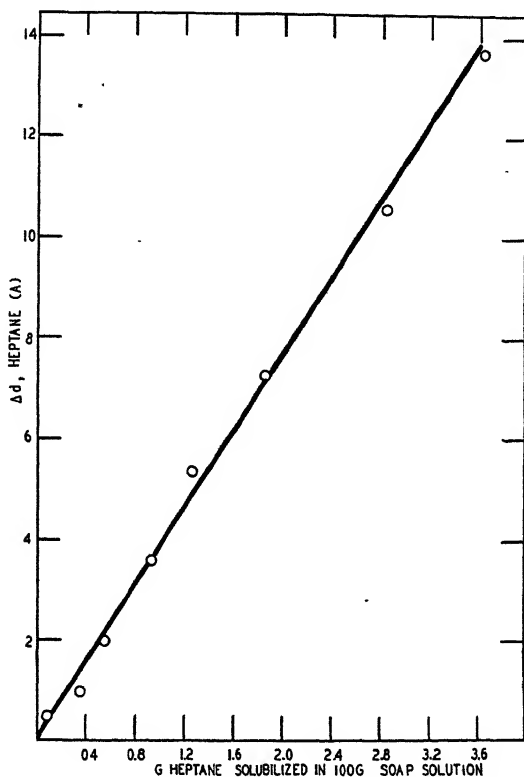


FIG. 7

Linear Relationship Between  $\Delta d$ , the X-Ray Increment, and the Weight of *n*-Heptane Solubilized per Unit Weight of Soap Solution

Table V and plotted in Fig. 8. As more triptane is solubilized, the intensity of the X-ray diffraction increases. All solutions X-rayed were clear, not turbid. By the method of least squares applied to the eight points of Fig. 8, the linear relationship between  $\Delta d$  and  $C$  was found to be

$$\Delta d = 0.154 + 3.87 C$$

(Ideally the line should go through the origin.)

TABLE V  
*Apparent Layer Thickness of Solubilized Triptane*

<i>C</i> G. triptane solubilized in 100 g. of 25.00% aqueous potassium laurate at 25°C.	<i>d</i> Micelle layer spacing, $\pm 1.0$ Å	$\Delta d$ Apparent triptane layer thickness $\pm 1.5$ Å
0	47.1 $\pm$ 0.5	0
0.48	49.6	2.5
1.22	51.8	4.7
1.45	52.5	5.4
1.67	53.0	5.9
1.83	54.3	7.2
2.69	58.5	11.4
2.70	57.7	10.6
3.47	60.7	13.6

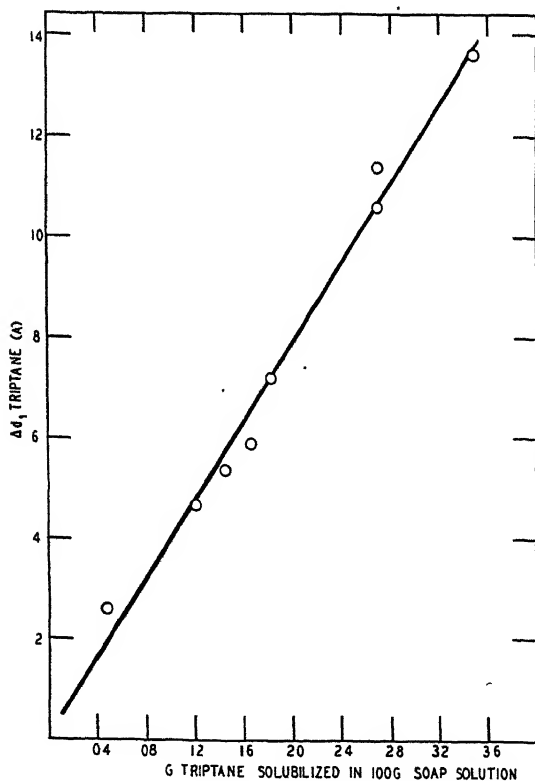


FIG. 8

Linear Relationship Between  $\Delta d$ , the X-Ray Increment, and the Weight of Triptane Solubilized per Unit Weight of Soap Solution

VII. Ratio of  $\tau$  to  $\Delta d$  for Undersaturated Solutions of *n*-Heptane and of Triptane in 25% Potassium Laurate

The values of the ratio  $\tau/\Delta d$  for solutions of *n*-heptane and triptane in a 25% solution of potassium laurate are given in Table VI. The values of the ratio are 0.405 and 0.384, respectively. It may be noted that the ratio increases slowly with concentration.

TABLE VI

A. Ratio of  $\tau$  to  $\Delta d$  for *n*-Heptane in 25% Solution of Potassium Laurate at 25°C.

(30 Å<sup>2</sup> taken as area per soap molecule in A, B, C.)

Soap area =  $94.95 \times 10^{22}$  Å<sup>2</sup>

$\Delta d = 3.82$  C

C = g. heptane/100 g. soap solution

C	$\tau$	$\Delta d$	$\tau/\Delta d$
.08449 <sub>7</sub>	.1281	.323	.396
.36108 <sub>9</sub>	.5521	1.379	.400
.55460 <sub>1</sub>	.8489	2.118	.401
.93761 <sub>0</sub>	1.439	3.581	.402
1.8632 <sub>6</sub>	2.869	7.118	.403
2.84955 <sub>2</sub>	4.402	10.885	.404
3.56519	5.522	13.619	.405

B. For Triptane in 25% Solution of Potassium Laurate at 25°C.

$\Delta d = 0.154 + 3.87$  C

.40082 <sub>6</sub>	.613	1.705	.360
.88658 <sub>5</sub>	1.353	3.585	.377
1.21690 <sub>1</sub>	1.854	4.863	.381
1.6657 <sub>61</sub>	2.530	6.600	.383
1.8262 <sub>89</sub>	2.772	7.222	.384
2.7024 <sub>63</sub>	4.083	10.613	.385
3.7320 <sub>99</sub>	5.599	14.597	.384

C. Ethyl Benzene in 15% Potassium Laurate at 25°C. (for comparison)

2.88	5.83	14.5	.402
------	------	------	------

The solubilization value, 2.88 g. ethyl benzene per 100 g. of 25% solution potassium laurate, was obtained by a turbidimetric technic to be described by Heller and Klevens.

VIII. Solubility of Styrene

Whenever an attempt was made to determine the X-ray oil spacing for styrene without the presence of an antioxidant, it was found that good agreement was not obtained in duplicate experiments, as the X-rays, even at room temperature, seem to catalyze the reaction of styrene to polystyrene. However, with 0.784 mole of soap, equimolar with respect to potassium laurate and myristate, per 1000 g. of solution,  $\Delta d$  was found as 16 Å for an oil which was a mixture of 75% isoprene and 25% styrene. This mixture does not initially polymerize as readily as styrene.

While styrene, when it does not polymerize, gives a layer spacing of about 15 Å, it was reported \* on June 6, 1944 that three identical solutions in 16.7% aqueous potassium laurate when rotated for 4, 14 and 24 hours gave oil spacings of 10.5, 3.2 and 1.5 Å respectively, while polymer appeared in the aqueous phase outside the micelles. When allowance is made for the amount of soap adsorbed by the polymer it was found that all of the styrene had disappeared from the micelles of the sample shaken 24 hours. This shows that the polymer formed segregates from the micelles. Many experiments have shown that it is difficult, or impossible, to get large molecules into micelles. Lauryl mercaptan in 16.7% potassium laurate gave a much larger layer spacing after shaking 4 hours than after 8 hours, while a blue color, possibly denoting the escape of dilauryl disulfide formed in this way into the water, is developed in the latter solution but not in the former.

### *IX. Laurylamine Hydrochloride and Aerosol AY*

A 14.9% aqueous solution of laurylamine hydrochloride gave a micelle layer spacing of 69.9 Å and a 9.7% solution, 96.2 Å. This indicates that the water layer is unusually thick for a molecule of its length, which is much the same as that of potassium laurate. The results show also that the thickness of the water layer changes with concentration even more rapidly than with sodium oleate.

A certain weight of the 9.7% solution was shaken with the same weight of lauryl mercaptan for 4 hours and then centrifuged for 15 minutes at 25,000 *g*. The lowest phase gave a layer spacing of 107.3 Å, so the apparent thickness of the lauryl mercaptan layer was  $107.3 - 96.2 = 11.1$  Å.

A 20% solution of Aerosol AY gave a very weak, broad diffraction with a spacing of 23 Å for the maximum of the diffraction pattern and 19 Å and 29 Å for the two edges of the diffraction. This indicates the presence of thin micelles with considerable disorder in such an Aerosol AY solution.

\* In reports of March 19 and 20, 1943, and in several later reports during the same year, it was shown that the principal initial locus of the polymerization reaction, when soap is present, is in the soap micelles and that the polymer particles thus formed, when they escape from the micelles, become the locus in which most of the polymer is formed. The polymer particles which escape are extremely small, much less than 100 Å in diameter, and, therefore, adsorb a considerable amount of soap from the micelles on their surfaces. The micellar material which is left, however, dissolves more monomer and thus the micelles continue, on a reduced scale, as a locus for the initiation of polymer particles.

Hughes, Sawyer and Vinograd, *J. Chem. Phys.* **13**, 131 (1945), found that solubilized styrene can be polymerized, but Vinograd and associates (Meeting of Am. Chem. Soc., Sept. 13, 1944) considered that the further course of the reaction is in the aqueous phase, while we consider it to be in the polymer-monomer particles (polymer phase).

*X. Diffraction from Aqueous Potassium Laurate with Nearly Spherical Molecules Solubilized*

Preliminary experiments have been made with a 15.0% aqueous potassium laurate solution, presumably undersaturated with nearly spherical oil molecules (tetrahedral symmetry), to determine the type of spectrum involved. Each solution with the "oil" added in excess was shaken vigorously at room temperature for 4 hours and then centrifuged 10 min. at 5000 *g* (except where noted). The aqueous phase was removed and X-rayed.

The X-ray diffraction from this soap solution with nearly spherical molecules solubilized differs from that with long linear molecules, *e.g.*, lauryl mercaptan, or flat molecules, *e.g.*, benzene, in two respects, as shown in Table VII:

TABLE VII

*Diffraction from Aqueous Potassium Laurate with Nearly Spherical Molecules Solubilized*

"Oil" added	$d_l$ Long layer spacing $\pm 1$ Å	Intensity	$\Delta d = d - 54.2$ Apparent "oil" layer thickness $\pm 2$ Å	$d_i$ Range for intermediate weak band	$d_s$ Range for short side spacing Å	$\sigma$ Range for equivalent molecular area, Å <sup>2</sup>
None	54.2	Strong	0.0	None	4.65 to 4.75	28.4 to 29.5
(C <sub>2</sub> H <sub>5</sub> ) <sub>4</sub> Pb	57.6	Weak	3.4	20.0 to 25.6	4.3 to 9.0	24.6 to 107
CCl <sub>4</sub>	58.4	Weak	4.2	21.0 to 25.4		
CHCl <sub>3</sub> *	54.0	Weak	-0.2	33.1 to 38.5	4.6 to 8.3	27.5 to 90
CH <sub>2</sub> Cl <sub>2</sub> *	53.8	Medium	-0.4	31.6 to 34.5	4.6 to 8.3	27.5 to 90

\* Not centrifuged

1. A new, intermediate, weak, broad, diffraction band appears, designated as  $d_i$ . This cannot be the second order of the regular long layer spacing diffraction,  $d_l$ .

2. The regular short side spacing diffraction,  $d_s$ , is broadened toward larger spacings. The fact that the apparent "oil" layer thickness,  $\Delta d$ , is so low and the side spacing,  $d_s$ , extends to larger values suggests that these nearly spherical molecules may accommodate themselves to some extent *between* the soap molecules of the soap layers in the micelles. More work is necessary for explanation of these effects. A 10-hour exposure on the fastest Eastman Type K film was necessary for the  $d_i$  and  $d_s$  diffractions.

*XI. Oil Layer Spacing and Molecular Volume*

While the X-ray increment,  $\Delta d$ , of the normal paraffins at saturation decreases rapidly with the length of the chain and thus with the volume

of the molecule, it is evident that this is due to the concomitant decrease of solubility. However, if the solution is not saturated and equimolar solutions of the oil are considered, it is to be expected that  $\Delta d$  should be proportional to the volume of the molecule. Thus, in the relation:

$$\Delta d = k \frac{\text{moles oil}}{\text{moles soap}}, \quad (1)$$

$k$  should be a constant for any one species of molecules but should vary as the molecular volume. The values for

$$\frac{\Delta d}{\text{moles oil/moles soap}} = k \quad (2)$$

for ethyl benzene and *n*-heptane were found to be 34 Å in 15% soap and 40 Å in 25% soap, while the molar volumes are 134 cm.<sup>3</sup> and 146 cm.<sup>3</sup> The dependence of  $k$  on soap concentration is not, as yet, known.

Equation (1) or (2) is found to express the relations for a single oil dissolved in a specific soap solution when the amount of oil dissolved is varied. The ratio of  $\tau$  to  $\Delta d$  seems to be essentially constant for a specific oil in a soap solution of a definite concentration, so these equations, but with a smaller value of  $k$ , are probably valid if  $\tau$  is substituted for  $\Delta d$ , except when the fraction of oil dissolved is very small.

## DISCUSSION

In this paper the model assumed for a soap micelle is that presented in 1937 by Hess and Gundersman (4) on the basis of measurements of X-ray spacings as interpreted by the theory of molecular orientation at interfaces. Prior to this the micelle was often considered to be a spherical aggregation of oriented molecules, as in the theory of Hartley (5), while McBain assumes the concomitant existence of different types of structure (6).

Even up to the present time, no one has been able to reconcile all of the known properties of soap solutions with any model, although a very great amount of attention has been given to this problem. The present paper adds to the knowledge of the subject but introduces a further complexity in the strange relations revealed in the ratio of the mean thickness ( $\tau$ ) of the oil layer, to the increment ( $\Delta d$ ) of the layer spacing caused by the oil as measured by X-ray.

In all cases the calculated mean thickness ( $\tau$ ) calculated from the volume of the oil is much smaller than the increment in the layer spacing ( $\Delta d$ ).

In the calculation of  $\tau$  it is assumed that the total area ( $\Sigma$ ) of the double layers of the micelles and therefore of the oil layer itself is not

greatly varied by the solubilization of the oil. It is difficult at present to see, on the basis of the model assumed, how the expansion ( $\Delta d$ ) of the micelle can be as high as over twice that which corresponds to the volume of oil added. The experiments with *n*-heptane show that the volume relations of soap solution and oil are nearly additive.

The deviations, except for the halogen compounds, are in the wrong direction to be explained by the assumption that a part of the oil is dissolved between the sides of the hydrocarbon chains instead of their ends. In addition, the value of the chain area (26 to 28 Å) is not increased by any of the following oils: ethylbenzene, styrene, benzene, *n*-hydrocarbons and lauryl mercaptan. It is only with spherical molecules of the type of tetraethyl lead that the side spacing has been found to be affected.

#### *Ejection of Large Molecules from the Oil Layers of Soap Micelles*

The work on solubilization reported in this paper has been incidental to researches related to "A General Theory of the Reaction Loci in Emulsion Polymerization" (*J. Chem. Phys.* 13, 381 (1945); also, January, 1946). Before this work was begun, the idea had been developed by Harkins, on the basis of work by Jordan and Ewing of the United States Rubber Company, that a monomer in the oil layer of a soap micelle undergoes polymerization and that the polymer molecules thus formed are ejected into the aqueous phase where they become loci for further polymerization.

Very soon after the experimental work of the project had begun, several lines of evidence indicated that this point of view is correct. In experiments by surface tension and other methods by Dr. Bernard Adinoff and others, it was found that almost all of the polymer particles produced in emulsion polymerization are formed while soap micelles are present and that relatively few are formed when they are absent. If polymerization is started with 3% of soap, practically all the micelles have disappeared by the time the yield of polymer attains a value of 12 to 13%. The disappearance of micelles is due to the fact that the polymer particles are extremely small and thus have a large interfacial area in comparison with the total volume of polymer.

Now, each polymer particle contains monomer obtained by diffusion from monomer droplets into the polymer particles. Each polymer-monomer particle is surrounded by a monomolecular layer of soap molecules with their polar groups oriented toward the water and the non-polar hydrocarbon groups oriented toward the polymer-monomer particle. Thus, the soap changes rapidly from the micellar to the adsorbed form. The evidence for the above relations cannot be presented here but will be given in an extensive paper on the relations of the polymerization reaction.



Numerous experiments were carried out with no monomer present except that which was solubilized and, therefore, almost wholly in the micellar oil layers.

In an interesting set of experiments of this type by R. S. Stearns 0.75 g. of styrene per 100 g. of solution was dissolved in potassium laurate solutions of soap concentrations from 6% to 21%. The styrene was completely solubilized. After complete polymerization the latex particles were so small that the solutions seemed almost completely transparent, and exhibited only a very slight scattering of light. The particles were also so small that no determination of their size could be made by the optical method in general use in this laboratory. A comparison with solutions in which the particle diameter is about 100 Å suggested that they are very much smaller than this (probably not over about 25 Å).

In this set of experiments the styrene was almost entirely present in the micellar oil layers of a mean thickness less than that of a molecule. However, at a soap concentration of 0.2%, which is below the critical concentration for micelles, the same amount of monomer gave an *excessively* turbid, *non-transparent* latex, as was also the case when no soap was present.

A few typical experiments of this type are described below. In a very large number of experiments it was found that the value of  $\Delta d$  for styrene or for a styrene-isoprene mixture is much smaller after long exposure to X-rays in the absence of an inhibitor of polymerization than when a very small quantity of inhibitor is present. This seems to indicate that the polymer molecules formed by X-ray irradiation escape from the micelles. It might be thought that the larger oil spacing was due to the inhibitor, but (1) the amount of inhibitor was small and (2) in the presence of ten times more inhibitor the value of  $\Delta d$  for ethylbenzene gave no indication of an increase.

In another type of experiment the value of  $\Delta d$  produced by styrene was entirely normal but on polymerization the spacing, when proper corrections were introduced, was found to be that of the soap alone, thus showing that the polystyrene produced had been spewed out by the micelle. On shaking this solution with ethylbenzene the long spacing was increased by 14 Å and with styrene by 16 Å above the long spacing of the soap.

Thus, micelles which have been utilized as loci for the formation of polymer may be used over and over again as the reaction proceeds, so that the soap micelles would continue as loci through the entire course of the polymerization reaction, if it were not for a factor introduced by the polymer particles formed. These contain monomer and the polymer-monomer particles adsorb a monolayer of soap. Thus, soap present in the micelles changes into adsorbed soap. This causes the disappearance of the

micelles at some yield of polymer, which, with the standard formula, appears to be below 20%.

Much more striking results are obtained with higher concentrations of soap, for example, with the 0.784 mole of soap, equimolar in potassium laurate and potassium myristate, per 1000 g. of soap solution, the initial long spacing with the soap alone was 58.4 Å. On shaking this with styrene at 25°C., the spacing increased to 74.4 Å. This indicates an oil layer spacing of 16.0 Å, which is a relatively thick layer of oil. On polymerization the long spacing was reduced to 60.7 Å. Thus, from this measurement alone it might be considered that the thickness of the oil spacing decreases from 16.0 to 2.3 Å.

However, when a calculation is made for the decrease in concentration of the soap solution by adsorption on the latex particles which are formed, it is found that, within the limits of error of experimental work, the initial oil spacing of 16 Å *has completely disappeared*.

Experiments of this type demonstrate that the oil layers of the micelles constitute the locus in which polymer particles are initiated but that the particles thus formed are not small enough to be able to remain in the micellar structure. However, the particles of polymer produced in this way are found to be extremely small after they appear in the aqueous phase. In a private communication McBain and Richards state that large molecules do not dissolve in micelles, but they do not designate what they consider as large. In this laboratory experiments by Corrin and Klevens indicate that pinacyanol of molecular weight 388 is solubilized in micelles of potassium laurate, although the concentration in the solution which they used was exceedingly small.\* It is possible that the slight solubilization of pinacyanol is due to the fact that its molecule is flat.

Discussion of relations presented in this paper is reserved until a considerable amount of other work now in progress is completed.

#### SUMMARY

1. The lamellar micelles formed by oriented double layers of soap molecules in water (Fig. 1) "solubilize" a layer of oil between the hydrocarbon ends of soap molecules in adjacent single layers of soap. The thickness ( $d_l$ ) of a double layer of soap and a single water layer, as determined by X-rays, may be considered to be given by the relation

$$d_l = d_0 + k \log (1/c)$$

in which  $c$  is the fraction of soap in the solution. In a solution saturated with  $n$ -dodecane in 20% potassium laurate at 25°C.,  $d_l$  is increased by

\* See Sheppard, S. E., and Geddes, A. L., *J. Chem. Phys.* **13**, 63 (1945). They used aqueous solutions of cetyl pyridinium chloride and found evidence for the solubilization of a minute amount of pinacyanol.

$\Delta d = 9$  Å, while with *n*-heptane and triptane in 25% potassium laurate  $\Delta d$  is 13.8 Å and 14.7 Å, respectively (triptane is the more soluble), and with *n*-hexane and *n*-pentane in 15% potassium laurate increasingly larger. Thus, at saturation with oil,  $\Delta d$  increases rapidly with decrease in length of the molecule of the solubilized oil.

2. For undersaturated and saturated solutions of *n*-heptane  $\Delta d = 0 + 3.82 C$  and for its isomer, triptane,  $\Delta d = 0.15 + 3.87 C$ , or the same within the limits of experimental error.

3. The area per soap molecule in the *layer* of soap is found to be 26–28 Å<sup>2</sup> (or constant within the limits of error) for close packing and independent of whether a solubilized hydrocarbon layer is present. However, the actual packing is shown by the X-ray diffraction to be that of a liquid, which gives a slightly larger area, which for purposes of calculation has been rounded off to 30 Å<sup>2</sup>.

4. Assuming the mean area of 30 Å<sup>2</sup> and that the total area ( $\Sigma$ ) of the double soap layers is given by  $\Sigma = 30 \times 10^{-16}(N/2)$  cm.<sup>2</sup>, where  $N$  is the total number of soap molecules present, a quantity  $\tau$ , a mean apparent thickness of the oil layer, is obtained. For *n*-heptane in 25% potassium laurate solution  $\tau$  is 40% of  $\Delta d$ , for triptane  $\tau/\Delta d$  is about 0.38, and for 2.9% ethyl benzene in 15% potassium laurate, 0.4. No explanation of this will be offered until other work now in progress is completed.

5. The apparent specific volume of 0.08% *n*-heptane solubilized at 25°C. in 25% potassium laurate is 1.4400, while with a saturated solution it is 1.470986, or practically the same as for *n*-heptane in bulk. With triptane, however, the reverse is true: the thickest layer departs most from the specific volume of the liquid, while this is approached as the layer gets thinner.

6. Monomer layers with  $\Delta d$  as high as 16 Å (75% isoprene and 25% styrene constituted the monomer layers in this particular case) were found to have this decrease to zero when polymerized by the action of a catalyst, and to exhibit a considerable decrease by the action of X-rays. This shows that the polymer molecules cannot be held by soap micelles. Thus, molecules may be too large to be held by micelles.

#### REFERENCES

1. HARKINS, W. D., MATTOON, R. W., AND CORRIN, M. L., *J. Am. Chem. Soc.* **68**, January, (1946).
2. KIESSIG, H., AND PHILIPPOFF, W., *Naturwissenschaften* **27**, 593 (1939).
3. SHEPARD, HENNE AND MIDGLEY, *J. Am. Chem. Soc.* **53**, 1948 (1931).
4. HESS, K., AND GUNDERMAN, J., *Ber.* **70**, 1800 (1937).
5. HARTLEY, J. S., *Aqueous Solutions of Paraffin Chain Salts*, Hermann et Cie., Paris (1936).
6. MCBAIN, J. W., *Trans. Faraday Soc.* **9**, 99 (1913), and many later papers.

# PHYSICAL-CHEMICAL PROPERTIES OF SOLUTIONS OF THE COLLOIDAL ELECTROLYTE HEXANOLAMINE OLEATE

Emanuel Gonick and James W. McBain

*From the Department of Chemistry, Stanford University, California*

*Received December 20, 1945*

## INTRODUCTION

No single kind of physico-chemical measurement alone can yield adequate characterization of the constitution of colloidal electrolytes. Only the combination of several kinds of measurement can lead to a satisfactory knowledge of this important class of compounds. This paper presents results of several different types of measurements made on aqueous solutions of hexanolamine oleate (the 4-methyl, 4-aminopentanol-2 salt of oleic acid) over a wide range of concentrations. Hexanolamine oleate differs from the ordinary soaps in that the monatomic cation has been replaced by a fairly large organic ion of complex structure, which is, however, of itself non-colloidal, as shown by the fact that aqueous solutions of the hydrochloride and of the free amine, 1.025  $N_w$  and 1.902  $N_w$ , respectively, give normal freezing point depressions (3.873° and 3.673°).

The phase diagram of the system hexanolamine oleate-water has already been communicated (1).

At room temperature, solutions containing over 39.5% and up to about 80% soap are homogeneous, anisotropic liquids of widely varying viscosity. The less concentrated anisotropic liquids are remarkable in that they flow freely under gravity, but at concentrations between 50% and 80% soap they are highly viscous. Below 28.8% soap, the solutions are all homogeneous and isotropic; while between 28.8% and 39.5%, the systems are a mixture of isotropic and anisotropic phases. In the isotropic range below 28.8% the system is again remarkable in that it passes gradually from liquid to jelly and back to liquid again as the concentration of soap is varied from zero to 28.8%. The maximum of rigidity occurs at approximately 12% soap, at which concentration a small beaker containing the solution can be inverted without any flow occurring. It remains a single homogeneous phase upon either concentration or dilution. It will be shown that the formation of this isotropic jelly is without effect on the electrical conductivity or the depression of freezing point.

## EXPERIMENTAL

The hexanolamine was a purified sample kindly supplied by the Shell Development Co., Emeryville, California. It was repurified by recrystallization as the sulfate, followed by vacuum distillation of the liberated and dried amine. Its boiling point is 60.2°C. at 6 mm. pressure. A small initial portion which came over below this temperature, as well as a small amount of higher-boiling residue, was discarded. The soap was made by mixing equivalent quantities of the amine and Kahlbaum's "purest" oleic acid. Its melting point is 58°C. All solutions were made up gravimetrically in Jena bottles with conductivity water of specific conductivity  $0.8 \times 10^{-6}$  or less. Concentrations are expressed as molalities or weight normalities,  $N_w$ .

Conductivities were measured at 25°C.  $\pm$  .005°C., using a grounded oil thermostat. A Jones-Dike bridge was used for measuring resistance, the null point being determined by earphones. Alternating current was supplied by a Leeds and Northrup No. 9842 sine wave oscillator adjustable to 500, 1000 and 2000 cycles. Varying the frequency had no effect on the resistance as measured. Most measurements were made at 2000 cycles. A conventional U-shaped conductivity cell, whose constant was 0.4745, was used for the dilute solutions.

For the more concentrated range, where jelly formation made it impossible to pour the solution, a special streamlined cell was constructed by fusing slightly conical platinum foil electrodes to the inner walls of a section of 8 mm. pyrex tubing, which was then drawn down and extended at each end with 5 mm. tubing, terminating with the male part of a standard tapered joint. The extensions were then bent to form a U with horizontal side arms. Electrical contact with the platinum was made by means of mercury wells through small holes blown through the glass before the electrodes were fused in. It was found most convenient to construct the cell in two separate halves, which were then fused together. Because of the continuous, streamlined shape of the interior of the cell, it was possible by suction to introduce the most viscous jellies and solutions free from air bubbles. Because of the rigid support of the electrodes, this cell was rugged and free from changes in its constant due to jarring and, because of its small size, the contents came to rapid thermal equilibrium with the thermostat. The cell was closed by stoppers made from the female parts of the standard tapered joints. The capacity of the cell was only about 2 cc. Its cell constant was 7.4313. Cell constants were determined with standard potassium chloride solutions made up according to the direction of Parker and Parker (2).

All conductivity measurements were corrected for alkalinity by subtracting the specific conductivity due to hydroxyl ions from that of

the solution as a whole, the remainder being the specific conductivity due to the ions and micelles of the soap itself. Hydroxyl ion concentrations were calculated from the pH as measured with a Beckman standard glass electrode assembly at 25°C.

Freezing point measurements in the dilute range below 0.01  $N_w$  were made in a precision freezing point apparatus modeled after that of Scatchard (3) and calibrated with pure potassium chloride solutions, using the freezing point data of Scatchard and Prentiss (4). The concentration of each solution withdrawn from the apparatus was determined by means of a Zeiss interferometer, using as standard a known solution of approximately the same concentration.

The freezing points of solutions above 0.01  $N_w$  were measured by the more rapid and convenient Beckmann method, the usual precautions being observed, and concentrations being corrected for the weight of ice formed as calculated from the amount of supercooling.

The Hittorf method was used for determining transport numbers. The apparatus and method were essentially that described by M. E. Laing (5) with the exception of the addition of a small auxiliary U-tube at the anode. This was made necessary by the fact that, unlike most soap solutions, those of hexanolamine oleate are less dense than the potassium sulfate guard solution and so float on top of the latter.

Relative viscosities were measured with an Ostwald type of capillary viscometer.

### *Experimental Results and Their Significance*

*Lowering of Freezing-Point.* Freezing-point results are most conveniently expressed as osmotic coefficients,  $g$ , given by the equation

$$g = \frac{\theta}{3.716 \times m} \quad (1)$$

i.e., the ratio of the observed freezing point lowering,  $\theta$ , to the theoretical lowering for a fully dissociated 1-1 electrolyte, where  $m$  is the molality or weight normality,  $N_w$ . The results up to 30% soap have been recorded in Table I and are shown graphically in Fig. 1. The so-called critical concentration, at which  $g$  begins to drop rapidly, is very low. Above 0.01  $N_w$ ,  $g$  drops more slowly to a minimum value of 0.090 at about 0.2  $N_w$  and thereafter rises gradually. This rise is attributable to hydration.

Although the critical concentration of hexanolamine oleate is considerably below the most dilute solution which could be measured, it can readily be calculated by making use of A. P. Brady's discovery that between the critical concentration and that at which the sharp drop in  $g$  ends, the osmotic coefficients of all colloidal electrolytes of the same

TABLE I

*The Osmotic Coefficients of Solutions of Hexanolamine Oleate from Lowering of Freezing Point*

$N_w$	$\theta$	$g$
(By Precision Apparatus)		
.001497	.00316°	.568
.001854	.00348	.505
.002100	.00363	.465
.002500	.00392	.422
.003047	.00422	.372
.004904	.00556	.305
.005763	.00611	.285
.009233	.00741	.216
(By Beckmann Method)		
.01359	.007°	.138
.02569	.0115	.120
.03392	.014	.111
.04846	.020	.111
.06316	.025	.106
.09302	.035	.101
.1154	.041	.096
.1745	.058	.090
.3092	.104	.0905
.4663	.164	.095
.6670	.260	.105
1.004	.420	.108

type (straight chain or branched chain) fall on the same curve if plotted against  $\log (m/m_{g=0.5})$ , where  $m_{g=0.5}$  is the molality at which the osmotic coefficient has the value 0.5 (6). The oleates behave as branched chain compounds, presumably because of the bend in the chain due to the double bond, oleic acid having the *cis* configuration. Fig. 2 shows the coincidence of the data for hexanolamine oleate with Brady's branched chain curve.

Thus, taking  $m_{g=0.908}$  as the critical concentration \* and noting that  $(m_{g=0.908}/m_{g=0.5})$  is a constant for all branched chain compounds, one may write for hexanolamine oleate and Catol 607 (7)

$$\left( \frac{m_g = 0.908}{0.001885} \right)_{\text{hexanolamine oleate}} = \left( \frac{m_g = 0.908}{m_g = 0.5} \right)_{\text{Catol 607}} = \frac{0.003235}{0.0102}$$

whence the critical concentration of hexanolamine oleate is 0.00060  $N_w$ , the lowest value reported for any colloidal electrolyte.

*Electrical Conductivities.* Electrical conductivities were measured over an extremely wide range of concentration, the highest of which, 4.086  $N_w$ ,

\* The so-called critical concentration is actually a short range of concentration, but a definite concentration has been taken for convenience.

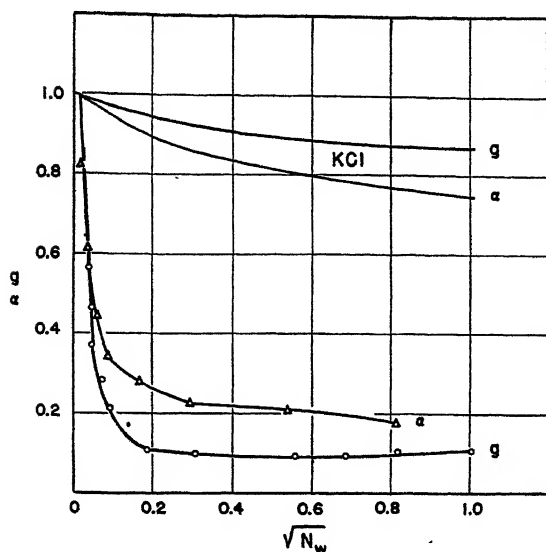


FIG. 1

The Osmotic Coefficient,  $g$ , and the "Arrhenius Coefficient,"  $\alpha = \Delta/\Delta_0$ , of Aqueous Hexanolamine Oleate Plotted Against Molality,  $N_w$ ; Those for Potassium Chloride are Shown for Comparison

$\alpha$  is typically greater than  $g$  at moderate concentrations owing to the presence of electrically charged micelles with negligible effect on the freezing-point of the solution

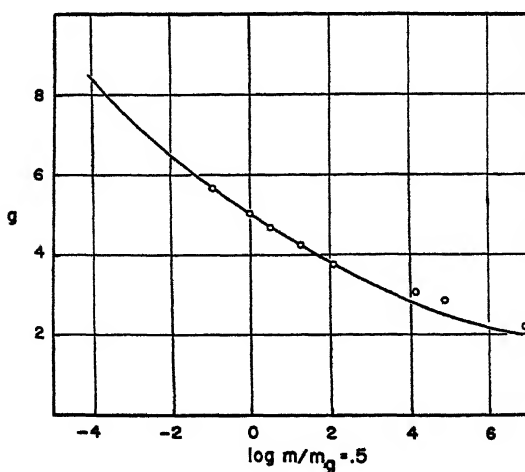


FIG. 2

Brady's Generalized Curve for Branched Chain Colloidal Electrolytes

The circles are the experimental points for hexanolamine oleate



TABLE II

*Electrical Conductivities and Viscosities,  $\eta$ , of Hexanolaminc Oleate Solutions*

$N_w$	$N_v$	$\Lambda$	$\Lambda_{corr.}$	$\eta^*$	$\alpha_{obs.}$
Isotropic Solutions					
.0003149	.0003140	42.10			.827
.0004896	.0004882	38.8 (from graph)			
.0007957	.0007933	32.72			.643
.001135	.001132	31.14			.617
.001742	.001736	25.71			.550
.002602	.002592	22.79			.448
.004551	.004528	19.68	19.82	1.007	.387
.005317	.005292	18.92	19.05	1.01	.372
.007214	.007170	17.44	17.66	1.02	.343
.01122	.01114	17.13	17.35	1.03	.337
.01466	.01453	15.81	16.24	1.027	.311
.01937	.01915	14.98	15.43	1.05	.294
.02702	.02663	14.28	15.14	1.09	.280
.04499	.04400	13.02	14.67	1.19	.256
.05324	.05101	12.50	14.66	1.27	.245
.06254	.06070	12.00	14.76	1.37	.236
.08540	.08209	11.51	17.61	1.9	.226
.1151	.1093	11.07			.217
.1491	.1395	11.02			.217
.2871	.2560	10.56			.207
.6563	.5099	8.881			.175
Liquid Crystalline Solutions					
2.034	1.084	4.721			.0928
2.302	1.166	2.819			.0552
2.867	1.284	2.653			.0521
4.086	1.482	1.173			.0230
7.32	1.74	.44			.0086
8.80	1.82	.50			.00098

\* Interpolated from Table III.

corresponds to approximately 78.5% soap; the range includes both isotropic and liquid crystalline systems. The experimental data, expressed as equivalent conductivities;  $\Lambda$ , are presented in the third column of Table II. A graphical representation is given in Fig. 3. Between the concentrations indicated by small arrows in the figure, the solution passes from fluid to rigid jelly and back to fluid again. The vertical arrow indicates the concentration at which the jelly is most rigid. It is evident that the conductivity is unaffected by this change in the physical properties of the solution, as is also the osmotic coefficient (Fig. 1). This phenomenon is consistent with the observation of Laing and McBain (7) that the conductivity, like the osmotic activity, has the same value for both sol and jelly forms of sodium oleate solution of any given concentration.

TABLE III

*Experimental Values of Relative Viscosities,  $\eta$ , of Dilute Solutions of Hexanolamine Oleate at 25°C.*

$N_w$	$N_o$	$\eta$
.03346	.03291	1.134
.04640	.04540	1.204
.05743	.05593	1.313
.06743	.06543	1.48
.08557	.08243	1.99

Inspection of Fig. 3 shows that the conductivity is of the same order of magnitude for liquid crystalline solutions as for isotropic solutions in spite of their difference in viscosity and internal organization. The isotropic solutions conduct fractionally better than the anisotropic solutions. Even an anomalously isotropic solution of 53.4% concentration conducted 46% better than the usual anisotropic solution of that composition.

It is also to be noted that the conductivity minimum, generally so characteristic of colloidal electrolytes, is absent in this case. It has been

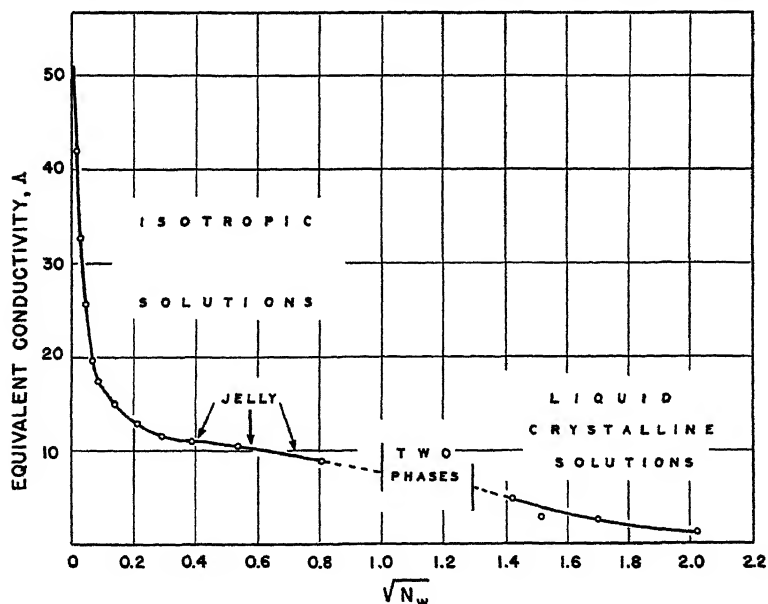


FIG. 3

The Equivalent Conductivity of Aqueous Hexanolamine Oleate at 25°C.  
Plotted Against Molality,  $N_w$

The vertical arrow marked "jelly" indicates the point of maximum rigidity of the jelly. On addition or removal of water, the solution changes progressively to a free-flowing liquid. The break in the curve represents the region between 28.8 and 39.5% oleate, where liquid crystalline and isotropic phases are in equilibrium.

found that the conductivity of a related compound, hexanolamine caprylate (8), is markedly lowered by the increasing viscosity of the solution with increasing concentration.\* Hence, putative corrected conductivities have been computed in Table II by multiplying the observed values by the  $2/3$  power of the relative viscosity and are listed in Table II under  $\Lambda_{\text{corr.}}$ . The corrections were carried only to  $0.08540 N_w$ , as at higher concentrations the viscosity is increased by incipient jellification,

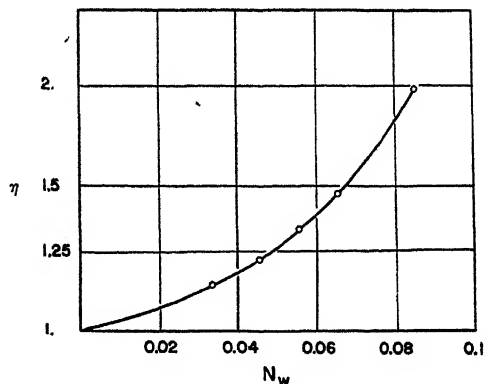


FIG. 4

The Relative Viscosity,  $\eta$ , of Dilute Solutions of Hexanolamine Oleate at 25°C.  
 $\eta$  is plotted on a logarithmic scale

which obviously does not at all comparably affect the conductivity, and perhaps, as in the cited example of sodium oleate (7), does not affect it at all. The correction applied to  $0.08540 N_w$  is, therefore, itself probably too high.

In the last column of Table II the "Arrhenius coefficients,"  $\alpha = \Lambda/\Lambda_0$ , are given. The value of  $\Lambda_0$  is taken as 50.9. The results are plotted in Fig. 2 to facilitate comparison with the osmotic coefficient.  $\alpha$  is seen to be typically higher than  $g$ . This indicates that the small colloidal micelles contribute very little to the freezing point depression, but do make a significant contribution to the conductivity.

*Transport Numbers.* A determination of the transport numbers in a  $0.1211 N_w$  solution gave  $-1.58$  for the cation and  $+2.55$  for the anion. The negative value of the cationic transport number is proof of the inclusion of hexanolammonium ions, as well as oleate ions, in the conducting micelles, though in lesser numbers. The transport of the cations incorporated in the micelles toward the anode is greater than the transfer

\* However, on the contrary, the conductivity of hexanolamine elaidate is apparently unaffected by the viscosity of the solution and shows the characteristic minimum. The flow behavior of the elaidate is anomalous, showing high shear elasticity.

of free cations in the normal direction, *i.e.*, toward the cathode. Thus, there is a net *decrease* in the amount of hexanolammonium ions in the solution around the cathode. A similar state of affairs was shown for soap solutions by McBain and Bowden (9), Quick (10), and Laing (5), and for other detergents by Hartley, Collie and Samis (11).

#### SUMMARY

1. Freezing-point, conductivity, viscosity and transport data have been given for aqueous solutions of hexanolamine oleate.

2. The osmotic coefficients have been shown to follow Brady's curve for *branched* chain compounds, and the "critical concentration" has been calculated therefrom.

3. The necessity for the existence in solution of "small micelles" or particles which contribute very little to the freezing point lowering but have a substantial conductivity is demonstrated by the fact that the conductivity ratio  $\Lambda/\Lambda_0$  is considerably higher than the osmotic coefficient.

4. The cationic transport number is found to be negative and that for oleate radical is greater than unity at moderate concentrations, a further demonstration of the presence of conducting micelles, which, moreover, must include hexanolammonium ions.

#### REFERENCES

1. GONICK, E., AND MCBAIN, J. W., *Isotropic and Anisotropic Liquid Phases in the System Hexanolamine Oleate-Water*, *J. Am. Chem. Soc.* (in press).
2. PARKER, H. C., AND PARKER, E. W., *J. Am. Chem. Soc.* **46**, 330 (1924).
3. SCATCHARD, G., JONES, P. T., AND PRENTISS, S. S., *J. Am. Chem. Soc.* **54**, 2676 (1932).
4. SCATCHARD, G., AND PRENTISS, S. S., *J. Am. Chem. Soc.* **55**, 4355 (1933).
5. LAING, M. E., *J. Phys. Chem.* **28**, 680 (1924).
6. MCBAIN, J. W., AND BRADY, A. P., *J. Am. Chem. Soc.* **65**, 2072 (1943).
7. LAING, M. E., AND MCBAIN, J. W., *J. Chem. Soc.* **117B**, 1506 (1920).
8. GONICK, E., *J. Am. Chem. Soc.* (in press).
9. MCBAIN, J. W., AND BOWDEN, R. C., *J. Chem. Soc.* **123B**, 2417 (1923).
10. QUICK, W. C., *J. Chem. Soc.* **127**, 1401 (1925).
11. HARTLEY, G. S., COLLIE, B., AND SAMIS, C. S., *Trans. Faraday Soc.* **32**, 795 (1936).



# THE CONTACT ANGLE BETWEEN WATER AND A MONOLAYER OF EGG ALBUMIN ON GLASS AS A FUNCTION OF FILM PRESSURE

George Jura and William D. Harkins

*From the Department of Chemistry, University of Chicago, and  
Universal Oil Products Company, Chicago, Illinois*

*Received November 11, 1945*

## INTRODUCTION

### *Angle of Contact against Water as Related to the Orientation of Groups in a Monolayer*

Let it be supposed that a monolayer of an  $n$ -long chain paraffin acid such as stearic acid is deposited on the plane surface of a solid subphase. If, as is probable if the subphase is glass or a metal, the non-polar groups are turned away from the surface of the solid, an outer surface of the general nature of a paraffin is formed. On the surface of solid paraffin the angle of contact with water is found, according to the nature of the paraffin, to be between  $104^\circ$  and  $111^\circ$ . If, now, the molecule of the paraffin acid is sufficiently long and the orientation of its molecules is perfect, the angle of contact of water with the surface of the monolayer should also be high and of this general order, provided the molecules preserve their orientation when in contact with water. If, however, the polar groups are all turned outward, the contact angle should be zero.

If a protein, whose molecules contain a large number of both polar and non-polar groups, is deposited, the angle should be high if the hydrocarbon residues are largely oriented outward, and low, if the polar groups have this orientation. An intermediate value would indicate that both polar and non-polar groups are oriented outward. Since the attraction of glass is much higher for polar than non-polar groups, an intermediate angle indicates that in the molecule the configuration is such that both polar and non-polar groups are oriented outward. A method analogous to that used by Blodgett (1) for depositing multimolecular films is described below, whereby a monomolecular layer of denatured egg albumin film can be deposited on a glass slide.

Measurements of the contact angle of water against deposited egg albumin films have been made by Bull (2) who did not succeed in obtaining equilibrium values. However, the writers have been able to do this by

the technique described later. It is found that the contact angle between water and the protein monolayer deposited on glass increases linearly with the film pressure of the monolayer while still on the surface of the water, before it is transferred to the surface of the glass.

## EXPERIMENTAL

### *Deposition of the Film and Measurement of the Contact Angle*

The egg albumin used was obtained from Professor Edwin J. Cohn of the Harvard Medical School. The water used for all experiments was doubly distilled, the second distillation being carried out over acid permanganate in a block tin still.

A single monolayer of egg albumin was transferred from the surface of water, buffered with acetate to give a pH of 4.67, which is close to the isoelectric point of the protein, to the clean surface of a glass slide by a vertical movement given by a rack and pinion of the latter upward (U or Y film). The mean thickness of the monolayer on the glass was varied by changing the film pressure of the monolayer on the surface of the water before it was transferred to the surface of the glass. The slide was cleaned before the deposition of a monolayer by immersion in warm cleaning solution followed by a thorough rinsing with doubly distilled water. After the film was deposited, the slide was dried by heating in an oven for one hour at 110° C. The barrier used for the compression of the film was of the type adopted in this laboratory in experiments on built-up films, *i.e.*, a short section of the barrier is replaced by a thread coated with vaseline.

The film was spread by the technique of Görter (3). One half an hour was allowed for spreading after the pipette was emptied. A piston oil was then placed behind the barrier. The film was then slowly compressed until the pressure of the albumin film was equal to that of the piston oil as indicated by the behavior of the thread. The value of this pressure was determined by the use of a horizontal type film balance.

The contact angle between the protein monolayer on the glass slide and the surface of doubly distilled water was determined by the apparatus of Fowkes and Harkins (4). In this apparatus the surface of the water is cleaned by sweeping. A small Wilhelmy balance, sensitive to a change in surface tension of 0.1 dyne cm.<sup>-1</sup>, is used to check the cleanliness of the water surface, which remained uncontaminated while the contact angle measurements were being made. After the slide was placed in position, the contact angle became constant at the end of fifteen minutes, the time necessary with the clean surface of graphite, and remained constant for a period of more than one hour thereafter. *The same value of the contact angle was obtained, regardless of whether the liquid was advancing or receding*

over the surface. The values of the contact angle as a function of the film pressure during deposition of the film are given in Table I and represented in Fig. 1.

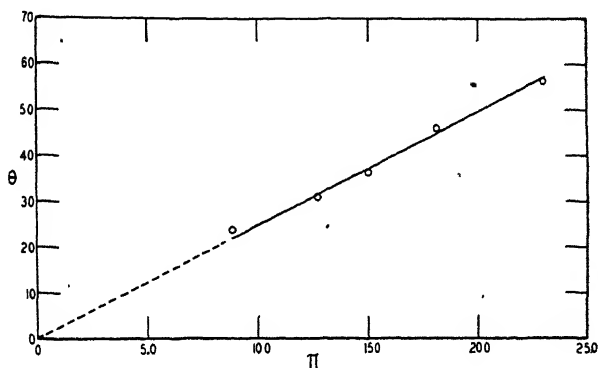


FIG. 1

The Contact Angle ( $\theta$ ) of Water against a Deposited Monomolecular Layer of Egg Albumin on the Surface of Glass as a Function of the Film Pressure ( $\pi$ ) of the Protein Monolayer Before Deposition While Still on the Surface of Water

TABLE I.

*The Contact Angle as a Function of Film Pressure of Water against a Monolayer of Egg Albumin on a Subphase of Glass as a Function of the Film Pressure*

$\pi$ dynes cm. <sup>-1</sup>	$\theta$	$t$ °C	Piston oil
3.5	0 < $\theta$ < 20°	33	
8.8	23.8 ± 0.6	33	Tricresyl phosphate
12.8	30.9 ± 0.8	33	Ethyl cinnamate
19.1	46.2 ± 0.7	27	Castor oil
15.0	36.2 ± 0.7	27	Myristic acid
23.0	56.4 ± 1.4	27	Oxidized nujol

The remarkable feature exhibited in Fig. 1 is that the contact angle is a linear function of the film pressure for all pressure values for which the contact angle could be measured. Because of the interference of the meniscus on the edge of the slide the contact angle could not be determined at film pressures below 3.5 dynes cm.<sup>-1</sup>. If the extrapolation of the observed linear relation is valid, then (1) the contact angle should be zero at zero film pressure, and (2) the film pressure would attain the value of 50 dyne cm.<sup>-1</sup> before the contact angle reaches 109°, that of paraffin. The first of these is true, since at zero film pressure the observed contact angle would be that of water against glass, which is zero (5). The film of egg albumin on water at pH 4.67 collapses at pressures of about 36 dynes cm.<sup>-1</sup> as determined independently on a horizontal film balance.



Thus, if the extrapolation to high film pressures is valid, then in the film of egg albumin, even at the highest pressures, some polar groups are oriented away from subphase. From the complexity of the molecule, this result is not surprising. Unfortunately, at the present time there is insufficient knowledge available to make it possible to give a more specific interpretation of the relations discovered.

#### SUMMARY

1. The contact angles of water against monolayers of egg albumin deposited on glass were found to vary from  $23.8^\circ$  to  $56.4^\circ$  as the film pressure of the egg albumin on water, from which it was deposited on the slide, varied from 8.8 to 23.0 dyne  $\text{cm}^{-1}$ . The contact angle of water against the protein film on the glass was found to be a linear function of the film pressure of the film on water.

2. The results indicate that at no pressure at which the film is stable does the outer surface of the monolayer, after transference to the glass, consist entirely of non-polar groups.

#### REFERENCES

1. BLODGETT, K. B., *J. Am. Chem. Soc.* **57**, 1007 (1935).
2. BULL, H. N., *J. Biol. Chem.* **125**, 585 (1938).
3. GÖRTER, E., AND GRENDL, F., *Proc. Acad. Sci. Amsterdam* **29**, 371 (1925).
4. FOWKES, F. M., AND HARKINS, W. D., *J. Am. Chem. Soc.* **62**, 3377 (1940).
5. RICHARDS, T. W., AND CARVER, E. K., *J. Am. Chem. Soc.* **43**, 827 (1921).

## SOME ASPECTS OF THE ELECTROCHEMISTRY OF CLAYS

J. N. Mukherjee and R. P. Mitra

*From the Physical Chemistry Laboratory, University College of Science  
and Technology, Calcutta*

*Received October 31, 1945*

### 1. INTRODUCTION

The term clay has been used in this paper to designate in general the clay fraction of soils and other natural deposits of clay materials such as bentonites, shales, kaolins and fuller's earths freed as far as possible from organic matter by the usual treatments. Following current usage, the acid forms of these systems will be called hydrogen clays. Also, in view of a markedly colloidal nature of the clay fraction its various ingredients will be referred to collectively as the colloid constituents.

The nature and content of the colloid constituents of clay materials determine to a large extent their uses in agriculture, structural engineering and the ceramic, rubber, petroleum and other industries. The importance of detailed investigations on these constituents by physical and chemical methods is now being increasingly felt for purposes of soil systematics, soil classification and standardization of clays for use in the various industries. While numerous investigations have cleared up the physical and chemical properties of clays it is only recently that the use of X-ray, thermal and optical methods have enabled us to obtain an insight into the chemical constitution of their ingredients. These methods have revealed that clays consist mostly of crystalline clay minerals with admixtures of silicon dioxide and the sesquioxides of aluminum and iron. The principal clay minerals belong to the groups hydrous micas, kaolinites and montmorillonites. The atomic structures of these minerals are now fairly well understood. Isomorphous replacements within the lattice can occur permitting wide variations in the mass chemical composition which is, therefore, of limited significance in characterizing clays. The lattice structure enables us to understand some properties of clays, *e.g.*, swelling, and it has also thrown light on the phenomenon of cation exchange. There is however a group of properties to be presently discussed which, more than anything else, determines their suitability for different uses and such aspects of their colloidal behavior as plasticity and anomalous viscosity, swelling and shrinkage, flocculation and deflocculation, and moisture absorption.

The clue to a systematic correlation of the physical and chemical properties of clays seems to lie in the recognition that their constituents are predominantly polar substances and consequently their electrochemical character should form the background of the interrelationships of the diverse aspects of clay behavior. Until recently, however, not much attention has been paid to the elucidation of the fundamental electrochemical character of either the clay fraction or the individual substances which enter into its make up. Vital to an understanding of the electrochemistry of clays is the manner of their interaction with acids, bases and salts, their properties of cation and anion exchange, and factors on which such interactions and properties depend. These aspects, by their nature, cannot be dealt with directly by X-ray and other physical methods, but these, in conjunction with electrochemical methods, should enable us to obtain much fuller information.

## 2. SOME ASPECTS OF RECENT DEVELOPMENTS OF THE ELECTROCHEMISTRY OF COLLOIDS

Clays being colloid systems, their electrochemical properties exhibit the characteristics of these. Attempts have been made to explain the electrochemical properties of colloids from the point of view of classical electrochemistry and the Debye-Hückel-Onsager theories of strong electrolytes. Limitations of such treatments have been discussed in previous papers (1) and repetitions will be avoided. It is perhaps necessary to reiterate the main point made in those papers, *viz.*, that colloidal systems show special features which require for their explanation that the electrical double layer be considered as such and in detail, *e.g.*, as regards the manner in which it is formed and affected by the adsorption and exchange of ions. The main object of the present paper is to illustrate this point by observations made during the past few years on hydrogen clays isolated from a large number of soils, bentonites and kaolins. Reference may be made in this connection to some special features observed comparatively recently with systems having a much simpler chemical constitution than the clays. These systems include various paraffin-chain acids and salts, and certain dyestuffs. It has been observed that the equivalent conductance of the paraffin-chain radical,  $\lambda_p$ , rapidly rises above a certain critical concentration and often attains values much greater than that at infinite dilution (2). The equivalent conductance of the oppositely charged ions (*gegenions* or counter ions of Pauli),  $\lambda_o$ , on the other hand, shows a sharp fall.  $\lambda_p$  and  $\lambda_o$  pass respectively through a maximum and a minimum value at about the same concentration. The activity coefficient of the *gegenions*,  $f_o$ , as also the total equivalent conductivity,  $\lambda$ , fall sharply at the critical concentration and remain practi-

cally constant (2) or increase to a small extent beyond a minimum value (3, 4). Somewhat different explanations of these observations have been given by McBain (5), Hartley (2, 6) and Lottermoser (3, 4). Opinion particularly differs as to the existence of one or several types of micelles and "neutral colloids," and in regard to the mechanism of the rise of the total equivalent conductivity at higher concentrations. Without going into these in detail it can be said that most of the above observations, especially the existence of a critical concentration, the rise in the total equivalent conductivity, and the activity coefficient of the *gegenions* after passing through a minimum value, and the fact that the equivalent conductance of the micelle ion attains a value greater than that at infinite dilution, are not meant to be dealt with by the Debye-Hückel theory. Equally foreign to the contents of this theory are some of the concepts introduced to explain the observations, *e.g.*, those of an adherence and a release or loosening of the *gegenions* at low and high concentrations respectively (2, 6). It may be mentioned that the idea of an adherence of *gegenions* runs closely parallel to the theory of secondary adsorption of ions postulated by one of us (7, 8).

### 3. EFFECT OF CONCENTRATION ON SOME ELECTROCHEMICAL PROPERTIES OF CLAYS

In the case of the systems mentioned above, a thermodynamic equilibrium is assumed to exist between the simple ions and the aggregates. No such equilibrium between monomeric and polymeric ions appears to exist in colloidal solutions of most clays and many other insoluble substances. For this reason they may be designated as "electrolytic colloids," an expression which, it is hoped, emphasizes their electrolytic character and at the same time serves to distinguish them from the true colloidal electrolytes where such an equilibrium exists. Some definite evidence of aggregate formation in dilute solutions of hydrogen bentonites has been obtained (9). The cataphoretic velocity, *c.v.*, has been found to increase rapidly with the concentration and, at the same time, there is a sharp fall in the total conductivity calculated per g. of colloid (Fig. 1). The sols show strong absorption and the extinction coefficient,  $\epsilon_m$ , decreases with increase in concentration and passes through a minimum. Somewhat similar changes have been observed with colloidal dyes (10) and ascribed to aggregate formation. The cataphoretic velocity, *c.v.*, of a large number of inorganic colloids has been found to increase before the coagulating concentration of an added electrolyte (11) has been reached. Such an increase in the *c.v.* also possibly results from an aggregation of the colloidal particles prior to complete coagulation. Microcataphoretic measurements also have shown that the *c.v.* increases with time to a maximum value as

the aggregation proceeds. There is a sharp drop in the *c.v.* when coagulation takes place (12).

Reference has previously been made to measurements of the activity coefficients of the counter ions in colloidal electrolytes. Earlier investigations in the field of electrolytic colloids led to the postulation of the so-called "suspension effect" by Wiegner and Pallmann (13). This effect has been studied by us over a wider range of concentrations of the colloid (0.01% to 18.0%) than hitherto used so as to include thick pastes and gels. The antimony electrode, and the quinhydrone electrode as used by

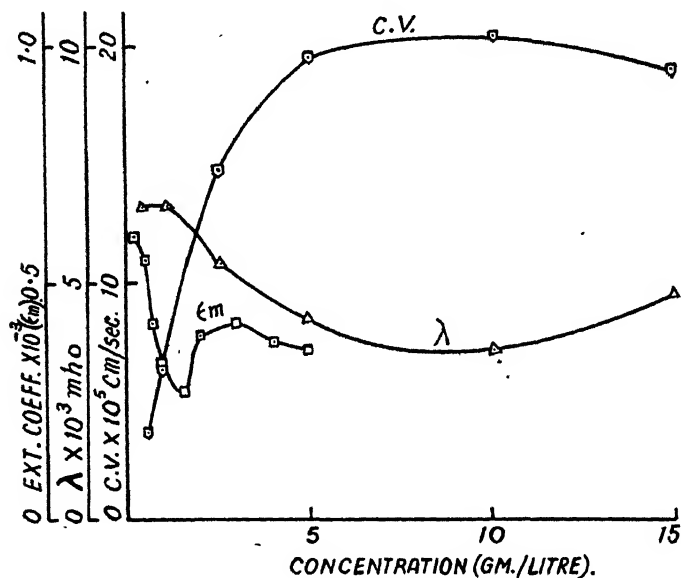


FIG. 1

Sanders (14), were found very convenient for measuring the pH of the most concentrated suspensions and pastes. Using a hydrogen bentonite\* which, on X-ray analysis by Mr. S. N. Bagchi of this laboratory, was found to contain no clay mineral other than montmorillonite, the  $H^+$  ion concentration,  $C_{H^+}$ , was found to increase linearly with the concentration of the colloid,  $C$ , till the latter attained a value of about 0.2%, and then the plot of  $C_{H^+}$  against  $C$  became concave toward the axis of concentration (Fig. 2a) and the slope  $\frac{dC_{H^+}}{dC} = \alpha$  rapidly decreased (15). At higher concentrations, the  $C_{H^+} - C$  curve became convex toward the axis of  $C$  and showed an inflection at a concentration of about 9.0% (Fig. 2b). The curve became increasingly flat at still higher values of  $C$ .

\* Isolated from the entire clay fraction of a deposit of bentonite in Kashmir.

The theory of the electrical double layer and of adsorption of ions as postulated by Mukherjee (7, 8) provides a consistent explanation of the curves given in Figs. 1 and 2. According to this theory, the colloidal particles of the sol are surrounded by electrical double layers whose outer sheets consist of  $H^+$  ions present in a mobile as well as bound, or second-

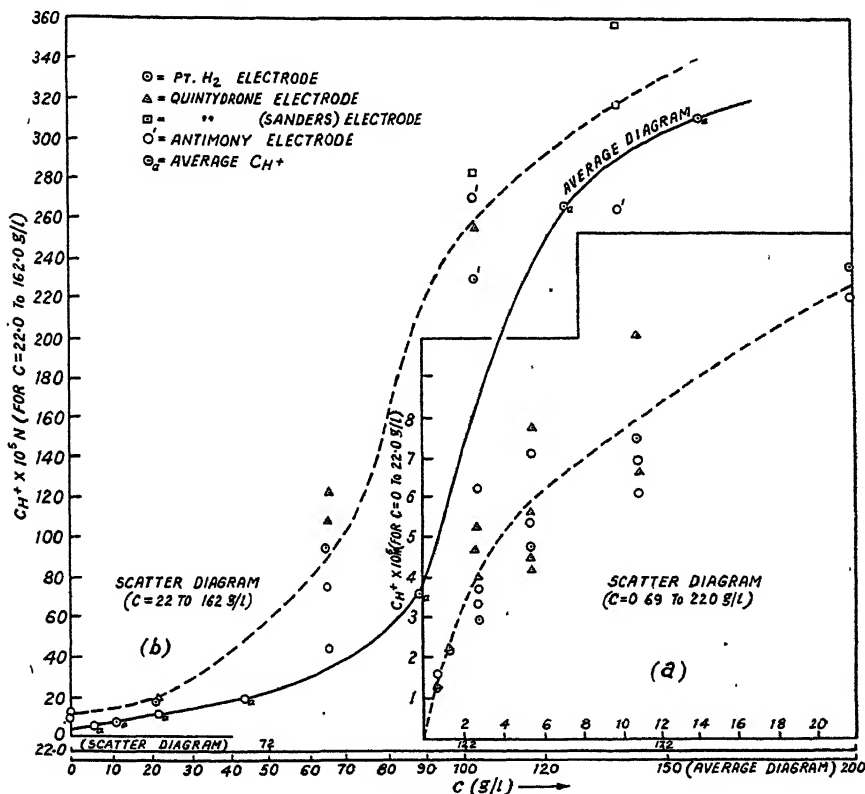


FIG. 2

arily adsorbed, condition. The mobile  $H^+$  ions are responsible for the observed  $H^+$  ion activity of the sol. An increase in the concentration of the sol above a value of approximately 0.2% causes a rapid change from the mobile to the bound condition of the  $H^+$  ions in the double layer. Formation of larger micelles above this concentration seems to be responsible for such a transformation. A rapid secondary adsorption of the  $H^+$  ions near the critical concentration would also reconcile the sudden fall in the conductivity per g. of colloid,  $\lambda$ , shown in Fig. 1. The contribution made by the particles to  $\lambda$  or, in other words, their *c.v.*, increases as a result of such aggregation. The secondary adsorption of the  $H^+$  ions caused by it, however, gives rise to a much more marked decrease in their con-

ductivity coefficient and consequently, as a net result, the total conductivity,  $\lambda$ , decreases. This secondary adsorption is probably also responsible for the fact that the *c.v.*, instead of increasing proportionately with the concentration, at higher values of the latter shows a maximum.

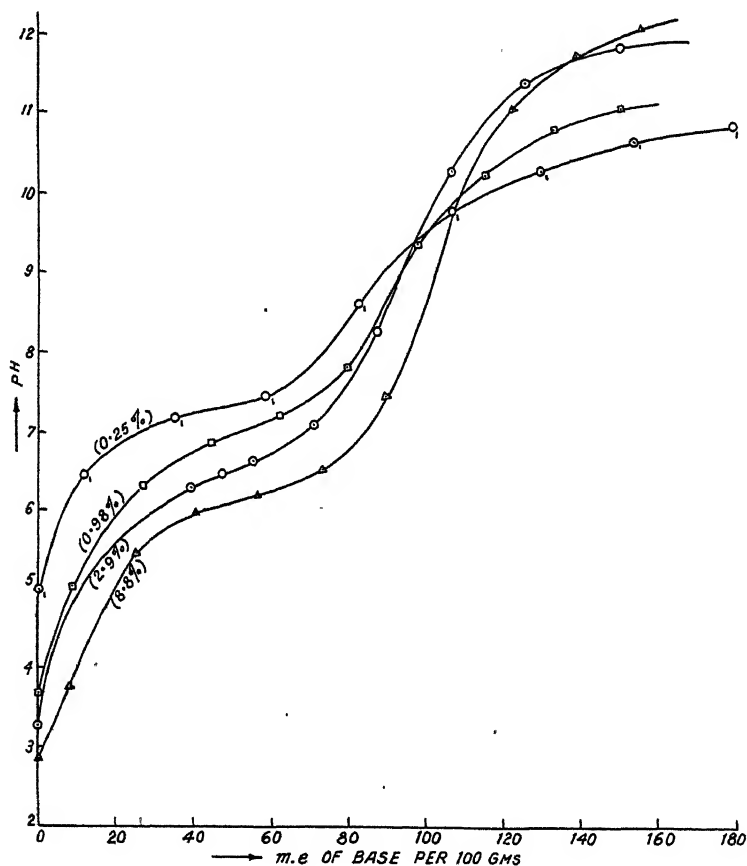


FIG. 3

At concentrations above 5.0%, the particles exert a strong mutual influence on one another as is indicated by a *rapid* rise in the viscosity of the sol above this concentration.\* It is possible that the electrical double

\* According to unpublished work of Dr. R. P. Mitra and Mr. S. Mandal, no such rapid rise in the viscosity could be observed in the case of a montmorillonitic hydrogen clay (isolated from a black cotton soil) up to the highest concentration studied (12.0%). The  $C_H^+$ —C curve of this hydrogen clay also did not show any sharp inflection although the curve became increasingly convex toward the axis of concentration above values greater than 6.0% of the latter.

layers overlap, causing a loosening of the secondarily adsorbed or bound  $H^+$  ions of the double layers and their passage into the mobile condition (1a). Such an effect would explain the convex portion of the curve in Fig. 2b and also the inflexion.

The total neutralizable acid, or the base exchange capacity, *b.e.c.*, of the above hydrogen bentonite calculated at the inflection point of its potentiometric titration curve\* with NaOH (Fig. 3) increased from 81.0 to 103.0 milliequivalents per 100 g. of oven dried material when the concentration of the sol was increased from 0.25 to 8.80%. Such an effect of the concentration on the *b.e.c.* has not been previously reported. This increase has also been observed by us using two subfractions of the above hydrogen bentonite having average equivalent spherical diameters, *e.s.d.*, 0.06 and  $< 0.05$  expressed in microns. A coarse subfraction with an average *e.s.d.* equal to  $1.10 \mu$ , and the entire clay fraction of another sample of bentonite, on the other hand, showed no variation of the *b.e.c.* with the concentration. Fuller discussion of the effect of the concentration on the *b.e.c.* and the other factors discussed above is deferred pending completion of investigations, now in progress, on hydrogen clays containing clay minerals other than montmorillonite.

#### 4. ADSORPTION OF IONS BY COLLOIDAL SOLUTIONS OF ACIDS AND THE FORMATION OF "ION PAIRS" ON THE SURFACE OF THE COLLOIDAL PARTICLES

The *b.e.c.* of hydrogen clays and, in fact, the so-called "total neutralizable acid" of colloidal acid systems in general, depend upon several factors discussed below. In contrast to acids in true solution, surface reactions depending on such factors as the energy of the reaction between the surface molecules and the alkali, the lattice energy of the solid acid, the stability of the resulting salt and, in case the salt is insoluble, its lattice energy, must be considered in dealing with interactions of colloidal acids with bases (*vide seq.*). The above factors include considerations of the adsorption of hydroxyl ions and exchange of the cations of the base for the hydrogen ions on the surface, types of interaction with the base which are distinct from the neutralization of acids in true solution. The classical concepts, as is to be expected, adequately explain the interaction of an acid with a base when equilibrium is established between definite phases. If, however, the anion of the resulting salt is not stable in solution and the lattice energy of the solid salt is too weak or its solubility too large to admit of the formation of a separate solid phase, then stable ion pairs, as explained below, are formed on the surface and an equilibrium is established between ions adsorbed on the surface and ions in the liquid

\* The features of the titration curves have been illustrated in Figs. 7, 8 and 9.



phase. Some of the adsorbed ions (the primarily adsorbed ions) are firmly built into the surface forming a layer of localized charges on the surface and they draw near them, by electrostatic forces, an equivalent amount of ions of opposite sign. Part of these ions may be fixed on the primarily adsorbed ions by purely electrostatic forces. Chemical valence or quasi-chemical and van der Waals' forces may also operate (7, 8). The energy with which the ions of opposite sign are adsorbed depends on the type of force operating. In the simplest case, where electrostatic forces alone are involved, the energy of adsorption is determined by the valency and diameter of the oppositely charged ion and is given by the electrical work,

$$W = \frac{N_1 \times N_2 \times E^2}{x \times D},$$

where  $N_1$  and  $N_2$  are the valencies of the primarily and secondarily adsorbed ions,  $D$  the dielectric constant of the medium intervening between them, and  $x$  the distance separating their centers, allowance being made for their hydration envelopes, if any. The lyotrope series of cations,  $\text{Th} > \text{Al} > \text{Ba} > \text{Ca} > \text{Mg} > \text{Rb} > \text{K} > \text{Na} > \text{Li}$ , follows from these considerations. The existence of surface conduction at the isoelectric point which, as rightly pointed out by McBain (16), cannot be explained from the theory of the double layer as postulated by Helmholtz and Smoluchowski, can be reconciled with the concept of ion pairs as stated above. At the isoelectric point the net charge per unit area of the surface is zero. If, however, the electrically adsorbed ions are of higher valency than the primarily adsorbed ions, then it follows from the above theory that, even at the isoelectric point, the surface carries equal amounts of positive and negative charges, and there are also present both cations and anions in equivalent amounts in the mobile sheet of the double layer. A "composite" double layer formed in this manner will show surface conduction. The existence of such composite double layers has been proved in the case of precipitated manganese dioxide (17). The sign of the charge (negative) on the precipitate has been found to be reversed by di- and trivalent cations, *e.g.*,  $\text{Ba}^{++}$ ,  $\text{Mg}^{++}$  and  $\text{Al}^{+++}$ , but even after the reversal the concentration of  $\text{H}^+$  ions liberated from the interfacial layers continued to increase. This observation definitely indicates that the reversal of the charge of the surface does not mean that all the acid groups on the surface have been converted into positively charged Ba- or Mg-complexes, but that some acid molecules are still left on the surface. At the isoelectric point the primarily adsorbed layer consists of positively charged ion pairs and also some primarily adsorbed anions which have not formed such ion pairs and consequently give an equal amount of negative charge

to the surface. The double layer therefore contains both cations (*viz.*,  $H^+$  ions) and anions (of the added salt) in its mobile sheet (Fig. 4).

If a colloidal solution of an acid were a heterogeneous system and if the product of its interaction with a base gave a salt which separates out as a well-defined solid phase, then its behavior, as deduced from considerations of solubilities, would be represented by the titration curves of

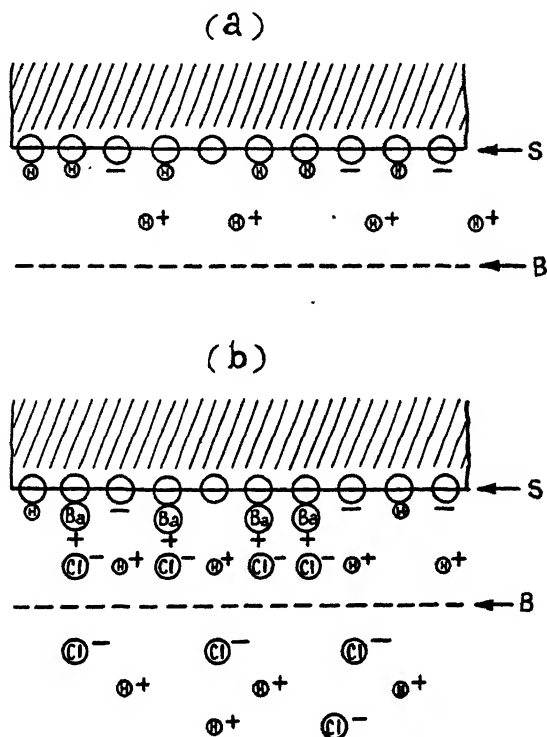


FIG. 4

S.—Surface of the colloidal particle  
B.—Boundary of the double layer

palmitic acid sols with alkaline earth hydroxides. Using  $Ba(OH)_2$ , the whole of the acid substance (as determined by analysis) reacts at a constant pH between 6.2 and 6.3 and, on further addition of the base, the pH shoots up as would happen if the base were added to pure water (18) (Fig. 5). The stoichiometric conversion of the acid into its Ba-salt is to be attributed to a marked difference between the lattice energies of solid palmitic acid and barium palmitate, in consequence of which the Ba-palmitate molecules peel off as the solid salt from the surface as fast as they are formed, once the solubility product of the salt has been reached.

Such a stoichiometric conversion at the inflection point of the titration curve is not to be found with silicic acid sols. Titration curves of these sols with dilute bases show an inflection point in the acid(1b,19a) (Fig. 6). The interaction with the base continues beyond the inflection point. Further, when a barium or calcium salt is added to the system an amount of neutralizable acid considerably larger than the total acidity at the inflection point is liberated (1b, 19b). The inflection point, there-

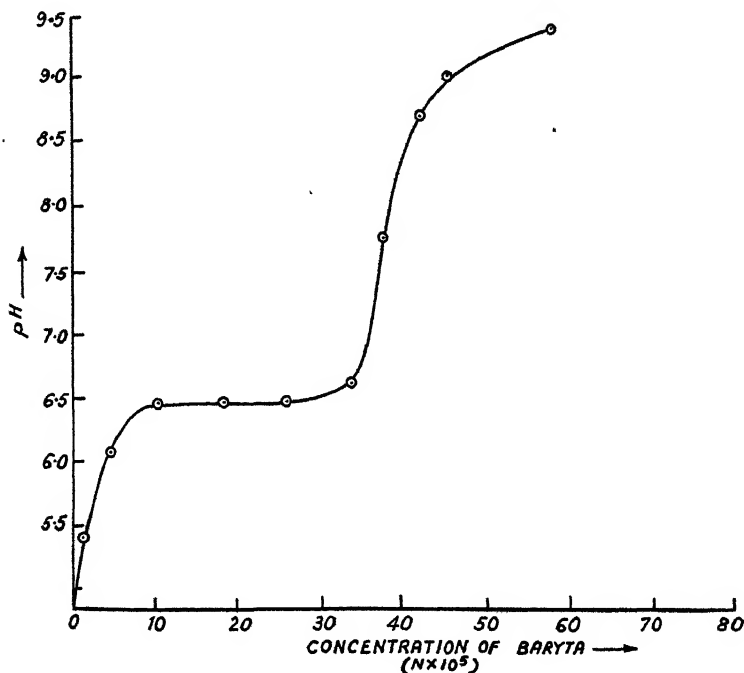


FIG. 5

fore, in no sense corresponds to the neutralization of all the  $H^+$  ions capable of reaction. Degrees of dissociation and dissociation constants calculated on the basis of the "total" acidity at the inflection point consequently do not have their usual significance. In addition to the  $H^+$  ions liberated by neutral salts, which pass into the ultrafiltrate, others are still present in the system. This is found on continued leaching, which gives an additional amount of  $H^+$  ions. Evidently, more ion pairs are formed on the surface by leaching with the salt solution than by a single treatment or by titration with a dilute base up to the inflection point in the acid region. Titration with concentrated NaOH gives a second inflection at about pH 11.5 and the total acidity obtained from this inflection agrees with the assumption of the dissolution of the particles to form the

acid metasilicate if silicic acid is considered to be dibasic (1b, 19a). The values of the buffer indices, however, show that the inflection point and the form of the curve at this stage have features which differ definitely from those of weak acids in true solution.

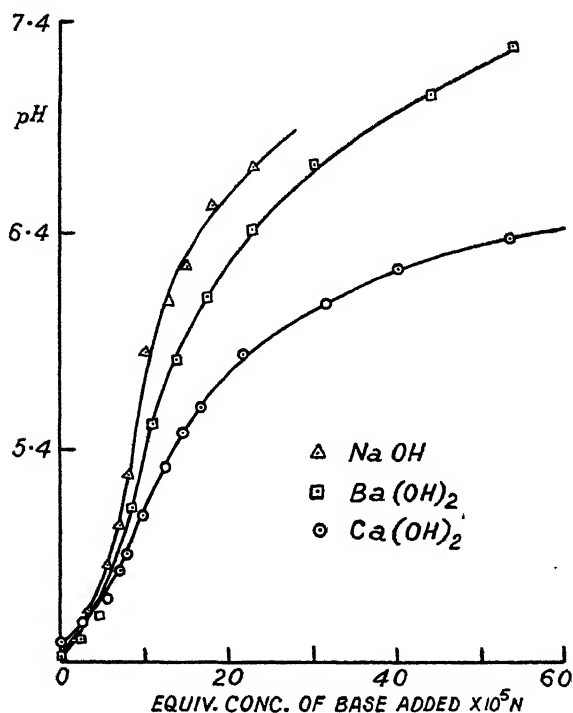


FIG. 6

The relative effects of  $Ba^{++}$  and  $Ca^{++}$  ions in their interactions with silicic acid sols are very interesting. In the interaction with neutral salts, as a result of which acid is liberated,  $Ba^{++}$  has a greater effect than  $Ca^{++}$ . This is in agreement with the theory of electrical adsorption. Considerations of solubilities would lead us to expect a greater effect of  $Ca^{++}$  than  $Ba^{++}$ , as Ca-silicate is more insoluble than Ba-silicate (20). In the interaction of the sols with bases which occurs in the weakly acidic and alkaline regions,  $Ca^{++}$  does react more strongly than  $Ba^{++}$ , as the slopes of the titration curves (Fig. 6) show. A similar reversal in the relative effects of  $Ba^{++}$  and  $Ca^{++}$  ions has been observed in the case of hydrogen clays isolated from soils (further discussed below) and with several other colloidal acid systems including humic acid (21), nucleic acid (22) and various gum acids (23).

## 5. THE ROLE OF THE ELECTRICAL DOUBLE LAYER AND OF ADSORPTION OF IONS IN THE ELECTROCHEMISTRY OF CLAYS

Studies of hydrogen clays isolated from several typical Indian soils, kaolins and bentonites have revealed a number of characteristic features of these systems (24-29). The more important of these which clearly bring out the part played by the electrical double layer and adsorption of ions, are discussed below.

### *a. Features of Titration Curves with Bases*

Hydrosols of the hydrogen clays show a pronounced acid character and give potentiometric and conductometric titration curves with bases

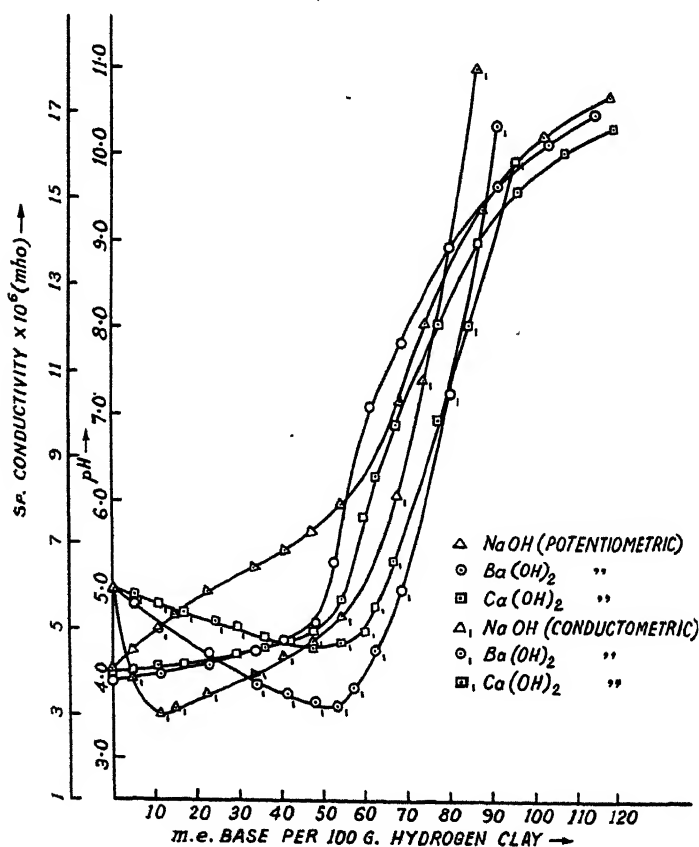


FIG. 7

having definite inflection points and breaks. The sols, however, show many striking differences from acids in true solution. Their titration curves with different bases have different forms. Potentiometric titration

curves with  $\text{Ba}(\text{OH})_2$  and  $\text{Ca}(\text{OH})_2$  have a comparatively flat initial run indicative of strong acids (Fig. 7). The corresponding  $\text{NaOH}$ -curve shows a much steeper initial rise and, in this respect, resembles that of a weaker acid. The slopes of the descending portions of the conductometric titration curves are in the order  $\text{NaOH} > \text{Ba}(\text{OH})_2 > \text{Ca}(\text{OH})_2$  indicating, in contrast with the potentiometric curves, a stronger acid character of the conductometric titration curve with  $\text{NaOH}$  than with  $\text{Ba}(\text{OH})_2$  or  $\text{Ca}(\text{OH})_2$ . These contradictory features are reconciled if it be assumed that the greater the electrical adsorption of the cations of the base the greater will be the amount of secondarily adsorbed  $\text{H}^+$  ions liberated from the double layer which consequently can react with the base. The greater the liberation of such  $\text{H}^+$  ions the smaller would be the slopes of the conductometric curves which will thus resemble that of a weaker acid. The liberation of  $\text{H}^+$  ions would also diminish the slope of the potentiometric curve but in this case a smaller slope indicates a stronger acid.

*b. The Base Exchange Capacity of Clays: Its Ill-Defined Character and Dependence on the pH and on "Cation Effects"*

The base exchange capacity, *b.e.c.*, of a given hydrogen clay is not a fixed quantity but depends on the pH, and on cation effects associated with the formation of ion pairs on the surface. Usually, the greater the pH the greater is the *b.e.c.* calculated from the titration curve. The cation effect is illustrated by (a) the dependence of the *b.e.c.* calculated at the inflection point of the titration curve on the cation of the base, or, more strikingly, at a fixed pH, *e.g.*, pH 7.0; (b) by the much higher *b.e.c.* obtained on titration in the presence of a large concentration of a neutral salt than in its absence; and (c) by the different effects of various neutral salts having a common anion. The titration curves given in Fig. 8 illustrate these points.

In the absence of salts the *b.e.c.* usually decreases in the order  $\text{Ca}(\text{OH})_2 > \text{Ba}(\text{OH})_2 > \text{NaOH}$  which, however, changes to  $\text{Ba}(\text{OH})_2 > \text{Ca}(\text{OH})_2 > \text{NaOH}$  when the sol is titrated in the presence of a fixed high concentration of the corresponding salts. As in the case of silicic acid sols (p. 151), this reversal in the relative effects of  $\text{Ba}^{++}$  and  $\text{Ca}^{++}$  ions has been traced to differences in the range of pH in which the acid-base interaction takes place in the presence and absence of salts. When the salt is present, the interaction with  $\text{Ba}(\text{OH})_2$  or  $\text{Ca}(\text{OH})_2$  takes place in the acid region up to the inflection point which occurs between pH 4.5 and 7.0; the greater part of the acid reacts between pH 3.5 and 5.5. In the absence of salts, the inflection point in the titration curves with  $\text{Ba}(\text{OH})_2$  and  $\text{Ca}(\text{OH})_2$  usually occurs between pH 6.0 and 7.5 and the reaction with these bases up to the inflection point is mainly confined within the

range of pH 5 to 6.5. A relatively greater amount of  $Ba^{++}$  than  $Ca^{++}$  has been found to be adsorbed by completely desaturated soils on the acid side of a pH ranging between 5.5 and 6.5 when the soils were repeatedly leached with normal solutions of  $BaCl_2$  and  $CaCl_2$  having different pH values; more  $Ca^{++}$  than  $Ba^{++}$  was adsorbed on the alkaline side of this pH (30).

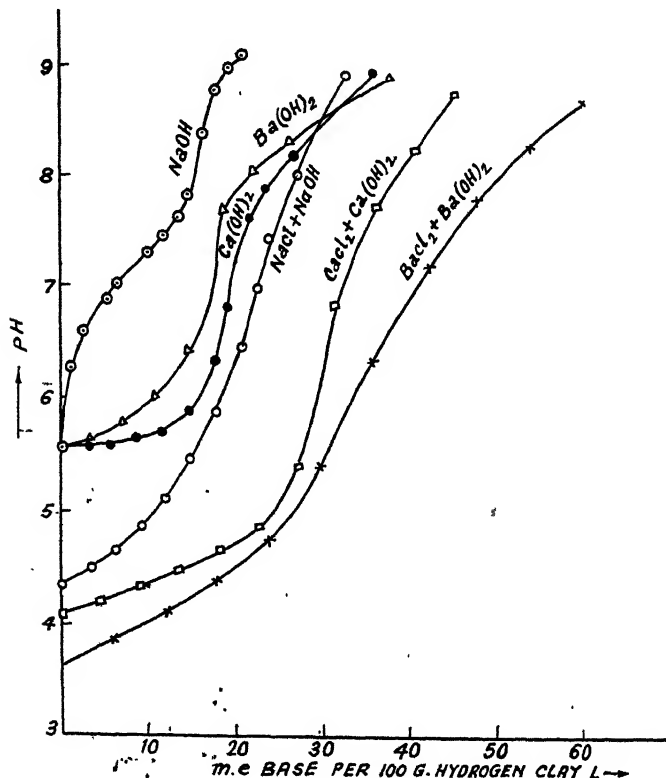


FIG. 8

In titrations in the presence of salts, the cation effect is regular in the sense that it follows the lyotrope series and is determined by the order of electrical adsorption of the cations together with their hydration envelopes (7, 8). At comparatively high pH in the absence of salts the cations are probably adsorbed in a dehydrated condition which accounts for the irregular or specific cation effect—irregular in the sense that it does not follow the lyotrope series—operating under these conditions.

The sol + salt mixture contains (1) free  $H^+$  and  $Al^{+++}$  ions (31, 32) displaced into the intermicellary liquid from the double layer, and (2)  $H^+$  ions (possibly also,  $Al^{+++}$  ions), free and bound, associated with the

flocs contained in the mixtures.\* When the mixture is titrated, the free  $H^+$  ions are at first neutralized and then, as the pH rises, more and more  $H^+$  ions are displaced from the surface in the presence of the salt to maintain equilibrium and are neutralized. The large number of cations present in the system materially helps this process and in consequence of this cation effect the sol *plus* salt mixture has a much larger *b.e.c.* compared with the sol itself. The  $H^+$  ions which are brought into a neutralizable condition on the addition of the salt to the sol are not all displaced into the intermicellary liquid. This is shown by the fact that a smaller *b.e.c.* is obtained on titrating the clear supernatant liquid above the coagula than on titrating the mixture itself, *i.e.*, the whole system containing the coagula and the supernatant liquid.

## 6. THE LATTICE STRUCTURE OF CLAY MINERALS IN RELATION TO THEIR ELECTROCHEMICAL PROPERTIES

Some characteristic differences between the electrochemical properties of hydrogen clays containing kaolinitic and montmorillonitic minerals as judged from X-ray and thermal analyses† have been observed.

The kaolinitic clays show a dibasic acid character within the range of pH 4–11 (33). The first inflection usually occurs between pH 7.0 and 8.0 and the second between pH 8.0 and 9.5 (Fig. 9).‡ The ratio of the *b.e.c.*'s at the two inflections is nearly 2.0 although the actual value of the *b.e.c.* varies in the case of different hydrogen clays and hydrogen kaolinites from 2.0 me. per 100 g. at the first inflection point, and from 4.0 to 40.0 me. per 100 g. at the second inflection.

Hydrogen clays containing only montmorillonitic clay minerals as judged from X-ray analysis usually show only one inflection between pH 7.1 and 8.8 in their titration curve with NaOH (Figs. 7 and 10) and between pH 5.2 and 7.5 when titrated with  $Ba(OH)_2$  and  $Ca(OH)_2$ . The *b.e.c.* calculated at this inflection varies from 55 me. to 120 me. per 100 g. for entire hydrogen clay fractions. A few montmorillonitic hydrogen clays having a dibasic acid character have been found but unlike kaolinitic clays, their first inflection occurs in the acid region (between pH 4.5 and 6.0) and the ratio of the *b.e.c.*'s at the two inflections is much greater than 2.0.

\* Displacement of  $Al^{+++}$  ions from hydrogen clays by neutral salts will be discussed in a later paper.

† By Mr. S. N. Bagchi of this laboratory.

‡ The points (represented by  $\Delta$ 's) in the titration curve beyond the first inflection represent pH values measured ten days after the addition of increasing amounts of NaOH to equal volumes of the sol taken in a series of jena glass bottles. Details will be published in a later paper.



Another criterion for differentiating kaolinitic clays from those containing montmorillonitic minerals has been found, and is based on the effect of addition of NaOH on the viscosity of aqueous suspensions of the hydrogen clays (34). On the gradual addition of the alkali to hydrosols of hydrogen bentonites and montmorillonitic hydrogen clays, their vis-

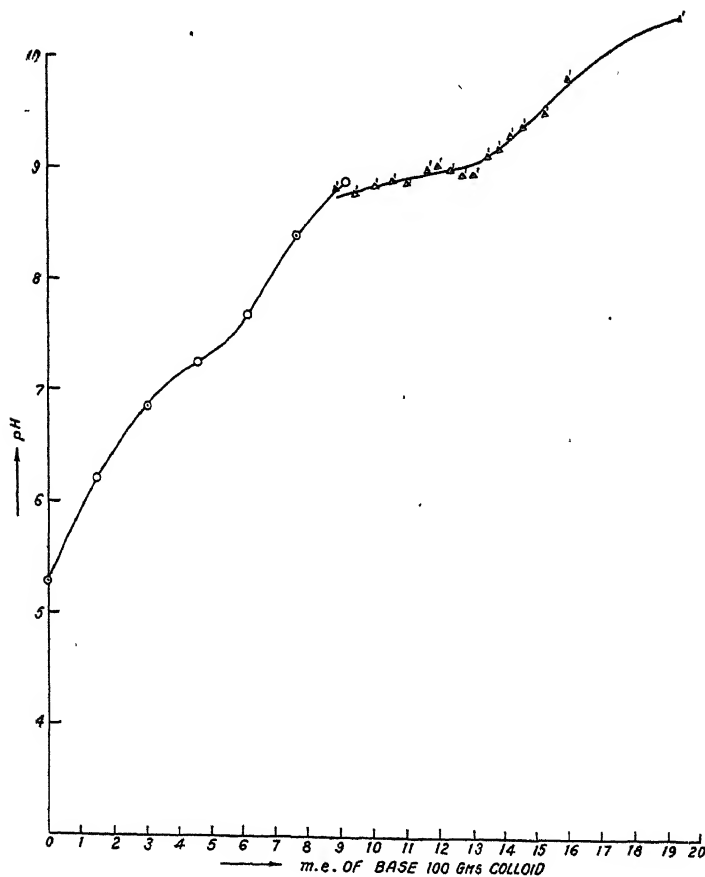


FIG. 9

cosity increases and passes through a maximum value at a point corresponding to about 75% neutralization of the amount of the acid given by the inflection point of the titration curve (Fig. 10). Apart from a slight initial decrease, the alkali has no marked effect on the viscosity of the hydrogen kaolinite and hydrogen clays containing kaolinitic minerals within the range of pH 4-11.

Work on the above lines on pure specimens\* of other clay minerals, *e.g.*, halloysite, illite and attapulgite is in progress.

Judging from the electrochemical and viscous criteria mentioned above (and from X-ray and thermal studies) hydrogen clays from entire clay fractions of some Indian laterite soils, *e.g.*, those obtained from a red earth from Coimbatore and a laterite soil from Belgaon (Bombay Presidency), have been found to contain only kaolinitic minerals. On the other

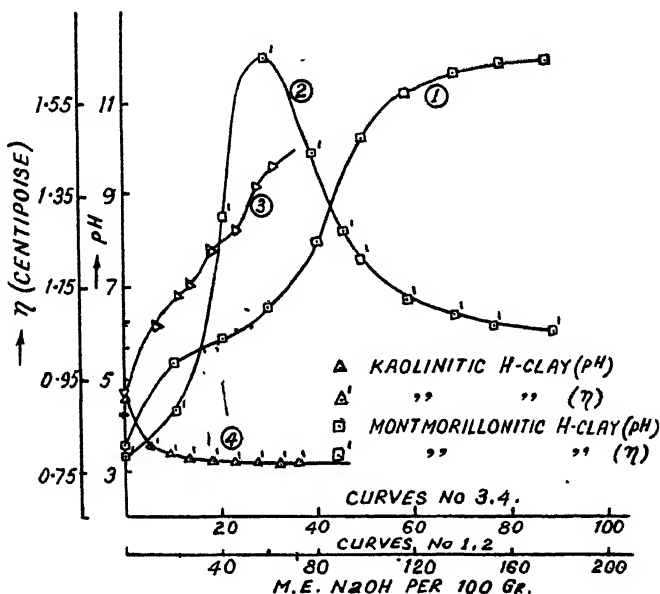


FIG. 10

hand, montmorillonite is the dominant and often the only mineral constituent of hydrogen clays from Indian "black cotton" soils, *e.g.*, those obtained from Government Farms at Satara in Bombay Presidency, and Nagpur, Akola and Raipur in the Central Provinces. Some lateritic soils of Bengal, *e.g.*, those from Dacca and Burdwan, and two acid soils from Jorhat and Latekujan in Assam have been found to contain mainly kaolinite and some montmorillonite in their clay fraction. Judging from investigations carried out so far, hydrous mica or illite does not appear to be as common a constituent of the clay fraction of Indian soils as kaolinite or montmorillonite. Only surface soils have been examined up to now. The work will soon be extended to include soil profiles.

\* Made available through the kindness of Dr. C. S. Ross of the U. S. Geological Department, Dr. G. Nagelschmidt of Rothamsted Experimental Station, England, and Dr. S. B. Hendricks of the Bureau of Chemistry and Plant Industry, U. S. A.

Subfractions of hydrogen clays, hydrogen kaolins and hydrogen bentonites, having particle sizes ranging between specified limits and mechanically separated from the same entire clay fraction, usually give similar titration curves with bases (35). Differences have also been observed, and in such cases the chemical composition, *b.e.c.* and mineralogical makeup are different from those of the other subfractions. In the case of some kaolins containing mainly kaolinite and some montmorillonite in the entire clay fraction, the latter mineral has been found to be concentrated in the finer subfractions judging from the electrochemical and viscous criteria mentioned above and also from X-ray and dehydration studies.

## REFERENCES

- 1.(a) MUKHERJEE, J. N., *Kolloid-Z.* **62**, 257 (1933); *ibid.* **63**, 36 (1933).  
 (b) MUKHERJEE, J. N., MITRA, R. P., AND MUKHERJEE, S., *Trans. Natl. Inst. Sci. India*, **1**, 227 (1937).
2. HARTLEY, G. S., COLLIE, B., AND SAMIS, C. S., *Trans. Faraday Soc.* **32**, 795 (1936).
3. LOTTERMOSER, A., AND PÜSCHEL, F., *Kolloid-Z.* **63**, 175 (1933).
4. LOTTERMOSER, A., AND FROTSCHER, H., *Kolloid-Beihfte* **45**, 303 (1937).
5. MCBAIN, J. W., AND BETZ, M. D., *J. Am. Chem. Soc.* **57**, 1909 (1935); see also *Colloid Chemistry*, edited by J. Alexander, Vol. 5, p. 102, Reinhold Publ. Corp., 1944.
6. HARTLEY, G. S., *Kolloid-Z.* **88**, 22 (1939).
7. MUKHERJEE, J. N., *Trans. Faraday Soc.* **16**, 103 (1921).
8. MUKHERJEE, J. N., *Phil. Mag.* **44**, 321 (1922).
9. MUKHERJEE, J. N., AND SEN GUPTA, N. C., *Nature* **145**, 971 (1940).
10. KÖRTUM, G., *Z. physik. Chem. B* **34**, 255 (1936).
11. MUKHERJEE, J. N., RAYCHAUDHURI, S. P., AND BHATTACHARYYA, A. S., *J. Indian Chem. Soc.* **5**, 735 (1928); see also No. 12.
12. MUKHERJEE, J. N., CHAUDHURI, S. G., AND GHOSH, B. N., *Trans. Natl. Inst. Sci. India* **1**, 47 (1935).
13. WIEGNER, G., AND PALLMANN, H., *Verhand. zwei. Komm. alk., Subkomm. Int. Bod. Ges.* **92**, 1929.
14. SANDERS, G. P., *Ind. Eng. Chem., Anal. Ed.* **10**, 274 (1938).
15. MUKHERJEE, J. N., MITRA, R. P., AND MANDAL, S. S., *Nature* **155**, 329 (1945).
16. MCBAIN, J. W., AND SALMON, C. S., *Proc. Roy. Soc. (London)* **97A**, 44 (1920).
17. GHOSH, B. N., *J. Chem. Soc.* **128**, 2605 (1926).
18. MUKHERJEE, S., *J. Indian Chem. Soc.* **14**, 17 (1937).
- 19.(a) CHATTERJEE, B., *J. Indian Chem. Soc.* **16**, 589 (1939); see also MUKHERJEE, J. N., AND CHATTERJEE, B., *Nature* **155**, 85 (1945).  
 (b) CHATTERJEE, B., *J. Indian. Chem. Soc.* **16**, 607 (1939).
20. JOSEPH, A., AND HANCOCK, J. S., *J. Chem. Soc.* **123**, 2022 (1923).
21. Unpublished work of Dr. B. Chatterjee.
22. } Unpublished work of Mr. J. N. Mukherjee.
23. }
24. MITRA, R. P., *Indian J. Agri. Sci.* **6**, 555 (1936).
25. MITRA, R. P., MUKHERJEE, S. K., AND BAGCHI, S. N., *Indian J. Agr. Sci.* **10**, 303 (1940).
26. MITRA, R. P., *Indian J. Agr. Sci.* **10**, 317 (1940).

27. MITRA, R. P., *Indian Soc. Soil Sci. Bull No. 4*, 41 (1941-42).
28. MUKHERJEE, J. N., AND MITRA, R. P., *Indian J. Agr. Sci.* **12**, 433 (1942).
29. MUKHERJEE, J. N., AND MITRA, R. P., *Nature* **154**, 824 (1944).
30. Unpublished work of Dr. S. K. Mukherjee.
31. CHATTERJEE, B., *Indian Soc. Soil Sci. Bull No. 4*, 148 (1941-42); see also MUKHERJEE, J. N., AND CHATTERJEE, B., *Indian J. Agr. Sci.* **12**, 105 (1941-42).
32. MUKHERJEE, J. N., AND CHATTERJEE, B., *Nature* **155**, 268 (1945).
33. MITRA, R. P., AND BISWAS, T. D., *Proc. 31st. Indian Sci. Cong.* **3**, 152 (1944); see also No. 29 and 27.
34. MITRA, R. P., INDRA, M. K., AND RAY, B. G., *Proc. 31st. Indian Sci. Cong.* **3**, 152 (1944); see also No. 29.
35. MITRA, R. P., BAGCHI, S. N., RAY, S. P., AND MUKHERJEE, S., *Indian J. Agr. Sci.* **13**, 18 (1943).



## SURFACE FILMS OF POLYMERS.

### PART II. FILMS OF THE COHERENT AND SEMI-CRYSTALLINE TYPE

D. J. Crisp

*From the Department of Colloid Science, The University, Cambridge, England*

*Received August 3, 1945*

#### INTRODUCTION

In the previous paper (Surface Films of Polymers, Part I) the properties of fluid surface films of polymers are described. The present paper deals with surface films of coherent and semi-crystalline types.

#### COHERENT TYPE OF FILM (GROUP II)

The mutual cohesion between the chains is considerably greater than in the previous groups (Part I), but dilute solutions can be spread at the air-water surface to give uniform films with reproducible force-area characteristics. The specific areas are usually low and the expanded region at low surface pressure is lacking. As long as the maximum surface pressure is not too high and the films are not held long at this pressure, the force-area curve can be retraced on reducing the pressure. Beyond a certain point, however, this ceases to be possible, hysteresis effects and some degree of permanent loss becoming apparent. The films gelate at low surface pressure (below 5 dynes/cm.), becoming increasingly coherent as the area is reduced and sometimes breaking up into islands with sudden drop in surface pressure when the area is increased. The surface viscosity and rigidity is of a very high order so that successful multilayer deposition is difficult or impossible, the film breaking and the base-plate emerging wet. Threads drawn from the collapsed film are inextensible and brittle.

#### SIMPLE METHACRYLIC ESTERS

Both in the solid state and in films, polymethacrylates show remarkable differences from polyacrylates. It is difficult to see how this could be caused simply by the increased van der Waals attraction of a single methyl group. Inspection of models reveals that acrylates possess a loose structure allowing flexure of the chain, but the addition of  $\alpha$ -methyl

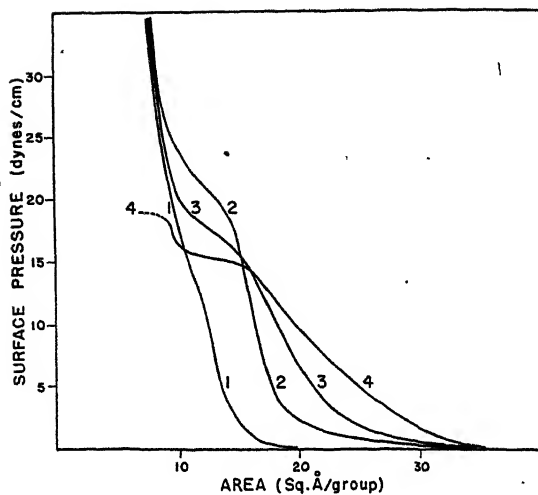


FIG. 1

Force-Area Curves for Polymethacrylates

- (1) Polymethyl Methacrylate; (2) Polyethyl Methacrylate; (3) Poly-*n*-propyl Methacrylate; (4) Poly-*n*-butyl Methacrylate

All readings taken slowly to avoid hysteresis

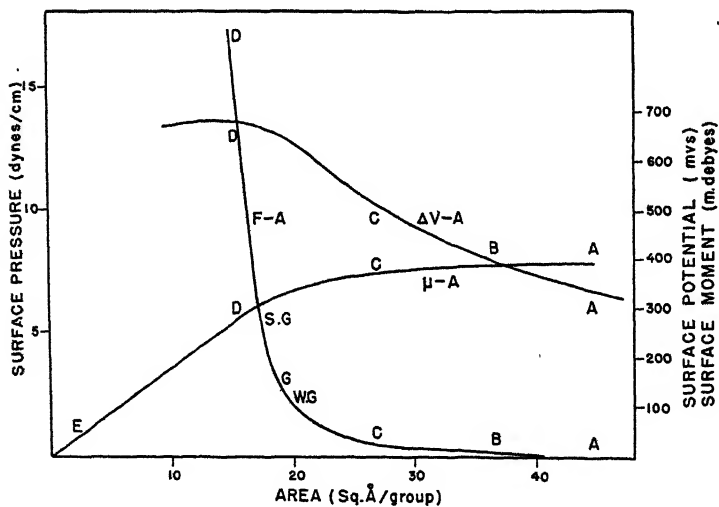


FIG. 2

Surface Pressure, Potential and Moment Data for Ethyl Methacrylate Polymer 18°C.  
(M.W.  $\approx$  100,000)

W.G. = weak gel; G = gelated; S.G. = strong gel

groups locks the main chain, restricting rotation and possible orientations very considerably. This will result in decreased kinetic movement except at much higher temperatures (Tuckett, 1942). Mead and Fuoss (1942) have shown that the moment of the methacrylate is less than that of the acrylate, has a positive temperature coefficient and broader dispersion maximum, all indicating limited dipole rotation.

Similar differences exist when these two series of compounds are spread at an air-water interface. Fig. 1 gives force-area curves of polymethyl, -ethyl, -*n*-propyl and -*n*-butyl methacrylates; Fig. 2 the surface potential and moment of polyethyl methacrylate as a typical example, which may be compared with the previous figure for polyethyl acrylate (Part I, Fig. 2). This comparison brings out two important differences. Firstly, the expanded region (BC) of low pressure and constant dipole moment is reduced, and secondly, the film shows elastic properties at very low surface pressures. It indicates the lack of freedom of the molecules to whip about in the surface, the chains being held by lateral van der Waals forces, supplemented by dipole forces when the film contains a significant proportion of collapsed residues. The area occupied by each molecule includes little free space between the chains when the surface micelles are brought into contact. Polypropyl and polybutyl methacrylates are somewhat transitional between Group I and Group II.

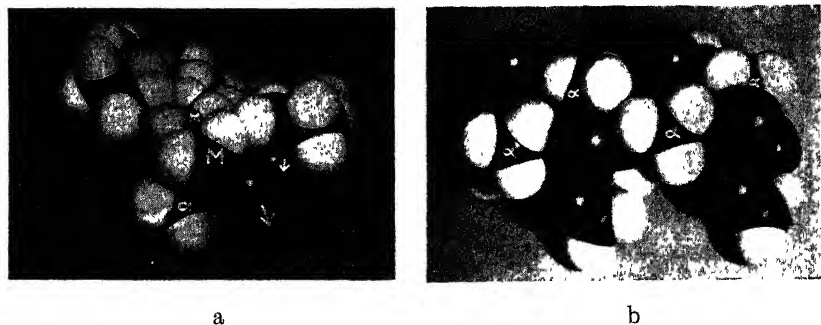


Fig. 3

Orientation of Methacrylate Polymers at the Air-Water Interface

(a) Ethyl Methacrylate, viewed along the chain; (b) Methyl Methacrylate, viewed from below showing methyl groups

The values of the maximum dipole moments in polymethacrylates are close to those of the corresponding polyacrylates, though in general slightly lower. Consequently, the configuration of the ester group must be essentially the same. The position suggested for the polyacrylates cannot be reached by twisting the polymethacrylate chain since steric hindrance is encountered by the  $\alpha$ -methyl groups. An orientation in which the main chain is less deeply immersed and the side chains forced



out laterally appears most probable, and is illustrated in Fig. 3. The moment calculated from this model is slightly less than that of the polyacrylates and the specific areas should increase with the addition of the first few  $\text{CH}_2$  groups, since these not only increase the absolute area of the residue by pushing outwards, but will also decrease the lateral attraction. This increase in area is verified by experiment (Table I).

TABLE I

Polymer	Area (calc.) (cis)	Moment (calc.) (cis)	Area (calc.) (trans)	Moment (calc.) (trans)	Area (obs.) from $\Delta F \rightarrow 0$	Area (obs.) from $\Delta\mu \rightarrow \mu_m$	Max. moment (obs.)
Polymethyl methacrylate	22.5 $\text{\AA}^2$	450 m.d.	20 $\text{\AA}^2$	200 m.d.	14.5 $\text{\AA}^2$	18.5 $\text{\AA}^2$	260-270 m.d.
Polyethyl methacrylate	27 $\text{\AA}^2$	450 m.d.	22 $\text{\AA}^2$	200 m.d.	19 $\text{\AA}^2$	22 $\text{\AA}^2$	390 m.d.
Poly- <i>n</i> -propyl methacrylate	28 $\text{\AA}^2$	450 m.d.	22 $\text{\AA}^2$	200 m.d.	23.5 $\text{\AA}^2$	26.5 $\text{\AA}^2$	445 m.d.
Poly- <i>n</i> -butyl methacrylate	28 $\text{\AA}^2$	450 m.d.	22 $\text{\AA}^2$	200 m.d.	27 $\text{\AA}^2$	28.5 $\text{\AA}^2$	470 m.d.

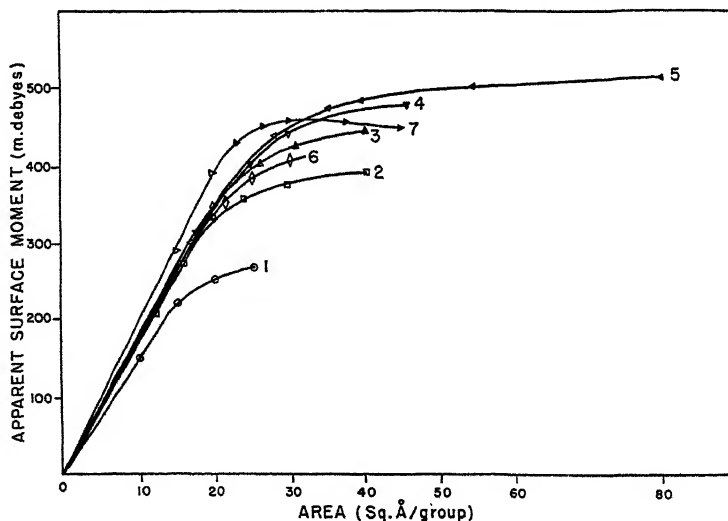


FIG. 4

Apparent Surface Moments of Polymethacrylates

1. Methyl; 2. Ethyl; 3. *n*-Propyl; 4. *n*-Butyl; 5. Ethoxyethyl;
6. Cyclohexylmethyl; 7. Octadecyl

Fig. 4 gives the apparent surface dipole moments of the methacrylates as a function of specific area. The curves show the same features as those of the acrylates, suggesting again that some of the residues in the lower

members are partially collapsed into a three-dimensional form at the lowest surface pressure. Interchain cohesion is, however, much stronger in methacrylates and it is possible that these lateral forces might constrain some of the ester groups toward the *trans* position, at least in methyl methacrylate, the conditions then bearing an analogy with condensed films of methyl and ethyl esters, where the attractions of the hydrophobic chains compress the ester group into a *trans* or an intermediate form (Alexander, 1942c). The observed moment is greater than that of the *trans* orientation however, and the maximum moments approximately in proportion to the limiting areas. It is therefore more likely that all the residues at the interface remain in the *cis* form.

The great resistance of methacrylate polymers to hydrolytic agents is therefore a little surprising. But Fig. 3(b) shows that the  $\alpha$ -methyl groups in the orientated molecules at the interface are directed toward the water, tending to shield the polar groups. This feature, coupled with the strong intermolecular forces, may prevent easy access to the ester group (Alexander and Schulman 1937, Schulman 1941).

#### OTHER METHACRYLIC ESTERS

*Poly- $\beta$ -Ethoxyethyl Methacrylate.* This substance differs from poly-*n*-butyl methacrylate only in the introduction of a polar group into the

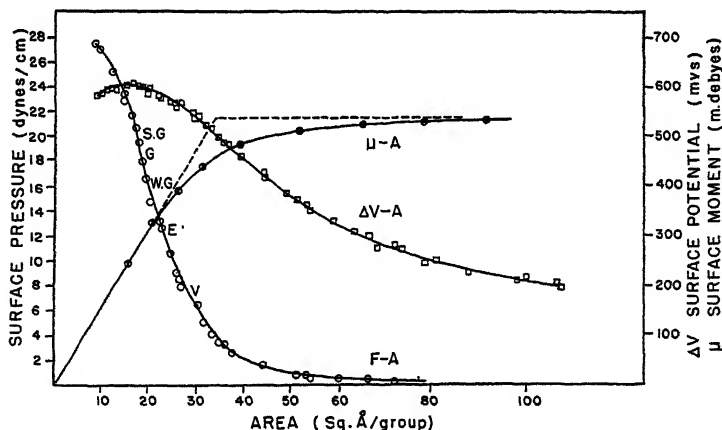


FIG. 5

Poly- $\beta$ -Ethoxyethyl Methacrylate (M.W. 33,000)

3 Sets of observations 15–18°C.; pH 2 & 3

V = Viscous, E = Elastic; W.G. = Weak gel; G. = gel; S.G. = strong gel

side chain. As can be seen from Fig. 5 the film might well be classified in Group I, there being a considerable expanded region with free space between the chains. In this region the moment is 525 m.d. compared

with 470 in polybutyl methacrylate; the ether group raises the moment by only 50 m.d. instead of 200 as would be expected from an independent ether group (Alexander 1942(b)). Within the range below 40 Å<sup>2</sup> per residue the moments are identical. This indicates that the greater surface pressure of the β-ethoxy compound represents the free energy required to force the ether oxygen atom out of its position of maximum moment, possibly away from the interface. At higher surface pressure the film gels at an area close to the gelation area of the simple methacrylates, as would be expected if the ether group were forced out of the way, allowing the main chains to approach. The rather small increment in  $\mu$ , due to the ether dipole, is explicable with the aid of molecular models. If this group is brought down to the surface the ester group tends to swing into the *trans* position, so that the full dipolar orientation of both groups is not possible.

*Polycyclohexylmethyl Methacrylate.* This substance spreads rather badly. The specific area obtained, 27–28 Å<sup>2</sup> per residue at zero pressure, is rather low since normally a cyclohexyl ring would itself occupy about this area excluding other parts of the molecule (Danielli and Adam, 1936). The moment is 430 m.d., again suggesting that spreading may not be complete. Careful experiments show that the area increases slightly when the spreading solution is diluted or spread over a larger initial area. The film is very unstable and highly coherent, gelating at zero surface pressure and collapsing slowly and irreversibly at 8–10 dynes per cm.

*Polyoctadecyl Methacrylate.* (Fig. 6.) The effect of introducing a long hydrophobic chain into a polyester is of considerable interest as it combines certain features of both polymer and long-chain films. The specific area and moment is of the same order as those of other methacrylic esters, the limiting area by extrapolation of the *F*–*A* curve being 30.5 Å<sup>2</sup>, and the moment 460 m.d.

The hydrocarbon chains compress down to about 21.6 Å<sup>2</sup> at 40 dynes/cm., but the film becomes rather unstable at higher surface pressures. The film is solid at 5 dynes/cm. and becomes increasingly rigid as the area is reduced. If the film is placed at about 10 dynes compression, and the temperature raised from 20 to 30°C. liquefaction sets in quite suddenly. Gel films of the lower polymethacrylates are weakened by raising the temperature, but, except with β-ethoxyethyl methacrylate, a rise from 20° to 65°C. did not succeed in bringing about complete liquefaction. This unique feature of polyoctadecyl methacrylate shows that the paraffin chains, which in the two-dimensional state melt at about this temperature, largely determine the state of the film. The form of the *F*–*A* curve is also significant, as it has a lower more compressible region up to 13 dynes/cm. and a less compressible region of close-packed chains up to its collapse point. It will be recalled that in long-chain

triglycerides and in pentaerythritol tetrapalmitate very similar conditions prevail; at low surface pressure the linked polar heads limit the area, but as the pressure increases these groups merely serve as anchors, the long chains compressing down to  $20 \text{ \AA}^2$  apiece.

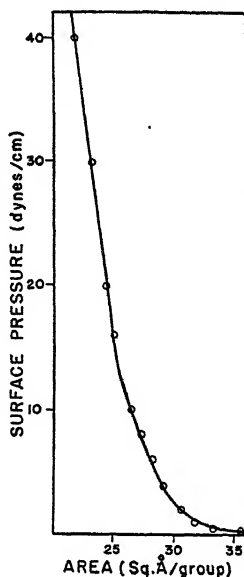


FIG. 6

Polyoctadecyl Methacrylate. Force-Area Curve

The moment of the film does not fall until the pressure has risen to 10 dynes/cm. and the area reduced to  $25 \text{ \AA}^2$  showing that the hydrophobic chains do in fact stabilize the molecule and prevent the collapse of polar groups from the plane of the surface.

#### EFFECT OF SIDE CHAINS ON THE STATE OF FILMS

Table II gives the area and surface pressure at which various stages of gelation set in for a series of polymethacrylates in which the side chain length is varied.

Increasing the length of the side chain causes a rise in the gelation pressure, which indicates that the internal forces between the main chains have been reduced and a greater external pressure is, therefore, required to bring the film molecules together. Nevertheless, the specific area at which gelation occurs does not increase markedly with the length of the side chain except from methyl to ethyl methacrylate. The packing in the film at isoelastic points is therefore similar.

When the side chain is either a very long hydrocarbon chain (polyoctadecyl methacrylate) or a ring (polycyclohexylmethyl methacrylate, "benvar"), interlocking of these groups can occur causing the film to become solid. It is interesting to note that the strong forces in octadecyl methacrylate can be eliminated by increasing the temperature above 30°C. or by spreading at an oil-water interface, where the film is fluid.

TABLE II  
*Gelation Areas (A) and Surface Pressures (F) in Polymethacrylates*

Condition	Methyl		Ethyl		Propyl		Butyl		$\beta$ -Ethoxyethyl	
	A	F	A	F	A	F	A	F	A	F
Elastic	20 Å <sup>2</sup>	0.1 dy./cm.	34 Å <sup>2</sup>	0.25 dy./cm.	21.5 Å <sup>2</sup>	5.0 dy./cm.	23.5 Å <sup>2</sup>	6.0 dy./cm.	22.4 Å <sup>2</sup>	12.0 dy./cm.
Weak gel	17 Å <sup>2</sup>	0.5 dy./cm.	23 Å <sup>2</sup>	1.0 dy./cm.	20.0 Å <sup>2</sup>	7.0 dy./cm.	21.3 Å <sup>2</sup>	8.0 dy./cm.	21.0 Å <sup>2</sup>	16.0 dy./cm.
Gel	15.7 Å <sup>2</sup>	1.0 dy./cm.	18.8 Å <sup>2</sup>	3.0 dy./cm.	19.0 Å <sup>2</sup>	8.0 dy./cm.	18.1 Å <sup>2</sup>	12.0 dy./cm.	18.5 Å <sup>2</sup>	18.5 dy./cm.
Strong gel	14.7 Å <sup>2</sup>	2.5 dy./cm.	17.4 Å <sup>2</sup>	6.0 dy./cm.	17.2 Å <sup>2</sup>	12.0 dy./cm.	16.5 Å <sup>2</sup>	15.0 dy./cm.	17.0 Å <sup>2</sup>	19.5 dy./cm.

Very similar differences in mechanical properties exist in the bulk state. The substitution of short side chains by flexible ones renders the plastic softer and more rubber-like (internal plasticization) while the introduction of long chains or rings causes secondary cohesions and greater rigidity. (E. I. du Pont de Nemours and Co., 1936.) There are, however, two differences between surface and bulk plasticization of polymers. Firstly, the introduction of polar side chains will have a very marked effect in expanding the film, whereas in the bulk only the size and flexibility of the side chains are important. Secondly, at the interface the hydrophobic chains tend to be orientated away from the interface and adlineated, but in the bulk they will be more randomly distributed. Consequently hydrocarbon chains have a greater condensing effect at the surface. Thus "Octvar" is more condensed and rigid than "Butvar" at the surface (Part I, Fig. 7) though in the bulk it is more rubber-like. Similarly, in polyacrylates, condensing effects due to the side chains set in as low in the series as butyl acrylate.

#### OIL-WATER INTERFACE MEASUREMENTS

The greatly increased cohesion in methacrylate films may be demonstrated by spreading at the oil-water interface, where the presence of oil molecules above the film reduces the lateral field of force. As a result the films are more expanded and fluid, and in some cases more fully spread.

The ideal method of expressing the degree of expansion of a film is to employ an equation of state which includes a term for the attractive forces along the plane of the surface, and can be applied both at the

oil-water and at the air-water interface (Alexander and Teorell, 1939). Unfortunately, no general formula of this type has been derived for a polymer film and such a method is, therefore, impossible. Differences in expansion can, however, be seen from a comparison of the areas per group, at a surface pressure of 5 and 10 dynes/cm. respectively.

Table III illustrates the much greater expansion of coherent films, particularly the unstable polymethyl and cyclohexylmethyl methacrylates, when brought to the cyclohexane-water interface, compared with

TABLE III  
*Comparison of Areas at Air-Water and Oil-Water Interface*

Film	Gelling pressure	Areas at 5 dynes/cm.		Areas at 10 dynes/cm.	
		Air-water	Oil-water	Air-water	Oil-water
Polymethyl acrylate	c. 18 dy./cm.	20.1 Å <sup>2</sup>	26.4 Å <sup>2</sup>	15.7 Å <sup>2</sup>	19.8 Å <sup>2</sup>
Polymethyl methacrylate	zero.	14.0 Å <sup>2</sup>	30.3 Å <sup>2</sup>	13.0 Å <sup>2</sup>	24.0 Å <sup>2</sup>
Polyethyl acrylate	fluid.	24.6 Å <sup>2</sup>	30.5 Å <sup>2</sup>	19.8 Å <sup>2</sup>	23.7 Å <sup>2</sup>
Polyethyl methacrylate	c. 1 dy./cm.	17.2 Å <sup>2</sup>	35.0 Å <sup>2</sup>	16.0 Å <sup>2</sup>	28.4 Å <sup>2</sup>
Polyisopropyl acrylate	fluid.	28.5 Å <sup>2</sup>	35.5 Å <sup>2</sup>	24.6 Å <sup>2</sup>	27.8 Å <sup>2</sup>
Poly- <i>n</i> -propyl methacrylate	c. 5 dy./cm.	21.1 Å <sup>2</sup>	36.3 Å <sup>2</sup>	18.2 Å <sup>2</sup>	29.2 Å <sup>2</sup>
Poly- <i>n</i> -butyl acrylate	fluid.	28.2 Å <sup>2</sup>	34.5 Å <sup>2</sup>	25.6 Å <sup>2</sup>	28.5 Å <sup>2</sup>
Poly- <i>n</i> -butyl methacrylate	c. 7 dy./cm.	25.5 Å <sup>2</sup>	41.6 Å <sup>2</sup>	19.8 Å <sup>2</sup>	33.0 Å <sup>2</sup>
Polycyclohexylmethyl methacrylate	zero.	24.4 Å <sup>2</sup>	42.7 Å <sup>2</sup>	21.8 Å <sup>2</sup>	31.0 Å <sup>2</sup>
Polyoctadecyl methacrylate	zero. fluid above 30°C.	28.1 Å <sup>2</sup>	37.8 Å <sup>2</sup>	—	—

the smaller degree of expansion of fluid acrylate films. Similar results were obtained at the benzene-water interface. The differences between force-area curves of polyacrylates and polymethacrylates are very much reduced at an oil-water interface, while, in an homologous series, the areas occupied at a given surface pressure do not vary greatly with increase in length of the side chain, only the lower members having appreciably smaller areas. The effect of the oil is to eliminate differences due to attractions along the surface.

The method of Alexander and Teorell (1939) is not favorable for the detection of transition points in the force-area curve. Nevertheless, results of a series of runs seemed to indicate that there was a discontinuity at a surface pressure close to the gelation point in films of methyl and ethyl methacrylates. Even interfacial films of polypropyl, polybutyl, polycyclohexylmethyl and polyoctadecyl methacrylates which did not gelate, showed discontinuities at areas corresponding with the onset of gelation at the air-water surface.

Certain films which are probably badly spread at the air-water interface can be spread efficiently by the method above. Fig. 7 illustrates a typical unstable film (cellulose acetate) at the air-water interface and the greatly expanded curve obtained at the cyclohexane-water interface. The film gels at the oil-water interface at  $65 \text{ \AA}^2$ , and the discontinuity is clearly seen in this region. The area obtained is identical with the limiting areas of cellulose ethers at the air-water interface (Adam 1933) and about

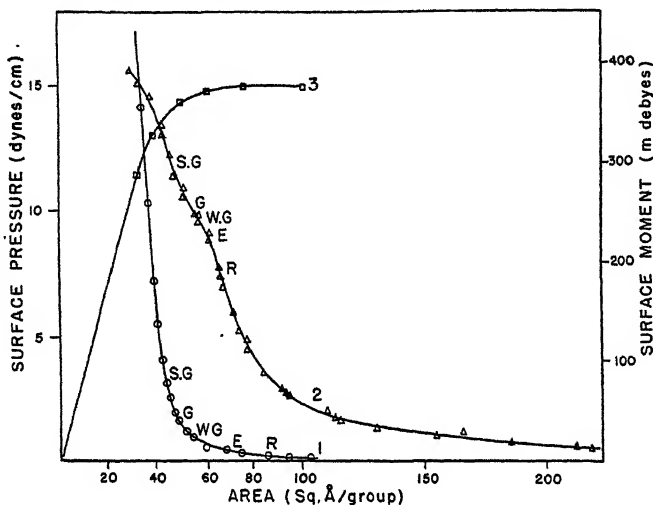


FIG. 7

Surface Pressure-Area Curves for Cellulose Triacetate  
 1. Air-Water interface; 2. Cyclohexane-Water interface;  
 3. Surface Moment at Air-Water interface

that of the pyranose rings lying flat. It may be concluded that the gelation area or discontinuity at the oil-water interface marks the limiting areas of the chains lying flat, further compression of the film results in polymer either passing into solution in the oil phase, or, if insoluble, forming a coherent skin.

### HYSTERESIS EFFECTS

Langmuir and Waugh (1940) describe a phenomenon of pressure aging in protein films, in which hysteresis loops appear in the high pressure region of the force-area curves. This they attribute to pressure displacement into an "underfilm" of certain of the more hydrophilic residues. Very similar processes are evident with all films of the coherent type. By studying the effect caused by differences in the nature of the plastic it has been possible to draw more definite conclusions with regard to the mechanism of the process.

The shape of the double inflexion in propyl and butyl methacrylate films is somewhat dependent on the rate at which the film is compressed (Fig. 1). With ethyl methacrylate the inflexion is not very evident unless

carefully timed readings of the surface pressure are taken. A series of hysteresis loops very similar to those given by Langmuir and Waugh are

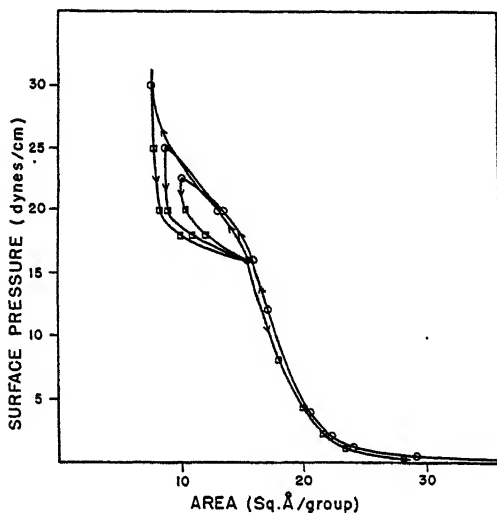


FIG. 8a

Hysteresis in Films of Ethyl Methacrylate

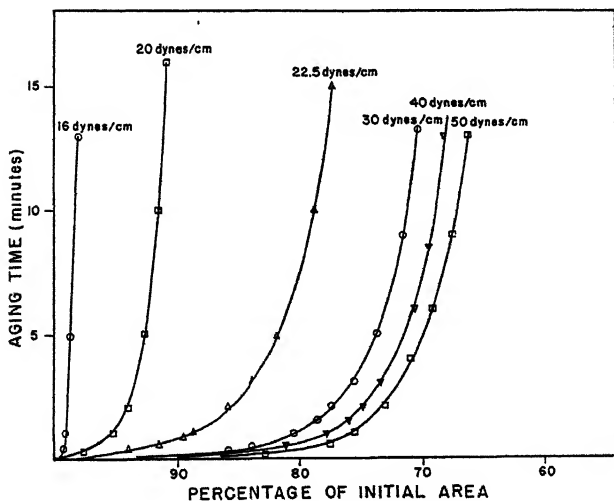


FIG. 8b

Pressure Aging in Films. Ethyl Methacrylate

shown in Fig. 8a while in Fig. 8b the effect of pressure aging on films of ethyl methacrylate is recorded. The film is kept at constant surface pressures up to 50 dynes/cm., and the area recorded at intervals. When



the film is re-expanded after this treatment a permanent reduction in area is observed, greater when the film has been held at higher surface pressure, but negligible below 10 dynes/cm., and a loss of only about 8% at 50 dynes/cm. aging pressure.

Films of methyl and cyclohexylmethyl methacrylate behave somewhat similarly, but the inflexion is less clearly marked and permanent collapse takes place more readily. Certain very unstable films described below (cellulose acetate, "benvar," nylon), which collapse spontaneously, do not give hysteresis loops since there is very little re-expansion when the pressure is reduced. On the other hand poly- $\beta$ -ethoxyethyl methacrylate retraces its  $F$ - $A$  curve up to 27 dynes without loss or hysteresis.

Thus the behavior of polymer films at high surface pressures falls into three classes:

- (1) No hysteresis or collapse, force-area curves reversible (Fluid type).
- (2) Hysteresis with little permanent collapse (Coherent type).
- (3) Permanent collapse without much hysteresis (Unstable type).

From the fact that these classes are not sharply distinguished, one may deduce that the process of collapse in coherent (Group II) films is not essentially different from that in fluid films (Group I), but owing to the high viscosity of coherent films the change does not take place rapidly until the imposed pressure is somewhat greater than the true collapse pressure. As would be expected, the more coherent the plastic and the lower its gelation pressure, the greater is its lag during collapse. As collapse continues the film thickens into a poly-layer, gradually acquiring the mechanical strength of the bulk polymer, which resists compression, accounting for the sharper rise in surface pressure at about  $10 \text{ \AA}^2/\text{group}$  (Fig. 1).

Direct evidence of collapse may be observed under the dark field illuminator, folds and streaks appearing in the region where the  $F$ - $A$  curve begins to turn over. There is no change in surface potential during the inflexion of the curve, again indicating collapse, the surface being unable to accommodate more polar groups.

With increasing molar cohesion the polymer units may become so strongly attached to each other (and possibly dehydrated) during collapse that they cannot be drawn back into the surface by their polar groups. Therefore, some degree of permanent collapse accompanies hysteresis; in the unstable type of film, re-expansion is scarcely in evidence at all.

Table V gives the collapse pressures of coherent films (measured by very slow increments in surface pressure) together with the energy required to compress the films ( $\int F dA$ ) from the lowest measured pressures up to the beginning of collapse (Column 3) and to the end of the double inflexion (Column 4). Column 5 gives Alexander and Schul-

man's (1942) data for the energy necessary to immerse the side chain of the corresponding palmitic ester. If Langmuir and Waugh's assumption of an "underfilm" were correct, the energy to immerse a residue should increase with the number of methylene groups in the side chain as in Column 5. This is clearly not the case. Moreover, the energy should be least for the more polar side-chains, whose collapse pressures should be lower. In actual fact the polar residue of  $\beta$ -ethoxyethyl methacrylate

TABLE V  
*Collapse Pressures and Energies in Methacrylate Films*

1 Side chain	2 Collapse pressure	3 Energy of collapsing film	4 Energy for completely collapsing film	5 Work to immerse side chain in palmitate
	<i>dynes/cm.</i>	<i>cals./residue</i>	<i>cals./residue</i>	<i>cals./g. mol.</i>
Methyl	10-15	20	90	0
Ethyl	18-25	50	200	205
<i>n</i> -Propyl	16-20	75	230	460
<i>n</i> -Butyl	14-16	105	190	590
$\beta$ -Ethoxyethyl	20-27	360	570	—
Cyclohexylmethyl	8-12	45	110	—

requires the greatest energy to collapse it, while methyl and cyclohexyl-methyl methacrylate, which are known to have very strong molecular cohesion, require the least. It is, therefore, concluded that the mechanism involves the formation of an overfilm and the energy required is that to remove a residue from the interface to the bulk.

#### FILMS OF SEMICRYSTALLINE POLYMERS

These polymers have been shown by X-ray and electron diffraction patterns to exist either normally or on stretching in a more highly orientated form than the amorphous type described above.

**1. Expanded Semicrystalline Type (Group IV).** Polyvinyl alcohol, polyacrylic and polymethacrylic acids differ from the other plastics studied in being freely soluble in water. For this reason they show some properties similar to proteins. Like proteins they may be spread directly from the solid owing to the solvent action of the water setting free the polymer molecules, or they may be spread from aqueous and dilute alcoholic solutions. They are strongly adsorbed at the air-water interface from very dilute aqueous solutions, polyvinyl alcohol forming a gel film on the surface of a moderately dilute solution ( $10^{-4}$  g./cc.).

*Polyvinyl Alcohol.* Polyvinyl alcohol may be spread from dilute aqueous solution after the method of Gorter and Grendle (1926) for

proteins; addition of 50% ethyl or 30% propyl alcohol improves spreading very slightly (see Part I).

Unfortunately the pure compound was not obtainable since polyvinyl acetate, from which it is normally prepared, is very intractable to complete hydrolysis. Purified specimens were prepared by repeated precipitation from aqueous solution by acetone, which tends to separate out those molecules having fewer acetate groups, and allowance was made in the force-area and surface potential curves for the small proportion (2-3%) of acetyl residues still remaining.

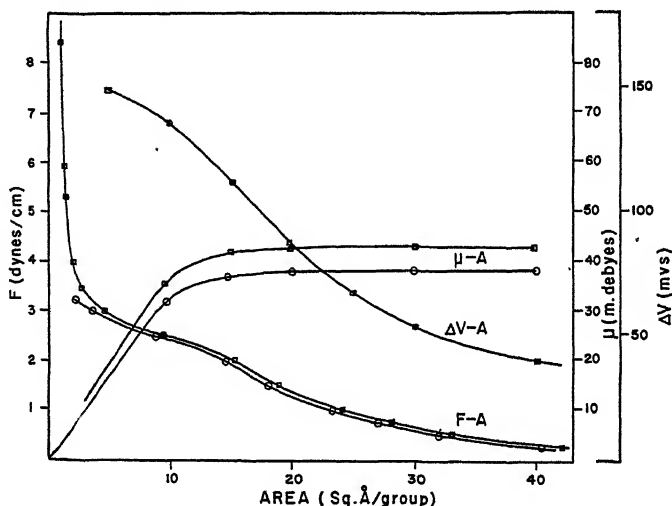


FIG. 9

Surface Pressure ( $F$ ), Potential ( $\Delta V$ ) and Moment ( $\mu$ ) for Polyvinyl Alcohol  
 $\square$  = Observed values;  $\circ$  = Value corrected for residual acetate groups

The film of polyvinyl alcohol is fluid and extremely compressible. At 2.5 dynes/cm. it shows a tendency to collapse, but on further reducing the area the surface pressure again rises, this time more sharply. This incompressible region has an exceedingly small specific area, and is due in part to the remaining acetate residues, and probably in part to collapsed polyvinyl alcohol. In this region gelation and solidification occur. The compressible region up to 20 Å<sup>2</sup>/residue is reversible, but it is difficult to establish accurately that no solution from the film occurs under pressure owing to the very small slope  $dF/dA$ . The film appears to be stable up to 2 dynes and no differences were found between samples prepared from polyvinyl acetates of different molecular weights.

As can be seen from Fig. 9, the film expands at low pressures to 40 or 50 Å<sup>2</sup> per residue; the moment is very small (40 m.d.), remaining

constant up to about  $20 \text{ \AA}^2$ . The very low value of the resolved moment is most remarkable, being less than a fifth that of a long-chain primary alcohol (Schulman and Hughes, 1932). On the other hand the area occupied is large, indicating a considerable free space between the chains. At 2-3 dynes/cm. the film collapses, both the collapse area and extrapolation of the  $\mu$ - $A$  curve give limiting areas of about  $12 \text{ \AA}^2$  per residue. Since the alcohol groups can be very compactly arranged the interchain distance across the surface will be  $4.8\text{--}5.0 \text{ \AA}^2$  and the inter-residue distance is  $2.5 \text{ \AA}$ , giving an area of  $12\text{--}12.5 \text{ \AA}^2$  per group. The moment of the alcohol group must be low either on account of its orientation, or because only a few alcohol groups are effectively present at the surface, the majority being above or below it. The second alternative does not accord with the relatively large areas observed. Nor is it likely that a film, which can be spread spontaneously from the solid, would contain a large proportion of unspread segments at very low surface pressure. Yet the moment remains low down to surface pressures less than  $0.2 \text{ dyne/cm}$ .

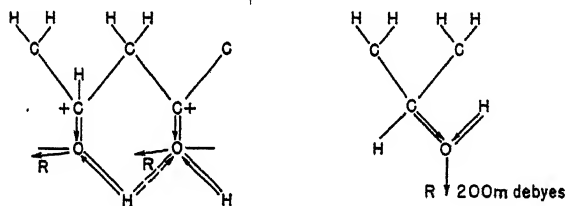


FIG. 10

Orientation of Alcohol Group; (1) in Polyvinyl Alcohol; (2) in Long-Chain Alcohol

It must, therefore, be concluded that the orientation of the  $:\text{CHOH}$  dipole in polyvinyl alcohol is quite different from that in a long-chain alcohol. In polyvinyl alcohol the  $-\text{OH}$  groups are situated very closely together. This must have two results: (a) the dipole interaction will be greater, there being a tendency for each dipole to swing the others out of the field; (b) the hydrogen atoms can be shared along the chain, these hydrogen bonds fixing the  $\text{C}-\text{OH}$  bond in the position shown in Fig. 10. In this position the contribution of the bonded alcohol group will be very small because the more powerful  $\text{H}^+-\text{O}^-$  dipole is directed against the field and the resultant moment horizontal. A similar mechanism may account for the low moment of  $\alpha$ -monoglycerides (Alexander, 1941). The proportion of residues bonded and freely orientated will depend on the bond energy, which may exceed that of liquid alcohols, or even water, since the distance separating the electronegative centers is less in polyvinyl alcohol ( $2.5 \text{ \AA}$ ).

The behavior of polyvinyl alcohol monolayers at collapse is of interest as the material is very soluble; up to at least 10% by weight. It would be expected, therefore, that the film would be unstable and pass into solution, especially when the film is compressed. This does not take place, however, since re-expansion of the film after compression is rapid and does not appear to be limited by a slow back diffusion from the substrate. Also, material is left in the surface after a very great reduction in area since it will form a visible surface gel. Thus equilibrium between the film and the overfilm or bulk phase is established much more rapidly than equilibrium between the surface and dissolved molecules, as has been noted in several other systems (Alexander, 1942c).

The very low collapse pressure indicates that the film passes into a microcrystalline state in which the internal energy is lowered by lattice forces. If the overfilm were amorphous, as in Group I polymers, a collapse pressure of the same order as the spreading pressure of simple organic alcohols would be expected; *viz.*, 40–50 dynes/cm.

*Polyacrylic and Polymethacrylic Acids.* These substances closely resemble polyvinyl alcohol but, as they may be prepared by catalytic polymerization of the monomer, their composition is definite. Both acids dissolve in water but not completely. On acid substrates spreading may be carried out as with polyvinyl alcohol, but on neutral substrate the film is unstable. The films closely resembled that of polyvinyl alcohol in all other respects. The dipole moment of polyacrylic acid was between 30 and 40 m.d., areas expanding out to 50 or 60 Å<sup>2</sup> but collapsing at about 3 dynes/cm. The condensed area found by extrapolating the  $\mu$ - $A$  curve was 22 Å<sup>2</sup> per residue, which is similar to that of a long-chain fatty acid. The films remain fluid up to very small areas, where gelation and secondary rise in pressure indicate the presence of a poly-layer. It is probable that the low dipole moment can again be accounted for by hydrogen bonding, the carboxyl groups pairing alternately along the chain, only a few being free to orientate.

Polymethacrylic acid collapses similarly at about 3 dynes/cm. This provides further evidence that collapse, even in soluble films, involves the formation of a microcrystalline phase above the surface rather than direct passage of the monolayer into solution. In the latter case the extra  $\alpha$ -methyl group of polymethacrylic acid should raise the collapse pressure considerably, but it would not necessarily alter the energy difference between the film and the crystal. If the pH of the substrate is increased, causing the films to become unstable and dissolve directly, the extra  $-\text{CH}_3$  group in methacrylic acid becomes effective.

Films of polyacrylic acid are stable up to pH 3, and the addition of  $M/2$  KCl had no effect on the observed areas. If solution were taking place during spreading, addition of salt would probably improve spreading as with proteins (Gorter, 1937). Between pH 3 and pH 4 the film dissolves out rapidly as it is spread, finally at pH 5 no film can be detected. If a few cc. of strong acid are injected beneath a collapsing film at pH 3.5, the film becomes stable and the area increases slightly, but not com-

pletely, indicating that some material had diffused away into the substrate. Polymethacrylic acid films are similarly affected by pH, the change occurring in a less acid range between pH 4.5 and 5. Kern's data (1939) on the ionization of these acids shows that polyacrylic acid dissolves from the film when about  $\frac{1}{10}$  ionized while methacrylic acid is  $\frac{1}{6}$  ionized. The film becomes unstable because the electrical potential set up by ionization lowers the energy of adsorption of the ionized residues. As a result, the net energy becomes too small to stabilize the film. Thus the degree of ionization necessary to render the film unstable depends on the adsorption energy of the neutral molecule. This being greater in methacrylic acid, the film is more fully ionized before solution occurs. Approximate calculations from the electrical data gave a reasonable value of about 700 cal./residue for the increment in energy of adsorption due to the  $\alpha$ -methyl group.

*Alginic Acid.* Neither alginic acid nor its salts were found to give stable films. Askew and Danielli (1936) have succeeded in spreading it at the bromobenzene-water interface, but even under these favorable conditions the film collapses readily.

*Poly- $\omega$ -Hydroxydecanoic Acid.* Polyesters in which the ester group lies in the main chain have been studied by Harkins, Carman and Ries (1935). They are classified here because their low collapse pressures (5–8 dynes) are associated with their greater degree of crystallinity compared with amorphous polyesters with side chains. They have a limiting area of 60 Å<sup>2</sup> per residue indicating a flat arrangement of the chains, and an apparent dipole moment of about 600 m.d. in the expanded condition before collapse. This is somewhat higher than in polyacrylates, possibly on account of greater freedom of the ester groups. Unfortunately the physical state of these films was not put on record.

**2. Coherent Semicrystalline Type (Group III).** When the polar groups are less strongly water-attracting, and strong lattice forces exist, the films are very unstable. Cellulose acetate, "benvar," and Nylon on neutral substrate are examples of this type of film.

*Nylon.* Nylon is the generic name given to linear polyamides having the structure  $((\text{CH}_2)_x\text{CO}\cdot\text{NH})_n$ . They resemble silk in physical properties, silk fibroin being the first member of the series where  $x = 1$ . They differ from proteins in having hydrocarbon groups in the main chain, and lacking side chains; hence, they provide useful material for examining the effect of a  $\text{CO}\cdot\text{NH}$  group in a polymer film.

The results of spreading films of Nylon ( $x = 4$ ) vary considerably with the substrate (Fig. 11). Except on strong acid the film is highly condensed, gelating at less than 1 dyne/cm. and collapsing readily. On neutral substrates there is some variation according to the initial area over which Nylon is spread, and the incompressible region, with an area of less than 10 Å<sup>2</sup> per residue, consists only of a thick collapsed skin. On a pH 2 substrate the film is still badly spread and coherent, but occupies a greater area, but on 3–5 *N* acid there is a marked expansion and the film is fluid up to 8 dynes/cm. pressure.

All these results can be related to the well known association of the keto-imino groups. There is considerable evidence that hydrogen bridges from the imino group of one residue to the carboxyl of another are stronger than the association between the peptide group and water. It is for this reason that, although strongly polar, the peptide link does not aid spreading or confer increased water solubility to the molecule. Thus, formamide absorbs heat on dissolving ( $\Delta H > 0$ ) and the solubility of polypeptides rapidly diminishes with chain length (Abderhalden and Fodor, 1916), in marked contrast

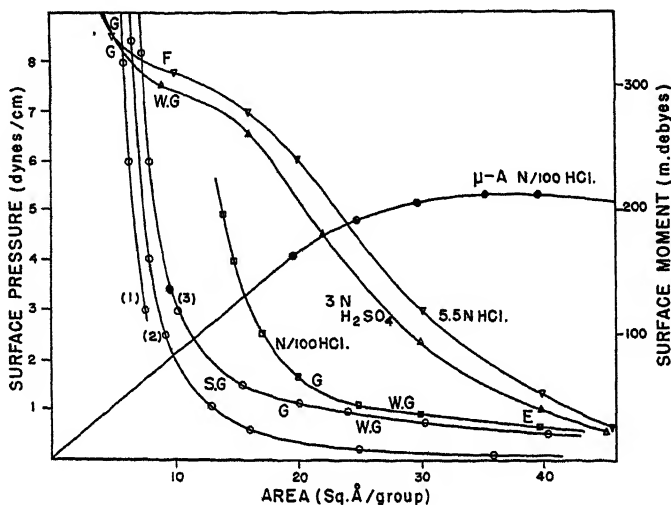


FIG. 11

Surface Pressure and Moment of Polyamide on Various Substrates

(1), (2), (3) on distilled water, spreading area 7.5, 25, and 100 Å<sup>2</sup> respectively

to vinyl alcohol or acrylic acid which remain freely soluble even when highly polymerized. Linear polyamides have considerable lattice energy attributable largely to hydrogen bondings at the peptide links since the softening point rises and specific polarization falls when the proportion of these links is increased (Baker and Yager, 1942). Hydrogen bonding in films of long-chain ureas and amides has been demonstrated by Alexander (1942) but this bonding is not spontaneous owing to the hydrocarbon chains which at low surface pressures prevent the ketonic oxygen and imino nitrogen atoms from approaching within 3 Å of each other. In a linear polyamide this hindrance is absent, the only opposing forces being the electrical field tending to swing the C=O moment vertically, thermal agitation, and the free carboxyl and amino groups at the ends of the molecule. The high bonding energy is sufficient to overcome these forces and collapse the film when the molecules are brought together. That hydrogen bonds are responsible for the collapse of the film is confirmed by the expanding action of strong acids which are known to break down this type of bond, probably by the formation of complexes with the peptide group (Meyer and Dunkel, 1931). When under these conditions the CO·NH groups have little attraction, the behavior is similar to that of poly- $\omega$ -hydroxy acids.

The dipole moment measured at pH 2 is about 200 m.d., which is similar to that of a protein (Schulman and Cockbain, 1939). The specific area measured by extrapolation of the  $\mu$ - $A$  curve is about  $30 \text{ \AA}^2$  per residue, while from the  $F$ - $A$  curve on strong acid it is  $38$ – $40 \text{ \AA}^2$ . Calculation from the fiber period ( $7.5 \text{ \AA}^2$ ) and interchain spacing ( $4.5 \text{ \AA}^2$ ) gives about  $34 \text{ \AA}^2$  per residue, in fair agreement with the above.

From the results obtained with Nylon it is possible to conclude that the  $-\text{CO}\cdot\text{NH}-$  groups of protein films will exercise a condensing effect by the formation of hydrogen bridges as first suggested by Mitchell (1937). Schulman and Cockbain criticized this view since they found no such interaction in mixed films of methyl stearamide and hexadecyl urea. But very different steric factors operate when long-chain compounds are employed and the negative result may well have been due to the spacing imposed by the hydrocarbon chains. It is interesting to observe that strong acids cause a similar expansion of protein films (Phillippi, 1936).

The greater stability of protein films compared with Nylon results from the presence of amino acid side chains which tend to keep the backbones apart and reduce the keto-imino interaction.

#### EFFECT OF TANNIC ACID

Schulman and Rideal have shown that injection of tannic acid beneath protein films causes rigidity and a reduction in the dipole moment. A similar action on amine films indicates that it is adsorbed by free amino groups forming a salt link (Schulman and Rideal, 1937), but it is not certain to what extent imino groups may take part in the tanning of the protein.

When tannic acid was injected beneath a film of heptadecyl acetamide at 15 dynes pressure, no change was observed in the area or potential of the film. At lower pressures tannic acid entered the film, but the action was no more pronounced than beneath an ethyl stearate monolayer with which interaction was unlikely. This result agrees with the similar experiments of Schulman and Cockbain on stearamide. When injected beneath a film of Nylon at low surface pressure, neither at pH 2 nor pH 7 was any marked tanning effect observed. Careful observations at pH 2 suggested that the film was slightly more condensed and less compressible, due perhaps to adsorption of tannic acid by the terminal amino groups of the polyamide. An observed reduction in surface potential of 30 mvs. with 0.01% tannic acid and 60 mvs. with 0.03% suggests a weak adsorption by the polyamide residues, in agreement with Schulman and Cockbain.



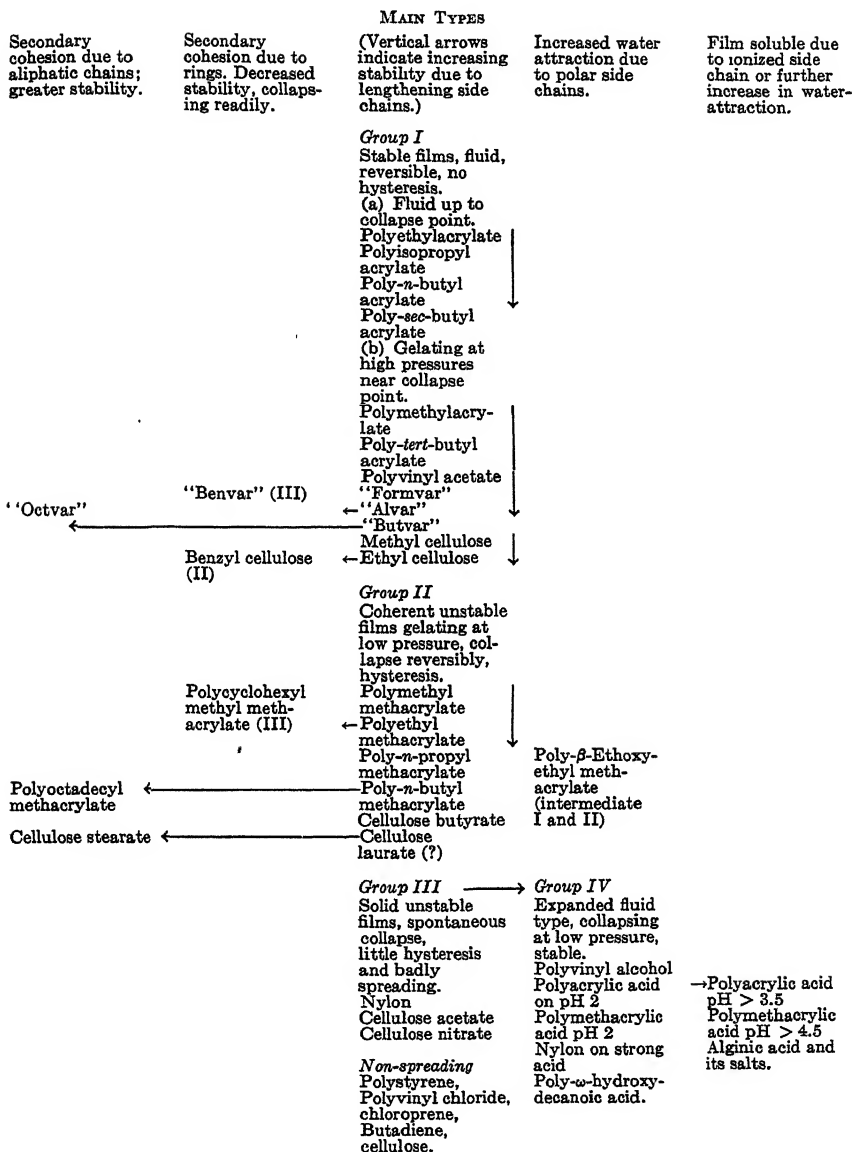
## DISCUSSION

The force area characteristics of long-chain films can usually be interpreted in terms of molecular packing. When the films are condensed the area may be limited either by the head group interaction or by the packing of the hydrocarbon chains. In the expanded state the head groups may be treated as a gas phase at the interface between the water and the hydrophobic chains, while gaseous and vapor films approximate to a relation  $FA = KT$  as dilution is increased. In all states of aggregation the molecules remain at the interface, although their orientation may vary; when collapse occurs it sets in sharply and usually at high surface pressures.

There is a good deal of evidence from the work described above that polymer films tend to collapse much more readily than long-chain films; while molecules as a whole remain at the interface, individual groups or segments may collapse. This tendency is least at low pressures, increasing at higher pressures until a complete overfilm of bulk polymer is formed. Thus collapse does not take place at one definite area but sets in gradually. As a result, it is not possible to interpret force-area curves solely in terms of molecular packing. A further consideration must be taken into account—the energy required to remove a group from the interface.

Until more knowledge is acquired concerning the surface-bulk phase equilibrium it may not be possible to obtain a general equation of a state to cover the collapse range of these systems, though it is possible that an expression might be deduced for the two-dimensional osmotic pressure of sinuously agitating threads of finite thickness to cover the low pressure region of the force-area curves. The two rather arbitrary methods of characterizing limiting areas, described in Part I, do meet with moderate success.

More valuable at present is the qualitative classification of these films. They exhibit a range of behavior which falls naturally into four main classes according to the lateral cohesion in the film, and the energy levels of film and bulk state. The stability of the film to surface pressure increases with the number of water-attracting groups, provided these are not sufficient to cause the whole film to dissolve, and is decreased by the internal cohesion of the polymer. This latter is generally decreased when short side chains are replaced by flexible ones, but increased by very large side chains or rings (Crisp, 1942). These factors are illustrated by the diagram below (which includes films of cellulose derivatives) and are clearly of importance in relating mechanical properties of individual plastics to their chemical constitution.



The conclusion that segments pass out of the surface layer above rather than below the main film is of some importance and the evidence on which it is based is summarized below:

1. Observations by dark-field illuminator at high surface pressures.
2. Threads of polymer can be spun off the surface when greatly compressed.

3. Films thickened by compression always show mechanical properties paralleling those of the bulk polymer.

4. No observable tendency for the films to undergo solution at high pressure unless the chain length is low or ionized groups are present. In the latter instance the whole molecule dissolves.

5. Measurement of the free energy required to collapse the film (or the equilibrium collapse pressure) shows that collapse is favored by strongly bonding groups (*e.g.*,  $C_6H_5$ ,  $C_6H_{11}$ , hydrogen bonds) and short side chains, while stability increases as the residue becomes more polar. Further, fluid amorphous films require more free energy to cause collapse than coherent films with the same polar group. If an "underfilm" were formed, more energy would be required to overcome the attraction of neighboring molecules in a coherent film, causing it to be immersed at a higher, not lower, surface pressure.

6. Calculations on the probable free energy of immersion of a number of residues constituting a segment of "underfilm" show this process to be very unlikely. On the other hand the energy difference between a close-packed film and the bulk state is not very great.

Protein films share many of the properties of other polymer films. They are particularly difficult to spread because they exist in two forms, the soluble globular form and the denatured film which probably consists of an insoluble thread with exposed hydrophobic groups. In the soluble form they tend to pass into solution unless carefully spread, preferably with addition of propyl alcohol or other spreading agent, on a substrate at the isoelectric point. After spreading, however, they may be two-dimensional fluids (*e.g.*, gliadin films) or they may form a network of chains which is solid even at zero pressure, and therefore be hindered by intermolecular cohesion from complete spreading, *e.g.*, ovalbumen (Phillippi, 1936), nerve protein (Fourt, 1939).

The forms of the  $F-A$  and  $\Delta V-A$  curves for proteins and polymers are very similar, and the same difficulties must exist when determining limiting areas. It is probable that, since the protein film contains a variety of residues, the more readily collapsing groups will pass first into the overfilm and the form of the  $F-A$  curve is determined by the successive collapse of the various types of residue into a thick gel. Attempts to relate the specific areas to particular configurations of the protein molecule are not, therefore, likely to prove successful.

High viscosity and gelation are not peculiar to protein films. They appear in all polymer films either (1) when powerful attractions exist between the monolayer units giving an approximately two-dimensional network (*e.g.*, methacrylates, ovalbumen), or (2) when the thickened polylayer formed by compression begins to show the bulk mechanical properties (*e.g.*, polyvinyl acetate, gliadin). It should be noted that only

the former process merits the term "surface gelation," and even so there is no strict analogy with bulk gelation. Owing to the very thin layer of matter present at the surface, much more powerful forces are necessary before the monolayer can exert visible mechanical rigidity. In "surface gels" the residues are separated by distances little greater than the van der Waals radii of the chains and the mechanical forces approach those of a solid polymer or protein, rather than those of a gelated solution.

Hysteresis phenomena at high surface pressures have been shown to exist in polymer as well as in protein films, and have been interpreted on the basis of collapse into an "overfilm." It is probable that proteins also form an "overfilm" rather than an "underfilm" as suggested by Langmuir and Waugh (1940). The distinction when the film is half collapsed is not purely verbal; there remains one important difference; the forces of the collapsing residues may be directed towards the water phase below or towards each other above the remainder of the monolayer. In the former case solution of the protein under high surface pressure would be conceivable, in the latter case a thick skin will be formed. Such a skin can in fact be spun off protein films after collapse, although it is possible that some degree of solution of elongated macromolecules also takes place (Lawrence, Miall, Needham and Shen, 1944). The argument that protein films with short hydrophilic side chains (*e.g.*, gelatin) collapse more readily than those with long side chains (*e.g.*, insulin) does not necessarily point to folding into an underfilm. The mutual cohesion of the main chains is increased when short side chains are present and collapse into an overfilm would, therefore, take place more readily.

My thanks are due to Professor E. K. Rideal, F.R.S., and Dr. A. E. Alexander for helpful discussions and encouragement throughout this work, to the Distillers' Co., Ltd., Messrs I.C.I., Ltd., and Messrs Shawinigen, Ltd., for a supply of the various polymers used, and to the Department of Scientific and Industrial Research for financial assistance.

#### SUMMARY

Polymer films which possess strong intermolecular forces are only slightly expanded and not very stable. When strongly hydrophilic groups are present (*e.g.*,  $-\text{OH}$ ,  $-\text{COOH}$ ), but the lattice forces are high, stable films exist only at surface pressures of a few dynes/cm. Without strongly hydrophilic groups the films tend to collapse spontaneously.

A series of polymethacrylate films illustrate the effect of the side chain on the film character. Short side chains result in strong intermolecular forces and coherent films; flexible side chains reduce these forces, giving a more expanded type, while large side chains introduce secondary cohesion.

High viscosity and intermolecular cohesion will account both for hysteresis and collapse phenomena in such films.

At the oil-water interface the intermolecular forces parallel to the surface are greatly reduced, and the differences between coherent and fluid films become less pronounced.

The low resolved surface dipole moment of polyvinyl alcohol and polyacrylic acid is attributed to hydrogen bonding. The effect of ionization of films of polyacids on their surface properties is described, solution of the film taking place when a sufficient proportion of residues become charged.

Polyamides form very coherent films due to bonding of the peptide link, and the bearing on this on the structure of protein films is discussed. Evidence is provided that films of proteins as well as other polymeric substances form a three-dimensional "overfilm" when they collapse.

#### REFERENCES

- ABDERHALDEN, E., AND FODOR, A., *Ber.* **49**, 561 (1916).  
ADAM, N. K., *Trans. Faraday Soc.* **29**, 108 (1933).  
ALEXANDER, A. E., (a) *Proc. Roy. Soc. (London)* **A179**, 470 (1942).  
ALEXANDER, A. E., (b) *Proc. Roy. Soc. (London)* **A179**, 486 (1942).  
ALEXANDER, A. E., (c) *Trans. Faraday Soc.* **38**, 54 (1942).  
ALEXANDER, A. E., AND SCHULMAN, J. H., *Proc. Roy. Soc. (London)* **A161**, 115 (1942).  
ALEXANDER, A. E., AND TEORELL, T., *Trans. Faraday Soc.* **35**, 727 (1939).  
ASKEW, F. A., AND DANIELLI, J. F., *Proc. Roy. Soc. (London)* **A155**, 695 (1936).  
BAKER, W. O., AND YAGER, W. R., *J. Am. Chem. Soc.* **64**, 21, 71 (1942).  
CRISP, D. J., *Trans. Faraday Soc.* **38**, 320 (1942).  
DANIELLI, J. F., AND ADAM, N. K., *Biochem. J.* **26**, 1233 (1936).  
E. I. DU PONT DE NEMOURS AND CO., *Ind. Eng. Chem.* **28**, 1160 (1936).  
FOURT, L., *J. Phys. Chem.* **43**, 887 (1939).  
GORTER, E., *Trans. Faraday Soc.* **33**, 1125 (1937).  
GORTER, E., AND GRENDLE, F., *Trans. Faraday Soc.* **22**, 477 (1926).  
HARKINS, W. D., CARMAN, E. F., AND RIES, H. E., *J. Chem. Phys.* **3**, 692 (1935).  
KERN, W., *Biochem. Z.* **301**, 338 (1939).  
LANGMUIR, I., AND WAUGH, D. F., *J. Am. Chem. Soc.* **62**, 2771 (1940).  
LAWRENCE, A. S. C., MIALL, M., NEEDHAM, J., AND SHEN, S. C., *J. Gen. Physiol.* **27**, 233 (1944).  
MEAD, D. J., AND FUOSS, R. M., *J. Am. Chem. Soc.* **64**, 2389 (1942).  
MEYER, K. H., AND DUNKEL, M., *Z. physik. Chem. (Bodenstein Festbd.)* 553 (1931).  
MITCHELL, J. S., *Trans. Faraday Soc.* **33**, 1129 (1937).  
PHILIPPI, G. T., *Thesis*, Amsterdam (1936).  
SCHULMAN, J. H., *Trans. Faraday Soc.* **37**, 134 (1941).  
SCHULMAN, J. H., AND COCKBAIN, E. G., *Trans. Faraday Soc.* **35**, 1266 (1939).  
SCHULMAN, J. H., AND HUGHES, A. H., *Proc. Roy. Soc. (London)* **A136**, 1938 (1932).  
SCHULMAN, J. H., AND RIDEAL, E. K., *Proc. Roy. Soc. (London)* **B122**, 29 (1937).  
TUCKETT, R. F., *Trans. Faraday Soc.* **38**, 313 (1942).

# THE HYDRATES OF CELLULOSE \*

P. H. Hermans and A. Weidinger

*From the Laboratory for Cellulose Research of the AKU and Affiliated Companies,  
Utrecht, Holland*

*Received Jan. 2, 1946*

## 1. INTRODUCTION

In this paper the "native" modification of the cellulose lattice will be designated as cellulose I and the "mercerized" modification ("hydrate cellulose") as cellulose II, a terminology which is, for several reasons, to be preferred.

J. Mercer believed that mercerized cellulose did contain chemically bound water and he termed it cellulose hydrate. We shall see that, contrary to the current opinion, Mercer was right.

## 2. X-RAY EVIDENCE ON THE EXISTENCE OF A TRUE CELLULOSE HYDRATE GIVING RISE TO "INTRAMICELLAR SWELLING"

In the literature it is generally stated that the swelling of cellulose in water is merely an "*intermicellar*" one and, hence, that the position of the interferences in the X-ray diagram of cellulose is not affected by swelling. The swelling of cellulose has often been cited as a classical example of intermicellar swelling. This is certainly correct for cellulose I but does not apply to cellulose II. The possibility of a small change in the X-ray diagram on swelling of cellulose II has been left open in the classical paper by Sponsler and Dore, discussed by Katz (1). Later, Sakurada and Hutino (2) reported quite positively on this point and found a slight shift of the paratropic  $A_0$  interference (101), indicating a decrease in the lattice distance of 0.3 Å on drying. We have confirmed this observation, which seems to have attracted insufficient attention (*cf.* experimental part).

Bone-dry mercerized ramie fibers, on moistening, show a shift of the  $A_0$ -lattice distance of 0.4 Å. We shall designate the two lattice modifications as "narrow" and "wide."

First the question arises as to whether the phenomenon is due to *intramicellar* swelling (hydrate formation) or to the existence of two different modifications of cellulose, the

\* Communication No. 22 from the Laboratory for Cellulose Research of the AKU and affiliated companies, Utrecht (Holland).

narrow one being stable at 100°C. (the temperature at which the fibers were dried) and the wide one being stable at room temperature, the transformation, however, requiring the presence of some water as a catalyst.

In the former case the transformation must be quantitatively connected with relative vapor pressure, in the latter it should be possible to obtain complete transformation with only traces of moisture present.

All experiments performed to check the second possibility turned out negative. Fibers dried at 100°C. and exhibiting the narrow lattice, when cooled and kept at room temperature in a dry atmosphere for many days did not show any change in the X-ray diagram. The presence of traces of moisture was attained by drying the samples at 100°C. over a mixture of anhydrous calcium chloride and its monohydrate (which at room temperature exhibits a vapor pressure corresponding to 1.5% rel. hum.). Fibers thus dried and then kept in sealed Keesom-capillaries at room temperature always exhibited the narrow lattice.

Fibers dried at room temperature to a low moisture content, and still exhibiting the wide lattice, were sealed into a Keesom-capillary and photographed in a heatable X-ray camera at 100°C. The lattice invariably remained wide.

These observations exclude the hypothesis of two lattice modifications transforming into each other under the influence of traces of moisture. On the other hand, experiments checking the hypothesis of hydrate formation were positive.

Well-dried mercerized ramie fibers were reconditioned to various moisture contents and X-ray diagrams taken at each regain. The  $A_0$ -lattice distance was derived from measurements on the film as well as on photometer curves. The results are shown in Table I.

TABLE I

*Lattice Distance of the  $A_0$ -Planes of Dried Cellulose II; No. 2-4 After Treatment with Moist Air at 100°C.; No. 5-8 After Treatment with Moist Air at 20°C.*

Exp. No.	Rel. hum. of air	Moisture content per cent	Lattice distance in Å	
			on film	on photom. curve
1	0	—	7.33	7.30
2	0.4 (100°)	—	7.37	7.30*
3	0.8 (100°)	—	7.37	7.29*
4	2.0 (100°)	1.5	7.46	7.46
5	7.5 (20°)	2.8	7.46	7.46
6	35 (20°)	6.6	7.50	7.52
7	65 (20°)	11.4	7.73	7.73
8	85 (20°)	17.0	7.73	7.70

\* Experiments with smaller film distance (40 mm.).

To produce low relative humidities easily for experiments 2, 3 and 4, air conditioned at 20°C. was led over the fibers enclosed in a vessel heated at 100°C. In experiments 5-8 conditioning was carried out in moist air at 20°C. The corresponding moisture content was read from the known absorption isotherm of mercerized ramie. (The isotherm at 100°C. not being known at low regain, the moisture content of the fibers in experiments 2 and 3 could not be given.)

It is seen that the widening of the lattice becomes detectable at 1.5% regain and has reached its maximum at 11.4%. (The experimental error in the figures of the last two columns was  $\pm 0.02 \text{ \AA}$ .)

It follows from these observations that *cellulose II shows intramolecular swelling and hence forms a true hydrate*. The water is taken up between the lamellar  $A_0$ -planes of the crystallites. Averaging over the best of our observations (only partially referred to above) we found for the lattice distance for the narrow lattice =  $7.32 \text{ \AA}$  and for the wide lattice =  $7.73 \text{ \AA}$ .

### 3. THE SECOND HYDRATE OF CELLULOSE

Another hydrate of cellulose II has been discovered and fully described by Sakurada and Hutino (2). It cannot be obtained from cellulose and water, but is always formed when other compounds of cellulose containing water are decomposed at low temperatures, *e.g.*, if alkaline cellulose I is washed with cold water or if cellulose xanthate is decomposed at low

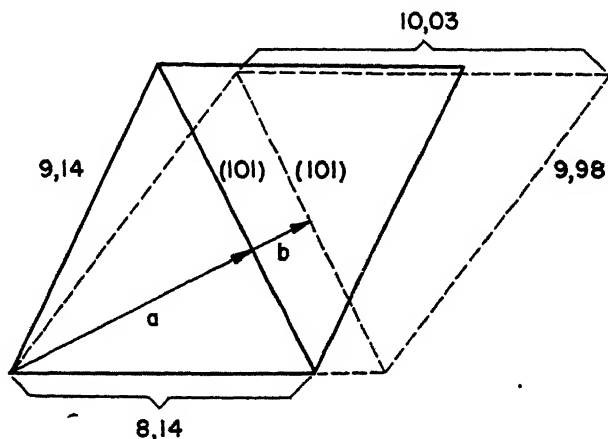


FIG. 1

temperatures. The  $\text{\AA}$  spacing of the planes in this hydrate was found to be  $8.92 \text{ \AA}$ , in conformity with the paper by Sakurada and Hutino. Kept at  $0^\circ\text{C}$ . this hydrate, called "water cellulose" by Sakurada and Hutino, remains unchanged for many days. In the long run, however, it slowly decomposes (more rapidly as the temperature is raised) producing the first hydrate with an  $A_0$ -spacing of  $7.73 \text{ \AA}$ . It has already been shown by the Japanese authors that the intensity maximum of the  $A_0$ -interference gradually shifts to its new position as the decomposition of the hydrate proceeds.\*

Fig. 1 shows the change in cross-section of the elementary cell perpendicular to its  $b$ -axis (fiber axis) on decomposition of water cellulose and

\* A theoretical explanation of this phenomenon was given by J. J. Hermans (3).



complete drying of the final product. The spacing of the  $A_0$ -planes decreases from  $a + b$  to  $a$ . The surface of the cross-section thereby remains practically proportional to the  $A_0$ -spacing (apart from a negligible correction of 1%). Since the lattice spacing in the direction of the  $b$ -axis remains constant, the volume change of the elementary cell is also proportional to the  $A_0$ -spacing. The formation of the hydrate referred to in section 2 represents only a small step on the path leading from dry cellulose II to the "water cellulose" of Sakurada and Hutino.

#### 4. LATTICE CONSTANTS OF THE TWO CELLULOSE HYDRATES

It is proposed that the first hydrate be termed *hydrate I* and the second, with the higher water content, *hydrate II*.

In Table II the dimensions of the elementary cells and the principal

TABLE II  
Lattice Constants of Cellulose II and Its Two Hydrates (in Å)

	$a$	$b$	$c$	$\beta$	101	10 $\bar{1}$	002
Cellulose II	8.14	10.3	9.14	62°	7.35	4.45	4.01
Hydrate I	8.58	10.3	9.38	59°	7.73	4.44	3.99
Hydrate II	10.03	10.3	9.98	52°	8.98	4.41	3.95

lattice spacings of cellulose II and both its hydrates are shown. It is seen that only the (101) or  $A_0$  interference changes position, whereas the other principal paratropic interferences (10 $\bar{1}$ ) and (002) remain practically unaltered on transformation.

#### 5. PROBABLE COMPOSITION OF THE TWO CELLULOSE HYDRATES

A possible way to compute the stoichiometric composition of the hydrates has been offered by Sakurada and Okamura (4). Let

- $\varphi_{cr}$  = the specific volume of dry cellulose II,
- $\beta$  = the coefficient of dilatation of the lattice on hydration,
- $a$  = the weight of hydrate water per g. cellulose,
- $\varphi_w$  = the spec. volume of the hydrate measured in water;

then

$$\varphi_w = \varphi_{cr}(1 + \beta) - a \quad (1)$$

since 1 g. cellulose in the form of the hydrate has a volume of  $\varphi_{cr}(1 + \beta)$  and a gram of water has penetrated in this volume. Hence,

$$a = \varphi_{cr}(1 + \beta) - \varphi_w. \quad (2)$$

If  $\varphi_w$  is measured,  $a$  can be calculated, since  $\beta$  is known from X-ray analysis. Now  $\varphi_w$  represents the reciprocal density of *crystalline* cellulose hydrate II in water. In the density determination, however, we are always concerned with the *amorphous* parts of the fiber also. We make the assumption that the density of this amorphous hydrate II in water is practically equal to that of the crystalline hydrate II in water. This assumption is a reasonable one, since the cellulose chains in this hydrate are practically completely surrounded by water molecules, irrespective of whether we are concerned with the crystalline or the amorphous parts. Moreover, a support is given by the density figures in Table III, which

TABLE III  
*Density of Various Preparations of Hydrate II Measured in Water*

Prepared from	Density observed		Mean
Fresh model filaments	1.6429	1.6407	1.6418
Reswollen model filaments	1.6423	1.6434	1.6424
Ramie fibers	1.6428	1.6424	1.6426
	General mean		1.6423

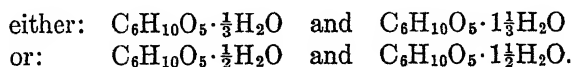
show that various fibers, if transformed into hydrate II, yield the same density in water, although (even in these mercerized fibers) the percentage of crystalline material changes to a certain extent with the nature of the fiber. Now, if we take  $\varphi_w = 1:1.6423 = 0.609$  and recalling that  $\varphi_{cr}$ , deduced from X-ray data, is 0.632, we get from equation (2)

$$a = 0.166.$$

This leads to a ratio of 1.49 mol  $H_2O$  per mol  $C_6H_{10}O_5$ .\*

Assuming that the water content of the hydrates is proportional to the coefficient of dilatation,  $\beta$ , of the lattice, which is 0.057 for hydrate I and 0.226 for hydrate II, the ratio of water to cellulose in the former is calculated to be 0.36 mol  $H_2O$  per mol  $C_6H_{10}O_5$ .

Allowing for the approximate character of the theory and for experimental errors, we can only conclude that the composition of the two hydrates is



There are some arguments in favor of the former alternative:

(a) According to Sakurada and Okamura the composition of the compound sodium cellulose IV, the X-ray diagram of which is almost identical with that of cellulose hydrate II, is  $C_6H_{10}O_5 \cdot 0.3NaOH \cdot H_2O$ . Hydrate II might then belong to the same type of substitution compound.

\* Sakurada and Okamura obtained a lower value. They have, however, used samples of hydrate II, which were already partially decomposed, as may be deduced from their X-ray data.

(b) If one calculates the density of hydrate I in water according to equation (1), substituting  $a = \frac{1}{2}$  and  $\alpha = \frac{1}{2}$ , one obtains 1.584 and 1.630, respectively. The density of a cellulose fiber, containing cellulose II would, hence, be greater than these figures, since the density of packing of cellulose and water in the amorphous parts will presumably be greater than that in the crystalline part. Now, we have found that the densities of regenerated fibers measured in water always lies between 1.610 and 1.620 (5). This would lead to the conclusion that the composition of hydrate I cannot be  $C_6H_{10}O_5 \cdot \frac{1}{2}H_2O$ .

## 5. DISCUSSION

The lattice energy of the native modification of cellulose, termed cellulose I, which according to the dimensions of the elementary cell has the greatest density (1.59), is apparently so large that water cannot penetrate into the lattice.

In the somewhat wider lattice of cellulose II (density according to X-ray data = 1.58), a small quantity of water can penetrate spontaneously and is bound there very tightly. The free energy of hydration is greater than the work necessary to widen the lattice.

Although the affinity of the cellulose molecule toward water is not exhausted after the formation of this first hydrate, hydrate II cannot be formed spontaneously in the crystalline state when starting from hydrate I, as its free energy of formation is surpassed by the remaining cohesive attractions in the lattice of hydrate I. In the amorphous part of the fiber, however, the cohesion between the chains is weakened at several spots, and it is reasonable to assume that hydrate II will also be formed here, provided the temperature is not too high. (This will also apply to dispersed cellulose where the chains are free.)

If cellulose crystallizes from an aqueous medium at low temperature, or if cellulose compounds containing water are decomposed, hydrate II appears in the crystalline form and then becomes detectable in the X-ray diagram. The chains composing the amorphous part of the fiber are then, of course, also hydrated to form the second hydrate. At higher temperatures, hydrate II is rapidly decomposed, while hydrate I is only decomposed on rigorous drying of the material.

On the other hand, if more and more water is gradually added to a fiber consisting of dry cellulose II, the first amount of water is tightly bound in the form of hydrate I in the crystallites as well as in the amorphous part of the fiber. More water is then bound in the amorphous part only, and the most obvious assumption is that this occurs in the form of hydrate II. This water is less strongly bound but still with an appreciable heat effect. The "chemical" affinity of water toward cellulose is now exhausted and further water will be bound by much weaker forces of the type of van der Waals bonds.

Considering fibers containing cellulose I, the same scheme can be visualized, with the difference that the first phase, the binding of water in the crystallites, does not occur. In the amorphous part of the fiber both hydrates will be formed if sufficient water is added.

In many respects the foregoing deductions throw a new light on the mechanism of absorption of water by cellulose. This point is discussed at length in another publication (5). The conclusion is reached that nearly all the water absorbed by cellulose fiber, when exposed to moist air up to about 50% relative humidity, consists of hydrate-water.

## EXPERIMENTAL

### 1. Shift of $A_0$ Line

In order to attain the highest possible precision in measuring the small shift of the  $A_0$  interference, a small quantity of the black mineral molybdenum sulfide ( $\text{MoS}_2$ ) was rubbed on the fibers. A sharp and intense interference line of this substance corresponding

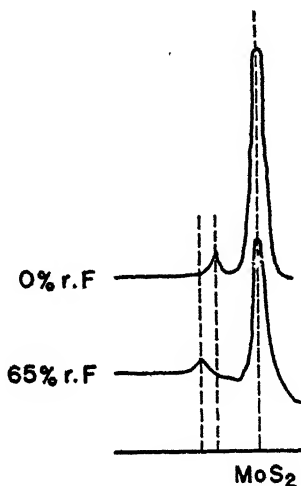


FIG. 2

Photometer Curves of Samples 4 and 7 from Table I (Shift of  $A_0$  Relative to the  $\text{MoS}_2$  Line) on Absorption of Water

to a spacing of  $6.33 \text{ \AA}$  then appeared in the diagram not far from the interference  $A_2$  ( $d = 5.36 \text{ \AA}$ ) of cellulose I or from the interference  $A_0$  ( $d = 7.33 \text{ \AA}$ ) of cellulose II alternatively.\* Moreover, another interference of  $\text{MoS}_2$ , corresponding to a smaller spacing, appeared outside the cellulose diagram. With the aid of these  $\text{MoS}_2$  lines the position of the cellulose interferences could be accurately measured. To that end, direct

\* According to O. Hassel (6), this  $\text{MoS}_2$  interference corresponds to a spacing of  $6.19 \text{ \AA}$ . In this mineral, however, the magnitude of the spacing seems to vary according to the origin of the sample. We have determined its actual position in comparing it with the lines  $2.81 \text{ \AA}$  and  $2.46 \text{ \AA}$  of zinc oxide powder. [Cf. J. D. Hamawalt, H. W. Rinn and L. F. Frevel (7).]

measurements of the mutual distances on the film, as well as measurements on photometer curves taken along the equator of the diagram, were performed. The photometer curves corresponded to a linear magnification of 3.9. In Fig. 2 the photometer curves of samples 1 and 7 from Table I are reproduced. The high intensity maximum at the right represents the  $\text{MoS}_2$  line 6.33 Å, the lower one on the left the  $A_0$  interference. The shift of the latter is distinctly visible. On the original scale of the photometer curves the shift of the  $A_0$  line amounted to 2.5 mm. If we allow for a maximum error of one tenth of this length, the figures in the last column of Table I are accurate within  $\pm 0.02$  Å. The radiation used was the usual filtered  $\text{Cu-K}_\alpha$  radiation.

The fibers were investigated sealed in thin-walled glass capillaries (so called Keesom-capillaries).

### 2. Technique of Drying and Conditioning

The samples were dried *in vacuo* over  $\text{P}_2\text{O}_5$  following the procedure shown in Fig. 3. The small glass apparatus is evacuated. Some  $\text{P}_2\text{O}_5$  is filled into the small bulb at 1, and a thin-walled Keesom capillary, 3, fused on at 2. After drying was complete the capillary at 2 was removed by heat and placed on the diaphragm of the X-ray camera.

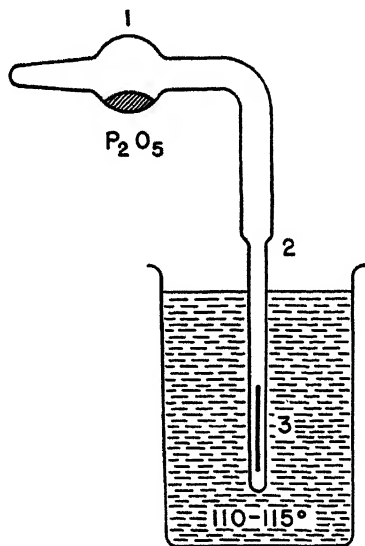


FIG. 3

Conditioning was performed similarly. The Keesom capillary remained open and a continuous slow stream of conditioned air was passed through it until equilibrium was reached, when the capillary was sealed at both ends.

### 3. Determination of the Density in Water

A sample of the fibers consisting of water cellulose II prepared at a temperature below  $5^\circ\text{C}$ . and corresponding to about 1 g. of dry material, was suspended from a hydrostatic balance by a platinum wire 0.02 mm. in diameter and weighed under water, the temperature of which was kept below  $5^\circ\text{C}$ . The capillary pull on the thin wire was less than 1 mg. and hence the influence of eventual fluctuations of the surface tension

of the water (which can hardly be excluded) could be neglected.\* Afterwards the fiber sample was dried and reweighed.

### SUMMARY

It is shown that the formation of true hydrates plays a part in the process of moisture absorption in cellulose fibers. The existence of two hydrates, called hydrate I and hydrate II, can be derived from X-ray data.

Crystalline hydrate I is formed when cellulose II (the modification of "mercerized" cellulose) is exposed to water vapor and hence this modification, in contrast to current statements in the literature, exhibits so-called "intramolecular" swelling. Cellulose I (native modification) does not show this phenomenon.

Crystalline hydrate II is identical with the "water cellulose" of Sakurada and Hutino. It is formed when other cellulose compounds containing water are decomposed at low temperature.

The lattice constants of both hydrates are given in Table II. If their composition be expressed by  $C_6H_{10}O_5 \cdot pH_2O$  the value of  $p$  is most probably  $\frac{1}{3}$  or  $\frac{1}{2}$  in hydrate I and  $1\frac{1}{3}$  or  $1\frac{1}{2}$  in hydrate II.

The point of view is adopted that the crystalline part of fibers consisting of cellulose II takes part in the process of sorption by the formation of hydrate I, whereas crystalline cellulose I does not. In the amorphous part of the fiber both hydrates are always formed if sufficient water is absorbed.

### REFERENCES

- (1) KATZ, J. R., *Röntgenspektrographie als Untersuchungsmethode*, Berlin-Wien 1934, p. 217.
- (2) SAKURADA, I., AND HUTINO, K., *Kolloid-Z.* **77**, 347 (1936).
- (3) HERMANS, J. J., *Rec. trav. chim.* **63**, 211 (1944).
- (4) SAKURADA, I., AND OKAMURA, S., *Kolloid-Z.* **81**, 199 (1937).
- (5) HERMANS, P. H., *Contribution to the Physics of Cellulose Fibers*, New York-Amsterdam (to appear soon).
- (6) HASSEL, O., *Z. Krist.* **61**, 42 (1925).
- (7) HANAWALT, J. D., RINN, H. W., AND FREVEL, L. F., *Ind. Eng. Chem.* **30**, 457 (1938).

\* A detailed description of the technique of the density determinations in water is given elsewhere (5).



# A VISCOMETER FOR MEASUREMENTS DURING THIXOTROPIC RECOVERY; RESULTS WITH A COMPOUNDED LATEX \*

M. Mooney \*\*

*From the General Laboratories, United States Rubber Company, Passaic, N. J.*

*Received November 28, 1945*

## INTRODUCTION

Various studies have been made of the break-down of thixotropic structure by stirring, and of the time required for recovery of structure under conditions of quiescence. However, there are certain operations, such as painting or dipping, in which the quality of the finished product depends in part on the flow properties of a thixotropic liquid under small but finite forces operating immediately after a rapid deformation, while thixotropic recovery is still in progress. The forces referred to are those of gravity and surface tension. The apparatus described in the present article is designed especially for studying the rheology of a thixotropic liquid immediately after a rapid deformation, and for determining, in particular, the rate of thixotropic recovery while the liquid is subjected to a low shearing stress. Experimental data are reported on a commercial type of compounded rubber latex.

In order to obtain essentially uniform shearing stress and rate of shear throughout the test material, a viscometer of the rotating cylinder type with small clearances between the cylinders is desired. It would be comparatively simple to design such an apparatus with driving speeds or driving torques which could be abruptly changed. However, it would not be easy to devise a set of bearings for the rotating cylinder which would function satisfactorily at high torques and yet would have sufficiently small friction to have a negligible effect on the observations when the torque is very greatly reduced. To avoid this difficulty, a viscometer has been designed in which the arrangement for stirring the liquid to break down its structure is distinct from the arrangement for measuring the viscosity.

## APPARATUS

The apparatus consists essentially of a hollow cylinder, called the rotor, suspended by a steel torsion ribbon in a narrow cylindrical channel,

\* Presented before the Society of Rheology, October 27th, 1945.

\*\* General Laboratories, United States Rubber Co., Passaic, N. J.



called the stator, which contains the test material. The novel feature of this apparatus lies in the fact that the inner wall of the stator is rotatable with respect to the outer wall. Therefore, by rapidly oscillating the inner wall, the liquid in the viscometer can be stirred, that is, sheared at a high rate. The torsional rigidity of the suspension is sufficiently low that the rotor practically moves with the liquid. In other words, it has roughly half the angular velocity of the inner wall of the stator. After stirring is completed, the inner wall remains stationary, and viscosity measurements are made with only the rotor moving.

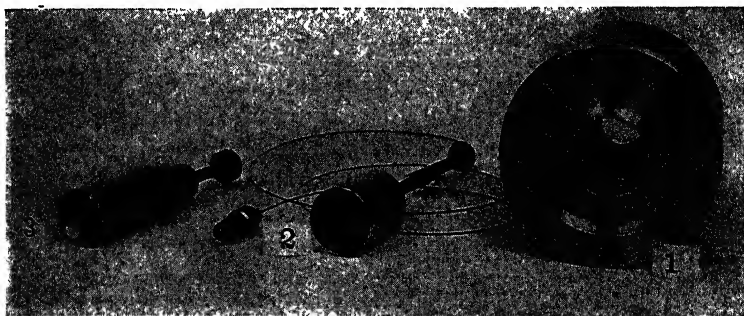


FIG. 1

- (1) Outer stator
- (2) Rotor
- (3) Inner stator

Fig. 1 is a photograph of the viscometer proper disassembled. It will be observed that the inner part of the stator (3) has a conical bearing at its lower end which fits into a corresponding conical bearing in the outer part (1). A light film of oil serves to lubricate the bearing and, at the same time, makes the system water tight. A photograph of the complete assembly is shown in Fig. 2.

The optical system includes 4 mirrors mounted  $90^\circ$  apart on the rotor, and 4 light sources. With this arrangement, a record can be obtained of any number of revolutions of the rotor; for as one light spot is passing beyond the end of the photographic paper within the camera, the light spot from another of the 4 sources comes onto the paper at the other end.

#### THEORY OF THE VISCOMETER

With small, nearly equal clearances on both sides of the stator, the rate of shear and shearing stress are both nearly uniform throughout the liquid. Therefore, the viscosity also is essentially uniform and we may neglect variations in the viscosity. Let  $\eta$  be the viscosity,  $\omega$  the

angular velocity of the rotor in radians/second;  $R_1, R_2, R_3, R_4$  the radii of the inner stator, the inside of the rotor, the outside of the rotor, and the outer stator, respectively;  $\tau_1, \tau_2, \tau_3, \tau_4$  the tractions \* at the corresponding points;  $L$  the immersed length of the rotor, and  $T$  the torque of the suspension. Then, by equations previously published, (1)

$$\eta\omega = \frac{\tau_1 + \tau_2}{2} \cdot \frac{R_2^2 - R_1^2}{R_2^2 + R_1^2}. \quad (1)$$



FIG. 2

- (1) Viscometer, outer stator
- (2) Leveling screws
- (3) Stirring handle, attached to rotatable inner stator
- (4) Mirror on rotor shaft
- (5) Suspension ribbon for rotor
- (6) Lights, clear bulb, straight filament
- (7) Camera box
- (8) Lens and shutter
- (9) Light-tight holder for drum in transporting to and from dark room
- (10) Gear box
- (11) Synchronous motor for rotating the drum
- (12) Thermal insulation for viscometer

When in use, the rotating drum, carrying photographic paper, is mounted inside the camera (7) coaxial with the holder (9).

\* The word "traction" as used in this article is synonymous with the more awkward phrase "shearing stress."

Also

$$\tau_1 R_1^2 = \tau_2 R_2^2. \quad (2)$$

Whence,

$$\eta\omega = \frac{\tau_2}{2} \frac{R_2^2 - R_1^2}{R_1^2}. \quad (3)$$

Likewise

$$\eta\omega = \frac{\tau_3}{2} \frac{R_4^2 - R_3^2}{R_3^2}. \quad (4)$$

Now by setting  $T$  equal to the sum of the moments due to  $\tau_2$  and  $\tau_3$ , we obtain from (3) and (4),

$$\eta = \frac{T}{4\pi L\omega \left[ \frac{R_4^2 R_3^2}{R_4^2 - R_3^2} + \frac{R_2^2 R_1^2}{R_2^2 - R_1^2} \right]}. \quad (5)$$

In addition to this equation for the viscosity, we require an equation for the mean traction. The mean traction in the inner space is  $\tau_{1,2} = (\tau_1 + \tau_2)/2$ ; and in the outer space  $\tau_{3,4} = (\tau_3 + \tau_4)/2$ . In calculating the over all mean traction it is slightly better to weight  $\tau_{1,2}$  and  $\tau_{3,4}$  by factors proportional to the volumes of the two corresponding clearance spaces, these factors being  $R_2^2 - R_1^2$  and  $R_4^2 - R_3^2$ . With this procedure the over all mean traction,  $\tau$ , can be expressed in terms of  $\eta\omega$  by using equations (3) and (4) and two similar equations for  $\tau_1$  and  $\tau_4$ . Elimination of  $\eta\omega$  by use of equation (5) then gives us:

$$\tau = \frac{T}{4\pi L} \cdot \frac{\frac{R_4^2 + R_3^2 + R_2^2 + R_1^2}{(R_4^2 - R_3^2) + (R_2^2 - R_1^2)}}{\frac{R_4^2 R_3^2}{R_4^2 - R_3^2} + \frac{R_2^2 R_1^2}{R_2^2 - R_1^2}}. \quad (6)$$

The dimensions of the present apparatus are:  $R_1 = 1.045$  cm.,  $R_2 = 1.13$  cm.,  $R_3 = 1.175$  cm.,  $R_4 = 1.265$  cm.,  $L = 3.50$  cm. The torque constant of the suspension is 50.0 dyne-cm./radian; and the moment of inertia of the rotor is 15.5 g-cm.<sup>2</sup>.

#### METHOD OF OPERATION

The apparatus, at room temperature, is filled with the latex to be tested and some water placed in the overflow channel of the stator. With the thermal insulation and cover in place, the water maintains high humidity under the cover and prevents skin formation by evaporation from the sample. The inner stator is oscillated by hand 8 to 10

times through an angle of about  $90^\circ$  at a rate of about 1 cycle per second. On the last oscillation, the handle is brought back to a positive stop against the frame of the viscometer; and at the same time the upper end of the suspension ribbon is given a sudden twist proportional to the desired shearing stress, or traction. From this time on, the rate of rotation of the rotor is determined by the torque due to the suspension ribbon acting against the viscosity of the liquid. In the present work, the photographic records terminate at 20 to 40 seconds.

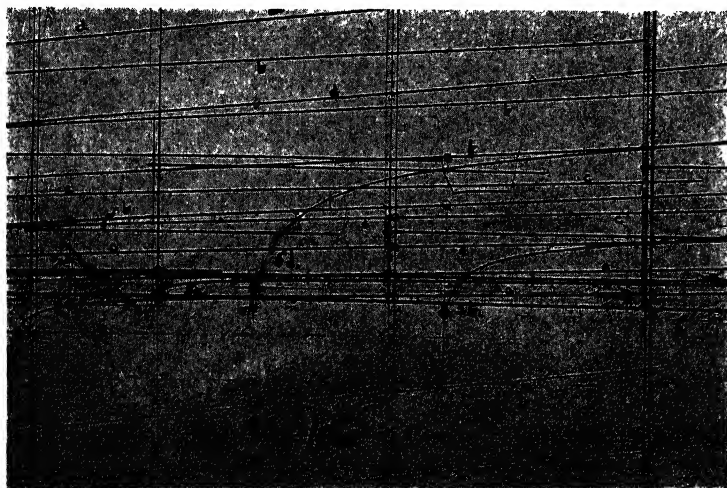


FIG. 3

## Photographic Traces

Horizontal displacement is time, full scale = 10 seconds. Vertical displacement is rotation of the viscometer rotor

Trace Number	Traction, $\tau$ dynes/cm. <sup>2</sup>
5a	1.33
5b	4.00
5c	2.67
5d	5.33

Fig. 3 shows four photographic traces on a single record paper. The velocity of the rotor at any instant is proportioned to the slope of the photographic trace. When the slope of the trace is changing rapidly, it is determined by fitting a tangent line to the curve. When the slope is nearly constant, best accuracy is obtained by measuring heights of the curve at different points.

## EXPERIMENTAL RESULTS

Measurements were made on a commercial latex compound containing 47.5% total solids. The stirring process described above is obviously not carried out with accurate controls. However, the reproducibility of the viscosity measurements show that with this latex the

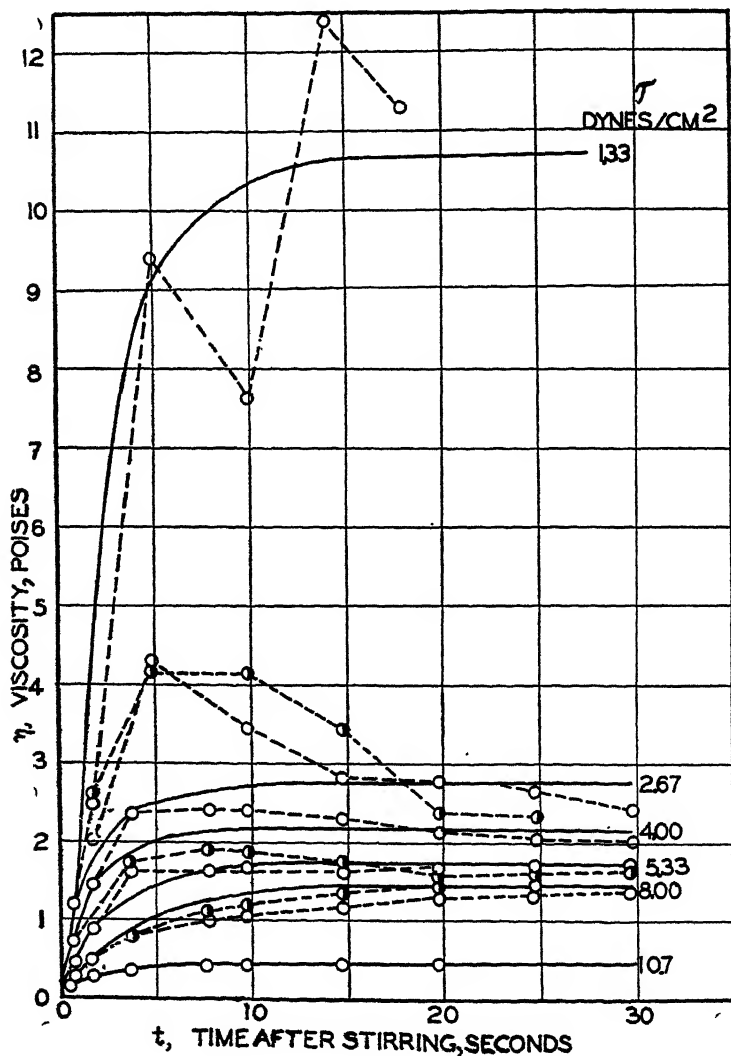


FIG. 4

Observed and Calculated Viscosity vs. Time After Stirring,  
for Various Values of  $\tau$ , the Traction

stirring process was sufficient to give reproducibility of break-down of the thixotropic structure. The initial twist in the suspension ribbon was such as to develop an initial traction between 1.3 and 10.7 dynes/cm.<sup>2</sup>. The traction in any experiment decreases with time as the rotor moves; but the percentage decrease was negligible in most cases and less than 6% in the worst case.

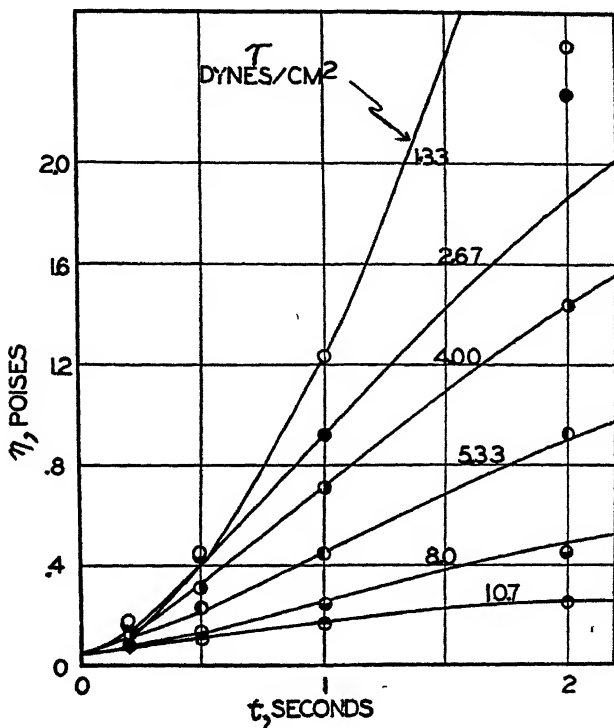


FIG. 5

Observed and Calculated Viscosity vs. Time After Stirring,  
for Various Values of  $\tau$ , the Traction

Figs. 4 and 5 show the viscosity as a function of time after the rapid shearing ceases for the range of tractions employed in viscosity measurement. Within experimental error, all curves start, by extrapolation, at the same initial viscosity of approximately .05 poises. Thus, in the stirred state the latex is a Newtonian liquid. This is strong evidence that the thixotropic structure is completely broken down in the stirring procedure employed.

The viscosity begins to increase immediately after stirring. The initial rate of increase and the ultimate viscosity attained both decrease as the stress used in the measurement is increased. The maxima in the

curves obtained with tractions of 2.7 to 5.3 dynes/cm.<sup>2</sup> are apparently reproducible and presumably real.

Fig. 6 is a graph of the fluidity at 20 seconds after stirring *vs.* the traction. This curve suggests a yield stress at about 1.0 dyne/cm.<sup>2</sup>. However, qualitative tests to detect a yield stress were not successful. In these tests, the apparatus was allowed to stand until the rotor assumed a steady position, when the rotor was turned through a few degrees and

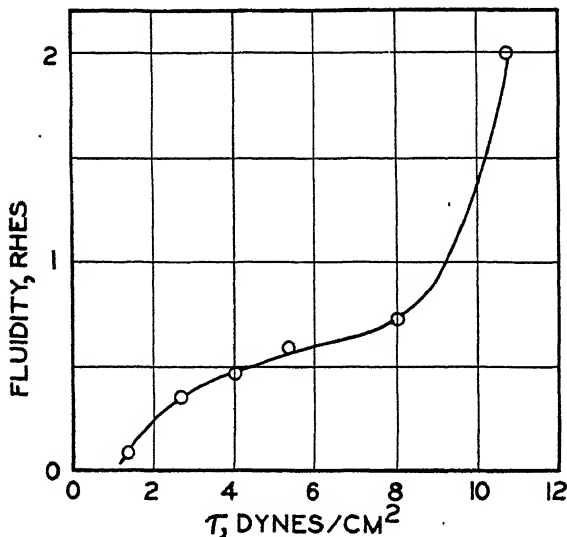


FIG. 6

Fluidity at 20 Seconds After Stirring *vs.* Traction,  $\tau$

permitted to come back to a steady position again. There was no observable difference between the two final positions of the rotor. Since this procedure would reveal a true yield stress of .01 dyne/cm.<sup>2</sup>, if it existed, we are forced to conclude that the yield stress suggested by Fig. 6 is only apparent.

#### INTERPRETATION OF THE DATA

A commercial latex consists of a suspension of rubber latex particles and various compounding ingredients of various particle sizes and densities, stabilized by a suitable adjustment of the pH and the addition of various stabilizing agents. The large difference in viscosity between the active or stirred latex and the quiescent latex indicates that these suspended particles form weak agglomerates which trap and immobilize considerable volumes of water, thus increasing the viscosity. In attempting a quantitative explanation of the experimental data, we shall assume

that the agglomeration process after stirring follows the Smoluchowski theory of slow coagulation (2), and that the relationship between viscosity and fractional volume of the solid material, that is, agglomerated material including trapped water, follows an empirical viscosity equation based upon Eilers' (3) experimental data. We must postulate also that the rate constant in Smoluchowski's coagulation equation will vary with the traction in the liquid, since the higher the stress, the less the probability that two newly attached particles will remain attached.

We assume that the stirring breaks down all thixotropic structure with the result that initially, that is, immediately after stirring ceases, the latex contains only elementary colloidal particles. Let there be  $N_0$  such single particles per unit volume, of average volume,  $v$ , per particle. As agglomeration proceeds, we take account of the water trapped in the agglomerates by defining a swelling factor,  $f$ , by the equation:

$$v_n = nvf \quad (7)$$

where  $v_n$  is the volume of an agglomerate of  $n$  elementary particles. Then  $V$ , the effective partial volume of the solids including the immobilized water, is

$$V = v[N_1 + f(N_0 - N_1)], \quad (8)$$

where  $N_1$  is the number of single particles left unagglomerated at any time,  $t$ , after stirring ceases.

By Smoluchowski's kinetic theory of coagulation,

$$N_1 = \frac{N_0}{(1 + bt)^2} \quad (9)$$

where  $b = kN_0$  and  $k$  is the velocity constant of the coagulation process. For "slow" coagulation,  $k \sim 8\pi DrP$ , where  $D$  is the diffusion constant of single particles,  $r$  is the particle radius, and  $P$  is the fractional number of impacts which result in permanent attachments. According to rough estimates, based on the value of  $b$  and other constants involved,  $P \sim 10^{-1}$ . This justifies describing the coagulation process as slow, even though the time to approach equilibrium is relatively short. Equations (8) and (9) give us

$$V = V_s \left[ f - \frac{f-1}{(1+bt)^2} \right], \quad (10)$$

where  $V_s = N_0 v$  = the true partial volume of the solids.

Lacking any direct measure of  $V$ , we must calculate it from the viscosity measurements. By combining equation (10) with Einstein's viscosity equation, Smoluchowski obtained a relationship between time and the viscosity of a coagulating system, the increase in apparent



volume of the coagulate being attributed to trapped water. However, there is no theoretical equation relating viscosity to  $V$  which has any validity at the large values of  $V$  involved in the present work. We must, therefore, employ an empirical equation. The best experimental data for our purpose are those obtained by Eilers in his measurements of the viscosity of aqueous suspensions of bitumen. An equation which fits his data very well has the form

$$\eta_r = \frac{\sqrt{1 + .5V}}{1 - V} \exp \left( \frac{1.25V}{1 - V} \right) \quad (11)$$

where  $\eta_r$  is the relative viscosity, or viscosity of the suspension/viscosity of water.

Fig. 7 shows that this equation fits Eilers' experimental data quite well. Eilers' own equation fits slightly better; but it has a singularity, giving infinite viscosity, at  $V = .78$ . The corresponding singularity in equation (11) is at  $V = 1$ . For this reason equation (11) seems preferable, although the choice is largely a matter of judgment and involves the assumption that the dispersion in particle or agglomerate size is greater in the agglomerated latex examined here than in the emulsion prepared by Eilers. Fortunately the choice is not crucial; and any reasonable method of extrapolating Eilers' data would give essentially the same results in the present application.

There is a discrepancy at Eilers' last point, where  $V = .7$ ; but the discrepancy is not large in terms of  $V$ . In this connection it may be remarked that there would be no point in concerning ourselves over small errors in  $V$ ; for it is certain that at high partial volumes the viscosity will vary considerably with the size distribution of the particles, aside from questions of shape; and there is no reason for believing that the size distribution will be the same in the agglomerated latex as in Eilers' Bitumen suspensions. Equations (10) and (11) involve three variables,  $\eta_r$ ,  $t$  and  $V$ ; and three parameters,  $f$ ,  $b$  and  $V_s$ . The parameters  $f$  and  $b$  may vary with the applied shearing stress, but  $V_s$  is the same for all curves. If we take the intercept in Fig. 5 as .052 poise, and the viscosity of water at room temperature as .009, we calculate the initial value of  $\eta_r$  to be 5.8. Then, by Fig. 7,  $V_s = .46$ .

The values of  $f$  and  $b$  were determined for each experimental curve so that the theoretical curve would have the proper asymptotic limit and would pass through the experimental point at  $t = 1$  second.

The various values thus determined are shown in Table I, and the corresponding theoretical curves of  $\eta$  vs.  $t$  are the full curves shown in Figs. 4 and 5. The curves agree satisfactorily with the data except for the maxima in some of the experimental curves. Especially noteworthy

is the fact revealed by Fig. 5, that the theoretical curves for the smaller tractions show an initial slope less than the slope at 1 second, which is in agreement with the data. Since this feature of the data was not used in determining the parameters of the equations, the agreement in this case may be taken as additional evidence in support of the theory.

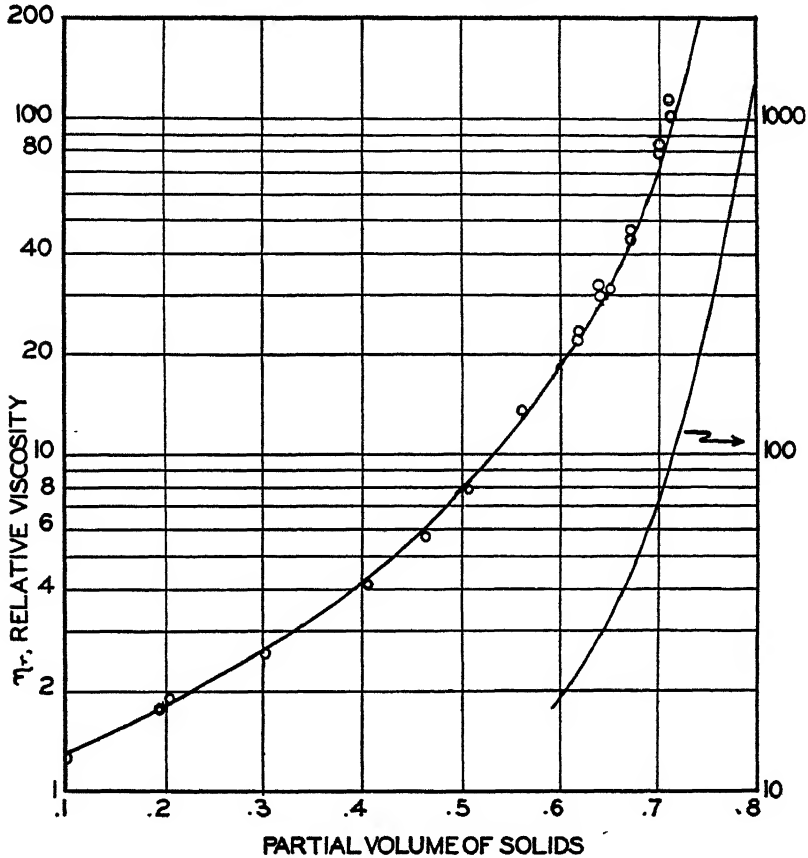


FIG. 7

Eilers' Experimental Data on Aqueous Suspensions of Bitumen Spheres, and the Empirical Equation

$$\eta_r = \frac{\sqrt{1 + .5V}}{1 - V} \exp. \left( \frac{1.25V}{1 - V} \right)$$

The maxima in the experimental curves reveal the presence of some important factor not included in the Smoluchowski theory of coagulation; and it appears highly probable that the large jump in  $\eta$  between  $\tau = 1.33$  and  $\tau = 2.67$  is due to this same factor. As a plausible explanation of the observed facts, the following hypothesis is submitted.

The initial agglomerates formed at a low traction are looser and contain more water than those formed at a high traction. These coagulates grow by accretion and coalescence until they occupy so much of the total volume that they are forced, in the shearing of the liquid, to approach very close or bump into each other. As a consequence of the resulting momentary, localized high stress, the looser agglomerates break into fragments; and in the final, steady state, the only agglomerates left will be those which are sufficiently dense and firm to withstand not only the average, continuous shearing stress, but also the occasional high stresses developed at bumping contacts. Thus, the maxima are to be attributed to the instability of the initial agglomerates under stresses which develop only after considerable agglomeration has occurred.

The apparent absence of a distinct maximum in the experimental curve at the lowest traction may indicate that even the bumping stresses in this case are insufficient to break up the loose agglomerates. This theory may appear to contradict the observation reported above that the quiescent latex has no yield stress greater than .01 dyne/cm.<sup>2</sup>. However, the theory can be reconciled with this observation if we assume further, that at very low tractions the agglomerates can undergo a very slow, continuous deformation of a viscous type in which reattachments are formed within the agglomerate as fast as they are broken.

## DISCUSSION

The partial volume of the solids in the latex is approximately 0.485, which is the figure obtained if we take the mean density of the solids to be 0.98. The value of 0.46 found for  $V_s$  therefore is slightly low, but is correct in magnitude and supports the assumption of no agglomeration in the stirred state.

Table I shows a general decrease in  $f$  as  $\tau$ , the traction, increases. This trend reflects the variation in the initial slopes of the  $\eta - \tau$  curves, and shows how the traction decreases the probability of permanence of new agglomerates.

The variation of  $f$  with  $\tau$  is quite small in comparison with the variation of  $\eta$ , but the matter becomes comprehensible when we note that the slope of the  $\eta - V_s$  curve in Fig. 7 is very high.

The Smoluchowski theory assumes that eventually all material in the suspension coagulates. Undoubtedly this assumption is not strictly valid in our problem; for we must expect that in the final, steady state attained at any constant traction, there will be a fraction of the material not agglomerated. Furthermore, this fraction will increase with the traction. In fact, the variation in final viscosity with traction might be explained entirely as the result of variation in the non-agglomerated fraction.

However, if this fraction were the only variable factor in the situation, and all agglomerates were of the same density and cohesion, it would be difficult to explain the variation with traction observed in the initial slopes of the  $\eta - \tau$  curves. If all agglomerates, both temporary and permanent, had the same cohesion strength, their rate of disruption by the stress would be proportional to the number existing. Hence, in the

TABLE I  
*Constants of the Agglomeration-Viscosity Equations*

$\tau$ , dynes/cm. <sup>2</sup>	1.33	2.67	4.00	5.33	8.0	10.7
$\eta_{\infty}$ , poise	1000.	260.	220.	175.	150.	50.
$\eta_1$ , poise	123.	92.	71.	45.	25.	17.
$V_{\infty}$	.790	.750	.746	.740	.732	.676
$V_1$	.726	.706	.698	.668	.626	.592
$f$	1.796	1.705	1.696	1.683	1.664	1.537
$b$	1.546	1.652	1.524	1.042	.660	.676

$V_0 = .44$  = the partial volume at zero time after stirring. The viscosity of water at room temperature is taken as .009 poises.

$\tau$  = traction, or shearing stress, during viscosity measurement.

$\eta_1$  = viscosity at 1 second after stirring.

$\eta_{\infty}$  = viscosity at infinite time.

$V_1$  = partial volume of agglomerates at 1 second after stirring.

$V_{\infty}$  = partial volume of agglomerates at infinite time.

$f$  = volume of flocculate/volume of solids in agglomerates.

$b = kN_0$ .

$k$  = velocity constant of agglomeration.

$N_0$  = initial number of single particles/cm.<sup>3</sup>.

beginning, when this number is small, their rate of increase would be determined by the agglomerating forces almost uninfluenced by the disrupting forces. The initial increase in viscosity with time would then be independent of the traction, which is contrary to experiment.

Apparently, then, the variation in the initial slopes of the  $\eta - \tau$  curves requires the postulate that, under zero stress, agglomerates form with a wide range in cohesive strength but, in the presence of stress, only those agglomerates can form which have a cohesion greater than a critical value which increases with the traction.

It appears from the foregoing arguments that the quantitative theory presented above takes account of the primary factors involved in the process of thixotropic recovery of the latex after stirring. Determination of secondary factors, particularly the amount of non-agglomerated solids in the steady state, will require further experiments which include additional treatments.

The experimental data reported in this paper were obtained by Mr. W. E. Wolstenholme, now a Lieutenant in the United States Navy.

## SUMMARY

A viscometer is described for measuring the viscosity of a liquid immediately after an abrupt reduction of the shearing stress to a very low value. A hollow cylinder on a torsion suspension is immersed in the liquid contained in a narrow annular channel. The inner wall of the channel is rotatable with respect to the outer wall, and by this rotation the liquid is stirred or sheared. After the stirring is stopped, the viscosity is measured by photographically recording the rotation of the hollow cylinder, driven by a nearly constant torque applied through the torsion suspension.

Measurements were made on a commercial compounded rubber latex containing 47.5% total solids. Immediately after stirring, the latex is a Newtonian liquid with a viscosity of .05 poises. Thereafter the viscosity increases at an initial rate and to an ultimate value both of which decrease as the shearing stress for measuring the viscosity is increased. The steady viscosity is attained approximately in 10 seconds. The observed extremes in steady viscosity were 11 and .5 poise, corresponding to the shearing stresses 1.3 and 10.7 dynes/cm.<sup>2</sup>.

The experimental data are fitted approximately by theoretical curves based on these assumptions: All aggregates of solid particles are broken up by the stirring. During subsequent thixotropic recovery, loose aggregates are formed which contain considerable trapped water. The rate of aggregation follows Smoluchowski's theory of slow coagulation, but both the coagulation rate constant and the *per cent* volume of water in the coagulates vary with the applied shearing stress. The relative viscosity of the suspension of aggregates follows an empirical law based on Eilers' data on aqueous suspensions of Bitumen spheres.

## REFERENCES

- (1) MOONEY, M., *J. Rheol.* **2**, p. 210 (1931).
- (2) SMOLUCHOWSKI, v., *Physik. Z.* **17**, 557, 583 (1916); *Z. physik. Chem.* **92**, 129 (1917).  
Also FREUNDLICH, *Colloid & Capillary Chemistry*, p. 433, E. P. Dutton & Co., New York.
- (3) EILERS, H., *Koll. Z.* **97**, 313 (1941).

## Book Reviews

**Photosynthesis and Related Processes, Vol. I.** By EUGENE I. RABINOWITCH. Interscience Publishers, Inc., New York City. 599 pages. \$8.50.

The process of photosynthesis in plants is recognized everywhere as the most important chemical reaction in nature, since the existence and maintenance of life depend upon it. Plant physiologists, organic chemists, biochemists, physical chemists and physicists made very important progress in this field, especially in the last ten years. From the time Spoehr's well known monograph was published in 1926, no comprehensive review on photosynthesis has appeared. Consequently, a new survey was sorely needed as an aid to research workers and students alike. The book of Eugene Rabinowitch, the first volume of which appeared recently, is splendidly fitted to remedy the situation. It is written by an author who possesses a rare combination of qualities. He is a photochemist of renown and, at the same time, a scientific writer known for his ability to survey critically a vast amount of material, to order it and to present it in a form in which it becomes palatable to a broader audience. The casual reader and the student who is eager to know at a glance where we stand at present may ask himself whether it was necessary to discuss not only the facts but also, with historical accuracy, all the theoretical interpretations of the phenomena, merely to show later that, and why, they are obsolete. But such a criticism is not just; the present status of the problem forced the author to discuss the whole literature in order to make it clear to the reader why a host of theories and pseudo-theories must be rejected. Only by such a procedure is a house-cleaning possible. This reviewer hopes that from now on most of the old theoretical equipment found unusable by the author may be eliminated for good from the literature. To solve the problem of photosynthesis, scientists of a great variety of training have to cooperate and learn to understand mutually their scientific language; until that is achieved we have to pass through a period of confusion. Rabinowitch's book is of considerable help in shortening that period.

The author approaches the problem from its most neglected angle—that of the photochemical changes, in which the light-absorbing chlorophyll molecule is involved. Experience, gained from his own work on the behavior of chlorophyll *in vitro*, enabled him not only to review with understanding the work of the investigators who contributed the new factual material during the last ten years, but to weigh the evidence, to provide competent criticism, and to put forward stimulating ideas for further research.

After an interesting historical introduction and a discussion of the total volume of photosynthesis on earth, the author proceeds to describe, in the first part of Volume I, the chemistry of photosynthesis and related processes in the living plant and outside it. The individual chapters deal with the over-all reaction and products of photosynthesis, the reactions of isolated chloroplasts, the photochemical reactions *in vitro* which bear a relation to true photosynthesis, and the metabolism of purple and colorless autotrophic bacteria and anaerobically adapted algae. Then the author deals in separate chapters with the primary photochemical process and the several known or inferred non-photochemical reactions in photosynthesis, such as the primary binding of carbon dioxide. This part is completed by two chapters dealing with the effects of various poisons, narcotics, ions and other chemical and physical agents.

The second part of Volume I is devoted to the structure and composition of the chloroplasts, and the structure and chemical properties of the pigments (chlorophyll,

carotenoids, phycobilins). It concludes with chapters dealing with the photochemical reactions of these pigments (including photooxidation reactions *in vivo*) and the relationship between photosynthesis, photooxidation and respiration.

Each chapter contains an exhaustive presentation of factual material in which the reliable older data receive adequate attention, together with the results of the more recent investigations. By means of comprehensive tables, the author has striven to economize in space and to enable the reader to make critical comparisons of the results of various observers.

The material is accompanied by a thorough discussion of the theoretical considerations the various investigators presented in their papers. Many an original thought of the writer of the book has been incorporated into these discussions, particularly those dealing with the photochemical problems.

A well organized table of contents, chronological bibliographies at the end of each chapter, and careful cross-references written in the book allow the reader to find his way through a wealth of data that, by necessity, are often heterogeneous. The difficulty that no generally accepted system of symbols and schemes exists in the literature was solved by the introduction of a system of the author's choice which is used consistently throughout the book.

Volume II, which is promised to appear within a year, must contain, as can easily be seen from what is missing in Vol. I, all the work on the kinetics of photosynthesis, the quantum yields and their theoretical implications, the induction phenomena, and the spectroscopy and fluorescence of plant pigment. It would be agreeable to have a chapter on experimental methods since the work clearly transcends the scope of a text book. As a handbook in the laboratory, it would save the worker time if such a chapter were added.

To authors of textbooks in the fields of biology, biochemistry, and photochemistry, it presents an opportunity of modernizing and correcting their pertinent chapters that usually abound with obsolete or downright erroneous statements.

Once completed, Dr. Rabinowitch's work will stand out as an example of how to write a monograph on a specialized and difficult subject. In this particular case, one may truly say it is just the kind of book which was needed in the field of photosynthesis. The reviewer ventures to predict that it will be of considerable influence in shaping the future development of this intriguing problem.

JAMES FRANCK

**Catalytic Chemistry.** By HENRY WILLIAM LOHSE, Chemical Publishing Company, Inc., Brooklyn, N. Y., 1945. xiv+471 pages. Price \$8.50

In writing this book the author has "aimed at a brief factual presentation of the underlying principles of catalytic phenomena and the application of catalytic reactions in industrial practice." The material included is subdivided into five chapters: I. Brief History of Catalytic Chemistry (5 pages); II. Catalytic Theory (105 pages); III. Nature and Properties of Catalysts (68 pages); IV. Specific Types of Catalytic Reactions (120 pages); and V. Industrial Catalytic Reactions (121 pages). The book opens with a foreword by E. Emmet Reid and an author's preface, and closes with a very complete author and subject index (47 pages).

The last three chapters present a good and well-annotated summary of catalysts, their properties, reactions in which they are effective and the industrial uses to which they are put. Particularly valuable is the survey of catalytic activity of elements and compounds in relation to the position of the elements in the periodic table (Chapter III), and the consideration of various types of reactions and the substances found to be catalytically active for them (Chapter III). The discussion of catalytic reactions in

industry is quite extended and as up-to-date as possible at present, although it is of some question to what degree process flow sheets and plant layouts contribute to the understanding and appreciation of catalytic phenomena.

The author's attempt to present all the theoretical aspects of catalysis within a span of 105 pages does not fare so well. This chapter opens with a statement of the Brønsted theory of reaction velocity and rushes on at breakneck speed through such topics as chemical purity, spectroscopy, Langmuir's work on surface reactions, negative and autocatalysis, chain and induced reactions, promoters, inhibitors, poisons, homogeneous catalysis in solution and gas phase, and heterogeneous catalysis in its various ramifications. About the only topic omitted is the Theory of Absolute Reaction Rates. A novice in the subject of catalysis could well learn in this manner nothing about everything. Further, the presentation contains statements and generalizations which are either misleading or fallacious. Thus, on page 19 we find the conclusion that "it takes a mechanism of chemical heterogeneity to make reactions start and to keep them going." On page 37 we learn that "it is undoubtedly quite general in homogeneous catalysis that the reaction products cause negative catalysis." Again, on page 41 it is stated that "in acid-base catalysis both the acid and base must be present before the reaction takes place," while on page 71 we find the conclusion that "anions of weak acids are likewise to be regarded as (generalized) acids." On page 73 the secondary salt effect is ascribed as "due to ions in common with catalyst or substrate," while on pages 74-75 the variation of activities with ionic strength is adduced as evidence for variation of the degree of ionization of weak acids on addition of neutral salts. In another chapter activity coefficients of gases are confused with fugacities (page 262). Still another curious deduction is reached on page 308. The author tabulates the equilibrium concentrations of  $\text{NH}_3$  present at equilibrium, as calculated from thermodynamic data on the assumption that  $K_p$  is identical with the thermodynamic equilibrium constant, and then points out that "at higher pressures, *i.e.*, 200-1000 atmospheres, more  $\text{NH}_3$  is found than is expressed by the equation above [ $\ln K = f(T)$ ], which is ascribed to the use of more efficient catalysts."

There are also some equations in the book which are incorrect (as equation 6, p. 60), which do not apply to the conditions given (p. 246), or in which the symbols are improperly explained (p. 236). Besides some obvious misprints, such as Irwing Langmuir (p. 25), Bailly for Bailey (twice on p. 36), and some others, Aston's name is consistently given as Ashton on pages 123, 129, 135, 145 and 149.

In the reviewer's opinion this book, despite some of its good features, is not the sort of volume which can be recommended to a beginner as an authoritative treatise on catalysis. To one familiar with the field the errors and misstatements are a source of annoyance. The price of the book also appears to be rather high for a work of this size and type.

SAMUEL H. MARON

**Atomic Energy in War and Peace.** By GESSNER G. HAWLEY and SIGMUND W. LEIFSON. Reinhold Publishing Corporation, New York City. 211 pages, 35 figures. \$2.50.

The definite political implications, as well as the possible economic significance, of the conversion by nuclear chemistry of comparatively large quantities of mass into destructive or useful radiant energy has developed a thirst in the average man for knowledge of the physics of the atom. The book, written in response to this demand, is intended for "those who have an elementary acquaintance with physics and who wish to obtain a fairly well-rounded view of the most remarkable scientific achievement in history, and the future possibilities of this new force in the economic life of the nation." The book is a "quickie . . . based on facts drawn from thoroughly reliable sources,"



the most important of which is the report prepared for the War Department by Prof. Smyth.

The entire text is interestingly presented and will engage at times the bewildered attention of the pedestrian reader. Several statements will also amaze the professional scientist. Thus, according to the authors, Dalton's Atomic Theory is an established fact capable of predicting the exact ratios in which the atoms combine. The impression is created (page 47) that, in contrast to rapid oxidation or ordinary chemical explosions, the rate of nuclear reactions may be slow and yet be capable of producing excessively high temperatures. This impression is later (pages 146, 164) corrected. Unfortunately, a clear statement is nowhere given of the relative values of the masses converted to radiant energy (in accordance with the Einstein equation) in ordinary and nuclear chemical reaction. Such a statement would immediately make evident the usual comparisons between tons of coal and unbelievably small amounts of radioactive or fissionable materials. According to a statement made (page 58), the reaction 2 protons plus 2 neutrons  $\rightarrow$  Helium plus 190,000 kilowatt hours if reversed would yield 190,000 kilowatt hours. Although the concept of half-time is very clearly presented, it is later used incorrectly to indicate a lag time between nuclear capture of a particle and a subsequent radioactivity.

Principles of such complicated instruments as the cyclotron and the mass spectrograph are very distinctly and understandably presented.

The authors' evaluation of possible future peace time uses of atomic energy is appropriately sensible and they exhibit unusual courage in their discussion of possible effects of the atomic bomb on naval warfare.

"The ability, courage, foresight, and hard work of all those who participated in the atomic energy development" are indeed praiseworthy but these qualities, this reviewer believes, should not be compared with those of the men who shouldered the guns. The virtues may be the same but the circumstances under which they were exhibited are too dissimilar to permit comparison.

The book is exceptionally well printed with a type easy to read. A convenient index is included and an appendix lists the personnel, participating Companies and Universities, of the Atomic Bomb project. The book is recommended to those for whom it was written.

FRANK BRESCIA

## STUDIES IN AMPHIPATHIC ADSORPTION.

### I. THE ADSORPTION OF POLYVINYL ALCOHOL ON SILVER BROMIDE \*

S. E. Sheppard, A. S. O'Brien and G. L. Beyer

*Communication No. 1067 from the Kodak Research Laboratories, Rochester 4, N. Y.*

*Received February 4, 1946*

#### INTRODUCTION

The term "amphipathic" was originally employed by Hartley (1) to refer to the dual character of particles, micelles and (macro) molecules which have both hydrophile and hydrophobe groups operative in the same structure or system. We have used the term in reference to adsorption for cases where the adsorption of an amphipathic molecule or micelle to a solid or liquid involves a primary step of one-sided irreversible adsorption (sometimes termed *pseudo*-adsorption), which we will distinguish as  $\psi$ -adsorption, followed by a secondary step of reversible adsorption, which we will distinguish as  $\theta$ -adsorption, effected by the anti-thetic side or aspect of the molecule or micelle in question. In most cases so far studied the primary  $\psi$ -adsorption has occurred by attachment of polar hydrophile groups to a polar surface, leaving a nonpolar hydrophobe grouping exposed as the new surface to which similar groups of free amphipathic molecules could attach themselves, in general reversibly, but with development of a new polar hydrophile surface.

The primary stage generally gives rise to coagulation and precipitation of the coated particles (to which is attributed the phenomenon of the "sensitization" of hydrophobic inorganic colloids by hydrophile organic colloids (2)), while the secondary  $\theta$ -adsorption leads to a peptization or deflocculation of the precipitated material.

The first example of such behavior examined in these laboratories was the adsorption of basic cyanine dyes to silver bromide (3), which gave a method for determining the specific surface of the dispersed phase of the silver bromide sol and, furthermore, estimates of the orientation of the adsorbed molecules to the surface. This procedure, in which the adsorbate consists, in selected cases, of molecularly dispersed particles of relatively low molecular weight (*ca.* M.W. 400), and of rather accurately

\* Beside that of gelatin (Sheppard, S. E., Lambert, R. H., and Swinehart, D., *J. Chem. Physics* **13**, 372 (1945)), a number of orientating investigations have been made by these Laboratories and will be reported on later.

known composition and constitution, is of great assistance in studying the  $\psi$ -adsorption of high molecular substances.

### EXPERIMENTAL

The silver bromide sol was prepared by slight modification of a procedure already described (4). It was  $0.020 M$  to  $AgBr$  and contained  $10^{-3} M$  bromide ion. Another sol containing  $10^{-3} M$  silver ion was prepared by a similar method.

Since PVA\* is not a material of unique and identically reproducible composition and constitution,† some particulars are in order as to the specimens used. *Material A* was prepared by the Organic Research Department of these Laboratories by alkaline deacetylation of a polyvinyl acetate of relatively low viscosity corresponding to a M.W. of about 20,000–25,000. It still contained 1.5% of undecomposed polyvinyl acetate and was unfractionated. *Material B* was a fractionated portion (by ace-

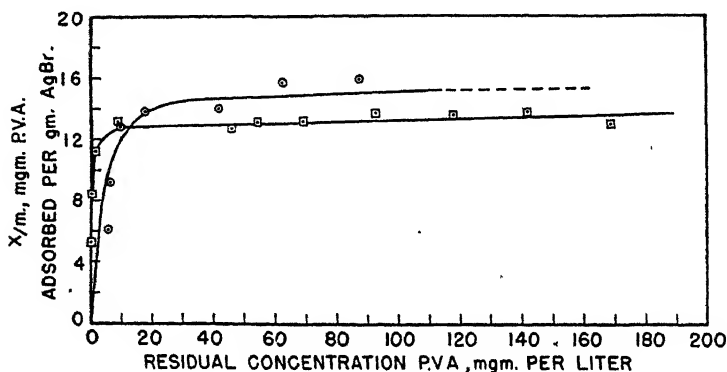


FIG. 1

Adsorption of Polyvinyl Alcohol on the Dispersed Phase of the Silver Bromide Sol

□  $10^{-3} M$  to Bromide Ion; ○  $10^{-3} M$  to Silver Ion

tone-water) of M.W. 47,000 prepared by the same laboratory by acid hydrolysis (deacetylation) of a polyvinyl acetate of correspondingly high M.W. It likewise contained a residual 1.5% of acetate and also about 3% of polyvinyl acetal.

*Material A* was used for the analytical adsorption experiments—Table I and Fig. 1, and Table II—while the coagulation and peptization cycles were carried out with both A and B. No significant difference of behavior was observed between them. It may be noted that these ad-

\* PVA is the abbreviation for polyvinyl alcohol.

† We thank Dr. C. J. Staud for calling our attention to this question and Dr. G. Waugh for supplying the data on composition.

sorption experiments are carried out on material in dilute aqueous solution. It is probable that the significant differences observed with different batches of PVA, which are connected with differences in the modes of preparation and, to some extent, with small differences in composition, appear with hydrogels and with sols and dopes of high concentration.

TABLE I

*Adsorption of PVA to the Dispersed Phase of the Silver Bromide Sol*

Mg. PVA Added per 25 ml. Sol	Mg. PVA Adsorbed per 25 ml. Sol	Residual Conc. PVA mg./liter	x/m mg./g.
In $10^{-3}$ M Bromide Ion			
0.50	0.50	0.0	5.3
0.80	0.80	0.0	8.5
1.10	1.05	1.2	11.2
1.60	1.24	8.9	13.2
3.00	1.19	45.3	12.7
3.40	1.24	54.0	13.2
3.70	1.58	53.0	16.8
4.00	1.24	69.0	13.2
5.00	1.29	92.7	13.7
6.00	1.28	118	13.6
7.00	1.30	142	13.8
8.00	1.22	169	13.0
In $10^{-3}$ M Silver Ion			
0.80	0.57	5.7	6.1
1.10	0.86	6.0	9.2
1.60	1.20	9.7	12.9
2.00	1.30	17.4	13.8
3.00	1.32	42.0	14.0
4.00	1.48	62.5	15.7
5.00	1.50	87.5	15.9

TABLE II

*Displacement of Adsorbed PVA by Dye IVb*

Mg. Dye Added	PVA Desorbed Mg./G.	Per Cent PVA Desorbed
0.48	2.4	18
0.80	6.6	51
1.12	9.0	69
1.60	—	—
2.08	9.4	72
2.56	—	—
3.20	9.9	76

The adsorption of PVA to the sol was tested as follows: To 50-ml. glass-stoppered centrifuge tubes were added known amounts of PVA solution, a constant amount of buffer at pH 6 and water to make a total volume of 15 ml. Then 25 ml. of silver bromide sol (containing 0.094 g. AgBr per 25 ml.) were added and the tubes were tumbled at room tempera-

ture for 16 hours, then centrifuged at 2200 r.p.m. for 1 hour. Portions of the supernatant liquid were analyzed for their PVA content by a method of permanganate oxidation to be described elsewhere (5).

Data for two series of experiments at pH 6, one at  $10^{-3}$  *M* silver ion and one at  $10^{-3}$  *M* bromide ion, are given in Table I, and graphically presented in Fig. 1.

For comparison, Fig. 2 represents the data obtained in the adsorption of Dye IVb to silver bromide sol which is  $10^{-3}$  *M* to bromide ion.

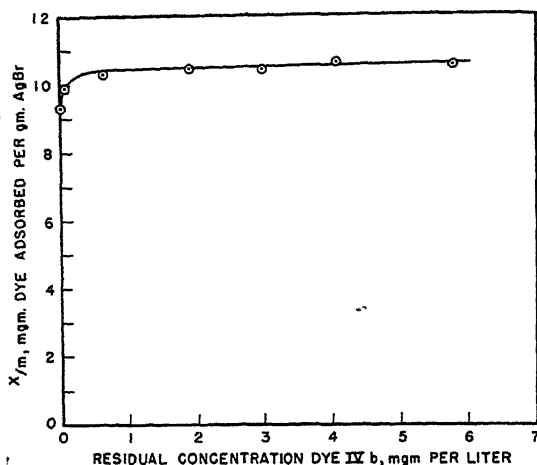


FIG. 2

Adsorption of Dye IVb to AgBr Sol  
 $10^{-3}$  *M* to Bromide Ion

#### EXPERIMENTS ON REVERSIBILITY

Attempts were made to reverse the adsorption by shaking in water at 25°C. After 45 hours, not more than 0.1–0.2 mg. of polyvinyl alcohol was removed per g., which is *ca.* 1–1.5% of the total adsorbed. Boiling the same quantities of polymer-coated silver bromide for 3 hours removed only 1.8 mg./g. AgBr, or *ca.* 13% of the 13–14 mg. originally adsorbed.

#### BEHAVIOR OF BASIC CYANINE DYE

Experiments in a medium  $10^{-3}$  *M* to bromide ion and at pH 6 showed that, when the silver bromide surface had Dye IVb (3,3'-diethyl-9-methyl thiacyanine bromide) adsorbed just sufficient to saturate the surface, PVA, in any concentration, was quite unable to displace any dye. Varying amounts of PVA were added to the dyed silver bromide in centrifuge tubes which were tumbled for 16 hours. Not only was no dye displaced from the silver bromide but no polymer was adsorbed from the

solution on the dye coating at any concentration of PVA. Thus, the dye completely "protected" the silver bromide against the PVA.

Similar experiments indicate also that the dye very largely (up to 75% at least) displaces PVA on the silver bromide surface, when just sufficient PVA had been added to saturate the surface.

#### AMPHIPATHIC ADSORPTION

In several respects the behavior of PVA on silver bromide is similar to that of gelatin (4). Some experiments, therefore, were made on the coagulation and peptization of the silver bromide sol by dilute PVA solutions by the procedure described in the reference above. The results are presented graphically in Fig. 3, and it will be seen that the curve is

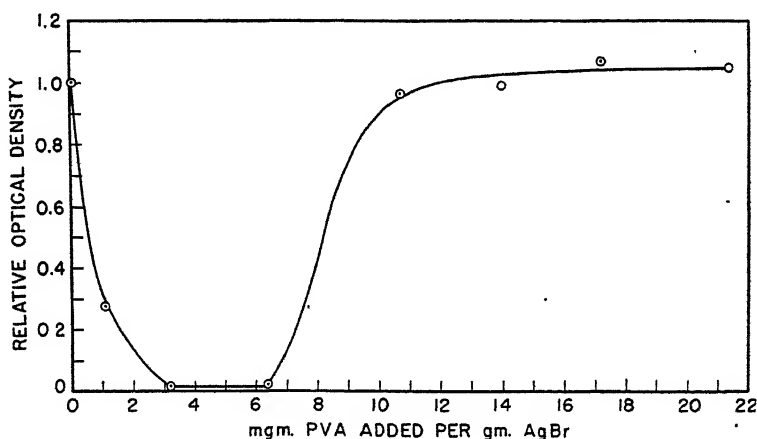


FIG. 3

Flocculation-Peptization of AgBr Sol by Polyvinyl Alcohol; pH = 4.9

generally similar to those obtained with gelatin but without pH effect. The peptization point is at 6.5–7.0 mg./g. AgBr for both *Materials A* and *B*, a value which must be taken as provisional until more data are obtained on different specimens of PVA.

#### EFFECT OF ADSORPTION TO SILVER BROMIDE ON POLYVINYL ALCOHOL

When the coagulated (precipitated) PVA-coated silver bromide was centrifuged prior to peptization in excess solution of PVA, it was observed that this material dissolved much more slowly in a saturated solution of potassium bromide than the original silver bromide particles uncoated with PVA, several hours in the cold plus about one hour at 80° to 90°C. being necessary. When the silver bromide was finally dissolved, the

polymer coating retained the form of the precipitated and centrifuged mass and floated in the solution of potassium bromide as a semitransparent disk. This was insoluble in cold water but dissolved readily when the temperature was raised to 60°C.

The observations suggest that, not only is PVA made relatively insoluble as and when adsorbed to a silver bromide surface, but it may have been made permanently less soluble after removal (or solution) of the silver bromide. The solution of potassium bromide, from the position of its ions in the lyotrope series, might be expected to have a peptizing rather than an insolubilizing effect on the PVA; the experiments will be repeated and diversified in an effort to specify and clarify more completely the meaning of "solubility," "melting point" and "minimum solution temperature" when applied to such substances as gelatin and polyvinyl alcohol.

### DISCUSSION

Examination of the data given in Table I and Fig. 1 shows that the adsorption of PVA to silver bromide resembles that of several cyanine dyes (3) in proceeding to an irreversible saturated layer. The saturation value found at 25°C. for the standard AgBr sol was 13-14 mg. PVA/g. AgBr, which is near that found, 10 mg./g., for the basic cyanine dye, IVb. The dye has a M.W. of *ca.* 400, and the PVA one of *ca.* 40,000, so that it is probable that the polymer axis or backbone would be lying parallel to the AgBr surface but the rest of the molecule more or less edgewise thereto. It is noteworthy that there seemed no tendency to formation of further layers over the primary layer at saturation. The fact that the weight/g. of this coating appears to be just twice the value for the "peptization point" (6-7 mg./g. AgBr) may be fortuitous, otherwise there are two interpretations:

(1) The peptization point represents a completed monolayer with a hydrophobe exterior, in which case the saturation level indicates a completed duplex layer, but both compound monolayers are irreversibly adsorbed; or

(2) The saturation level represents a monolayer, but one such that hydrophile properties appear at 50% coverage.

The structure suggested from X-ray diffraction data (6) for orientated PVA is not inconsistent with a duplex layer (7) which might have an alternate folding, whereby —OH polar groups are effectively presented to both the silver bromide surface and to water.\* Some quasi-electronic

\* A further, perhaps equivalent, kind of hydrogen bonding might be occurring somewhat in the fashion suggested by L. Michaelis (8) for the polymerization of the free

continuity of the —OH groups of PVA is suggested by recent observations that the intensity of the electrical anisotropy of stretched PVA films is considerably increased by previous impregnation of the PVA sheet with precipitated silver bromide.\*

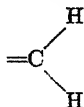
The behavior of PVA on silver bromide shows that the phenomenon of agglutination  $\rightarrow$  peptization consequent on addition of an amphipathic molecule or macromolecule to a hydrophobe sol may involve variants in the mechanism, even though this seems to be fundamentally a matter of alternation of polar and nonpolar interactions.

So far, the rate of adsorption in the primary phase ( $\psi$ -adsorption) has appeared, in absence of other interfering bodies, to be very rapid, but it is likely that the later phases of the adsorption act involve relatively slow processes of diffusion and molecular accommodation (orientation) on the surface of the solid. It is hoped to gain some information about these by time-studies of the interfacial tension and contact angle of water and, *e.g.*, cyclohexane, at the evolving surface.

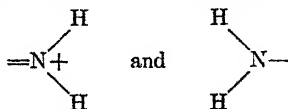
The pseudo-adsorption or irreversible adsorption dealt with in this and related studies need not be considered as contradicting the broad principle embodied in the Gibbs Theorem, but as standing in much the same relation thereto as crystallization or precipitation to the behavior of a solution, *i.e.*, essentially as a discontinuity in any functional representation. The adsorbed dye or colloid, which becomes insoluble in the liquid from which it is deposited, is bonded to the adsorbent by chemical forces of high magnitude, greater than any existing between water and the hydrophobe organic part of the adsorbed molecule.

### SUMMARY

The adsorption of polyvinyl alcohol to silver bromide has been measured and found to be irreversible ( $\psi$ -adsorption). No secondary reversible radicals of Würster dyes. In the case of PVA, it would have to be assumed that



groups attached to —OH groups, which themselves, when in orientated chains (in the polymer), form resonating systems, take on properties similar to the alternate of



Michaelis's configuration. Naturally, this remains speculation until electron diffraction studies can be made of the adsorbed PVA. Something similar may be present in the polymeric structures of boron hydride and of aluminum trimethyl (9).

\* Unpublished experiments of S. E. Sheppard and P. T. Newsome.



adsorption appeared to occur but there was precipitation of silver bromide sol followed by peptization with excess polyvinyl alcohol. The peptization point was found to occur at an adsorption value 6.5 to 7.0 mg./g., just half that at which saturation occurred.

Adsorbed basic (cyanine) dye is not displaced from silver bromide by PVA but the latter is very largely displaced by basic dye.

#### REFERENCES

1. HARTLEY, G. S., *Trans. Faraday Soc.* **37**, 130 (1941).
2. SHEPPARD, S. E., *Nature* **155**, 266 (1945).
3. SHEPPARD, S. E., LAMBERT, R. H., AND WALKER, R. D., *J. Chem. Phys.* **7**, 265 (1939).
4. SHEPPARD, S. E., LAMBERT, R. H., AND SWINEHART, D., *J. Chem. Phys.* **13**, 372 (1945).
5. Paper in preparation, by A. S. O'Brien.
6. MOONEY, R. C. L., *J. Am. Chem. Soc.* **63**, 2828 (1941).
7. SHEPPARD, S. E., AND NEWSOME, P. T., *J. Chem. Phys.* **12**, 513 (1944).
8. MICHAELIS, L., AND GRANICK, S., *J. Am. Chem. Soc.* **65**, 1747 (1943).
9. BURAWOY, A., *Nature* **155**, 328 (1945).

# EFFECT OF DIVERSE ANIONS ON THE pH OF MAXIMUM PRECIPITATION OF "ALUMINUM HYDROXIDE"

Stephen P. Marion and Arthur W. Thomas

*From the Department of Chemistry, Columbia University, New York 27, N. Y.*

*Received February 8, 1946*

## INTRODUCTION

Certain observers have reported diverse values for the pH of optimum precipitation of aluminum hydroxide. Theriault and Clark (1), using a time study of the "best and most rapid" method of floc formation from a potassium alum solution, conclude that this is at a pH value of 5.5 to a pH value of 5.6. They found that in this region the floc appeared first and possessed the qualities of rapid settling and abundance in the highest degree. Miller (2), continuing the study along similar lines, found that the most complete precipitation from an alum solution occurs between the pH values of 6.7 and 7.0.

Hatfield (3), precipitating the hydroxide from alum, reported a minimum of aluminum in the filtrate between the pH values of 6.1 and 6.3. He also observed that added anions shifted the location of the zone of coagulation. In the presence of oxalate ion, for example, aluminum precipitated only in the range of 8.5 to 9.5, whereas in the presence of chromate ion a broad range of coagulation from pH 5 to pH 10 was found. He attributed these effects to a specific "coagulating effect" of the anion, and concluded that, in general, polyvalent anions are more efficient than monovalent anions in aiding the sodium hydroxide to produce coagulation. Hatfield refers to his pH values of 6.1 to 6.3 (for a minimum of aluminum in the filtrate) as indicating the isoelectric point of aluminum hydroxide.

Mattson (4), investigating the laws of soil colloidal behavior, prepared some isoelectric mixtures of aluminum hydroxide and added salt, and concluded that "the sulfated hydroxides are isoelectric at a lower pH than the chloridated complex, and that the sulfate content of the former is higher than the chloride content of the latter." He made further studies on the shift of the isoelectric point when phosphate and silicate ions were added. "The entrance of phosphate and silicate ions into the sesquioxide complex lowers the isoelectric pH because these ions displace the diffusible acid anions as well as the hydroxyl ions." (4)

These widely differing results cannot be attributed to experimental error. It is to be noted that, while the various authors refer to the behavior of "aluminum hydroxide," it is at once obvious that the material under study is not just aluminum hydroxide but some combination of hydrous alumina complexes with added anion, since the varied results of the optimum precipitations are due, in the main, to the fact that the "hydroxide" was precipitated in the presence of different anions.

It is the intention of the authors to submit an explanation for the various pH values of optimum precipitation on the basis of the formation of Werner complexes. Inasmuch as aluminum exhibits the co-ordination number of six, the hydrated ion can be considered to be  $[\text{Al}(\text{H}_2\text{O})_6]^{+++}$ .

In accordance with the ideas on the hydrolysis of aluminum salts suggested by Pfeiffer (5), when hydroxyl ion is added to such a solution it has the ability to attract hydrogen ion from the co-ordinatively bound water molecules. Thus in solution we have the possibility of the existence of the following substances:  $\text{Al}(\text{OH})(\text{H}_2\text{O})_5^{++}$ ,  $\text{Al}(\text{OH})_2(\text{H}_2\text{O})_4^{+}$ ,  $\text{Al}(\text{OH})_3(\text{H}_2\text{O})_3^{\circ}$  (aluminum hydroxide),  $\text{Al}(\text{OH})_4(\text{H}_2\text{O})_2^{-}$  (aluminate ion) (6), and also solated complexes. There is no evidence for the ability of hydroxyl ion, even in concentrated solutions, to remove more than four hydrogen ions per aluminum ion (7).

If foreign anions are added, these may displace aquo groups and occupy some of the co-ordination positions formerly held by them. The effect of added hydroxyl ion cannot be easily predicted since the hydroxyl ions might completely replace the bound anions, replace them in part, or perhaps not at all. With this viewpoint in mind the following experiments were conducted.

#### PROCEDURE

To freshly prepared 0.02 *M* aluminum chloride solution was added the calculated amount of the solid potassium salt of the anion under investigation. One hundred ml. portions of the resulting solution were then pipetted into "Non-Sol" glass bottles and 100 ml. portions of sodium hydroxide solution were added as rapidly as possible to each bottle containing the aluminum chloride-added salt solution. These were then rotated at room temperature for a period of three days at 12 r.p.m.

It was found that there was a considerable drift in the pH value of the contents of any one bottle for the first few hours. One sample changed from pH 6.18 to pH 6.81 in seven hours. After two days this had changed to 6.82 and then remained constant to within 0.05 pH unit for two weeks.

A series of such bottles was prepared at one time. Each bottle contained the same concentration and the same amount of aluminum chloride plus added salt but differed from the next in the quantity of sodium hydroxide. Preliminary experiments indicated the approximate amount of sodium

hydroxide needed to obtain maximum yield of precipitate. The concentrations of added sodium hydroxide in any series were then so adjusted that this maximum precipitation appeared near the center of the series, that is, on either side of this maximum the weight of precipitate diminished.

After three days the rotator was stopped and the pH of the supernatant liquid in each case measured by means of a glass electrode. The solutions were filtered through quantitative filter paper, washed with 2% aqueous ammonium nitrate solution three times, ignited and weighed. This is substantially the procedure for determining aluminum as proposed by Blum (9).

In some cases the aluminum content of the filtrates was determined by destroying the added anion where necessary, usually by boiling with a mixture of nitric and sulfuric acids. The aluminum was precipitated with 8-hydroxyquinoline and determined by means of standard bromate-bromide solution according to the method of Knowles (8).

In some cases only an aliquot portion was treated in the manner described. Remaining aliquots were used to determine the anion content of the filtrate. Oxalate was determined by titrating against standard potassium permanganate, while sulfate was determined gravimetrically as barium sulfate. Fluoride determinations were made for low concentrations of added fluoride ion only, to avoid precipitation of  $\text{Na}_3\text{AlF}_6$ . The precision of all measurements was  $\pm 0.5\%$  or better.

One of the techniques employed by other observers (10) for determining the pH of optimum precipitation has been to precipitate the "aluminum hydroxide" in graduated tubes and, instead of determining the aluminum gravimetrically, the point of optimum precipitation has been judged by the largest volume of precipitate. It was found in this investigation, however, that there is generally no definite relationship between the volume and weight of the precipitate. This is due to the fact that aluminum hydroxide occurs both in a gelatinous and a compact form. Added anions influence the form of flocc, such anions as fluoride and sulfate producing a compact crystalline type while other anions, such as citrate and tartrate, produce a voluminous gelatinous "aluminum hydroxide." The transition for any added anion is gradual and varies with the amount of anion added, the larger the amount of added anion, the lower the pH at which the crystalline form is obtained. Aluminum hydroxide precipitated from an aluminum chloride solution without added anion is most voluminous at pH 5.5 but is precipitated most completely at pH 7.7.

It has been found, however, that with anions which produce the very gelatinous aluminum hydroxide, such as citrate and tartrate, there is a very close relationship between the pH of optimum precipitation obtained

by both methods. This is to be expected when one realizes that with these anions the compact, powdery form of aluminum hydroxide is not obtained. •

In addition to the freshly prepared aluminum chloride solutions, "aged" basic aluminum chloride solutions were also studied. These "aged" basic solutions were prepared by partially neutralizing the aluminum chloride solution with sodium hydroxide and boiling for three or four hours to accelerate the formation of polynuclear complexes, *i.e.*, increasing the number of "ol" and "oxo" bridges in the complex basic aluminum ions or micelles (11) (12).

### RESULTS

Figure 1 summarizes the measurements made in this investigation. Individual curves were plotted for each series, the curves recording the change in weight of precipitate with change in pH. As examples, figures 2, 3 and 4 illustrate this behavior when the added anion is fluoride, sulfate and oxalate, respectively. Each of the curves on these figures

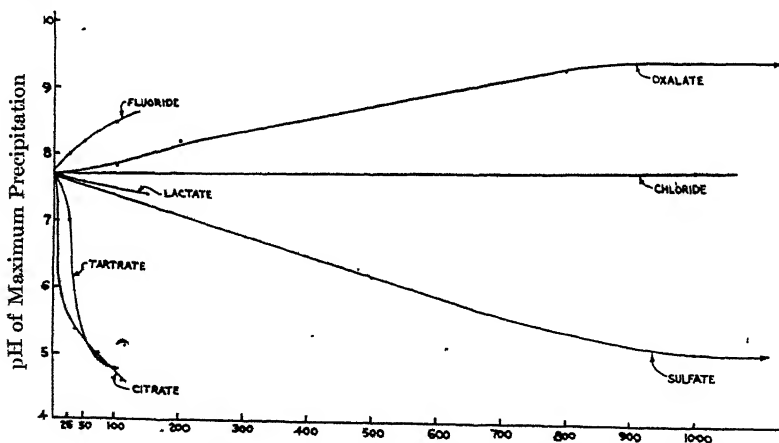


FIG. 1

Concentration of Added Anion in Equivalents per Liter ( $\times 10^4$ )

possesses a maximum which indicates the pH value at which maximum precipitation was obtained for that concentration of added anion. The pH values of these maxima are plotted as a function of the change of concentration of added anion (Fig. 1). From this summary curve it can be seen that each added anion exhibits its individual effect on the shift of the pH of maximum precipitation. The pH at which aluminum hydroxide precipitated from a 0.01 *M* aluminum chloride solution with no added anion other than the hydroxyl ion has been carefully determined. This appears to be at  $\text{pH } 7.7 \pm 0.05$ .

Adding fluoride ion causes this pH of maximum precipitation to rise sharply. Added oxalate ion produces a change in the same direction, but the change is not quite as rapid.

Citrate ion causes the pH of maximum precipitation to decrease very sharply. When the ratio of citrate ion to aluminum ion reaches a value

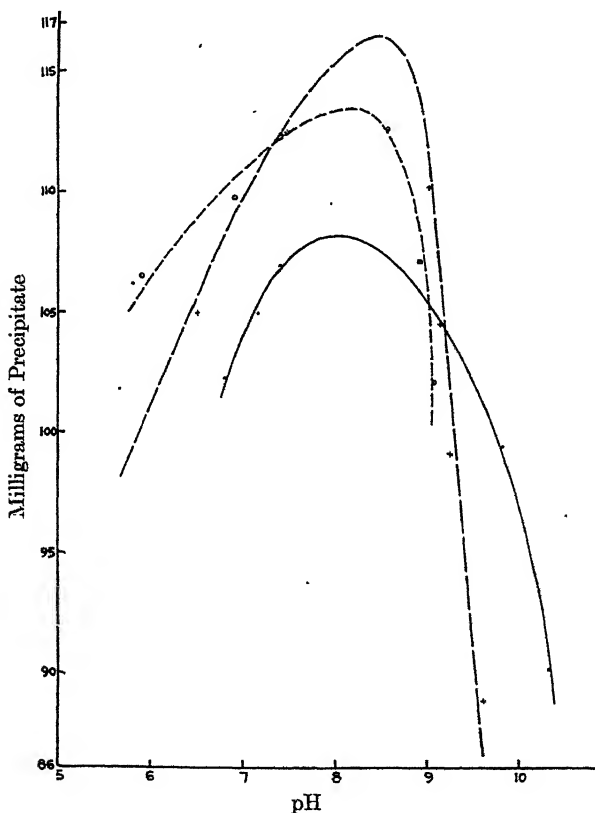


FIG. 2

- 0.0025 *M* fluoride; pH = 8.0
- - - 0.005 *M* fluoride; pH = 8.2
- · - 0.010 *M* fluoride; pH = 8.5

greater than 0.35 mole to 1 (for a 0.01 *M* aluminum chloride solution), no precipitate can be obtained, regardless of the concentration of the added hydroxyl ion. Evidence in accord with this data is furnished by Hanus and Quadrat (13).

Tartrate ion also causes the pH of maximum precipitation to drop sharply as the concentration of tartrate ion is increased. It is to be noted,

however, that the slope of the curve is not quite as great as that of the citrate ion curve. Like the latter, there is a concentration of tartrate ion above which it is impossible to precipitate the aluminum by addition of hydroxyl ion. This concentration is one in which the molar ratio of tartrate to aluminum is greater than 0.5 to 1 for a 0.01 *M* concentration of aluminum ion (13).

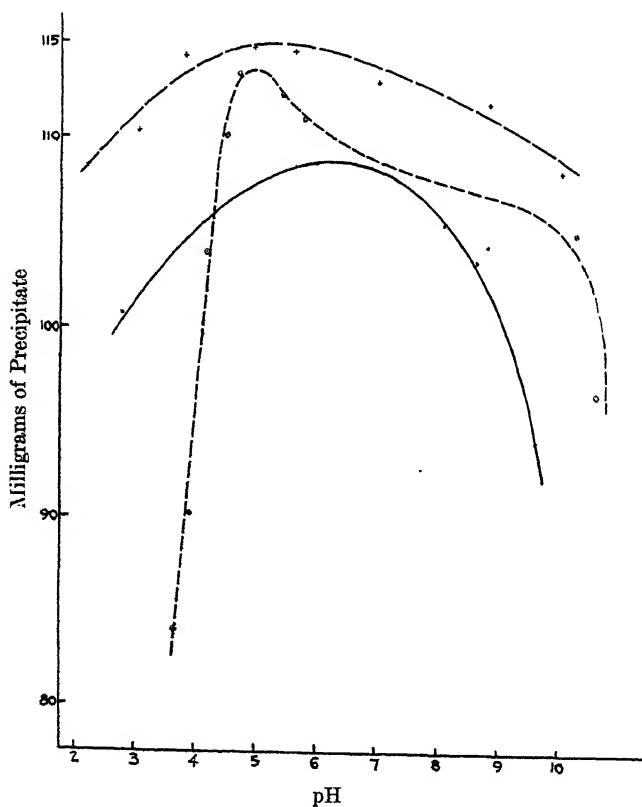


FIG. 3

1. ————— 0.025 *M* sulfate; pH = 6.2
2. - - - - - 0.05 *M* sulfate; pH = 5.1
3. — · — · — 0.1 *M* sulfate; pH = 5.2

When sulfate, chloride or lactate ions are added, the pH of maximum precipitation also drops. Although the sulfate curve drops faster than the other two, all three drop at a gradual rate and in no manner as steeply as the curves describing the effect of the citrate and tartrate ions. Unlike the behavior in presence of citrates and tartrates, there appears

to be no concentration of sulfate, chloride or lactate which prevents the precipitation of "aluminum hydroxide"; on the contrary, increasing the sulfate concentration seems to make the floc more crystalline and compact.

When the precipitate was formed in the presence of certain anions the weight of the ignited aluminum oxide at the point of maximum precipitation was greater than that obtained when no added anions were present. For the concentration and volume of the aluminum chloride solution used, the theoretical yield of the ignited precipitates (expressed as  $\text{Al}_2\text{O}_3$ ) should have been 102 mg. This divergence was most noticeable

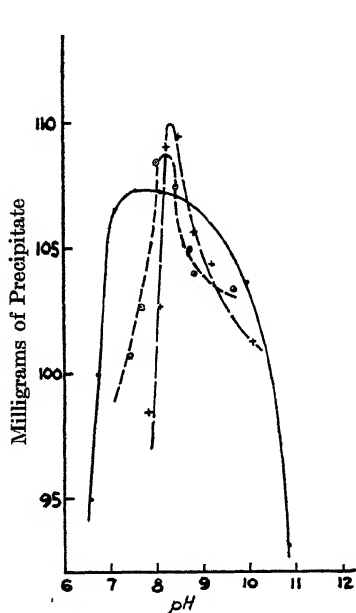


FIG. 4a

1. ——— 0.005 M oxalate; pH = 7.8
2. - - - - 0.01 M oxalate; pH = 8.2
3. — · — 0.02 M oxalate; pH = 8.4

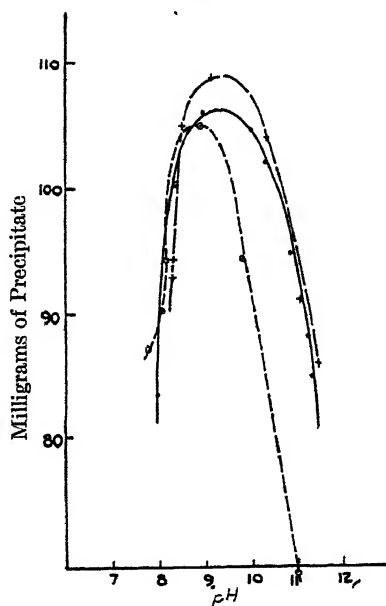


FIG. 4b

1. ——— 0.04 M oxalate; pH = 9.3
2. - - - - 0.04 M oxalate  $\frac{2}{3}$  Basic; pH = 8.8
3. — · — 0.06 M oxalate; pH = 9.4

where large concentrations of sulfate were present. It is obvious, therefore, that the ignited precipitates were not in all cases aluminum oxide alone. Kolthoff and Sandell (14) state that sulfate is difficult to remove from aluminum oxide by ignition.

A double oxalate of aluminum and sodium has been reported (15) with the formula  $3\text{Na}_2\text{C}_2\text{O}_4 \cdot \text{Al}_2(\text{C}_2\text{O}_4)_3$  and it is believed, from the results of this investigation, that a small quantity of this and the corresponding potassium salt are formed when oxalate is the added anion. When a large sample of precipitate (prepared from twenty identical smaller



samples to facilitate washing) was dissolved in nitric acid very positive flame tests were obtained for both sodium and potassium although the nitric acid and the ammonium nitrate (the latter used for washing) gave no significant tests for either of these ions. Upon ignition, small quantities of sodium and potassium oxides are formed which account for the high results of the oxalate curves. For a similar reason, the fluoride results may be high due to the precipitation of a compound such as  $K_2AlF_6$  (16).

The presence of citrate and tartrate did not increase the weight of the precipitate, but rather caused this weight to diminish. When the filtrates were analyzed the expected amount of aluminum to make up the difference was found.

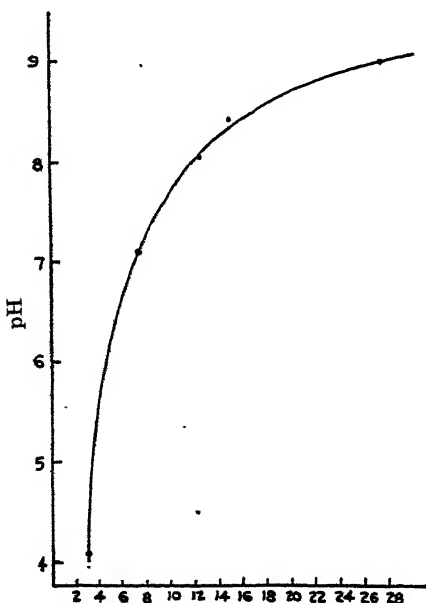


FIG. 5

Moles Al per Mole Sulfate  
in the Precipitate  
(System Described by Curve 1, Fig. 3)

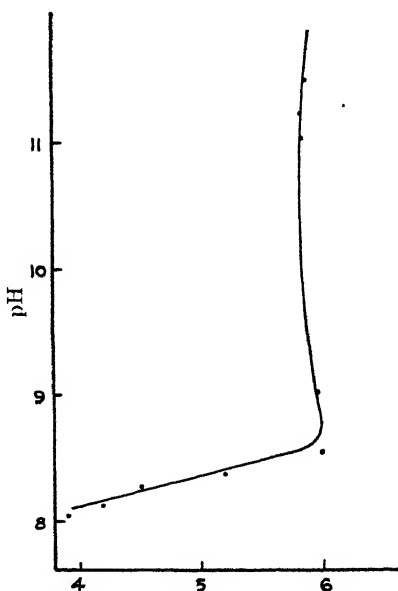


FIG. 6

Moles Al per Mole Oxalate  
in the Precipitate  
(System Described by Curve 1, Fig. 4)

Figures 5 and 6 show the change in the molar ratio of aluminum to sulfate ion in the precipitates (Fig. 5) and the change in the molar ratio of aluminum to oxalate ion in the precipitates (Fig. 6), with the change in pH values. As the pH values increase, the molar ratio of aluminum to sulfate increases from 3.2 at pH 3.9 to 31 at pH 9.1. At pH values higher than this no sulfate can be detected in the precipitate. Thus, it is apparent that hydroxyl ion displaces sulfato groups, or prevents sulfate becoming

bound to the aluminum ions or micelles when present at suitable concentration.

The molar ratio of aluminum to oxalate also increases at first with an increase in the pH value. The change is very slight, however, in comparison to the change exhibited by aluminum and sulfate, the molar ratio of aluminum to oxalate increasing from 3.9 at pH 8.1 to 6 at pH 8.5. Above the latter pH value the molar ratio of aluminum to oxalate remains constant. It is evident that hydroxyl ion cannot displace the oxalate ion as completely as it can displace sulfate ion, or cannot prevent the oxalate from becoming bound to the aluminum ions or micelles.

### DISCUSSION

From a purely chemical viewpoint one would predict that in the presence of strongly co-ordinating anions (those which have a decided tendency to form complex ions with aluminum), less hydroxyl ion would be required to precipitate the aluminum, owing to the fact that these strongly co-ordinating anions already neutralize part of the charge on the aluminum ion. In other words, they might occupy co-ordination places which the hydroxyl ion might ordinarily take. This was realized with tartrate and citrate ions. However, the action of oxalate and fluoride ion was contrary to this simple prediction.

It is known that the citrate and tartrate complexes of aluminum are very stable and quite resistant to the action of hydroxyl ion. Oxalate ion does not form as stable a complex. Although the complex corresponding to the formula  $\text{Al}(\text{C}_2\text{O}_4)_3^{3-}$  is known, if hydroxyl ion is added in the proper concentration, a voluminous precipitate is formed in which the aluminum is precipitated quantitatively.

This difference in behavior toward hydroxyl ion, it is believed, may account for the opposite effects that oxalate (and fluoride) and tartrate (and citrate) ion have on the shift of the pH of optimum precipitation. When hydroxyl ion is added to the aluminum chloride solution, in which the molar ratio of citrate to aluminum is not greater than 1 to 3, a precipitate is obtained. That the precipitate contains bound citrate is indicated by charring when treated with sulfuric acid. But, instead of the necessary three moles of hydroxyl ion per mole of aluminum to precipitate "aluminum hydroxide," only two moles were needed. Since a smaller quantity of hydroxyl ion was added, and since the amount of citrate present was too small to exert much buffer action, the pH at which optimum precipitation is obtained, as predicted, is lower than the corresponding pH for a system containing aluminum chloride with no added anion other than hydroxyl.

When hydroxyl ion is added to aluminum chloride solutions containing a given amount of added oxalate, varying amounts of precipitates

are obtained (Fig. 4). The composition of the precipitate varies with the amount of hydroxyl ion added. Fig. 6 shows that, as the pH rises, the molar ratio of aluminum to oxalate increases, and above a pH of 8.5 this ratio remains practically constant. It is evident, therefore, that up to pH 8.5 the hydroxyl ion is displacing some of the oxalate ion which had become co-ordinatively bound to the aluminum.

Since the oxalato aluminate complex is soluble, and since the aluminum hydroxide is insoluble, there must be an intermediate stage where the oxalate concentration in the complex is low enough and the hydroxyl ion concentration high enough to form a precipitate. But the oxalate ion displaced from the complex can pick up a proton to form the  $\text{HC}_2\text{O}_4^-$ . The pH of optimum precipitation rises because, at the stage where we have added enough hydroxyl ion to form a precipitate, the total base added (hydroxyl ion plus the anion) is sufficient to make the system definitely alkaline. It can be seen, therefore, that not only must the anion be replaceable by hydroxyl ion, but that the anion must be very basic. That this is a necessary condition is substantiated in the behavior of added sulfate ion. Sulfate is also a moderately strong co-ordinator with aluminum, although a much weaker complex ion former than the organic ions already discussed. This is shown by Fig. 5 where it can be seen that, as the pH increases, the molar ratio of aluminum to sulfate in the precipitate also increases. Beyond pH 9.2, precipitates were obtained in which no sulfate could be detected, showing that the hydroxyl ion had completely displaced all the sulfate.

Since sulfate ion is a weaker base than oxalate ion, there will be less tendency for the pH of the system to be affected by anything other than the added hydroxyl ion. But since, as the sulfate ion concentration in the solution is increased, the amount of added hydroxyl ion needed for precipitation decreases, for reasons discussed before, it can be seen that the pH of optimum precipitation will decrease as the anionic concentration increases. However, this is not as pronounced as the effect obtained with very strong co-ordinative binders such as tartrate and citrate for two reasons: first, because smaller amounts of sulfate become bound to the aluminum due to a weaker co-ordinative binding affinity, and secondly, because these bound groups can be later displaced by added hydroxyl ion, thus tending to form precipitation maxima at pH values higher than those obtained with the non-displaceable strongly co-ordinating anions.

Ions which are only weakly bound to the aluminum ion, such as chloride and lactate, will occupy few of the co-ordination positions. As a result, the pH of optimum precipitation will not be very different from the pH of optimum precipitation of aluminum chloride with no added anion, other than the hydroxyl ion.

Therefore, from the evidence submitted, it can be expected that the effect of added anion on the pH of optimum precipitation will be as follows:

- A. If the anion is a strong co-ordinator with aluminum, and is not replaced by hydroxyl ion, the pH of optimum precipitation will drop sharply as the concentration of that particular anion is increased.
- B. If the anion is a strong co-ordinator with aluminum but can be displaced by added hydroxyl ion, then the pH of optimum precipitation will rise if the particular anion is very basic, while the pH will drop if the particular anion is weakly basic.
- C. If the anion is a weak co-ordinator with aluminum, its effect on the pH of optimum precipitation will be comparatively slight and in the direction of lower pH values.

#### EFFECT OF INCREASED DEGREE OF OLATION

The complex colloidal systems from which the aluminum is precipitated have been profitably considered in this laboratory to be polynuclear complexes of which the "ol" and "oxo" groups act as connecting links between the metallic ions, and these complexes have been considered to contain aquo and hydroxo groups. Since the degree and rate of oxolation and olation are increased by elevation of temperature (17), it was indicated that boiling of basic aluminum chloride solutions would, among other things, shift the reactions  $\text{aq} \rightarrow \text{hydroxo} \rightarrow \text{ol} \rightarrow$  (and possibly  $\text{oxo}$ ) to the right, thus diminishing the number of aquo and hydroxo groups per aluminum ion and, as a consequence, reducing the opportunity for other anions to become co-ordinatively bound through displacement of aquo and hydroxo groups. Thus the effect of the added anion on the pH of maximum precipitation should be reduced.

This was found to be experimentally true. In the case of the freshly prepared 0.01 *M* aluminum chloride solution with an oxalate concentration of 0.04 *M*, the pH of maximum precipitation was found to be 9.3 (Fig. 4b, Curve 1). With an aluminum chloride solution which had been made two-thirds basic (two-thirds of the stoichiometric amount of hydroxyl ion needed to precipitate  $\text{Al}(\text{OH})_3$  was added) and boiled for four hours, the pH of maximum precipitation for the same aluminum and oxalate ion concentration as above was 8.8 (Fig. 4b, Curve 2). Thus the effect of increased olation and oxolation of the aluminum micelles is to shift the pH value of maximum precipitation in the presence of added anion toward the pH value of optimum precipitation found in the absence of added anion.

Studies were made on the behavior of citrate additions to the "aged" basic aluminum chloride solutions, similar to the experiment described above. Curves 1-3, Fig. 7, summarize this action. From Curve 1 (Fig. 7) it is seen that, for an aluminum concentration of  $0.01\ M$  and a citrate ion concentration of  $0.0025\ M$ , the pH of maximum precipitation is 5.0.

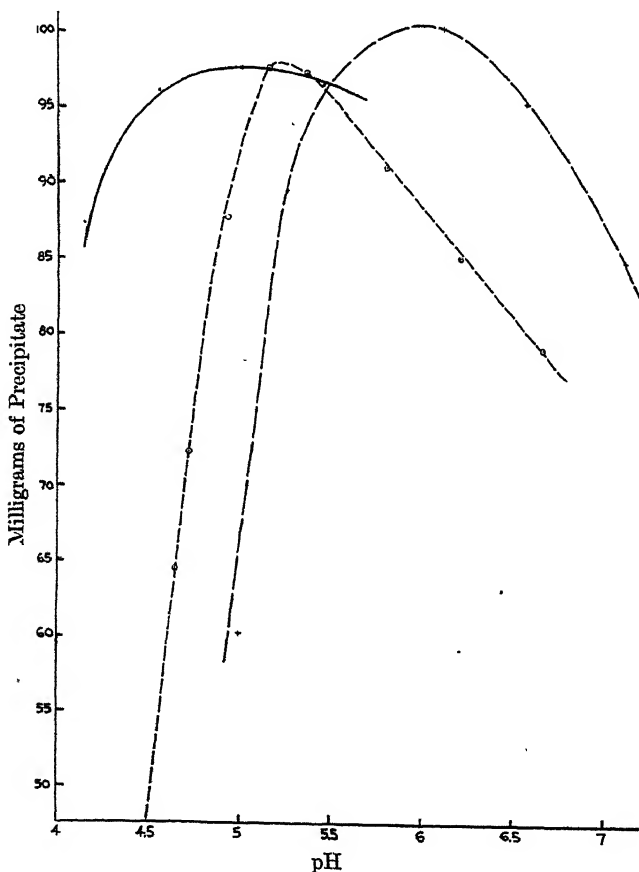


FIG. 7

1. ——— 0.0025  $M$  citrate; pH = 5.0
2. - - - 0.0025  $M$  citrate— $\frac{1}{3}$  Basic; pH = 5.2
3. — · — 0.0025  $M$  citrate— $\frac{2}{3}$  Basic; pH = 6.0

For the same concentrations, with the exception that the solution was made one-third basic and boiled for four hours prior to the addition of the citrate, the pH of maximum precipitation was 5.2 (Curve 2, Fig. 7). When a similar experiment was performed with the "aged" two-thirds basic aluminum chloride solution (Curve 3, Fig. 7), the pH of optimum

precipitation rose to 6.0. This latter experiment illustrates that the effect of added anion is further diminished when the number of groups around the aluminum ion available for displacement becomes less owing to increased olation and/or oxolation.

### CONCLUSIONS

The pH value of maximum yield of "aluminum hydroxide" resulting from the addition of hydroxyl ion to solutions of aluminum ion is not a constant, but varies with the nature and concentration of the anion present. For the anions studied, this effect is as follows: fluoride or oxalate raises the pH at which maximum precipitation is obtained, sulfate, lactate and chloride gradually lower this pH value, while citrate and tartrate cause a sharp drop in the pH of maximum precipitation.

A mechanism is advanced for the behavior of these anions based on the basicity of the anion, the co-ordinative binding affinity of the anion for aluminum and the resistance of bound anion to displacement by added hydroxyl ion. It has been demonstrated that if the anion is:

- A. A strong co-ordinator with aluminum and is not replaced by hydroxyl ion, the pH of optimum precipitation will drop sharply as the concentration of the particular anion is increased.
- B. A strong co-ordinator with aluminum but can be displaced by added hydroxyl ion, then the pH of optimum precipitation will rise if the particular anion is very basic, while the pH of optimum precipitation will drop if the particular anion is weakly basic.
- C. If the anion is a weak co-ordinator with aluminum, its effect on the pH of optimum precipitation will be comparatively slight and in the direction of lower pH values.

It is shown that "aged" basic aluminum chloride solutions differ from freshly prepared aluminum chloride solutions in their behavior toward added anion, the pH value for optimum precipitation of aluminum from "aged" solutions approaching that of a freshly prepared aluminum chloride solution in the absence of that particular anion. An explanation for this effect is offered.

### REFERENCES

1. THERIAULT, E. J., AND CLARK, W. M., *U. S. Pub. Health Service, Pub. Health Rept.* **38**, 181 (1923).
2. MILLER, L. B., *U. S. Pub. Health Service, Pub. Health Rept.* **38**, 1502 (1923).
3. HATFIELD, W. D., *J. Am. Water Works Assoc.* **11**, 554 (1924).
4. MATTSO, S., *Soil Science* **30**, 459 (1930).
5. PFEIFFER, P., *Ber.* **40**, 4036 (1907).
6. HAMMETT, L. P., *Solutions of Electrolytes*, 2nd ed., p. 111. McGraw Hill Publishing Co.

7. PARTINGTON, J. R., Textbook of Inorganic Chemistry, p. 879. Macmillan and Co. (1930).
8. KNOWLES, H. B., *Bur. Standards J. Research* **15**, 87 (1935).
9. BLUM, W., *J. Am. Chem. Soc.* **38**, 1282 (1916).
10. MILLER, L. B., *U. S. Pub. Health Service, Pub. Health Rept.* **992** (1925).
11. STIASNY, E., *Collegium* **670**, 41; **677**, 413 (1926); **682**, 81; **691**, 505 (1927).
12. THOMAS, A. W., AND WHITEHEAD, T. H., *J. Phys. Chem.* **35**, 27 (1931).  
THOMAS, A. W., AND TAI, A. P., *J. Am. Chem. Soc.* **54**, 841 (1932).  
THOMAS, A. W., AND VON WICKLEN, F. C., *ibid.* **56**, 794 (1934).  
THOMAS, A. W., AND VARTANIAN, R. D., *ibid.* **57**, 4 (1935).  
THOMAS, A. W., AND KREMER, C. B., *ibid.* **57**, 1821, 2538 (1935).  
THOMAS, A. W., AND OWENS, H. S., *ibid.* **57**, 1825, 2131 (1935).  
THOMAS, A. W., AND H. S. MILLER, *ibid.* **58**, 2526 (1936).
13. HANUS, J., AND QUADRAT, O., *Z. anorg. allgem. Chem.* **63**, 306 (1909).
14. KOLTHOFF, I. M., AND SANDELL, E. B., Textbook of Quantitative Inorganic Analysis, Macmillan Co. (1936).
15. ABEGG, S., Handbuch der Anorganischen Chemie **III**, 93 (1906).
16. WEINLAND, R., LANG, I., AND FIKENTSCHER, H., *Z. anorg. allgem. Chem.* **150**, 47 (1925).
17. PERKINS, B. H., AND THOMAS, A. W., Stiasny Festschrift, p. 307. Ed. Roether Verlag, Darmstadt (1937).

# THE BEHAVIOR OF RUBBERLIKE MATERIALS WHEN STRETCHED \*

J. J. Hermans

*From the Laboratory for Cellulose Research of the AKU and Affiliated Companies,  
Utrecht, Holland*

*Received January 2, 1946*

## INTRODUCTION

In long-chain molecules the atoms may be arranged in a variety of ways. If the line joining two successive monomeric groups has a given direction in space, the position of the next group is restricted only by the magnitude of the valency angle and by conditions imposed upon the atom by steric factors and interaction energies. These conditions differ for different types of macro molecules and are usually unknown or only known incompletely. To arrive at a simple general treatment of rubber elasticity, Kuhn (1) introduced the so-called statistical chain-element. Each chain-element comprises a certain number of successive monomeric groups, and this number must be so chosen that the orientations of the different chain-elements in space are practically independent. Under these conditions the spatial arrangements of the chain-elements in a molecule allows of a simplified statistical treatment (*cf.* Recapitulation on stress-strain).

In Kramers' (2) method the macro molecule is treated as a pearl necklace of atoms which are connected by weightless rods of length  $L$ . It is assumed that these atoms are subject to forces which derive from a potential  $U$ , a condition which makes it possible to apply the method of statistical mechanics. Let  $q, p$  be the (generalized) coordinates and impulses and  $\tau = \frac{1}{2} \sum a_{ki} \dot{q}_k \dot{q}_i$  the kinetic energy. The distribution in  $(q, p)$ -space will be given by Boltzmann's expression

$$\exp \left( - \frac{\tau + U}{kT} \right) dp dq.$$

The average value of a function  $F(q)$  of the coordinates  $q$  alone has the form (3)

$$\bar{F} = \frac{\int F \exp (- U/kT) \sqrt{A} dq}{\int \exp (- U/kT) \sqrt{A} dq}, \quad (1)$$

\* Communication No. 26 from the Laboratory for Cellulose Research, AKU and Affiliated Companies, Utrecht, Holland.



where  $A$  is the determinant of the coefficients  $a_{ki}$ . The value of  $A$  determines the correlation between the orientations of the various links in the molecule. If  $A = 1$ , no correlation exists.

The simplest case is that in which all links are free to turn independently. The links are then more or less similar to Kuhn's chain-elements. If there are  $N$  links, the coordinates  $q$  are: the three coordinates of the center of gravity of the molecule and the  $2N$  angles defining the orientation of the connective rods in space. Even in this simple case Kramers finds the determinant  $A$  to differ from zero. The correlation, however, is not very pronounced and has no great influence on the average value of the functions  $F$  which are of importance in the present investigation. We will therefore always substitute the value 1 for  $A$ . It may be remarked in this connection that our model represents only a rough approximation (see section on stress-strain relationship in particular). Before going into the subject of rubber elasticity, we will first discuss a subject which has no direct bearing upon the problem. It serves, however, as an introduction to the above mentioned section and, moreover, has some features of general interest which make discussion desirable.

#### ZWITTERIONS IN AN ELECTRIC FIELD

As an application of Kramers' method, which at the same time serves as an introduction to the subject treated in a later section, we consider a solution of long-chain molecules which carry two opposite charges,  $e$  and  $-e$ , one at each end. (Such molecules are called Zwitterions.) Let  $\gamma_i$  be the cosine of the angle between the  $i$ -th link (or chain-element) and an external electric field  $E$ . If  $L$  is the length of a link, the projection of the molecule in the direction of  $E$  will be  $z = L\sum \gamma_i$  and the potential energy will be  $-eEz$ . Considering functions  $F$  which depend on the coordinates  $\gamma$  only, it is obvious that in equation 1 we may omit all coordinates other than  $\gamma$ . Abbreviating:

$$\lambda = \frac{eEL}{kT}, \quad (2)$$

$$s = \gamma_1 + \gamma_2 + \cdots + \gamma_N \quad (3)$$

and the average moment per molecule becomes, therefore,

$$e\bar{z} = eNL\bar{\gamma} = eNL \frac{\int_{-1}^1 \cdots \int_{-1}^1 d\gamma_1 \cdots d\gamma_N \gamma_1 e^{\lambda s}}{\int_{-1}^1 \cdots \int_{-1}^1 d\gamma_1 \cdots d\gamma_N e^{\lambda s}}$$

which gives:

$$e\bar{z} = eNL \left( \text{Cth } \lambda - \frac{1}{\lambda} \right) \cong \frac{1}{3} eNL\lambda = \frac{e^2 L^2 N}{3kT} E.$$

If  $\epsilon_0$  is the dielectric constant of the pure solvent,  $\epsilon$  that of the solution, and  $G$  the number of macro molecules in unit volume, we have

$$\frac{\epsilon - 1}{\epsilon + 2} - \frac{\epsilon_0 - 1}{\epsilon_0 + 2} = \frac{4}{3} \pi G \frac{e^2 L^2 N}{3kT}, \quad (4)$$

or, if the concentration  $G$  is low:

$$\epsilon - \epsilon_0 = \frac{(\epsilon_0 + 2)^2 4}{3} \pi G \frac{e^2 L^2 N}{3kT}.$$

Let us further calculate the double refraction imposed by the external electric field. For simplicity, we assume that the contribution of a link (or chain-element) to the polarization tensor shows cylindrical symmetry. Let  $\alpha_1$  be the polarizability in the direction of the link and  $\alpha_2$  that perpendicular to the link. From simple tensor calculus it is obvious that the contribution of a molecule to the difference between the polarizabilities along  $E$  and perpendicular to  $E$  may then be expressed by an orientation factor  $f$ :

$$\alpha_{11} - \alpha_{\perp} = (\alpha_1 - \alpha_2) N f \quad (5)$$

where  $f$  is determined<sup>1</sup> by the cosines  $\gamma$ :

$$f = -\frac{1}{2} + \frac{3}{2} \overline{\gamma^2}. \quad (6)$$

Applying equation 1 to the function  $F = \gamma_1^2$ , we find

$$f = 1 - \frac{3}{\lambda} \text{Cth } \lambda + \frac{3}{\lambda^2} \cong \frac{\lambda^2}{15}.$$

The difference between the two polarizabilities per unit of volume becomes

$$(\alpha_{11} - \alpha_{\perp}) G = (\alpha_1 - \alpha_2) G N f$$

and hence the double refraction

$$n_{11} - n_{\perp} = \frac{(n_0^2 + 2)^2 4}{6n_0} \frac{4}{3} \pi G N L^2 \frac{\alpha_1 - \alpha_2}{15} \left( \frac{eE}{kT} \right)^2. \quad (7)$$

A similar formula was derived by W. Kuhn and H. Kuhn (4), who considered long-chain molecules carrying an ionized group at one end. These molecules are dragged through the liquid by the electric force  $eE$  and so acquire a birefringence which is much akin to the one considered here. Formulas 4 and 7 are of some interest in that they enable us to eliminate the unknown quantity  $NL^2$ . We are then left with a relation containing only one constant which is typical for the type of macro

<sup>1</sup> For a simple derivation of formula (6) see, for instance, P. H. HERMANS, Contribution to the Physics of Cellulose, Amsterdam 1946.

molecule concerned, to wit  $\alpha_1 - \alpha_2$ :

$$\frac{n_{11} - n_{\perp}}{\epsilon - \epsilon_0} \frac{1}{E^2} = \frac{(n_0^2 + 2)^2}{2n_0(\epsilon_0 + 2)^2} \frac{\alpha_1 - \alpha_2}{kT}. \quad (8)$$

Measuring the dielectric constant on the one hand and the double refraction at a given field strength  $E$  on the other hand, we are thus in a position to compute  $\alpha_1 - \alpha_2$ . In the birefringence of flow and the double refraction when stretched, which were discussed in earlier papers (4, 5), a direct determination of  $\alpha_1 - \alpha_2$  was impossible, since one always had to resort to an estimate of  $N$  and  $L$ .

#### RECAPITULATION OF EARLIER WORK ON THE STRESS-STRAIN RELATION IN RUBBER

It is fairly generally accepted that a large number of gels consist essentially of a network of macro molecules. The knots of this network may be formed by chemical bonds or associative links. For shortness the monomeric groups between two successive knots are said to constitute a molecule. The average molecular weight in the gel depends, therefore, on the number of knots in unit volume. It is assumed that these molecules conform to the rules which apply to randomly kinked structures. If a stretch is applied to the material, the molecules themselves are subject to a stretch and change their (average) shape. A quantitative treatment of this phenomenon meets with many difficulties, chiefly because it is impossible to satisfactorily account for the effect of neighboring molecules. The theories known at present have simply neglected this effect and have treated the molecules essentially as free systems. We have adopted a similar point of view in the present paper.

In the statistical treatment of randomly kinked macro molecules as developed by Kuhn, each molecule is said to consist of  $N$  chain-elements of a given (average) length  $L$ . The number  $\nu$  of monomeric groups in a chain-element is so chosen that the orientation of each chain-element may be considered as practically independent of that of all other chain-elements. Consequently, the probability of finding a distance  $r$  between the two ends of the molecule is proportional to the probability of reaching a distance  $r$  by making  $N$  successive steps of length  $L$  in arbitrary directions, and is found to be (5)

$$W_0 \sim e^{-\mu^2/2} \quad (9)$$

where

$$\mu^2 = \frac{3}{2NL^2}. \quad (10)$$

If, now, a stretch is applied to a material consisting of macro molecules, the randomly kinked structures are deformed. The tension which opposes the stretch results from a tendency to reestablish the equilibrium

distribution (equation 9). As is well known, the modulus of elasticity derived in this way is proportional to the absolute temperature (1).

In later work the present author (6) made an attempt to explain the initial curvature of the stress-strain diagram. The argument given was the following: If the force acting on a cross-section of the material is  $K$ , the end-point of each molecule will, on the average, be subject to a force  $p$  in the direction of the stretch (Fig. 1). It is clear that this model

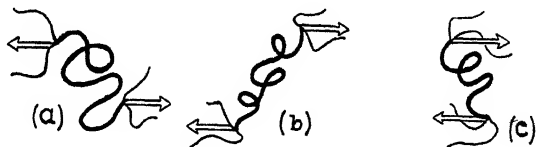


FIG. 1

Randomly Kinked Molecules Exposed to a Stretching Force

represents only a very rough approximation. The force  $p$  is a kind of overall force, whose physical meaning remains somewhat obscure.

For convenience, we imagine that one end of each molecule is fixed at the origin of coordinates; the other end-point is then subject to a force  $p$  in the direction of the stretch  $z$ , *i.e.*, to a potential  $-pz$ . If we introduce the quantity

$$\rho = \frac{p}{2\mu kT} \quad (11)$$

we will have, instead of equation 9, the following distribution of end points:

$$W \sim e^{-\mu^2 r^2 + 2\mu p z} \quad (12)$$

Let  $G$  be the number of molecules in unit volume and  $\bar{z}$  the average projection of the molecule in the direction of the stretch. Then  $\sigma G \bar{z}$  molecules intersect a cross-section  $\sigma$ , and hence

$$K = \sigma G \bar{z} p. \quad (13)$$

It is further assumed that we need only consider positive values of  $z$ . Molecules which are subject to a pair of forces such as shown in Fig. 1c (positive force and negative  $z$ ) are rare and their influence is neglected. From the distribution (equation 12) the stress-strain relation and the double refraction at stretch can be derived. They are best expressed in terms of the parameter  $\rho$ . Since, in equation 13,  $\bar{z}$  is proportional to the length of the stretched material and, thus,  $\sigma \bar{z}$  is proportional to the volume and, since further,  $G$  is inversely proportional to the volume, it is obvious that  $\sigma G \bar{z}$  remains constant throughout the stretching process.<sup>2</sup> Comparing with equation 11 we find, therefore, that the parameter  $\rho$  is proportional to the total force  $K$  on a cross-section. In other words, if

$v$  denotes the degree of stretch, *i.e.*, the ratio between the length of the stretched material and its original length, the  $\rho - v$ -diagram is nothing but a force-strain diagram in which all forces have been multiplied by a constant factor. This factor depends on the number  $G$  of molecules in unit volume and on the magnitude of  $\mu$  (*i.e.*, on  $NL^2$ ). The relation between  $\rho$  and  $v$  is universal for all materials. It was found that this relation is represented by the curve of Fig. 2, which shows a curvature towards the  $v$ -axis at low values of the stretch (for particulars see (6)). In principle this explains the S-shaped diagrams found in practice, since the behavior of the actual substance will deviate from that of the simplified model at more advanced degrees of stretch. In fact, it will become

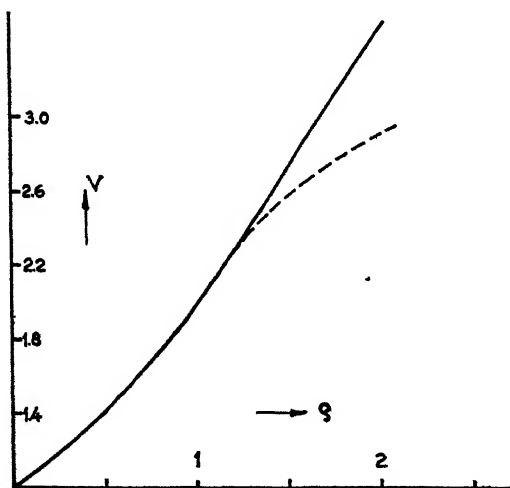


FIG. 2

Force-Strain Diagram According to Earlier Theory

clear in the following section that the relation between  $\rho$  and  $v$  shown in Fig. 2 must be considered as an *asymptotic* relation for very large values of  $N$ . The finite value of  $N$  results in a deviation from the straight line in Fig. 2 (dotted curve). We will see presently how this deviation can be quantitatively accounted for.

While this paper was written, the author became acquainted with the work of Wall (7) and Treloar (8) who published a result obtained from a direct extension of Kuhn's theory. Assuming constant volume, they obtain the following relation between the force  $K$  and the degree of stretch  $v$ :

$$K = GkT \left( v - \frac{1}{v^2} \right).$$

This relation agrees within experimental error with that shown in the curve of Fig. 2. Their theory, however, does not allow of an extension to finite values of  $N$ . (See, however, the note added in proof.)

#### STRESS-STRAIN RELATION FOR FINITE VALUES OF $N$

We adopt the same view point as described in our earlier paper (6) and briefly sketched in the preceding section. We assume that the behavior of a network of macro molecules under the influence of an external tension may be described as if all molecules were completely free and the end-points subject to a force  $p$  in the direction of the stretch. Consequently, the total force  $K$  on a cross-section  $\sigma$  of the material is given by equation 13, where  $\bar{z}$  is the length of a molecule in the direction of the stretch and  $G$  the number of molecules in unit volume. The potential energy is  $-pz$ . Introducing the coordinates (compare section on zwitterions) and abbreviating

$$\lambda = \frac{pL}{kT}, \quad (14)$$

$$s = \gamma_1 + \gamma_2 + \cdots + \gamma_N. \quad (15)$$

We find the following expression for  $\bar{\gamma}$ :

$$\bar{\gamma}(\lambda) = \frac{\int \cdots \int d\gamma_1 \cdots d\gamma_N \gamma_1 e^{\lambda s}}{\int \cdots \int d\gamma_1 \cdots d\gamma_N e^{\lambda s}} = \frac{Q_N(\lambda)}{P_N(\lambda)}. \quad (16)$$

There is an important difference between the integrals in equation 16 and those discussed under zwitterions. In that section the integration had to be made for all values of  $\gamma$  from  $-1$  to  $+1$ . As will be clear from the preceding section, in equation 16 we are to integrate only over values of  $\gamma$  which make  $s$  positive. Let us first consider the denominator  $P_N$ . The value of  $Q_N$  follows from that of  $P_N$ , since  $Q_N = 1/N \cdot dP_N/d\lambda$ . We shall distinguish between  $P_N(\pm)$ ,  $P_N(+)$  and  $P_N(-)$ , where the index  $\pm$  denotes that the integration is to be performed over all values of  $\gamma$  irrespective of the value of  $s$ ;  $+$  denotes that the integration must be performed for positive values of  $s$  only, while  $-$  indicates that the integral extends over  $\gamma$ -values which make  $s$  negative. It is obvious that

$$P_N(\pm) = \left( \frac{2Sh\lambda}{\lambda} \right)^N. \quad (17)$$

To compute  $P_N(-)$  we make use of the following integral:

$$e^{\lambda s} = \frac{2}{\pi} \int_0^\infty du \frac{\cos su}{\lambda^2 + u^2}; \quad \text{provided } s < 0.*$$

\* For  $s > 0$  the right-hand side becomes  $e^{-\lambda s}$ .

This means that  $P_N(-)$  is equal to the integral  $C(-)$ , which is defined by the following equation:

$$C(-) = \frac{2\lambda}{\pi} \int \cdots \int d\gamma_1 \cdots d\gamma_N \int_0^\infty du \frac{\cos su}{\lambda^2 + u^2},$$

where the integration must be performed over  $\gamma$ -values, which make  $s$  negative. It is at once obvious, however, that  $C(+) = C(-)$ , and therefore  $C(-) = \frac{1}{2}C(\pm)$ , integrated over all values of  $\gamma$ . In other words,

$$P_N(-) = \frac{\lambda}{\pi} \int_{-1}^1 \cdots \int_{-1}^1 d\gamma_1 \cdots d\gamma_N \int_0^\infty du \frac{\cos su}{\lambda^2 + u^2}.$$

Integrating first over the coordinates  $\gamma$ , this reduces to

$$P_N(-) = \frac{2^N}{\pi} \int_0^\infty du \left( \frac{\sin u}{u} \right)^N \frac{\lambda}{\lambda^2 + u^2}.$$

Consequently,

$$P_N(\lambda) = 2^N \left( \frac{Sh\lambda}{\lambda} \right)^N - \frac{2^N}{\pi} \int_0^\infty du \left( \frac{\sin u}{u} \right)^N \frac{\lambda}{\lambda^2 + u^2} \quad (18)$$

or also

$$P_N(\lambda) = 2^N \left( \frac{Sh\lambda}{\lambda} \right)^N - \frac{2^N}{\pi} \int_0^\infty dt \left( \frac{\sin \lambda t}{\lambda t} \right)^N \frac{1}{1 + t^2}. \quad (18a)$$

To begin with, we shall consider the relation between the present result and that obtained in our earlier work. In view of equations 10, 11 and 14 we have

$$\lambda = \rho \sqrt{\frac{6}{N}}. \quad (19)$$

If in equation 18a the parameter  $\lambda$  becomes very small while  $N$  becomes very large, in such a way that  $\lambda\sqrt{N/6} = \rho$  remains finite, we obtain the following asymptotic results:

$$\left( \frac{Sh\lambda}{\lambda} \right)^N \cong e^{\rho^2}; \quad \left( \frac{\sin \lambda t}{\lambda t} \right)^N \cong e^{-\rho^2 t^2}.$$

Further, we have

$$\int_0^\infty \frac{dt}{1+t^2} e^{-\rho^2 t^2} = \sqrt{\pi} e^{\rho^2} \int_\rho^\infty d\omega e^{-\omega^2} \quad (\text{since } \rho \text{ is positive}).$$

This gives

$$P_N \cong 2^N e^{\rho^2} \int_{-\rho}^\infty d\omega e^{-\omega^2}. \quad (20)$$

This same integral is obtained by integrating the distribution  $W$  in equation 12 over half the  $x, y, z$  space, where  $z > 0$ . This shows that the earlier theory results from the present one in the limit of very large  $N$  values or very small values of the stress.

Returning to the expression 18a and  $P_N(\lambda)$ , we derive  $Q_N(\lambda)$  by differentiation:

$$Q_N(\lambda) = 2^N \left( \frac{Sh\lambda}{\lambda} \right)^N \left( \text{Cth } \lambda - \frac{1}{\lambda} \right) + \frac{2^N}{\pi} \int_0^\infty du \left( \frac{\sin u}{u} \right)^{N-1} \frac{\sin u - u \cos u}{u(\lambda^2 + u^2)}. \quad (21)$$

The degree of stretch,  $v$ , is obviously given by the ratio

$$v = \frac{\bar{\gamma}(\lambda)}{\bar{\gamma}(0)} = \frac{Q_N(\lambda)}{P_N(\lambda)} \cdot \frac{P_N(0)}{Q_N(0)}. \quad (22)$$

There is no difficulty in finding  $P_N(0)$  and  $Q_N(0)$ . From equation 18a it follows that  $P_N(0) = 2^{N-1}$ . Further, equation 21 reduces to

$$Q_N(0) = \frac{2^N}{\pi} \int_0^\infty du \left( \frac{\sin u}{u} \right)^{N-1} \frac{\sin u - u \cos u}{u^3}.$$

This gives  $Q_1(0) = 1/2$ ;  $Q_2(0) = 2/3$ ;  $Q_3(0) = 13/12$ . As we will see presently, for  $N > 3$  we may use the asymptotic formula

$$Q_N(0) \cong 2^{N-1} \sqrt{\frac{2}{3\pi N}}. \quad (23)$$

This asymptotic formula may be obtained directly from the integral expression for  $Q_N(0)$ .

It is further obvious, since the highest possible value of  $\bar{\gamma}$  is 1 (*viz.*, for  $\lambda \rightarrow \infty$ ), that the maximum degree of stretch is  $1/\bar{\gamma}(0)$  or  $P_N(0)/Q_N(0)$ . For  $N > 3$ , we have, therefore, practically:

$$v_{\max} = \sqrt{\frac{3\pi N}{2}} = 2.17\sqrt{N}. \quad (24)$$

This asymptotic value is approached very rapidly, as is seen from the following table:

$N = 1$	2	3
$v_{\max} = 2$	3	3.70
asymptotic value (equation 24) = 2.17	3.06	3.75

With small values of  $N$ , a direct integration of equation 18 may be carried out, giving, for instance,

$$P_1(\lambda) = \frac{1}{\lambda} (e^\lambda - 1), \quad (25)$$

$$P_2(\lambda) = \frac{1}{\lambda^2} (e^{2\lambda} - 1 - 2\lambda), \quad (26)$$

$$P_3(\lambda) = \frac{1}{\lambda^3} (e^{3\lambda} - 3e^\lambda + 2 - 3\lambda^2). \quad (27)$$



Derivation with respect to  $\lambda$  leads to  $Q_1$ ,  $Q_2$ ,  $Q_3$  and, thus, applying equation 22, to the degree of stretch  $v$ . A graph is given in Fig. 3. With larger  $N$  values we resort to graphic integration. To that end we first make a rough estimate of  $N$  from the experimental value of  $v_{\max}$ .<sup>3</sup>  $P_N(\lambda)$  and  $Q_N(\lambda)$  are then determined by graphic integration for a few  $N$  values in the neighborhood of the estimated one. This method is not so laborious

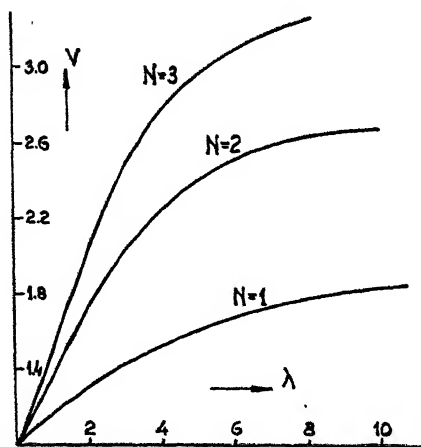


FIG. 3

Force-Strain Diagram for Small Values of  $N$

as it might seem at first sight. The integrals  $P_N(-)$  and  $Q_N(-)$  soon become very small compared with  $P_N(\pm)$  and  $Q_N(\pm)$ , respectively, if  $\lambda$  is increased, which means that in practice we need go no further than to integrate  $P_N(-)$  and  $Q_N(-)$  for a few  $\lambda$  values below  $\lambda = 3$ . Moreover, since  $N$  is a fairly large number, the integrand in  $P_N(-)$  and  $Q_N(-)$  decreases rapidly with increasing integration variable  $u$ , so that it suffices to calculate this integrand for a small range of  $u$  values only. For each  $N$  value we thus obtain a  $v - \lambda$  curve. The curve found in practice is a  $v - K$  curve. Since  $\lambda$ , for a given value of  $N$ , is proportional to the total force  $K$  on a cross-section of the material, the ratio  $K/\lambda$  should be a

<sup>3</sup> TRELOAR, L. R. G., Reports on Progress in Physics (Physical Society) 9, 134 (1943), states that formula (24) leads to values of  $v_{\max}$  which are 2 to 4 times larger than the experimental one. He applies the equation, however, to the number of monomeric groups instead of chain-elements. According to our experience equation (24) gives a result of the right order of magnitude if applied to the number  $N$  of chain-elements in the molecule. For instance, the rubber mentioned in Fig. 4a showed a maximum extensibility of 1000% as compared to 1100% in theory. That of the rubber of Fig. 4b was 900% instead of 800%, as calculated.

constant. It is, therefore, possible to select the best value of  $N$ , *viz.*, that which makes  $K/\lambda$  a constant over the largest possible range of stretches. This procedure was followed for two species of vulcanized rubber, one with a low sulfur content, the other with a comparatively high degree of vulcanization. These samples were measured by Wildschut (9) (Delft), who kindly put his experimental results at the author's disposal. A graph is given in Fig. 4. It is interesting to observe that Wildschut (9) used a second degree equation with 4 arbitrary constants to represent the stress-strain diagram. In the present theory only two constants,  $N$  and  $K/\rho$ , are free to be disposed of, and, moreover, one of these constants is related to the other.

To show this, let us return to equation 13 for  $K$ . We mentioned previously that  $\sigma G \bar{z}$  is constant. Using the index  $o$  to denote the original unstretched state and substituting the value from equation 11 for  $p$ , we may therefore write

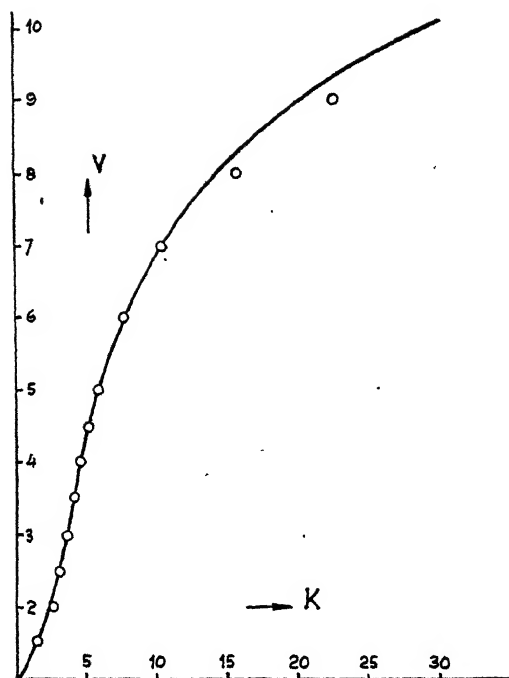
$$\frac{K}{\rho} = \sigma_o G_o \bar{z}_o 2 \mu k T = \sigma_o G_o \bar{z}_o \frac{k T}{L} \sqrt{\frac{6}{N}}.$$

Here  $\bar{z}_o = NL\bar{\gamma}_o = NL/v_{\max}$ , which, according to equation 24, is practically  $L\sqrt{2N/3\pi}$ . It follows that

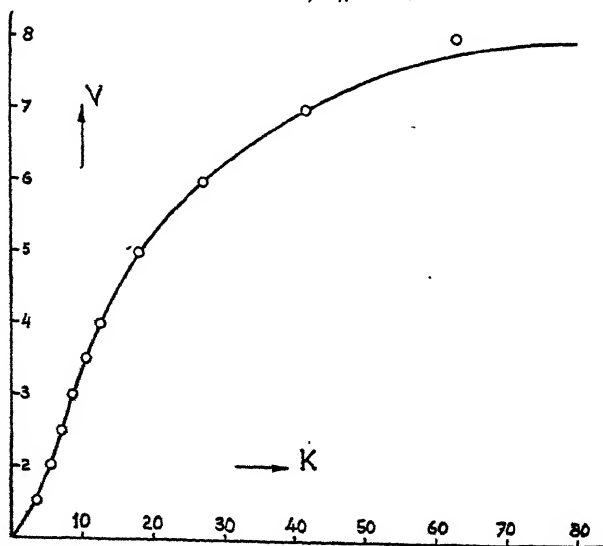
$$\frac{K}{\rho} = \sigma_o \frac{2}{\sqrt{\pi}} k T G_o.$$

In other words, the ratio  $K/\rho$  is determined by the number of molecules per  $\text{cm}^3$  of the unstretched material. Now, the number of monomeric groups per unit volume follows directly from the density of the substance and the molecular weight of the monomeric group. Comparing with  $G_o$  we are, therefore, in a position to calculate the number of monomeric groups in a molecule (*i.e.*, the degree of polymerization between junction points in the network). Since we also know the number  $N$  of chain-elements per molecule, we find the number  $\nu$  of monomeric groups per chain-element. This number must tally with that derived from measurements on viscosity or birefringence of flow (10).

From the density 0.9 of rubber and the molecular weight 68 of the monomeric group it follows that there are  $90 \times 10^{20}$  monomeric groups per  $\text{cm}^3$ . In the sample of Fig. 4a we find  $G_o = 0.44 \times 10^{20}$  (molecules per  $\text{cm}^3$ ), *i.e.*, 200 monomeric groups per molecule. With  $N = 30$ , we find  $\nu = 6.5$  for the number of monomeric groups in a chain-element. Similarly, in the sample of Fig. 4b we have  $G_o = 1.1 \times 10^{20}$  or 82 monomeric groups per molecule. Which gives  $\nu = 5$ . These figures for  $\nu$  tally well with the value 5-7 derived from viscosity determinations.



(a) Time of vulcanization 90 min. (100 R, 8 S) drawn curve calculated with  $N = 30$ ;  $K/\rho = 2.0$ .



(b) Time of vulcanization 240 min. (100 R, 8 S) drawn curve calculated with  $N = 17$ ;  $K/\rho = 5.4$

FIG. 4  
Force-Strain Diagram of Vulcanized Rubber

## DOUBLE REFRACTION AT STRETCH

The value of  $\bar{\gamma}^2$  can be derived by similar reasoning to that used for  $\bar{\gamma}$ . This leads to the expression

$$\bar{\gamma}^2 = \frac{R_N}{P_N}, \quad (28)$$

$$R_N = 2^N \left( \frac{sh\lambda}{\lambda} \right)^N \left( 1 - \frac{2 \operatorname{Cth} \lambda}{\lambda} + \frac{2}{\lambda^2} \right) - \frac{2^N}{\pi} \int_0^\infty du \left( \frac{\sin u}{u} \right)^N \left( 1 + \frac{2 \cotg u}{u} - \frac{2}{u^2} \right) \frac{\lambda}{\lambda^2 + u^2}. \quad (29)$$

Here again, a graphic integration is not very difficult, since the integral need only be evaluated for a few  $\lambda$  values below 3. In addition, we mention the expressions for  $R_1$ ,  $R_2$  and  $R_3$ :

$$R_1 = \left( \frac{1}{\lambda} - \frac{2}{\lambda^2} + \frac{2}{\lambda^3} \right) e^\lambda - \frac{2}{\lambda^3}, \quad (30)$$

$$R_2 = \left( \frac{1}{\lambda^2} - \frac{2}{\lambda^3} + \frac{2}{\lambda^4} \right) e^{2\lambda} - \frac{2}{3\lambda} - \frac{1}{\lambda^2} - \frac{2}{\lambda^3} - \frac{2}{\lambda^4}, \quad (31)$$

$$R_3 = \left( \frac{1}{\lambda^3} - \frac{2}{\lambda^4} + \frac{2}{\lambda^5} \right) e^{3\lambda} + \left( \frac{-3}{\lambda^3} + \frac{2}{\lambda^4} - \frac{6}{\lambda^5} \right) e^\lambda - \frac{5}{6\lambda} + \frac{4}{\lambda^5}. \quad (32)$$

Using the relation 6 this gives the orientation factor  $f$ , which determines the ratio between the double refraction at the stretch considered and that at complete orientation of all the chain-elements. A graph is given in Fig. 5 which shows that for  $N < 4$ ,  $f$  is an almost universal function of  $\lambda$ . Eliminating  $\lambda$  from Fig. 3 and Fig. 5 we obtain the  $f - \nu$  diagram of Fig. 6. Finally, Fig. 7 gives  $f$  as a function of  $\lambda\nu$  for  $N = 25$ . Since  $\lambda$  is proportional to the force  $K$  on the total cross-section,  $\lambda\nu$  is proportional to the tension per cm.<sup>2</sup> of the stretched material, provided the volume is not changed at stretch. This Fig. 7 is of interest in connection with earlier work. According to the theory given in (6), the double refraction is proportional to the tension throughout the whole stretching process. This only applies, however, to the asymptotic expression for infinite  $N$  values or very small degrees of stretch. Fig. 7 shows that deviations from this rule will occur at more increased stretches.

To conclude, it may be remarked that the theory developed in the present paper must by no means be considered as an attempt to give a definite answer to all the problems which present themselves in the stretch of rubber-like substances. The influence of crystallization, for instance, is completely left out of account. Conversely, however, it must be considered as a point of considerable interest, that a simplified theory, such as that put forward by us, is able to give a quantitative explanation

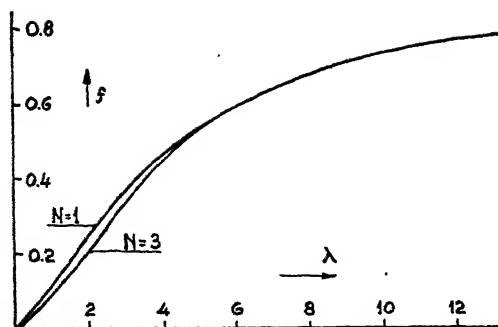


FIG. 5

Orientation Factor  $f$  Plotted Against Force-Parameter for  $N = 1, 2$  and  $3$

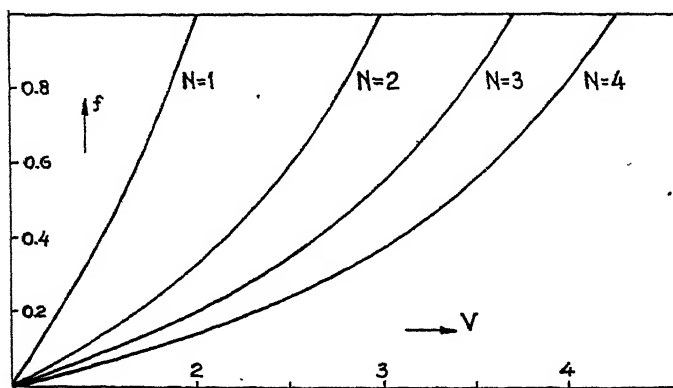


FIG. 6

Orientation Factor  $f$  Plotted Against Degree of Stretch  $v$  for  $N = 1, 2$  and  $3$

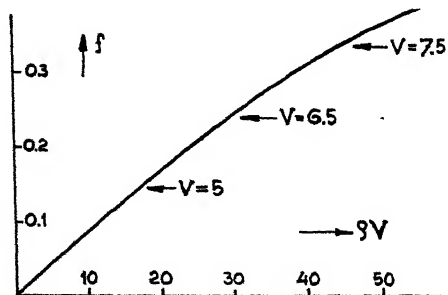


FIG. 7

Orientation Factor  $f$  Plotted Against Tension  $Kv$  for  $N = 25$

of the stress-strain diagram over almost the entire range of stretches. This suggests that the effect of crystallization is considerably less pronounced than it is usually believed to be.\*

The expressions for  $P_N$  and  $R_N$  with  $N = 1, 2, 3$  with the corresponding Figs. 3, 5 and 6 were added because the author hopes to deal with cellulose in a later paper. The gels of this macro molecular substance show a behavior at stretch which is, on the whole, in fair agreement with the present theory if to  $N$  we assign values between 1 and 3, values which, of course, need not necessarily be integers.

The author is much indebted to W. Opechowski for his interest in this work and his helpful suggestions.

### SUMMARY

Kuhn's method of computing the relationships existing between stretch, tension and double refraction in rubber-like substances has recently been extended by Wall, by Treloar and by the author. These treatments assume randomly kinked structures consisting of an (effectively) *infinite* number of chain-elements. In Kramers' method no assumption regarding the number of chain-elements is made. The present paper attempts to apply Kramers' theory to (1) long-chain "zwitterions" in an electric field and (2) a network of macro molecules in unidirectional extension.

It is shown that the earlier theory of rubber elasticity is a result of the present one within the limit of a very large number of chain-elements per molecule, or a very small stress.

It is found that the stress-strain diagram of rubber conforms closely to the requirements of the theory. A few results for molecules consisting of 1, 2 or 3 chain-elements, together with some graphs, are added with a view to their application to cellulose in the near future.

The Editor of this journal kindly drew my attention to a paper of James and Guth (11), whose treatment of rubber elasticity has some features in common with the method developed in the present article. These authors have also used a potential energy of the type given in equation (14), which leads to the introduction of an exponential factor  $\exp(\lambda s)$ , (compare equation 16). In particular, they also point out the analogy with electric or magnetic dipoles in an electric or magnetic field (compare section on zwitterions). On the other hand they neglect the restriction:  $s > 0$  in the integrations (equation 16), which accounts for the situation represented by Fig. 1. This does not affect the results ob-

\* This was also emphasized by L. R. G. TRELOAR, *Trans. Faraday Soc.* 38, 293 (1942). It may be due partly to two effects which, to a certain extent, cancel: crystallization in itself has a "hardening" effect (increasing the modulus of elasticity) but at the same time the total *amount* of amorphous elastic material is reduced.

tained at high values of the stress and, in fact, at advanced degrees of stretch both the James-Guth theory and the present one approach the following result (using the symbols of the present article):

$$\frac{\nu}{\nu_{\max}} = C\theta\lambda - \frac{1}{\lambda}.$$

A further common feature is the fact that the final stress-strain relation contains two arbitrary constants, one dependent on the total number of junction points ( $G$  in equation 13) and one depending on the maximum extensibility ( $N$  in, for example, equation 24).

A somewhat unsatisfactory feature of James and Guth's treatment is the one-dimensional character of their considerations. On the other hand their final formula is simpler than ours and their highly interesting analysis of the network structure may eventually be helpful in an attempt to obviate the introduction of the overall force  $p$ .

#### REFERENCES

1. KUHN, W., *Kolloid-Z.* **68**, 2 (1934); **76**, 258 (1936). KUHN, W., AND GRÜN, F., *Kolloid-Z.* **101**, 248 (1942).
2. KRAMERS, H. A., *Physica* **11**, 1 (1944).
3. GIBBS, W., Principles of Statistical Mechanics.
4. KUHN, W., AND KUHN, H., *Helv. Chim. Acta* **27**, 493 (1944).
5. KUHN, W., AND GRÜN, F., *Kolloid-Z.* **101**, 248 (1942); KUHN, W., AND KUHN, H., *Helv. Chim. Acta* **26**, 1394 (1943); HERMANS, J. J., *Kolloid-Z.* **103**, 210 (1943); **106**, 22 (1944); *Rec. trav. chim.* **63**, 25 (1944); *Rec. trav. chim.* **63**, 205 (1944).
6. HERMANS, J. J., *Kolloid-Z.* **103**, 210 (1943).
7. WALL, F. T., *J. Chem. Physics* **10**, 485 (1942).
8. TRELOAR, L. R. G., *Trans. Faraday Soc.* **39**, 36, 241 (1943).
9. Compare also WILDSCHUT, A. J., *Physica* **10**, 111 (1943).
10. HERMANS, J. J., *Kolloid-Z.* **106**, 22 (1944); *Rec. trav. chim.* **63**, 25 (1944); KUHN, W., AND KUHN, H., *Helv. Chim. Acta* **26**, 1394 (1943); see, in connection with their paper, HERMANS, J. J., *Rec. trav. chim.* **63**, 205 (1944).
11. JAMES, H. M., AND GUTH, E., *J. Chem. Physics* **11**, 455 (1943); *J. applied Phys.* **15**, 294 (1944), see also E. GUTH, Publ. No. 21 of the Am. Assoc. Adv. Sci., p. 103.

# OPTICAL PROPERTIES OF THE SYSTEM CELLULOSE-WATER \*

(A Contribution to the Optics of Swollen Gels)

P. H. Hermans, J. J. Hermans and D. Vermaas

*From the Laboratory for Cellulose Research of the AKU and Affiliated Companies,  
Utrecht, Holland*

*Received January 2, 1946*

## 1. INTRODUCTION

Up to the present, attempts to account quantitatively for the influence of moisture on the refractive indices of cellulose have been unsuccessful.

Meyer and Frey-Wyssling (1) measured the refractive indices of moist ramie fibers and reported that the results were not in conformity with the formula of Wiener or with other formulae tested. A few years later Hermans and Platzek (2) in their studies on isotropic model filaments arrived at the same conclusion.

We are now in a position to reconsider the problem, and we will see in the present paper that the earlier attempts failed only because the volume relationships in the system cellulose-water were not properly accounted for. It will be shown that up to a moisture content of about 20% the refractive indices of moist cellulose conform closely to the simple formula of Gladstone and Dale. Beyond 20% regain deviations begin to occur, which probably are due to a "double refraction of shape" in Wiener's sense (compare section 4).

Our experiments comprise isotropic model filaments, steamed isotropic model filaments, stretched model filaments and ramie fibers. In the experiments with model fibers we examined a series of moisture contents ranging from 0 to 78%. The ramie fibers were examined in the bone-dry state and at 65% relative humidity. The results obtained with a variety of rayons at 65% relative humidity will be recorded elsewhere (3).

Details of the experimental procedure for determining the refractive indices have been described in another communication (3). The fiber samples were conditioned to the desired humidity in thin walled capillaries, about 1 mm. in diameter, through which a stream of air of exactly controlled relative humidity was passed. Then the immersion liquid (if necessary dried or conditioned beforehand) was sucked into the capillary and the latter sealed at both ends. Mixtures of butyl stearate and tricresyl phosphate were used for this purpose.†

\* Communication No. 23 from the Laboratory for Cellulose Research of the AKU and affiliated Companies, Utrecht (Holland).

† A detailed description of the manner in which the capillaries were mounted for microscopic examination, and all further details of the technique are given in the publication cited in ref. (3).



## 2. ISOTROPIC MODEL FILAMENTS

Isotropic fibers should have only one refractive index:  $n_{iso}$ . However, since most isotropic filaments show a small residual optical anisotropy of about 1 unit in the third decimal, we always measured both refractive indices and calculated  $n_{iso}$  according to the formula

$$n_{iso} = \frac{1}{3}(n_{||} + 2n_{\perp}). \quad (1)$$

Here  $n_{||}$  is the refractive index for oscillations in the direction of the fiber axis, while  $n_{\perp}$  is that for oscillations perpendicular to the fiber axis. The refractive index of dry fibers conforms to the formula of Gladstone and Dale:

$$\frac{n_{iso} - 1}{d} = K. \quad (2)$$

where  $d$  is the density (3). For brevity, we introduce the notation "refractivity" for the quantity  $n - 1$ . The formula (2) expresses that if the refractivity of a certain amount of a substance in a volume  $v$  is  $n - 1$ , that of the same amount of substance in a volume  $v'$  will be

$$n' - 1 = (n - 1) \frac{v}{v'}. \quad (3)$$

The application of Gladstone and Dale's rule to moist cellulose may now be formulated as follows. Let 1 g. of dry cellulose with a volume  $v_0$  absorb  $a$  g. of water and thereby acquire a volume  $v_a$ . If  $n_0$  is the refractive index of the dry cellulose, the contribution of the cellulose to the refractivity of the gel will be  $(n_0 - 1)v_0/v_a$ . Since the refractive index of water at 20°C. is 1.333 and its volume is  $a$ , the contribution of the water to the refractivity of the gel is  $0.333a/v_a$ . The total refractivity is, therefore,

$$n_a - 1 = (n_0 - 1) \frac{v_0}{v_a} + 0.333 \frac{a}{v_a}. \quad (4)$$

Or also

$$(n_a - 1)v_a = (n_0 - 1)v_0 + 0.333a. \quad (5)$$

In other work (3) we have recorded the values of  $v_a$  for isotropic model filaments and steamed isotropic model filaments in dependence on regain. Table I and graph 1 give the corresponding values of  $n_a$ . To check the equation (5) we have plotted  $(n_a - 1)v_a$  against  $0.333a$  in Fig. 2. The curve obtained is a straight line with unit slope. The point of intersection with the ordinate determines the value of  $(n_0 - 1)v_0$ . Beside this geometrical check we may calculate  $n_0$  from the experimental figures for  $n_a$  and  $v_a$ , using equation (5) and the experimental value  $v_0 = 0.661$ . This leads to the  $n_0$  values in the last column of Table I. They are ob-

TABLE I

*Observed Refractive Indices,  $n_a$ , of Isotropic Model Filaments and Steamed Model Filaments Containing a g. of Water per g. of Dry Cellulose*

*1. Ordinary Isotropic Fibers;  $v_0 = 0.661$*

$a$	$v_a$	$n_a$ obs.	$n_a$ calc.
0	0.661	1.544 <sub>8</sub>	1.544 <sub>8</sub>
0.022	0.674	1.545 <sub>4</sub>	1.545 <sub>2</sub>
0.026	0.677	1.545 <sub>9</sub>	1.545 <sub>3</sub>
0.035	0.682	1.544 <sub>4</sub>	1.544 <sub>0</sub>
0.044	0.688	1.546 <sub>4</sub>	1.545 <sub>8</sub>
0.050	0.692	1.544 <sub>2</sub>	1.543 <sub>7</sub>
0.098	0.731	1.537 <sub>2</sub>	1.544 <sub>0</sub>
0.156	0.784	1.526 <sub>1</sub>	1.543 <sub>7</sub>
0.242	0.867*	1.510 <sub>3</sub>	1.543 <sub>5</sub>
Average:			1.544 <sub>4</sub>

*2. Steamed Filaments;  $v_0 = 0.659$*

0	0.659	1.544 <sub>5</sub>	1.544 <sub>5</sub>
0.034	0.680	1.547 <sub>2</sub>	1.547 <sub>7</sub>
0.040	0.682	1.547 <sub>0</sub>	1.546 <sub>0</sub>
0.054	0.692	1.545 <sub>4</sub>	1.545 <sub>8</sub>
0.083	0.716	1.541 <sub>2</sub>	1.546 <sub>2</sub>
0.135	0.763	1.530 <sub>4</sub>	1.546 <sub>0</sub>
0.204	0.827	1.517 <sub>0</sub>	1.545 <sub>8</sub>
Average:			1.546 <sub>0</sub>

\* Interpolated (see reference 3).

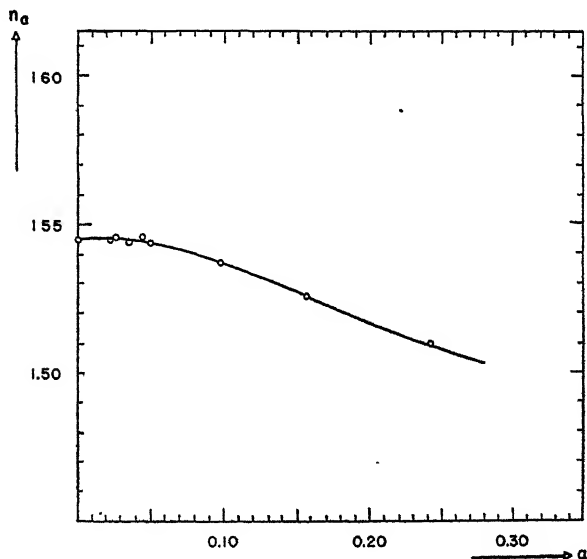


FIG. 1

Refractive Index of Ordinary Isotropic Model Filaments in Dependence on Regain.  
(The curve for steamed fibers is very similar)

viously constant within experimental error. The average figures 1.546<sub>0</sub> and 1.544<sub>4</sub> represent the most probable values for the refractive indices of steam-treated and untreated dry cellulose. They compare well with the densities:  $(n_0 - 1)v_0$  is 0.359<sub>0</sub> for both the steam-treated dry cellulose and the untreated one (3).

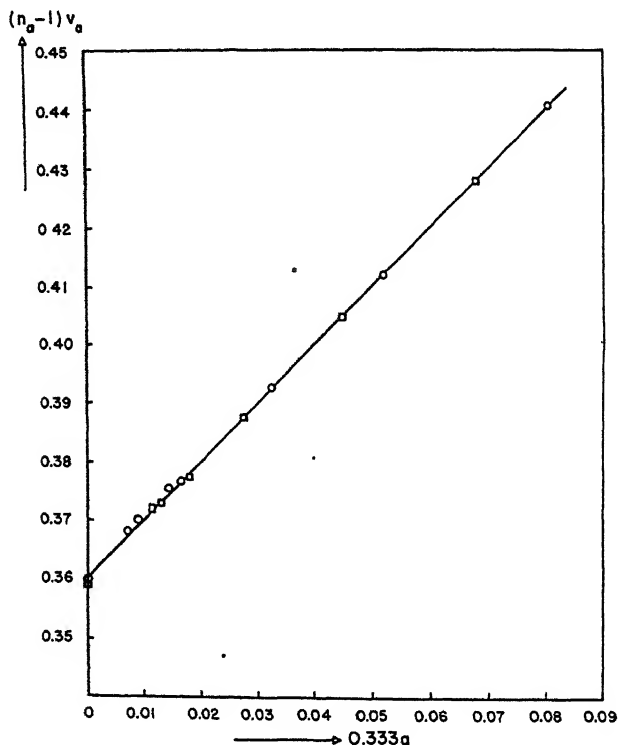


FIG. 2

The value of  $(n_a - 1)v_a$  plotted against  $0.333a$ .

○ = ordinary isotropic fibers, □ = steamed (HMF) fibers

### 3. ANISOTROPIC FIBERS

Model filaments which underwent a 100% stretch as xanthate and were later decomposed to cellulose, were conditioned at various relative vapor pressures. The refractive indices  $n_{11}$  and  $n_{\perp}$  of these orientated filaments are given in Table II and Fig. 3. These refractive indices conform quantitatively to the same simple relations as that given by equation (5):

$$(n_{11} - 1)v_a = (n_{11} - 1)v_0 + 0.333a, \quad (6)$$

$$(n_{\perp} - 1)v_a = (n_{\perp} - 1)v_0 + 0.333a. \quad (7)$$

TABLE II

*Observed Refractive Indices,  $n_{11}$  and  $n_{\perp}$ , of Orientated Filaments in Dependence on Regain*

$a$	$v_a$	$n_{11}$ obs.	$(n_{11})_0$ calc.	$n_{\perp}$ obs.	$(n_{\perp})_0$ calc.
0	0.659	1.573	1.573	1.532	1.532
0.023	0.670	1.574	1.572	1.534	1.531
0.038	0.679	1.573	1.571	1.535	1.531 <sub>s</sub>
0.055	0.692	1.570	1.571	1.531	1.530
0.092	0.721	1.565	1.572	1.529	1.532
0.135	0.761	1.555	1.572	1.519	1.531
0.198	0.821	1.541 <sub>s</sub>	1.574 <sub>s</sub>	1.506 <sub>s</sub>	1.533

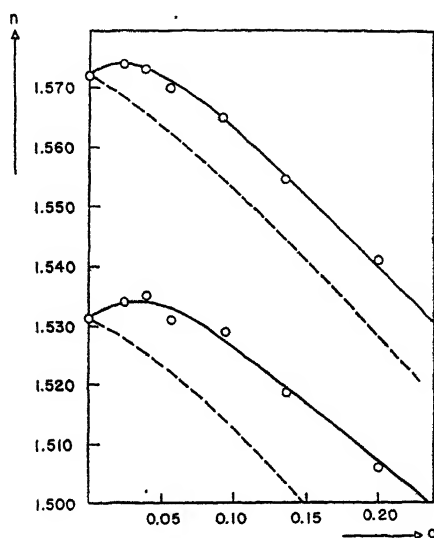


FIG. 3

Refractive Indices of Anisotropic Model Fibers in Relation to Moisture Content.

The dotted curves represent refractive indices calculated according to Wiener's formula (see section 4)

This is apparent from Fig. 4, where  $(n_{11} - 1)_{av}$  and  $(n_{\perp} - 1)_{av}$  are plotted against moisture content. We have also calculated  $(n_{11})_0$  and  $(n_{\perp})_0$  on the basis of equations (6) and (7). The values of  $(n_{11})_0$  and  $(n_{\perp})_0$  obtained in this way are shown in the 4th and 6th columns of Table II. It is clear from this table, and also from Fig. 4, that the equations (6) and (7) apply up to about 15% regain, which is demonstrated by the constant value of  $(n_{11})_0$  and  $(n_{\perp})_0$ . At 19.8% regain the constancy is somewhat less satisfactory. Although the deviation found here is hardly more than the possible experimental error, we have reason to believe that it is real (compare section 4).

From equations (6) and (7) it follows immediately that

$$(n_{11} - n_{12})_a = (n_{11} - n_{12})_0 \frac{v_0}{v_a} \quad (8)$$

Introducing the degree of swelling  $q = v_a/v_0$  (ratio between volume of swollen and that of dry fiber), we may write

$$(n_{11} - n_{12})_a = \frac{(n_{11} - n_{12})_0}{q} \quad (9)$$

In other words, the double refraction of the fiber is inversely proportional to its degree of swelling, a relation which was used in earlier work by

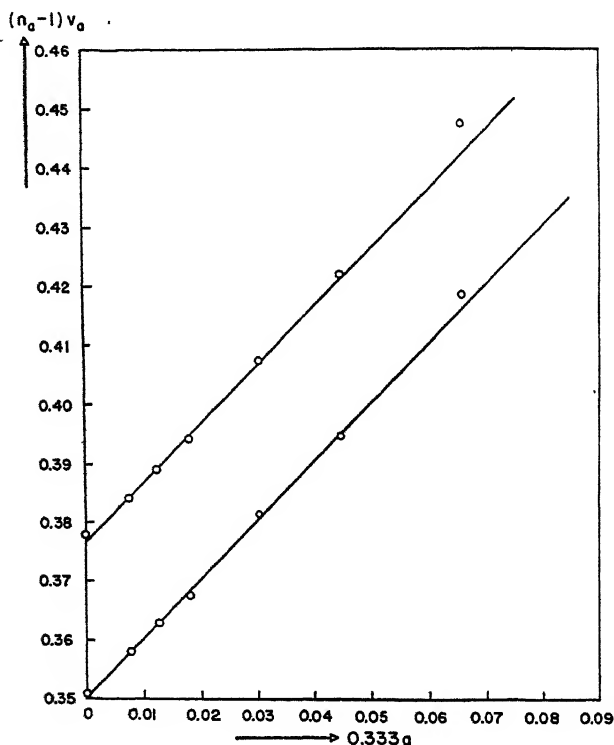


FIG. 4

The Values of  $(n_{11} - 1)_a v_a$  and  $(n_{12} - 1)_a v_a$  plotted against  $0.333a$   
(Anisotropic Model Fibers)

Kratky and Platzek (4). This relationship assumes that the double refraction of the gel is determined by that of the cellulose alone. The part played by the water is that of a diluting medium only. This result is in conformity with the conclusions arrived at in other work (3). The

water is absorbed in the so-called amorphous parts of the fiber, where it is distributed uniformly in the substance, and the gel obtained has the properties of a solution of water in cellulose. Conversely, the applicability of Gladstone and Dale's rule definitely conflicts with the point of view adopted by those authors who have tried to describe the behavior of moist cellulose in terms of rod-shaped particles immersed in water (see section 4).

It is obvious from our results that the water absorbed does not contribute to the anisotropy of the gel. From the experiments carried out by Neubert (5) and Mohring (6), and recently by Vermaas (7), we know that double refraction may result from orientated adsorption. Such a "birefringence of adsorption" apparently plays no part in the system cellulose-water. This is surprising in a way because the anisotropy of the water molecule is quite considerable (8). A simple calculation reveals that the influence of this anisotropy on the refractive indices of the fiber would amount to more than 10 units in the third decimal at 13% regain if all the water were bound anisotropically.

The results obtained so far are not confined to model filaments alone. We have also ascertained that the refractive indices of ramie at 8% regain (65% relative humidity) can be computed from those of dry ramie with the aid of equations (6) and (7). This is shown by the following table: \*

TABLE III  
*Observed and Calculated Refractive Indices of Moist Ramie Fibers*

	$n_{11}$	$n_{\perp}$	$n_{11} - n_{\perp}$
Bone-dry fiber	1.602	1.532	0.070
With 8% H <sub>2</sub> O, obs.	1.595	1.526 <sub>s</sub>	0.068 <sub>s</sub>
With 8% H <sub>2</sub> O, calc.	1.594	1.527	0.067

#### 4. STRUCTURAL BIREFRINGENCE OF SHAPE

If parallel cylindrical particles, which are thin compared with the wave-length of light but thick compared with molecular dimensions, are immersed in a medium, they give rise to a double refraction (rodlet birefringence), which was calculated by Wiener (9). The refractive indices  $n_{11}$  and  $n_{\perp}$  of the mixture depend on the refractive indices and on the volume fractions of the two components. Due to the classical work of Ambronn (10) it is known that the optical behavior of cellulose gels containing a variety of liquids conforms (at least qualitatively) to Wiener's theory. In this work the volume fractions of the two components are identified with the quantities

$$\delta_1 = \frac{1}{q} \quad \text{and} \quad \delta_2 = 1 - \frac{1}{q}$$

where  $q$  is the degree of swelling. Using these relations, Wiener's expres-

\* The volume  $v_0$  of the dry ramie was measured. The volume  $v_a$  of the moist fiber was calculated from  $n_{iso}$ , using equations (1) and (4).

sions may be written as follows:

$$n_{11}^2 = \frac{n_1^2 + (q-1)n_2^2}{q}, \quad (10)$$

$$n_{\perp}^2 = n_2^2 \frac{(q+1)n_1^2 + (q-1)n_2^2}{(q+1)n_2^2 + (q-1)n_1^2}. \quad (11)$$

Here  $n_{11}$  refers to oscillations along the axis of the cylindrical cellulose particles,  $n_1$  in formula (10) represents the refractive index of dry cellulose along this axis, *i.e.*,  $(n_{11})_0$  in our notation, while  $n_{\perp}$  in formula (11) is the refractive index of dry cellulose perpendicular to this axis, *i.e.*,  $(n_{\perp})_0$ . The quantity  $n_2$  is the refractive index of the dispersing medium (water), which is assumed to be isotropic. We have carried out this calculation and found the dotted curves in Fig. 1 for  $(n_{11})_a$  and  $(n_{\perp})_a$ . Their decrease with increasing moisture content is much too rapid.

A simpler approach to the problem is the following. We write

$$(n_{11} - n_{\perp})_a = \frac{(n_{11} - n_{\perp})_0}{q} + (n_{11} - n_{\perp})_w, \quad (12)$$

*i.e.*, we consider the double refraction as additively composed of a double refraction by the cellulose itself (*Eigendoppelbrechung*) and a birefringence of shape in Wiener's sense. According to calculations carried out by Möhring (6) this is permissible if the Wiener component  $(n_{11} - n_{\perp})_w$  is calculated from equations (10) and (11) using the value  $(n_{iso})_0$  for  $n_1$ . Here  $(n_{iso})_0$  is obtained from  $(n_{11})_0$  and  $(n_{\perp})_0$  according to equation (1). Doing so, we get the figures of Table IV, which shows that the Wiener

TABLE IV

*Birefringence of Rods According to Equations (10) and (11) if Applied in Möhring's Sense*

% Water	2.3	3.8	5.5	9.2	13.5	19.8
$(n_{11} - n_{\perp})_w$	0.000 <sub>6</sub>	0.001 <sub>2</sub>	0.001 <sub>8</sub>	0.003 <sub>0</sub>	0.004 <sub>1</sub>	0.005 <sub>8</sub>

component calculated in this way considerably surpasses the experimental error. We are forced to conclude that this Wiener component does not exist for regains below 15%. It may be responsible, however, for the small discrepancy of about  $2 \times 10^{-3}$  units which was observed at 19.8% regain. In fact, this discrepancy was also found—to a larger degree—at 78% moisture content. To that end, we measured the double refraction of the swollen orientated filaments in liquid water, using a quartz compensator, and found 0.0234. Since the degree of swelling was 2.12, the double refraction according to equation (9) would have been 0.0193. If this discrepancy is attributed to a double refraction of shape, we find  $(n_{11} - n_{\perp})_w = 0.0041$ . Applying equations (10) and (11) according to Möhring we get 0.0085. Thus, here again the birefringence of shape is

noticeably smaller than the calculated value. This cannot be due to incomplete orientation in the fiber, since we know from X-ray investigations (3) that this orientation amounts to almost 90%.

As regards a possible interpretation of these results, let us consider more closely some of the assumptions underlying Wiener's theory. It is assumed that the components cellulose and water are separated by a well-defined interface: layers of cellulose several molecules in thickness must alternate with layers of water which also comprise a large number of molecules. We know at present that the water in cellulose gels at low values of regain shows molecular dispersion, thus leading to the applicability of Gladstone and Dale's rule. From the fact that most *organic* liquids in cellulose give rise to a double refraction which is in qualitative agreement with Wiener's formulae, we are inclined to conclude that these liquids are *not* molecularly dispersed, but form comparatively thick layers which alternate with cellulose layers.

How then are we to explain the structural birefringence which appears to exist at higher values of regain in the system cellulose-water? This question cannot be answered with any degree of certainty. We know from other work (3) that the cellulose chains at about 20% regain are more or less completely covered with water molecules and that, therefore, water layers of more than one molecule in thickness are likely to occur in the amorphous part of the fiber at moisture contents beyond 20%. A system of this nature will probably show a structural birefringence, but the magnitude of this birefringence cannot be derived from Wiener's formulae. A quantitative theory of such systems, where the dispersion is molecular, or lies somewhere in between a molecular dispersion and a colloid, is not available at the present time.

So far we have left out of consideration the possible rôle of the crystalline parts of the fiber. The amount of water absorbed by the crystals, if any, is very small (11) and the refractive index of the amorphous parts will, therefore, soon drop below that of the crystals. Thus, a possible interpretation of the structural birefringence observed consists in assuming that it results from crystalline rodlets imbedded in a homogeneous medium consisting of amorphous cellulose and water. In the dry substance the difference between the refractive indices of crystalline and amorphous cellulose is so small that the corresponding Wiener effect is negligible. It is only at comparatively high moisture contents that the refractive index of the amorphous parts falls below that of the crystalline material to such an extent that a double refraction becomes measurable. Using the figure of approximately 25% crystalline material, arrived at in other work (3), it can be shown that the Wiener component observed has the order of magnitude which is required by this assumption. The accuracy of the measurements, however, is insufficient and the uncer-



tainties in our interpretation are as yet too great to allow of an evaluation of the percentage of crystalline material from the optical data.

### SUMMARY

The refractive index of moist isotropic model filaments conforms quantitatively to Gladstone and Dale's rule for mixtures. This also applies to the two refractive indices in ramie and in anisotropic model fibers below approximately 15% regain. At high moisture contents discrepancies occur, which are probably due to a structural birefringence in Wiener's sense. This Wiener component, however, is considerably smaller than that calculated for cellulose rods immersed in water.

The results obtained are in accordance with the picture of water absorption arrived at in our earlier work. The absorption of water in cellulose essentially represents the formation of a homogeneous binary mixture of water and the amorphous portion of the fiber substance (in which hydrate formation may play a rôle). It should not be considered as due to a surface action of a colloidal structure.

### REFERENCES

- (1) MEYER, M., AND FREY-WYSSLING, A., *Helv. Chim. Acta* **18**, 1408 (1935).
- (2) HERMANS, P. H., AND PLATZEK, P., *Rec. trav. chim.* **58**, 1001 (1939).
- (3) HERMANS, P. H., Contribution to the Physics of Cellulose Fibers, New York-Amsterdam (in press).
- (4) KRATKY, O., AND PLATZEK, P., *Kolloid-Z.* **84**, 268 (1938).
- (5) NEUBERT, H., *Kolloidchem. Beihefte* **20**, 244 (1925).
- (6) MÖHRING, A., *Kolloidchem. Beihefte* **23**, 152 (1927).
- (7) VERMAAS, D., Thesis. Utrecht (1941) (in Dutch); *Z. physik. Chem.* **B52**, 131 (1942).
- (8) STUART, H. A., *Molekülstruktur*. Berlin, 1934, p. 190.
- (9) WIENER, O., *Abhandl. math.-phys. Klasse sächs. Akad. Wiss. (Leipzig)* **32**, 508 (1913).
- (10) AMBRONN, H. *Ber., sächs. Ges. Wiss.* **63**, 249 (1911); *Kolloid-Z.* **18**, 90, 273 (1916); **20**, 173 (1917).
- (11) HERMANS, P. H., AND WEIDINGER, A., *J. Colloid Sci.* **1**, 185 (1946).

# THE TERMINOLOGY OF INTRINSIC VISCOSITY AND RELATED FUNCTIONS

L. H. Cragg

*From the Department of Chemistry, McMaster University, Hamilton, Ontario*

*Received February 19, 1946*

## INTRODUCTION

Although Staudinger is rightly given the credit for demonstrating the value of viscosity measurements in the study of high polymers, many workers over a period of many years have contributed ideas and techniques which together have made viscosity a function of great importance in this field. Human nature being what it is, these workers have not always been willing to use the symbols and nomenclature proposed by earlier workers; the terminological confusion that has resulted now rivals that in thermodynamics. Anyone working in this field must be aware of this confusion, but only those who have fresh memories of a survey of the literature will realize how chaotic the situation actually is.

## HISTORICAL BACKGROUND

Recently, interest has more and more centred in the "intrinsic viscosity,"  $[\eta]$  (or, sometimes,  $\eta_i$ ), and the viscosity functions closely related to it. The term "intrinsic viscosity" was introduced by Kraemer\*; in 1938 (29) he applied it to the quantity  $[\eta]$  defined by the expression

$$[\eta] = \left( \frac{\ln \eta_r}{c} \right)_{c \rightarrow 0}$$

where  $\eta_r$  = viscosity of the solution, relative to that of the solvent

$c$  = concentration, g. solute/100 cc. solution.

In 1935 Kraemer and Lansing (30) had used the symbol  $[\eta]$  for  $\lim_{c \rightarrow 0} [(\eta_r - 1)/c]$  without, however, giving it a name.† That the functions

\* So far as I have been able to discover, the term first appeared in print in a paper by Kauppi and Bass (*Ind. Eng. Chem.* **29**, 800 (1937)) where it was applied to a function that may readily be shown to be identical in value with Kraemer's. Nevertheless, Dr. Bass in a private communication (March, 1946) states that the name "intrinsic viscosity" originated with Kraemer.

† It has frequently been stated (43) or implied (13) that in this paper Kraemer proposed the name intrinsic viscosity for  $[\eta]$ . He did recognize the need for a name for this function (see the footnote on p. 157) but did not attempt to fill it. Nor did he introduce it in the paper published with Lansing (33) (*cf.* Gee (16)) or in the paper published with VanNatta (31) (*cf.* Mead and Fuoss (41)).

$(\ln \eta_r)/c$  and  $(\eta_r - 1)/c$  (or, as this function is more usually written,  $\eta_{sp}/c$ ) are in the limit ( $c \rightarrow 0$ ) identical had been proven several years earlier by Hess and Sakurada (21) and reaffirmed by Kraemer and VanNatta (31).

The recognition that it is desirable to use these extrapolated values in precise work had been a gradual development. The function  $\eta_{sp}/c$  became of interest after Staudinger had proposed his well-known rule (48) relating the "specific viscosity,"  $\eta_{sp} (= \eta_r - 1)$ , of the high polymer solution to its concentration and to the molecular weight of the polymer:  $\eta_{sp}/c = K_m \cdot M$ . Objections to the rule in its original form were soon forthcoming, among them that  $\eta_{sp}/c$  varies with concentration and that it is the limiting value,  $\lim_{c \rightarrow 0} (\eta_{sp}/c)^*$ , that has most theoretical (and practical) significance. Similarly, an empirical viscosity-concentration relationship discovered by Arrhenius (3) and used by Duclaux and Wollman (10, 11) (among others) in the form  $(\log \eta_r)/c = K_c$  was applied to linear high polymers by Staudinger (48) in the form  $(\log \eta_r)/c = M/K_{cm}$ . This relation has been widely used, either as written or as the equivalent  $(\ln \eta_r)/c = K'M$ . The function  $(\ln \eta_r)/c$  [or  $(\log \eta_r)/c$ ] varies much less with concentration than does  $\eta_{sp}/c$  (14, 24) (and is therefore preferred by many workers). It is not, however, independent of concentration, and in precise work an extrapolation to zero concentration is still necessary. The greater significance (23) of the limiting values of  $\eta_{sp}/c$  and  $(\ln \eta_r)/c$  is emphasized by the fact of their identity. Since, moreover, the slope of the relative viscosity-concentration curve  $d\eta_r/dc$  at zero concentration is identical with these limiting values of  $\eta_{sp}/c$  (31) and  $(\ln \eta_r)/c$  (14, 39), the intrinsic viscosity

$$[\eta] \equiv \lim_{c \rightarrow 0} \left( \frac{\eta_{sp}}{c} \right) \equiv \lim_{c \rightarrow 0} \left( \frac{\ln \eta_r}{c} \right) \equiv \lim_{c \rightarrow 0} \left( \frac{d\eta_r}{dc} \right)$$

would certainly seem to have a more fundamental meaning than any of the unextrapolated functions.†

#### THE EXISTING CONFUSION

The importance of  $[\eta]$  in molecular studies of high polymers and for the characterization of commercial high polymeric material may be taken for granted here. What we are more concerned with is the confusion that exists in the naming of  $[\eta]$  and related functions. This arises from:

\* The limiting value of  $\eta_{sp}/c$  is also symbolized variously as  $(\eta_{sp}/c)_{c \rightarrow 0}$ ,  $(\eta_{sp}/c)_{c=0}$ ,  $(\eta_{sp}/c)_0$  and  $\eta_{sp}/c_0$ . In this paper all these will be written  $\lim_{c \rightarrow 0} (\eta_{sp}/c)$ .

† The intrinsic viscosity of a high polymeric substance is, however, not so fundamental as to be independent of the solvent, of temperature, and of the rate of shear (see, for example, the discussion in *Trans. Faraday Soc.* **40**, 274 (1944)). These, and other, conditions of measurement should, therefore, always be described.

### 1. Uncertainty as to the Meaning of the Symbols

(a)  $\eta$  is generally accepted as the symbol for the coefficient of viscosity (the absolute viscosity) measured in centipoises. In the investigation of high polymers in solution, however, the property of interest is usually not  $\eta$  but  $\eta_r$ , the relative viscosity, *i.e.*, the ratio  $\eta/\eta_0$  of the viscosity of the solution to that of the pure solvent. But  $\eta_r = \eta/\eta_0 = \nu d/\nu_0 d_0$  where  $\nu$  and  $\nu_0$  are the kinematic viscosities,  $d$  and  $d_0$  the densities, of solution and solvent respectively. As the kinematic viscosity is the function more directly related to the flow time of a capillary viscometer ( $\nu_r = t/t_0$  if kinetic energy corrections are negligible), it is more convenient to determine  $\nu_r$  than  $\eta_r$ . Indeed, in many determinations of  $\eta_r$  the assumption is made that the solution is dilute enough to justify the neglect of the  $d/d_0$  term (5, 27, 51) (*i.e.*, that  $d = d_0$ ); the quantity actually measured is therefore  $\nu_r$ , the relative kinematic viscosity. When it has been proven experimentally that the density term may safely be neglected this usage of  $\eta_r$  is justified; but if no such proof of the equivalence of  $\eta_r$  and  $\nu_r$  is given, misunderstanding would be avoided if, as Wall (52) has suggested, the symbols  $\nu_r$ ,  $\nu_{sp}$ ,  $[\nu]$ , *etc.*, were used in place of the less correct but more usual  $\eta_r$ ,  $\eta_{sp}$ ,  $[\eta]$   $\cdots$  (or, when kinetic energy corrections are appreciable but are yet not made, the symbols  $t_r$ ,  $t_{sp}$ ,  $[t]$   $\cdots$ ).

(b) In  $\eta_{sp}/c$  and  $(\ln \eta_r)/c$  the symbol  $c$  invariably represents concentration. But that still leaves considerable scope for rugged individualism; in recent publications,  $c$  has meant the concentration expressed in the units: monomoles (Staudinger's "grundmoles")/l. of solution (22, 27, 41), monomoles/kg. of solution (15), g./100 cc. of solvent (50), g./100 cc. of solution (13, 29, 34, 36, 40), g./100 g. of solvent (7), g./100 g. of solution (38, 44), g./l. of solvent (12), g./l. of solution (35), cc./cc. of solution (5), cc./100 cc. of solution (37), cc./l. of solution (1).

It is true that the units are usually explicitly stated, but it is also true that the statement is too often in such ambiguous terms as "volume %," "volume fraction," "g./litre," and "base molality."\* It would be most helpful if workers would agree on a standard usage: fortunately a preference for the units "g./100 cc. of solution" (as recommended by Kraemer in his definitions of  $[\eta]$  (29, 30)) is now becoming apparent.

(c) The familiar confusion involving natural and common logarithms also arises here. Notations like  $\log_{10}$ ,  $\log_e$ ,  $\ln$ , are unambiguous, but some authors persist in the use of the unadorned "log." That this

\* In a recent paper (53), for example, an otherwise unusually careful and precise definition,

$$\text{"intrinsic viscosity"} = \frac{\log_e \left( \frac{\text{viscosity of soln.}}{\text{viscosity of solvent}} \right)}{\text{concn. of polymer (g./100 cc.)}},$$

is marred by the omission of the noun after g./100 cc.

may cause serious misunderstanding is strikingly illustrated by Gee's (18) misreading of the definition of  $[\eta]$  as given in Davis and Blake (8), a mistake that made necessary a later correction and revision of a published paper.

## 2. Uncertainty as to the Meaning of the Names\*

Again the best proof is illustration. Representative examples of names that have been applied to some of the important viscosity functions are listed in Table I.

TABLE I

<i>Function</i>	<i>Name</i>	<i>Reference</i>
$\eta_{sp}$	specific viscosity	36, 48
	intrinsic viscosity	47
$\frac{\eta_{sp}}{c}$	reduced viscosity	32, 42
	viscosity number	46
	intrinsic viscosity	37
	specific viscosity	28
	specific viscosity constant	12
$\lim_{c \rightarrow 0} \left( \frac{\eta_{sp}}{c} \right)$	intrinsic viscosity	19, 36
	limiting viscosity	42
	viscosity number	49
	specific increase in relative viscosity	31
$\frac{\ln \eta_r}{c}$ ( or $\frac{\log \eta_r}{c}$ )	specific viscosity	9, 10, 11
	specific viscosity constant	6
	equivalent viscosity	41
	intrinsic viscosity	17, 53
	reduced viscosity	4
	concentration reduced solution viscosity	4
	viscosity average index	50
$\lim_{c \rightarrow 0} \left( \frac{\ln \eta_r}{c} \right)$	intrinsic viscosity	29
$\frac{d\eta_r}{dc}$	relative viscosity concentration coefficient	14
$\lim_{c \rightarrow 0} \left( \frac{d\eta_r}{dc} \right)$	relative viscosity concentration	
	coefficient at infinite dilution	14
	or viscosity concentration coefficient	14
	coefficient of viscosity	20
	viscosity constant	45

Many of these names that are used are good, but it is not good that so many of them are used. And it is worse when the same name is used by different workers (or by the same worker at different times) with different meanings. Thus, as we have seen, *specific viscosity* is used for

\* "The question is," said Alice, "whether you *can* make words mean so many different things."

$\eta_{sp}$  (36), for  $\eta_{sp}/c$  (28) and for  $(\log \eta_r)/c$  (11) (although, as Kraemer has pointed out, it might have been more suitable if given to  $\lim_{c \rightarrow 0} (\eta_{sp}/c)$ .\* Similarly *intrinsic viscosity*, although generally reserved for  $\lim_{c \rightarrow 0} [(\ln \eta_r)/c]$  or  $\lim_{c \rightarrow 0} (\eta_{sp}/c)$  or  $\lim_{c \rightarrow 0} (d\eta_r/dc)$ , has also been used for  $\eta_{sp}$  (47), for  $\eta_{sp}/c$  (37), and, with increasing frequency, for  $(\ln \eta_r)/c$  (17, 53) especially when  $\eta_r < 1.40$ .† (There is some justification for this latter usage, for in many instances  $(\ln \eta_r)/c$  is roughly constant over a relatively wide concentration range (13, 25); but there is not enough justification for it, for in many others  $(\ln \eta_r)/c$  varies considerably with  $c$  (4, 35, 41), and in very few indeed is it independent.)

Now surely, if names are to be given these functions (and they will be, if only to facilitate talking about them), the names should mean the same to all workers. It is not necessary—fortunately—that each name be apt and informative; it is necessary (or at least highly desirable) that it have a unique significance.‡ As none of those who have earned the right to recommend have yet done so, the following suggestions are made in the hope that they may provoke discussion and subsequent action.

### Proposed Terminology

One name is suggested for each function, and one function for each name.

- |                           |  |
|---------------------------|--|
| (a) $\eta_{sp}$           | <i>Specific viscosity</i><br>This use of the name is winning general acceptance.   |
| (b) $\frac{\eta_{sp}}{c}$ | <i>Reduced viscosity</i><br>This seems to be the best of the names that have been used; it can be thought of as a shortened version of "concentration reduced specific viscosity" (cf. Baker (4)). (The name has also been used for $(\ln \eta_r)/c$ but at a later date.) |

\* According to Staudinger (48),  $\eta_{sp}$  is the "increase in viscosity which a dissolved substance produces in a solvent"; in other words it is the specific contribution to the relative viscosity that the solute makes. In that sense, then, it is a specific viscosity. But  $\eta_{sp}$  varies with concentration; if "specific viscosity" is to have a meaning analogous to that of specific gravity, specific volume, specific conductance (cf. ref. 30), etc., it should be an intensive property of the solute. Dividing  $\eta_{sp}$  by  $c$  should theoretically give a function of this type, but unfortunately  $\eta_{sp}/c$  itself varies with concentration. On the assumption that "ideal" conditions obtain at infinite dilution, the "true" specific viscosity would be  $\lim_{c \rightarrow 0} (\eta_{sp}/c)$ . It may be for this reason that Kraemer regretted that the name specific viscosity had been preempted; be that as it may, it is probably just as well that another name had to be found, for, as it turned out,  $[\eta]$  is not independent of the solvent used (16, 26), and a multivalued property could scarcely be considered a truly specific property.

† "When I make a word do a lot of work like that," said Humpty Dumpty, "I always pay it extra."

‡ In another connection, Mueller (2) has made the sage remark that "good usage is essentially a compilation of the mistakes habitually made by the right people."

$$(c) \lim_{c \rightarrow 0} \left( \frac{\eta_{sp}}{c} \right)$$

*Intrinsic viscosity (limiting reduced viscosity)*

The name intrinsic viscosity should be reserved strictly for this and the equivalent functions  $\lim_{c \rightarrow 0} [(\ln \eta_r)/c]$  and  $\lim_{c \rightarrow 0} (d\eta_r/dc)$ ; the temptation to use it for  $\eta_{sp}/c$  and especially for  $(\ln \eta_r)/c$  is strong but should, on that account, be the more carefully avoided (lest one fairly good custom should corrupt the word\*).

"Limiting reduced viscosity" follows from (b). It is not to be regarded as an alternative but rather as a supplement to intrinsic viscosity, of value in describing the method used in evaluating  $[\eta]$ ; e.g., "the intrinsic viscosity, determined as limiting reduced viscosity. . ."

$$(d) \frac{\ln \eta_r}{c}$$

*Inherent viscosity*

Many names have been used for this function yet none of them seem particularly suitable: in general they are misleading or have other better established meanings. The exception, "viscosity average index," recently proposed by Tamblin *et al.*, certainly has value for use as recommended, but does not suggest the close relationship between this function and  $[\eta]$ . The name "inherent viscosity" is suggested because it is free of other associations and because, as a synonym of intrinsic viscosity, it serves as a reminder that  $(\ln \eta_r)/c$  is (usually) very nearly but not quite the same as  $\lim_{c \rightarrow 0} [(\ln \eta_r)/c]$ .

$$(e) \lim_{c \rightarrow 0} \left( \frac{\ln \eta_r}{c} \right)$$

*Intrinsic viscosity (limiting inherent viscosity)*

Intrinsic viscosity is the name given this function by Kraemer and is now well established. The expression in brackets would be of value in recalling the means used to evaluate  $[\eta]$ , (compare (c)).

$$(f) \frac{d\eta_r}{dc}$$

*(Relative) viscosity concentration coefficient*

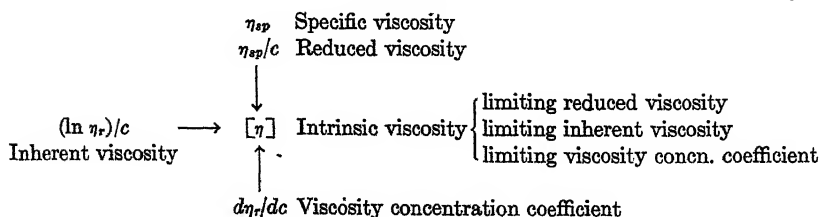
$$(g) \lim_{c \rightarrow 0} \left( \frac{d\eta_r}{dc} \right)$$

*Intrinsic viscosity (limiting viscosity concentration coefficient)*

The latter phrase, although cumbersome, is almost self explanatory. Its value, as a supplement to "intrinsic viscosity," is comparable to that of limiting reduced viscosity or limiting inherent viscosity.

The relationships between these functions are summarized in Table II.

TABLE II



In accordance with Wall's suggestion (52) the symbols should be written with  $\nu$  in place of  $\eta$  where kinematic viscosities are determined

\* With apologies to Tennyson.

and it is not clearly shown that these are numerically equal to viscosities\*; similarly, the word kinematic should, under these circumstances, be added to each of the names. When, in addition, kinetic energy corrections are not made (and in the routine determination of these functions they usually are not) confusion would be avoided, and the purpose of the investigation would be equally well served, if use were made of the terms and symbols (52): relative flow time  $t_r$ , specific flow time  $t_{sp}$ , reduced flow time  $t_{sp}/c$ , inherent flow time  $(\ln t_r)/c$ , intrinsic flow time  $[\eta]$ , etc.—unless of course it is proven that the kinetic energy correction is truly negligible.

It will be noted that with one exception the names recommended here are not new but have been chosen from those already in use. An attempt has been made to choose the most satisfactory, and it is hoped that the selections may prove generally acceptable. The important thing, however, is not *what* choice is made but that a choice *be* made. A name need not be etymologically sound but it should certainly be definitive. The first man satisfactorily performed his first task when he gave a name—any name—to each of the animals over which he had been given dominion. "And whatsoever the man called every living creature, that was the name thereof." †

#### ACKNOWLEDGMENT

The assistance given by Miss Hanna Hammerschlag, especially in locating examples of diversified usage, is greatly appreciated, as is the benefit derived from discussions with Dr. R. P. Graham. Grateful acknowledgment is also made of the suggestions of Dr. F. T. Wall and his permission to incorporate them in this paper.

#### SUMMARY

The confusion existing in the use of symbols and names for Kraemer's "intrinsic viscosity" and other functions related to it is illustrated and deplored.

The reasonable plea is made that one name be adopted for each function and that it be used with no other meaning. To stimulate discussion and ultimate action, the following names are proposed: "specific viscosity" for  $\eta_{sp}$ ; "reduced viscosity" for  $\eta_{sp}/c$ ; "inherent viscosity" for

\* The difference between intrinsic kinematic viscosity  $[\nu]$  and intrinsic viscosity  $[\eta]$ , though real (52), is very slight and may generally be neglected.

† Not "those were the names thereof"!!

My attention has been drawn to a paper by H. Fromm (*Kolloid-Z.* **102**, 86 (1943)) in which some carefully considered recommendations for the standardization of German usage in this field are made. Because of the difference in language, many of his proposals will not be directly helpful to English-speaking workers. It is, however, the primary purpose of the present paper to encourage just such careful consideration of our problems of nomenclature, and, should a committee be formed to standardize the nomenclature, it would do well to give careful attention to Fromm's proposals.



$(\ln \eta_r)/c$ ; and "intrinsic viscosity" for  $[\eta]$ , whether determined as "limiting reduced viscosity"  $\lim_{c \rightarrow 0} (\eta_{sp}/c)$ , or as "limiting inherent viscosity"  $\lim_{c \rightarrow 0} [(\ln \eta_r)/c]$ , or as "limiting viscosity concentration coefficient"  $\lim_{c \rightarrow 0} (d\eta_r/dc)$ .

Often, especially in routine practice, it is the relative kinematic viscosity  $\nu_r$  that is determined; unless this is shown to be numerically equal to the relative viscosity  $\eta_r$ , the symbols and names of the derived functions should be modified accordingly: thus,  $(\ln \nu_r)/c$  inherent kinematic viscosity,  $[\nu]$  intrinsic kinematic viscosity. Frequently, also, kinetic energy corrections are neglected; under these circumstances the suggested usage is  $t_r$  relative flow time,  $t_{sp}/c$  reduced flow time,  $[t]$  intrinsic flow time, etc.

*Editorial Note:* The Journal and author will welcome comments on this paper and on the general problem of standardizing terms and notations in the field of colloid chemistry wherever confusion exists.

#### REFERENCES

1. ALFREY, BARTOVICS AND MARK, *J. Am. Chem. Soc.* **65**, 2319-2323 (1943).
2. American Institute of Physics, Temperature, Its Measurement and Control in Science and Industry, p. 162. Reinhold Pub. Corp., New York (1941).
3. ARRHENIUS, *Z. physik. Chem.* **1**, 285 (1887).
4. BAKER, FULLER AND HEISS, *J. Am. Chem. Soc.* **63**, 3316 (1941).
5. BARTOVICS AND MARK, *J. Am. Chem. Soc.* **65**, 1901 (1943).
6. BERL AND BÜTTLER, *Z. ges. Schiess. Sprengstoffw.* **5**, 82 (1910); ref. 30, 48.
7. CONRAD, *Ind. Eng. Chem., Anal. Ed.* **13**, 526 (1941).
8. DAVIS AND BLAKE (EDS.), Chemistry and Technology of Rubber, p. 232. Reinhold Pub. Corp., New York (1937).
9. DOBRY AND DUCLAUX, *Compt. rend.* **197**, 1318 (1933).
10. DUCLAUX AND WOLLMAN, *Compt. rend.* **152**, 1580 (1911); ref. 30.
11. DUCLAUX AND WOLLMAN, *Bull. soc. chim.* [4], **27**, 414 (1920).
12. EVANS AND YOUNG, *Ind. Eng. Chem.* **34**, 461 (1942).
13. FLORY, *J. Am. Chem. Soc.* **65**, 372 (1943).
14. FLORY AND STICKNEY, *J. Am. Chem. Soc.* **62**, 3032 (1940).
15. FROSS, *J. Am. Chem. Soc.* **63**, 2401 (1941).
16. GEE, *Ann. Repts. Progress Chem. (Chem. Soc. London)* **39**, 7 (1942).
17. GEE, *Trans. Faraday Soc.* **36**, 1162 (1940).
18. GEE, *Trans. Faraday Soc.* **38**, 108 (1942).
19. GEE, *Trans. Faraday Soc.* **40**, 261 (1944).
20. GOUJON, *Chimie & industrie* **43**, Suppl. to No. 8, 229 (1939).
21. HESS AND SAKURADA, *Ber.* **64**, 1183 (1931).
22. HUGGINS, *J. Am. Chem. Soc.* **64**, 2716 (1942).
23. HUGGINS, *Ind. Eng. Chem.* **35**, 980 (1943).
24. KEMP AND PETERS, *J. Phys. Chem.* **43**, 1063 (1939).
25. KEMP AND PETERS, *Ind. Eng. Chem.* **33**, 1263 (1941).
26. KEMP AND PETERS, *Ind. Eng. Chem.* **34**, 1097, 1192 (1942).
27. KEMP AND PETERS, *Ind. Eng. Chem.* **35**, 1108 (1943).

28. KERN AND FERNOW, *J. prakt. Chem.* **160**, 296 (1942); *Rubber Chem. Tech.* **18**, 267 (1945).
29. KRAEMER, *Ind. Eng. Chem.* **30**, 1200 (1938).
30. KRAEMER AND LANSING, *J. Phys. Chem.* **39**, 153 (1935).
31. KRAEMER AND VAN NATTA, *J. Phys. Chem.* **36**, 3175 (1932).
32. KRATKY AND SAITO, *Cellulosechem.* **16**, 85 (1935).
33. LANSING AND KRAEMER, *J. Am. Chem. Soc.* **57**, 1369 (1935).
34. LOVELL, *Ind. Eng. Chem., Anal. Ed.* **16**, 683 (1944).
35. LOVELL AND HIBBERT, *J. Am. Chem. Soc.* **62**, 2140 (1940).
36. LYONS, *J. Chem. Phys.* **13**, 43 (1945).
37. MARK, *Physical Chemistry of High Polymeric Systems*, p. 280. Interscience Pub., Inc., New York (1940).
38. MARTIN, cited by Pfeiffer and Osborn, in Ott (ref. 43), p. 967.
39. MATTHES, *Angew. Chem.* **54**, 517 (1941); *Chem. Abs.* **36**, 6874<sup>2</sup> (1942).
40. MATTHES, *J. prakt. Chem.* **162**, 245 (1943); *Chem. Abs.* **38**, 2546<sup>8</sup> (1944).
41. MEAD AND FUOSS, *J. Am. Chem. Soc.* **64**, 277 (1942).
42. MEYER, *Natural and Synthetic High Polymers*, p. 23. Interscience Pub., Inc., New York (1942).
43. OTT (ED.), *Cellulose and Cellulose Derivatives*, Interscience Pub., Inc., New York (1943).
44. OWENS, LOTZKAR, MERRILL AND PATERSON, *J. Am. Chem. Soc.* **66**, 1178 (1944).
45. PHILIPPOFF, *Kolloid-Z.* **98**, 90 (1942).
46. SCHULZ AND BLASCHKE, *J. prakt. Chem.* **158**, 130 (1941); *Chem. Abs.* **36**, 17<sup>9</sup> (1942).
47. SIMHA, *J. Applied Phys. (U.S.S.R.)*, **13**, 147 (1942). (Cf., however, *J. Chem. Phys.*, **13**, 188 (1945)).
48. STAUDINGER, *Die hochmolekularen organischen Verbindungen*, Julius Springer, Berlin (1932) (lithoprinted Edwards Bros., Ann Arbor (1943)).
49. STAUDINGER AND JÖRDER, *J. prakt. Chem.* **160**, 166 (1942).
50. TAMBLYN, MOREY AND WAGNER, *Ind. Eng. Chem.* **37**, 573 (1945).
51. THOMAS, ZIMMER, TURNER, ROSEN AND FROLICH, *Ind. Eng. Chem.* **32**, 299 (1940).
52. WALL, private communications (Dr. F. T. Wall, University of Illinois, June 1944, July 1945).
53. YOUNG AND HARNEY, *Ind. Eng. Chem.* **37**, 675 (1945).



# ADSORPTION ISOTHERMS OF SOME SUBSTITUTED BENZOIC ACIDS

Robert J. Hartman\*, Raymond A. Kern†  
and Edward G. Bobalek\*

*From Colloid Laboratory, Indiana University, Bloomington Indiana*

*Received December 14, 1945*

*Revised manuscript received March 21, 1946*

## INTRODUCTION

The investigations of Bartell and Miller (1) have established that a charcoal adsorbent has a varying adsorption capacity for differently substituted benzoic acids in aqueous solutions. These observations suggest that results of considerable interest should be obtained from an investigation of the adsorption capacity of a constant type of charcoal surface in solutions of solvents and solutes of systematically varying degrees of complexity.

The preliminary studies of this program involved the determination of the Freundlich adsorption isotherms (2) of some benzoic acids in benzene at several temperatures. The acids selected were benzoic, *o*-toluic, *m*-toluic, *p*-toluic, *o*-chlorobenzoic, *o*-hydroxybenzoic and *o*-aminobenzoic. Because of their limited solubility in benzene, the adsorption of other halogen, hydroxy, nitro or amino substituted benzoic acids could not be measured with sufficient accuracy by using the techniques applicable to the more soluble acids.

## EXPERIMENTAL

*Charcoal Adsorbent.* The charcoal adsorbent was prepared by charring recrystallized sucrose for two hours in an electric muffle furnace at 200–250°C. The charring was carried out in a fused silica dish. The carbon thus obtained was then ground in a "mullite" mortar to pass through a 100 mesh sieve and finally purified according to the method of E. J. Miller (3). After this preliminary purification, the charcoal was ground in a flint ball mill to pass through a 200 mesh sieve. The charcoal purification procedure was again repeated. This second treatment reduced the ash content from .04% to .0075% by weight. The charcoal was activated in a manner similar to that employed by Bartell and Lloyd (4). The activation was carried out at 600°C. in an atmosphere of dry nitrogen. Cooling to room temperature was also effected in the presence of dry nitrogen.

Several samples of charcoal, prepared by this procedure, were tested for constancy by measuring the reproducibility of the adsorption isotherms for benzoic acid in benzene

\* Present Address: The Arco Company, Cleveland 4, Ohio.

† Present Address: Harmenting Manufacturing, Inc., Indianapolis 2, Indiana.

at 30°C. The standard deviation of the results, obtained with the different charcoal samples, was equal to, or less than,  $\pm 2\%$  of the values reported for  $x/m$  (Fig. 2).

*Solvent (benzene).*—Thiophene-free C. P. benzene was refluxed over phosphoric anhydride for three hours and then distilled, retaining only the middle fraction. Precautions in the storage and transfer of the benzene were taken to assure a minimum of moisture content. The physical constants of the benzene were as follows:

$d_{25}^{25^\circ\text{C.}} = 0.8763$  (0.8772);  $n_D^{25} = 1.4979$  (1.49794); B.P. 79.94 (80.093)°C. The comparison values in parentheses were listed in the International Critical Tables (5).

*Acid solutions.*—The C. P. acid solutes, namely, benzoic (120–121°C.), *o*-toluic (104–105°C.), *m*-toluic (109–111°C.), *p*-toluic (178–180°C.), *o*-hydroxy (157–159°C.), *o*-chloro (139–140°C.) and *o*-amino (146–147°C.), were obtained from Eastman Kodak and were further purified by triple recrystallization. The values in parentheses are the measured melting points of the recrystallized acids. Storage of the acids in a desiccator over phosphoric anhydride assured a minimum moisture content. The concentrations of the benzene solutions of these acids were determined by titration with barium hydroxide.

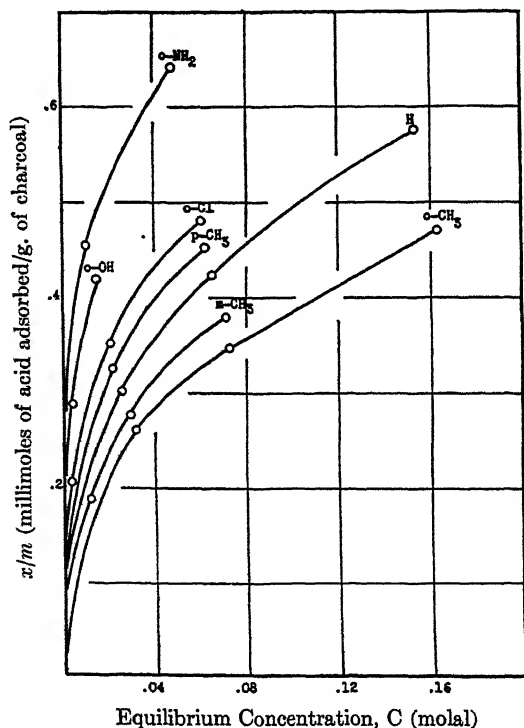


FIG. 1  
Adsorption Isotherms (20°C.) of Benzoic and Substituted Benzoic Acids.

*Procedure.* The acid adsorbates were weighed into oven-dried 125 ml. glass-stoppered Erlenmeyer flasks. The quantities of acids employed were such that molal concentrations of the order 0.010, 0.025, 0.050, 0.100 and 0.200 were obtained. Into the flasks were then introduced the acid solution (approximately 25 g.) and the charcoal adsorbent (2 g.  $\pm$

0.4 mg.). The flasks were tightly sealed with collodion solution and immersed in constant temperature oil baths ( $\pm 0.05^\circ\text{C}.$ ) and permitted to remain 30 hours with intermittent shaking. This time was determined to be sufficient for the establishment of adsorption equilibrium. The average of triplicate experimental results is reported.

### DATA AND RESULTS

The adsorption isotherms ( $20^\circ\text{C}.$ ), obtained by plotting  $x/m$  (the ratio of the millimoles of acid adsorbed to the weight of charcoal in g.) as ordinate and  $C$  (equilibrium molal concentration of acid) as abscissa (Freundlich equation), for the seven acids included in this study are shown in Fig. 1:

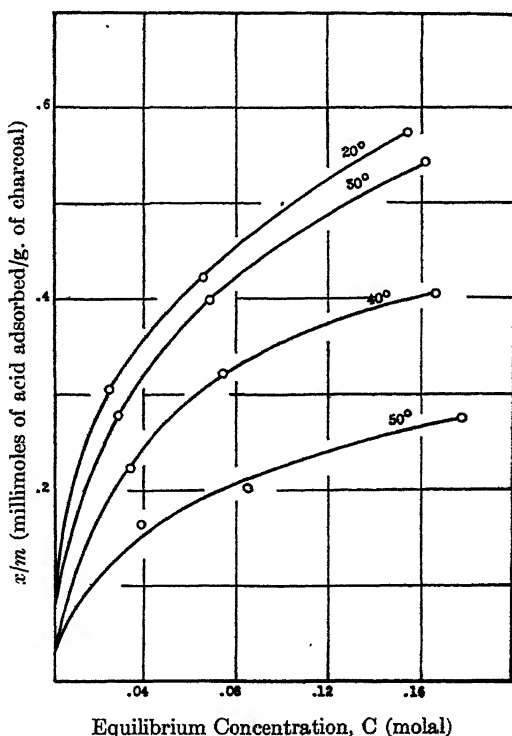


FIG. 2

Adsorption Isotherms of Benzoic Acid at 20, 30, 40 and  $50^\circ\text{C}.$

The adsorption isotherms of the same acids were also determined at 30, 40 and  $50^\circ\text{C}.$  and the isotherm for each acid was found to retain the same relative position with respect to the others at all temperatures. Fig. 2, which illustrates the adsorption isotherms for benzoic acid at 20, 30, 40 and  $50^\circ\text{C}.$ , is typical of the isotherm group for each of the acids studied.

The values of  $1/n$  and  $\log k$  of the linear form of the Freundlich equation ( $\log x/m = \log k + (1/n) \log c$ ) for the acids studied at 20, 30, 40 and 50°C. are given in Table I.

TABLE I  
*1/n and log k Values*

Acids	$1/n$	20°	30°	$\log k$ 40°	50°
Benzoic	0.3680	0.0613	0.0265	-0.1091	-0.2551
<i>o</i> -Chlorobenzoic	0.4060	0.2208	0.1834	0.1303	0.0936
<i>o</i> -Aminobenzoic	0.3693	0.3472	0.3031	0.2678	0.2218
<i>o</i> -Hydroxybenzoic	0.3840	0.2700	0.2385	0.2091	0.1844
<i>o</i> -Toluic	0.3879	-0.0215	-0.0719	-0.2510	-0.5232
<i>m</i> -Toluic	0.3581	-0.0092	-0.0582	-0.1791	-0.3732
<i>p</i> -Toluic	0.3696	0.1351	0.0762	-0.0324	-0.1886

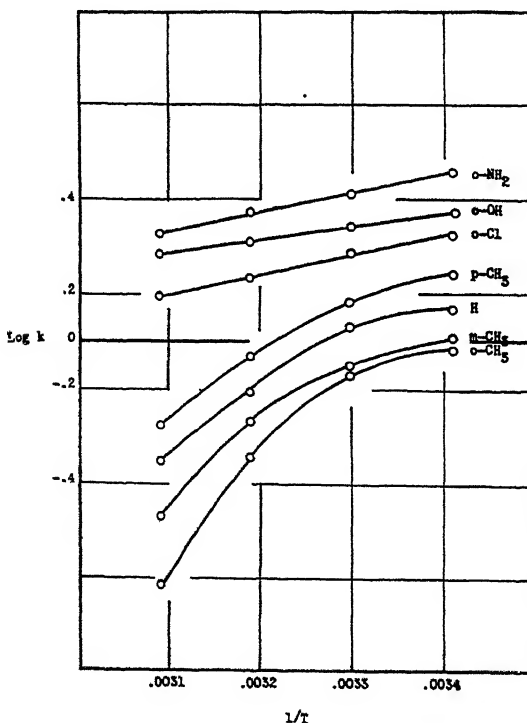


FIG. 3

$\log k$  (Freundlich) as a function of  $1/T$

The variations of the Freundlich constants with temperature are described in Fig. 3, wherein the values of  $\log k$  (Freundlich) for each acid

are plotted *vs.* the reciprocal of the absolute temperature. The slopes of the curves at each temperature, expressed as  $-d(R \ln k[\text{Freundlich}])/d(1/T)$  in calories, are listed in Table II. Although the quantities of Table II may be related to the heats of adsorption, no such positive

TABLE II

*Values of  $d(R \ln k [\text{Freundlich}])/d(1/T)$  in calories at 20, 30, 40 and 50°C.*

Acid	20°	30°	40°	50°
Benzoic	375	2770	7070	7950
<i>o</i> -Chlorobenzoic	1850	1850	1850	1850
<i>o</i> -Aminobenzoic	1810	1810	1810	1810
<i>o</i> -Hydroxybenzoic	1280	1280	1280	1280
<i>o</i> -Toluic	29	4560	11000	11400
<i>m</i> -Toluic	53	3240	6740	9610
<i>p</i> -Toluic	1700	3300	6070	7600

significance is attached to these values at this time. Until the theoretical significance of this or similar types of calculations for these types of systems can be established with greater clarity, the data of Table II have value chiefly as a basis of comparison of the adsorption tendencies of different adsorbates over a range of comparable experimental conditions.

These data are too limited to permit extensive generalization concerning the relation of chemical structure to adsorption. At this time it can be noted that, as compared to benzoic acid, the order of the adsorption tendencies of the amino and hydroxy substituted acids is the reverse in benzene of the order prevailing in aqueous solutions (1). It is certain also that the factors influencing solubility cannot be related in any obvious manner to the order of adsorption tendencies in even the more simple solvents. For example, in the order of increasing solubility in benzene we can list *o*-hydroxybenzoic acid, *o*-aminobenzoic acid, *o*-chlorobenzoic acid, *p*-toluic acid, *m*-toluic acid, *o*-toluic acid and benzoic acid. Reference to the adsorption data can produce no sequence that is related obviously to this solubility ordering.

#### SUMMARY

The adsorption isotherms (20°, 30°, 40° and 50°C.) for *o*-aminobenzoic *o*-hydroxybenzoic, *o*-chlorobenzoic, benzoic, *o*-toluic, *m*-toluic and *p*-toluic acids on charcoal from benzene solutions are presented. These acids are adsorbed in the following descending order: *o*-aminobenzoic, *o*-hydroxybenzoic, *o*-chlorobenzoic, *p*-toluic, benzoic, *m*-toluic and *o*-toluic.

The constants  $d(R \ln k(\text{Freudlich}))/d(1/T)$  have been evaluated for this series of acid in the temperature range of 20–50°C.



## REFERENCES

1. BARTELL, F. E., AND MILLER, E. J., *J. Phys. Chem.*, **28**, 992 (1924).
2. FREUNDLICH, H., *Colloid and Capillary Chemistry*. E. P. Dutton & Co., New York (1922).
3. MILLER, E. J., *J. Phys. Chem.*, **30**, 1031 (1926).
4. BARTELL, F. E., AND LLOYD, L. E., *J. Am. Chem. Soc.*, **60**, 2120 (1938).
5. *International Critical Tables*. McGraw-Hill, New York.

## NEW ELECTROCAPILLARY PHENOMENA <sup>1</sup>

A. Frumkin

*From the Institute of Colloid and Electrochemistry, Academy  
of Sciences, U.S.S.R., Moscow*

*Received April 26, 1946*

When a metal comes in contact with a solution, chemical forces acting on the atoms of the metal and the ions of the solution give rise to a double layer of electrical charges which exerts a far-reaching influence on a number of physico-chemical properties of the metal, such as its surface energy, wettability, adsorptive properties and behavior in various electrode processes.

The subject of the present paper is the description and analysis of the influence of the double layer on what might, perhaps, be called the simplest physical properties of a metal: its dynamic behavior in the liquid state and mechanical hardness in the solid state. These phenomena have recently been investigated in the Institute of Colloid- and Electrochemistry of the Academy of Sciences of the U.S.S.R. by B. Levich and myself on the one hand, and by P. Reh binder and co-workers on the other.

If a charged sphere of radius  $\alpha$  is placed in an electric field of intensity  $E$ , then, as follows from elementary physical considerations, it will acquire a velocity equal to

$$U = \frac{2}{3} \frac{\epsilon E \alpha}{\mu} \quad (1)$$

where  $\epsilon$  is the surface density of the charge and  $\mu$  the viscosity of the medium. In the case of a liquid sphere this expression will have a slightly different numerical coefficient, which for a liquid sphere moving in a medium whose viscosity considerably exceeds that of the sphere itself becomes:

$$U = \frac{\epsilon E \alpha}{\mu} \quad (2)$$

Inasmuch as the density of the charges spontaneously arising in the electric double layer is greater by many orders of magnitude than the density which can be attained by artificially charging the particle, one might expect that particles in an electrolyte solution subject to the action

<sup>1</sup> Address delivered on June 18, 1945 at the Jubilee session of the Chemistry Section of the Academy of Sciences of the USSR in celebration of the 220th anniversary of the Academy.

of an external electric field would acquire exceedingly high velocities. Actually, this is not so. The electrokinetic movement arising from application of a tangential electric field to the interface between a liquid and a foreign solid or liquid particle has long been known. It was discovered in 1807 by Reuss in Moscow, has since been the object of a great number of investigations, and has found applications in colloid chemistry, technology and biology. However, although the methods of investigating electrokinetic movement have progressed considerably since the time Reuss used a battery composed of 92 silver rubles and an equal number of zinc plates to create his electric field, no such large velocities as those mentioned above have ever been observed. Actually, the velocity of electrokinetic movement is very small and for  $E = 1$  volt./cm. only amounts to several  $\mu$ /sec. in aqueous solutions. The reason for this becomes apparent if one turns to the theory of electrokinetic movement, developed especially by Helmholtz and Smoluchowski, and analyzes this movement in greater detail. The charges of the double layer, in contradistinction to those which we have placed on our sphere, are not free, the double layer containing equal amounts of charges of opposite sign which make up its two sheets. The electric forces acting on these sheets are equal in magnitude and opposite in sign. If the charge per unit surface area on the metal is  $\epsilon$ , then that of the outer part of the double layer in the solution is  $-\epsilon$ , and the corresponding forces are  $\epsilon E$  and  $-\epsilon E$ , it being assumed that the field intensity is the same at small distances on both sides of the interface, as in the case of a dielectric particle. The points of application of these forces are separated by a very small distance equal to the thickness of the double layer  $d$ , *i.e.*, of the order of  $10^{-7}$  cm. As a result, even small velocities of the relative motion of the particle and liquid suffice to give rise to large velocity gradients in the liquid near the particle surface and, hence, large viscous stresses which counterbalance the applied forces. For a particle whose dimensions are large compared with the thickness of the double layer the theory leads to the following expression for the velocity of the electrokinetic motion:

$$U = \frac{\epsilon E d}{\mu}. \quad (3)$$

Inasmuch as  $d \ll a$ , this velocity is, in order of magnitude, much smaller than that of a particle carrying a free charge; for a particle of radius  $10^{-2}$  cm. in a  $0.1 N$  solution this ratio comprises  $10^{-5}$ . The question arises as to whether or not it is possible to find conditions under which the high velocities which are ordinarily damped by the viscous stress in the double layer could be realized.

As far back as 1903 Christiansen (1) described another group of motions which can be observed when an electric current is passed through

a solution of an electrolyte containing a drop of mercury. Christiansen's explanation of the phenomena was as follows.

Under ordinary conditions the mercury surface in contact with the solution is positively charged. The double layer on the solution-mercury interface affects the magnitude of the interfacial tension making it less. When an electric current passes through the solution and the drop, as in an ordinary capillary electrometer, the initial positive charge of the mercury is decreased at the point where the current enters the drop while the interfacial tension increases here. At the point where the current goes from the drop to the solution the positive charge increases and

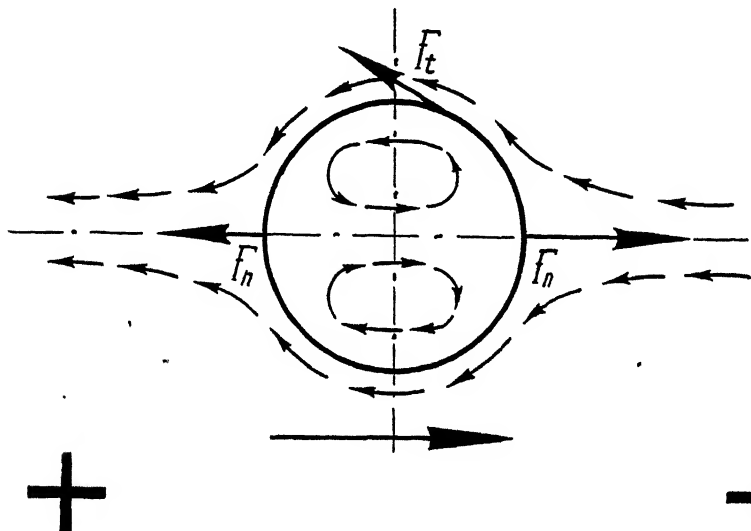


FIG. 1

Motion of a Mercury Drop in an Electrolyte Solution under the Influence of an Electric Field. The small arrows denote the direction of flow of the solution and the mercury at each point; the large arrow underneath the figure shows the direction of motion of the drop as a whole.

the interfacial tension falls off. As a result a flow of the liquid arises along the surface in the direction of increasing interfacial tension, *i.e.*, opposite to the electric field as depicted in Fig. 1. Due to this movement the drop as a whole is repelled from the surrounding mass of liquid and migrates by a reaction movement in the direction of the field.

This qualitative explanation of the electrocapillary motion of the drop, as it is usually called, must, on the whole, be considered correct in the light of our present-day concepts. However, in such an interpretation, the relation between electrocapillary and electrokinetic movement is still not clear. In the subsequent literature these two groups of phe-

nomena were usually treated completely independently; the few attempts to compare them (Craxford (2) Antweiler and Stakelberg (3)) did not, in the writer's opinion, throw sufficient light on the problem. Moreover, neither Christiansen nor the other authors gave a quantitative theory of electrocapillary movement. B. Levich and the present author have recently developed a quantitative theory of the dynamic behavior of charged metal surfaces (4) which makes an attempt to explain the relations between electrokinetic and electrocapillary movement and brings out some unexpected features of the latter. In the present communication the fundamentals of the theory are set forth, a detailed exposition is shortly to appear elsewhere.

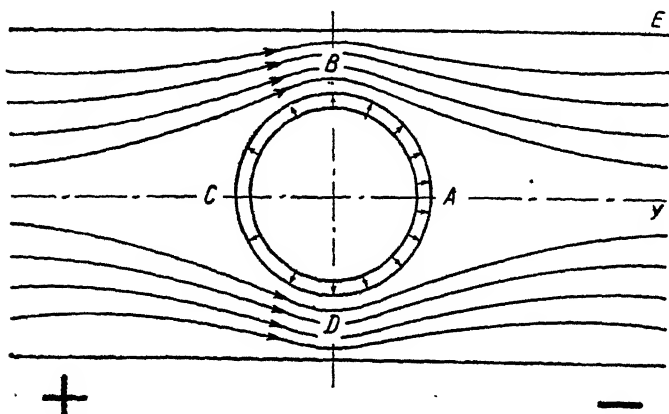


FIG. 2

Schematic Representation of the Double Layer of a Completely Polarizable Metal Particle in an External Electric Field. The arrows denote the direction of the lines of force.

Let us consider more closely the forces acting on a metal particle in a medium through which an electric current is flowing. We shall limit ourselves to the simple case when the particle can be regarded as "completely polarizable," *i.e.*, when ions of the solution cannot become neutralized nor atoms of the metal ionized at the metal-solution interface. In this respect the metal particle behaves as if it were covered with a thin layer of a perfect insulator. A mercury drop in a potassium chloride solution from which all the dissolved oxygen has been removed can be considered as satisfying the condition of complete polarizability. If this condition is not satisfied, some corrections must be made in the relations deduced; these do not greatly affect their essential features, but weaken the observed effects. The distribution of the lines of force in the case of a completely polarizable positively charged particle is shown in Fig. 2

using the simplest model of a Helmholtz double layer in the form of a plate condenser. The current through the solution flows past the drop. Due to metallic conductance the potential inside the drop is everywhere constant, the external field merely causing a redistribution of the charges in the double layer. Under the influence of the external field the double layer becomes polarized so that the potential difference between metal and solution becomes greater on the right-hand side of the drop than on the left-hand side. Consider now the forces acting on a surface element  $ds$  at point B or D. The outer sheet of the double layer is subject to a force  $-E_i eds$ , where  $E_i$  is the field intensity at the surface of the sphere (as is well known  $E_i = \frac{3}{2}E$ , where  $E$  is the intensity at a great distance from the drop); inside the metal, however, the field intensity is zero, hence the force on the inner sheet of the double layer is also zero and cannot counterbalance the force on the outer sheet, as in the case of a dielectric particle. As a result, a tangential force  $F_t$  arises as is shown in Fig. 1. On the whole, however, inasmuch as our sphere carries no free charges, the sum of the forces acting on it is zero and, therefore, the point of application of the forces acting in the opposite direction should be in another part of the sphere. This is easily seen if one considers the forces  $F_n$  normal to the surface at the points A and C. They are determined by the field intensity inside the double layer. The forces acting on the inner and outer sheets are opposite in sign. Since the curvature of the surface is slightly greater at the boundary of the inner sheet then, according to the equations of the field of a spherical condenser, the corresponding force is also slightly greater and the resultant of the forces of interaction between the charges is directed from the drop outward. Reverting to the usual terminology, one can say that the electric field, by decreasing the interfacial tension, reduces the Laplace pressure directed toward the center of the sphere. It is essential, however, that this force can be determined directly from the distribution of the electric field, without introducing the concept of interfacial tension, *i.e.*, by the same procedure as is used in the theory of ordinary electrokinetic movement. Since the density of the field of the double layer is greater on the right- than on the left-hand side of the drop, the components of the electric force normal to the surface for the surface elements near A and near C give a resultant force which coincides with the direction of the external field and is applied to the middle part of the drop. If one takes the sum of all the tangential and normal forces acting on the surface of a polarized metal drop, one gets, of course, zero. However, in contradistinction to the case of a non-conducting particle where this sum was zero for each surface element, here such a result holds only for the surface as a whole. On surface elements farther removed from the  $y$ -axis there is a predominance of the forces acting in the direction opposite to that of the field, while for the surface elements lying closer to the

$y$ -axis there is a predominance of the forces acting in the direction of the field; the order of magnitude of these forces per unit surface area is  $E\epsilon$ , as was shown for the tangential force at the points B and D. In the case of a solid particle, these forces cannot affect the translatory motion of the particle as a whole, inasmuch as their sum is zero, and only give rise to strains in the particle. A different result is obtained for a liquid metal particle. The forces bring the liquid into motion which, as is easily seen, must take place as shown in Fig. 1. The viscous stresses for a drop of radius  $a$  in the surrounding medium and in the mercury are equal in order of magnitude to  $\mu/a$  and  $\mu'/a$ , where  $\mu'$  is the viscosity of the mercury. The velocity of motion of the surface and, hence, the velocity of the movement of the particle as a whole due to reaction should therefore be equal, in order of magnitude, to  $\epsilon Ea/(\mu + \mu')$ . The complete hydrodynamic theory yields the more exact result:

$$U = \frac{\epsilon Ea}{2\mu + 3\mu'}, \quad (4)$$

*i.e.*,  $U$  is of the same order of magnitude as for a drop carrying a free charge of density  $\epsilon$ . In particular for a drop moving in a medium of comparatively high viscosity (like glycerine) for which  $\mu \gg \mu'$ ,

$$U = \frac{1}{2} \frac{\epsilon Ea}{\mu},$$

*i.e.*, the velocity acquired equals one-half the value for a liquid drop with a free charge of density  $\epsilon$ . The above consideration shows that whereas, in the case of a non-conducting particle the influence of the external field on the charges of the double-layer gives rise to ordinary electrokinetic movement, in the case of a liquid metal drop it induces electrocapillary motions, which, due to the properties of the polarized double layer, make it possible to realize experimentally high values of the velocity corresponding, in order of magnitude, to the total charge of a sheet of the double layer. Although Christiansen's data cannot be utilized for a quantitative check of the relations derived, nevertheless they definitely show that the velocity of electrocapillary movement is greater than that of electrokinetic movement by several orders of magnitude. In this Institute I. Bagotzkaya recently made measurements of the deviations in an electric field of mercury droplets falling in water-glycerine solution of sodium chloride. These experiments, which are still in progress, give values of the mobility of the order of magnitude which follows from the theory here developed. Thus, for example, the mobility of a droplet of radius  $a = 2.8 \times 10^{-2}$  cm. in a solution of viscosity  $\mu = 2.5$  is  $6 \times 10^{-1}$ , whereas the ordinary electrokinetic mobility at the same viscosity would

not have exceeded  $\sim 3 \times 10^{-6}$  cm./sec. per volt/cm. The existence of such high mobilities in a viscous medium in which the rate of fall and the current density in the solution for a given field are small makes it possible to perform a number of interesting experiments with drops falling in an electric field. In addition to the effects described by Christiansen the following phenomena can be observed which have been investigated by I. Bagotzkaya. If the end of the capillary from which the mercury is dropping is placed between the electrodes, the application of an electric field greatly reduces the size of the drops formed; thus, a field of 8 volts/cm. caused a decrease in the diameter of the drops from 0.1 to 0.05 cm. It is possible in this manner to obtain very homogeneous, exceedingly small mercury droplets, which would be difficult to procure by other methods. If the solution in which the drops are falling is initially freed from oxygen by passing hydrogen through it, one can charge the drops positively or negatively, the charge communicated remaining practically constant throughout the time of fall, as evidenced by the rectilinear path of the drops in a homogeneous electric field. Positively charged drops are attracted to the cathode and, with a sufficiently strong field, strike it; the sign of the charge is then reversed and the drops bounce off the electrode as if reflected from it. This can be especially well observed with electrodes of platinized platinum. In a similar manner, negatively charged drops migrate toward the anode and, at certain values of the field, may reach it. In this case, however, an additional phenomenon is observed. The solution surrounding the anode is saturated with oxygen, so that the negatively charged drops can interact with the  $O_2$  molecules and change their charge to positive before reaching the anode. This causes a change in the direction of motion and the drops recede from the anode, describing an arc, as depicted in Fig. 3. Under certain conditions, alternating changes in the sign of charge can be observed several times during the fall of one droplet.

It follows from equation (4) that the problem of determining the influence of the total charge on dynamic processes, which was formulated in the beginning of this communication, may be solved. If however, we attempted to get the greatest profit from this result and, following the procedure generally adopted in the study of electrokinetic phenomena, went over to highly dilute and weakly conducting solutions of electrolytes, in which it is easy to create comparatively strong fields, we should be somewhat disappointed. As the solution is diluted, the electrocapillary mobility falls off and finally approaches the ordinary electrokinetic values. This is the second interesting feature of these movements. The cause thereof becomes evident if we consider the motion of a mercury surface in a solution of electrolyte in the absence of an electric field, under the action of some other force, for example, gravity, as in the flow of mercury from



a capillary. A mercury drop coming out of a capillary is shown in Fig. 4. If the surface of the mercury behaved say like a free water surface, then motions would arise in the mercury drop as denoted by the arrows in Fig. 4. These motions are directly related to the process of drop formation itself and, as Antweiler has shown, are actually observed when a drop of water flows out of a capillary. They must also be communicated to the solution, as shown in Fig. 4. However, such motions are not generally observed when mercury flows into an electrolyte solution. This follows in particular from the circumstance that the quantitative basis of polarographic analysis, the Ilkovič-Rideal-MacGillavry equation of the diffu-

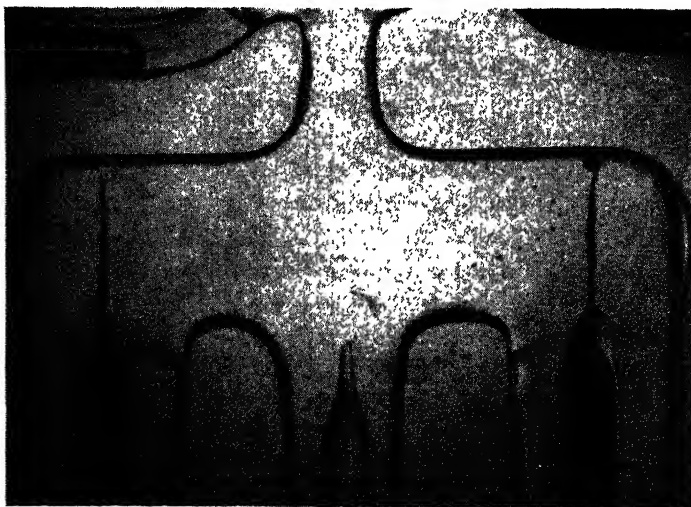


FIG. 3

Motion of Negatively Charged Mercury Drops in an Electric Field. The drops move toward the anode but, upon approach, the sign of their charge is reversed due to the action of dissolved oxygen and they change the direction of their motion.

sion current of a dissolved substance to the surface of a growing drop, which was derived on the assumption that such motions are absent, is excellently borne out by experiment. In the derivation of this equation it is assumed that the drop grows similarly to a soap bubble or an inflated rubber balloon, *i.e.*, that all the motions take place normal to the surface. However, as was comparatively recently shown by Krjukova and Kabanov (5) tangential motions of the mercury surface caused by the flow process still do take place and radically affect the form of the polarographic curves if the mercury falls into a sufficiently concentrated solution (above 0.1 N KCl). These effects usually disappear in more dilute

solutions. In such systems, under certain conditions, as is well known, one can observe motions of the surface due not to the process of flow but to the inhomogeneity of the electric field of the polarizing current. These motions, which play an important rôle in polarography, should not be confused with the phenomena here described.

How can this influence of the concentration on the dynamic properties of the surface be explained? Let us examine what happens to the charges of the double layer during the motion of the surface. As is evident

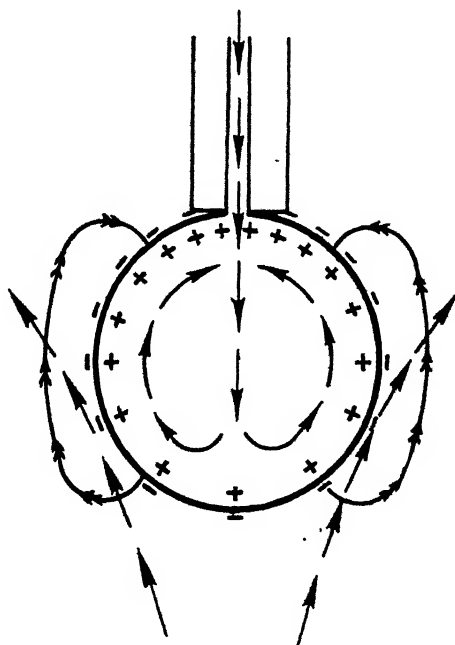


FIG. 4

Emergence of a Mercury Drop from a Capillary. The single arrows show the direction of flow of the mercury and of the solution; the double arrows—the direction of the lines of force of the electric field.

from Fig. 4, the flow of the liquid carries the charges to the upper part of the drop where, consequently, the charge density increases. As a result, an electric field is set up between the upper and lower parts of the drop which retards the motion of the surface. The direction of the field is shown by the double arrows in Fig. 4. This field induces an electric current in the solution which equalizes the potential difference and decreases the accumulation of charges. In sufficiently conducting solutions the potential differences are almost completely equalized and the described

motion of the surface can develop without hindrance. On the contrary, in dilute, weakly conducting solutions, the induced potential differences almost completely stop the tangential motion and the drop actually grows like an inflating rubber balloon.

A quantitative analysis of the problem shows that the mode of motion depends on the magnitude of the dimensionless coefficient  $\frac{\epsilon^2}{\kappa(2\mu+3\mu')}$ , where  $\kappa$  is the electrical conductivity of the solution. If  $\frac{\epsilon^2}{\kappa(2\mu+3\mu')} \ll 1$ , *i.e.*, in the case of a weakly charged surface or well conducting solution, the damping effect is absent. If  $\frac{\epsilon^2}{\kappa(2\mu+3\mu')} \gg 1$ , damping sets in and the tangential motions disappear. T. Krjukova was recently able to confirm these conclusions by direct observations of the velocity of motion of the solution near the surface of growing mercury drops over a wide range of concentrations and potentials. She showed, in particular, that whereas in a normal potassium chloride solution these motions are observable at all potentials, in a  $10^{-4}$  *N* KCl solution they can be observed only for very small charges in the immediate neighborhood of the electrocapillary zero and practically disappear at a distance of 0.2 volt from this point. The application of the theory to the case of falling drops also brings forth a number of interesting conclusions as, for example, that the velocity of fall of mercury drops in an electrolyte solution at constant viscosity should depend on the electrical conductivity of the solution. In a sufficiently viscous medium, such as glycerine, with an increase in conductivity, the velocity of fall should increase one and a half times. As droplets fall through a column of liquid the presence of the mobile double layers on their surface gives rise to a rather considerable electric current in the liquid whose strength increases with the electrical conductivity of the medium. These conclusions were checked quantitatively by comparison with the results of measurements of currents of falling drops by N. Bach (6).

Let us now return to the consideration of the motion of a drop under the influence of an external electric field. The motion of the surface in this case (Fig. 1) evidently leads to results analogous with the case of the motion under the influence of gravity, namely to an accumulation of charges on one part of the drop (the left-hand part here) and to their depletion in another part, *i.e.*, to the appearance of a local electric field of the drop which will counteract and weaken the external field. In this manner the "self-damping" effect arises. This effect may also be described somewhat differently by introducing the concept of the convective conductivity of the mobile charged metal surface, which weakens the

external field; the final result, however, is the same.<sup>2</sup> A quantitative analysis of these phenomena shows that equation (4) must be corrected to account for the effect of self-damping; it then takes the following form:

$$U = \frac{\epsilon E a}{2\mu + 3\mu' + \frac{\epsilon^2}{\kappa}} \quad (5)$$

For small values of  $\frac{\epsilon^2}{\kappa(2\mu + 3\mu')}$ , in particular for good conducting solutions, equation (5) goes over into (4), which was discussed above. In dilute solutions as a rule  $\frac{\epsilon^2}{\kappa(2\mu + 3\mu')} \gg 1$  and equation (5) goes over into

$$U = \frac{E a \kappa}{\epsilon} \quad (6)$$

so that the mobility should fall off rapidly with dilution. It should be observed that for a given solution expression (5) has a maximum at a certain value of the charge  $\epsilon = \kappa^{\frac{1}{2}}(2\mu + 3\mu')^{\frac{1}{2}}$  so that the velocity of the drop first increases with the charge and then falls off. A maximum of the mobility was actually found in the experiments of I. Bagotzkaya.

The most interesting field of application of the theory here developed is given by the so-called polarographic maxima, which, under certain conditions, appear on the current-voltage curves of the dropping mercury electrode. Due to the varying resistance of the solution along the paths of the current and to the different conditions of supply of the substances reacting on the cathode, potential differences set in between various parts of the drop, thus inducing electrocapillary motions similar to the ones here described. Upon these are superimposed the motions which are related to the process of dropping itself. On the other hand, the existence of a definite movement affects the supply of the substances reacting at the electrode and, hence, the polarization conditions and the potential differences arising between various parts of the drop. Thus, the representation of the motions on a dropping mercury electrode on the passage of a current is far more complicated than in the case of completely polarizable drop, or even in the more general case of any drop which is not an electrode, i.e., for which the currents entering the drop and going from the drop to the solution are equal. It appears however, that a consistent application of the theory here developed to the case of a

<sup>2</sup> Smoluchowski (7), Bikerman (8) and others considered a similar correction for the convective conductivity of the double layer in the theory of electrokinetic movement. In this case, however, due to small mobility, this correction is considerably smaller and should be taken into consideration only in highly dilute solutions.

dropping electrode will still help us to an understanding of all the effects involved; but this is outside the scope of the present communication.

It follows from the preceding that the presence of a double layer on the surface of a liquid metal gives rise to very well-defined easily observed effects. For solid metals the electrocapillary motions disappear and, until lately, we were limited in this case to numerous, but indirect methods of observing the influence of the double layer on the properties of the metal surface. Recently P. Reh binder and co-workers (9) discovered a phenomenon which very strikingly demonstrates the influence

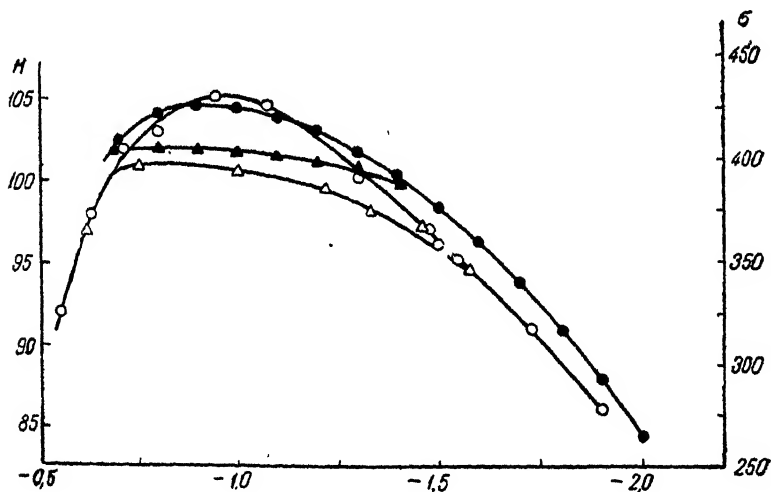


FIG. 5

Hardness,  $H$ , of Thallium and Interfacial Tension,  $\sigma$ , of Thallium Amalgams in Electrolyte Solutions as Functions of the Potential,  $\varphi$ , Referred to the Normal Calomel Electrode.

- Hardness of thallium in 1  $N$   $Na_2SO_4$ ,
- △—The same in 1  $N$   $Na_2SO_4$  +  $i$ - $C_6H_{11}OH$ , 0.185 mols/liter
- Interfacial tension of thallium amalgam (41.5% Tl) in 1  $N$   $Na_2SO_4$ ,
- ▲—The same in 1  $N$   $Na_2SO_4$  +  $i$ - $C_6H_{11}OH$ , 0.175 mols/liter

of the double layer on the behavior of solid metals and consists in a lowering of the hardness by the appearance of an electric field on the surface of the metal. According to the theory of the disintegration of solid bodies, as developed by Reh binder, any factor reducing the interfacial tension of the internal surface of the microscopic cracks which arise in the process of disintegration, lowers the hardness of the body. Hardness is understood in a generalized sense as the resistance of the body to various deformations, both elastic, brittle and plastic. This theory thus presents us with an opportunity of determining the electrocapillary curves of solid metals from the variation of the hardness with polarization. In the

experiments of Reh binder and Wenstrem the hardness was measured by the decrease in the amplitude of a pendulum pressing upon the body under investigation by means of a glass ball of small radius. A drop of a conducting solution was placed on the part of the surface which came in contact with the pendulum, so that the metal could be polarized with the aid of an external electromotive force. The greater the disintegration of the metal, the greater the amount of the energy of the pendulum absorbed, and the more rapid the decrement of the oscillations. The hardness  $H$  was determined quantitatively as the reciprocal logarithmic decrement of the oscillation amplitude. The curves in Fig. 5 give the hardness as a function of the potential for metallic thallium in various solutions, according to Reh binder and Wenstrem; for comparison are shown the electrocapillary curves of a thallium amalgam containing 41.5% of thallium, which were obtained from direct measurements of the metal-solution interfacial tension by Frumkin and Gorodetskaya (10). The potentials are referred to the normal calomel electrode. The striking similarity be-

TABLE I

	Maximum of the curve of hardness	Maximum of electrocapillary curve
Tellurium	+0.79	+0.70
Graphite (in NaCl)	+0.13	—
Mercury	—	(0.0)
Lead	-0.37	-0.37
Zinc	-0.42	-0.45
Thallium	-0.49	-0.57

tween the curves of hardness and the true electrocapillary curves, which holds even for the curves of complex form observed in the presence of adsorbed organic substances, leaves no doubt that we are dealing in both cases with the same phenomenon and confirms the correctness of the views developed by Reh binder. We should observe also that according to the data of Karpachev and Stromberg (11) obtained from measurements with molten electrolytes, the electrocapillary curves of concentrated thallium amalgams and of pure molten thallium differ comparatively little. The curves of hardness were obtained for a number of metals, as well as for graphite and tellurium (9). Table I gives the values determined up to now for the potentials at the maxima of these curves in  $N$   $Na_2SO_4$  solution, referred to the potential at the maximum of the electrocapillary curve of mercury in the same electrolyte. The second column gives the potentials at the maxima of the electrocapillary curves for molten metals in  $KCl + LiCl$  measured by Karpachev and Stromberg at 420–450° C. (550° C. in the case of tellurium) and referred to the maximum of the electrocapillary curve of mercury at 420° C. in the same medium.

The electrocapillary curve of molten carbon could not, of course, be measured but, from the dependence of the wettability on the potential, the maximum of the electrocapillary curve for graphite according to the measurements of Bruns and Chuginov (12) should be at 0.28 on our scale. As is evident from Table I, there is a satisfactory agreement between the results of measurements of the hardness and the interfacial tension of various substances. We are thus forced to the conclusion that measurements of the hardness as a function of the polarization represent an effective method of determining the point of zero charge, *i.e.*, the potential at which the charge of the double layer becomes zero and the accompanying decrease in the metal-solution interfacial tension vanishes.

The potential difference which remains between metals in electrolyte solutions when the charges of the double layers become zero should be regarded as analogous to the Volta potential between metals *in vacuo* (except for a correction related mainly to the possibility of a different orientation of the water molecules at the surface of various metals (13)). Thus, measurements of the hardness as a function of the potential allow us in a number of cases to solve the problem which has occupied electrochemists from the time of Volta's experiments and which was formulated with such remarkable lucidity by Langmuir (14), namely the determination of the extent to which the electromotive force of galvanic circuits depends on the contact potential difference between the metals.

#### SUMMARY

In the present communication the mechanism of certain phenomena connected with the presence of a double layer at a metal-solution interface is discussed. The forces acting on a completely polarizable metal particle placed in an electric field in electrolyte solutions are considered. It is shown that the same action of an external field on the charges of the double layer which in the case of a dielectric gives rise to the usual electrokinetic movement, induces electrocapillary movement in a liquid metal drop. The theory of these movements has been developed by B. Levich and the author. Quantitative expressions are given for the velocity of the electrocapillary movement. In highly conducting solutions or at low values of the charge this velocity approaches the velocity of a particle bearing a free charge equal to that of the inner sheet of the double layer. The nature of the damping effect exercised by the charges of the double layer on the movement of the liquid metal surface is considered. This effect brings a decrease in the mobility with increasing dilution, and the appearance of a maximum on the curve representing the velocity of movement as a function of the surface charge.

The values of the potentials corresponding to zero surface charge, as determined by Reh binder and Wenstrem, from the relation between the

hardness of metals and polarization are compared with the values of the potentials at the maxima of the electrocapillary curves of molten metals according to Karpachev. It is shown that there is a satisfactory agreement between the results of the measurements by the two methods.

## REFERENCES

1. CHRISTIANSEN, *Ann. Phys.* [4] **12**, 1072 (1903).
2. CRAXFORD, *Phil. Mag.* **16**, 268 (1933); CRAXFORD, GATTY AND MCKAY, *ibid.* **23**, 1079 (1937).<sup>3</sup>
3. ANTWEILER, *Z. Elektrochem.* **44**, 719, 831, 888 (1938); STACKELBERG, *ibid.* **45**, 490 (1939).<sup>4</sup>
4. FRUMKIN AND LEVICH, *Acta Physicochim. U.R.S.S.* (in print).
5. KRJUKOVA AND KABANOV, *J. Phys. Chem. (U.S.S.R.)* **15**, 475 (1941).
6. BACH, N., *Acta Physicochim. U.R.S.S.* **1**, 27 (1934).
7. SMOLUCHOVSKI in Graetz, *Handb. der Elektrizität u. des Magnetismus*, **9**, 296 (1914).
8. BIKERMAN, *Z. physik. Chem.* **163**, 378 (1933); **171**, 209 (1934); *Trans. Faraday Soc.* **36**, 154 (1940).
9. REHBINDER AND WENSTREM, *J. Phys. Chem. (U.S.S.R.)* **19**, 1 (1945); *Acta Physicochim. U.R.S.S.* **19**, 36 (1944) and unpublished data.
10. FRUMKIN AND GORODETZKAYA, *Z. physik. Chem.* **136**, 451 (1928).
11. KARPACHEV AND STROMBERG, *Acta Physicochim. U.R.S.S.* **12**, 523 (1940); **16**, 331 (1942).
12. BRUNS AND CHUGUNOV, *Acta Physicochim. U.R.S.S.* **18**, 351 (1943).
13. FRUMKIN, *J. Chem. Phys.* **7**, 552 (1939).
14. LANGMUIR, *Trans. Faraday Soc.* **29**, 15 (1916).

<sup>3</sup> The authors arrive at the conclusion that a metal particle in a field  $E$  is subject to a net force  $E\theta$ , where  $\theta$  is the total surface charge of the metal (corresponding in our notations to  $4\pi a^2 e$ ). In reality the net electric force acting on the particle as a whole is equal to zero.

<sup>4</sup> Antweiler and Stackelberg came nearer than any other authors to a qualitatively correct comparison of the mechanisms of electrokinetic and electrocapillary motions. However, their assumption that the process of electrolysis on the metal-solution interface is indispensable for the appearance of electrocapillary motions is incorrect and has affected a number of their conclusions. Contrary to their assumption the best conditions for the development of electrocapillary motions are realized in the case of a completely polarizable surface.





## BOOK REVIEWS

**Advancing Fronts in Chemistry. Vol. I. High Polymers.** Edited by SUMNER B. TWISS, Department of Chemistry, Wayne University. Reinhold Publishing Corporation, 330 West 42nd St., New York, 1945. 196 pp. 16×24 cm. Price \$4.00.

The general subject of polymers has been expanding at such a rapid rate in recent years that it is becoming difficult for one interested in any particular aspect of the field to keep abreast of current developments in all the others. The large number of symposia on polymers, sponsored by different universities and learned societies, has been evoked by the need for exchange of information. This volume presents, in condensed form, a series of ten lectures given by Wayne University during the Spring of 1944, under the Chairmanship of Dr. Neil E. Gordon. The reviewer hopes that more of these and similar symposium programs will be made available in printed form, both for later reference for those who were present at the lectures, as well as for the benefit of those who were unable to attend.

Authors and titles of the present collection are: 1. Herman F. Mark, *Molecular Structure and Mechanical Behavior of High Polymers*; 2. Samuel S. Kistler, *The Relation Between Structure and Physical Properties of High Polymers*; 3. Edgar C. Pitzer, *Some Applications of Catalysis to Hydrocarbon Reactions of Importance in the Synthesis of High Polymers*; 4. Charles C. Price, *Some Aspects of the Mechanism of Addition Polymerization*; 5. Frank R. Mayo, *Polymerization as a Study of Reactions of Free Radicals*; 6. Walter H. Stockmayer, *Molecular Size Distribution in High Polymers*; 7. Emil Ott, *Effect of Chain Length on Physical Properties of Cellulose Derivatives*; 8. William O. Baker, *Nature of the Solid State of Chain Polymers*; 9. John D. Ferry, *Mechanical Properties of Concentrated Solutions of High Polymers*; 10. Milton Harris, *Some Concepts of Textile Fibers*.

The two introductory chapters seem shorter than they might have been, considering the importance of the subjects and the ability of the authors, and lack bibliographies. The third chapter on catalysis is also quite brief, which is regrettable, because it covers a significant field related to that of polymer chemistry, with which the average polymer chemist is quite unfamiliar. The remaining seven chapters, especially 7 and 8, are excellent summaries of the fields covered, with competent bibliographies. A number of the authors present not only the current status of their particular subjects, but indicate along which lines further work would be profitable. An interesting and commendable feature of the book is the inclusion of photographs and biographies of the lecturers.

This volume is recommended for the reference shelf of research workers on polymers, and, in the opinion of the reviewer, could serve very efficiently as a source book for a graduate seminar course on polymers.

RAYMOND M. FUOSS

**Plastics, Scientific and Technological.** By H. RONALD FLECK. Chemical Publishing Co., Inc., Brooklyn, N. Y. 1945. x+325 pp. 76 figs. Price \$6.50.

The purpose of this book, according to the author's preface, is to present "a critical survey of the literature and a correlation of scattered data." Considering the enormous volume of scientific, technological and patent literature at present available on the general subject of plastics, it was obviously necessary to make a rather arbitrary selection of material in order to compress the text into three hundred and twenty-five pages.

In the reviewer's opinion, the project was too ambitious. The author was confronted with the dilemma of omitting significant work in order to save space on the one hand and of writing a highly specialized treatise on the other. As a consequence, the book is too advanced to be used as a college text (as C. M. Massopust suggests in the foreword), and is too sketchy to serve the technologist who wants more than a very brief survey of a given topic. The book can, however, be recommended to workers in other fields who would like to get a general idea of this subject; the style is good and the organization of the material is systematic. The bibliography, unfortunately, is weak; very frequently, a historical reference from the 1800's is followed immediately by one from the '30's or '40's.

The book contains fifteen chapters, with roughly one-third of the space devoted to each of the general fields of the chemistry, physics and technology of plastics. The allotment of space to the different topics does not always seem to be in proportion to their relative importance: camphor and cellulose each have one page in the chapter on raw materials; copolymerization is very hastily dismissed with two paragraphs on page 78 while natural proteins, polypeptides and amino-acids are treated in some detail in the same chapter on the chemistry of plastic materials. The section on molecular weights only mentions distribution of molecular weights casually and omits all reference to the work of Flory and Huggins on thermodynamic properties. Boiling point and freezing point methods are placed on a par with osmometry, and in regard to the latter, it is stated that "the most suitable apparatus for carrying out this determination is that devised by Pfeffer"! A long discussion of viscosity is given which merely by implication suggests that viscosity measurements can give only relative values of molecular weights, and then only when the structures of the compounds investigated are known to be similar. Other regrettable omissions include references to the work of Melville, Marvel and Wall.

The physical properties (Chapters VII and VIII) of polymeric systems are, on the whole, given a much better treatment than their chemical properties. Again, lack of space caused some omissions: the electrical properties of several bakelites are given, but no mention is made of these properties for rubbers and thermoplastic materials. Approximately the last third of the book deals primarily with the technology of plastics and their practical applications. These chapters are well written, and can be useful to academic researchers who should have some knowledge of this aspect of polymers.

RAYMOND M. FUOSS

**Wood Chemistry.** Edited by LOUIS E. WISE with chapters by: HARRY P. BROWN, CARL C. FORSAITH, RICHARD D. FREEMAN, WILLIAM M. HARLOW, L. F. HAWLEY, W. OUBRY HISEY, EDWIN C. JAHN, ERVIN F. KURTH, HERMANN MARK, A. G. NORMAN, MAX PHILLIPS, ALFRED J. STAMM, SELMAN A. WAKSMAN. Reinhold Publishing Corporation, New York. 900 p. 1944. Price \$11.50.

This volume, edited by Dr. L. E. Wise, is the cooperative work of 14 authors, all of whom are specialists in their respective fields. The text is divided into 6 parts, each containing from one to as many as 9 chapters, dealing with related topics.

By way of introduction to the subject of wood chemistry, the monograph starts out with a discussion of tree growth and anatomy of wood, followed by a discourse on the physical properties of wood. This approach is to be highly commended, inasmuch as chemical utilization is considerably affected by the cellular characteristics and physical properties of the raw material involved, in this case, wood. Considering the practical significance of variations in density and the importance of moisture content, fuller discussion of these topics might have been in order.

Part II of the text is entitled "Components and Chemistry of the Cell Wall." The

principal components of the wood cell wall—cellulose, hemicelluloses and lignin—are dealt with by different authors. A certain amount of overlapping is to be noted in this section of the book. However, as the editor justly points out in the preface, the same material was frequently presented “with quite a different emphasis by different authors.” In this section again a balance is achieved by inclusion of a chapter on physical properties of cellulose and another on “The Chemistry of the Cell Walls of Wood.” In the latter, the author, after pointing out that “the chemical utilization of wood is dependent not only upon a knowledge of the amount of certain substances in wood but also upon where they are located in the cell wall, and how the complicated cell aggregate (wood) behaves when chemically treated with various réagents,” gives a thorough review of techniques employed in such studies and their relative reliability.

Part III, consisting of one chapter, presents a very complete discussion of the extraneous components of wood. A special feature of this chapter is a chart presenting “A Scheme for the Separation of Wood Extractives,” and a table of volatile oils and their constituents from oleoresins in native and foreign species.

Part IV treats with “Surface Properties of Cellulose Materials.” Consideration of surface properties of cellulose and wood has until recently been largely neglected, even though these phenomena control to a considerable degree the various treatments, to which wood and cellulose are subjected in the course of their preparation for use. This discussion, much of which is based on original work by the author and his associates, is a valuable contribution to a subject, the practical importance of which, as the author points out, has been recognized only since 1926.

The 5th part, entitled “The Chemical Analysis of Wood,” though divided into a number of chapters, is, with a single exception—the determination of lignin—the work of one author. The treatment stresses methods of sampling and analysis, and interpretation of analytical data. Those readers looking for a detailed analysis of different species, may be disappointed to find that only a brief section is devoted to this subject. This, however, is in keeping with the editor’s statement that “the present volume does not strive to emulate” the detailed discussion of the chemistry of individual species in Carl G. Schwalbe’s book “Die Chemie der Hölzer.”

The last part of the text is devoted to a discussion of “Wood as an Industrial Raw Material.” Again, readers who expect to find in this section detailed treatment of different methods of wood conversion by chemical means and the products thus obtained are due for a distinct disappointment. The approach chosen by the authors is that of confining the discussion largely to that of basic reactions involved, leaving out the detailed treatment of technical aspects of wood conversion. An exception is the chapter on “Chemical Behavior of Wood,” in which brief but specific references are made to industrial processes and the products derived.

A notable feature of this text are extensive and, in most cases, quite up-to-date lists of references, placed conveniently at the end of each chapter.

This text is definitely not for the uninitiated. It is primarily a reference book for cellulose chemists, who will find in this volume a thorough and up-to-date treatment of each selected topic, handled expertly by men who have painstakingly reviewed the available literature and blended it skilfully with their own experience. In thus coordinating their composite knowledge the editor and the authors have performed an outstanding service for those who are not in a position to keep constantly in touch with all the sources of information in the field of wood chemistry. As a reference volume, “Wood Chemistry,” no doubt, will take its place among other well known monographs of quality, for which the American Chemical Society Series are well recognized.

A. J. PANSHIN, Michigan State College

**Casein and Its Industrial Applications.** By EDWIN SUTERMEISTER AND F. L. BROWNE. 405 pages. Reinhold Publishing Corp., New York, N. Y. Price \$6.50.

To devote space to the review of a book that was published seven years ago requires explanation and justification beyond the fact that the subject matter is of interest to the readers of this journal. This span of time, particularly since most of it was occupied with the frenzy of war-time research, will make any chemical text out-of-date at least in some particulars. However, in Sutermeister we have a work which was originally done on such a high level that much of its value is permanently maintained, and the careful compilation and organization of chapters by Browne gave to this second edition a quality which could only be heightened by the inclusion of a relatively small addendum dealing with certain new developments and refinements to bring it up-to-date. Very little would need to be added to the chapters on isolation, physical chemistry, manufacture and storage of casein, and to those chapters dealing with the use of casein in plastics, glue, paper and leather. The chapter on The Organic Chemistry of Casein, while one of the most intriguing chapters in the book, will be in a subsequent edition, whenever this might be prepared, surely expanded in view of the great amount of research which has been done in recent years in modifying casein through organic chemical reactions, particularly by those who have contributed to the development of casein fiber. The exacting demands for casein as a filament-forming material have also brought about some refinements in the testing and analysis of casein. A new chapter in casein paints would be written with emphasis on the emulsion types of paint. The chapter on medicinal uses of casein would include new material on the hydrolysates of this protein and in fact there would be more attention paid to hydrolysis reactions and products throughout other chapters as well. Miscellaneous uses of casein might well have been described in greater scope in the present edition, though perhaps at the risk of including certain uses more hoped for than actual.

Following a logical sequence, the chapters deal first with the state of casein as it exists in milk, followed by discussion of the organic and physical chemistry of the protein. A chapter on manufacture is followed by chapters on testing, analysis and storage. These chapters account for almost half of the book. The remainder is devoted to applications, each section written by an authority in one or other of the consumer industries. Indeed, the book is largely the work of representatives of the users of casein, and therefore bears the stamp of reliability as regards the methods of handling casein. In addition to the more practical information based upon the author's actual experiences, most chapters are the result of much effort in presenting a thorough picture of the various developments, with references generously provided. The colloid chemistry of casein is covered by Browne in Chapter I. The many investigations that have been made to establish the state of existence of casein in milk are systematically reviewed. Destabilizing agencies causing coagulation are explained. The special methods of producing pure casein are presented.

Although today's main problems in casein are economic rather than technical, this protein is well established in world commerce and its further progress in industry will be in part due to continued use of this singular reference work. The indexes are excellent and the binding is of the usual fine quality found in the American Chemical Society Monographs.

H. K. SALZBERG

**Formaldehyde.** By FREDERIC WALKER. American Chemical Society Monograph No. 98. 393 pages. Reinhold Publishing Corp., New York, N. Y., 1945. Price \$5.50.

The author, who is with the Electro-Chemicals Department of E. I. du Pont de Nemours & Company at Niagara Falls, N. Y., deserves the thanks of American chemists

for this comprehensive book which is recognized as authoritative on the subject. Chemists have been handicapped for years because of the lack of a central source of information concerning the chemical and physical properties of formaldehyde. Many can now discard their collected bibliographies and files in favor of this book, which not only covers the field completely but also arranges the information so logically that it may be readily consulted. In addition each chapter closes with a satisfactory reference file of the original articles for further detailed reading if necessary. This part alone is the crowning result of an arduous task of literature search.

The chapters devoted to the physical properties of formaldehyde and its solutions are lucid, thorough and intelligible. Some of the information was never published before and all of it brings the chemist up to date.

The reader will welcome the chapter on the polymers of formaldehyde as being the first clear account of the complex chemistry of polymeric formaldehyde to appear in English. It is a terse synopsis of the classic research of Auerbach and Marshall followed by that of Staudinger, who came about a quarter of a century later, and others.

It was necessary to include an account of synthetic resins, so the author made a brave attempt to cover this subject in one chapter. As far as he went he was successful, but any one wanting to master this subject will naturally consult books devoted exclusively to it and not expect to find it in a book on formaldehyde.

In the chapters on the chemistry of formaldehyde and its reactions with various classes of compounds possessing active hydrogen, each class separately dealt with, Dr. Walker has collected under one cover a vast amount of information, which was hidden in foreign language literature. This disclosure should stimulate research in unexplored fields of organic synthesis, and ultimately increase the use of this important chemical. It may also explain certain behaviors that have vexed researchers using it. No longer will the chemist need to thumb through abstruse literature in quest of methods for the detection and analysis of formaldehyde, its polymers and hexamethylene tetramine, because the book contains all the proven methods.

In order to emphasize the scope of the work, the titles of the twenty chapters are as follows: Formaldehyde Production, Monomeric Formaldehyde, State of Dissolved Formaldehyde, Commercial Formaldehyde Solutions, Physical Properties of Pure Aqueous Formaldehyde Solutions, Distillation of Formaldehyde Solutions, Formaldehyde Polymers, Chemical Properties of Formaldehyde, Reactions of Formaldehyde with Inorganic Agents, Reactions of Formaldehyde with Aliphatic Hydroxy Compounds and Mercaptans, Reactions of Formaldehyde with Aldehydes and Ketones, Reactions of Formaldehyde with Phenols, Reactions of Formaldehyde with Carboxylic Acids, Acid Anhydrides, Acyl Chlorides, and Esters, Reactions of Formaldehyde with Amino and Amido Compounds, Reactions of Formaldehyde with Hydrocarbons and Hydrocarbon Derivatives, Detection and Estimation of Small Quantities of Formaldehyde, Quantitative Analysis of Formaldehyde Solutions and Polymers, Hexamethylenetetramine, Uses of Formaldehyde, Formaldehyde Polymers and Hexamethylenetetramine, Part I, and Uses of Formaldehyde, Formaldehyde Polymers and Hexamethylenetetramine, Part II. A complete author and subject index is included.

Like so many other volumes in the A.C.S. Monograph Series, this book becomes a "must" in the chemist's reference shelf.

ROBERT J. MOORE

**Surface Active Agents.** By C. B. F. YOUNG AND K. N. COONS. Chemical Publishing Company, New York City. 370 pages. \$6.00.

The stated objective of this book is to "present information as to the origin, effects, and utilization of surface-tension phenomena in a diversity of industrial fields in the hope that the transfer of knowledge from one field to another may bear fruit in easing

the problems of some worker, or in providing the germ of an idea which may improve some process or solve some problem." In titling this book, the authors implicitly use the broader significance of "surface-active agents," rather than the restricted meaning of agents which reduce surface tension. Though such usage accords with this reader's personal preference, it is not popularly accepted; the reader should have been put on guard by explicit prefatorial comment.

The book is divided into two parts. The first part deals with the theory and determination of surface tension and the structure of wetting and specific surface-tension agents. The second part is devoted to industrial applications under such topics as emulsions, plating, metal cleaning, cosmetics, leather, flotation, inks, textiles, cutting oils, adhesives, foods, lubrication and soldering, brazing and welding.

Proofreading errors occur more frequently than is usual; e.g., "considerating" on p. 8, lettering of fig. 3 to correspond to text, chemical formulae on p. 222, etc. Errors due to misinterpretation and/or misunderstanding also occur too frequently; e.g., dimensions of equation on p. 6, the drop-number method on p. 40, detergent additives p. 346, conditioners p. 226, etc. The reader soon becomes acutely aware of a change of pace in method of presentation and emphasis. This derives partly from the wholesale verbatim reproduction of other published matter, e.g., p. 68-86, and partly from the yielding of the authors to their specialties. The overall impression is one of a job hurriedly done.

The objective of the authors would have been better served had they more clearly presented the functioning of the surface-active agents in the different industrial applications. In those cases where mechanism is in dispute presentation of opposing views with their respective arguments would have been informative. The insistence of the authors that the surface-active agents reduce surface tension and that this is an essential of the mechanism, e.g., flotation, lubrication, etc. requires argument when cited in the face of contradictory evidence.

This book may satisfy the needs of a reader desirous of getting a quick survey of the fields of industrial application, it probably will not satisfy the reader who is seeking more detailed and suggestively organized knowledge.

M. D. HASSIALIS

# PHASE RELATIONS IN THE [SYSTEM: SODIUM STEARATE-CETANE \*

Todd M. Doscher † and Robert D. Vold

*From the Department of Chemistry of the University of  
Southern California, Los Angeles*

*Received April 16, 1946*

## INTRODUCTION

This study was undertaken to supplement the information already obtained by the macroscopic investigation of this same system (1), as well as to lay the foundation for a broader study of the theoretical and technical behavior of soap-oil base systems; i.e., greases, emulsions, ointments, creams, etc.

Different compositions of the binary system, sodium stearate-cetane, were investigated with the polarizing microscope and the change in visual appearance or aspect recorded between room temperature and  $T_i$  (temperature at which the system forms an isotropic liquid). The aspects were compared to the appearances of the various phases of the system sodium oleate-water and of anhydrous sodium palmitate, which have already been published (2, 3).

The results have been plotted on a temperature-composition diagram, and seem to suggest a theoretically valid phase diagram, which in turn, has led to tentative conclusions concerning the generalized behavior of soap-oil systems as well as to point the way to further experiments.

## APPARATUS AND MATERIALS

*Chemicals.* The sodium stearate and cetane were the same as used in an earlier investigation (1). Indeed, wherever possible the identical samples of that investigation were used—others being made only to fill gaps along the composition axis or to check observations.

*Apparatus.* The flat capillaries used to hold the microscopic sample were prepared from 12 mm. heavy wall pyrex tubing. A piece of the tubing is heated in an oxygen-gas flame on diametrically opposite sides over a length of 1 to 1½ inches. This is done by turning the tubing through 180° about every 20 seconds. Before the glass sags under its own weight, it is removed from the flame and drawn out to a length of about 100 mm. The center 60 mm. of this capillary were then cut off and divided in half, making two flat

\* Presented at the Atlantic City meeting of the American Chemical Society, Apr., 1946.

† Colgate-Palmolive-Peet Co., Research Fellow in Colloid Chemistry.



capillaries which tapered internally from about 0.8 mm. to 0.4 mm. Each capillary was sealed at its wider end.

*The Cold-Box.* Systems containing less than 50 to 60% soap were not sufficiently solid at room temperature to permit the maintenance of homogeneity while working them in the filling operation to be described below. Hence, it was necessary to work with them at a lower temperature. The cold-box, Fig. 1, is a simple device which permits

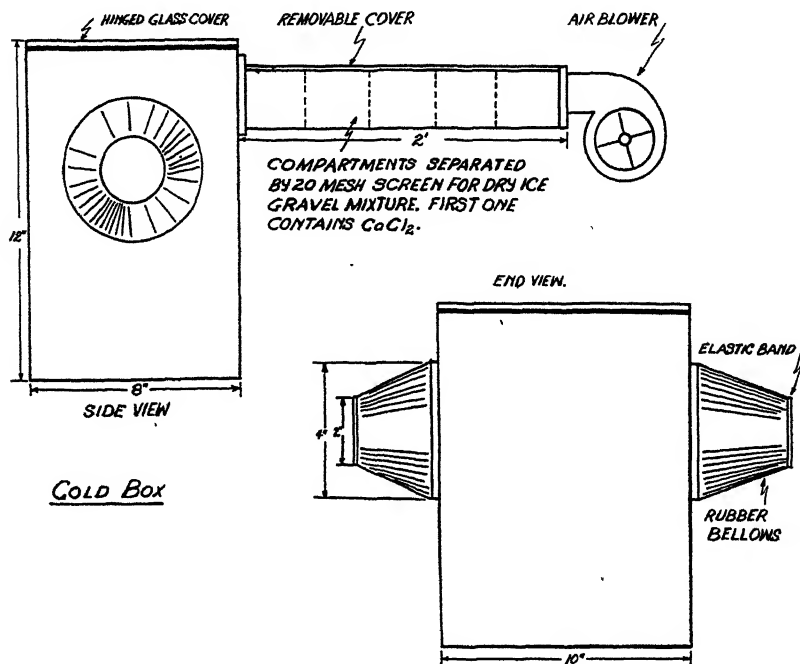


FIG. 1

handling these systems in a cold ( $-10^{\circ}\text{C.}$  to  $0^{\circ}\text{C.}$ ), dry atmosphere. The calcium chloride is used to remove most of the water vapor from the air since otherwise the dry ice would form a solid cake-like mass upon contacting the moist air. Even with the use of calcium chloride, the chopped dry ice is mixed with a fairly coarse gravel to prevent the occurrence of such caking, which would reduce the efficiency of the cooling tunnel. The filling operation is conducted entirely within this box by inserting rubber-gloved hands through the bellows at both sides of the box.

*Polarizing Microscope.* A Bausch & Lomb Chamot chemical microscope was used. A disk of Polaroid J film was used in place of the cap-nicol to permit the viewing of a wider field. A  $10\times$  objective was used in conjunction with a  $12.5\times$  eyepiece in practically all observations.

*Hot-Stage.* A hot stage developed for this investigation, which insured a uniformity of temperature along the capillary to within  $\pm 0.2^{\circ}\text{C.}$ , is described in detail elsewhere (4).

#### EXPERIMENTAL TECHNIQUE

##### *Preparation of the Micro Samples*

*Samples Containing more than 80% Sodium Stearate.* The macro samples were homogenized by heating them above their  $T_i$  points and cooled with constant shaking

as previously described (1). The tube was broken open and the surface of the solid scraped off; then a few grains were cut out with a knife-sharp nickel spatula and the capillary filled as for making a melting point determination. The material was packed into the bottom of the tube with the aid of a piece of stainless steel wire to a depth of about 5 to 8 mm. The tube was then sealed by drawing it out about 10 mm. away from the sealed end, by using a very fine pointed oxygen-gas flame. This operation requires passing the tube through the point of the flame while pulling at both ends. This effectively seals the capillary; however, to strengthen the seal, the tip of the capillary is passed through the tip of the flame two or three times more, melting it into a bead of glass. The tube must only be passed through the flame and not permitted to remain in the flame for more than a few seconds lest it explode.

*Samples Containing between 80 and 45% Soap.* These systems exhibit marked syneresis when cooled to room temperature. Hence, after homogenizing the sample, the tube was quickly cooled in ice water. The tube was removed from the oven with an asbestos-tipped forceps and submerged lengthwise and rotated until the contents had solidified. This technique was necessary to prevent the development of inhomogeneity during the quenching process. The homogeneity of the resulting quenched sample was confirmed by preparing micro samples from different parts of the macro sample.

The tube was dried, broken open, and the open narrow end of a flared capillary was gently forced down into the solid to a depth of 1 to 2 mm. The capillary was then extricated and the material which had been forced into the mouth of the capillary was pushed down with a stainless steel wire. This operation could be performed without the separation of liquid (syneresis) since the capillary widened toward the bottom and excessive pressures were not developed due to compression of air or compaction of the material. This operation was repeated until about 5 to 8 mm. of material were contained in the tube. In these systems the material was not packed solidly as in those of higher soap content. The capillary was then sealed as described above.

*Systems below 45% Sodium Stearate.* It is doubtful whether samples in this range quenched in ice-water are homogeneous, since they exhibit syneresis under the slightest pressure at room temperature. Hence, after homogenizing, the samples were dropped lengthwise into a bath of dry ice and acetone. The tubes were dried and placed in the cold box described above in which the capillaries were filled. The capillaries used for these systems were modified slightly from those previously described. A glass rod about 10 cm. long was attached to the sealed end so that a minimum of heat was transferred from the hands to the capillary. For the same reason the stainless steel wire used for packing the samples was cemented to the tip of a glass rod. Systems containing more than 10% soap were filled much like the tubes containing more than 80% soap, whereas those containing less than 10% soap were filled like those in the middle range (45–80%). After filling and sealing the capillary, the glass rod was snapped off.

#### *Microscopic Examination*

*Scope of the Method.* The use of the polarizing microscope to investigate phase transitions implicitly assumes that a succession of phases will present a succession of visual aspects. This has long been known to be true in the case of inorganic systems of salts and metals, and has been verified in the case of soap systems in the course of previous investigations (2, 3). The identification of the various phases in the system under discussion has been based on the recorded appearance of the various phases observed in these previous systems, since in every case they were directly comparable.

*Preliminary Preparation.* The micro-tubes were first homogenized by heating above  $T_i$  in the hot stage, as the mechanical working of the system in the filling operation masked much of the appearance below 100–150°C., and then allowed to cool spontaneously to room temperature over a period of about 15 minutes. For systems containing

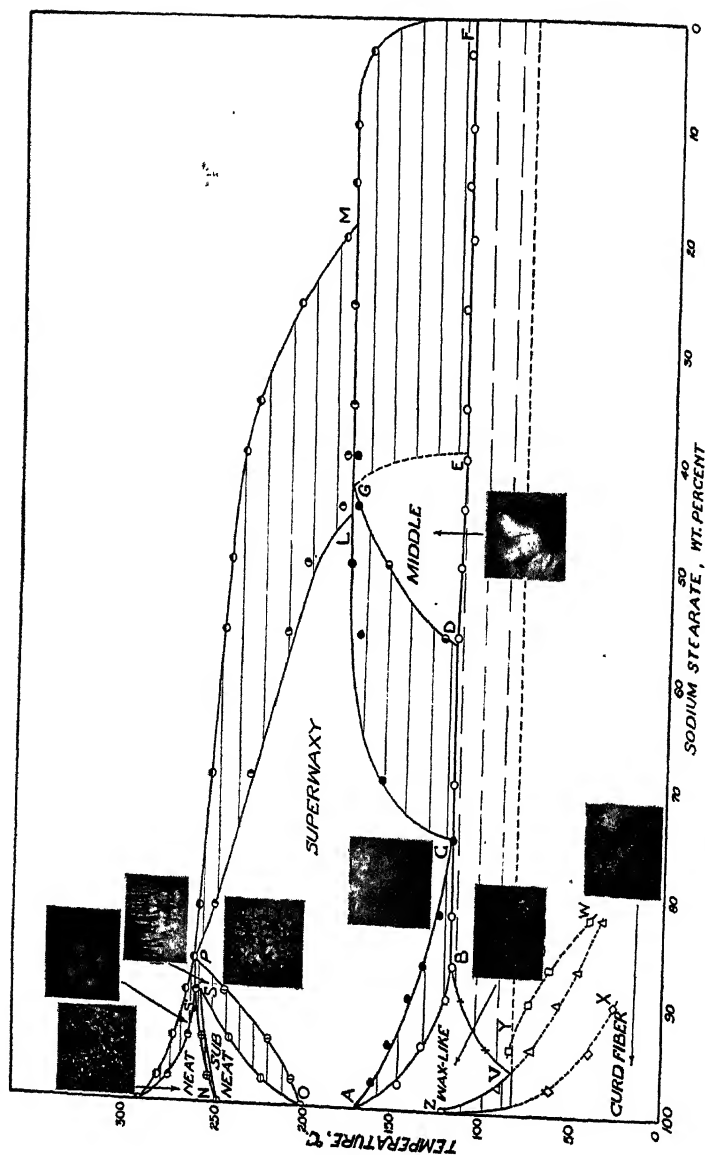


Fig. 2

The System: Sodium Stearate-Cetane

●,  $T_i$ ; ○, Initial appearance of isotropic liquid; ○, ○, superwaxy-subneat solidus and liquidus; ○, brightening, mixture from middle soap; ■, uniform superwaxy appearance; ●, formation of middle and superwaxy appearance of curd fibers; □, appearance of free liquid; +, absorption of free liquid above 90% soap; ◇, disappearance of curd fibers; △, slight brightening.

Photomicrographs are from *J. Am. Chem. Soc.* 61, 810 (1939) and *J. Phys. Chem.* 43, 1221 (1939).

more than approximately 50% soap, the microscopic examination could be begun immediately after cooling to room temperature. However, it was found that, with those systems containing less than 50% soap, it was necessary to allow the micro-tubes to age at room temperature for about 24–48 hours in order to overcome the effects of supercooling in this region and obtain an equilibrium state capable of giving reproducible transition temperatures.

*Systematic Microscopic Examination.* Preliminary investigations indicated that most changes in appearance or transformations could be obtained at reproducible temperatures ( $\pm 1$ – $2^{\circ}\text{C}.$ ) only if the heating rate is lowered to about  $1.5^{\circ}\text{C./minute}$ , and in many cases the heating had to be arrested and the temperature held constant for 30 minutes to 4 hours in order to complete the transformation.

To avoid the possibility of mis-recording a transition temperature, or recording some transitions as occurring over a wider range than they would under equilibrium conditions, all systems were run at least in duplicate. The first run was made at a uniform heating rate of  $1.0$ – $1.5^{\circ}\text{C./minute}$ , and then during the second run the heating rate was arrested at intervals for as much as two hours at temperatures starting somewhat below the point where transitions seemed to begin in the first run. In this manner, the equilibrium temperature of slow transformations, structural growth, absorption of a second phase, *etc.*, could be determined.

Isotropic liquid may appear in these systems in two different ways. At a solidus curve, the liquid appears as isotropic patches throughout the system. Below  $100^{\circ}\text{C}.$ , however, the liquid appears as films on the surface of the anisotropic solid or in the free spaces of the capillary. This effect is not due to distillation of liquid to cooler parts of the tube since the very places where the liquid appears are, if anything, the hotter parts of the tube (the walls of the capillary).

In addition to the difficulties and precautions outlined above, there remains the possibility of orientation at the walls of the capillaries, the effect of dust on the small samples, the inclusion of traces of moisture during the filling operation, *etc.* This last effect must have been negligible since the microscopic  $T_i$  curve agrees so very well with the curve obtained in a previous macroscopic investigation (1).

#### SUMMARY OF OBSERVATIONS

*Below  $110^{\circ}\text{C}.$*  In concentrated systems in this temperature range transitions occur in the binary system between curd-supercurd, and supercurd and one of the waxy phases. It is the most difficult region to analyze with the microscope, since introduction of cetane masks completely any difference in appearance between the curd and supercurd, or between subwaxy and waxy phases. In Fig. 2 no effort is made to differentiate waxy and subwaxy fields, both being labeled "wax-like." Addition of small amounts of cetane to anhydrous sodium stearate also seems to decrease the transmission of light by system. Nevertheless, the following systematic changes are exhibited below  $110^{\circ}\text{C}.$  by systems containing more than 80% soap.

(1) At room temperature, the appearance of the field is due to the presence of the curd fiber and a wax-like phase. The curd fiber phase (Cf. plates I-III, *J. Am. Chem. Soc.* **61**, 810 (1939)) is typified by the appearance of a net work of dark, irregular strings or fibers against a lighter background. The waxy phases are identified by the presence of dark, unevenly stippled areas, which give an over all blotchy appearance (Cf. plates IV-VI, *ibid.*).

(2) Upon raising the temperature, the curd fibers appear to vanish (line ZX, Fig. 2) and eventually a temperature is reached at which the system has only a wax-like appearance (line YW, Fig. 2).

(3) Shortly above this temperature, free liquid is observed, except in those systems containing more than 94% soap. As noted above, this free liquid appears as droplets on the surface of the solid and at the walls of the capillary. The liquid is reabsorbed in the 94% system at 105°C. and, in those containing less than 90% soap, within a degree or two of 118°C.

In those systems containing less than 80% sodium stearate, and below 110°C., there is little to be ascertained from the microscopic appearance. The presence of free liquid is definite and this fact contributes greatly to the masking of the field. A slight increase occurs in the amount of free liquid in systems between 60 and 80% soap as the temperature is raised toward 80°C. At this temperature, the amount of free liquid appears to remain constant or even to decrease slightly. The solid has a dull, yellow color throughout this range. In systems between 50% and 20% soap the solid appears to brighten slightly at about 80°C. This effect is small but was consistently observed. In systems containing less than 20% soap, the anisotropic material has a white, amorphous appearance and appears as clumps in an isotropic phase.

110°C. to 120°C. It had been observed that the microscopic appearance of anhydrous soap brightens somewhat continuously on heating over the lower range, with larger changes in brilliance or transmission of light at the transitions (2). However, in the 98% soap-cetane system, and in all those down to 75% soap, the brightening is confined chiefly to one transition, line ABC, which is at 144°C. for the 98% system, and drops to 118°C. for the 90% system, where it remains substantially constant down to 75% soap. The subwaxy-waxy transition, if any occurs in this system, is entirely masked; the aspect above YW being somewhat brighter and less intensely stippled but of the same nature as the subwaxy phase of anhydrous sodium stearate.

Between 70 and 20% soap, the systems seem to brighten at a slightly lower temperature and over a short range of temperature, 111-116°C., whereas below 20% soap, the amount of the isotropic phase is so great that there is no possibility of observing such a brightening.

Free liquid is reabsorbed spontaneously within a degree or two of

118°C. in systems containing between 75% and 90% soap, which is seen to be concurrent with the brightening observed in these systems. In systems containing between 40% and 75% soap, the reabsorption of free liquid can only be effected by maintaining the temperature constant for at least thirty minutes and, at the lower end of this concentration range, for as long as two hours. The reabsorption in this concentration range again occurs concurrently with the brightening mentioned above, *i.e.*, over the temperature range 111–116°C. Below 40% soap, the free liquid is never completely reabsorbed but the amount present drops sharply at 111–115°C.

The appearance of the material following this transition band is a function of the soap content:

(1) *Above 75% Sodium Stearate.* The material which begins to form along the line *ABC* is wax-like in character. It has a dull golden, mottled appearance and is similar to the photographs of sub-waxy soap (*Cf.* plate VI, *J. Am. Chem. Soc.* 61, 810 (1939)). However, careful examination revealed fairly large areas of mottled gold interspersed with ill-defined, darker patches (description of true waxy), and still other areas which had a uniform golden brilliance, typifying the superwaxy phase. Upon passing the line *AB* there is a gradual increase in the brilliance and uniformity of the system until, at the line *AC*, the brightness increases sharply. The appearance of the field is now completely uniform and that of the superwaxy phase (*Cf.* plate 2, *J. Phys. Chem.* 43, 1221 (1939)).

(2) *Between 75% and 57% soap,* this transformation does not lead to the exclusive formation of wax-like phases. First of all, just prior to the general brightening, and accompanying a significant decrease in the amount of free liquid (107–115°), the systems appear to develop structured areas in the isotropic phase. This phenomenon was particularly evident where the finer droplets had coalesced to form a continuous area of isotropic liquid. It was noted in several samples that these structures could be produced in the isotropic areas by jarring the hot stage although at the expense of any previously existing structures. These transitory structures were those of inverted focal conics and crossed droplets (*Cf.* plate 13, *J. Phys. Chem.* 43, 1221 (1939)). However, by arresting the temperature rise for 2–4 hours all the free liquid could be absorbed at 116–7°C. Secondly, the appearance above this transition consists in part of structured areas similar to those seen in subneat and middle soap in previously studied systems (2, 3). The structured areas are recognized by their polarization colors and the focal conic contours. The focal conic structures are quite small and not too distinct in this temperature-composition range whereas the rainbow-hued colors permit ready distinction from the wax-like phases.

These characteristic phenomena are not observed if the rate of heating is too rapid. Thus, in the first series of runs the liquid was not completely reabsorbed at 117°C. when heating at 1.5°C. per minute, nor did the anisotropic material exhibit any kind of structured appearance. Instead, the golden, granular superwaxy phase appeared in equilibrium with the isotropic liquid. Only at a considerably higher temperature, 130–40°C., did the change occur in part to structured areas together with the gradual absorption of free liquid.

Above the line *CD* the structured areas transform gradually into a uniform mottled golden appearance similar to that appearing at *AC*, above 75% soap, until at line *CL* the material has entirely the characteristic superwaxy appearance.

(3) *Between 57 and 40% soap*, massive focal conic structures develop directly on heating above 115°C. provided the heating rate is very slow, and coarsen with further rise in temperature. The focal conic structures developed here are similar to those seen in the middle soap phase of the sodium oleate-water system (Cf. plate 9, *J. Phys. Chem.* **43**, 1221 (1939)). They give the impression of being large, multi-colored patches of velvet. It was consistently noted in this region that entrapped air bubbles assumed an elongated appearance—at times being drawn out into cylindrical shape.

(4) *Between 40 and 20% soap*, appreciable isotropic liquid is also present together with the large focal conic structures described above. With increasing cetane content, the structured areas lose their sharp contours and eventually (*ca.* 20–30% soap) appear as isolated patches of anisotropic material—gold, blue and white in color—with irregular outlines.

(5) *Below 20% soap* the behavior of the anisotropic material is quite extraordinary: The white, amorphous anisotropic material existing in equilibrium with an isotropic phase at temperatures below 110°C. apparently begins to decrease in quantity at about 110–112°C., this decrease continuing up to about 115–120°C. In this temperature range the anisotropic material is observed to form a type of palisadic structure. This is recognized by the formation of more or less parallel, irregularly outlined rods, which usually form at right angles to the axis of the capillary (Cf. plate 10, *J. Phys. Chem.* **43**, 1221 (1939)). At about 118–20°C. all permanent anisotropy seems to have disappeared in favor of orientation anisotropy, viz., the anisotropic bars appear isotropic upon rotating the cell through 90° and other, originally isotropic, areas appear anisotropic after this manipulation. The oriented areas are not fixed but shift slightly with time at constant temperature.

*120°C. to  $T_i$ .* In systems containing more than 75% sodium stearate, the bright mottled golden aspect at *ACL* begins to coarsen as the tem-

perature is raised. This coarsening is gradual, is accompanied by an increase in translucence and consists in the segregation or sectioning of the field. Its development is suggestive of the formation of crystallites. The appearance above  $170^{\circ}$  is "granite-like" (Cf. plate 6, *J. Phys. Chem.* **43**, 1221 (1939)). There is no determinably sharp demarcation between any stage of this coarsening nor any consistent rate of coarsening.

In systems of high soap content, the line *OP* represents the appearance of palisadic structures. These persist only over a narrow range of temperature and are completely transformed into subneat soap at *OS*. The subneat phase transforms quite sharply into neat soap at *NS*, which in turn transforms into isotropic solution over a short temperature range.

Below 90% sodium stearate neither neat nor subneat soap is formed but, instead, the granite-like appearing material begins to melt directly to isotropic liquid at *PL*, and the system is completely isotropic at the  $T_i$  curve. Below 90% soap none of the classic focal conic structures exhibited by neat soap in equilibrium with isotropic liquid, such as crossed droplets, batonnets, etc., were generally observed, although the crossed droplet occasionally had a transitory existence in systems above 75% soap. The anisotropic solid upon melting breaks off in small clumps which expand and whiten before turning isotropic.

In systems containing more than 50% soap any structured areas of the middle soap that had formed in the neighborhood of  $115^{\circ}\text{C}$ . (brightening transition) transform into the granite-like appearance of the superwaxy phase beginning at the line *DG* and the transformation is complete at *CL*. The superwaxy phase, in turn, begins to form isotropic liquid at a higher temperature, *PL*. However, in the 45% soap system, and those containing less, there occurs an almost simultaneous transformation of middle soap into superwaxy soap and isotropic liquid. As noted with other transitions involving middle soap, equilibrium is not attained rapidly and the systems must be kept at  $170\text{--}5^{\circ}\text{C}$ . for several hours for the transition to be completed. The amount of isotropic liquid present increases with further rise in temperature until a uniform isotropic solution is formed at  $T_i$ .

$T_i$  drops rapidly between 40 and 20% soap and below 20% is substantially constant at  $170^{\circ}\text{C}$ . Below 20% soap the anisotropic material in equilibrium with the isotropic solution appears to be substantially unaltered in overall appearance when compared to the same systems at lower temperatures. However, above  $120^{\circ}\text{C}$ . there has been a still further increase in the orientation anisotropy of the system.

All the foregoing transitions above approximately 50% soap can be obtained quite satisfactorily on cooling the isotropic melt. Below this composition supercooling is very pronounced and the transformations cannot be obtained at reproducible temperatures on cooling.



## THE PHASE DIAGRAM

Below 110°C. the results are not sufficiently definitive to establish the position of phase boundaries. Dotted lines are drawn in as suggested by the following: *XZ*, temperature at which curd fiber begins to disappear; *VW*, temperature at which a slight brightening occurs; *YW*, temperature at which free liquid is apparent; *VB*, temperature at which free liquid is absorbed between 90 and 94% soap.

*AB* is the temperature at which a fairly sharp brightening occurs due to the transformation of the wax-like material to a mixture of superwaxy and the wax-like phase (which are distinguished primarily by the uniformity and brilliance of the former). *BCD* is an extension of *AB*, although here absorption of free liquid also occurs. At *CD* superwaxy soap and a 'structured' soap phase (middle soap) are formed rather than the superwaxy phase as at *BC*.

It is unlikely that this structured phase is continuous with the middle soap phase observed in the soap-water systems (2) despite the great similarity in microscopic appearance. However, it is believed that this similarity is probably due to structural similarities and hence this phase too will be tentatively called a "middle soap." *DE* represents the lower temperature limit for existence of middle soap and *EF* the temperatures at which it is formed in systems of lower soap content. The fact that the transitions along *DE* and *EF* were recorded over a range of temperature (111–6°C.) is attributed to the slow rate of attainment of equilibrium, and the transition is drawn as a single valued temperature line. This conclusion has been confirmed by syneresis experiments in progress in this laboratory.

*AC* and *CL* separate the homogeneous superwaxy phase from the two-phase areas where it occurs in admixture with wax-like and middle soap phases, respectively. *DG* separates the field of middle soap from the mixture of middle and superwaxy phases. The other boundary of this region, *GE*, must exist even though no observed points were determined for it. That it is approximately correctly located is indicated by the fact that systems to its right have isotropic liquid present whereas those to its left do not. At *LM* middle soap is transformed into superwaxy with a concurrent increase in the quantity of isotropic liquid.

*PL* indicates the initial appearance of isotropic liquid in equilibrium with the superwaxy phase. Since it seems likely that some isotropic liquid is formed in the system before it can be observed the phase boundary *PL* is drawn in a few degrees lower than these points. The reality of the two-phase area between *PL* and *T<sub>i</sub>*, and the validity of the boundaries as drawn, was confirmed macroscopically by keeping a 45% system at 210°C. and then at 225°C. for 24 hours in a flat-bottomed tube. The

observed volume distribution between liquid and solid was 60:40 and 80:20 compared to 54:46 and 75:25 demanded by calculation by the law of tie lines from the indicated phase boundaries. In view of the uncertainties in the measurement (incompleteness of phase separation, undetermined density differences between the phases, *etc.*) the agreement is satisfactory.

The superwaxy—subneat transitions as well as the neat soap-isotropic liquid transitions are obvious. However, it is necessary to split the line *NS*, representing the observed transition of subneat soap to neat soap, into two lines, *NS* and *NS'*, in order to conform to the phase rule.

The one-phase superwaxy area merits further consideration. As shown in Fig. 2, it is continuous with the superwaxy phase of anhydrous sodium stearate and extends to the *T*<sub>1</sub> curve. The boundary has been drawn in this manner because no definite transition points could be detected, although the anisotropic material at *PL* has a different appearance from that at *ACL*. As already described, the change between *ACL* and *PL* is gradual and suggestive of "crystal growth" or an orientation phenomenon. There are also no observable macroscopic changes in this region, and preliminary studies on the ternary system, sodium-stearate-cetane-water also seem to demand that this area be a single-phase region.

## DISCUSSION OF RESULTS

### *Correlation with Grease Technology*

Lubricating greases prepared from paraffin oil and saturated sodium soaps are relatively unstable. This might have been deduced from the fact that anhydrous systems with the soap content of typical grease formulae at temperatures below 120°C. fall in a two phase region, which consists of the paraffin oil and a soap fiber phase containing less than 20% oil. Solvation of the soap by the paraffin hydrocarbon chain does not occur until the soap lattice is "opened up" by thermal energy.

Such an alteration in the physical structure of the grease system has been clearly demonstrated by experiments on the structural viscosity of grease systems (5). Below 120°C., 4% suspensions of sodium stearate in paraffin oil did not exhibit any yield value; and, further, the viscosity of the suspension was only slightly greater than that of the pure oil and decreased with rising temperature at the same rate as the latter. At 125°C., however, a sharp increase in viscosity occurred simultaneously with swelling of the dispersed soap. The viscosity of the suspension then decreased with further rise in temperature. For systems containing less than 40% soap this is the temperature at which transformation occurs to the more highly solvated and more viscous middle soap.

*Interpretation in Terms of Colloidal Structure*

The curd fiber phase has been established as consisting of a disordered array of crystals or crystallites consisting of parallel double molecules of sodium stearate fairly tightly bound by intermolecular forces (6). Cetane held in this phase can be attributed to sorption on the crystal surfaces and in the interstices of the solid. Up to 110°C. there seems to be a slight but regular decrease in the amount of cetane bound by the soap. This may be attributed to an increase in the specific volume of the liquid which results in squeezing some out of the capillary spaces, together with the lowering of the forces of physical adsorption at the surface.

The formation of the various waxy phases is due to a weakening to some extent of the intermolecular forces, and this weakening is assumed to occur along the length of the hydrocarbon chains and not at the polar heads of the molecules. Direct evidence for this assumption is the much larger heat effects associated with the curd fiber-waxy transitions than with any of the other mesomorphic transitions, and the correspondence between chain length and magnitude of the thermal effect at these transitions (7). The occurrence of this weakening of the inter-chain forces (which can be thought of as a pseudo- or partial liquefaction) may be expected to permit the solution of cetane or other geometrically compatible hydrocarbon molecules between the tails of sodium stearate. This concept, it should be noted, is different from that of the usual mechanism for solubilization (8, 9). Non-polar material solubilized in soap solutions is usually considered to be held between the ends of the hydrocarbon tails of the soap micelles, although recent evidence (10) indicates that globular molecules may enter between the hydrocarbon chains.

The coincidence of the temperature at which large amounts of cetane are incorporated into the soap lattice with the temperature range over which the inter-chain forces diminish in sharply defined steps in the anhydrous soap (curd fiber  $\rightarrow$  subwaxy  $\rightarrow$  waxy  $\rightarrow$  superwaxy) makes the assumption tenable that the cetane dissolves between the soap chains. This hypothesis is rendered even more plausible by the fact that the stable phase above this transition temperature at the higher soap concentrations is superwaxy soap, in which the chain forces have been reduced to a low value as shown by the fact that deBretteville and McBain (11) report from X-ray work that subwaxy and waxy phases of anhydrous sodium stearate are definitely crystalline while the superwaxy phase more nearly resembles the liquid crystalline forms.

This explanation of the extension of superwaxy soap to fairly high cetane concentration (approximately 50 mole %) may also account for the non-smectic character of the superwaxy phase in this system. The smectic phases are characterized by an arrangement of molecules such

that their ends lie on equidistant planes, with successive planes mutually parallel. The arrangement within these planes is completely random and is sufficiently loose so that continuity over a very large number of molecules without break or irregularity of any kind is improbable. The focal conic structures which characterize the true smectic phase arise from the way in which a set of planes with normals in a given direction adjust themselves to a set with normals in some other direction. The regions of adjustment in which planes are bent into optically non-homogeneous regions are the focal conic sections, and are bounded by geometrical configurations known as Dupin's cyclides (12). This geometrical configuration, together with the observed optical properties of the smectic phases, requires that the molecules in the layers be at right angles to the layers.\* The inclusion of cetane molecules between the chains of the soap lattice at a temperature where the attractive forces between the polar terminals is still relatively high, can be expected to deform the parallel alignment of the lattice and, in turn, prevent the formation of a smectic phase. That attractive forces between the polar heads in the superwaxy phase are still appreciable is confirmed by the fact that a 70% soap system cannot be made to flow under moderate pressures at temperatures as high as 175°C., nor can threads be drawn from it with a glass rod (13). Dissolution of the forces between the polar heads has been shown to be necessary for extended fiber (thread) formation under these conditions (14).

The occurrence of the apparently smectic phase, middle soap, at lower temperatures and higher cetane concentration therefore requires some explanation. In these mesomorphic phases the balance between the polar forces holding the heads together and the nonpolar attraction between the tails and the added cetane is important. As the proportion of cetane is increased the polar forces are overcome resulting in a looser structure which again permits of perpendicular alignment of the tails with respect to the polar planes. If this is the case, then we should expect the middle soap gel to be readily deformed, and this is actually true in this oil system. Not only is the middle soap gel (45% sodium stearate at 120°C.) readily deformed, but it can be forced into the pores of a filter paper under a pressure of about 10 lbs./sq. in. Under the same pressure at temperatures below the transition to middle soap this system loses

\* K. Hermann has questioned this theoretical requirement since he found the long spacing of both thallium stearate and thallium oleate to decrease in a liquid crystalline state, which he deemed to be smectic (15). More recently McBain and deBretteville (11) reported the same effect with sodium stearate. Bernal has in turn questioned the assumption that a true smectic phase is obtained in these anhydrous soaps, or whether they are of a closely related liquid crystalline type (16). It is evident that continued X-ray work on polycomponent soap systems is necessary for a satisfactory analysis of this problem.

only-cetane leaving the soap as a cake (13). Gallay *et al.* have also noted the fact that fibers may be formed from dilute soap-paraffin oil systems above 125°C., but that these break up as the temperature is lowered below the transition.

The stability and colloidal characteristics of lubricating grease systems are thus seen to be closely related to the phase relations prevalent under a given set of conditions. This work is being extended to include more complex systems.

### SUMMARY

The system sodium stearate-cetane has been investigated with a polarizing microscope in a specially designed hot stage, and a partial phase, diagram constructed from these data.

The change from synerectic to non-synerectic systems, together with the accompanying change in rheological properties, has been shown to be related to the existence of a unique phase transition.

An attempt is made to correlate these effects with the internal structure of the phases.

### REFERENCES

1. VOLD, R. D., AND PHILIPSON, J., *J. Phys. Chem.* **50**, 39 (1946).
2. VOLD, R. D., *J. Phys. Chem.* **43**, 1213 (1939).
3. VOLD, R. D., AND VOLD, M. J., *J. Am. Chem. Soc.* **61**, 808 (1939).
4. DOSCHER, T. M., AND VOLD, M. J., *Ind. & Eng. Chem., Anal. Ed.* **18**, 154 (1946).
5. GALLAY, W., PUDDINGTON, I. E., AND TAPP, J., *Can. J. Research* **22B**, 66 (1944).
6. THIESSEN, P. A., AND EHRLICH, E., *Z. physik. Chem.* **165A**, 453 (1933).
7. VOLD, R. D., *J. Am. Chem. Soc.* **63**, 2015 (1941).
8. MCBAIN, J. W., in *Advances in Colloid Science*, pp. 123ff. New York (1942).
9. HESS, K., PHILIPPOFF, W., AND KIESSIG, H., *Kolloid-Z.* **83**, 40 (1939).
10. HARKINS, W. D., *J. Colloid Sci.* **1**, 105 (1946).
11. MCBAIN, J. W., AND DEBRETTEVILLE, A., *J. Chem. Phys.* **11**, 426 (1943).
12. BRAGG, W., *Trans. Faraday Soc.* **29**, 1056 (1933).
13. DOSCHER, T. M., unpublished experiments in this laboratory.
14. GALLAY, W., *et al.*, *Can. J. Research* **21B**, 211 (1943).
15. HERMANN, K., *Trans. Faraday Soc.* **29**, 972 (1933).
16. BERNAL, J. D., *Trans. Faraday Soc.* **29**, 1073 (1933).

# EFFECT OF METHOXYL CONTENT OF PECTIN ON THE PROPERTIES OF HIGH-SOLIDS GELS

Harry S. Owens and W. Dayton Maclay

*From the Western Regional Research Laboratory,<sup>1</sup> Albany, Calif.*

*Received March 26, 1946, revised copy received May 31, 1946*

## INTRODUCTION

Since their discovery in 1790 (1), pectin gels have become commercially important and the subject of considerable investigation. At the present time four types of gels have been developed from the various available pectins. The first is a high-solids gel (about 65% total solids) prepared from rapid-set pectin which is extracted from citrus or apple wastes and forms gels before the gel mixture has cooled appreciably after the required amount of acid is added. The second is a high-solids gel prepared from slow-set pectin which is partly de-esterified either by alkali (2-5) or acid (6) while the pectin is *in situ* or after it has been extracted. The gel mixture does not set until some cooling has occurred. The period of time required depends on the methoxyl content of the pectin used (7) when other factors are constant. These two types comprise the common jellies of the food industry. The third is a gel that usually contains 10-40% total solids and requires the use of low-methoxyl pectins which have been de-esterified by alkali (8, 9), acid (10, 11, 12), or enzymes (12). These gels, prepared with calcium pectinate, are becoming important for use in desert, salad and other similar food gels (12-20). The fourth one is prepared from so-called "fibrous" sodium pectate (13) or low-methoxyl pectins (8, 14) with a suitable nutrient for use in the identification of strains of bacteria and as an agar substitute (15, 16).

So much interesting and fundamental work has been published on these gels that it cannot be reviewed here and, hence, reference is made to some of the more recent investigations for details (14, 21, 22, 23, 24). There appears to be a lack of some experimental detail which would make comparison of the properties of the gels more quantitative; consequently an investigation has been undertaken to examine pectin gels prepared under different conditions with devices that measure the modulus of rigidity, modulus of elasticity in compression, and the breaking limit. Such information is believed to be necessary to permit study of wider

<sup>1</sup> Bureau of Agricultural and Industrial Chemistry, Agricultural Research Administration, U. S. Department of Agriculture.

application of the gels and to develop a more comprehensive theory of pectin gel formation. In this paper comparisons of gels of the first two types prepared at different pH values and in the presence of calcium ion are reported.

### EXPERIMENTAL METHODS

Most of the pectinic acids in Table I were described previously (25, 26, 27). Sample 10.5 was extracted from lemon peel and de-ashed by precipitation in acidified ethanol, then washed free of chloride in ethanol-water mixtures. Samples 7.4E and 4.5E were also prepared from lemon peel and were partly de-esterified by citrus pectinesterase while *in situ*. A nearly ash-free commercial citrus pectin was used for sample 10.1. It was treated with ammonium hydroxide at 5°C. to prepare all the "B" samples.

TABLE I  
*Description of Pectins Used in the Investigation*

Number <sup>a</sup>	Uronic Anhydride	Ash	$[\eta]$	$\bar{M}_n$	$\bar{M}_w$ <sup>b</sup>
10.5	82	0.2	7.9	3.9	11.0
7.4E	80	0.4	5.5	—	8.0
4.5E	81	0.5	5.2	—	7.6
10.1	84	0.6	4.3	3.3	6.7
8.5B	85	0.6	3.6	—	5.9
7.4B	85	0.5	3.5	—	5.8
6.2B	86	0.5	3.3	2.3	5.5
5.8B	86	0.5	3.3	—	5.5
5.2B	86	0.4	3.2	—	5.4
4.8B	87	0.5	3.2	—	5.4
3.5B	87	0.5	3.1	2.1	5.2
8.0A	86	1.2	4.2	—	6.6
10.9	84	0.2	5.7	2.7	8.2

<sup>a</sup> The number refers to the methoxyl content; the letter indicates the method of de-esterification: A = acid, B = base, and E = esterase.

<sup>b</sup> These values were interpolated from viscosity data (26) and from the molecular weights reported by S  verborn (32).

Sample 8.0A was prepared from a commercial citrus pectin by the acid method of Hills, White and Baker (12). Sample 10.9 is a commercial apple pectin de-ashed in an ion-exchange column (28).

The analytical, viscometric, and osmotic pressure (a measure of the number-average molecular weight,  $\bar{M}_n$ ) methods have been described (26). Some of the osmotic pressure measurements were made with osmometers designed by Bull (29). The solvent (0.155 M sodium chloride) and the temperature (25°C.) at which the viscosities and osmotic pressure measurements were made, were the same as had been used previously (26). The results are summarized in Table I.

Gel strengths were measured with three instruments. All three measurements were performed on the same sample after standing 18–24 hours at room temperature, which was  $24 \pm 2^\circ\text{C}$ . The temperature at which the measurements are made is not so critical with pectin gels where the change in strength is less than 0.2%/degree (23) as it is with gelatin gels where the change in strength is as much as 5%/degree (30).

A torsion-type instrument similar to the one designed by Brimhall and Hixson (31) (called a rigidometer hereafter) to obtain absolute measurements of the modulus of rigidity was made with a serrated steel cylinder 1 cm. in diameter and 10 cm. long. The gel was cast in a 400-ml. beaker containing a layer of mercury to reduce end effects and covered with a layer of mineral oil to reduce evaporation. The torsion head was turned by a constant-speed motor at 0.043 rpm. The suspension was a piano wire 0.047 cm. in diameter and 20 cm. long. Its torsional moment was determined from the period of oscillation of brass weights fastened to a brass rod suspended from the wire. The torsion head was turned through  $10^\circ$  and the displacement of the cylinder was measured with a telescope and scale. Investigation here and elsewhere has shown that pectin gels obey Hooke's law for small displacements (32); therefore, single measurements were deemed sufficient to establish the modulus.

Routine measurements were made with a blade 1 by 5 cm., which could be inserted into the gel without the necessity of casting it in the gel. The gels were allowed to form in jelly glasses with tape sideboards (33). Results seldom differed more than  $\pm 2\%$  on duplicate gels.

The second tester was a sagometer (33), which under certain conditions is a measure of the modulus of elasticity in compression, and was used as described by the inventors. The glasses had an inside height of 8.76 cm. Results are reported in unit compression values, measured after the gels had sagged for a period of 2 minutes; they seldom varied more than  $\pm 2\%$  on duplicate gels.

The third tester was a Tarr-Baker plunger-type instrument (34) which yields information on the breaking limit. The values reported are in cm. of carbon tetrachloride required to force a copper-clad plunger with an area of 3.14 cm.<sup>2</sup> and a weight of 19.7 g. through the bottom of an inverted gel. Results usually varied no more than  $\pm 5\%$  on duplicate gels.

Gels were prepared in a uniform way. Eighty g. of sucrose and a weighed amount of pectinic acid were stirred into 300 ml. of boiling water containing sodium citrate (from 1.5 to 15 m.eq.) in a tared pan. A timer was started as soon as the pectin was wet. Two minutes later the remaining sucrose (400 g.) was added rapidly. The pan and its contents were adjusted to weight at the end of 4 minutes and again at 5 minutes when the mixture weighed 740 g., including the weight of the acid. Between 1.5 and 43 m.eq. of citric acid or 6-12 m.eq. of hydrochloric acid was divided between two glasses and the hot gel mixture poured into them. The entire mixture was then stirred vigorously for a few seconds and allowed to set. Calcium chloride, when used, was added during the last 10 seconds of the boiling period. A flowmeter was used on the gas inlet to the burner to insure maintenance of a constant heating rate.

## RESULTS

The calibration of the blade against the results with the cylinder is shown in Fig. 1, where shear modulus in g./cm.<sup>2</sup> is plotted against deflections of the blade in cm./ $10^\circ$  turn of the wire. Each cm. of the scale was equivalent to  $0.58^\circ$ . Relaxation effects, which are receiving further study, influence the values obtained.

A plot of sagometer readings made at the end of 2 minutes in cm. depression/cm. height of gel *vs.* shear moduli is given in Fig. 2. It is noteworthy that at small values of unit compression, the modulus of elasticity follows the theoretical equation derived by Chree (35, 36) for a cylinder supported on its base sagging under its own weight  $E_c = hd/2e$ , where  $E_c$



is the compression modulus,  $h$  is the height of the gel,  $d$  is the density of the gel and  $e$  is the unit compression. To calculate shear modulus, a value of 0.5 was assumed for Poisson's ratio in the equation  $E_s = E_c/2(1 + \nu)$ , where  $E_s$  is the shear modulus and  $\nu$  is Poisson's ratio (36). Deviations from theory are narrowed considerably by allowing the gel to sag for longer periods of time. For example, a typical gel with an  $E_s$  of 8.8 g./cm.<sup>2</sup>

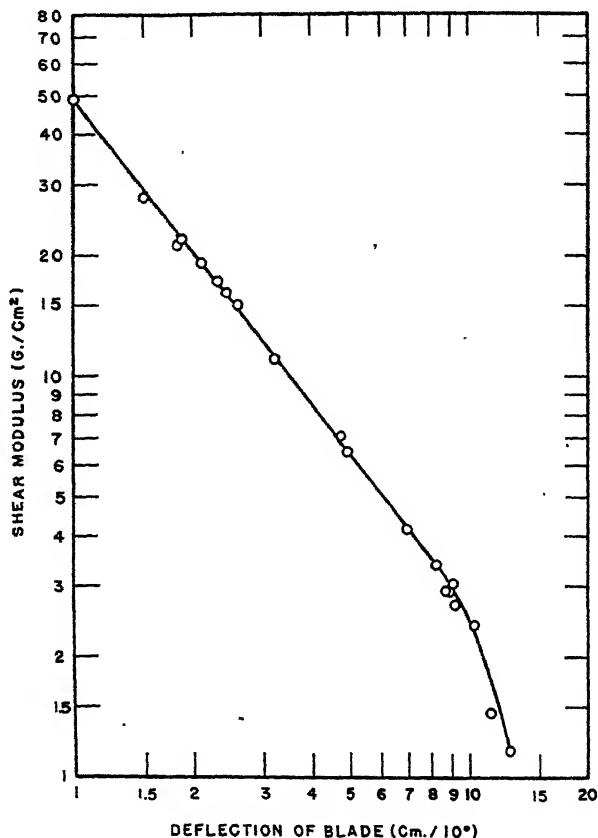


FIG. 1

Deflection of Blade Used in Rigiditymeter as a Function of Shear Modulus of Various Gels

sagged 0.135 cm./cm. in 2 minutes, 0.185 in 22 hours, 0.204 in 72 hours, 0.213 in 120 hours, and 0.224 in 192 hours. Theoretical is 0.227 cm./cm. Similar results were noted with other gels.

The effect of pH on the modulus of rigidity of 65% sucrose gels containing 0.70% pectin is illustrated in Fig. 3. There is an upper limit of pH at which pectin will form a gel, as reported by previous investigators

(14, 22, 34, 37, 38). This upper limit can be changed only slightly by changing the concentration of pectin or by changing its molecular weight as shown in Fig. 4, which is a plot of moduli *vs.* pH at a pectin concentration of 0.35%. The upper limit is decreased markedly by decrease in the methoxyl content of the pectin used, as shown in Figs. 3 and 4, and by the work of Hinton (22). Baker and Goodwin observed a minimum

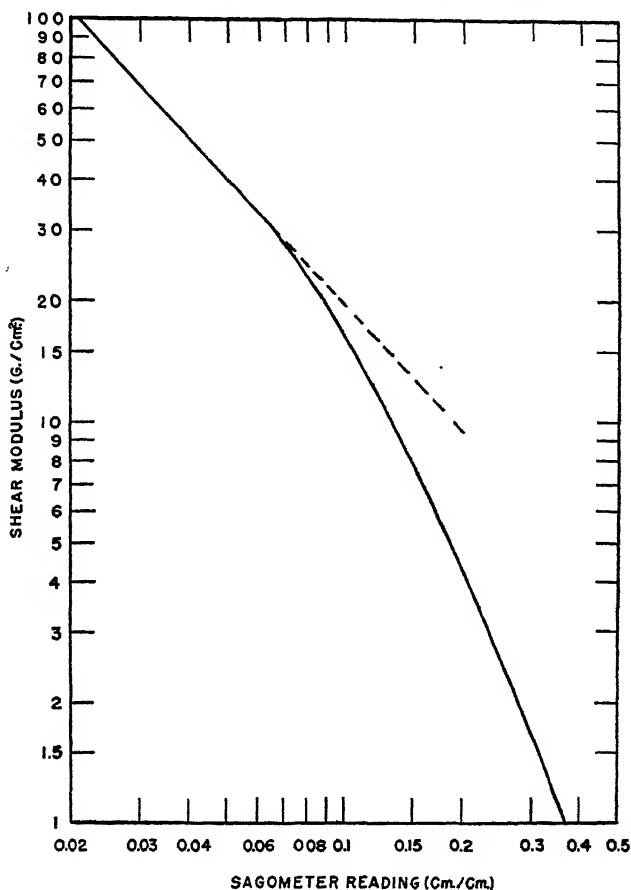


FIG. 2

Depression of Gels in a Period of 2 Minutes as a Function of the Shear Modulus

initial pH requirement at about 7% methoxyl. Considering the high ash content of their pectins, it is believed that some polyvalent cations were present which permitted gelation at the higher pH values with pectins which had methoxyl contents below 7%.

Examination of the molecular weights given in Table I and the gel strengths given in Figs. 3 and 4 indicate that gel strength is strongly

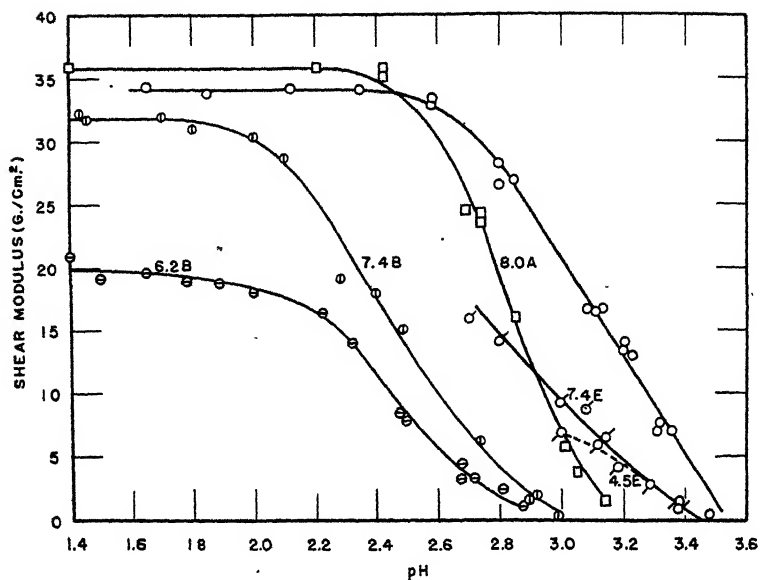


FIG. 3

Effect of Methoxyl Content of Pectinic Acids at 0.35% Concentration  
on the Shear Modulus vs. Gel pH Curves

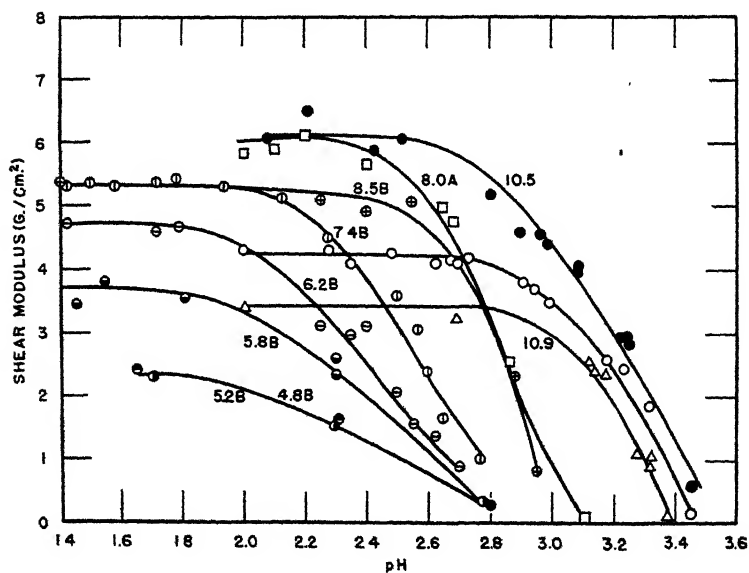


FIG. 4

Effect of Methoxyl Content of Pectinic Acids at 0.7% Concentration  
on the Shear Modulus vs. Gel pH Curves

influenced by change in molecular weight. Speiser and Eddy (24) found that gel strength could be correlated with weight-average molecular weight of pectin nitrates derived from the pectin used in their gel study. The data presented here are not so definite. With pectins of the same methoxyl content and from the same source, no choice may be made between weight-average or number-average molecular weights. If comparison of pectins from different sources or of different methoxyl contents is made, then the gel strength seems to vary more directly with the number-average molecular weight. The exceptions to these statements are presented by the enzymatically de-esterified pectinic acids. They form much weaker gels than would be expected either from weight- or number-average molecular weight. This will be discussed further.

Decreasing the methoxyl content influences the characteristics of the gels formed near the upper pH limit. Table II illustrates change in sago-

TABLE II

*Unit Compression Values as Influenced by pH at a Constant Modulus of Rigidity*

Number	2.2	2.50	pH 2.75	3.90	3.05
At $E_s = 1 \text{ g./cm.}^2$					
6.4B	.375	—	.485	—	—
7.2B	.375	.390	.440	.490	—
10.1	.375	.375	—	—	.375
At $E_s = 3 \text{ g./cm.}^2$					
6.4B	.230	.260	.310	—	—
8.0A	.230	.230	—	—	.265
4.5E	—	—	.235	—	.280
7.4E	—	—	.230	—	.240

meter readings at constant rigidometer reading at different pH values of gels prepared with various pectins. It will be noted that gels containing partly de-esterified pectins tend to sag more rapidly than those prepared from the untreated pectin. This difference can be eliminated by decreasing the pH at which the gels are prepared, as indicated in Fig. 4.

Although sagometer readings increase with gels prepared from partly de-esterified pectins at higher pH values, Fig. 5 shows that the elastic limit is not decreased in the same way. The figure is a plot of readings with the Tarr-Baker tester *vs.* shear moduli and indicates that the rate of settling of the gels prepared near the maximum pH values is sufficiently different to change the calibration of the sagometer when a 2-minute period of measurement is used.

Table III shows the influence of calcium added to gels prepared with pectin 7.4B at different pH values. The untreated pectin 10.1 acted simi-

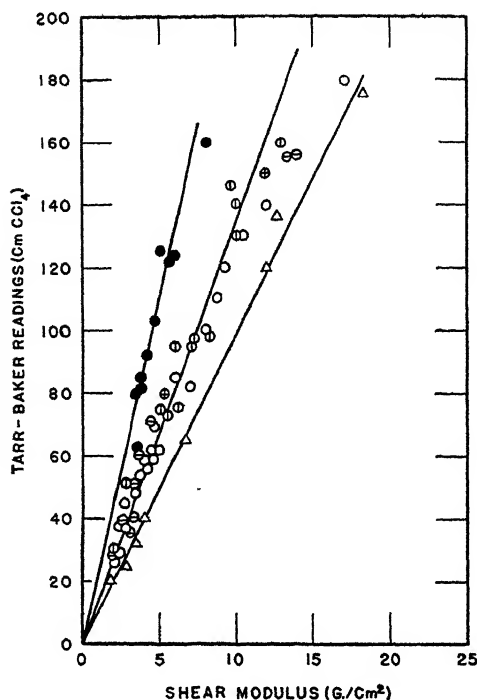


FIG. 5

Plot of Tarr-Baker Readings Against Shear Moduli of Gels (●, No. 10.5; Δ, No. 10.9; ○, No. 10.1; ⊙, No. 7.4B; ⊗, No. 6.2B)

TABLE III

*Effect of Calcium Ion on the Shear Modulus (g./cm.<sup>2</sup> of Gels Prepared with Pectinic Acid 7.4B)*

pH	mg. Ca/g. pectinic acid				
	0	5	10	20	40
1.9	30	—	33	33	31
2.7	6.5	15	22	28	28
3.1	0	5.6	5.6	24	21

larly with calcium at the higher pH values, which is expected from perusal of results already in the literature (22, 37, 39). Calcium ion also removed the difference between the sagometer and rigidometer readings noted in Table II.

### DISCUSSION

The data that have been given show several interesting effects of removal of methoxyl groups on the properties of high-solids gels. The maximum pH at which a gel can form decreases with decreasing methoxyl

content. Near the maximum pH the sag of the gels prepared from partly de-esterified pectinic acids is greater than with untreated pectin at the same shear modulus. The difference in the character of the gels can be removed by decreasing the pH or by addition of calcium ion.

These observations can be explained by a few refinements of the theory of pectin gel structure that have been developing from the ideas originally expressed by Fremy (40). The sucrose, or other similar added agent, decreases the solubility of the pectin, causing formation of a fibrillar network. These agents may also act as bridges across pectin molecules further strengthening the gel structure (41). For the most part, the water and sucrose are probably held to the fibrils without entering directly into the framework (42). This assumption appears reasonable, inasmuch as glycerol and sucrose form gels of about the same strengths, at equal weight concentrations, despite the marked difference in size of the molecules (32).

Olsen (21) proposed that added acid served to decrease the negative charge on the pectinic acid, permitting closer contact between the molecules. Hinton (37) modified this proposal further by pointing out that fewer carboxyl groups need be ionized in partly de-esterified pectins to prevent gelation and to require a lower pH before gelation occurs. He did not consider the forces that may be acting between the molecules but based his arguments on the solubility of pectin and its degree of dissociation, both of which he measured to prove his point tenable. This hypothesis offers an explanation for the maximum pH effect noted but is insufficient to account for the different properties of the gels near the maximum pH and for the difference in time or temperature of set.

To offer an explanation for the properties of the gels, it appears necessary to make assumptions concerning the types of forces operating between the pectinic acid molecules constituting the gel network. Schneider and Bock (43) proposed that carboxyl groups were the centers of crystallization in the gel structure. Meyer (44) disagreed with that proposal and, indeed, Hinton's evidence that pectin with 13.5% methoxyl content forms strong gels is argument against it (22). In this case about 5% of the carboxyl groups are available for bonding if it is assumed that there is 83% uronic acid anhydride in the samples of pectin used by him. Although the centers of crystallization may be the methyl ester groups (44), the forces of attraction between them are probably van der Waals' forces and are very weak. They may be supplemented, however, by hydrogen bonding between the hydroxyl groups and, possibly, by water and sucrose bridges (41). This would explain the findings of Hinton satisfactorily. It will also explain why the enzymatically de-esterified pectins have about the same maximum pH as the untreated pectin. If it is assumed that the enzyme acts on adjacent ester groups in the molecule (25) or in a non-

random manner (41), the portions not acted upon would have properties like the untreated pectin. If gel networks were built from those portions of the chains they would be weaker, despite the high molecular weight of the pectin, since fewer centers of crystallization are available and the gel structure could not be so uniform.

If a sufficient number of ionized carboxyl groups are available, the repulsive forces between them overcome the aggregative tendencies of the methyl ester, alcohol groups, and unionized carboxyl groups. If the pH is lowered to the point that gels will barely form, the repulsive forces are overcome but they may be sufficiently strong to require the pectin molecules to be in certain preferred positions before the interaction forces are effective. This assumption would explain the time delay noted before gelation occurs with the partly de-esterified pectins. The sag characteristics of such gels in which many of the carboxyl groups are free to rotate should be somewhat different in showing greater elasticity (44) than gels prepared from high-methoxyl pectins, which appears to be true at pH values near the maximum where the carboxyl groups are less likely to be involved in hydrogen bonding.

As the pH is decreased further, the carboxyl groups contribute materially to the attractive forces between the pectin molecules. Hydrogen bonding between the carboxyls would occur (24), accounting for the strong gels prepared with samples 6.2*B* and 7.4*B*. Theoretically, this would require that there be no maximum in the strength-*vs.*-pH curves unless the anion of the added acid interferes with hydrogen bonding between pectinic acid molecules.

Another way to cause the carboxyl groups to enter into the gel structure is to add polyvalent cations. This technique has been used to prepare low-methoxyl, low-solids gels (13, 14, 15, 16) and is effective with high-solids gels as well (22). Säverborn (32) used the complex hexamminocobalt ion for this purpose and has found it very effective. In these cases ionic bonds between the carboxyl groups and the cations are formed and it seems probable that such gels would be stronger than those depending upon hydrogen bonds and van der Waals' forces. Säverborn's (32) results verify that assumption. It is believed that some coagulation or presetting occurred with calcium ion as used in the experiments reported in Table II which prevented attainment of the maximum possible gel strength. Otherwise, the calcium gels should have been stronger in all cases than the ones depending only on hydrogen bonding.

The pH effects noted in this paper can be explained qualitatively by assuming that, first, the repulsive forces of the ionized carboxyl groups must be suppressed before unionized carboxyl and alcohol groups are close to similar groups of other molecules in sufficiently large numbers to form a stable structure. And second, if the suppression is sufficient,

that most of the carboxyl groups are available for hydrogen bonding between chains.

Some time ago (18) it was noted that polymetaphosphates and polyphosphates decreased the viscosity of pectin solutions to minimal values. It was believed that this depression was due to a reduction in the charge effects of the pectin and to sequestering of polyvalent cations which might react with it. This has since been confirmed (27). It seemed that such agents could be added to pectin solutions, the viscosity of the solutions determined, and a simple relationship to jelly grade obtained. Preliminary work on commercial pectins was favorable, but when various extraction conditions were used, the relationship did not hold. From the data presented here, the reason appears to be that the modulus of rigidity varies more directly with the number-average molecular weight than with the molecular weight measured by viscosity and changing conditions of extraction probably changes the shape of the molecular weight distribution curve.

Säverborn (32) noted a high-molecular weight sugar-beet pectin which formed only weak gels. This pectin had a high non-uronide content which may have been attached through side chains which would hinder the interaction effects emphasized above.

The high gel strength obtained with pectins that have low number-average molecular weights may be due to the extended chain structure (26, 32). With molecules 1000 Å. long, the concentration need be only 0.02% to cause overlapping of the spheres of revolution made by the macromolecules in solution. At the concentrations used in preparing gels, it is conceivable that every pectin molecule could take part in the structure.

The shape of the rigidity-*vs.*-pH curves is somewhat similar to those obtained by Lampitt and Money (23) and by Olsen (21) when lower pour-temperatures were used. Other workers have reported maxima or optima at various pH values (14, 22, 24, 34, 38). In one of these cases (22) the curve presented to show a maximum at pH 2 could be redrawn to remove the maximum without increasing the average deviation of the experimental points from the curve. The importance of presetting has been well established (21, 45). The pour temperature and the amount of setting before stirring has ceased are such important factors that the shape of the curves obtained with the untreated pectins below pH 2.6 is believed to be characteristic of the method used and not of the pectin. For the partly de-esterified pectins, the shape is more nearly characteristic of the pectin, since the setting time is fairly long and presetting does not occur immediately after the gel mixture has been stirred with the acid. Pour temperature, however, is still a factor and will receive further consideration.



It is interesting that the assumption of a value of Poisson's ratio of 0.5 appears to be justified when unit compression values with a sagometer are 0.06 or less. This value for the ratio is the same as that found for gelatin gels (46). The deviation at greater unit compressions was shown to be due, in part, to the fact that measurements of sag were made before equilibrium was reached and possibly due, in part, to a change in the value of Poisson's ratio likely to be obtained at greater deformations.

The value of 0.235 for the unit compression used as the standard of firmness by Cox and Higby (33) yields a value of about 3 g./cm.<sup>2</sup> for the shear modulus. It might be well for the industry to consider some such standard value with a standard procedure, in order to establish objective standards by which pectin may be sold. From the work presented here, a more reliable measurement would result if a slightly stiffer gel were chosen for the standard. A value of 4 g./cm.<sup>2</sup> would be more desirable.

The merits of the three gel testers reported on for fundamental and practical work may be compared on the basis of the data presented. The rigidometer has the advantage that gel strengths can be measured in absolute units. A simplified type that could be readily used in routine work can be easily constructed. The sagometer is simple to operate but under certain conditions the calibration curves may be different for slow-setting pectins. For simplicity of operation, glasses of the same heights must be used. The Tarr-Baker apparatus is more time-consuming in operation. It could be made nearly automatic in operation but this refinement may not be worthwhile.

#### ACKNOWLEDGMENT

The authors are indebted to A. D. Shepherd for many of the samples used, to J.R. Hoffman and J. C. Jacobsen for machining the gel testers, to H. A. Swenson for the analyses and to T. M. Shaw for many valuable suggestions.

#### SUMMARY

The maximum pH at which high-solids pectin gels can form, decreases with decreasing-methoxyl content. It is about 3.5 for purified pectins containing 10–11% methoxyl and about 2.9 for pectins containing around 5% methoxyl, providing alkali or, possibly, acid is used as the catalyst.

Pectins de-esterified *in situ* by citrus pectinesterase form gels at maximum pH values near those for untreated pectins.

The pH maximum is not markedly influenced by molecular weight or concentration of the pectin.

No optimum pH value was observed in the moduli-*vs.*-pH curves.

The modulus of rigidity of pectin gels is related to the molecular weight of the pectin.

Measurement of the moduli of rigidity is rapid, reliable, and appears to be amenable to use in industrial work.

The modulus of elasticity in compression can be related to that in shear if a Poisson ratio of 0.5 is assumed when small deformations are observed.

## REFERENCES

1. VAUQUELIN, *Ann. chim.* **5**, 92 (1790).
2. JOSEPH, G. H., *U. S. Patent* 2,061,158 (1938).
3. COLE, G. M., AND COX, R. E., *U. S. Patent* 2,109,792 (1938).
4. COX, R. E., *U. S. Patent* 2,133,273 (1938).
5. MACDOWELL, R. H., *Br. Patent* 541,528 (1941).
6. PLATT, W. C., *U. S. Patent* 2,020,572 (1929).
7. OLSEN, A. G., STUEWER, R. F., FEHLBERG, E. R., AND BEACH, N. M., *Ind. Eng. Chem.* **31**, 1015 (1939).
8. MCCREADY, R. M., OWENS, H. S., AND MACLAY, W. D., *Food Industries* **16**, 794 (1944).
9. MACDOWELL, R. H., *Br. Patent* 555,842 (1943).
10. OLSEN, A. G., AND STUEWER, R. F., *U. S. Patent* 2,132,577 (1938).
11. BAKER, G. L., AND GOODWIN, M., *U. S. Patent* 2,233,574 (1941).
12. HILLS, C. H., WHITE, J. W., AND BAKER, G. L., *Proc. Inst. Food Tech.* **1942**, 47-58.
13. KAUFMAN, C. W., FEHLBERG, C. R., AND OLSEN, A. G. *Food Industries* **141**, 1257 (1942); **15**, 158 (1943).
14. BAKER, G. L., AND GOODWIN, M. W., *Univ. Del. Agr. Exp. Sta. Bull.* **234** (1941); **246** (1944).
15. MCCREADY, R. M., OWENS, H. S., AND MACLAY, W. D., *Food Industries* **16**, 906 (1944).
16. POLLARI, V. E., MURRAY, W. G., AND BAKER, G. L., *Fruit Products* **25**, 6 (1945).
17. BAIER, W. E., AND WILSON, C. W., *Ind. Eng. Chem.* **33**, 287 (1941).
18. OWENS, H. S., MCCREADY, R. M., AND MACLAY, W. D., *Ind. Eng. Chem.* **36**, 936 (1944).
19. MCCREADY, R. M., OWENS, H. S., AND MACLAY, W. D., *Science* **97**, 428 (1943).
20. BAIER, W., AND MANCHESTER, T. C., *Food Industries* **15**, 794 (1943).
21. OLSEN, A. G., *J. Phys. Chem.* **38**, 919 (1934).
22. HINTON, C. L., *Fruit Pectins*. 1st Am. Ed. Chemical Pub. Co. (1940).
23. LAMPITT, L. H., AND MONEY, R. W., *J. Soc. Chem. Ind.* **56**, 290T (1937); **58**, 29T (1939).
24. SPEISER, R., AND EDDY, C. H., *J. Am. Chem. Soc.* **68**, 287 (1946).
25. SCHULTZ, T. H., LOTZKAR, H., OWENS, H. S., AND MACLAY, W. D., *J. Phys. Chem.* **49**, 554 (1945).
26. OWENS, H. S., LOTZKAR, H., SCHULTZ, T. H., AND MACLAY, W. D., *J. Am. Chem. Soc.* In press.
27. LOTZKAR, H., SCHULTZ, T. H., OWENS, H. S., AND MACLAY, W. D., *J. Phys. Chem.* **50**, 200 (1946).
28. OWENS, H. S., LOTZKAR, H., MERRILL, R. C., AND PETERSON, M., *J. Am. Chem. Soc.* **66**, 1178 (1944).
29. BULL, H. B., *J. Biol. Chem.* **137**, 143 (1941).
30. POOLE, H. J., *Trans. Faraday Soc.* **21**, 114 (1925).
31. BRIMHALL, B., AND HIXSON, R. M., *Ind. Eng. Chem., Anal. Ed.* **11**, 358 (1939).
32. SÄVERBORN, S., Contribution to the Knowledge of the Acid Polyuronides. Dissertation, Uppsala (1945).

33. COX, R. E., AND HIGBY, R. H., *Food Industries* **16**, 441 (1944).
34. TARR, L. W., *Univ. Del. Agr. Exp. Sta. Bull.* **142** (1926).
35. CHREE, C., *Trans. Cambridge Phil. Soc.* **15**, 313 (1892).
36. TIMOSHENKO, S., *Theory of Elasticity*. McGraw-Hill Book Co., Inc., New York (1934). P. 217 presents a derivation of the stretching of a beam by its own weight; p. 10 gives the formula relating shear and compression moduli.
37. HINTON, C. L., *Biochem. J.* **34**, 1211 (1940).
38. ECKART, H., AND GYALÖKAY, A. V., *Konservenindustrie* **14**, 37 (1927).
39. HALLIDAY, E. G., AND BAILEY, G. R., *Ind. Eng. Chem.* **16**, 595 (1924).
40. FREMY, E., *J. pharm. chim.* **3**, 2 (1847).
41. HILLS, C. H., MOTTERN, H. H., NUTTING, G. C., AND SPEISER, R., Sept. Meeting Am. Chem. Soc., New York (1944).
42. SUCHARIPA, R., *J. Assoc. Off. Agr. Chem.* **7**, 57 (1923).
43. SCHNEIDER, G. G., AND BOCK, H., *Ber.* **71**, 1353 (1938).
44. MEYER, K. H., *Natural and Synthetic High Polymers*. Interscience Pub., Inc., **4**, 372 (1942).
45. COLE, G. M., COX, R. E., AND JOSEPH, G. H., *Food Industries* **2**, 219 (1930).
46. SHEPPARD, S. E., SWEET, S. S., AND BENEDICT, A. J., *J. Am. Chem. Soc.* **44**, 1857 (1922).

# ELASTICITY, PLASTICITY AND FINE STRUCTURE OF PLANT CELL WALLS

Otto Treitel

*From the Botanical Laboratory, University of Pennsylvania,  
Philadelphia, Pa.*

*Received May 31, 1946*

I. Introduction.....	327
II. Method.....	328
III. Measurements of Elasticity and Plasticity.....	329
1. Definitions.....	330
2. Longitudinal Direction.....	330
3. Transverse Direction.....	337
4. Forces Acting on the Stem of a Plant When the Stem is Ruptured.....	340
IV. Equations of Elasticity and Plasticity Curves.....	342
1. Rubber Elasticity.....	342
(a) Mooney's Theory.....	342
(b) Wall's Theory.....	343
(c) Structure of Rubber, Wool and Protoplasm.....	346
2. Metallic Elasticity.....	348
(a) Longitudinal.....	348
(b) Transverse.....	348
3. Equations of Elasticity and Plasticity Curves in the Case of Plant Tissues.....	349
V. Influence of Tension, Humidity and Temperature on the Value of Young's Modulus of Cylindrical Plant Tissues.....	356
(a) Influence of Tension on the Value of Young's Modulus.....	357
(b) Influence of Humidity on the Value of Young's Modulus.....	358
(c) Influence of Temperature on the Value of Young's Modulus.....	359
(d) Change of Structure Produced by Change of Young's Modulus.....	360
VI. Relation between Tension and Temperature for Plant Tissues and Sub- microscopic Structure in Cell Walls of Higher Plants.....	361
VII. Summary.....	366
References.....	368

## I. INTRODUCTION

Experiments carried out (25) on rhizomes of *Equisetum fluviatile* revealed a striking similarity between the elastic behavior of this plant tissue and rubber. In certain other plant tissues there is a slow change from an S-shaped stress-strain curve to a straight line, that is, from rubber-like elasticity to metallic elasticity (26). The laws governing the elastic behavior of rubber and metals may be applied to plant tissues, or at least to their cell walls. Application of the laws of metallic elasticity to ex-

tensible elastic plant tissues reveals a linear relationship between Young's modulus of elasticity and the specific gravity of these tissues (27). The properties of rubber are especially important in a study of extensible elastic plant tissues because these substances have small Young's moduli of elasticity.

Investigation of rubber is very important for understanding the elasticity of many biological materials, such as gelatin, glue, wool, silk and muscle (12, p. 305).

A study of the elastic and plastic deformations of substances makes possible a better understanding of their structure. Thus, a study of deformations of plant tissues indicates the structure of cell walls.

The structure of cell walls is microscopic, submicroscopic or amicroscopic. The structure is microscopic when determined by using the microscope, submicroscopic when determined by using the electron microscope or the X-ray diffraction picture, and amicroscopic when it is only determinable theoretically.

The importance of the relation of elasticity and structure is found in a remark of Szent-Györgyi: "It is evident that muscle function must be explained by structure. The elementary process of contraction and relaxation takes place in molecular or micellar dimensions" (21).

The following experiments were carried out from July 1945 until March 1946 at the University of Michigan Biological Station and at the Botanical Laboratory of the University of Pennsylvania. I wish to express my appreciation to Dr. A. H. Stockard, Director of the Station, and to Dr. W. Seifriz, Professor of Botany at the University of Pennsylvania, for the use of laboratory facilities.

## II. METHOD

Most cells in cylindrical plant tissues, especially in the woody state, have the form of long cylinders, and by far the greater proportion are arranged parallel to the axis of the cylindrical tissue (27). Stems of wood will, therefore, require less thrust to flatten the cells parallel to the axis across the diameter of the stem than to compress them longitudinally. Hence, for cylindrical plant tissues there are two moduli of elasticity, one for the longitudinal and one for the transverse direction. These two moduli must be measured to understand the elastic properties of cylindrical plant tissues.

The device used in the experiments reported here is composed of two parts. The first part, for measuring the longitudinal modulus of elasticity is similar to the device used by me in 1942, 1943 and 1944 (25, 26, 27). The second part is so constructed that the transverse modulus of elasticity may be measured. In addition, plasticity in this direction may also be measured.

For measuring the properties of the plant tissue in the longitudinal direction, the tissue to be studied is held horizontally between two binding posts (Fig. 1). One end of the plant tissue is clamped in the first binding post, the other end, for convenience, passes through the hole of the second post and is clamped in a movable clamp. To avoid friction the movable clamp has two runners which slide on a glass plate. The movable clamp is connected to a pan and weights by a steel wire. Thus, strain and stress measurements can be made in the longitudinal direction.

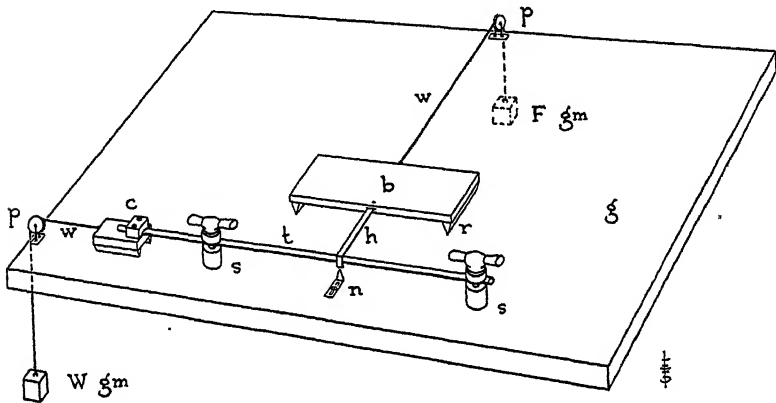


FIG. 1  
Device for Experiments

$p$ = pulley	$s$ = binding post
$w$ = steel wire	$n$ = indicator point
$h$ = copper hook	$t$ = cylindrical plant tissue
$b$ = sliding board on runners	$g$ = glass plate
$c$ = sliding clamp on runners	$r$ = runner

For measuring the elastic and plastic properties of the tissue in the transverse direction, the tissue horizontally held between the two posts is pulled aside at its center by a copper hook. The hook is connected to a board with two runners sliding on a glass plate. This board and a second pan with weights are connected by another steel wire. In this manner measurements of deflection and force can be made in a transverse direction.

### III. MEASUREMENTS OF ELASTICITY AND PLASTICITY

The following tissues were investigated: petioles of *Nymphaea*, rhizomes of *Equisetum fluviatile*, stems of *Brasenia schreberi*, woody roots of *Rhus glabra*, sclerenchymatous plates of rhizomes of *Pteris aquilina*, branches of *Salix* and, for comparison, bands of rayon and raw catgut.

### 1. Definitions

Elasticity is that property of a body by virtue of which it recovers its original size and shape after deformation.

Plasticity is that property of a body by virtue of which the body retains a permanent deformation.

### 2. Longitudinal Direction

The elastic properties of the plant tissues investigated in the longitudinal direction are found by constructing stress-strain curves. For obtaining these curves one measures stress and strain.

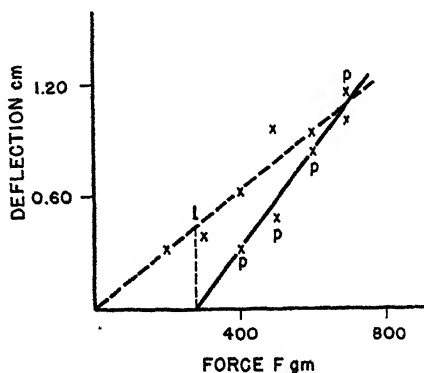


FIG. 2

Force-Deflection Curve of a Petiole of *Nymphaea odorata* 0.37 cm. Thick  
Elasticity curve-dashes, *l* = elastic limit  
Plasticity curve-solid line, *p* are experimental points of the plasticity curve

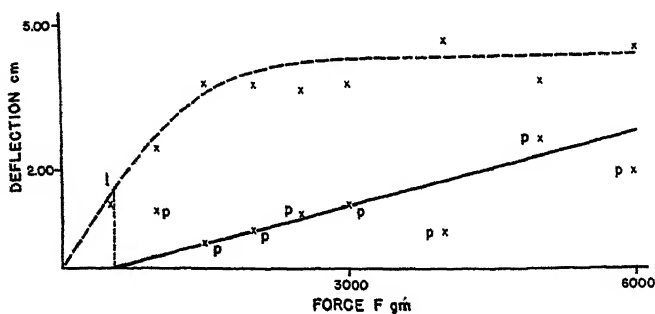


FIG. 3

Force-Deflection Curve of a Rhizome of *Equisetum fluviatile* 0.63 cm. Thick  
Elasticity curve-dashes, *l* = elastic limit  
Plasticity curve-solid line, *p* are experimental points of the plasticity curve

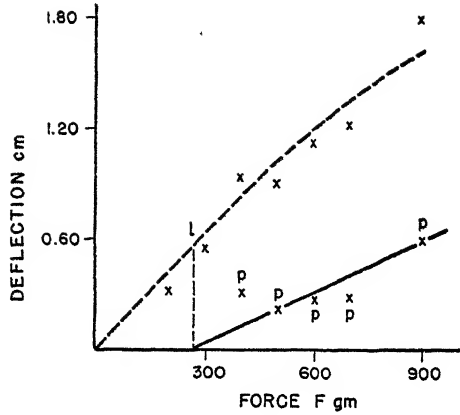


FIG. 4

Force-Deflection Curve of a Stem of *Braseniaschreberi* 0.29 cm. Thick

Elasticity curve-dashes, *l* = elastic limit

Plasticity curve-solid line, *p* are experimental points of the plasticity curve

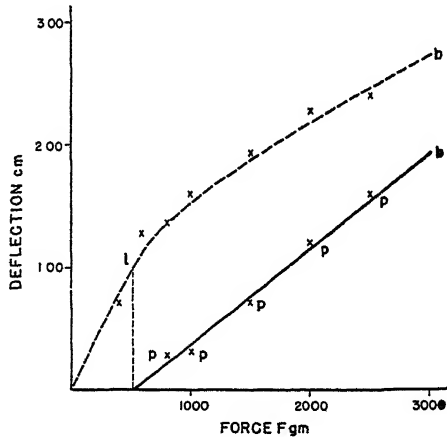


FIG. 5

Force-Deflection Curve of a Woody Root of *Rhus glabra* 0.38 cm. Thick

Elasticity curve-dashes, *l* = elastic limit, *b* = breaking point

Plasticity curve-solid line, *p* are experimental points of the plasticity curve,  
*b* = breaking point

The weight, of *W* g. (Fig. 1), acts as stress  $\sigma = \frac{w \cdot 980}{A'} \frac{\text{dynes}}{\text{cm}^2}$ , where  $A'$  cm.<sup>2</sup> is the solid area of the cross section of the cylindrical plant tissue. The corresponding strain of the plant tissue of *l* cm. length is strain  $\epsilon = e/l$ , where *e* cm. is the elongation produced by weight *W* g.

If we plot a curve with  $\epsilon$  as abscissa and  $\sigma$  as corresponding ordinate we get the longitudinal stress-strain curve.



A cylindrical plant tissue has metallic elasticity if the stress-strain curve is a straight line in the first or elastic part of the curve (Fig. 6). Here Hooke's law is valid.

A cylindrical plant tissue has rubber-like elasticity if the stress-strain curve is an S-shaped curve (Fig. 13). Then Young's modulus of elasticity =  $\frac{\text{stress}}{\text{strain}}$  at the elastic limit.

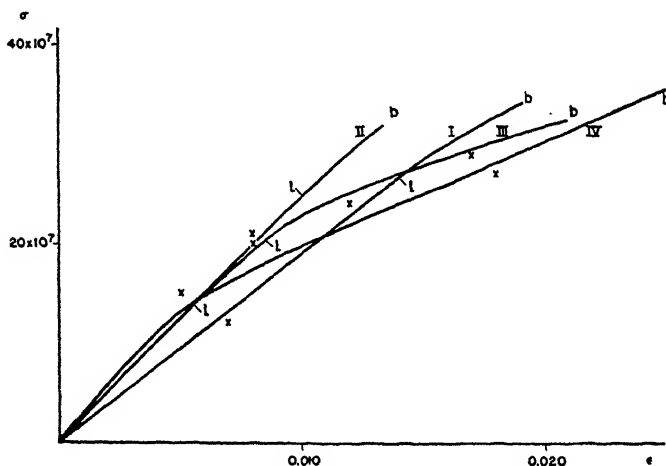


FIG. 6

Longitudinal Stress-Strain Curves of Branches of *Salix babylonica*

$\epsilon$  = strain

$\sigma$  = stress in dynes/cm.<sup>2</sup>

$l$  = elastic limit

$b$  = breaking point

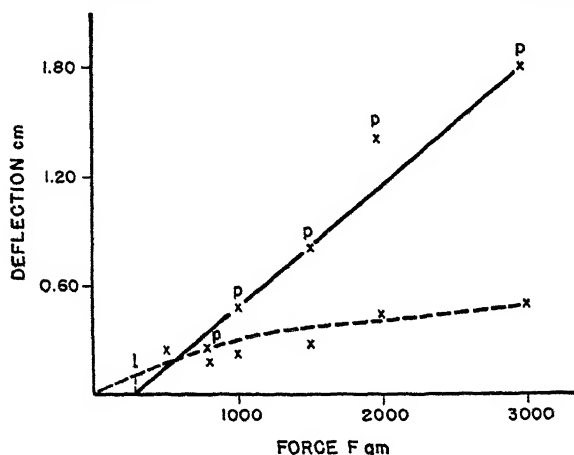


FIG. 7

Force-Deflection Curve of a Branch of *Salix lucida* 0.33 cm. Thick

Elasticity curve-dashes,  $l$  = elastic limit

Plasticity curve-solid line,  $p$  are experimental points of the plasticity curve

The elastic limit separates the elastic part of the stress-strain curve from the non-elastic part. In the elastic part of the curve the deformation completely disappears after the stress is removed; in the non-elastic part, the deformation does not fully disappear after the stress is removed.

Several general laws may be formulated from a study of the longitudinal elasticity (26, 27). Some of these laws were mentioned in the introduction; others are:

(a) Young's modulus of elasticity of plant tissues increases with increasing hardness.

(b) The Gough-Joule effect is to be observed for rubber, some animal tissues and rubber-like elastic plant tissues.

A consequence of (a) is that, in the case of a low Young's modulus, most cell walls are soft and, in the case of a large Young's modulus, most

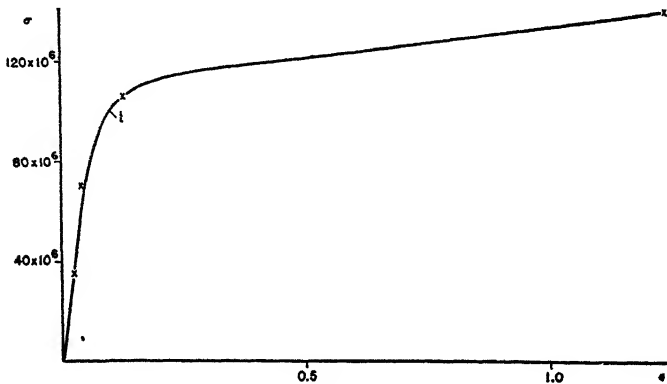


FIG. 8  
Longitudinal Stress-Strain Curve of a Band of Rayon

$\epsilon$  = strain

$\sigma$  = stress in dynes/cm.<sup>2</sup>

$l$  = elastic limit

cell walls are hard. This means that there is a relationship between the microscopic structure of plant tissues and Young's modulus.

To the longitudinal stress-strain curves constructed in 1942 and 1943 (25, 26) for tissues is now added the ascending parabolic stress-strain curve of a rayon band (Fig. 8). The parabolic stress-strain curve is characteristic for material which is slightly elastic and chiefly plastic (26). By using Fig. 8, we find that Young's modulus of elasticity for rayon is  $10 \times 10^8$  dynes/cm.<sup>2</sup> (see Table I in IV, 3).

The rubber-like S-shaped stress-strain curve of raw catgut (Fig. 10) gives a value of  $344 \times 10^8$  dynes/cm.<sup>2</sup> for Young's modulus of elasticity for this material.

The stress-strain curves of branches of *Salix babylonica* (Fig. 6) are straight lines in the elastic range. They are, therefore, examples of metallic

elasticity. To construct the curves, the cross section of the branches must be known. The willows are diffuse porous woods, the pores or vessels being scattered throughout the growth ring (20, p. 44). From the cross sections of branches of *Salix babylonica* the solid area of the cross section may be calculated. Then, from Fig. 6, Young's modulus of elasticity for branches of *Salix babylonica* is found to be  $233 \times 10^8$  dynes/cm.<sup>2</sup>. In all the foregoing determinations of elasticity of plant tissues the elasticity

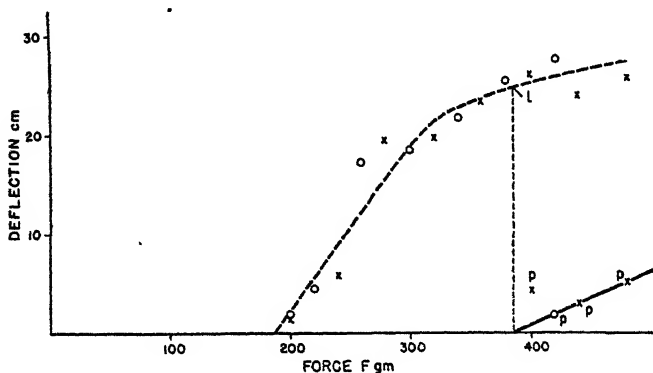


FIG. 9

Force-Deflection Average Curve of a Band of Rayon

Width of band 0.14 cm., height 0.02 cm.

Elasticity curve-dashes,  $l$  = elastic limit

Plasticity curve-solid line,  $p$  are experimental points of the plasticity curve

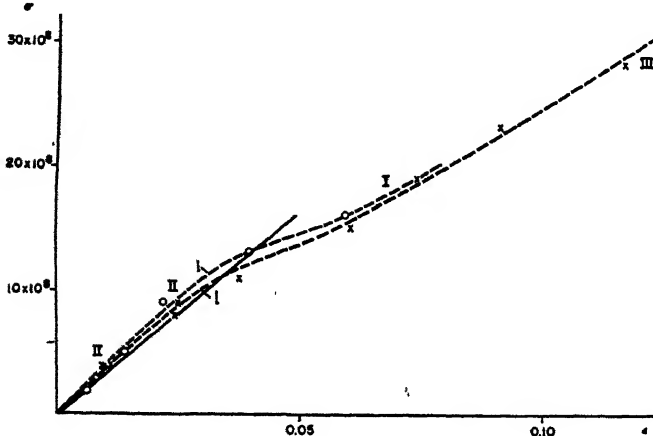


FIG. 10

Longitudinal Stress-Strain Curves of Raw Catgut

Experimental curves-dashes

$\epsilon$  = strain

Theoretical curve-solid line

$\sigma$  = stress in dynes/cm.<sup>2</sup>

$l$  = elastic limit

of the cell walls is measured. The protoplasm in the cells adds little or no elasticity (27).

Cellulose is the chief substance in the cell walls of higher plants. The structure of the cell wall is determined by the cellulose it contains (see VI). The importance of cellulose in the cell wall is understandable when it is known that mild chemical treatment of native cellulosic fibers does not affect the cellulose greatly, although it affects other substances in the fiber (7).

The stress-strain curves for cellulose fibers of ramie and cotton are almost straight (14, p. 248). They do not have a tail like the stress-strain curves of branches of *Salix babylonica* (Fig. 6). This means that fibers of ramie and cotton are not plastic but merely elastic. Young's moduli of elasticity for these fibers are very high. For fibers of ramie, Meyer and Lotmar (17) found Young's modulus of elasticity to be about  $6000 \times 10^8$  dynes/cm.<sup>2</sup>.

Meyer and Lotmar used an acoustic method for the measurement of Young's modulus of cellulosic fibers. The equation used for such measurements is  $v = \sqrt{\frac{E}{s}}$ , where  $v$  is velocity of sound,  $s$  is density and  $E$  is Young's modulus.

According to the acoustic method, the maximum amount of Young's modulus for cellulosic fibers of flax is  $11000 \times 10^8$  dynes/cm.<sup>2</sup>.

Meyer and Lotmar tried to compute this maximum amount on a theoretical basis. For the computation they assumed that cellulose in flax fibers is pure and well oriented. They used both the structural model of cellulose established by Meyer and Mark, and Raman spectra. The coincidence of experimental and theoretical values of Young's modulus for flax was good. This computation proves the correctness of the structural formula of cellulose. It proves that cellulose is composed of ring-shaped glucose units. This is an important result for the amicroscopic determination of the cell wall structure of higher plants, as regards cellulose, obtained by knowing the characteristics of elasticity for plant tissues.

Meyer and Lotmar's acoustic method for measuring Young's modulus of cellulosic fibers was improved by Ballou and Silverman (4) who used an electrical device for sound measurements in fibers.

Native cellulosic fibers consist chiefly of chain molecules of cellulose which are well oriented in fibrils. When natural cellulosic fibers are chemically treated rayon is produced. As a consequence of treatment we find a lack of organized structure with respect to the fibrils of native fibers. Besides, in rayon, the chain molecules of cellulose are shortened (7). The paraffin hydrocarbons have chain molecules of different lengths. We find the short chains in gases, the longer chains in liquids, and the

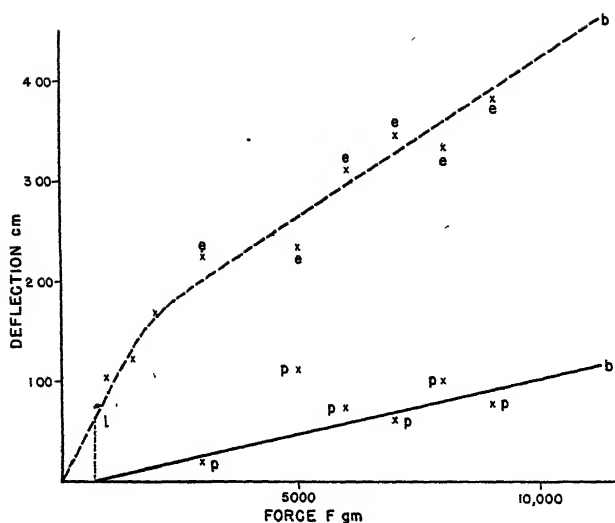


FIG. 11

Force-Deflection Curve of Raw Catgut. Thickness of sample 0.07 cm.  
 Elasticity curve-dashes, *e* are experimental points of the elasticity curve,  
*l* = elastic limit, *b* = breaking point  
 Plasticity curve-solid line, *p* are experimental points of the plasticity curve,  
*b* = breaking point

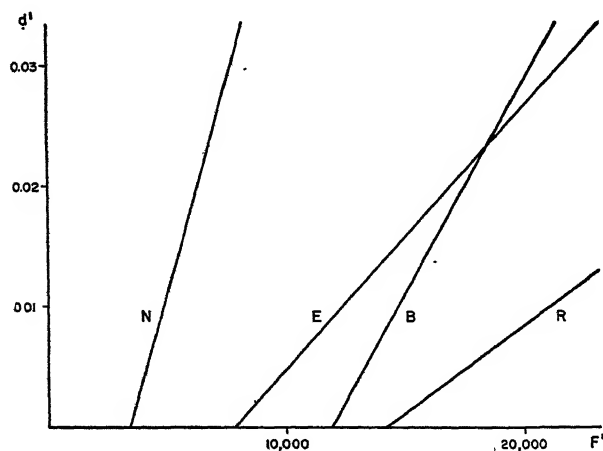


FIG. 12

Plasticity Curves in the  $(F', d')$  System

- N = plasticity curve for petioles of *Nymphaea odorata*
- E = plasticity curve for rhizomes of *Equisetum fluviatile*
- B = plasticity curve for stems of *Brasenia schreberi*
- R = plasticity curve for woody roots of *Rhus glabra*

longest chains in solids. Here the physical properties are determined by chain length (1, p. 357).

In a similar way, we understand that rayon, with short and poorly oriented chain molecules of cellulose, is only slightly elastic and very plastic. The native cellulosic fibers of ramie, cotton and flax with long, well oriented chain molecules of cellulose are very elastic and not plastic.

So again we find a relation between the physical properties of elasticity and plasticity and amicroscopic structure.

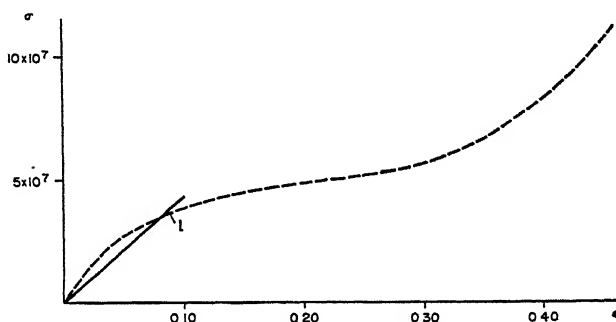


FIG. 13

Average Longitudinal Stress-Strain Curve of Rhizomes of *Equisetum fluviatile*

Experimental curve-dashes

Theoretical curve-solid line

$l$  = elastic limit

$\epsilon$  = strain

$\sigma$  = stress in dynes/cm.<sup>2</sup>

### 3. Transverse Direction

The elastic and plastic properties of the plant tissues investigated in the transverse direction are determined by constructing deflection-force curves. For obtaining these curves we must measure deflection and force.

The weight  $F$  g. (Fig. 1) acts as force. The corresponding deflection of the plant tissues of 21 cm. length is  $d$  cm., as the distance between the two binding posts (Fig. 1) is 2.1 cm.

For small forces,  $F$  g., we get deflections  $d$  cm. =  $e$  cm., which completely disappear when the force is removed.

For greater forces,  $F$  g., we get deflections which do not completely disappear when the force is removed. This deflection  $d$  cm. is composed of two parts, an elastic deflection  $e$  cm. and a plastic deflection  $p$  cm., therefore,  $d = e + p$ . By subtracting  $p$  cm. from  $d$  cm., both easily measured, one arrives at the value of  $e$  cm.:  $e = d - p$ .

Because of the "creep," or time effect, deflections must be measured when no visible change of deflection has been found for several minutes.

If we plot a curve with  $F$  g. as abscissae and  $e$  cm. as corresponding ordinates, we get the elasticity curve for transverse direction. The elas-

ticity curves for transverse direction of all tissues investigated are ascending curves whose initial parts are straight lines (Figs. 2, 3, 4, 5, 7, 9, 11). In all cases Hooke's law is valid. This is interesting because, in the longitudinal direction, elastic properties of plant tissues are determined by three kinds of stress-strain curves, ascending parabolic curves (petioles of *Nymphaea tuberosa*, rayon), S-shaped curves (stems of *Brasenia schreberi*, rhizomes of *Equisetum fluviatile*, catgut) and ascending curves the initial parts of which are straight lines (roots of *Rhus glabra*, sclerenchymatous plates of rhizomes of *Pteris aquilina*, branches of *Salix babylonica*) (25, 26, Figs. 6, 8, 10).

If we plot a curve with  $F$  g. as abscissae and  $p$  cm. as corresponding ordinates we get the plasticity curve for transverse direction. This is a straight line (Figs. 2, 3, 4, 5, 7, 9, 11). In the case of woody roots of *Rhus glabra* the straight line is obvious (Fig. 5). In the other cases the straight line is more or less probable.

Several elasticity and plasticity curves were constructed for every tissue investigated. The computations of the next section (see IV, 3) are based on all curves, not only on the figures of this article.

The plasticity curves always intersect the  $F$  axis at a point to the right of the origin. The ordinate of this point intersects the elastic curve at the elastic limit.

In transverse direction, for all tissues investigated, we find ascending elasticity curves and straight line plasticity curves.

The separation of elasticity and plasticity is readily determined in the transverse direction; in the longitudinal direction, however, the separation of elasticity and plasticity is difficult. Consequently, only stress-strain curves, the last part of which is the non-elastic range, were constructed.

It may thus be concluded that the elastic and plastic properties of cylindrical plant tissues differ in the longitudinal and transverse directions.

Plant tissue is anisotropic with respect to longitudinal and transverse direction. This is also true for metallic elasticity in both directions because the two moduli of elasticity are quite different (see IV, 3).

It is possible to assume that the structure of the cylindrical plant tissue is more solid in the lengthwise direction than in cross-section. Later we shall prove this conclusion. We shall find that the longitudinal modulus of elasticity is always much greater than the transverse modulus of elasticity (see IV, 3). Thus, we arrive at the conclusion that the structure of the cell walls of cylindrical plant tissues is determined by chain molecules of cellulose which are more or less oriented parallel to the axis of these tissues.

This result is to be expected because of the effect of thrust parallel and perpendicular to the axis (see II).

According to Sponsler and Dore (24, pp. 196, 197) cellulosic fibers of ramie, on absorption of water, usually show no swelling longitudinally but swell considerably in the lateral direction. Sponsler and Dore assume that the chain molecules of cellulose lie in the direction of the fiber. Since the linkages in the direction of the fiber length are by primary valences, there is no opportunity for water molecules to enter between the glucose units and no longitudinal swelling can occur. On the other hand, water molecules can be absorbed on the oxygens by the action of secondary valence forces. The spacing between the chain molecules, then, necessarily becomes wider to accommodate the water molecules, and lateral swelling occurs.

According to Meyer and Lotmar (17) the water molecules surround the OH groups, not the oxygens. But this does not change the conclusion about the direction of the cellulose molecules in fibers of ramie.

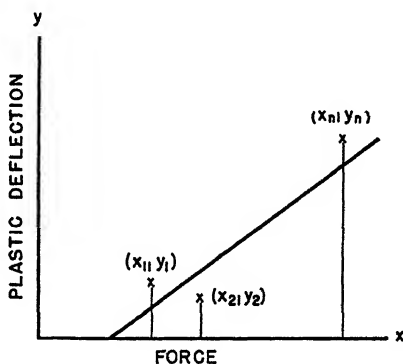


FIG. 14

Plastic Straight Line Determined by the Method of Least Squares

This result again substantiates our conclusion regarding cellulose molecules in cylindrical plant tissues.

As stated, the plasticity curve in the transverse direction is probably a straight line. The plasticity curves of tissues with a large Young's modulus of elasticity are difficultly determined because the plasticity in these cases is usually small (see IV, 3). Hence we determined the plastic straight lines in the case of raw catgut and of sclerenchymatous plates of rhizomes of *Pteris aquilina* by using the method of least squares.

In the case of the plastic straight line of raw catgut (Fig. 11) we may assume that the sum of the squares of deviations in the direction of the Y-axis (plastic deflection) will be a minimum (Fig. 14). This is equivalent to assuming that the X-measurements (force measurements) are exact, and that only the values of the dependent Y-variable (plastic deflection) are liable to error (32, pp. 238-240).



The equation of the plastic straight line is (Fig. 14)

$$y = a + bx \quad (1)$$

$(x_1, y_1), (x_2, y_2), \dots (x_n, y_n)$  are the coordinates of points which represent measurements of force and of plastic deflection. Then

$$\Sigma(y_n - y)^2$$

shall be a minimum.

A simple computation shows:

$$a = \frac{\Sigma x_n^2 \cdot \Sigma y_n - \Sigma x_n \cdot \Sigma x_n y_n}{n \cdot \Sigma x_n^2 - (\Sigma x_n)^2} = -0.08, \quad (2)$$

$$b = \frac{n \cdot \Sigma x_n y_n - \Sigma x_n \cdot \Sigma y_n}{n \cdot \Sigma x_n^2 - (\Sigma x_n)^2} = 0.115 \times 10^{-3}. \quad (3)$$

If (2) and (3) are substituted in (1), then the correct equation for the plastic curve in the case of raw catgut is obtained:

$$y = -0.08 + 0.115 \times 10^{-3}x.$$

This line is the one shown in Fig. 11.

One must remember that not all six points  $(x_n, y_n)$  have the same weight, and thus understand that we did not use the second point  $(x_2, y_2)$  in Fig. 11. In the case of the second point the points  $p$  and  $e$  are very close, and this probably is impossible.

The measurements in the transverse direction for sclerenchymatous plates of rhizomes of *Pteris aquilina* are to be used only if we assume different weights for all measurements. Under these conditions we might get a correct plastic straight line in this case.

#### 4. Forces Acting on the Stem of a Plant when the Stem is Ruptured

If we pick a shrub branch by pulling the branch sideways, then we have values of forces and deflections roughly similar to the values measured in our experiments on the transverse direction. But, for a complete analogy, the branch to be picked must be connected with the shrub at one end and entangled with other branches at the upper end. Such a branch corresponds to the tissue held horizontally between the two posts of our device. If we pick this branch by pushing it aside, we might then expect almost similar values of forces and deflections as those measured in our experiments across the diametral direction.

We might break petioles or stems in the open air or in water and we might break roots or rhizomes in the ground under conditions similar to those existing in the experiments on the transverse direction. The forces and deflections observed in all these cases can be found by using

the elasticity and plasticity curves for the transverse direction (Figs. 2, 3, 4, 5, 7, 9, 11). The general picture is always the same. We have ascending elasticity curves, for which Hooke's law is valid, and straight plasticity curves intersecting the  $F$ -axis to the right of the origin.

There must be a general law in nature by which sideward breaking of plants always proceeds in the same way if an increasing force acts perpendicularly to the plant.

It has been shown (III, 2) that the structure of cylindrical plant tissues is more solid longitudinally than transversely. Hence, it seems reasonable to suppose that, because of identical structure, there is a general law governing sideward breakage of plants.

The force acting on all living substance is the force of gravity. It might be that, under the influence of geotropism, the structure of stems became more solid in their lengthwise direction. The branches, petioles and roots are so influenced from the stem that again the same structural arrangement is formed.

According to the theory of rubber elasticity there are S-shaped stress-strain curves in the longitudinal direction. It is particularly interesting to note the theoretical prediction that rubber should obey Hooke's law for shear in the transverse direction (29). This is a result similar to that found experimentally while investigating the elasticity of plant tissues in the transverse direction.

We may consider a horizontal root of *Rhus glabra*, 4 mm. thick, partly dug out and fixed in the ground at both ends. According to Fig. 5 the process of breaking by pushing this to the side with our hands might proceed as follows: Our hands push with increasing force, The deflection in the transverse direction increases until we reach the point of elastic limit with a force of 520 g. and a deflection of 1 cm. Up to this point the root always snaps back to the original position if released. If the force exerted by our hands increases beyond 520 g., the deflection is composed of an elastic component and a plastic one. This deflection disappears only partly when the root is released and the remaining deflection is plastic. The deflection which disappears is elastic. If the force of our hands increases still more, we reach the breaking point for the root with a force of about 3 kg. At the breaking point the deflection is composed of the elastic component, 2.7 cm., and the plastic component, 2 cm. Beyond the elastic limit the elastic deflection is at first much greater than the plastic deflection; at the breaking point the plastic deflection is nearly equal to the elastic deflection. The plastic deflection then becomes so great that, at the rupture point of the root, the force of rupture, 3 kg., becomes greater than the force of cohesion, and the root must then tear.

Because of some importance to surgery let us consider the conditions for breaking raw catgut 0.7 mm. thick.

According to Fig. 11, the process of breaking for raw catgut held horizontally between two posts, is similar to that for cylindrical plant tissues. The force at the elastic limit is 700 g. and the deflection at this limit is 6 mm. In the case of catgut at the breaking point, the plastic deflection is one-fourth of the elastic deflection. The force at the breaking point is about 11 kg., the elastic deflection is 4.6 cm., and the plastic deflection is 1.2 cm.

#### IV. EQUATIONS OF ELASTICITY AND PLASTICITY CURVES

We found that different cylindrical plant tissues investigated longitudinally have stress-strain curves which slowly change from S-shaped curves to straight lines with a tail (26). Hence, the elastic behavior of plant tissues is between two limits. The lower limit is given by the elastic behavior of rubber, the upper limit by the elastic behavior of metals.

##### 1. Rubber Elasticity

The classical theory of elasticity is based on the concept of continuum. By using this theory Mooney was able to solve the problem of the elasticity of rubber to a certain extent (18). Mooney's conclusion is that the S-shaped stress-strain curve of rubber requires no molecular peculiarities of rubber for its explanation. Indeed, we shall see that the equations derived by Mooney are very useful for elastic plant tissues.

A more thorough study of elasticity of rubber is based on the molecular structure of rubber. This study shows that there is an important temperature dependency for elastic deformations of rubber. Mooney could not find this dependency using the classical theory of elasticity. In addition, the structural theory of rubber elasticity is important for understanding the structure of living tissues. To be logical we will first consider Mooney's non-molecular theory and then treat of Wall's molecular theory. Other theories exist which are related only to the molecular structure of rubber but Wall (29) tried to correlate his theory with the macroscopic theory of Mooney. This application is important for plant tissues.

(a) *Mooney's Theory.* Mooney used the following experimental facts for deriving his theory. A cylindrical sample of rubber is stretched. The resulting curve is not a straight line. If the sample is sheared, Hooke's law is valid.

Deformations of rubber are produced without any appreciable change in volume, that is, rubber behaves like a liquid.

Now Mooney computes an expression for work,  $W$ , done by deforming a rubber cylinder. He finds:

$$W = \frac{G}{4} \left[ \lambda^2 + \frac{1}{\lambda^2} + 2 \cdot \left( \lambda + \frac{1}{\lambda} \right) - 6 \right] + \frac{H}{4} \left[ \lambda^2 - \frac{1}{\lambda^2} - 2 \left( \lambda - \frac{1}{\lambda} \right) \right] \\ + \left[ \frac{G}{4} \left( \lambda + \frac{1}{\lambda} \right) - \frac{H}{4} \left( \lambda - \frac{1}{\lambda} \right) \right] \gamma^2,$$

where  $G$  and  $H$  are constants of the material,  $\lambda$  is the ratio of the final length of the rubber cylinder to the initial length, and  $\gamma$  is shear in the plane normal to the direction of the stretch  $\lambda$ .

For shearing we have only to set  $\lambda = 1$  and we get

$$W = \left[ \frac{G}{4} \cdot 2 - \frac{H}{4} \cdot 0 \right] \gamma^2 = \frac{1}{2} G \gamma^2;$$

then, by differentiating

$$\frac{dW}{d\gamma} = G\gamma,$$

or

$$\tau = G\gamma,$$

or shearing stress = modulus of rigidity  $\times$  shear (Hooke's law). For stretching we have only to set  $\gamma = 0$ ; when

$$W = \frac{G}{4} \left[ \lambda^2 + \frac{1}{\lambda^2} + 2 \cdot \left( \lambda + \frac{1}{\lambda} \right) - 6 \right] + \frac{H}{4} \left[ \lambda^2 - \frac{1}{\lambda^2} - 2 \left( \lambda - \frac{1}{\lambda} \right) \right].$$

By differentiating we find

$$\text{stress } f = \frac{dW}{d\lambda} = \frac{G}{2} (\lambda + 1) \left( 1 - \frac{1}{\lambda^3} \right) + \frac{H}{2} (\lambda - 1) \left( 1 - \frac{1}{\lambda^3} \right).$$

The molecular theory of Wall predicts  $G = H$  (29)

By substituting  $G = H$  in the last equation we have:

$$\text{stress } f = G \cdot \left( \lambda - \frac{1}{\lambda^2} \right), \text{ where } \lambda = 1 + \text{strain}.$$

This is the equation for the S-shaped stress-strain curve without upward curvature.

From Mooney's theory equations for shearing in the transverse direction and for stretching in the lengthwise direction result. These equations are fairly well checked by experiments. The theoretical longitudinal stress-strain curve is an ascending curve which coincides with about two thirds of the experimental S-curve.

(b) *Wall's Theory*. Wall (30), in his third paper on "Statistical Thermodynamics of Rubber," derives equations for the stretching and shearing of vulcanized rubber by applying a network structure and a minimum of postulates.

Rubber behaves to a certain extent like a gas. Therefore, corresponding to the kinetic theory of gases there is a kinetic theory of rubber elasticity. According to this theory, because of thermal motion of the atoms, the thread-like molecules of rubber are greatly folded if the rubber cylinder is unstretched; if the rubber cylinder is stretched, the chains of the molecules approach straight lines.

Wall uses the methods of statistical physics. For unstretched rubber the distribution of the molecules of length  $x$  is given by the formula

$$p(x) \cdot dx = \frac{\beta}{\sqrt{\pi}} \cdot e^{-\beta^2 x^2} \cdot dx$$

where  $p(x)$  is the probability of finding a molecule of length  $x$  in the range  $x$  to  $(x + dx)$ , and  $\beta$  is a constant.

The statistical state is given by

$$P = \frac{N!}{N_0! N_1! N_2! \dots} \cdot p_0^{N_0} p_1^{N_1} p_2^{N_2} \dots p_i^{N_i} \dots$$

where  $N$  is the total number of molecules.

$$N = N_0 + N_1 + N_2 + \dots + N_i + \dots$$

$N_i$  molecules have  $x$  values in range  $dx_i$ , and  $p_i$  is defined similarly to  $p(x)$ .

According to Flory (8) the equation for  $p$  must be replaced by

$$P = p_0^{N_0} p_1^{N_1} p_2^{N_2} \dots p_i^{N_i} \dots$$

Then Wall uses Boltzmann's relation

$$\text{entropy } S = k \cdot \ln P_{\max},$$

where  $k$  is Boltzmann's constant.

Wall finds

$$S = N \cdot k \cdot \ln \alpha - \frac{1}{2} N k (\alpha^2 - 1),$$

where

$$\alpha = \frac{l}{l_0} = \frac{\text{final length of rubber cylinder}}{\text{initial length}}$$

Now using the first and second laws of thermodynamics:

$$dE = dW + dQ,$$

or change in energy of the system = work done + change in heat (first law), and

$$dQ = T \cdot dS,$$

or change in heat = absolute temperature  $\times$  change in entropy (second law). The deformation considered is such that

$$dE = 0.$$

This means that there is no change in the thermal energy of molecular motion. Then we have

$$\begin{aligned} 0 &= dW + T \cdot dS, \\ dW &= -T \cdot dS. \end{aligned}$$

But work done = stress  $f \times$  change in length, or

$$dW = f \cdot dl.$$

By differentiation of  $S$  which is a function of  $\alpha$ , we get

$$\begin{aligned} f \cdot dl &= T \left[ \frac{Nk}{l_0} \left( \alpha - \frac{1}{\alpha} \right) \right] dl, \\ f &= \frac{NkT}{l_0} \cdot \left( \alpha - \frac{1}{\alpha} \right). \end{aligned}$$

In the last equation only one dimension is considered. By extension to three dimensions and using the fact that rubber is incompressible, we get

$$= \frac{NkT}{l_0} \left( \alpha - \frac{1}{\alpha^2} \right),$$

where  $\alpha = 1 + \text{strain}$ . This again is the S-shaped stress-strain curve without upward curvature. If we compare this result with Mooney's result (IV, 1a), we find

$$\frac{NkT}{l_0} = G = \text{modulus of rigidity, and } \alpha = \lambda.$$

By using shear  $\gamma = \alpha - \frac{1}{\alpha}$  we get, for the entropy of shearing,

$$S = -\frac{1}{2}Nk\gamma^2.$$

Hence, by differentiation, we find

$$\tau = \frac{NkT}{l_0} \cdot \gamma,$$

or

$$\tau = G \cdot \gamma,$$

or shearing stress = modulus of rigidity  $\times$  shear. Hooke's law is obeyed with respect to shear (see III, 3). From Wall's theory we get the same equations for stretching and shearing which Mooney found. But we find the interesting result that the validity of Hooke's law in the transverse

direction is a consequence of Wall's theory. For Mooney this consequence was a postulate to his theory.

Wall's theory shows that there is a relationship between molecular network structure and elastic properties of vulcanized rubber.

(c) *Structure of Rubber, Wool and Protoplasm.* From the structural theory of rubber elasticity, one may deduce a network structure for vulcanized rubber. According to Flory (8), Fig. 15 represents an attempt to draw a portion of the network structure of vulcanized rubber. Of course, the diagram is oversimplified. According to the kinetic theory of elasticity, the rubber molecules are meandering, they are spiral threads if the vulcanized rubber is in an undeformed state.

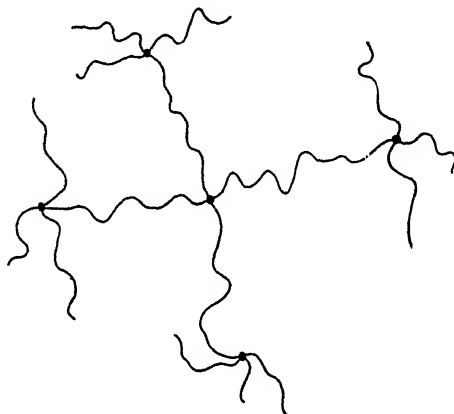


FIG. 15

Portion of the Molecular Network Structure of Vulcanized Rubber

It is generally assumed that vulcanization of rubber by using sulphur involves a cross-linking process between molecular chains of raw rubber. But the proof of the chemical structure of the cross links is lacking. Hence, the proof may be found by comparing the properties of vulcanized and raw rubber with those of wool before and after the rupture of the disulfide groups of its amino acid cystine. By chemical treatment of wool, rupture of the disulfide groups is produced (13). It seems well established that the disulfide groups form cross links in wool between molecular chains.

The stress-strain behavior of raw rubber is similar to the stress-strain behavior of wool in which the disulfide cross linkages have been ruptured. In both cases the stress-strain curves longitudinally are very flat and Young's moduli of elasticity are very low. With cross linking, both wool and vulcanized rubber have steeper stress-strain curves and higher Young's moduli of elasticity. These facts prove that rubber is to be vulcanized by cross links between the molecular chains of raw rubber.

It is an interesting result that rubber without cross links between molecular chains is elastic.

A growing wool fiber consists of the living portion, the root, and of the non-living portion, the shaft. The material in the root is comparable to raw rubber. When the cells of the root die, the disulfide groups of the woolshaft are formed. The soft, plastic material of the root becomes the tough, elastic wool fiber.

Thus we may conclude that, on the basis of elastic properties, the structure of the shaft of wool is produced by adding cross links to the molecular chains of the root of wool.

According to Astbury (1, p. 139) unstretched vulcanized rubber is amorphous, it has no micelles. In unstretched wool we find micelles. Both stretched vulcanized rubber and stretched wool contain micelles. Evidence of the presence of micelles is found in X-ray diffraction photographs.

Because of the similar elastic behavior of rubber and wool we may assume that the structure of wool, like that of vulcanized rubber, is formed by a network of thread-like molecules. The micelles in unstretched wool are thin. Later (VI) we shall see that unstretched vulcanized rubber may have micelles too.

The molecular chains of rubber consist of isoprene units, the molecular chains of unstretched wool are polypeptide chains of  $\alpha$ -keratin. In the unstretched state both wool and vulcanized rubber have spiral chain molecules.

According to Astbury (1, p. 151) and Frey-Wyssling (10, p. 255), the molecular network structure of the protein chains of wool is easily changed by treating wool with hot water for various lengths of time.

For studying the elasticity of protoplasm Seifriz and Freundlich investigated the elasticity of gelatin (9). They found that gelatin, when swollen with water, is elastic. Because gelatin is a fibrillar protein and because protoplasm is composed chiefly of proteins, we may assume that protoplasm is also elastic.

The device of the experiments of Seifriz and Freundlich was an electromagnet which acted on a particle of nickel in gelatin. The nickel particle, when attracted by the electromagnet, pulled some gelatin with it toward the magnet. Then the particle, together with the gelatin, returned to its original position when the electromagnet ceased to act. Thus a measure of the elasticity of gelatin was obtained.

Seifriz (11) proved the elasticity of protoplasm by using an onion cell and a microneedle. He found that gel-like protoplasm is elastic (slightly extensible) because, when the protoplasm is stretched by pulling it out of the cell, it easily snaps back (22, p. 232).

Similar experiments performed by Seifriz with slime molds and a



microneedle proved that sol-like protoplasm is also elastic (highly extensible) (23, p. 250).

According to Treloar (28), gelatin, when swollen with water, has rubber elasticity. Hence we must conclude that protoplasm has rubber elasticity too.

The structure of gel-like protoplasm is, therefore, very probably a network of thread-like protein molecules roughly similar in shape to the molecular network of vulcanized rubber. The structure of the sol-like protoplasm must likewise be more similar to the structure of raw rubber. These conclusions are approved by Frey-Wyssling (10, p. 137-139).

According to Frey-Wyssling the molecular network of unstable protoplasm is very easily changed, as is well known for the molecular structure of wool. The polypeptide chains of the structure of protoplasm are more or less movable. But never does all linking in the structure disappear. Free mobility of all polypeptide chains of the structure would result in the death of protoplasm by liquefaction. Therefore, sol-like protoplasm approaches the structure of raw rubber, but never has the structure of raw rubber. Presumably there are no micelles in protoplasm.

According to Banga and Szent-Györgyi, nature applies the globular proteins when a mobile protein is needed and rod-shaped proteins when a solid structure is to be produced (5). This remark again checks our theory of protoplasm structure, where we assume linear protein chains.

## 2. *Metallic Elasticity*

Our task now is to derive stress-strain relationships for a solid metal rod in longitudinal and transverse direction by using the methods of the classical theory of elasticity.

(a) *Longitudinal Direction.* If a metal rod of length  $l$  cm. and cross section  $1 \text{ cm.}^2$  is stretched by the stress  $\sigma$ , then the rod will increase its length by strain  $\epsilon$ . Because strain  $\epsilon$  increases with increasing stress  $\sigma$ , Hooke's law,  $\sigma = E \cdot \epsilon$ , is valid.

In this formula  $E$  is the proportionality factor, or Young's modulus of elasticity.

When a metal rod is stretched longitudinally within the elastic range, then, according to Hooke's law, stress = Young's modulus of elasticity  $\times$  strain.

(b) *Transverse Direction.* If the force  $F$  acts perpendicularly to a metal rod at the center, the rod being fixed at its two ends (Fig. 16), then the rod is bent, and a deflection  $d$  results. It is obvious that  $F$  is proportional to  $d$ . Besides  $F$  increases with increasing Young's modulus of elasticity  $E$ , and  $F$  might also increase with increasing cross-section  $A$  of the rod, then

$$F = c \cdot E \cdot A \cdot d,$$

where  $c$  is a proportionality factor.

A more thorough study of the problem of the "bending beam" shows that cross section  $A$  must be replaced by the moment of inertia,  $I$ , of the cross section with respect to an axis passing through the center of the rod. This axis is perpendicular to the force  $F$  and to the rod. Hence, in the elastic range

$$F = c \cdot E \cdot I \cdot d,^*$$

or

$$EI = \frac{1}{c} \cdot \frac{F}{d},$$

or

$$EI = k \cdot \frac{F}{d},$$

where  $k = 1/c$  is the proportionality factor. Hence

$\frac{F}{d} = k' = \text{constant}$ , because  $E$  and  $I$  are constants of the material.

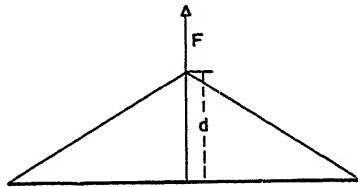


FIG. 16  
Metal Rod Deflected by Force  $F$

The deflection-force curve for the metal rod in the elastic range is a straight line passing through the origin. Hooke's law is valid. This is checked by our experiments in the transverse direction for cylindrical plant tissues (III, 3). In addition, Hooke's law is valid for vulcanized rubber when sheared in the transverse direction (IV, 1).

For a metal rod fixed at its ends, and deflected transversely at its center, we have the two important equations in the elastic range:

$$EI = k \cdot \frac{F}{d} \text{ and } F = k' \cdot d.$$

### 3. Equations of Elasticity and Plasticity Curves in the Case of Plant Tissues

We assume that, in the case of the longitudinal stress-strain curve of our tissues, Hooke's law (IV, 2) is valid in the form.

Young's modulus of elasticity  $E = \frac{\text{stress}}{\text{strain}}$  at the elastic limit (1) (see

\* An exact analysis of the problem, including forces resulting from elongation as well as bending, would be quite difficult. Therefore, the equation for  $F$  is only approximately correct.

III). Hence we can compute Young's modulus of elasticity for all tissues investigated.

As shown in III, 3, only the elasticity and plasticity of plant tissues were distinguished in the transverse direction. Therefore, the equations for elasticity and plasticity curves for cylindrical plant tissues must still be established with regard to the transverse direction. The curves to be investigated are given in section III, 2. These are ascending elasticity curves and straight line plasticity curves in the ( $F$ ,  $d$ ) system (Fig. 17).

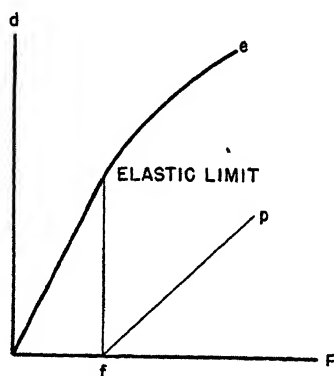


FIG. 17

Force-Deflection Curve of a Cylindrical Plant Tissue

$e$  = elasticity curve

$p$  = plasticity curve

From Fig. 17 the equation of the elasticity curve for all plant tissues investigated is in the elastic range

$$F = k' \cdot d.$$

From what has been said in section IV, 2b, this equation is correct for the deflection of a metal rod. Therefore, the transverse elastic behavior of cylindrical plant tissues is metal-like. The length of the plant tissue is  $2l$  which is the distance between the two binding posts in Fig. 1. Now we have

$$\frac{F}{\text{cross section}} = \mu \cdot \frac{d}{2l}, \quad \text{where} \quad k' = \frac{\mu}{2l} \cdot \text{cross section},$$

and where the cross-section of the plant tissue,  $2l$ , and  $\mu$  are constants. The constant  $\mu$  may be defined as the modulus of elasticity in the transverse direction. This transverse modulus of elasticity,  $\mu$ , is dependent on Young's modulus. The "real modulus of elasticity in transverse direction" is probably different for metals. But for cylindrical plant tissues  $\mu$  might be near the real value. Indeed, the modulus of rigidity for rhizomes

of *Equisetum fluviatile* and  $\mu$  are not very different (see later). We make

$$\frac{F}{\text{cross section}} = F', \quad \frac{d}{2l} = d',$$

and get as the equation of the elasticity curve in the elastic range transversely in the  $(F', d')$  system,

$$F' = \mu \cdot d'.$$

According to IV, 1, for a rubber cylinder  $\tau = G\gamma$ . It may be assumed that for rubber-like elastic cylindrical plant tissues the same equation is correct. The equation in the case of rhizomes of *Equisetum fluviatile* for a small deflection  $d$  is

$$\frac{F}{\text{cross section}} = G \cdot \frac{d}{2l}. \quad (a)$$

In this case  $\frac{F}{\text{cross section}}$  is shearing stress and  $\frac{d}{2l}$  is shear, the copper hook of Fig. 1 acts on the end of the rhizome near the binding post. Later on it is found that  $G = 1.6 \times 10^8$  dynes/cm<sup>2</sup>.

If the copper hook of Fig. 1 acts on the center of the rhizome and  $d$  is the same small deflection, then

$$\frac{F}{\text{cross section}} = \mu \cdot \frac{d}{2l}. \quad (b)$$

Later in Table I it is found that  $\mu = 1.1 \times 10^8$  dynes/cm<sup>2</sup>. The equations (a) and (b) are very similar because  $d$  has the same value and  $\mu$  and  $G$  are not very different. Hence, in the case of rhizomes of *Equisetum fluviatile*,  $\mu$  is well defined as the transverse modulus of elasticity. Now  $f$  is the distance between the origin and beginning of the plasticity curve (Fig. 17) and one may write:

$$f' = \frac{f}{\text{cross section}}. \quad (2)$$

The yield value is defined by (2) because a force which is a little greater than  $f$  produces a deflection which does not completely disappear if the force is removed (Fig. 17). Then we have for the transverse modulus of elasticity

$$\mu = \frac{f'}{d''}, \quad (3)$$

where

$$d'' = \frac{\text{deflection at elastic limit of the elasticity curve (Fig. 17)}}{2l}.$$

According to Fig. 17 the equation of the plasticity curve for all plant tissues investigated is:

$$d = \phi'(F - f),$$

where  $\phi'$  is constant. Now

$$\frac{d}{2l} = \phi \cdot \frac{F - f}{\text{cross section}},$$

where the cross section of the plant tissue,  $2l$  and  $\phi$  are constants. If we define  $\phi$  as the coefficient of plasticity, then the equation for the transverse plasticity curve in the  $(F', d')$  system is

$$d' = \phi \cdot (F' - f') \quad (4)$$

and the coefficient of plasticity becomes

$$\phi = \frac{d'}{F' - f'} \quad (5)$$

From Fig. 17 it is evident that plant tissue is very plastic if a small force  $(F' - f')$  produces a large plastic deflection  $d'$ . Then, by the last formula  $\phi$  is large, and hence  $\phi$  defines the coefficient of plasticity.

The definitions for  $\mu$ ,  $\phi$  and  $f'$  are not general. Our definition of  $\mu$  for cylindrical plant tissues demands dependency of the transverse modulus of elasticity on Young's modulus. Such a dependency is to be expected because all cylindrical plant tissues have structure. This dependency is stated by our equation for  $\mu$  if, in nature, cylindrical plant tissues are fixed at two ends. This is true for horizontal rhizomes of *Equisetum fluviatile* covered with loose sand between two stems. The same is true for horizontal roots of *Rhus glabra* between two stems. Because all cylindrical plant tissues have similar structure, we may conclude that

TABLE I

Substances	Longitudinal Direction		Transverse Direction		
	Strain at elastic limit	Young's modulus dynes/cm. <sup>2</sup>	Modulus of elasticity g./cm. <sup>2</sup>	Yield value g./cm. <sup>2</sup>	Coefficient of plasticity cm. <sup>2</sup> /g.
Petioles of <i>Nymphaea</i>	0.02	$5 \times 10^8$	$1.7 \times 10^5$	3434	0.00000673
Rhizomes of <i>Equisetum fl.</i>	0.1	$4.1 \times 10^8$	$1.1 \times 10^5$	7717	0.000002016
Stems of <i>Brasenia</i>	0.02	$28.5 \times 10^8$	$3.4 \times 10^5$	11868	0.000003196
Roots of <i>Rhus gl.</i>	0.02	$54 \times 10^8$	$3.9 \times 10^5$	14110	0.000001293
Sclerench. plates of rhizomes of <i>Pteris</i>	—	$115.9 \times 10^8$	$6.5 \times 10^5$	28760	0.0000003166
Branches of <i>Salix</i>	0.01	$233 \times 10^8$	$7.1 \times 10^5$	6831	0.00000319
Band of rayon	—	$10 \times 10^8$	$0.7 \times 10^5$	71430	0.000006516
Raw catgut	0.03	$344 \times 10^8$	$57.7 \times 10^5$	194900	0.0000002806

our equations for  $\mu$ ,  $\phi$  and  $f'$  at least give approximate values in all cases observed by us.

By using equations (1), (2), (3) and (5), and Figs. 6, 8, 10, 2, 3, 4, 5, 7, 9 and 11, other available figures and older values (25, 26), we obtain

(a) In the case of rayon a constant tension of 200 g. was applied longitudinally for obtaining values in the transverse direction. In the case of raw catgut a constant tension of 500 g. was applied lengthwise for getting values in both directions.

(b) Branches of *Salix babylonica* were used for obtaining longitudinal values and branches of *Salix lucida* for transverse values. The branches of the two species of *Salix* have similar cross sections.

(c) The second column of Table I shows that nearly all cylindrical plant tissues have strains at the elastic limit in the longitudinal direction of 0.01–0.02. According to Astbury (1, p. 127) this strain is 0.01–0.02 for cellulosic fibers. This coincidence might be understood because cellulose is the main substance in the cell walls of higher plants and determines the structure of these walls.

(d) The modulus of elasticity in the transverse direction indicates the rigidity of bending. Therefore, petioles of *Nymphaea odorata* are more flexible than stems of *Brasenia schreberi* (see Table I). This is important for the ecology of these aquatic plants. The more flexible plants of *Nymphaea odorata* are usually nearer the shore in lakes than the less flexible plants of *Brasenia schreberi*. The more flexible waterlilies secure a place in the sun in spite of competition with many shore plants. The less flexible *Brasenia* plants do not have so much competition.

In the shore water of Black Lake, Michigan, we collected the plants of *Brasenia schreberi* and *Nymphaea odorata* which we used for our experiments. In the region of *Brasenia schreberi* plants we measured the length of numerous stems of *Brasenia*. Thus, we found the depth of the lake in this region to be about 35 inches. Here the growth of water plants was not very dense. In the region of *Nymphaea odorata* plants we found, by measuring the length of petioles of *Nymphaea*, that the depth of the lake was about 27 inches. Here the growth of water plants was very dense. According to the measurements of depth the second region was nearer the shore than the first region. Our ecological results for *Nymphaea* and *Brasenia*, therefore, checked well.

Cellulosic fibers of flax have a Young's modulus of  $11,000 \times 10^8$  dynes/cm.<sup>2</sup>, and contain a large amount of cellulose. It is probable that branches of *Salix babylonica* with a relatively large Young's modulus (see Table I) contain a great amount of cellulose. According to Ott (19, pp. 295, 296) solid cellulose is more flexible the nearer its approach to a state of solution. We may then understand that branches of *Salix babylonica* with a great deal of cellulose become very flexible in the plastic

condition because they have a great coefficient of plasticity (see Table I). The tough branches of *Salix babylonica* hang down because of positive geotropic response. It might be that the great flexibility of these branches due to plastic condition facilitates their hanging down. Tough willow branches are used for making baskets. This is reasonable because of the great flexibility of the branches in the plastic condition.

Thus, we find that there are two kinds of flexibility for plant tissues. Soft cylindrical plant tissues are flexible because they have a small modulus of elasticity in the transverse direction. This kind of flexibility is like that of wet paper. Cylindrical plant tissues, which, in the normal condition, are hard, may be readily flexible in the plastic condition because they have a great coefficient of plasticity. Such a plant tissue is in the plastic condition if the force acting on it in the transverse direction is greater than the yield value.

We now wish to find the relationship of the equation for the S-shaped rubber stress-strain curve to the equation for S-shaped longitudinal stress-strain curves for our tissues.

According to Mooney and Wall we have as equation for the S-shaped stress-strain curve for a rubber cylinder (IV, 1)

$$\text{stress } f = G \times \left( \alpha - \frac{1}{\alpha^2} \right),$$

where

$$\alpha = 1 + \text{strain},$$

or, if we use stress  $\sigma$  and strain  $\epsilon$ , we get the equation of the curve in the  $(\epsilon, \sigma)$  system

$$\sigma = G \times \left( 1 + \epsilon - \frac{1}{(1 + \epsilon)^2} \right).$$

Fig. 13 contains the experimental S-shaped stress-strain curve for rhizomes of *Equisetum fluviatile* (25) in the  $(\epsilon, \sigma)$  system. We may assume that the equations for the S-shaped stress-strain curve are the same for the rubber cylinder and for rhizomes of *Equisetum fluviatile*.

The computation of  $G$  from Fig. 13 in the case of rhizomes of *Equisetum fluviatile* is given in the Table at top of page 355.

The average value for  $G$  is  $1.6 \times 10^8$  dynes/cm.<sup>2</sup>.

The theoretical longitudinal stress-strain curve for rhizomes of *Equisetum fluviatile* is given by the equation

$$\sigma = 1.6 \times 10^8 \times \left[ 1 + \epsilon - \frac{1}{(1 + \epsilon)^2} \right].$$

$\epsilon$	$1 + \epsilon - \frac{1}{(1 + \epsilon)^2}$	$\sigma \frac{\text{dynes}}{\text{cm.}^2}$	$G = \frac{\sigma}{1 + \epsilon - \frac{1}{(1 + \epsilon)^2}} \frac{\text{dynes}}{\text{cm.}^2}$
0.02	0.0588	$1.4 \times 10^7$	$2.4 \times 10^8$
0.04	0.1154	$2.35 \times 10^7$	$2.0 \times 10^8$
0.06	0.1700	$3.0 \times 10^7$	$1.8 \times 10^8$
0.08	0.2226	$3.5 \times 10^7$	$1.6 \times 10^8$
0.14	0.3705	$4.4 \times 10^7$	$1.2 \times 10^8$
0.24	0.5896	$5.2 \times 10^7$	$0.9 \times 10^8$

The following table shows how well the theoretical and experimental curves coincide.

$\epsilon$	$\sigma \frac{\text{dynes}}{\text{cm.}^2}$ (computed)	$\sigma \frac{\text{dynes}}{\text{cm.}^2}$ (experimental)
0.02	$0.9 \times 10^7$	$1.4 \times 10^7$
0.04	$1.8 \times 10^7$	$2.35 \times 10^7$
0.06	$2.7 \times 10^7$	$3.0 \times 10^7$
0.08	$3.6 \times 10^7$	$3.5 \times 10^7$
0.14	$5.9 \times 10^7$	$4.4 \times 10^7$
0.24	$9.4 \times 10^7$	$5.2 \times 10^7$

In Fig. 13 we have both the experimental and theoretical stress-strain curve. The curves coincide to some extent to slightly beyond the elastic limit of the experimental curve. The greatest deviation 30% with respect to the ordinate is for  $\epsilon = 0.02$ . We cannot expect much more because the rubber equation is derived on the assumption that rubber behaves like a liquid. It is obvious that this assumption is no more correct for the rhizomes of *Equisetum fluviatile*. The theoretical curve for rubber

$$\sigma = G \times \left[ 1 + \epsilon - \frac{1}{(1 + \epsilon)^2} \right],$$

also coincides with only two-thirds of the experimental rubber curve. The equality of the equations for the theoretical rubber curve and the theoretical curve for the rhizomes, and the partial coincidence of theoretical and experimental curves in the case of the rhizomes permit us to assume to a certain extent that there is a similarity in the structures of vulcanized rubber and the cell walls of rhizomes of *Equisetum fluviatile*.

The modulus of rigidity  $G$  (IV, 1) for the rhizomes is  $G = 1.6 \times 10^8$  dynes/cm.<sup>2</sup>.

There is an important difference between plant walls and rubber. Undeformed rubber is isotropic, while undeformed plant walls are, in



general, highly anisotropic. Hence, we may understand that coincidence is less for cell walls of rhizomes of *Equisetum fluviatile* than for catgut (see Fig. 13 and Fig. 10).

By using the same assumptions and computations in the case of the S-shaped stress-strain curve for raw catgut (Fig. 10) we find  $G = 113 \times 10^8$  dynes/cm.<sup>2</sup>.

The theoretical longitudinal stress-strain curve for raw catgut is given by the equation

$$\sigma = 113 \times 10^8 \times \left[ 1 + \epsilon - \frac{1}{(1 + \epsilon)^2} \right].$$

The theoretical and experimental curves again coincide fairly well to slightly beyond the elastic limits of the experimental curves. One can, therefore, expect some similarity in structure between vulcanized rubber and raw catgut.

Catgut consists of collagen fibrils from the intestinal walls of sheep. According to Clark (6, pp. 1340, 1341) collagen in the normal condition has a crystalline structure but on heating it contracts and becomes elastic, like rubber. The crystalline structure of collagen disappears similarly to the phenomenon occurring when stretched and frozen rubber is heated. Thus, we must assume that heated collagen and unstretched rubber have the same molecular network structure. Furthermore, protein collagen yields gelatin on hydrolysis, and gelatin, swollen with water, is rubber-like. Hence, our postulation that there is a similarity in structure between vulcanized rubber and raw catgut is checked.

From the foregoing the modulus of rigidity  $G$  (IV, 1) for raw catgut is found to be  $G = 113 \times 10^8$  dynes/cm.<sup>2</sup>.

To formulate a law for the values in Table I the plasticity curves for the first 4 plant tissues might be considered. By using equation (4) and Table I the equations for the 4 transverse plasticity curves in the ( $F'$ ,  $d'$ ) system may be determined.

Petioles of *Nymphaea odorata*;  $d' = 0.00000673$  ( $F'$ -3434).

Rhizomes of *Equisetum fluviatile*;  $d' = 0.000002016$  ( $F'$ -7717).

Stems of *Brasenia schreberi*;  $d' = 0.000003196$  ( $F'$ -11868).

Roots of *Rhus glabra*;  $d' = 0.000001293$  ( $F'$ -14110).

In Fig. 12 these plastic straight lines are plotted.

The slopes of the plasticity lines in Fig. 12 generally decrease with increasing Young's modulus of the plant tissues. We also recognize that the yield values become greater (Fig. 12).

From Table I the following law may be derived: The cylindrical plant tissues in Table I increase in hardness in the order enumerated. Generally, with increase in hardness, there is an increase in Young's modulus, the

transverse modulus of elasticity and yield value, and a decrease in the coefficient of plasticity. This means that soft plant tissues are slightly elastic and very plastic, and hard plant tissues are highly elastic and slightly plastic. The transverse moduli of elasticity of cylindrical plant tissues are much less than the corresponding values for Young's modulus. Therefore, cylindrical plant tissues have anisotropic structures longitudinally and transversely (see III, 2).

#### V. INFLUENCES OF TENSION, HUMIDITY, AND TEMPERATURE ON THE VALUE OF YOUNG'S MODULUS OF ELASTICITY FOR CYLINDRICAL PLANT TISSUES

We found that, for a metal cylinder fixed at its ends and deflected transversely at its center, within the elastic range (IV, 2, b),

$$EI = k \cdot \frac{F}{d},$$

where  $E$  is Young's modulus,  $I$  is the moment of inertia of the circular cross section with respect to an axis through the axis of the cylinder,  $F$  is the acting force, and  $d$  the deflection.

The similar equation

$$F = k' \cdot d$$

is to be used not only for metal rods but also for all our cylindrical plant tissues and catgut (IV, 3). Therefore, the equation

$$EI = k \cdot \frac{F}{d}$$

is to be used for cylindrical plant tissues and catgut fixed in the binding posts of Fig. 1.

##### 1. Influence of Tension on the Value of Young's Modulus

Young's modulus of plain catgut was found to be  $200 \times 10^8$  dynes/cm.<sup>2</sup> (26). Tension was obtained by applying  $W = 500$  g. and  $W = 800$  g. to catgut fixed in the binding posts of the apparatus shown in Fig. 1. In the case of  $W = 500$  g., deflections  $d$  cm. produced by forces  $F$  g. (Fig. 1) were measured. Then from equation:

$$EI = k \cdot \frac{F}{d},$$

we get

$$EI = k \cdot 200,$$

for tension 500 g. Similarly, in the case of  $W = 800$  g. we obtain

$$E'I = k \cdot 236$$

for a tension of 800 g.  $E$  is Young's modulus for the low tension (500 g.) and  $E'$  is Young's modulus for the high tension (800 g.). Dividing, we find

$$\frac{E'}{E} = \frac{236}{200} = 1.2,$$

or

$$E' = 1.2 \times E$$

for plain catgut 0.4 mm. thick. Young's modulus for catgut increases with increasing tension.

Petioles of *Nymphaea gladstonia* were investigated in the same way as catgut. Young's modulus for petioles of *Nymphaea odorata* is  $5 \times 10^8$  dynes/cm.<sup>2</sup>. If  $E$  is Young's modulus for the low tension 1500 g., and  $E'$  Young's modulus for the high tension 2000 g., in the case of *Nymphaea gladstonia*; then

$$E' = 1.9 \times E$$

for petioles of *Nymphaea gladstonia* 7 mm. thick. Young's modulus for petioles of *Nymphaea gladstonia* increases with increasing tension.

Finally, branches of *Salix babylonica* were investigated and Young's modulus was found to be  $233 \times 10^8$  dynes/cm.<sup>2</sup>. Again, if in the case of *Salix babylonica*,  $E$  is Young's modulus for the low tension 1500 g., and  $E'$  for the high tension 2000 g., then:

$$E' = 1.2 \times E$$

for branches of *Salix babylonica* 1.5 mm. thick. Therefore, Young's modulus for branches of *Salix babylonica* increases with increasing tension.

After drying a branch of *Salix babylonica* 1.5 mm. thick in an electric oven at 40° C. for 24 hours,  $F$  and  $d$  were measured for two different tensions. The dry branch was 1.4 mm. thick. After 48 hours drying the thickness was the same and the values of  $F$  and  $d$  for both tensions remained practically unchanged. In both cases we got

$$E' = 1.1 \times E.$$

The weight of the fresh branch was 1.123 g., the weight of the dry branch was 0.687 g., and the weight of the very dry branch was 0.547 g. We may assume that the dry branch was still living and that the very dry branch was dead. This means that Young's modulus does not change its value for a cylindrical plant tissue, living or dead, on condition that the water content does not change to any great extent. Therefore, the cell walls, and not the protoplasm, are responsible for the elasticity of plant tissues (see III, 2 and 27).

The following general law may be stated:

Young's modulus for cylindrical plant tissues increases with increasing tension. Meyer and Lotmar found for cellulosic fibers that the value of

Young's modulus generally increases with tension (17). Hence, our result for plant tissues is supported.

## 2. Influence of Humidity on the Value of Young's Modulus

Again using the equation:

$$EI = k \cdot \frac{F}{d}$$

and the device of Fig. 1, branches of *Salix babylonica* were investigated. For a fresh branch of *Salix babylonica* 0.15 cm. thick with a tension of 1500 g. we obtained

$$EI = k \cdot 750.4.$$

For a branch 0.14 cm. thick dried in an electric oven at 40°C. for 24 hours, with a tension of 1500 g. we obtained:

$$E_1 I_1 = k \cdot 690.5,$$

where  $E_1$  and  $I_1$  are values for the dry branch. The moment of inertia  $I$  of a solid circular cross section of radius  $a$  with respect to an axis passing through the center of the cross section is  $\frac{\pi a^4}{4}$ . Hence, in our case, we have

$$\frac{I_1}{I} \sim \frac{0.07^4}{0.075^4}$$

$$I_1 = 0.76 \times I.$$

Then for a tension of 1500 g.

$$E_1 \cdot 0.76 \cdot I = k \cdot 690.5.$$

Then we have

$$\frac{E_1 \times 0.76 \times I}{EI} = \frac{k \cdot 690.5}{k \cdot 750.4},$$

or

$$\frac{E_1}{E} = \frac{690.5}{0.76 \times 750.4} = 1.2,$$

$$E_1 = 1.2 \times E \text{ for a tension of 1500 g.}$$

$E$  refers to the wet branch and  $E_1$  to the dry branch. In a similar manner we obtained for the same branch  $E_1' = 1.2 \times E'$  for a tension of 2000 g.  $E'$  refers to the wet branch, and  $E_1'$  to the dry branch. The result is the same for both tensions. From this we have the general law: Decrease in the amount of water in a cylindrical plant tissue increases the value of Young's modulus.

Meyer and Lotmar (17) found a similar result for cellulosic fibers. In the case of fibers of raw hemp they found the value for Young's modulus to

be 3500 kg./mm.<sup>2</sup> for the wet fiber and a Young's modulus of 5800 kg./mm.<sup>2</sup> for the dry fiber. Therefore, for fibers of raw hemp we have the equation

$$5800 = 1.7 \times 3500.$$

Thus, our deduction for plant tissues

$$E_1 = 1.2 \times E$$

is checked.

### 3. Influence of Temperature on the Value of Young's Modulus

Using the equation

$$EI = k \cdot \frac{F}{d}$$

and the device of Fig. 1 for the influence of temperature, branches of *Salix babylonica* were again investigated. If a branch of *Salix babylonica* is surrounded by water at 25°C., then for a branch 0.15 cm. thick at a tension of 1500 g. we obtained

$$EI = k \times 743.$$

If the same branch is surrounded by water at 55°C., then, for the heated branch 0.15 cm. thick at a tension of 1500 g., we obtained

$$E_1 I = k \times 696,$$

where  $E_1$  is the value for the heated branch. Dividing, we find:

$$\frac{E_1}{E} = \frac{696}{743} = 0.9,$$

$$E_1 = 0.9 \times E$$

for a thickness of 0.15 cm. and a tension of 1500 g.  $E$  refers to the low temperature 25°C. and  $E_1$  to the high temperature 55°C. We have the general law:

Young's modulus decreases with increase in temperature for cylindrical plant tissues.

Again Meyer and Lotmar (17) found similar results for cellulosic fibers. They found for "crin artificiel": 850 kg./mm.<sup>2</sup> =  $0.6 \times 1350$  kg./mm.<sup>2</sup>, and for cellophane: 380 kg./mm.<sup>2</sup> =  $0.5 \times 740$  kg./mm.<sup>2</sup>. On the left side of the two equations we have Young's modulus for high temperature, and, at the right Young's modulus for low temperature. Hence our result for plant tissues

$$E_1 = 0.9 \times E$$

is checked by the results of Meyer and Lotmar.

#### 4. Change of Structure Produced by Change of Young's Modulus

According to Meyer and Lotmar (17) increase of tension solidifies loose spots of a cellulosic fiber. Therefore, increase of tension acts on cell walls of a plant tissue so that soft spots are solidified. The plant tissue becomes harder. Young's modulus then becomes greater (26). This must be the case according to the general law that Young's modulus increases with increasing tension. Hence, our explanation that soft spots of a plant tissue are solidified by increased tension, is correct.

According to Meyer and Lotmar, in cellulosic fibers the OH groups of the cellulose molecules are easily surrounded by water molecules. In this case the interstices between OH groups filled by water become larger. The structure of the fiber becomes weaker. A wet fiber is, therefore, weaker or softer than a dry fiber. Young's modulus becomes smaller. This must be the case according to the law of change of humidity and of change of Young's modulus.

In the cylindrical plant tissues investigated the vessels are filled with water. After some drying the vessels are less full. The plant tissue becomes harder and Young's modulus becomes greater. This is correct according to the law of change in amount of water and change of Young's modulus. Hence, in the case of humidity, the explanations are different for fibers and cylindrical plant tissues.

At last we must consider the case of heating a cylindrical plant tissue surrounded by water. The heat probably loosens the structure of the tissue, the tissue becomes softer and Young's modulus becomes smaller. This is checked by the general law of change of Young's modulus with change of temperature.

#### VI. RELATIONSHIP BETWEEN TENSION AND TEMPERATURE FOR PLANT TISSUES AND SUBMICROSCOPIC STRUCTURES IN CELL WALLS OF HIGHER PLANTS

Meyer and Lotmar (17) investigated cellulosic fibers of length  $l$  and determined whether an increase of tension  $F$  is related to an increase or decrease of temperature  $T$ . They found that  $(\partial F/\partial T)_l$  is negative for native cellulosic fibers. Such fibers and metal rods have large values for Young's modulus. Their longitudinal stress-strain curves are straight lines with a tail in accordance with Hooke's law. Metals and native cellulosic fibers have a crystalline structure. It must, therefore, be assumed that  $(\partial F/\partial T)_l$  is negative for cylindrical plant tissues which have metal-like longitudinal stress-strain curves. Such metal-like elastic plant tissues are woody roots of *Rhus glabra*, sclerenchymatous plates of rhizomes of *Pteris aquilina* and woody branches of *Salix babylonica*.

(a) The submicroscopic structure of the secondary cell walls of metal-like elastic plant tissues is determined by crystallites or micelles of cellulose.

The primary cell walls have a rubber-like submicroscopic structure (see later).

For fibers of amorphous cellulose (17) and for rubber cylinders  $(\partial F/\partial T)_l$  is positive. Meyer and Ferri (16) found this true for rubber over a very wide range of temperature, between  $-50^\circ\text{C}$ . and  $70^\circ\text{C}$ . The fact that  $(\partial F/\partial T)_l$  is positive for rubber, was one of the main reasons for introducing the kinetic theory of elasticity for rubber. According to Astbury (1, p. 139) and Flory unstretched rubber is amorphous, but Treloar (28) shows that, under certain conditions, unstretched vulcanized rubber is partly micellar and partly amorphous. The longitudinal stress-strain curve for a rubber cylinder is S-shaped. Rubber and amorphous cellulosic fibers have a molecular network structure, but rubber may also have micelles. It may probably be assumed, therefore, that  $(\partial F/\partial T)_l$  is positive for cylindrical plant tissues which have S-shaped or rubber-like longitudinal stress-strain curves. Such rubber-like elastic plant tissues are petioles of *Nymphaea odorata*, rhizomes of *Equisetum fluviatile* and stems of *Brasenia schreberi*. The validity of the Gough-Joule effect for rhizomes of *Equisetum fluviatile* (26) proves that  $(\partial F/\partial T)_l$  is positive for these rhizomes.

(b) The submicroscopic structure of the secondary cell walls of rubber-like elastic plant tissues is a molecular network of cellulose with some micelles. As was shown in section IV, 3, this same submicroscopic structure is applicable to the secondary cell walls of rhizomes of *Equisetum fluviatile* and to raw catgut.

According to Bailey, the microscopic structure of cell walls of higher plants is as follows (2, 3): "The cell wall is composed of the middle lamella, the thin primary cell wall and the thick secondary cell wall. The secondary cell wall of fibers is often composed of three layers. These layers sometimes contain fine lamellae. The lamellae are composed of fibrils. In all cases the secondary wall resolves itself ultimately into a system of fine fibrils, which are more or less extensively coalesced." This means that the secondary cell wall is always composed of fibrils. Such a microscopic structure of cell walls is correct for cells of metal-like elastic plant tissues.

Cellulose forms a high percentage of the volume of the solid cell wall of higher plants. Primary cell walls which are dry may contain 42% of cellulose, secondary cell walls with water may contain 75% cellulose (11). Because cellulose constitutes such a large proportion of the cell walls of higher plants, it is obviously responsible for the submicroscopic structure of cell walls.

By applying the two conclusions (a) and (b) on the submicroscopic structure of cell walls just mentioned, the correctness of the following more general deduction for higher plants may be assumed: The submicroscopic structure of secondary cell walls of plant tissues is composed of partly crystalline and partly amorphous cellulose.

In the case of rubber-like elastic cylindrical plant tissues, the amount of amorphous cellulose in the secondary cell walls is greater than the amount of crystalline cellulose. For such generally soft plant tissues  $(\partial F/\partial T)_i$  is positive and the Gough-Joule effect is valid.

In the case of metal-like elastic cylindrical plant tissues the amount of crystalline cellulose in secondary cell walls is greater than the amount of amorphous cellulose. For such generally hard plant tissues  $(\partial F/\partial T)_i$  is negative and the Gough-Joule effect is not valid.

For the rubber-like elastic cylindrical plant tissues we get a low ratio between Young's modulus and the transverse modulus of elasticity. According to Table I this ratio is:

- 3 for petioles of *Nymphaea odorata*;
- 4 for rhizomes of *Equisetum fluviatile*;
- 8 for stems of *Brasenia schreberi*; and
- 6 for raw catgut (animal tissue).

The ratio between Young's modulus and the modulus of elasticity in the transverse direction for metal-like elastic cylindrical plant tissues is large. From Table I this ratio is:

- 14 for roots of *Rhus glabra*;
- 18 for sclerenchymatous plates of rhizomes of *Pteris aquilina*; and
- 33 for branches of *Salix babylonica* (lucida).

The small ratios between Young's modulus and the modulus of elasticity in the transverse direction for cylindrical rubber-like elastic plant tissues correspond to the values less than 1 for the ratio between the amounts of crystalline and amorphous cellulose in secondary cell walls of these tissues.

The large ratios of the two moduli of elasticity for cylindrical metal-like elastic plant tissues correspond to the values greater than 1 for the ratio between the amounts of crystalline and amorphous cellulose in secondary cell walls of these tissues.

This correspondence of two ratios, one between two properties of elasticity and one between two properties of structure, makes it probable that our deductions assumed for the submicroscopic structure of various secondary cell walls are correct.

In 1929 and 1930 Meyer and Mark found that the micelles or crystallites of cellulose in secondary cell walls were rods of 600 Å length and



50 Å width. Such micelles or crystallites of cellulose are those which have been considered up to this point. These micelles are bundles of molecular cellulose threads. Staudinger found that the molecules of cellulose have a length of 15000 Å. Such long cellulose molecules do not fit into the micelles. Therefore, according to Meyer and Mark, the submicroscopic structure of secondary cell walls is composed of micelles which are connected with each other by cellulose threads. Hence, the same chain of cellulose can pass through a crystalline area, a micelle, enter an amorphous portion, pass right through this and enter another crystallite. Such a structure of the secondary cell wall is partly crystalline and partly amorphous (15, pp. 39, 40). It was Mark's picture of partly crystalline and partly amorphous cellulose which influenced Treloar to use the same picture for rubber.

Thus we have shown the correctness of our result that the submicroscopic structure of secondary cell walls is composed of crystalline and amorphous cellulose.

In 1936 Frey-Wyssling (11) gave another picture of the submicroscopic structure of secondary cell walls. According to him the micellar rods of cellulose of Meyer and Mark are fused together in a colloidal particle of crystalline structure, which is called a micelle by Frey-Wyssling. It is composed of the parallel crystallites of Meyer and Mark. In many cases in the secondary cell wall Frey-Wyssling's micelle forms one system, and lignin forms another. The two penetrate each other greatly in the secondary cell wall.

Bailey (2) found by experiment that, in the case of a heavily lignified secondary cell wall, it is possible to remove the cellulose and leave a firmly coherent residue of lignin, and conversely, it is possible to remove the lignin and leave the coherent matrix of cellulose. This is the picture in the secondary wall. Now it is reasonable to assume that, by grading down, we get the same picture inside the fibrils. This proves the correctness of the structure of Frey-Wyssling's micelle and of the submicroscopic structure for the secondary cell wall of woody plant tissues. But woody plant tissues belong to the group of metal-like elastic plant tissues.

We find, then, that the submicroscopic structure of the secondary cell wall of metal-like elastic plant tissues of high Young's modulus is determined by Frey-Wyssling's micelles of cellulose.

This partly proves the assumption that the submicroscopic structure of secondary cell walls of metal-like elastic plant tissues is determined by a ratio greater than 1 for the amounts of crystalline and amorphous cellulose.

We shall find that primary cell walls have only amorphous cellulose in their submicroscopic structure.

The submicroscopic network structure of amorphous cellulose, such as occurs in soft primary cell walls, constitutes the lower limit of submicroscopic structure. The other, upper limit, is formed by the submicroscopic structure of Frey-Wyssling's micelles in the secondary walls of cellulosic fibers. Between these two limits lie the submicroscopic structures of the secondary cell walls of higher plants.

The submicroscopic structure of a specific secondary cell wall is dependent on:

- (a) the percentage of cellulose in the secondary wall,
- (b) the ratio between the amounts of crystalline and amorphous cellulose in the wall, and
- (c) the orientation of the cellulose molecules in the wall.

Of course, the secondary cell walls of various cells of a specific plant tissue are quite different. But we assume that there is an average secondary cell wall, the submicroscopic structure of which corresponds to certain elastic and plastic properties of the plant tissue considered.

By applying these various assumptions, we arrive at a general law for the submicroscopic structure of the cylindrical plant tissue of higher plants. The greater the ratio between moduli of elasticity for a cylindrical plant tissue, the greater is the ratio between the amounts of crystalline and amorphous cellulose in the average secondary cell wall, the greater the percentage of cellulose in this wall, and the more the cellulose molecules in the wall are oriented parallel to the axis of the plant tissue.

The correctness of the theory of submicroscopic structure for cell walls depends in large measure on our knowledge of the occurrence of amorphous cellulose in cell walls. There is not much known about this matter.

Bailey (letter to Dr. Seifriz) is quite skeptical regarding the whole matter of the occurrence of amorphous cellulose in cell walls. He is willing to admit that microfibrils of cellulose are less compactly aggregated and less symmetrically oriented in primary than in secondary cell walls.

According to Frey-Wyssling (11) the submicroscopic structure of walls of the parenchymatic cells of *Avena* coleoptiles, which are primary walls, is a network of fibers. But he does not assume that the fibers are chain molecules of cellulose. According to him they are small rods of cellulose. Frey-Wyssling at least grants the possibility of a submicroscopic structure of cellulose in primary cell walls similar to that postulated in accordance with our theory for very soft rubber-like elastic plant tissues.

According to Wergin (31), primary cell walls contain rods of cellulosepectin surrounded by fat and wax. Wergin does not find micelles in primary cell walls. The plasticity of the primary walls is very great because of the occurrence of fat and wax. Soft primary cell walls with fat and wax

must have small Young's moduli and great plasticity according to our experiments. Because of this high plasticity of primary cell walls meristematic cell walls are able to grow. According to Wergin (31), the strong network of cellulose assumed by Frey-Wyssling in primary walls and kept together by "*Haftpunkte*," is too rigid. This network makes the wall strong, but not plastic enough for the growth of meristematic cells. We may, therefore, assume that the molecular network of cellulose in the submicroscopic structure of primary walls is similar to the network in raw rubber, namely, without cross linkage. This means that the chain molecules of cellulose in primary walls are tangled as the branches of a shrub may be tangled with each other. We use only a part of Wergin's picture for primary cell walls by assuming that the meshes of the network contain fat and wax.

By using Frey-Wyssling's and our own assumptions (11) we get the following explanation for the process of growth in meristematic cells: Protoplasm and primary cell walls have similar submicroscopic network structures. It is, therefore, easily understood that rings of glucose pass from the protoplasm to the meshes of the network of primary cell walls. In these meshes cellulose is formed by the aggregation of glucose units. The meshes of the network of entangled molecular chains in the primary cell walls, containing fat and wax, are then expanded in a plastic way by the formation of more cellulose. The turgor pressure in meristematic cells may be the force which moves glucose rings from protoplasm to primary cell walls. According to our experiments this force must be greater than the yield value of the wall if plastic deformation in the primary cell wall is possible.

Longitudinal growth is probably a much more complicated process than that postulated above, but at least the physical side of growth as a general phenomenon may be explained in this way.

## VII. SUMMARY

1. The elementary process of elastic and plastic deformations in living tissues is closely related to their submicroscopic structure. Therefore, an attempt was made to arrive at a general picture of the submicroscopic structure of cylindrical plant tissues.

2. Because cylindrical plant tissues have different elastic behavior longitudinally and transversely, an experimental device was constructed which permitted determination of two moduli of elasticity. Stretching horizontal cylindrical plant tissues gives three kinds of stress-strain curves and, therefore, Young's modulus also. These three stress-strain curves are parabolic, S-shaped and straight lines with tails. The S-shaped curves belong to rubber-like elastic plant tissues, the straight lines with tails

belong to metal-like elastic plant tissues. By forcibly deflecting the cylindrical plant tissue at its center, force-deflection curves are obtained. The force-deflection curve for all cylindrical plant tissues consists of two parts, an ascending elasticity curve and a straight line plasticity curve. From these two curves we can compute the transverse modulus of elasticity, the coefficient of plasticity and the yield value for cylindrical plant tissues.

3. Because all cylindrical plant tissues yield the same force-deflection curve, we may deduce the general law that in nature sideward breaking of plants always proceeds in the same way if a growing force is acting perpendicular to the plant.

4. From the elastic and plastic quantities computed, the following new laws may be stated:

(a) Soft plant tissues are slightly elastic and very plastic, hard plant tissues are highly elastic and slightly plastic.

(b) The structure of cylindrical plant tissues is more solid longitudinally than transversely. The submicroscopic structure of the cell walls of cylindrical plant tissues is determined by linear molecules of cellulose which are more or less oriented parallel to the axis of these tissues.

5. By using the elastic and plastic quantities computed, we find that plant tissues have two kinds of flexibility. Soft cylindrical plant tissues have the flexibility of wet paper. A second group of cylindrical plant tissues is flexible only in the plastic condition.

6. By using the molecular network structure of rubber, the theoretical equation for the S-shaped stress-strain curve for rubber is found to be:

$$f = G \left( \alpha - \frac{1}{\alpha^2} \right)$$

where  $f$  = stress,  $\alpha = 1 + \text{strain}$ ,  $G$  is the modulus of rigidity. This theoretical curve coincides fairly well with the experimental curve for rubber. Hence, we find that there is a relationship between the molecular network structure and the elastic properties of vulcanized rubber.

7. Because of similar elastic behavior of wool and vulcanized rubber we conclude that both substances have a similar molecular network structure. In addition there are thin micelles in wool. The network structure of wool is easily changed by heat.

8. Because protoplasm has rubber-like elasticity, we postulate a rubber-like molecular network structure for protoplasm. The network structure of the very unstable protoplasm is easily changed, as is known to be true for wool.

9. By using the theoretical equation for the S-shaped rubber curve in the case of the experimental S-shaped stress-strain curve for rhizomes of

*Equisetum fluviatile* we conclude that there is a similarity of submicroscopic structure for vulcanized rubber and for cell walls of rhizomes of *Equisetum fluviatile*. In a similar way we find that there is a similarity of structure for raw catgut and vulcanized rubber.

10. (a) The submicroscopic structure of secondary cell walls of plant tissues of higher plants is composed of partly crystalline and partly amorphous cellulose.

(b) In the case of rubber-like elastic cylindrical plant tissues the amount of amorphous cellulose in secondary cell walls is greater than the amount of crystalline cellulose. For such a plant tissue we have the fact that the ratio between Young's modulus and the modulus of elasticity transversely is small.

(c) In the case of metal-like elastic cylindrical plant tissues the amount of crystalline cellulose in secondary cell walls is greater than the amount of amorphous cellulose. For such a plant tissue we have the fact that the ratio between Young's modulus and the modulus of elasticity transversely is great.

(d) The greater the ratio between the moduli of elasticity for a cylindrical plant tissue, the greater is the ratio between the amounts of crystalline and amorphous cellulose in the average secondary cell wall of the tissue, the greater the percentage of cellulose in this wall, and the greater the orientation of cellulose molecules parallel to the axis of the plant tissue in this wall.

11. The submicroscopic structure of the highly plastic primary cell wall is given by a molecular network of cellulose. In this network there is no cross-linking, the chain molecules of cellulose are only entangled with each other.

12. The physical part of growth of primary cell walls is explained by passage of glucose units from protoplasm to the meshes of the cellulose network in the primary wall. The plasticity of this wall is great because the meshes contain fat and wax and because the loose molecular chains of cellulose are easily moved. The pressure of turgor producing the motion of glucose to the primary wall must be greater than the yield value for this wall. In this case a plastic deformation of the wall is possible.

13. The influences of humidity, temperature and tension on the value of Young's modulus in cylindrical plant tissues were investigated. The results are:

(a) Decrease in the amount of water in a cylindrical plant tissue increases the value of Young's modulus.

(b) Increase of temperature for a cylindrical plant tissue decreases the value of Young's modulus.

(c) Young's modulus for a cylindrical plant tissue increases with increasing tension.

The foregoing three cases are to be expected if there is no change in the submicroscopic structure of the plant tissue generally. Thus, by increased tension macroscopic soft spots of a plant tissue are solidified and Young's modulus is increased. According to Meyer and Lotmar it is not possible to assume a change in the orientation of the cellulose molecules in cellulosic fibers by increased tension thus causing Young's modulus to become greater (17). From the work of Kratky the influence of deformation on the amount of orientation of cellulose molecules is known. But, in the case of influence of tension on cellulosic fibers, the elongations are only 2-3%. These small elongations do not produce observable orientation of cellulose molecules.

Therefore, we must conclude that the submicroscopic structure of plant tissues generally is not changed by the influences of humidity, temperature or tension.

#### REFERENCES

1. ASTBURY, W. T., *Fundamentals of Fibre Structure*. Oxford University Press, London (1933).
2. BAILEY, I. W., *Am. Assoc. Adv. Sci., Pub. No. 14*, 31-43 (1940).
3. BAILEY, I. W., *Ind. Eng. Chem.* **30**, 40-47 (1938).
4. BALLOU, J. W., AND SILVERMAN, S., *J. Acoustical Soc.* **16**, no. 2, 113-119 (1944).
5. BANGA, I., AND SZENT-GYÖRGYI, A., *Science* **92**, 514-515 (1940).
6. CLARK, G. L., in GLASSER, O., *Medical Physics*. The Year Book Publishers, Chicago, Ill. (1944).
7. COMPTON, J., *Ind. Eng. Chem.* **31**, 1250-1259 (1939).
8. FLORY, P. J., *Chem. Rev.* **35**, 51-75 (1944).
9. FREUNDLICH, H., AND SEIFRIZ, W., *Z. physik. Chem.* **104**, 233-261 (1923).
10. FREY-WYSSLING, A., *Submicroscopische Morphologie des Protoplasmas und seiner Derivate*. Bornträger, Berlin (1938).
11. FREY-WYSSLING, A., *Protoplasma*, **25**, 261-300 (1936).
12. GUTH, E., in ALEXANDER, J., *Colloid Chemistry, Theoretical and Applied*, Vol. 5. Reinhold Publishing Corp., New York (1944).
13. HARRIS, M., MIZELL, L. R., AND FOURT, L., *Ind. Eng. Chem.* **34**, 833-838 (1942).
14. HOUWINK, R., *Elasticity, Plasticity and Structure of Matter*. Cambridge University Press (1937).
15. MARK, H., in BURK, R. E., AND GRUMMITT, O., *The Chemistry of Large Molecules*. Interscience Publishers, New York (1943).
16. MEYER, K. H., AND FERRI, C., *Helv. Chim. Acta* **18**, 570-589 (1935).
17. MEYER, K. H., AND LOTMAR, W., *Helv. Chim. Acta* **19**, 68-86 (1936).
18. MOONEY, M., *J. Applied Physics* **11**, 582-592 (1940).
19. OTT, E., in BURK, R. E., AND GRUMMITT, O., *The Chemistry of Large Molecules*. Interscience Publishers, New York (1943).
20. RECORD, S., *The Mechanical Properties of Wood*. John Wiley and Sons, New York (1914).
21. SZENT-GYÖRGYI, A., *J. Colloid Sci.* **1**, pp. 1-19 (1946).
22. SEIFRIZ, W., *Protoplasm*, 1st. Ed. McGraw-Hill Book Co., New York (1936).
23. SEIFRIZ, W., *A Symposium on the Structure of Protoplasm*. Iowa State College Press, Ames, Iowa (1942).

24. SPONSLER, O. L., AND DORE, W. H., Colloid Symposium Monograph. Chemical Catalog Co. New York (1926).
25. TREITEL, O., *Trans. Kansas Acad. Sci.* **46**, 122-132 (1943).
26. TREITEL, O., *Trans. Kansas Acad. Sci.* **47**, 219-239 (1944).
27. TREITEL, O., *Trans. Kansas Acad. Sci.* **48**, 186-197 (1945).
28. TRELOAR, L. R. G., *Repts. Progress Phys.* **9**, 113-136 (1943).
29. WALL, F. T., *J. Chem. Phys.* **10**, 485-488 (1942).
30. WALL, F. T., *J. Chem. Phys.* **11**, 527-530 (1943).
31. WERGIN, W., *Biol. Zentr.* **63**, Heft 7/8 (1943).
32. WORTHING, A. G., AND GEFFNER, G., *Treatment of Experimental Data*. John Wiley and Sons, New York (1943).

# FUNDAMENTALS OF DYE ABSORPTION

S. M. Neale

*From the College of Technology, Manchester, England*

*Received May 28, 1946*

## INTRODUCTION

During the last ten or fifteen years scientific effort, emerging from a highly successful empirical attack on the synthesis of artificial coloring matters, has been increasingly directed toward the problem of understanding how and why the colors become fixed to the fibers.

Industry, pioneered by the academic research worker, has evolved and selected by a long and painstaking process of trial and error, substances which possess the necessary attributes of high color intensity, resistance to sunlight, and affinity for the fiber. The understanding of the last named, which is essentially a physico-chemical problem, has now reached the stage where we may profitably pause and survey the ground thus far gained.

Before 1930, the description of dye affinity was qualitative, depending on comparative color tests (so called "dyeing trials"), interpreted by the unaided human eye and classified, by a wholly subjective process, as "good," "medium" or "poor." It was, therefore, apparent that no useful attempt could be made to apply the principles of physical chemistry to the problem, since verification always depends upon quantitative data, which in this case were lacking.

## THE ESTIMATION OF DYE ABSORPTION

The first serious attempt to remedy this defect was made by Knecht (1), who devised a chemical method (reduction by titanous chloride solution), whereby many dyes could be estimated quantitatively. The process, however, demands such relatively massive amounts of dye (of the order of tenths of a gram), as to be unsuitable for routine analysis of dye absorption on a practical laboratory scale.

The most obvious and characteristic property of any dye is its color, and the estimation of dye absorption could be solved by elevating the use of color from a qualitative to a strictly quantitative basis. This was achieved in about 1931 by Neale and co-workers (2-12) and by Boulton and co-workers (13, 14) who employed aqueous pyridine as a solvent capable of stripping "direct" dyes from any form of cellulose. In this way



the absorbed dye can be estimated in solution at the optimum concentration, and the insoluble complications of converting direct optical measurements in the fiber into weights of dyestuff may be avoided. Many of the vat colors and other insoluble dyes can be stripped from cellulose by the use of boiling *o*-chlorophenol.

The corresponding problem of stripping the "acid" colors from silk and wool has, however, not yet been solved, so that quantitative data in this field are scanty and depend upon optical estimation of the degree of

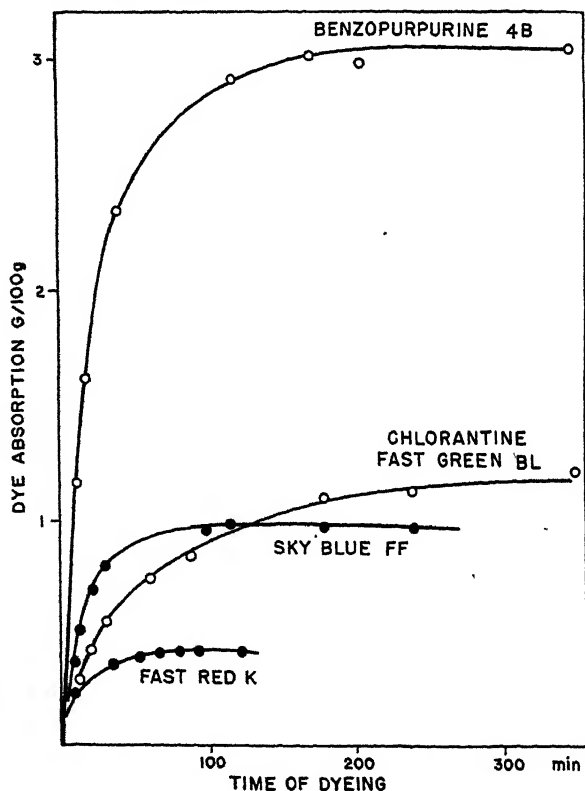


FIG. 1  
Absorption of Dyes G Cellophane (3 mg./cm.<sup>2</sup>) at 90°C.  
Dye 0.05 g./l.  
NaCl 5.0 g./l.

exhaustion of the original dye bath. Measurements of the time rate of dyeing from a bath of constant composition are, therefore, not possible.

Making use of the stripping method for the determination of dye absorption, several workers have made quantitative examinations of the effect of the various experimental factors upon the take-up of direct dyes

by cellulose. Neale and Stringfellow (5) showed that the rate-determining process could be regarded as the slow diffusion of color ions through the "meshes" of the cellulose structure and that the diffusion equations could be used to represent the variation of absorption with times of dyeing and thickness of the cellulose sheet.

They also showed that after a time of about 4 hours at 90°C. the absorption of dye reached an equilibrium (see Fig. 1) which was strictly

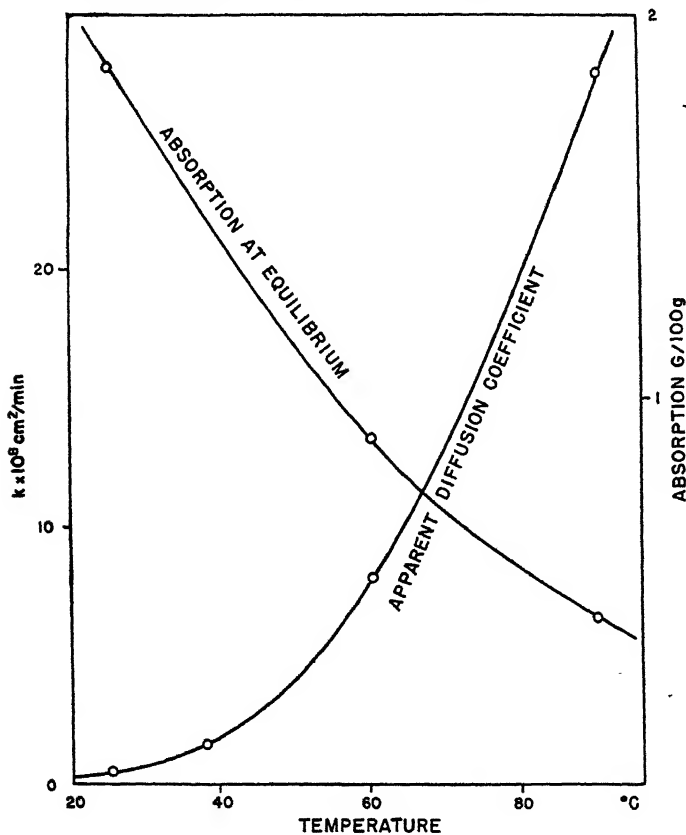


FIG. 2

Effect of Temperature on Dyeing of Cellophane with Fast Red K.

reversible. Garvie and Neale (11) later showed that the use of Fick's diffusion law was merely a first approximation, for the rate of diffusion, when more closely examined, was found to vary not only in proportion to the gradient of concentration, but also depended on the local concentration as such. Fick's law is, however, even in a simple system such as potassium chloride in water, merely a rough approximation to the truth (see McBain and Liu (15)).

The rate of diffusion for a direct dye through cellulose has been found to depend upon:

- (a) the local concentration,
- (b) the local concentration gradient,
- (c) the temperature, the diffusion rate rising rapidly with rising temperature (see Fig. 2), and
- (d) the concentration of added salt, the rate of diffusion being zero in the absence of added salt, and increasing rapidly with the salt concentration.

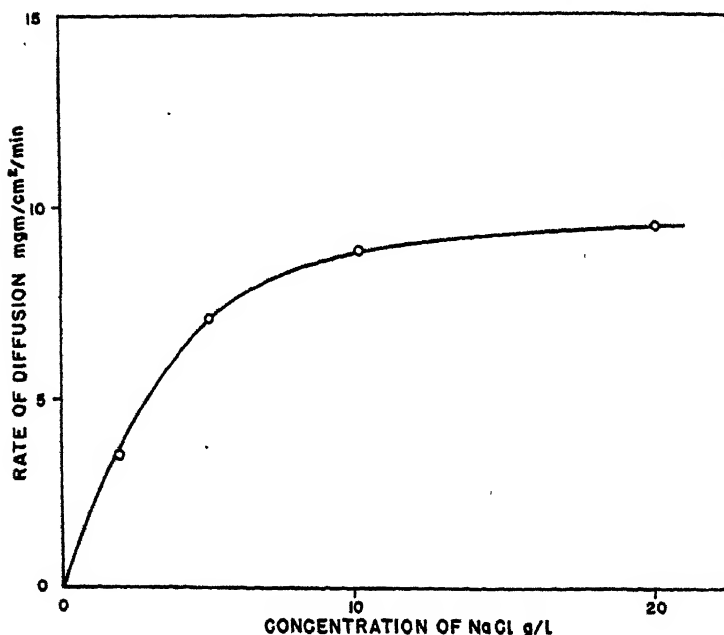


FIG. 3

Rate of Diffusion of Sky Blue FF through Cellophane at 90°C. (3 mg./cm.<sup>2</sup>)  
Dye Concentrations. 0.5 and 0 g./l.

Neale and his collaborators (2-12) showed that for many direct cotton dyes the "apparent diffusion coefficient" rose to a maximum and then fell as the salt concentration was increased. This fall at high concentration does not occur if the coefficient of diffusion be calculated in terms of the concentration of dye in the *solution*. It is found (see Fig. 3.) that the actual diffusion rate of dye through cellophane is immeasurably small in the absence of salt and simply approaches a maximum with increasing concentration of added salt. This is a striking and important fact, for it enables us to dismiss the commonly held idea that aggregation of the dye

produced by the addition of salt is the prime cause of the increased absorption. The dye molecules or ions are relatively large units, and their entry into the meshes of the cellulose structure must be a matter of some difficulty. It would clearly be made more difficult by aggregation, so that, on this theory, addition of salt should *decrease* the rate of diffusion.

The fact that salt addition actually *increases* the diffusion rate very greatly, can be explained if one allows that the mobile particles of dye are the negatively charged anions, and that these have difficulty in sur-

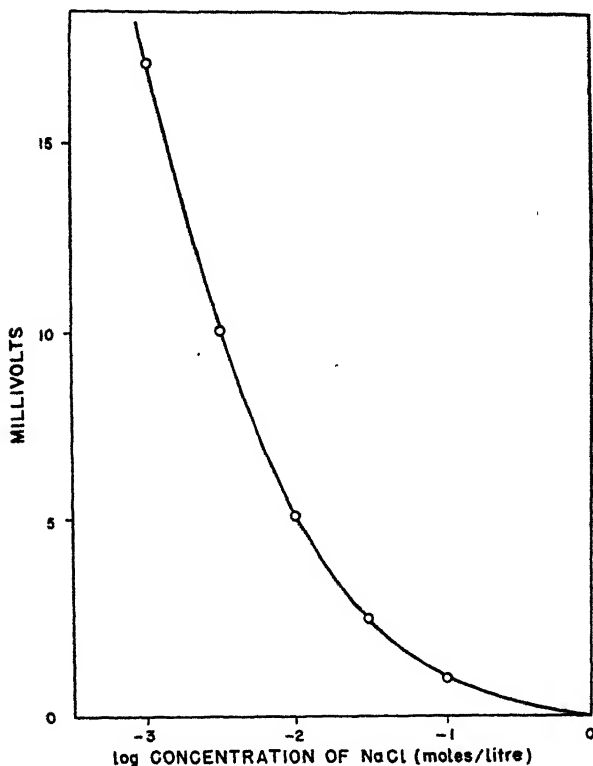


FIG. 4

ζ Potential of Cotton in NaCl Solutions

mounting the electrical potential barriers existing in the pores of the negatively charged cellulose. The origin of this negative charge is not known, but electrokinetic measurements show it to be real and quite large (16, 17, 18).

The zeta potential of cotton is about  $-18$  mv. in  $10^{-3}$  M NaCl, but only about  $-1$  mv. in  $10^{-1}$  M NaCl (17, 18) (see Fig. 4). Since one ion of a tetrasulphonic dye carries a net charge of  $4 e$  units of negative

electricity, the electrical work to be done on bringing one ion up to the cellulose surface is, therefore,

$$= 4 \times 4.77 \times 10^{-10} \times \frac{18}{300,000} \text{ ergs.}$$

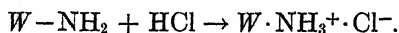
$$= 16,500 \text{ cal./mole. in } N/1000 \text{ NaCl, but only 1000 calories in } N/10 \text{ NaCl.}$$

The effect of the negative potential of 18 mv. is, therefore, almost entirely to prevent the dye ion approaching close to the surface—hence the absence of dyeing, or even of diffusion through a cellulose membrane, in absence of added salt.

The effect of salt in decreasing the negative potential of the surface follows at once from any theory of the diffuse double layer. In terms of three dimensions, it is perhaps better known as the Debye-Hückel effect.

It may be simply expressed by saying that the potential of any charged body is decreased by concentrating a neutral electrolyte in its environment, for the provision of local excess of ions of opposite sign to that of the body is accomplished with a less expenditure of energy in a more concentrated solution. The more localized this excess, *i.e.*, the closer to the surface, the less is the range of the electric field of the charged body and, hence, the lower the potential difference between it and the solution at "infinity" (in effect at distances over 100 Å.U.).

A complete explanation of the effect of salt in the dyeing of cellulose can, therefore, be deduced simply from classical electrical theory. The dyeing of wool with acid dyes from an acid bath provides an interesting variation, for here the salt effect is reversed, addition of salt decreases absorption. The explanation is simply that, below pH 3.1, wool becomes positively charged, owing to the reaction



In consequence, as the acid dyes are anionic, the electrical forces now assist the dyeing and, being again diminished by addition of salt, a lighter dyeing results. The absorption of substantive basic dyes by cellulose is again in line with this theory (see Fig. 5). In this case the fiber is negatively, the dye ions positively charged and when salt is added, the absorption, and also the rate of diffusion of these colors in cellulose, decrease, as long as sufficient dye has not been absorbed to reverse the intrinsic negative charge of cellulose.

There is, therefore, no need to assume aggregation as a major factor in the behavior of dyes. There is indeed little or no real evidence of its existence at the temperatures commonly used in technical dyeing. More or less implicitly recognizing the importance of the electrical "work terms" in the theory of dyeing, various investigators have attempted to avoid its direct measurement by considering the thermodynamics of a

process in which the dye anion is adsorbed while the equivalent quantity of cations also enter the equipotential region, so that the electrical work term cancels out. This was first done by Hanson, Neale and Stringfellow (10), who showed that the hypothesis of specific adsorption of the dye *anion* led to a simple explanation of the salt effect. Similar treatments have been put forward by Willis, Warwicker, Standing and Urquhart (19), and by Gilbert and Rideal (20). It would seem that further progress in the theoretical study of dye absorption now awaits measurements from some entirely new angle, and that attempts further to elaborate the mathematical treatment of the absorption—dye concentration—salt concentration—temperature relationship may be premature.

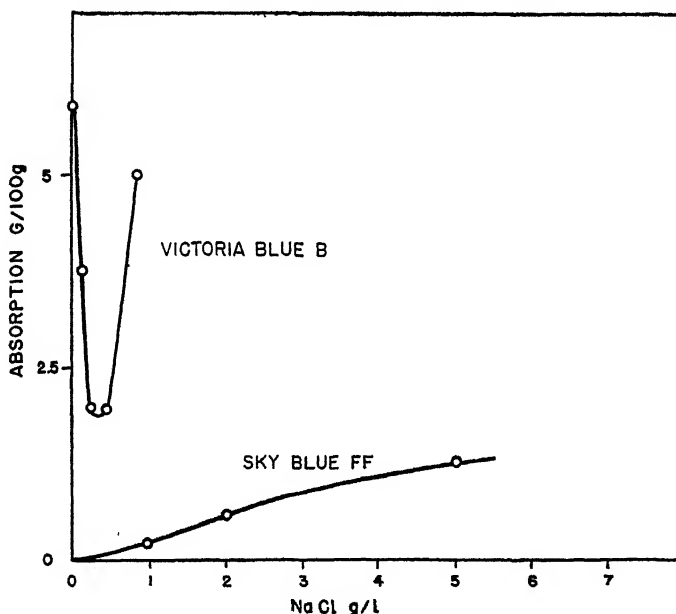
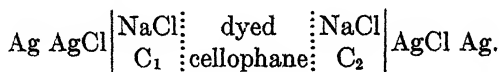


FIG. 5  
Effect of NaCl on Absorption of Victoria Blue B (Cationic)  
and of Sky Blue FF (Anionic) by Cellophane at 70°C.

Wahbi and Usher (21) made a useful attempt to throw fresh light on the problem by measuring the distribution of ammonium and chlorine ions between cellophane dyed with Sky Blue FF and the solution in which it was immersed. They used direct chemical analysis by titration, but the unavoidable errors of experiment were such as to make the results of little more than qualitative value. The work, however, is of fundamental importance, in establishing by direct chemical analysis, that the concentration of chloride ion in the dyed cellophane was definitely lower than in the external solution.

Neale has more recently attempted (22) to extend such analysis into a lower range of concentration, where the effect of the adsorbed dye anions in expelling other anions from the cellulose phase should be much more marked, by making use of a concentration cell:



The potential difference across such a membrane should be

$$\begin{aligned} E_m &= E_1 - E_2 + E_a \\ &= \frac{RT}{F} \left\{ \sinh^{-1} \frac{A}{2c_2} - \sinh^{-1} \frac{A}{2c_1} + u \ln \frac{x_2/A + u}{x_1/A + u} \right\} \end{aligned} \quad (i)$$

where

$$u = \frac{U - V}{U + V}, \text{ and } E_a \text{ is the diffusion potential}$$

and  $A$  is the concentration of immobile (*i.e.*, adsorbed) dye anions in the membrane. E.M.F. measurements were in good agreement with this equation, which was deduced on the assumption that adsorbed dye anions, together with mobile cations and anions of the dye and of the added electrolyte, are in an equipotential region consisting of the cellulose with its imbibed water. This was the fundamental assumption made by Hanson, Neale and Stringfellow (10) in their application of the Donnan membrane equilibrium to the problem of dyeing. Gilbert and Rideal also, in their thermodynamic treatment (20) of the adsorption of acid dye by wool, assume the adsorbing "surface" to be equipotential, and Willis, Warwicker, Standing and Urquhart (19) are, after some preliminary mathematical elaboration on a more general basis, forced to assume an equipotential space in their treatment of the absorption of Chrysophenine G by cellophane.

Some further advance beyond this point, in the direction of a more precise evaluation of the potential-distance function in the system, may be anticipated from the comparison of electrochemical and electrokinetic potentials at the surface of dyed fibers. Theoretical prediction unsupported by experimental evidence, may well be, in so complex a system, worse than useless. Neale and Peters (18) have indicated a direction in which the measurement of electrokinetic potential may proceed. The possibility of measuring the electrochemical potential of Cellulose also follows from equation (i).

For if KCl be the electrolyte and saturated KCl be used on one side of the membrane,

$$\text{then} \quad E_2 \approx 0$$

$$\text{and} \quad E_a \approx 0$$

so that  $E_1$  the potential between cellulose and solution (1) may be measured directly.

There are experimental difficulties in the way which have not yet been overcome, but the "cellulose electrode" is not altogether an impossibility.

#### REFERENCES

1. KNECHT AND HIBBERT, *New Reduction Methods*, 2nd Ed. (1925).
2. NEALE, *J. Soc. Dyers Colourists* **49**, 216 (1933).
3. NEALE, *J. Soc. Chem. Ind.* **52**, 881 (1933).
4. NEALE AND STRINGFELLOW, *J. Textile Inst.* **24**, P145 (1933).
5. NEALE AND STRINGFELLOW, *Trans. Faraday Soc.* **29**, 1167 (1933).
6. GARVIE, GRIFFITHS AND NEALE, *Trans. Faraday Soc.* **30**, 271 (1934).
7. HANSON AND NEALE, *Trans. Faraday Soc.* **30**, 386 (1934).
8. GRIFFITHS AND NEALE, *Trans. Faraday Soc.* **30**, 395 (1934).
9. NEALE AND PATEL, *Trans. Faraday Soc.* **30**, 905 (1934).
10. HANSON, NEALE AND STRINGFELLOW, *Trans. Faraday Soc.* **31**, 1718 (1935).
11. GARVIE AND NEALE, *Trans. Faraday Soc.* **34**, 336 (1938).
12. NEALE, *J. Soc. Dyers Colourists* **52**, 381 (1934).
14. BOULTON, DELPH FOTHERGILL AND MORTON, *J. Textile Inst.* **24**, 113 (1933).
15. MCBAIN AND LIU, *J. Am. Chem. Soc.* **53**, 59 (1931).
16. GORTNER AND CO-WORKERS, *J. Phys. Chem.* **32**, 641 (1928); **32**, 675 (1928); **34**, 1509 (1930); **35**, 309 (1931); **35**, 700 (1931); **42**, 641 (1938); **43**, 721 (1939).
17. NEALE, *Trans. Faraday Soc.* In press.
18. NEALE AND PETERS, *Trans. Faraday Soc.* In press.
19. WILLIS, WARWICKER, STANDING AND URQUHART, *Trans. Faraday Soc.* **41**, 506 (1945).
20. GILBERT AND RIDEAL, *Proc. Roy. Soc. (London)* **182A**, 335 (1944).
21. WAHBI AND USHER, *J. Soc. Dyers Colourists* **58**, 221 (1942).
22. NEALE, *Trans. Faraday Soc.* In press.





## BOOK REVIEWS

**Plastic Molding and Plant Management.** D. A. DEARLE. 196 pages. Chemical Publishing Co., Brooklyn, N. Y., 1944. Price \$3.50.

This interesting book describes the technique of compression and injection molding for the executives, engineers and foremen of the plastics molding industry. It is aimed particularly at production and managerial problems, discussing die design, costs, materials and methods. While emphasizing certain fundamentals of the industry, it points out many specific precautions which will save considerable time and expense for those who make use of them.

Chapters 1 and 2 review the types of plastics used. Chapter 3 is given over entirely to molds, their material, design, hobs, knock out mechanisms, etc. Chapters 4 and 5 give many hitherto little publicized details of compression and injection molding. Chapters 6 to 9 discuss, with the benefit of experience, problems of production, cost control, custom and proprietary molds, and plant management. These latter chapters are well written and are a distinct addition to the many recent books on the general subject of plastics. Mr. Dearle writes as a molding specialist and demonstrates an excellent knowledge of the inside conditions of such a plant.

Chapter 10 lists a series of questions and answers on design, production and costs. The final chapter, 11, points out future applications in various fields.

For general subject matter, especially on the materials of plastics, this book should be augmented by additional reading, such, for example, as "The Technology of Plastics and Resins" by Mason and Manning; D. Van Nostrand, 1945.

Mr. Dearle has not attempted to give a comprehensive picture of the materials of plastics. Occasionally this detracts from the text. For example, on page 9 he describes phenolic molding board as merely a mechanically mixed phenolic resin and fiber, which does not depict properly this material. But in his principal subject of molding procedures and costs he has made a distinct contribution to the literature on plastics.

DAVID M. BUCHANAN

ROBERT J. MOORE, Bakelite Corporation

**Advances in Carbohydrate Chemistry.** Edited by W. W. PIGMAN AND M. L. WOLFROM, with 13 contributors. xii + 374 pages, 15 × 23 cm. Academic Press, Inc. 125 E. 23rd St., New York 10, New York, 1945. Price \$6.00.

This is the first of a projected annual series dealing with topics in the field of carbohydrates. Eleven chapters, 15 to 52 pages in length, make up the present volume and each has been done both critically and well. Careful editorial scrutiny is evident from the uniformity found in the various chapters. The topics themselves, however, are widely separated including as they do such extremes as pure organic chemistry, high polymers, and carbohydrate metabolism. Each chapter is a critical and historical review such as we are accustomed to find in "Chemical Reviews."

Tipson's chapter on *Chemistry of the Nucleic Acids* is the longest one and is presented with exceptional clarity. Schoch's treatment of *The Fractionation of Starch* is an authoritative treatment. Hudson's discussion of *The Fischer Cyanohydrin Synthesis* includes hitherto unpublished material from Emil Fischer's records. Workers intending to enter the field of polyuronides will find helpful the discussion of methodology by Anderson and Sands. Each of the other chapters also cover relatively inaccessible topics: "The Altrose

Group" (Richtmyer), "Carbohydrate Orthoesters" (Pacsu), "Thio and Seleno Sugars" (Raymond), desoxy sugars derived from "Cardiac Glycosides" (Elderfield), "Metabolism of Sugar Alcohols" (Carr and Krantz), "Starch Esters" (Whistler), and "Cellulose Organic Esters" (Fordyce).

The typography of the book is excellent. A minor feature, but one appreciated by the reviewer, is that references are placed at the bottom of each page instead of being lumped at the end of the chapter. The reviewer has no doubt but that the hope of the editors, expressed in the preface, will be realized: "We hope that the "Advances" will receive the whole hearted support of carbohydrate chemists in particular and of the chemical profession as a whole." Doctors Pigman and Wolfrom are to be congratulated.

CHARLES D. HURD

✓ **Advances in Protein Chemistry. Volume II.** By M. L. ANSON AND JOHN T. EDSALL (Editors). xiii + 443 pages. Academic Press Inc., Publishers, 125 East 23rd Street, New York 10, N. Y.; 1946. Price \$6.50.

The second volume of this excellent new serial exceeds the promise of the first in fine discrimination as to timeliness and quality. As in the case of its predecessor, contributions to this volume are largely of a descriptive nature and may be described as exceedingly usable and some times exhaustive catalogues of the rapidly accumulating multiplicity of facts in this rich and varied field. As often in the past, protein chemistry has recently appeared to develop rapidly on its empirical periphery where it touches immunology, physiology, enzymology, physical chemistry, and technology. Progress within its own boundaries—discovery of the features of protein structure and of the laws characterizing the behavior of this particular class of macromolecules, is slower and less certain, and often characterized by premature (although temporary) acceptance of analogies with other branches of theoretical chemistry in terms of oversimplified physical models. It is a welcome feature of the present series that it concentrates on phenomena. Much of the recent solid progress in the field is due to the discovery of unsuspected phenomena sought, for example, by the disinterested immunologist, or discovered as a consequence of the development of new techniques.

The ten contributions to Volume II range in quality from excellent to adequate. In the category of excellent because of their completeness and critical balance are the articles by C. R. Dawson and M. F. Mallette on "The Copper Proteins"; Karl Myer's review "Mucoids and Glycoproteins"; and "The Reactions of Formaldehyde with Amino Acids and Proteins" by Dexter French and John T. Edsall. A noteworthy compendious review of the "Analytical Chemistry of the Proteins" (63 pages and 771 references) also requires special notice. Other contributions are: "The Microbiological Assay of Amino Acids" (Esmond E. Snell), "The Amino Acid Composition of Food Proteins" (Richard J. Block), "The Relationship of Protein Metabolism to Antibody Production and Resistance to Infection" (Paul R. Cannon), "Terminal Amino Acids in Peptides and Proteins" (Sidney W. Fox), "Wheat Gluten" (M. J. Blish), "Protein Denaturation and the Properties of Protein Groups" (M. L. Anson), and "X-Ray Diffraction and Protein Structure" (I. Fankuchen).

Of the nineteen contributions to the two volumes already published, only eight are by medical biochemists (members of medical school faculties). Government research institutes and agricultural laboratories, and the chemistry department of universities and technological institutes are well represented among the other contributors. The inclusion of contributions from industrial laboratories is particularly noteworthy. There is no more certain sign that protein chemistry is enlarging its horizons. It is inevitable that we should soon hear about a greater variety of reactive properties, and about a more widely representative group of substances than the classical egg albumen and serum

proteins. It is more than likely that this trend will lead to new discoveries, and ultimately to a better understanding of protein behavior and structure.

JACINTO STEINHARDT

**Analysis of Foods.** By ANDREW L. WINTON AND KATE BARBER WINTON. John Wiley & Sons, Inc., New York, N. Y., 1945. 946 pages plus 53-page index, 208 illustrations. Price \$12.

This book is an extensive compilation of methods of analysis applicable to foods, containing over 1000 methods and modifications, not only those accepted by the A.O.A.C., but also many methods, developed and tested by other laboratories, as published in chemical journals.

The contents are divided into two sections. Part I, on general methods of analysis, includes the discussion of all groups of foods under the accepted six major classifications of water, protein, fat, "nifext," fiber, and ash; and, in addition, directions for the determination of organic elements, alcohols, vitamins, coloring matter and food preservatives. In Part II, special methods and modifications applying to specific foods are taken up under the main types of foodstuffs, namely,—cereals, fats, vegetables, fruits, saccharine foods, dairy products and animal foods; and included also are methods of analysis of alcoholic beverages, alkaloids, food flavors, leaven and salt.

Introducing the section on general analytical methods are three special features of interest, i.e.,—a suggested short course in food analysis, equipment useful in the field, and reagents needed.

The suggested short course includes comprehensive assignments covering the common items of food analysis. It is of more value from a practical than from an academic viewpoint, since, in some instances, the analyses listed are somewhat lengthy and repetitious, especially for students well-versed in quantitative technique, and since the course does not take into consideration determinations of the vitamins.

This volume is a useful handbook of reference for those experienced in the field and offers a beginner a quick survey of available methods. However, since, for the most part, the discussions of methods (especially those on vitamin determinations) do not include a critical comparison or precautions to be observed, the book is limited in use for the beginner.

Winton's "Analysis of Foods" shows an arduous research into the literature and great breadth of subject matter. It should prove very useful in the field because of the wealth of material included in one volume.

M. IRENE BAILEY

✓ **The Microscope and its Use,** By F. J. MUÑOZ AND H. A. CHARIPPER. Chemical Publishing Co., Brooklyn, N. Y. 1943.

Probably no other precision instrument is used as widely in education, research, medicine and industry as the microscope. And certainly no other instrument is so commonly misused out of ignorance or neglect. Fortunately, in recent years several books have been published which explain in simple and adequate language the theory of the microscope and give practical advice for its proper use. The book by Muñoz and Charipper was designed especially for the general user of the microscope, for students and technicians. Emphasis is laid, therefore, on the practical side and the discussion of optics is restricted to a bare minimum.

The first chapter contains a very interesting account of the history of magnifiers and microscopes, from the rock crystal discovered in the ruins of Nineveh to the electron microscope. The next chapter introduces the modern microscopes and describes the various optical and mechanical parts. This is the weakest chapter of the book. Even

the general user of the microscope should know more about the optics of this wonderful instrument than is presented here. Furthermore, in the attempt to reduce technical explanations to a minimum many new terms are introduced without defining them. Many can thus be understood only much later in the book or not at all. This makes a real understanding of the parts of the microscope very difficult. The most common sins against the microscope have to do with illumination and so a special chapter on lamps and their use is certainly justified. This is a good chapter, making it very clear how to illuminate a microscope and why this has to be done so carefully if we want the lenses to give us their best. Most microscopists will have to use a microtome. A chapter is devoted to this instrument and the detailed instructions for its use and the discussion of all possible troubles and their remedies should prove very useful to the student.

A straightforward chapter on the care and use of the compound microscope and one on the dissecting microscope follow.

Specialized types of the microscope like the metallurgical and the polarizing microscope are discussed at some length. Next we are told briefly about some accessories like special objectives and oculars, measuring devices, counting chambers, camera lucida, comparison and demonstration oculars. The few pages on photomicrography are too short and inadequate even for an elementary and practical book. The last chapter lists a series of common errors in the use of the microscope and will be a great help to the beginner.

The glossary and index are good and make up for didactic shortcomings of some chapters. The book is well illustrated with photographs and diagrams, though there is perhaps too much emphasis on Spencer equipment. Paper and print are excellent. The book can be recommended as a first introduction to the microscope and especially to people who are mainly interested in the practical application and want a short and simple guide. Those however who are also interested in the optics of the microscope, who use it in research, in photomicrography, etc., will expect more than is offered here and will find books like Allen or Shillaber better suited to their needs.

HANS RIS,  
New York, N. Y.

## QUATERNARY AMMONIUM SALTS AS COLLOIDAL ELECTROLYTES

H. F. Walton, E. N. Hiebert and E. H. Sholtes

*From the Chemical Laboratory of Northwestern University, Evanston, Illinois*

*Received June 27, 1946*

### INTRODUCTION

In recent years quaternary salts of the long-chain alkyl-benzylammonium type have come into use as germicides (1) and surface-active agents. They are colloidal electrolytes in aqueous solution and, like other salts with long-chain cations, have received less study than colloidal electrolytes with long-chain anions. One such salt, dodecylbenzyltrimethylammonium chloride, was available to the authors in pure form and was chosen for study. Tests were also made with the corresponding hexadecyl salt. The object was to determine their critical concentrations and osmotic behavior, and to study the association of the chloride ions with the positively charged micelles. Freezing point depressions were determined for the dodecyl salt, and the activity of hydrochloric acid was measured in solutions of each quaternary salt.

### MATERIALS

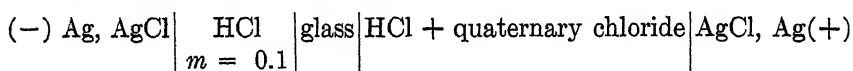
*Dodecylbenzyltrimethylammonium chloride* was, in part, prepared by Drs. Romeo Gauley and Byron Riegel of this laboratory from benzyl chloride and dodecyltrimethylamine and, in part, supplied by the Stillman Company, Aurora, Illinois. It was a light, colorless, crystalline powder which, after recrystallization from ethyl acetate, melted at 47.0°–48.0°C.; it was freely soluble in water at room temperature, giving clear solutions. The chloride ion content of the recrystallized material, determined by electrometric titration, was 97.0% of the theoretical for  $C_{12}H_{25} \cdot C_6H_5CH_2 \cdot (CH_3)_3NCl$ . On long storage, the melting point fell to 41°C., with an accompanying fall in chloride content and a slight rise in the acidity of the aqueous solutions. The salt appeared to undergo slow hydrolysis, but this was not investigated thoroughly.

*Dodecylbenzyltrimethylammonium Sulfamate.* An aqueous solution of this salt was prepared by mixing equivalent amounts of solutions of the chloride and silver sulfamate and removing the silver chloride centrifugally.

*Hexadecylbenzyltrimethylammonium chloride* was obtained from the Röhm and Haas preparation "Triton K-60," which is a paste containing 21% of this salt and 4% of hexadecyl alcohol. The paste was mixed with warm water and the hexadecyl alcohol extracted, first with ether and then with hexane. (In one attempted extraction a thixotropic gel formed, but otherwise two liquid layers resulted). The hexane was removed by heating in the air in an open dish. The resulting solution was opalescent at 50°C., the temperature at which measurements were made, and deposited solid at lower temperatures. Its chloride ion concentration was determined by conductivity titration.

#### APPARATUS

The freezing point depressions were determined by the Beckmann method. The activity of hydrochloric acid in the solutions was found from the electromotive force of the cell



A Leeds and Northrup "Std. 1199" glass electrode, diameter 22 mm., was used; the electromotive force was read to 0.1 millivolt, using a Leeds and Northrup student potentiometer with direct current amplifier. The temperature of the cell was controlled manually to  $\pm 0.2^\circ\text{C}$ . The glass electrode showed a perfect hydrogen electrode function against solutions of hydrochloric acid; its asymmetry potential was very small and was checked at every run. The electrodes came to equilibrium rapidly with the solutions.

#### RESULTS

##### *Freezing Point Depressions*

The data for the dodecyl quaternary chloride and sulfamate are given in Table I, and the osmotic and activity coefficients (the latter calculated by the method of Randall) are shown in Fig. 1. They should be regarded as preliminary, since the Beckmann technique was used. The Scatchard method would give more accurate results.

McBain and Brady (2) have shown that, if the osmotic coefficient  $g$  is plotted against  $\log(m/m_{0.5})$ , where  $m_{0.5}$  is the molal concentration at which  $g = 0.5$ , several different straight-chain colloidal electrolytes give points falling on one curve, while different branched-chain colloidal electrolytes give points falling together on a second curve, which is less steep than that for straight-chain compounds. If the values of  $g$  for the chloride given in Table I are so plotted, a curve is obtained which falls midway between the straight and branched chain curves of McBain and Brady.

TABLE I

*Freezing Point Depressions of Dodecylbenzyltrimethylammonium Salts in Water*

Salt	Molality	$\sqrt{m}$	Freezing point depression	Osmotic coefficient
	<i>m</i>		$^{\circ}\text{C.}$	$\phi$
Chloride	0.00760	0.087	0.0295	1.04
	0.00855	0.092	0.033	1.03
	0.0157	0.125	0.043	0.735
	0.0184	0.136	0.0425	0.62
	0.0199	0.141	0.045	0.605
	0.0316	0.178	0.049	0.415
	0.0321	0.179	0.048	0.40
	0.0395	0.199	0.053	0.36
	0.0413	0.203	0.053	0.345
	0.0467	0.216	0.0545	0.315
	0.0773	0.278	0.065	0.225
	0.0797	0.282	0.074	0.250
Sulfamate	0.023	0.152	0.070	0.25
	0.046	0.214	0.084	0.49
	0.093	0.305	0.088	0.82

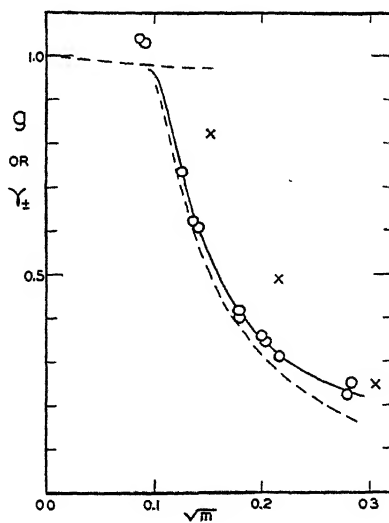


FIG. 1

Osmotic and Activity Coefficients of Dodecylbenzyltrimethylammonium Salts.

Circles, chloride; crosses, sulfamate. Circles and crosses, osmotic coefficients; broken line, activity coefficient of chloride.



The sulfamate salt is much less associated in dilute solutions than the chloride salt. No systematic study of the influence of the counter-ion on the association of colloidal electrolytes has yet been made, although it is known in a qualitative way that the nature of the counter-ion has an effect, especially with salts of long-chain cations.

### *Hydrochloric Acid Activities*

(a) *At Constant Total Molality.* One series of measurements was made in which the ratio of hydrochloric acid to dodecylbenzyltrimethylammonium chloride was varied over a wide range with constant total molality of 0.100. The results are shown in Fig. 2. The variation of activity

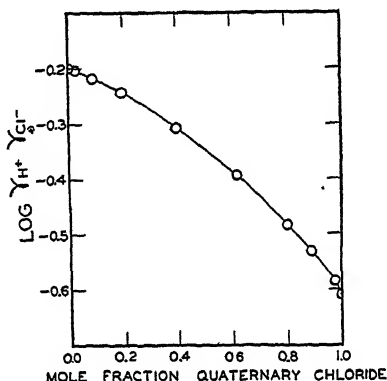


FIG. 2

Activity Coefficient of Hydrochloric Acid in Mixtures with Dodecylbenzyltrimethylammonium Chloride of Total Molality 0.100 at 25°C.

coefficient with composition is very different from that found with mixtures of hydrochloric acid and simple electrolytes, *e.g.*, potassium chloride. In the latter case, the relation between ( $\log \gamma$ ) and mole fraction is linear, and the total change in activity coefficient is relatively small (3). The effect of the quaternary ammonium salt in reducing the stoichiometric activity coefficient of hydrochloric acid is very marked. This may be partly an electrostatic effect, but there is evidence that the "ionic strength" of colloidal electrolyte solutions, once micelle formation is fully established, is not very different from that of an equimolar binary electrolyte (2). It seems likely, therefore, that this reduction in activity is mainly due to association of chloride ions with the micelles.

If one postulates that the true (as distinct from stoichiometric) activity coefficients of the hydrogen and chloride ions are the same in the quaternary salt solution as in hydrochloric acid of equal molality, and also that no hydrogen ions enter the micelle, then the difference between

$\log \gamma_{H^+} \gamma_{Cl^-} (m_{H^+} = 0.1)$  and  $\log \gamma_{H^+} \gamma_{Cl^-} (m_{H^+} = 0)$  is equal to  $\log (\text{free } Cl^- / \text{total } Cl^-) = -0.41$ , whence the ratio of free  $Cl^-$  to total  $Cl^-$  in the quaternary salt solution is 0.39.

By plotting  $\gamma_{H^+} \gamma_{Cl^-}$  against mole fraction, a nearly straight line is obtained, indicating that the proportion of chloride ions bound by the quaternary cations does not change much with the mole fraction of quaternary salt.

(b) *At Low HCl-Quaternary Salt Ratios.* The great majority of measurements were made with the mole fraction of hydrochloric acid from 0.05 to 0.005. Solutions of quaternary salt of different molalities were made up, and successive small quantities of hydrochloric acid added from a microburette, as in a previous work by one of the authors (4). The limiting activity coefficients of hydrochloric acid for zero acid concentration and different salt concentrations are shown in Fig. 3. The dodecyl

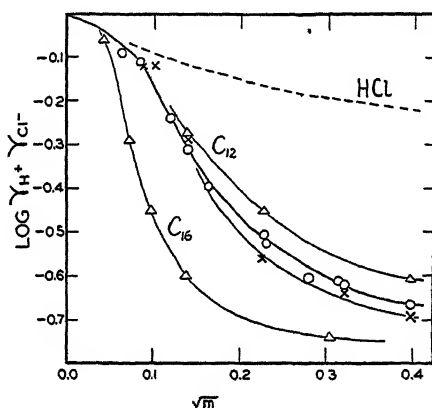


FIG. 3

Activity Coefficient of Hydrochloric Acid in Quaternary Salt Solutions.

$C_{12}$ , dodecylbenzyltrimethylammonium chloride;  $C_{16}$ , the hexadecyl salt. Triangles, 50°C.; circles, 25°C.; crosses, 0°C. Abscissas are square roots of molalities of quaternary salt.

salt was run at 0°, 25° and 50°C.; the hexadecyl salt at 50°C. only, because of its low solubility at lower temperatures. Tests showed, incidentally, that solubilization of hexadecyl alcohol by the hexadecyl salt did not affect these activity measurements. From the graphs the following conclusions can be drawn:

1. Hexadecylbenzyltrimethylammonium chloride starts to associate at about one-quarter the critical concentration of the dodecyl salt. This agrees with a general observation (5) that the addition of two carbon atoms to a hydrocarbon chain roughly halves this critical concentration.

2. Neither the critical concentration nor the activity of hydrochloric acid is greatly affected by temperature, although there is evidence of slightly increased dissociation of the micelles as the temperature rises. This effect of temperature has been noticed by other workers (6).

3. At the higher concentrations,  $\log \gamma_{H^+} \gamma_{Cl^-}$  in both cases begins to level off while  $\log \gamma_{\pm}$  of the dodecyl salt continues to fall rapidly. The activity of the dodecyl salt remains almost constant as the concentration is increased, while the activity of the hydrochloric acid, and hence, presumably, that of the chloride ion, rises in nearly direct proportion to concentration. The concentration of the unassociated quaternary cation is apparently *falling* as the concentration rises. A similar effect was noticed in an investigation of dodecanesulfonic acid (4).

From the data given,  $\gamma_{H^+}/\gamma_{M^+}$  can be calculated, where  $M^+$  is the dodecyl quaternary cation. This ratio is 13 for 0.1 molal salt, and at this point is increasing as the square of the molal concentration.

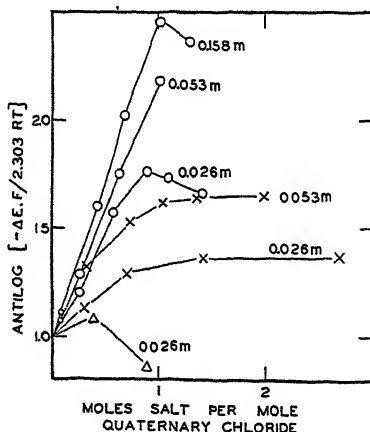


FIG. 4

Effect of Salts on Electromotive Force.

$\Delta E$  = increase in E.M.F. Circles, sodium perchlorate added; crosses, potassium nitrate; triangles, potassium sulfamate. The molal concentrations of the quaternary chloride are given.

(c) *Effect of Added Simple Salts at Low HCl-Quaternary Salt Ratios.* If a salt such as potassium nitrate is added to a solution of quaternary salt containing a little hydrochloric acid, the activity of the latter rises, as is shown by a fall in electromotive force of the cell. The electrostatic effect of increased salt concentration is to *lower* all activities, so it would seem that the potassium nitrate is increasing the concentration of hydrogen or chloride ions. Presumably the nitrate ions displace chloride ions from the micelles. If this is so, we can form an estimate of the proportion of

chloride ions bound in the micelles by adding an excess of nitrate and observing the maximum rise in hydrochloric acid activity. The method will give an *underestimate* of the bound chloride ion, because (a) the salt addition will reduce the true activity coefficients, (b) the displacement of chloride by nitrate ions may not be complete.

Experiments were made in which solid potassium nitrate was added to two dodecyl quaternary salt solutions of different molalities, each containing some 2 moles *per cent* of added hydrochloric acid. The results are shown in Fig. 4. The tests were confined to the lower quaternary salt concentrations because at higher concentrations the quaternary nitrate separated as an oil. It was hoped to avoid this limitation by using potassium sulfamate, since the quaternary sulfamate is very soluble but, as will be seen from Fig. 4, the sulfamate caused little or no increase in hydrochloric acid activity. It was to test the hypothesis that this corresponded to a low affinity of sulfamate ions for the micelles that the freezing point measurements, given above, were made with the quaternary sulfamate.

Similar tests were made in which anhydrous sodium perchlorate was added to dodecyl salt solutions containing 2 moles *per cent* of hydrochloric acid. In this case, the sparingly soluble quaternary perchlorate was precipitated and the hydrochloric acid activity rose, due to liberation of the micellar chloride ions. The addition of sodium perchlorate in effect substituted sodium chloride for quaternary chloride at constant total molality. The ionic strength was probably lowered, rather than increased, and hence the maximum rise in hydrochloric acid activity is believed to give a slight *overestimate*, rather than an underestimate of the bound chloride ions.

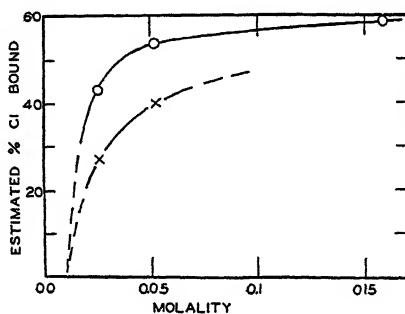


FIG. 5

Displacement of Bound Chloride.

The maximum ( $-\Delta E$ ) of Fig. 4 are considered to give the increase in chloride ion concentration due to displacement of chloride from the micelles. Ordinates are estimated proportions of total chloride bound in the micelles. Circles, sodium perchlorate added; crosses, potassium nitrate.

The results of all the salt addition tests are shown in Fig. 4. The ordinates are ( $\text{antilog } -\Delta E.F/2.303 RT$ ), that is, the factor by which the hydrochloric acid activity is multiplied through addition of salt. If the maximum value of this factor is  $B$ , then  $(B-1)/B$  is the estimated fraction of chloride ions bound by the positive micelles; this fraction is plotted against concentration in Fig. 5. It is concluded that, as the dodecyl quaternary ammonium salt concentration increases, the proportion of chloride ions bound in the micelle tends to a maximum of about 55–60%. This is about the same as the estimated proportion of micellar hydrogen ions in dedocanesulfonic acid solutions (4).

#### SUMMARY

1. Freezing point depressions in solutions of dodecylbenzyltrimethylammonium chloride and sulfamate have been measured. The osmotic coefficients of the chloride fall midway between the generalized curves of McBain and Brady for straight and branched chain compounds. The sulfamate is less associated in dilute solutions than the chloride.

2. The activity of hydrochloric acid has been measured electrometrically in mixtures of the above quaternary chloride and hydrochloric acid having constant total molality.

3. Activity coefficients of hydrochloric acid have been measured at 3 temperatures in solutions of dodecylbenzyltrimethylammonium chloride and its hexadecyl homologue containing a small proportion of added hydrochloric acid.

4. The effect of simple salts on the activity of hydrochloric acid in such solutions has been investigated.

5. From the data it is concluded that, in the concentration range where micelles are fully established, about 60% of the chloride ions are combined in the micelles of the dodecyl salt. It also appears that the concentration of simple quaternary cations falls as the quaternary salt concentration rises in this range.

#### ACKNOWLEDGMENTS

We are indebted to Romeo Gouley and Byron Riegel of this laboratory, the Stillman Company and the Röhm and Haas Company for supplying materials. This investigation was in part supported by a grant from the Abbott Fund of Northwestern University.

#### REFERENCES

1. KUHN, R., JERCHEL, D., AND WESTPHAL, O., *Ber.* **73**, 1095 (1940).
2. MCBAIN, J. W., AND BRADY, A. P., *J. Am. Chem. Soc.* **65**, 2072 (1943).
3. GUNTELBERG, E., *Z. physik. Chem.* **123**, 199 (1926).
4. WALTON, H. F., *J. Am. Chem. Soc.* **68**, 1182 (1946).
5. SCOTT, A. B., AND TARTAR, H. V., *J. Am. Chem. Soc.* **65**, 692 (1943).
6. WRIGHT, K. A., AND TARTAR, H. V., *J. Am. Chem. Soc.* **61**, 544, 549 (1939).

# MICELLAR ASSOCIATION OF IONIC AND NON-IONIC DETERGENTS IN NON-IONIZING SOLVENTS

Emanuel Gonick \*

*From the Department of Chemistry, Stanford University, California*

*Received June 25, 1946*

## INTRODUCTION

Aqueous solutions of paraffin chain fatty acid and amine salts are characterized by the association of the solute into colloidal micelles. This behavior, along with many of their other characteristic properties, may be explained by the dual nature of these molecules: the hydrocarbon body confers upon them the hydrophobic solubility characteristics of a hydrocarbon, while the ionic "head" confers the hydrophilic properties of an ordinary soluble inorganic electrolyte. The question arises: would this dual nature operate to cause similar behavior in a non-ionizing solvent such as benzene or cyclohexane?

Measurements of freezing point depressions produced by two soluble soaps in benzene, viz., hexanolamine oleate and hexanolamine caprylate, are presented here, to show that this association indeed occurs. In addition, evidence is presented showing that the non-electrolytic detergent, nonaethyleneglycol (mono) laurate† is associated in cyclohexane. However, it is not associated in benzene where the apparent molecular weight is 600 as compared with the formula weight, 597. Data to be reported elsewhere demonstrate that this compound forms micelles in water.

## EXPERIMENTAL

Freezing point depressions were determined by the Beckmann method with the usual precautions.

Thiophene-free benzene and Eastman Kodak Company white label grade cyclohexane were used. Both solvents were thoroughly dried over Drierite ( $\text{CaSO}_4$ ) and redistilled, the middle portions being taken. Solutions were made up gravimetrically. Concentrations are expressed in moles of solute/1000 g. of solvent. The hexanolamine salts are the same as those used in previous work on aqueous solutions (1, 2). The hexanolamine, from which the salts were made by direct combination with the acids, is 4-methyl-4-aminopentanol-2.

\* Bristol-Myers Company Postdoctorate Research Fellow in Chemistry.

† Kindly supplied by the Glyco Products Co., 230 King St., Brooklyn, N. Y.

The results summarized in the following table are expressed in terms of the osmotic coefficient,  $g$ , the ratio of the observed freezing point depression to the theoretical depression for a non-ionizing solute of the same concentration in the non-ionizing solvent. The calculations are based on a cryoscopic constant of  $5.12^{\circ}\text{C.}$  for benzene and  $20.0^{\circ}\text{C.}$  for cyclohexane. Its reciprocal,  $1/g$ , gives a number average degree of association of the micelles present.

*Freezing Point Depressions and Osmotic Coefficients*

Compound	Solvent	Conc.	Freezing point depression	Osmotic coefficient
Hexanolamine oleate	Benzene	0.1576 <i>m</i>	$\theta$ 0.310°	$g$ 0.384
Hexanolamine oleate	Benzene	.08892 <i>m</i>	.179	.393
Hexanolamine caprylate	Benzene	.07242 <i>m</i>	.097	.262
		.0511 <i>m</i>	.058	.221
Nonaethyleneglycol (mono) laurate	Cyclohexane*	.1014 <i>m</i>	.493	.242
Nonaethyleneglycol (mono) laurate	Benzene	.1187 <i>m</i>	.603	1.00

\* Containing 0.239 moles water/1000 g. of cyclohexane. See text.

The data for the two hexanolamine salts in benzene show that the average degree of association of the oleate is approximately three-fold and that of the caprylate is about four-fold. Presumably this represents a mixture of simple molecules with colloidal particles of varying sizes.

The results obtained with nonaethyleneglycol (mono) laurate present features of special interest inasmuch as this compound by itself is insoluble in cyclohexane, but can be brought into solution by the addition of water, which also goes into solution. The solution was thus 0.1014 molal in the laurate and 0.239 molal in water. If each exerted its full effect on the freezing point lowering, that due to the laurate would be  $2.028^{\circ}$  and that due to the water  $4.78^{\circ}$ , a total of  $6.81^{\circ}$ . In contrast to this the observed freezing point lowering was only  $0.493^{\circ}$ , less than one-fourth as much as would be expected from the fully dispersed laurate alone.

If the water is assumed to have no effect on the freezing point of the solution, an osmotic coefficient of 0.242 is obtained for nonaethyleneglycol (mono) laurate in cyclohexane. The correctness of this interpretation is supported by two lines of evidence: (1) the freezing points of aqueous solutions of soaps are unaffected by solubilized hydrocarbons, these being incorporated within the micelles; and (2) parallel results since obtained Dr. S. R. Palit \* in this laboratory showing that the freezing points

\* To be communicated to *J. Soc. Chem. Ind.*, London.

of electrolytic detergents in benzene are unaffected by solubilized water. This shows that the blending of benzene with water by detergents involves micelle formation.

#### SUMMARY

The detergents hexanolamine oleate and caprylate are associated in anhydrous benzene solution.

The non-electrolytic detergent nonaethyleneglycol (mono) laurate consists of simple molecules in benzene. However, it is associated in cyclohexane containing 0.43% water, the freezing point lowering being only one-fourth of that which would be caused by detergent alone if all were present as simple molecules, or one-tenth of that due to simple water molecules alone, or 7% of their sum. This shows that water blended with cyclohexane is solubilized in colloidal particles of detergent.

#### REFERENCES

1. GONICK, E., *J. Am. Chem. Soc.* **68**, 177 (1946).
2. GONICK, E., AND MCBAIN, J. W., *J. Colloid Sci.* **1**, 127 (1946).





# INVESTIGATION OF THE FORMATION OF CHROMIUM SALT COMPLEXES BY MEANS OF ORGANOLITES

K. H. Gustavson

*From C. J. Lundbergs Läderfabriks A.B., Valdemarsvik, Sweden*

*Received July 8, 1946*

## INTRODUCTION

Information regarding complex formation by chromium salts, primarily basic chlorides and sulfates, is theoretically, as well as practically, important, particularly for the theory of the chrome tanning process. The methods available for the quantitative determination of the charged complexes formed in aqueous solutions of these salts are rather unsatisfactory and uncharged complexes can neither be separated nor directly determined (1). Reference is made to the literature regarding our present knowledge of the chemistry of these basic chromium compounds (1).

The composition of cationic chromium complexes in chlorides and sulfates has been investigated by means of base-exchanging zeolites (sodium and ammonium permutits) which remove cationic complexes from solution (2). By analysis of the "chromium-permutit" formed and from the exchange ratio of sodium ions and chrome-complex cations, the number of acid groups in the chromium complex and its average charge were obtained. However, the permutit method shows many weaknesses. Only positively charged complexes are removed. Further, the theoretical treatment of such complicated and changing systems as those of alkali permutit in solutions of salts of sodium and chromium is exceedingly difficult and, above all, the acid-sensitive permutit is attacked and partly decomposed by the free acid resulting from the hydrolysis of solutions of these basic chromic salts. This may lead to disturbance of the hydrolysis of the solution of chromic salt and even to the precipitation of insoluble chromium compounds.

By the introduction of acid resistant, highly efficient ion exchangers of the synthetic resin type (organolites) (3), the shortcomings inherent in mineral exchangers were removed. Extensive investigations of chromium salts during the last six years (4), employing organolites, show that quantitative separation of positively, negatively and uncharged chromium complexes and information concerning their composition and properties may be obtained by interaction of organolites with solutions of these salts. An outline of the technique and some typical results will be given in this paper.

Organolites have been employed in analytical chemistry for removal of disturbing ions, particularly by *Samuelson* (5). As far as the author is aware, this convenient tool for determining the composition of complex salts has not been utilized previously.

### MATERIALS

As a cation exchanger, a sulfonic acid of phenol-aldehyde resin (*Wofatit KS*) was used (6). The technical product, commonly employed as a water softener, was purified by repeated digestions in 3 *N* solution of HCl. The treated stock was washed free from Cl<sup>-</sup> and used in H ion saturated state. Its exchange capacity, measured by titration of liberated H ions by treatment with 2*M* NaCl-solution, was 2.0 milliequivalent H<sup>+</sup>/1 g. of dry substance. It did not fix any measurable amounts of non-cationic chromium in special tests with solutions of such compounds. *Wofatit M*, a commercial anion exchanger, consisting of the hydrochloride of condensed aliphatic and aromatic amino compounds served as anion exchanger. It was also pretreated with HCl. This organolite possesses slight affinity for certain cationic chromium complexes.

Basic chromic salts are characterized by their *per cent acidity* which gives the percentage of valencies of chromium compensated by acid groups. In a basic salt, for instance, the type  $[\text{Cr}_2(\text{OH})_2\text{SO}_4]\text{SO}_4$ , the "over all" acidity of the sulfate is  $\frac{2 \times 2}{2 \times 3} \times 100 = 67\%$  and the acidity of the cationic complex (sulfato-complex)  $= \frac{2}{2 \times 3} = 33\%$ .

The basic chromic sulfates employed were prepared from C.P. grades of sodium bichromate and sulfuric acid, reduced with sucrose in concentrated, boiling solution. The chromic sulfate *without* neutral sulfate was obtained by reducing a mixture of 2 *M* chromic acid and 2 *M* sulfuric acid with a 30% solution of H<sub>2</sub>O<sub>2</sub> slowly (24 hrs), at a temperature of 6–8° C. The highly basic sulfates were obtained from the 67% acid sulfate by addition of sodium carbonate, followed by boiling the solutions. The chlorides corresponding in composition to the empirical formula  $\text{Cr}_2(\text{OH})_2\text{Cl}_4 \cdot 2 \text{NaCl}$  were prepared by the method given for chromic sulfate. The basic chloride without sodium chloride was obtained by dissolving freshly precipitated hydrous chromic oxide in HCl (1:1). The highly basic chlorides were prepared by addition of soda to the 67% acid chromic chloride.

### METHOD

Portions of 25–30 g. moist organolite (ca. 50% dry substance) were packed in a 16 mm. wide burette 500 mm. high, the bottom and top of

the layer being covered with glass wool. Fifty ml. portions of solutions containing 1-4 milliequivalents (meq.) of Cr were slowly percolated through the water-covered cation exchanger during 10-15 min., followed by 50 ml. of water at the same rate. The filtrates were collected in a 100 ml. volumetric flask. The chrome content of the filtrate (non-cationic Cr) was determined. In the first run with fresh organolite, certain difficulties in the oxidation of chromium by sodium peroxide may be experienced, probably caused by organic substances dissolved out from the organolite. In a used organolite regenerated with HCl, such complications are less evident. The filtrate is *immediately* titrated with 0.1 N NaOH (methyl red) and further in *boiling* solution using phenolphthalein as indicator. The former value gives the ionic acid groups in the original chromium salt and the difference in values between the two titrations represents the complexly bound acid groups in the noncationic complexes. It is necessary, especially with sulfates, to carry out these titrations *immediately* after the collection of the filtrate, since sulfato-groups gradually leave the complex. On the other hand, chloro-groups in noncationic complexes are rather stable. The difference between the amount of total hydrolyzable acid groups in the original solution and the amount obtained by titrating the boiling solution is equal to the amount of acid groups directly attached to chromium in the positively charged complexes.

These are removed from the organolite by percolation of 50 ml. solution of hydrochloric acid (1:1 by volume), followed by 50 ml. water, during 25-40 min. time through the layer. In certain instances twice that amount of acid is required. In the collected filtrate chromium is determined. Also a gravimetric determination of sulfate held in the complex may be carried out (after precipitating chromium as chromium hydroxide, redissolving, reprecipitating and collecting the filtrates) as a check on the indirectly obtained value. For removal of chromium chloride complexes from organolite, 10%  $\text{H}_2\text{SO}_4$  is used if a direct determination of complexly held Cl-groups in the cationic complexes is required. The acid-treated organolite is freed from mineral acid by profuse percolation of water at a rapid rate through the column. It is then ready for further use.

The total exchange capacity of the layer of cation exchanger was 35-50 meq. It was thus present in great excess over the chromium compound, only 2-6% of its exchange capacity being utilized. In analysis of solutions of chromic salts containing neutral salts, as those prepared from sodium bichromate, commonly used for tanning, the first filtrate also contains an amount of H ions equivalent to the neutral salt content (exchanged Na ions). A correction is made for this acid; indirectly, for salts of known previous history, and by direct determination of the neutral salt in other instances. The use of ammonium or sodium salt of sulfonic acid organolite is advantageous in many cases, and required in

analyses of acid-sensitive complexes, such as sulfito chromiates. Further, the use of alkali organolites is advisable, if a subsequent separation of non-cationic complexes of the filtrate into uncharged and negatively charged constituents is planned, by taking the filtrate through the anion exchanger. This method has usually been employed for isolation of uncharged complexes in solutions of strongly basic chromic chlorides.

The anionic chromium complexes are determined by filtering the solution of chromic salt (1-4 meq.) through a layer of anion exchanger and determining the nonanionic chromium in filtrate. The fixed anions are removed by HCl (1:1) and the chromium content determined, thus serving as a control of the value obtained indirectly. Further, the exchange of Cl ions for anionic chromium is estimated.

This method gives values of high precision for the acidity of cationic and noncationic complexes (eq. acid groups on 1 eq. Cr in %), the average charge of the complexes and the content of various forms of the same, within a few hours' time. Duplicate analyses in different tubes, run side by side, generally showed a deviation of not more than 2% of the total amount of chromium present. The isolation and direct determination of uncharged complexes, heretofore not feasible, is especially valuable. A detailed characterization and information of the "aging factor" of solutions in a given concentration range are rapidly obtained by simple means.

## RESULTS

### *Composition of Basic Chromic Chlorides and Sulfates*

Two examples of typical analyses will be given. A solution of 67% acid chromium sulfate, corresponding in composition to the empirical formula  $\text{Cr}_2(\text{OH})_2(\text{SO}_4)_2 \cdot \text{Na}_2\text{SO}_4$ , containing 8.0 eq./l. Cr, was diluted to 0.4 eq. and *directly* analyzed. A portion = 5.0 ml. (2 meq. Cr), diluted to 50 ml., was pipetted into the organolite burette and filtered as described. The figures given are based on 1.0 meq. Cr and correction has been applied for the H ions derived from exchange of Na ions ( $\text{Na}_2\text{SO}_4$ ); in this instance, 0.33 meq.  $\text{H}^+$ . The filtrate contained 0.64 meq. noncationic Cr. The methyl red titration gave 0.12 meq.  $\text{SO}_4$  ions and the phenolphthalein titration in boiling solution 0.57 meq.  $\text{SO}_4$ . Thus,  $(0.57 - 0.12) = 0.45$  meq.  $\text{SO}_4$  is held in the noncationic complexes. Their average acidity is  $\frac{0.45}{0.64} \times 100 = 70\%$ . The acidity of the cationic sulfato-chromium complex

is  $\frac{0.67 - 0.57}{0.36} \times 100 = 28\%$ . The total acidity of the cationic chromium

sulfate is then  $\frac{0.12 + 0.10}{0.36} = 61\%$ . Analysis by the anion exchanger gave

0.10 meq. anionic chromium, containing 0.095 meq.  $\text{SO}_4$ . Its acidity is figured to be 95% and that of the uncharged complexes to 66%. The composition of the compound is: 36% of cationic complexes of the type  $(\text{Cr}_2(\text{OH})_2\text{SO}_4)^{2+}$ ; 10% of anionic complexes of the type  $(\text{Cr}_2(\text{OH})_2(\text{SO}_4)_3)^{2-}$  and 54% of uncharged complexes, empirically written as  $(\text{Cr}_2(\text{OH})_2(\text{SO}_4)_2)^0$ . Upon 24 hrs. aging of the diluted solution (0.4 eq./l. Cr) no anionic chrome was present. The content of uncharged chromium had decreased to 21%. After 4 weeks aging, equilibrium was practically attained. The percentage of cationic chromium was then 96%, the rest being in the uncharged state. The sulfato groups in the noncationic complexes are rather weakly held in contrast to such groups in cationic complexes. The basic chromium chlorides show the opposite degree of stability of chloro groups in the two forms of complexes, those in noncationic ones being firmly attached.

As an example of a basic chromic chloride, data are given for a 30% acid compound, prepared by the addition of sodium carbonate to a 67% acid chromic chloride of the type represented by the formula  $\text{Cr}_2(\text{OH})_2\text{Cl}_4 \cdot 2\text{NaCl}$ . An aged solution, containing 0.4 eq./l. Cr, was used. The filtrate contained 0.81 meq. noncationic Cr; found by anionic exchange to consist entirely of uncharged complexes. The titrations showed 0.13 meq. Cl-ions and 0.14 meq. Cl held in the uncharged complex. Thus, the cationic complex contained 0.03 meq. Cl on 0.29 meq. Cr which gives an average acidity of chloro-chromium complexes of 10%. The acidity of the uncharged portion was 17%. Its composition corresponds to the empirical formula  $(\text{Cr}_2(\text{OH})_2\text{Cl})$ . This complex did not diffuse through cellophane membranes. The cationic salt had an acidity of 84%. Solutions of highly basic chromic chlorides consist *mainly* of extremely basic, rather large, uncharged complexes, containing stable chloro groups. The rest is the normal type of cationic complex. It is interesting to note that *Bjerrum* and *Faurholt* (7) as well as *Manegold* and *Hofmann* (8) have found by quite different methods that the main constituents of excessively boiled, extremely basic chlorides and nitrates of chromium are two extremes: (1) a high-molecular, semi-colloidal fraction, and (2) simple hexaquo-chromium ions. Because of the high stability of Cl-groups in uncharged complexes, the composition of highly basic chlorides of chromium is practically independent of the concentration of the solutions; a solution of 6.0 eq./l. Cr, giving practically the same percentages of the two forms of chromium as the dilute solution (0.4 eq./l Cr).

Data on the different types of complexes present in solutions of various chlorides and sulfates of chromium are given in Table I.

It is evident from these data that chromic chlorides of acidities > 67% only contain cationic complexes. In dilute solutions of these salts, no chloro complexes are present but concentrated solutions contain

TABLE I

*The Composition of Solutions of Basic Chlorides and Sulfates of Chromium  
(at attained equilibrium at 20°C.)*

No.	Per- cent- age Acid- ity	Conc. eq./l. Cr	Composition corresponding to	Per cent cationic	Per cent un- charged	Per cent anionic	Per cent acidity of acido-Cr cations
				Chromium complexes			
Chlorides							
1	100	0.4	$\text{Cr}(\text{OH})_2\text{Cl}_3$	100	0	0	0
2	67	0.4	$\text{Cr}_2(\text{OH})_2\text{Cl}_4$	100	0	0	0
3	67	6.0	"	98	2	0	0
4	67	0.4	$\text{Cr}_2(\text{OH})_2\text{Cl}_4 \cdot 2\text{NaCl}$	100	0	0	2
5	67	6.0	"	96	4	0	10
6	50	0.4	$\text{Cr}_2(\text{OH})_3\text{Cl}_3 \cdot 3\text{NaCl}$	82	18	0	not determined
7	42	0.4	$\text{Cr}_4(\text{OH})_7\text{Cl}_5 \cdot 7\text{NaCl}$	61	39	0	" "
8	33	0.4	$\text{Cr}_2(\text{OH})_4\text{Cl}_2 \cdot 4\text{NaCl}$	30	70	0	" "
9	33	6.0	"	27	73	0	" "
10	26	0.4	$\text{Cr}_4(\text{OH})_9\text{Cl}_3 \cdot 9\text{NaCl}$	14	86	0	" "
Sulfates							
11	100	0.4	$(\text{Cr}_2(\text{OH})_2)_{12}(\text{SO}_4)_3$	100	0	0	8
12	83	0.4	$\text{Cr}_4(\text{OH})_2(\text{SO}_4)_5 \cdot 2\text{Na}_2\text{SO}_4$	92	8	0	32
13	67	0.4	$\text{Cr}_2(\text{OH})_2(\text{SO}_4)_2$	98	2	0	27
14	67	6.0	"	90	10	0	29
15	67	0.4	$\text{Cr}_2(\text{OH})_2(\text{SO}_4)_2 \cdot \text{Na}_2\text{SO}_4$	93	7	0	30
16	67	8.0	"	36	54	10	29
17	50	0.4	$\text{Cr}_4(\text{OH})_6(\text{SO}_4)_3 \cdot 3\text{Na}_2\text{SO}_4$	90	10	0	24
18	50	8.0	"	46	46	8	27

hydroxo-chloro complexes. In solutions of acidities < 60%, uncharged complexes are formed and their percentage increases rapidly with increasing basicity. The main constituent in extremely basic chlorides (acidities 20–35%) is uncharged chloro chromium complexes of an average composition corresponding to the empirical formula  $(\text{Cr}_2(\text{OH})_5\text{Cl})$ . Anionic complexes are not formed, even in the presence of high molarities of sodium chloride. In concentrated solutions of basic chromic sulfate of the type  $\text{Cr}_2(\text{OH})_m(\text{SO}_4)_n \cdot \text{Na}_2\text{SO}_4$  (No. 16), all 3 types of complexes are present. The main constituent of dilute solutions is the cationic type, only small amounts of neutral complexes being shown. The acidity of the sulfato-Cr-cations varies from 20–40%. In dilute solutions of pure basic sulfates, the content of noncationic forms is very slight. With increasing chrome concentration the amount of cationic complexes is well main-

tained (No. 14), just the reverse of the behavior of the corresponding sulfate containing sodium sulfate (No. 16).

It has been proved that non-cationic chromic sulfates possess rather low affinity for hide protein, compared to the cationic type. (9). It may be pointed out, that the different effect of the chrome concentration of the tanning bath upon chrome fixation by collagen, shown by basic chlorides, basic sulfates *with* and *without* sodium sulfate, should, in the light of these findings be less enigmatic, since the general trend of their fixation curves (10) shows striking similarity to the curves representing the amount of *cationic* chromium as a function of the concentration of chromic salt. The directing influence of the constitution of the chromic compounds is clearly perceptible. This interesting aspect will be treated in another connection.

#### *The Effect of Neutral Salts and Complex Formers*

A number of problems have been investigated by means of the organolite method. Only the effect of certain alkali metal salts on solutions of basic chromic salts will be exemplified. By one min. boiling of a solution of pure basic chromic sulfate (No. 13), cooling and immediate analysis, the content of uncharged chromium increased to 10%, after 4 weeks aging, 2%. The same solution, made *M* in  $\text{Na}_2\text{SO}_4$ , which had received the very same treatment contained 28% cationic, 48% uncharged and 24% anionic complexes. Upon 24 hrs. "aging" of this solution, the figures were: 43, 50 and 7 and, after 4 weeks (equilibrium reached), 66, 34 and 10, respectively. Addition of sodium sulfate to the cold solution (No. 13), making it *M* in respect to  $\text{Na}_2\text{SO}_4$ , raised the percentage of uncharged complexes from 2 to 11. Also, the addition of neutral chlorides, as  $\text{NaCl}$ , has a similar, but less marked effect. By the addition of  $\text{Na}_2\text{SO}_4$  to cold solutions of basic chromic chlorides, anionic complexes are formed in addition to uncharged ones. The presence of large amounts of  $\text{NaCl}$  results in a stabilization of chloro groups and increased the number of complexly held  $\text{Cl}$  groups. These findings are of special interest for the theory of the neutral salt effect in tanning.

The action of alkali metal salts of organic acids, possessing pronounced complex-forming power, may be illustrated by a few examples. The addition of sodium formate to solutions of basic chromic sulfates leads to the formation of both uncharged and negatively charged complexes. Sodium acetate only gives the uncharged form, whereas the addition of sodium oxalate in moderate amounts favors the formation of both forms of non-cationic complexes; large amounts give a practically complete formation of negatively charged chromium complexes.

By the application of the organolite method a number of unsettled problems in the theory of chrome tanning will probably be elucidated,



especially the different degrees of affinity of various chromium salts and complexes toward hide protein, by analysis at short intervals of the solution of tanning systems, containing mixtures of such complexes.

### SUMMARY

1. Separation and quantitative determination of positively and negatively charged, as well as uncharged, complexes present in solutions of basic chromium chlorides and sulfates are obtained by filtering the solution through layers of cation- and anion-exchanging organolites. By titration of the filtrate from the cation exchanger, containing eventually present noncationic chromium, which is oxidized and determined, the number of acid groups in the cationic complex removed by the cation exchanger, is obtained, also the number of acid groups present in ionic form in the original solution and the acid groups complexly held in the noncationic part. The cationic chromium complexes are removed by percolating a solution of HCl (1:1) through the organolite layer. For the separation of anionic and uncharged complexes an anion exchanger is used. The organolites are regenerated, washed and used again.

2. The application of this technique shows that solutions of chromic chlorides of acidities  $> 67\%$  mainly consist of cationic complexes, chloro-complexes being formed by increasing chrome concentration. The main constituent of extremely basic chromic chlorides is uncharged chloro-complexes of high molecular weight of an average composition given by the empirical formula  $(Cr_2(OH)_5Cl)^0$ . The rest consists of cationic complexes of normal type. The Cl group is firmly attached to chromium in uncharged complexes. The composition of solutions of basic chromic chlorides is practically independent of their concentration.

3. Dilute solutions of basic chromic sulfates, containing sodium sulfate, consist chiefly of cationic complexes with sulfato acidities of 20–40%. In concentrated solutions the overwhelming constituent is uncharged complexes. The composition of solutions of basic sulfates is largely governed by the concentration of chrome and neutral sulfate.

4. The effect of neutral salts and complex-formers on the complex composition of chromic salts is exemplified. The versatility and usefulness of the organolite method are stressed.

### REFERENCES

1. STIASNY, E., *Gerbereichemie*. Steinkopff, Dresden (1931).  
GRASSMANN, W., *Handbuch der Gerbereichemie*. Springer, Vienna (1939), II/2 (Chapter II by *Balanyi*).
- MERRY, E. W., *The Chrome Tanning Process*. Harvey, London (1936).
2. GUSTAVSON, K. H., *J. Am. Leather Chem. Assoc.* **19**, 446 (1924); *Ind. Eng. Chem.* **17**, 577 (1925); *Collegium* **1926**, 97.

3. ADAMS, B. A., AND HOLMES, E. L., *J. Soc. Chem. Ind.* **54**, T1 (1935); *Brit. Pat.* 450308; 474361.  
BURRELL, H., *Ind. Eng. Chem.* **30**, 358 (1938).
4. GUSTAVSON, K. H., *Svensk Kem. Tid.* **56**, 14 (1944).
5. SAMUELSON, O., *Svensk Kem. Tid.* **51**, 195 (1939); **52**, 115, 241 (1940); **53**, 422 (1941); **54**, 124 (1942). Complete literature references in *Thesis*, Stockholm (1944).
6. GRIESSBACH, R., *Angew. Chem.* **52**, 215 (1939).
7. BJERRUM, N., AND FAURHOLT, C., *Z. physik. Chem.* **130**, 584 (1927).
8. MANEGOLD, E., AND HOFMANN, R., *Kolloid-Z.* **51**, 308 (1930).
9. GUSTAVSON, K. H., *J. Intern. Soc. Leather Trades' Chem.* **30**, No. 10 (1946).
10. See e.g., STIASNY, E., *Gerbereichemie*. p. 457.  
GRASSMANN, W., *Handbuch der Gerbereichemie*. II/2, pp. 217-226.



# THE CONTRIBUTION OF ENTROPY TO THE ELASTIC PROPERTIES OF KERATIN, MYOSIN AND SOME OTHER HIGH POLYMERS

H. J. Woods

*From the Textile Physics Laboratory, Department of Textile Industries,  
The University, Leeds, England*

*Received July 25, 1946*

## INTRODUCTION

The contribution of entropy changes to the elastic properties of highly extensible long-chain polymers has been the subject of a number of investigations (1); in these, attention has naturally been focused chiefly on the rubber-like materials in which the entropy effect is generally of predominating importance. The success of the theory in explaining rubber-like elasticity in terms of entropy has created a tendency for this type of behavior to be regarded as the only kind of high elasticity, in spite of the unambiguous evidence afforded by X-ray studies of keratin, which show that in normal hair entropy can be expected to play little part in the elastic mechanism. For the group of protein fibers generally, little information of a direct kind is available, apart from the results reported by Bull (2) for human hair. These observations are themselves sufficient to emphasize the clear distinction between the elastic mechanism in rubber and that in keratin: on one hand we see high elasticity depending on the large entropy changes accompanying extension and, on the other, high elasticity due almost entirely to internal energy.

In this paper we shall be concerned with certain modifications of keratin in which the X-ray evidence does not afford so clear a lead. We shall show that under certain conditions it is possible to obtain a relatively large entropy effect in keratin, but that, in order to do so, we must largely destroy its character as an oriented chain structure. Otherwise, under quite a large range of treatments, the essentially *energetic* nature of the elastic phenomena is preserved. In oriented myosin, too, the entropy effects are small, although unoriented myosin, as might be expected, is more rubber-like. It will also be shown that there exists a class of high-polymers which are, to coin a phrase, *hyper-entropic*; in these the entropy effect is more than sufficient to account for the loads developed when the specimens are stretched. Nylon shows this kind of effect over a restricted range of extension, but a more striking example is casein, in

which the phenomenon persists over a considerable part of the possible extension range.

There is no need here to do more than recapitulate briefly the thermodynamic results on which these investigations are based. If the total load on the specimen is  $K$  when its extended length is  $L$ , then, for reversible changes we have

$$K = \left( \frac{\partial U}{\partial L} \right)_T - T \left( \frac{\partial S}{\partial L} \right)_T = K_u + K_s \dots \dots \dots (1)$$

and

$$\left( \frac{\partial S}{\partial T} \right)_L = - \left( \frac{\partial K}{\partial L} \right)_T \dots \dots \dots (2)$$

By (1) the load is analyzed into two components:  $K_u$ , depending on the internal energy  $U$ , and  $K_s$ , depending on the entropy  $S$ . Equation (2) makes possible the experimental determination of the entropy contribution, since  $(\partial K / \partial T)_L$  is the observable temperature coefficient of the load at constant length.

In rubber-like substances  $K_u$  is, except at low extensions, generally unimportant in comparison with  $K_s$ , and may, in fact, be negative in some regions of the extension range. Bull's results for human hair in water indicate a negative value of  $K_s$  for extensions up to about 12%, with  $K_u$ , of course, positive; at higher extensions  $K_s$  becomes positive, but remains numerically insignificant compared with  $K_u$ .

It is advisable here to point out that the conditions under which equation (2) is used to determine the entropy effect are of such a nature as to render the interpretation of (1) more difficult than might appear casually. Equation (2) holds for reversible changes; it is, therefore, necessary to bring the specimen to a condition in which a reversible temperature cycle can be performed and to estimate  $(\partial K / \partial T)_L$  during such a cycle. Since the kind of material in which we are interested shows time effects in its elastic properties, it is thus necessary to limit our experimental investigations to specimens which have been allowed to relax to such an extent that the load will not change further during the time necessary to make the observations. It is then possible to take the specimen through a temperature cycle at the end of which the load is the same as at the beginning. The experimental data will refer, then, to specimens which have undergone some considerable degree of relaxation, and not to normal unrelaxed material. Strictly speaking, there is no way out of this difficulty. If, however, we assume (and there is ample evidence of an indirect kind to support the assumption, in the case of keratin, at least) that relaxation is a process involving chiefly the internal energy, we shall be able to obtain at least an approximate picture of the elastic mechanism in the normal substance.

It may also be pointed out in this connection that equation (1) may not be integrated to obtain the total internal energy and entropy changes during any real extension process, since the derivatives in (1) refer to reversible length changes, and the changes during any actual extension are irreversible. Looking at it from a physically simpler point of view we see that there would be omitted from the integral of (1) any internal energy and entropy changes which occur solely because of relaxation, and, therefore, do not contribute to the derivatives in (1). To a certain extent we may resolve this difficulty also by the same assumption as before, that relaxation involves chiefly the internal energy, and, to an order of approximation depending on the validity of this assumption, obtain the total entropy change during any extension process.

### EXPERIMENTAL

Measurements were made on a torsion balance type of extensometer in which the load was recorded by observing the deflection of a beam of light reflected by a mirror mounted on the arm of the torsion balance. All experiments were carried out with the specimens mounted in water. The general procedure was to allow the specimen to remain stretched in water at the highest temperature used until the rate of relaxation had fallen to a small enough value, and then change the water bath for one at a lower temperature. The reversibility of the load changes was finally checked by replacing the original water bath, and no such changes were accepted until the reversibility was perfect within the limits of the experimental error of the apparatus. The full cycle of temperature changes could be completed within a time of the order of 1 minute.

The lower end of the specimen was clamped to a rod which was immersed in the water bath. To reduce as far as possible any error due to thermal expansion of this rod, it was made of fused quartz, as was the hook used for holding the upper end of the specimen. This precaution was necessary, since the thermal expansion of glass or metal was found to introduce appreciable errors in the recorded load changes.

### *Keratin*

Fig. 1 shows the results obtained for a Cotswold wool fiber stretched in water and allowed to relax at different extensions at 40°C. until the cycle 40°–20°–40° could be completed reversibly. The same fiber was used for the whole of the extension cycle, the extension being increased or decreased after each recording of  $K$  and  $(\partial K/\partial T)_L$ . No particular significance attaches, therefore, to the shape of the load/extension curve, although it is fairly typical for a fiber stretched rather slowly at moderate temperature. For comparison, part of the curve (a) for quick extension

at 20°C. of a fiber of the same diameter is shown. In the contraction part of the cycle the loads shown are, of course, for a fiber which has undergone considerable relaxation, and are, therefore, much lower than would have been obtained for a fiber stretched quickly and allowed to recover without much relaxation.

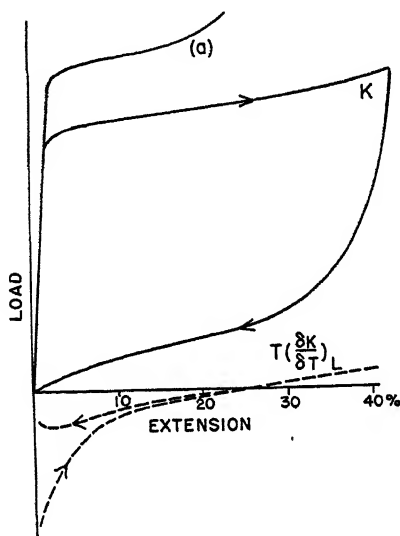


FIG. 1

Cotswold Wool Fiber Stretched in Water to an Extension of 40% and Allowed to Recover in Water.

Temperature range 20°–40°C. Full line:—total load; broken line:—entropy contribution. Curve (a) is the ordinary load/extension curve for quick stretching in water at 20°.

These results are essentially the same as those reported by Bull for human hair; the extension at which  $K_e$  changes sign is, however, very much higher (25%) than his value (12%). In general, there is good agreement with what we should expect from our knowledge of the molecular structure derived from X-ray and related investigations. These indicate that normal  $\alpha$ -keratin consists of well-oriented chains in various stages of organization up to that which can be recognized by X-rays as "crystalline," and that the elastic mechanism is one involving a transformation from the folded  $\alpha$ -configuration to the straightened  $\beta$ -form whatever the degree of organization, although the X-ray results themselves, on which the transformation theory is based, relate only to the crystalline parts of the complex. The transformation itself must involve an increase in the entropy, at least at first, when the regularity of the intra-molecular fold is disturbed. Ultimately, when the chains approach their final straightened

form, we should expect a decrease in the entropy; and these are just the tendencies shown by the entropy effect in Fig. 1. The good general fit with the consequences of the  $\alpha$ - $\beta$  transformation theory is satisfactory in confirming again the validity of ascribing the transformation to the less well-organized as well as to the crystalline keratin, for during the first 20% of extension the latter plays no significant part in contributing to the extension, and this is just the range in which the entropy effect is negative.

It is, perhaps, inadvisable to lay much stress on the hysteresis shown by the entropy load during the cycle. From what has been said above it does not *necessarily* follow that there has been an increase in the entropy as a result of the elastic cycle, although a small increase would be a reasonable consequence of the relaxation which has taken place. In any case, the amount of the hysteresis appears to be small enough for any such effect to be regarded as of little importance.

We may note finally that in Fig. 1 the internal energy load is positive at all points of the cycle, and the mechanism of elastic recovery must very largely involve the internal energy. In fact, over a considerable part of the recovery, the rôle played by the entropy is of a kind tending to oppose contraction. Since the loads shown by a fiber recovering after a quick extension are greater than those in Fig. 1, although the values of  $K_s$  are not very different, this argument applies with even greater force to the plastic recovery of normal fibers.

Although these results are satisfactory in confirming our previous deductions with regard to the elastic mechanism in more or less normal

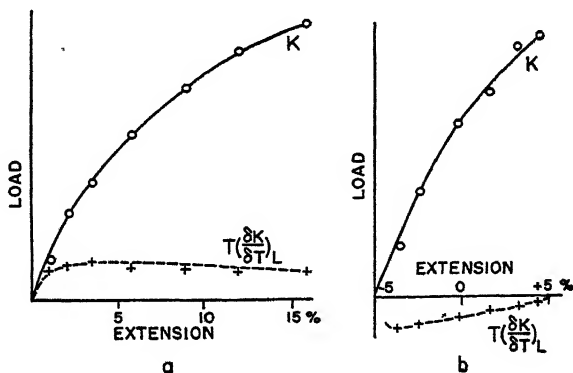


FIG. 2

The Entropy Contribution to the Load for Highly Relaxed Cotswold Wool Fibers Stretched in Water.

Temperature range 20°–40°C. Circles:—total load; crosses:—entropy contribution.

(a) and (b) represent the extremes of behavior observed in this series of experiments.



keratin, the real interest in a study of the entropy effect may more properly be taken to be in connection with the highly relaxed and moderately supercontracted states, to which Figs. 2 and 3 relate. In Fig. 2 are shown the results for two fibers relaxed for 15 mins. in 1% aqueous caustic soda at an extension of 80% and then allowed to contract in the alkali before being thoroughly washed. Fibers treated in this way are in the labile state in which supercontraction ensues if they are treated with hot water or steam, and the degree of relaxation may be judged from the fact that the load necessary to stretch them at low extensions is of the order of 20% of that for normal fibers. The entropy effect for such fibers is generally small, but may be either positive or negative: Fig. 2 (a) and (b) are the extremes which have been observed in these experiments. It seems probable that there is a uniform transition from the "normal" state in which the entropy effect changes sign at about 25% extension, through the state of Fig. 2(b) to that of Fig. 2(a), according to the precise nature and extent of the relaxation process.

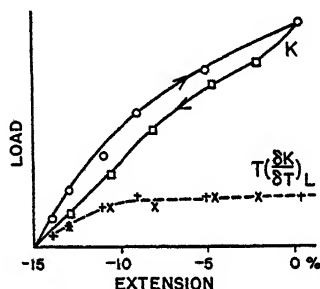


FIG. 3

Cotswold Wool Fiber Supercontracted by 15% of the Initial Length.

Stretched in water. Temperature range 20°–40°C. Full line:—total load; broken line:—entropy contribution (+—+ during extension; ×—× during contraction).

We see this carried a stage further in Fig. 3, which refers to a fiber relaxed in the same way as those used in the preceding experiments, but finally treated without tension in water at 80°C. for a few minutes. Under these conditions we have found that the X-ray photograph remains one of well-oriented  $\alpha$ -keratin; there is, indeed, a small amount of angular dispersion of the crystallites apparent in the photograph (Fig. 4), but this is quantitatively quite inadequate to account for the contraction of nearly 20%. It follows, therefore, that the crystalline parts of the keratin complex take little part in the supercontraction (so long as this is limited to not more than about 20%), and we must regard the phenomenon, within the range considered here, as being a property of the less highly organized keratin. There can be no doubt that this supercontrac-

tion is due to folding of the polypeptide chains into shorter lengths than in  $\alpha$ -keratin; the question is, "To what extent is this folding of a random nature?"

There is nothing in the way of direct evidence supporting a regular "sub- $\alpha$ -keratin" type of folding, and the data of Fig. 3 indicate folding of a less regular kind. For there can be no doubt that the entropy does play more part in the elastic behavior of moderately supercontracted keratin

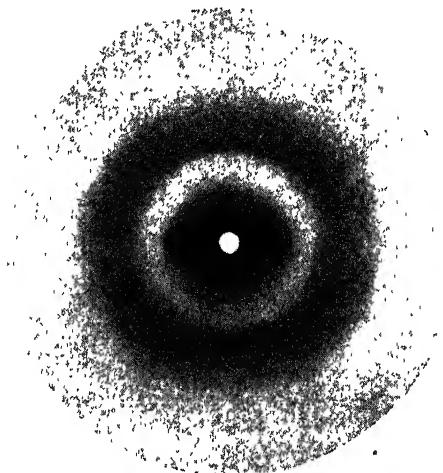


FIG. 4

X-ray Photograph of Cotswold Wool Fibers Treated Similarly to the Fiber Used for the Experiment of Fig. 3, to Induce a Supercontraction of 20% of the Initial Length.

than in that of normal keratin. Part of this increase in the entropy effect, however, may be already apparent in the relaxed fibers before supercontraction (*cf.* Fig. 2(a)) where the elastic behavior is still determined by the  $\alpha$ - $\beta$  transformation. It must, therefore, be ascribed, to this extent at least, to a general loss of organization in consequence of the drastic relaxation necessary to bring the fibers into the labile state. But, allowing for this, there still remains a small positive entropy effect to suggest some irregularity in the folding. On the other hand, it is quite clear from Fig. 3 that the internal energy still plays the predominating rôle, and it appears that the nature of the folding is determined primarily by internal energy considerations: the entropy effect is, from this point of view, incidental. It should be noted that in Fig. 3 the internal energy contribution to the load is still positive during the contraction of the fiber after stretching, so that it is not necessary to invoke the entropy in order to account for the reversible elasticity.

When high supercontractions have been induced by the action of steam on highly relaxed fibers, the entropy effect increases still more in importance and, over the initial stages of the extension, is large enough to account completely for the load on the fiber (Fig. 5). The increased

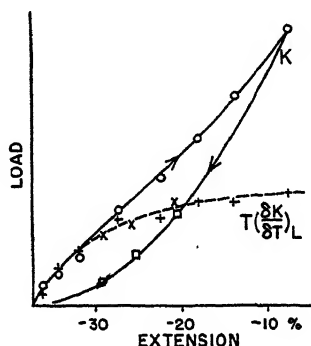


FIG. 5

Cotswold Wool Fiber Contracted in Steam by 37% of the Initial Length after Relaxation in Caustic Soda Solution.

Stretched in water. Temperature range 20°–40°C. Full line:—total load; broken line:—entropy contribution (+—+ during extension; ×—× during contraction).

entropy effect is clearly related to the appearance in the X-ray photograph of partially disoriented  $\beta$ -keratin; and although, by the procedure described, we never reach the degree of randomness shown by denatured proteins, something of this kind of randomness must undoubtedly be present. The process of recovery from strain is further distinguished in these highly supercontracted fibers by the occurrence of a positive internal energy load only during the initial stages of the recovery. For the fiber of Fig. 5, contractions greater than about 20% must be associated with the entropy.

### *Myosin*

The elastic properties of myosin are less uniform than those of keratin, but the available data indicate a strong resemblance between the properties of highly relaxed "generalized" keratin and myosin prepared by the technique of Astbury and Dickinson (4), which X-rays show to be in the oriented  $\alpha$ -configuration. An important difference between them is that, in myosin, supercontraction may be induced by only moderate increase of temperature, and may, in fact, be observed in water at temperatures as low as 40°C. To eliminate disturbing effects of this kind, the present experiments were carried out at temperatures below 25°C.

Myosin presents several difficulties which make it unsuitable for very precise work on its elastic properties, particularly in the kind of experi-

ment necessary for estimating the entropy effect. The most serious of these is in connection with the relaxation which must be allowed to take place to enable the specimen to approach a state in which reversible temperature cycles may be performed. The time of this relaxation is greatly prolonged in myosin as compared even with generalized keratin, and it was found that this extended relaxation was accompanied by considerable internal slipping, since the specimens did not show perfect elasticity when allowed to contract. (For quick stretching in water vapor, such slipping is almost absent; the effect noted here is a consequence of *prolonged* relaxation in water.)

Consequently, the results for myosin are less satisfactory than those for keratin. They showed, rather unexpectedly, that the entropy effect in oriented  $\alpha$ -myosin is more nearly parallel to that of "normal" keratin than to that of highly-relaxed keratin, which it more closely resembles in its general behavior. The entropy effect in  $\alpha$ -myosin is generally small and, for the most part, negative; in particular, it remains negative for extensions up to 50%. It must be remembered, however, that the conditions of these experiments were not comparable with those in which the ordinary  $\alpha$ - $\beta$  transformation has been shown to take place. The internal slipping, in consequence of which the specimens were no longer perfectly elastic, introduces a considerable element of doubt into the value of the real extension (due to the  $\alpha$ - $\beta$  transformation) at any extension of the specimen. For example, one film, which had been stretched during these experiments by 36% of the initial length, had a residual "set," when released in water, of 25%, so that the effective extension, assuming that the "set" was entirely due to internal slipping, was no more than 11% instead of the observed 36%. It may, therefore, be supposed, with some justification, that the negative entropy effect at high extensions in these experiments corresponds in reality to the effect at extensions below 25% in keratin, and that the non-appearance of any positive entropy load is due to the internal slipping limiting the real "molecular" extension to relatively low values.

Because of their possible relation to the elastic effects in muscle (5), the supercontraction properties of myosin are also important. In this series of experiments supercontraction was induced by treating oriented  $\alpha$ -myosin in 0.05% caustic soda solution for 5 mins. and then washing thoroughly. Specimens thus treated showed contractions of the order of 15% (*cf.* Astbury and Dickinson (4)). The entropy effects in such films depended on whether they were now allowed to dry before being tested. If they were not, they appeared to behave similarly to moderately supercontracted keratin; that is, both  $K_s$  and  $K_u$  were positive, but the former was generally the smaller at most extensions. But films which were allowed to dry and were rewetted before the load measurements were made,

showed a much smaller, and generally negative, value of  $K_s$ . It appears, therefore, that the drying process is accompanied by the formation of stable linkages whose action is to enhance the energy effect and reduce the entropy effect. It may be noted in this connection that the amount of lateral swelling in water of these supercontracted films was also very much reduced by the drying; the lateral dimensions after drying and rewetting were smaller than before drying. This observation also supports the idea of the formation of stable lateral linkages during drying.

On the whole, the results for myosin indicate that the entropy effects are of the same order of importance as in keratin, and that the elastic mechanism is thus chiefly dependent on the internal energy. This, of course, applies only to the oriented  $\alpha$ -myosin. In the unoriented myosin as originally prepared, the entropy effect is positive at all extensions and greater than the total load for extensions up to about 20%; at higher extensions the value of  $K_s$  decreases somewhat, while the total load continues to increase. The molecular changes which accompany the extension of this unoriented myosin are orientation and a partial  $\alpha$ - $\beta$  transformation, generally in this order but with considerable overlap between the two processes (4). The orientation, as might be expected, is responsible for a large positive entropy load; the appearance of a positive  $K_u$  is an indication of the approaching end of the orientation process and the start of the  $\alpha$ - $\beta$  transformation.

### Casein

We have seen that in keratin and myosin, where the normal elastic mechanism is the intramolecular  $\alpha$ - $\beta$  transformation, there is a strong tendency for the internal energy to determine the general run of the elastic properties. It is, therefore, of interest to compare and contrast these fibers with casein, which differs from most denatured proteins on account of the small degree of aggregation of the chains into parallel bundles in the  $\beta$ -configuration. In ordinary unstretched casein, such chain bundles as exist are disoriented with respect to the fiber axis and, although some degree of orientation is produced by stretching to high extensions, this is never even approximately perfect. The general sort of picture indicated by the X-ray results is of a rather poorly crystalline complex in which the chains for the most part are folded in a highly irregular manner.

Fig. 6 shows the results obtained in an experiment on a fiber of commercial casein in water. The extraordinarily large positive entropy load (necessitating a negative value for  $K_u$ ) is particularly noteworthy; casein is, in comparison with the ideal rubber, *plus que parfait* over a considerable extension range. In view of the X-ray indications of an irregular chain system in casein, we should expect some degree of chain

orientation on stretching and consequently a positive entropy load, but the appearance of such a strongly negative internal energy load is unexpected. In this case it can hardly be attributed to crystallization on stretching, for such an effect receives no support from the X-ray evidence, and in any case is more likely to happen at high extensions (as in rubber,

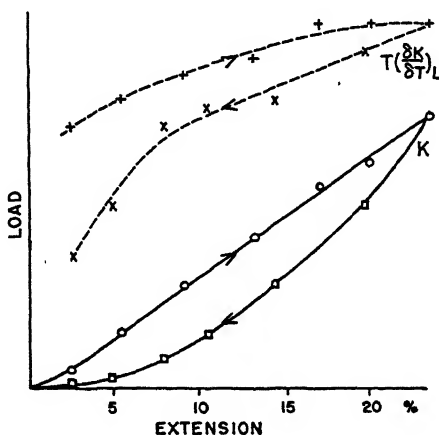


FIG. 6

Casein Stretched in Water.

Temperature range 20°–40°C. Full line:—total load; broken line:—entropy contribution.

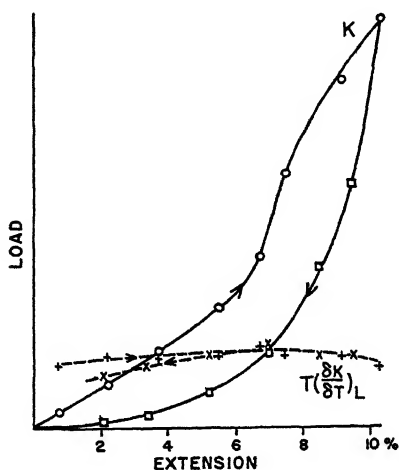


FIG. 7

Nylon Stretched in Water.

Temperature range 20°–40°C. Full line:—total load; broken line:—entropy contribution.

for instance) whereas the observed negative internal energy load in casein is eliminated at high extensions. It must, therefore, be due to something in the nature of an internal compression developed by the strongly contractile effect of the entropy. In the absence of molecular repulsions, the chains would presumably take up an even more random configuration than they in fact do, with the result that the unstretched system possesses molecular potential energy which decreases when the fiber is stretched.

The same phenomenon of a negative internal energy load also appears in nylon stretched in water, but here the effect is evident only within the first few *per cent* of the extension range, as may be seen in Fig. 7. Indications of a similar effect have been observed as well in supercontracted keratin and in disoriented myosin. The recognition of a class of high polymers behaving in this way completes the picture of a range of elastic mechanisms characterized by different values of  $K_u$ : in the keratin type, positive; in the ideal rubber, zero; and in the casein type, negative. High elasticity is not associated preferentially with any of these.

### *Nylon*

The occurrence of a negative internal energy load at low extensions in nylon is in accord with the result obtained in the complementary experiment by Leaderman (7), who observed in nylon a negative thermal expansion coefficient at zero load. Nylon is also interesting because of the fact that during the contraction part of the load/extension cycle  $K_u$  again becomes negative when the amount of the contraction reaches a few *per cent* of the initial length. The elasticity of form of nylon must thus be ascribed chiefly to entropy; in determining the resistance to stretching, however, the internal energy plays the more important part, except at the lowest extensions.

### *Addendum*

Since the above was written, a paper by Jordan Lloyd and Garrod (3) has appeared in which the entropy effects in some highly swollen protein fibers are described. The results for keratin in formic acid confirm the general conclusion here, that the entropy is of little importance in determining the elastic behavior in this fiber. From their data for elastin in water and silk in formic acid, it appears that these fibers under these conditions behave similarly to casein in water, in that the entropy load is greater than the total load.

In conclusion it may be pointed out that in the theory leading to equations (1) and (2) on p. 408 any reference to changing water adsorption with temperature is omitted. It is possible, therefore, that correction to the results given may become necessary when the appropriate data are available.

## REFERENCES

1. MEYER, High Polymers, 4. (1942).
2. BULL, *J. Am. Chem. Soc.* **67**, 533 (1945).
3. JORDAN LLOYD AND GARROD, *J. Soc. Dyers & Colourists*, Symposium on Fibrous Proteins, May, 1946.
4. ASTBURY AND DICKINSON, *Proc. Roy. Soc.* **129B**, 307 (1940).
5. ASTBURY, Royal Society, Croonian Lecture, 1945.
6. ASTBURY, *Chem. and Ind.*, **1945**, 114.
7. LEADERMAN, Elastic and Creep Properties of Filamentous Materials and Other High Polymers. Textile Foundation, Washington, D. C. (1943).





# STUDIES ON THE SURFACE LAYERS AND THE FORMATION OF THE FERTILIZATION MEMBRANE IN SEA URCHIN EGGS

John Runnström, Ludwik Monné and Elsa Wicklund

*From Wenner-Gren's Institute for Experimental Biology,  
University of Stockholm, Sweden*

*Received July 23, 1946*

## INTRODUCTION

The formation of the fertilization membrane constitutes the most easily recognizable change following the fertilization of the sea-urchin egg. Although the literature dealing with this process is extensive, its mechanism has not as yet been satisfactorily elucidated; for a brief survey of the literature cf. Runnström, Monné and Broman (1). The majority of workers in this field seem to have entertained the idea that the fertilization membrane corresponds to the vitelline membrane of the unfertilized egg. This membrane was considered to be elevated by an osmotic attraction of water exerted by a substance exuded between the surface of the granular cytoplasm and the vitelline membrane. During its elevation, however, the membrane, as generally recognized, undergoes considerable change in its chemical and mechanical properties. The cortical granules were first studied by Hendee (2) and Lindahl (3) but the credit for having first pointed out their importance in the process of membrane formation is due to Moser (4, 5). According to this author, the breakdown of the granules was a necessary condition for the membrane formation. Furthermore, he presented experimental evidence to the effect that Ca was necessary for the breakdown of the granules.

Moser submitted the hypothesis that the formation of the perivitelline space resulted from a transformation of the cortical granules to vacuoles and fusion of the latter. The vacuolar walls were believed to form an inner coating of the fertilization membrane as well as a new covering of the egg surface.

Runnström (6) found that the fully formed fertilization membrane presented a beautiful birefringence and was thus able to draw some conclusions concerning the submicroscopic structure of the membrane, cf. also Schmidt (7). Some quantitative data were later given, cf. (1). The present paper will report on a number of data concerning the structure of the surface layers in the sea-urchin egg and on their rôle in the formation

of the fertilization membrane. Particularly, we arrived at the conclusion that the cortical granules were included in the fertilization membrane and contributed greatly to its submicroscopic structure. This view has been presented in a preliminary form (8) and will be expanded in the present paper.

### MATERIAL AND METHODS

This research was carried out on the eggs of the sea urchins *Psammechinus miliaris* P. L. S. Müller, *Echinocardium cordatum* Penn and *Strongylocentrotus droebachiensis* Müll., available on the west coast of Sweden. The two former species have their breeding season during the summer, the last one in the early spring (March). The sperm of *Echinus esculentus* L. in some cases served as material for the preparation of antifertilizin.

The eggs were kept in bowls with an upper diameter of 5 cm., narrowing towards the bottom, where the diameter was only 2.5 cm. The height was 2.5 cm. The bowls, provided with about 2 ml. sea-water or other solutions, could be placed directly on the stage of the microscope where the cells could be observed with a 10× objective or a 40× water-immersion objective.

For special purposes the eggs were transferred into a drop of water enclosed between a slide and coverslip, the latter provided with wax supports. The phase contrast equipment from Zeiss was at our disposal, a sodium lamp serving as light source. The birefringence, its sign, and the value of retardation were determined with a Leitz polarizing microscope provided with a rotating mica plate/1/19\/. A powerful mercury lamp was used, with or without filters. The diaphragm opening was kept narrow. Care was taken that the plane of polarization of the light reflected from the mirror lay in the plane of the polarizer.

In many experiments the eggs were rendered jelly-free in the customary way by brief treatment with acidified sea-water. Naked eggs were prevented from adhering to the glass by addition of one to two drops of 0.1% serum albumin to 2 ml. sea-water (1).

On the preparation of antifertilizin cf. below p. 426 and on that of sperm lysin cf. (26, 27, 28).

### *On the Optical Properties of the Cortex and the Extraneous Coats of the Sea-Urchin Egg*

Eggs in different stages of development were examined with the polarizing microscope. Owing to the rather high refractive index of the surface, the eggs were delimited by a bright diffraction fringe. If, however, all optical disturbances were eliminated a very regular neutral or positive cross could be observed on the surface of the egg. The retardation of the cortex of the mature unfertilized eggs of *Strongylocentrotus* amounted to about 8.1 mμ. The corresponding value for *Echinocardium* was found to be  $8.7 \pm 0.4$  mμ. The cortical birefringence was present even in the oocytes. In *Psammechinus* the retardation was seen to increase with growth of the oocytes from about  $6.6 \pm 0.5$  to  $9.5 \pm 0.17$  mμ, the latter value also being found in the mature eggs. The cortical granules, which appear only in connection with maturation (9), evidently play no rôle in the birefringence.

The cortical birefringence, always positive in the radial direction was

also found in fertilized eggs with a fertilization membrane, in the blastomeres of the two- and multicellular stages, in the cells of the blastula, and in the polar bodies, even when these latter were abnormally large. No noticeable quantitative difference was found when unfertilized and fertilized eggs were compared (1). A small papilla or pit was present at the animal egg pole. Sometimes a similar, though less marked papilla could also be detected at the vegetal egg pole. These observations refer especially to *Echinocardium* eggs (cf. also *Jenkinson* (10) and *Lindahl* (11)). The base of the papillae appeared between crossed nicols as a straight line with a stronger retardation than the rest of the cortex. These observations indicate that the cortex may possess a special structure at the polar regions. The cortical granules, however, also proved to be present within these regions. *Monroy and Monroy* (12), in a paper which appeared after our first report, described the birefringence of the cortex of *Paracentrotus lividus* and *Arbacia pustulosa*. Moreover *Monroy* (13) reported observations of regular variations in the birefringence following fertilization, which were not observed in the species studied by us.

The vitelline membrane of the mature fertilized eggs is very susceptible to the action of trypsin (cf. below). Even after removal of the vitelline membrane by the action of trypsin the egg presents its normal birefringence. The positive birefringence of the egg surface thus resides in the cortical layer and not in the vitelline membrane.

The cortical birefringence was not changed in mature unfertilized eggs which had been subjected to a gravity field of 10,000 *g*.

Bee venom, owing to its content of lecithinase (cf. 14), attacks the phosphatides of the egg-surface (cf. (1) and (15)). In eggs subjected to treatment by the venom, lipids were separated from the cell structure. Under these conditions the cortical birefringence was considerably lowered or disappeared. This observation, in conjunction with the positive sign of the birefringence in the radial direction, favors the opinion that the birefringence is due chiefly to ordered layers of lipids present in the cortex, a conclusion at which *Monroy* arrived independently.

The lipids leave the eggs in the form of hyaline blisters. In favorable cases a weak birefringence, positive with respect to the radial direction, could be demonstrated on the surface of the blisters.

The vitelline membrane of the oocytes was visible as a rim around the surface and became still more distinct upon exposure of the eggs to a hypertonic solution (9). Following maturation, the vitelline membrane in the *Psammechinus* and *Strongylocentrotus* eggs became so intimately connected with the plasma membrane that it did not become visible even when the eggs were exposed to the hypertonic solution. In *Echinocardium* eggs, on the other hand, the vitelline membrane appeared as a rim distinct from the plasma membrane in a hypertonic medium.

When the eggs were transferred to sea-water diluted with about 75% distilled water, they ruptured at one point. The cytoplasm flowed out to a greater or lesser extent, and a thin elastic membrane became visible. This evidently represented the vitelline membrane which showed a rather low retardation, *in maximo* 4-5  $m\mu$ , *cf.* (1).

On the basis of numerous observations it seems probable that the vitelline membrane *in situ* does not exhibit any birefringence. The birefringence observed in the vitelline membrane detached from the plasma membrane might have been of a secondary nature.

The retardation of the fully formed fertilization membrane amounted, as previously (1) described, to  $12.5 \pm 0.13 m\mu$  (*Psammechinus* eggs). It was possible to observe how the retardation increased during elevation of the fertilization membrane. Its birefringence was always negative in the radial direction. We are chiefly concerned in this case with a birefringence of form which owes its origin to a lamellar structure of the fertilization membrane, *cf.* (6).

The hyaline layer which appeared on the surface of the egg about 10 minutes after fertilization (*Psammechinus* eggs, 20°C.) did not exhibit any birefringence while *in situ*. Especially in the two-cell stage the hyaline layer may be partially and temporarily lifted off between the blastomeres. Under these circumstances a certain birefringence of the layer was demonstrable. It was negative in the radial direction. The hyaline layer also presented a distinct negative birefringence when it was lifted from the egg surface by external means. Fertilized eggs, for example, were subjected to the action of hypertonic sea-water (2 ml. sea-water  $\pm$  0.6 ml. 2.5 *N* NaCl). By rotating the mica plate it was possible to show that the cortex presented a positive cross at the same time as the hyaline plasma layer, and the fertilization membrane exhibited a negative one. The retardation of the cortex had increased to  $14.2 \pm 0.4 m\mu$  and that of the hyaline layer to  $6.2 \pm 0.4 m\mu$ .

The hyaline layer lifted off in Ca-free hypertonic sea water is either isotropic or very weakly birefringent. As has been well known since the work of Herbst (16), the hyaline layer has a tendency to dissolve in Ca-free sea-water.

Below the vitelline membrane (in the unfertilized egg) or the hyaline layer (in the fertilized egg), the protoplasmic surface or "plasma membrane" (Danielli (17)) is found. It appears in the dark field as a luminous layer (*cf.* 6, 9, 15 and 18). This layer is white in the oocyte and in the fertilized egg, whereas it presents a yellow color in the mature, unfertilized egg. On maturation the color change occurs gradually, whereas the change is momentary at fertilization, starting from the entrance point of the spermatozoon. The color of the egg surface remained unchanged even when the eggs were submitted to the action of a solution of trypsin,

which destroys the vitelline membrane of the unfertilized or the hyaline layer of the fertilized egg. This proves that the luminous layer does not correspond to the extraneous coats but to the plasma membrane proper. The luminous layer is sensitive to attack by lysocithin or bee venom (*cf.* 15). This is in keeping with the view that the luminosity on the dark field is due chiefly to lipids present in the cortex.

The cortical granules could easily be distinguished in the living egg by means of the phase contrast method. The cortical granules appeared as dark spots when the surface of the egg was focused. The diameter of the cortical granules was of the order of  $0.5\text{--}1\ \mu$ . The number of cortical granules present in a *Psammechinus* egg was roughly estimated at 30,000.

The phase contrast method also confirmed that the cortical granules were absent in the immature as well as in the fertilized egg, *cf.* (9). In the egg of *Asterias rubens*, the cortical granules are formed, however, a long time before maturation, *cf.* (19).

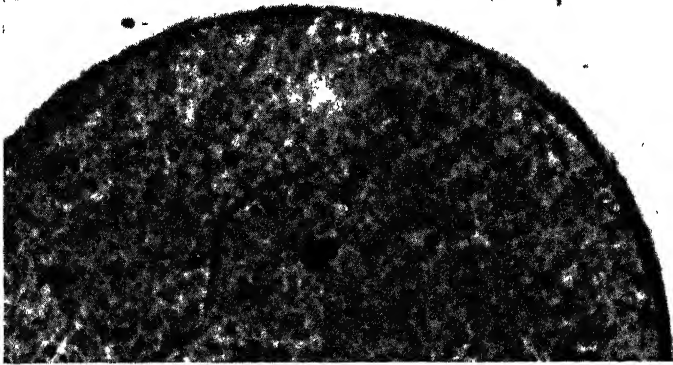


FIG. 1

Section of a Mature Unfertilized Egg of *Psammechinus* Showing Cortical Granules

Numerous eggs were fixed in Bouin's or Flemming's fluids. In the eggs of *Echinocardium* and *Psammechinus*, the cortical granules were stained with Heidenhain's iron hematoxylin (*cf.* Fig. 1) only after fixation with Flemming's fluid. In these eggs the vitelline membrane was frequently detached from the cortex under the influence of the fixing fluid, while the granules remained unchanged within the cortex. The detached vitelline membrane could be stained with eosin or pyronin. The stained preparations give the impression that the vitelline membrane contained numerous very minute granules. They were not stainable by iron hematoxylin and had nothing to do with the cortical granules.

*On the Formation of a Fertilization membrane  
in the Presence of Sperm Extract*

According to Frank (20), an inhibition of fertilization and development occurred in the presence of an extract obtained by heating a sperm suspension in sea water. The main characteristics of the extract were its agglutinating effect on the eggs and its neutralizing action on the sperm-agglutinating egg secretion, the "fertilizin" of F. Lillie (21). The egg-agglutinating factor has, therefore, been designated *antifertilizin* by Tyler (22).

The antifertilizin<sup>1</sup> was prepared as follows. The spermatozoa filtered through bolting silk were freeze-dried by the method of Flosdorf and Mudd (24). The dry powder was extracted with methanol. The residue was suspended in sea-water and subjected to a temperature of 85–90°C. for 3–5 minutes. The insoluble part was centrifuged off. Electrophoresis of the dialyzed solution revealed only one component, which, of course, does not guarantee uniformity of the solute, *cf.* (25) and (26).

The strength of the antifertilizin preparation was determined by observing its ability to produce precipitation of the jelly layer at different dilutions. At higher concentrations of antifertilizin, a contraction of the jelly layer soon took place (*cf.* (20)). The strengths of the preparations obtained by the procedure outlined above varied between 20 and 30, i.e., when the *original solution* was diluted 20–30 times no precipitation occurred. Beyond these dilutions, however, the jelly layer was certainly affected. A more or less definite agglutination occurred and the jelly became more brittle. These changes were less suitable as a basis for a quantitative assay which, however, was only approximate even with the method adopted.

Antifertilizins were prepared from the spermatozoa of *Strongylocentrotus*, *Echinocardium*, *Echinus* and *Psammechinus*. In general, the eggs of the last-named species were used as test material. The eggs of *Echinocardium* served as next best for this purpose. A species specificity with respect to the action of antifertilizin on the jelly layer has not been conclusively demonstrated thus far in our material, *cf.* (25). If it is present, the specificity must overlap considerably. While Frank reports that his extracts inhibited the fertilization, we found a subnormal fertilization of the eggs in the presence of our preparation. The spermatozoon penetrated

<sup>1</sup> In previous papers we have used the terminology introduced by Hartmann (23). We have felt it more convenient, however, to adopt the classical designations "fertilizin" and "antifertilizin." Furthermore, we propose the designation "sperm lysin" for what was called "androgamone III or AIII" in previous papers, *cf.* (26, 27 and 28). This designation directly characterizes the origin and action of this substance. It may prove convenient to use "gamones" (Hartmann) as a comprehensive designation for substances which presumably interact at the fertilization.

and a fusion of the pronuclei occurred, but the cortical reaction was more or less incomplete. The fertilization membrane either was not formed or presented abnormal features.

The interference with the cortical reaction occurred in much greater dilutions of antifertilizin than those giving rise to the precipitation of the jelly layer. In the experiments on the influence of antifertilizin on the membrane formation, eggs were, in general, used which had previously been deprived of their jellies.

In one experiment, *Echinus* antifertilizin was used in the following dilutions of the original solution:

1 1:50; 2 1:100; 3 1:150; 4 1:200; 5 1:250; 6 1:300. Jelly-free *Psammechinus* eggs were inseminated in these solutions. In the corresponding control in sea-water, a well-elevated membrane appeared subsequent to the insemination. In 1 the membranes were granular all round and the perivitelline space was often narrower than in the control. From 4 onward the majority of eggs had membranes without granules. Eggs were

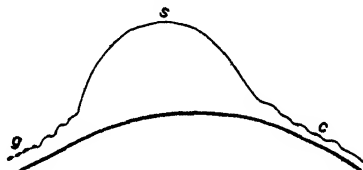


FIG. 2

Diagrammatic Representation of an Abnormal Fertilization Membrane Consisting of a Smooth Bulging (s), a Granular (g) and a Curled or Corrugated (c) Part

This latter appearance is due to the presence of numerous small bulges.

often found, however, with one part of the membrane granular and any other part faintly curled or corrugated. Also greater bulging parts with smooth contour occurred in these membranes, cf. Fig. 2 (g. granular, c corrugated part). A somewhat varying percentage of jelly-free eggs presented, even in absence of antifertilizin, a curled or corrugated appearance. Eggs surrounded by their jelly coats, on the other hand, had, almost without exception, a smooth contour.

From numerous observations, we infer that the corrugated shape of the membrane corresponds to a stage preceding the final one with smooth contour. Thus the removal of the jelly coat in certain cases inhibits the full development of the membrane.

A varying number of eggs in the above-mentioned experiment showed only nuclear but no cytoplasmic division in the antifertilizin dilutions 1:50, 1:100 and 1:150. This, no doubt, was due to the close attachment of the membrane to the egg surface by which the movements occurring at the cleavage were inhibited. Sometimes the cleavage furrow was in-



1—in *Echinocardium* eggs—merely by a number of more or less irregular ridges. As soon as the membrane was elevated from the surface, a more normal cleavage was observed. The membrane remained granular however. When diluted more than 200 times the anti-in, in general, did not impair the development.

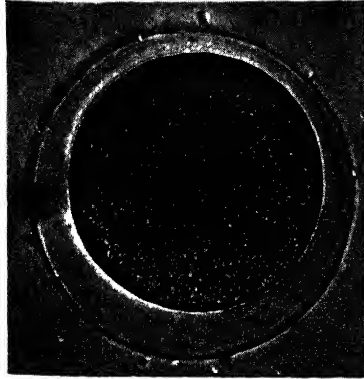


FIG. 3

Fertilized *Psammechinus* Egg with Smooth Membrane

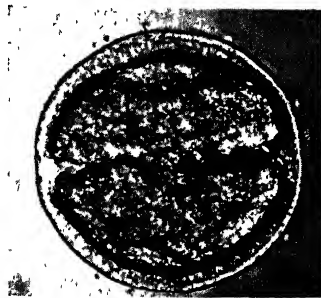


FIG. 4

*Psammechinus* Egg Fertilized in Presence of Antifertilizin, Immersed in Hypertonic Medium Sixty Minutes After Fertilization

In any experiments, more concentrated solution of antifertilizin than mentioned above were used. Jelly-free *Psammechinus* eggs were, for example, immersed in 1:2, 1:4, 1:8 and 1:16 antifertilizin solutions. In these solutions no membrane formation occurred, but the spermatozoa entered the eggs and a fusion of the pronuclei ensued. The activated nature of the eggs inseminated in the presence of antifertilizin was revealed by the occurrence of plasmolysis that occurred under hypertonic conditions; 0.6

ml. of 2.5 *N* NaCl was added to 2 ml. egg-suspension 20–30 minutes after the insemination. The eggs showed the angular or polyhedral type of plasmolysis characteristic of the fertilized state (cf. for references (1, 9, 18)). In many eggs the membrane failed to appear even under hypertonic conditions. In other cases a membrane became visible which was connected with the cytoplasmic surface by a hyaline layer presenting a fine radial striation. No perivitelline space was present.

Fig. 3 represents a normal *Psammechinus* egg with a smooth membrane, Fig. 4, an egg fertilized in antifertilizin of the dilution 1:16. Thereafter, the solution was made hypertonic at the beginning of the



FIG. 5

*Psammechinus* Egg From the Same Experiment as that Represented in Fig. 4

two-cell stage about 60 minutes after fertilization. The egg belonged to the type with a striated hyaline layer continuous with the membrane and with the egg surface. More or less clearly recognizable granules are present below the membrane. In some cases the membrane appeared partly delaminated from the hyaline layer. Below the bulging delaminated part of the membrane, a perivitelline space was visible. The two eggs in Fig. 5 were in contact at the bulging parts of their membranes. These parts were also provided with one layer of granules.

Fig. 6 represents some eggs which were inseminated in the presence of antifertilizin 1:128. The photograph was taken about 40 minutes after the fertilization. Three of the eggs are in contact through the bulging

parts of their membranes. In the lower egg and in that to the left, the greater part of the bulge is smooth, while in the upper egg, the bulge is more or less granular. In the egg to the left, the smooth area is continuous with a granular region which is visible in optical section on the upper part of the figure. In the lower egg also, the transition from the relatively thick smooth membrane to the thin granular part is clearly visible on the left side of the photograph. The transition from the smooth to the granular state observed in numerous cases was more or less gradual. The

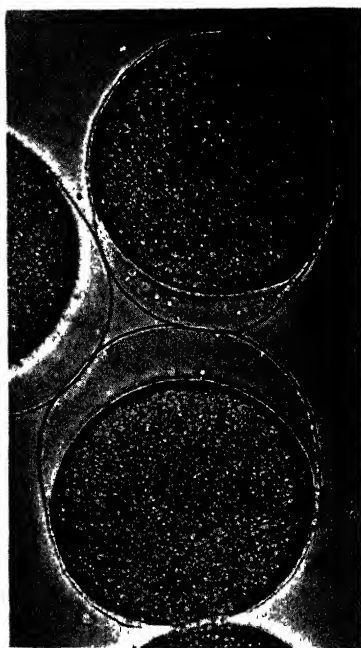


FIG. 6

*Psammochinus* Eggs Fertilized in Presence of Antifertilizin  
Wholly or partly granular fertilization membranes

granular parts of the membranes in the eggs represented in Fig. 6 were, on the whole, very close to the egg surface. By immersing the eggs in a hypertonic solution, it was shown that the membrane was separated from the egg surface even in its granular part. Sometimes, however, fine strands of filaments were seen extending between the egg surface and the membrane. Filaments were occasionally observed, even in cases where the whole membrane was smooth and the perivitelline space had almost normal width.

In some cases, a strand was directly observed to break into two fragments which contracted. The outer fragment merged into the membrane,

the inner into the egg surface. Occasionally droplets were observed to adhere to the inside of the membrane, cf. Fig. 7. They certainly correspond to strands which have not been wholly included in the membrane. Fig. 8 shows the granular membrane of an early blastula from an egg which had been fertilized in the presence of antifertilizin. The fixative was Flemming's solution, and the sections were overstained with iron hematoxylin to render the granules clearly visible. On closer examination, the granules are seen to be of different sizes. The larger ones in reality represent groups of aggregated granules. Some of the granules are slightly allongated in a tangential direction, which probably represents a stage in the normal transformation of the granules.



FIG. 7

Diagrammatic Representation of Droplets Attached to the Fertilization Membrane



FIG. 8.

Section of a Blastula Reared from a *Psammechinus* Egg Fertilized in Presence of Antifertilizin Granular Membrane.

Smooth parts of membranes, such as those represented in Fig. 6, gave the normal retardation values, *i.e.*,  $\sim 12.5 \mu$ ; the granular parts, on the other hand, showed various considerably lower values, whereas no appreciable difference was found between the retardation values of smooth and corrugated parts of the membrane. Membranes corrugated all round did not differ from smooth membranes with respect to the retardation, although they gave the appearance of being thinner than the latter.

Eggs of *Psammechinus* which had formed a granular membrane upon fertilization in the presence of antifertilizin were transferred to normal

sea-water. The membranes, however, remained granular. In some preliminary experiments, the Ca-content of the sea-water was increased (0.3 ml.  $M$   $\text{CaCl}_2$  solution, for example, was added to 20 ml. sea-water), and eggs with granular membranes were transferred into this medium, but the state of the membranes seemed to be irreversible even under these conditions.

At low concentrations of antifertilizin, the following observations were sometimes recorded for *Echinocardium* eggs. A granular membrane appeared upon insemination, but within less than one minute, the granular membrane was transformed into a smooth one showing the normal retardation value. Especially significant observations were made on *Strongylocentrotus* eggs which were inseminated in the presence of antifertilizin 1:10 in sea-water. Granular membranes appeared which adhered closely to the plasma membrane. On certain parts, however, the membrane was elevated in the form of blisters or bulges. Eggs with membranes of this type were transferred to solutions of 0.001% bee venom. Some extremely striking phenomena were now displayed. The membrane separated from the plasma surface. The granules gradually disappeared and the membranes passed, in the course of five minutes, through the corrugated to the normal smooth stage.

It was especially obvious in these experiments that the corrugated appearance was brought about by the presence of numerous bulges. In the beginning, these have the shape of convex half spheres. The surface area of the bulges was thus about twice that of the cross-sectional area at their base. Sometimes concave bulges were also observed. These arose at spots where filamentous connections with the plasma surface still existed.

The merging of the granules with the membrane contributed evidently to the formation of the bulges. The granules were often more or less flattened or lens-shaped which must be regarded as a step in the process of merging with the membrane. One or two granules were sometimes observed in the walls of the bulges. These had a fairly uniform height of 3–3.5  $\mu$ . When the membrane approached full elevation, the bulges were flattened and the membrane assumed more of a curled appearance until the smooth stage was finally attained.

In some cases, small groups of granules were observed to be present in a membrane which was otherwise smooth and well elevated. In one case, the granules were watched continually until they finally disappeared, evidently merging with the membrane.

The radius of the fully formed membrane measured about 95–96  $\mu$ , while the radius of the egg was 64–65  $\mu$ . This means that the surface area of the elevated smooth membrane was about twice that of the egg surface. The same relationship between the surface area of the membrane and that of the egg also holds for the *Psammechinus* egg.

Eggs of *Strongylocentrotus* which had been inseminated in the presence of antifertilizin were immersed in a hypertonic solution (2 ml. sea water + 0.6 ml. of 2.5 *N* NaCl). The diagram in Fig. 9a represents the granular membrane connected with the plasma surface by a finely striated hyaline layer, which became visible on exposure to the hypertonic medium. After 10 minutes, 0.05 ml. of a 0.1% bee venom solution was added. A breakdown of the tender filaments forming the hyaline layer now ensued. The membrane was elevated. During this process, the granules merged more or less completely with the membrane. Fig. 9b shows diagrammatically how the conditions represented in Fig. 9a changed on addition of the venom. Some few granules were still visible in an otherwise smooth part of the membrane.



FIG. 9a

Granular Fertilization Membrane Connected with the Plasma Surface  
by a Striated Layer

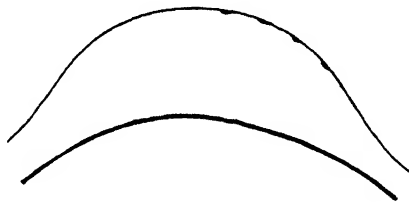


FIG. 9b

Following Exposure to Bee Venom the Filaments Disappeared  
and a Membrane was Elevated

It may be briefly stated that addition of sperm lysin<sup>1</sup> (1 mg. dry substance/ml.), for example in the dilution 1:4, was found to exert an action similar to that of the bee venom. Granular membranes adhering to the surface of fertilized *Strongylocentrotus* eggs were elevated. The granular state was gradually transformed into the corrugated. Only rarely, however, was the final smooth stage obtained. The action of the lysin was thus less complete than that of bee venom. In both cases, however, eggs were found which were more or less responsive to the venom or the lysin.

#### *Influence of Clupein on the Formation of the Fertilization Membrane*

Clupein has the same precipitating action on the jelly layer as antifertilizin, *cf.* (26). It was, therefore, of interest to investigate whether

<sup>1</sup> *Cf.* (26, 27, 28). New designation for androgamone III (A III) *cf.* above p. 426, footnote.

clupein interfered with the membrane formation in the same way as anti-fertilizin.

A 0.1% solution of clupein sulphate in sea-water was prepared and neutralized to pH 7.8. In one experiment, for example, the following dilutions of the standard solution were used: 1 1:4; 2 1:16; 3 1:30; 4 1:60; 5 1:120; 6 1:240; 7 1:480. Eggs of *Psammechinus* were transferred to these solutions; 10 minutes later, the eggs were inseminated. In 1-3, the eggs were fertilized but no membranes were visible. In 4, the membrane adhered to the plasma surface but local elevations of the membrane were observed in some cases, similar to those shown in Fig. 6. The membrane was granular or corrugated. In 5-7, the effect of clupein was slighter but

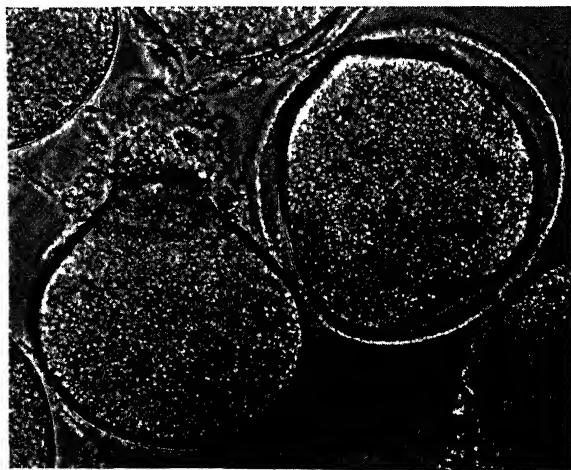


FIG. 10

*Psammechinus* Eggs Fertilized in Presence of Clupein, Immersed in Hypertonic Solution and then Returned to Sea-water

Granular fertilization membrane. In one of the eggs a crumpled ruptured membrane

still pronounced. Smooth elevated parts were continuous with corrugated or granular parts of the membrane. The samples 1-3 were made hypertonic (0.6 ml. of 2.5 *N* NaCl to 2 ml. egg suspension) 20 minutes after the insemination. A plasmolysis of the angular type (cf. above p. 429) was observed as in normally fertilized eggs of the same stage. No membrane, but a granular rim appeared, which closely followed the angular contour of the egg surface. The eggs subjected to the hypertonic solution were returned to normal sea-water after about 15 minutes. A membrane separation occurred in many eggs subsequent to the treatment with the hypertonic solution. The membrane formed was granular. Certain of these eggs exhibited irregular movements. They elongated and retracted again. In connection with these changes of form, the membrane often ruptured

and was rubbed off the egg. A crumpled membrane was finally visible in contact with a more or less bulging part of the egg surface (*cf.* Fig. 10), which part often underwent cytolysis. The rupture of the membrane was probably caused by the movements of the eggs, since the granular membrane does not possess nearly the strength of a smooth membrane. Fig. 11 represents a granular membrane which had been rubbed off the egg without crumpling. A local cytolysis was observed on the part of the egg surface that was still adjacent to the membrane. The granules were beautifully visible, not only in optical section, but also on focusing the surface of the membrane.

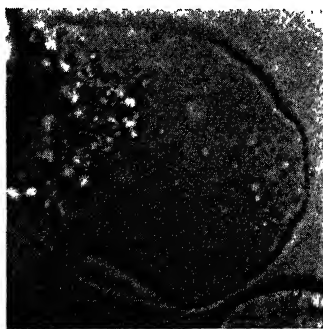


FIG. 11

Granular Fertilization Membrane Rubbed off a *Psammechinus* Egg Treated in Same Way as the Eggs Represented in Fig. 10

By use of phase-contrast microscopy, it was possible to demonstrate that the cortical granules were always absent from the cortex, as soon as a granular membrane had formed.

A well-defined substance, such as clupein, combines the two effects exerted by the antifertilizin, *viz.*, the precipitating effect on the jelly coat and the inhibiting effect on membrane formation. This indicates that the active principle present in the antifertilizin also has a uniform nature.

#### *The Influence of Antifertilizin and Clupein on the Unfertilized Eggs*

According to Frank (20), the jelly-free eggs were agglutinated by his sperm extract. Our antifertilizin preparation has similar effects. In experiments with *Psammechinus* eggs deprived of their jelly layers, the agglutination was never found to be quantitative. Certain groups of agglutinated eggs formed, especially when the eggs were rolled on the bottom of the bowl. The agglutination occurred only in antifertilizin of fairly high concentrations (above 1:32), the minimum concentration, however,



being somewhat variable in different experiments. The agglutination involves, indeed, a profound change of the egg surface as the following observation showed. The eggs were left in contact with the antifertilizin solution for 30 minutes, and the medium then rendered hypertonic by addition of 0.6 ml. of 2.5 *N* NaCl solution to 2 ml. of the egg suspension. In a control sample without antifertilizin, but otherwise treated in the same way, the eggs soon presented numerous small wrinkles on the surface. After a shorter or longer time (20–60 minutes) the surface of the eggs became smooth. Simultaneously more or less numerous vacuoles appeared below the egg surface. These vacuoles never appeared in immature or fertilized eggs upon treatment with hypertonic solution (cf. (18)).



FIG. 12

*Psammochinus* Eggs Agglutinated under the Influence of Clupein  
Exhibiting Angular Plasmolysis  
Below two singly spaced smooth eggs

The agglutinated eggs exhibited, upon exposure to the hypertonic solution, the angular type of plasmolysis characteristic of activated eggs, cf. Fig. 12. Furthermore, it was observed that no vacuoles appeared in the agglutinated eggs when the angular surface gradually changed into a smooth one. This is a further similarity to activated eggs. The number of angular eggs which appeared upon exposure to a hypertonic solution varied between a few and about 25%. Only in a few instances did the number of angular eggs amount to 50%. Not only the concentration of antifertilizin, but also the character of the egg material, influenced the number of eggs responding in the manner described.

The non-agglutinated eggs almost always behaved like the control eggs. However, the wrinkles had a tendency to disappear earlier in the eggs treated with antifertilizin.

The following table gives a record of the state of the eggs 3–4 minutes after their exposure to hypertonic sea-water.

Antifertilizin in sea-water	0	1:4	1:8	1:16	1:32	1:64	1:128	1:256
Percentage of angular eggs	—	20–25	20	10–15	10–15	5	0	0

The non-angular eggs were finely wrinkled or, in a few cases, smooth. In one experiment, it was found that, in presence of antifertilizin 1:4, 1:8, 1:16 or 1:32, the singly spaced eggs presented a smooth surface after exposure to the hypertonic medium for 20 minutes. In the stronger dilutions of antifertilizin (1:64, 1:128, 1:236) or in the control, about 50% of the eggs were still wrinkled. The small vacuoles appeared even in the presence of antifertilizin when the wrinkled, singly spaced eggs became smooth. Only in rare cases did singly spaced eggs exhibit angular plasmolysis, and then no vacuoles appeared.

A closer examination revealed the presence of a rim on the surface of each egg which underwent angular plasmolysis. The situation was similar to that found in eggs which were fertilized in the presence of antifertilizin. A membrane appeared upon exposure of the eggs to a hypertonic medium but was connected with the egg surface by a palisade of fine filaments. The cortical granules could be distinguished more or less clearly in the membrane. When the phase-contrast method was used, the granules often appeared somewhat elongated in a tangential direction. They had probably assumed a more rod-like shape. In some cases a granular membrane was separated from the egg surface, but the perivitelline space remained narrow and the retardation was much lower than in a normal fertilization membrane.

Antifertilizin preparations made from *Psammarchinus*, *Echinocardium* or *Strongylocentrotus* spermatozoa all acted in the same way. The species specificity, if present at all, must be very limited.

Clupein was shown to exert the same action on the egg surface as antifertilizin. Its action was even more pronounced and regular than that of the latter. *Psammarchinus* eggs were immersed in the following dilutions of a 0.1% clupein solution:

1 1:10; 2 1:50; 3 1:100.

A certain agglutination was observed, whereas, in a parallel control in sea-water, all the eggs were singly spaced. After about 15 minutes, the samples (each containing 2 ml. egg suspension) were rendered hypertonic by addition of 0.6 ml. sea-water. In 1 and 2 all the eggs presented angular plasmolysis; a radially striated rim or a granular membrane with a narrow perivitelline space became visible.

In 3 about 85% of the eggs exhibited angular plasmolysis, whereas about 15% were smooth. These latter eggs showed superficial vacuoles, which, as usual, were absent in the angular eggs.

Control eggs and eggs from sample 1 were transferred from the isotonic medium to distilled water. After 3 minutes, the eggs from the control began to burst at one point, and a great exovate was formed while a curled vitelline membrane appeared. Conversely, the membrane

of the eggs from 1 proved to be more resistant. It was not seen to burst; nevertheless, a part of cytolized material escaped from the interior of the egg. Following treatment with antifertilizin, the membrane also exhibited a greater resistance toward distilled water. The membrane seems to stiffen to a certain degree under the action of antifertilizin or clupein.

Eggs of *Echinocardium* were also deprived of their jellies and exposed to the action of different dilutions of antifertilizin as in the experiments with *Psammechinus* eggs. The peculiar pear-shaped form of the *Echinocardium* eggs has been briefly described in several papers from this laboratory (cf. Gustafson (29)). When the eggs were deprived of their jellies, they flattened and a number of more or less parallel wrinkles or ridges appeared on the surface of the somewhat anisodiametric egg (longer axis 135  $\mu$ , shorter axis 103  $\mu$ ), cf. Fig. 13. As usual 1-2 drops of 0.1% serum albumin were added to prevent the eggs from adhering to the glass (cf. p. 422). Even in presence of serum, the eggs of *Echinocardium*



FIG. 13

*Echinocardium* Egg Deprived of its Jelly Hull

adhere to the glass when they are immersed in samples containing antifertilizin. The eggs were anisodiametric as in the control, but the surface generally became smooth. When the samples were rendered hypertonic by the customary addition of 2.5 N NaCl, a granular membrane appeared. The adhesion to the glass was evidently due to the same change of the surface which brought about the agglutination of the *Psammechinus* eggs. Indeed, the *Echinocardium* eggs also were sometimes found to adhere in groups, i.e., to agglutinate, under the action of antifertilizin.

In one experiment, *Echinocardium* eggs with jelly coats were immersed in an 1:4 antifertilizin solution. In this special case, no precipitation of the jelly occurred, despite the presence of antifertilizin, the titer of which had probably decreased during storage. In a great number of eggs, however, a granular membrane formed, which was well elevated from the egg surface. The granules were quite evenly distributed over the membrane and of uniform size. They evidently represented the cortical granules. *Echinocardium* eggs become spherical on normal fertilization 10-15 seconds after the elevation of the membrane. The spherical shape

was not, however, assumed by the eggs from this experiment. They retained, as shown in Fig. 14, their anisodiametric form with an extrusion marking the animal pole. On the dark field, the surface color was as yellow as in the eggs of the untreated control, *i.e.*, the color change which normally accompanies activation did not take place. In this experiment, some special conditions possibly prevailed. At all events, the effect was not reproduced as clearly in repeated experiments. Despite this, some important conclusions can be drawn from the present observations. It is evident that the change of color of the plasma membrane, as well as the change of form of the egg, are independent of the extrusion of the cortical granules. It is further evident that the membrane may be considerably elevated from the egg surface without dissolution of the cortical granules (*cf.* also Fig. 6). The birefringence was not studied in this special experiment, but we know by experience that membranes with evenly distributed granules as in the present case give a retardation which is only about 25% lower than that of a normal fertilization membrane.

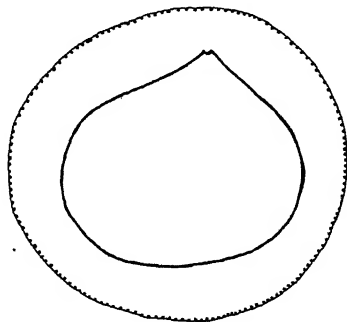


FIG. 14

Anisodiametric *Echinocardium* Egg with a Finely Granular Membrane

A great number of experiments were also carried out in which *Psammechinus* or *Echinocardium* eggs were exposed to a combined action of antifertilizin and sperm lysin, the surface-active agent which was extracted from the spermatozoa (*cf.* above). In other experiments, antifertilizin was combined with different detergents which act in the same way as the sperm lysin, for example, Duponol, *cf.* (27). Under the combined action of antifertilizin and sperm lysin, a type of membrane formation always occurred in high percentage. The membranes were granular, but showed many different stages of elevation. In a mixture containing 1:4 antifertilizin and 1.4 sperm lysin, eggs of *Echinocardium* showed a particularly interesting feature. A hyaline membrane adhering without any interspace to the plasma membrane was visible. This membrane contained the cortical granules. It seems rather probable that we are con-

cerned here with a stage which is passed rapidly under normal conditions but which has been stabilized under the circumstances prevailing in the experiment in question. In other cases the development advanced a step further; a more or less narrow perivitelline space appeared. The conditions prevailing in these eggs are represented in the diagram of Fig. 15b.

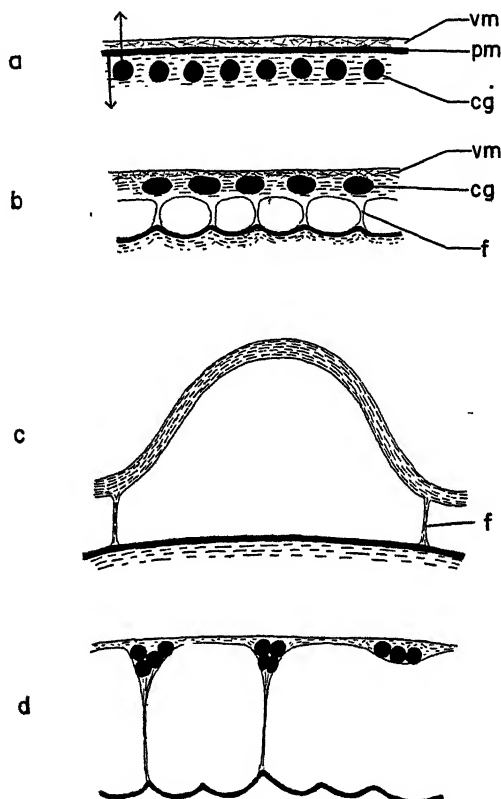


FIG. 15 a-d

Diagrammatic Figures Serving to Illustrate Various Phases of the Formation of the Fertilization Membrane

Vitelline membrane (vm), plasma membrane (pm), cortical granules (cg), filament (f)

FIG. 15a. Conditions in the Mature Unfertilized Egg

FIG. 15b. Early Stage of the Membrane Formation

FIG. 15c. A Bulging Smooth Part of the Fertilization Membrane

FIG. 15d. Granular Membrane Formed in a Hypertonic Solution.

### *Membrane Formation in Unfertilized Eggs Subjected to a Hypertonic Solution*

The reaction of unfertilized *Psammechinus* eggs to a hypertonic solution (2 ml. sea-water  $\pm$  0.6 ml. of 2.5 N<sub>s</sub> NaCl) has repeatedly been

described, (*cf.* 1, 9, 18). Membranes were often formed by a certain number of the eggs while these still remained in the hypertonic solution. The eggs of certain females formed no membrane, while in other cases a greater or smaller number of the eggs reacted by membrane formation. This process occurred only rarely in percentages higher than 20-30. The membrane formation began only after an exposure to the hypertonic solution of at least 5-10 minutes.

The membranes formed by *Psammechinus* eggs in the hypertonic solution were always granular. The granules seemed to be attached inside the membrane. The number of granules was variable. So too was the retardation of the membrane which attained *in maximo* half the value of the retardation prevailing in a normal fertilization membrane. What appeared as one granule in the membrane formed under the action of hypertonic solution, often corresponded to a group of aggregated cortical granules, *cf.* the diagrammatic Fig. 15d. Owing to these circumstances, the granules in the membrane often appeared coarser and less regular than the cortical granules of the intact unfertilized eggs.

In contradistinction to the eggs of *Psammechinus*, those of *Echinocardium* were able to form a normal fertilization membrane under the influence of hypertonicity. During its elevation, the membrane at first formed local bulges which, however, soon coalesced to a uniform smooth membrane showing the normal value of retardation. Intermediate granular stages were also observed more or less distinctly. In the presence of antifertilizin, the membrane remained granular, *although it was well separated from the egg surface by a perivitelline space of almost normal width.*

#### *The Influence of Diluted Serum on Membrane Formation*

The eggs of *Psammechinus*, as well as those of *Echinocardium*, were often found to be refractive to fertilization. Many experiments were, therefore, designed with the aim of finding procedures which would render the eggs fertilizable. It was soon found that the addition of diluted serum from rabbit or sheep to the sea-water (*e.g.*, 1 part serum  $\pm$  9-15 parts sea-water) often had a most surprising effect on the refractive eggs. The untreated eggs sometimes formed no membranes, whereas all those which had remained in contact with the serum mixture formed well-elevated membranes. It was soon revealed that the serum caused a swelling of the jelly coats. These were often fairly narrow on eggs freshly brought from their habitat into the laboratory. Under these circumstances the jelly counteracted the elevation of a membrane; consequently, the segmentation of the cytoplasm was also inhibited or, at least, showed an abnormal course. The eggs of the littoral form of *Psammechinus* (*cf.* (1)) have a diameter of about 98  $\mu$ ; the jelly coat has a varying thickness.

When it is 20–25  $\mu$  thick, it is tough enough to prevent normal membrane elevation. A jelly coat of 30–40  $\mu$ , on the other hand, has so changed its physical state as to allow normal membrane formation. Under the influence of the diluted serum, the jelly coat may attain a thickness of 80–90  $\mu$ . A number of amino acids proved able to exert the same influence on the jelly coat as that of the serum. Histidine caused a considerable swelling, even in the concentration 0.0025% in sea-water. Five-hundredth to 0.1% glycine solution in sea-water was frequently used to swell the jelly coats and render the eggs normally fertilizable. Cysteine, tryptophan and glutamic acid in the same concentration range also exerted the swelling effect.

The jelly coats of *Echinocardium* eggs responded in the same way to the serum and the amino acids as recorded above for *Psammechinus*. During these experiments, it was found that the formation of a perfect fertilization membrane often occurred upon treatment of *Echinocardium* eggs with diluted serum. The serum used was generally inactivated, i.e., warmed to 56°C. for one-half hour. A membrane formation upon treatment with serum was never observed in *Psammechinus* eggs. In the experiments with diluted serum, a slight hypotonicity prevailed. To exclude any effect from this circumstance, isotonic serum was used prepared by dialysis against sea-water. Alternatively rabbit serum was freeze-dried. The dry serum was dissolved before use in 22 *per mille* sea water and brought to the original volume. Including the serum salts, the solution could be regarded as having a salinity of about 30 *per mille*. The serum thus obtained was diluted with sea water before the experiments. The formation of a membrane occurred both in the isotonic serum-sea water mixture and in the slightly hypotonic one.

The first change observable in the presence of serum was a fine wrinkling of the surface, which recalled the first changes following the fertilization. A separation then occurred of the membrane, which, during its elevation, formed a number of bulges. The membrane gradually became uniformly elevated and now gave the same or even higher retardation than a normal fertilization membrane, which it resembled in all other respects. The egg also assumed the spherical form and showed in the dark field the same change of surface color as followed fertilization. The migration of the nucleus to the center of the egg and an increase in its volume sometimes occurred, but attempts at nuclear and cytoplasmic division were rarely observed. The elevation of the membrane took place at a lower rate than at fertilization. In certain cases, the membrane formation took as long as about 15 minutes, although generally but 1–2 minutes. In a number of cases, a granular state was distinguishable at the beginning of the elevation, followed by a corrugated or smooth stage. These observations confirm the fact that the granular and corrugated

membranes represent intermediate stages of membrane formation. In the normal fertilization, these stages occur so rapidly that they escape observation.

In experiments with *Psammechinus* eggs, it was proved that serum to a considerable extent counteracts the inhibitory effect exerted by antifertilizin. The eggs were made jelly-free and immersed 1, in different dilutions of antifertilizin or 2, in similar solutions but with, for example, 1:10 sheep serum, and then inseminated. In the presence of 1:16 antifertilizin, the membranes were granular, sometimes exhibiting transitions to the corrugated stage. In the presence of serum, the membranes were more elevated and usually smooth, although in some cases somewhat corrugated. In 1:32 antifertilizin, the membranes were still chiefly granular; upon addition of serum, however, they were almost as well developed as in the control.

Eggs which had formed a granular membrane in the presence of antifertilizin were transferred to a 1:10 serum. This after-treatment with serum was, however, quite ineffective. An improvement evidently occurs only when the treatment with serum is applied in connection with the fertilization.

Eggs with a normal fertilization membrane were transferred to undiluted serum which had been dissolved in the dry state in sea water. The perivitelline space then disappeared and the membrane apparently adhered to the egg surface. A closer examination revealed, however, that no decrease of the surface of the membrane had taken place. The surface was laid in numerous folds. Garrey (29) made an analogous experiment in which Witte peptone was used instead of serum. This author did not mention any folding of the membrane. His description might, therefore, convey the impression that the membrane is an elastic structure, the elastic stress being counterbalanced by the osmotic pressure of the perivitelline space. Our observations show that such conclusions would be erroneous. It is also obvious from previous observations that the fully formed fertilization membrane possesses a low degree of elasticity, cf. Peterfi (32). The osmotic pressure of the perivitelline space certainly plays a rôle in the elevation of the membranes and also in the maintenance of the distended state of the membrane, but this is an auxiliary factor, since an important part must also be ascribed to the structural conditions prevailing in the membrane itself.

#### *The Action of Trypsin on the Membrane Formation*

It has been reported earlier for experiments with *Psammechinus* eggs that fertilization could occur in the presence of 0.1–0.4% trypsin (1). The preparation used was from Merck (Darmstadt) and contained at least 40,000 Fuld-Gross units/g. No fertilization membrane was formed,



however, under these conditions. Furthermore, the hyaline layer failed to appear and, as a consequence, the blastomeres fell more or less apart. In other experiments, the eggs exposed to trypsin were washed with pure sea water several times immediately after the fertilization. The results were not very different from those described above. Even under these conditions the hyaline layer failed to appear or developed in a defective manner.

In one experiment, spermatozoa were added to a 0.4% trypsin solution in sea-water. The mobility of the sperm was in no way affected by the presence of trypsin. Two minutes later, eggs were added and, after the lapse of a further 1.5 minutes, the eggs were washed with pure sea-water. No membrane formation occurred, but about 50% of the eggs segmented. In this case, however, a hyaline layer appeared. It became especially visible when the eggs were immersed in a hypertonic solution.

Perhaps more important in relation to our problem were the experiments earlier reported in which unfertilized eggs were subjected to a treatment with trypsin for various periods, then washed free from trypsin and inseminated. No membrane appeared provided the exposure to trypsin had not been too brief. In many cases, a pre-treatment with trypsin for 2-3 minutes was sufficient to suppress membrane formation. The immediate effect of the exposure to trypsin is certainly a disturbance of the structure of the vitelline membrane (*cf.* (1)). Our results prove that the vitelline membrane must be extremely sensitive to the attack by trypsin. Furthermore, it is evident that the presence of an intact vitelline membrane is a prerequisite for the formation of the fertilization membrane. The exposure to trypsin does not change the appearance which the eggs present when viewed with dark-field illumination. The surface of the egg is yellow; upon fertilization the color changes to silvery white. With the aid of phase-contrast microscopy, it could be established that the cortical granules of unfertilized eggs were not broken down under the action of trypsin.

Subsequent to fertilization of the eggs pretreated with trypsin, the granules were extruded, even when the membrane formation was suppressed. With the phase-contrast method, it could be observed that the granules remained more or less attached to the egg surface. Eggs fertilized in the presence of trypsin were fixed in Flemming's solution, sectioned and overstained with iron hematoxylin. The extruded cortical granules were found to adhere to the surface of the eggs. It was obvious that a flattening of the granules had occurred. In many cases a regular layer of flattened granules was observed. Traces of the vitelline membrane seemed to be present, and these perhaps served as a support for the granules.

The *Echinocardium* eggs reacted, on the whole, in the same way as the *Psammechinus* eggs to treatment with trypsin. As described above, the *Echinocardium* eggs deprived of their jelly coats are anisodiametric

and show ridges or wrinkles on their surface (*cf.* Fig. 13). Upon immersion in 0.025–0.4% trypsin, the egg surfaces became smooth, and the eggs assumed a more or less pronounced spherical form. When the eggs remained in contact with a 0.05–0.1% trypsin solution for 1–2 hours, the nucleus migrated to the center of the egg and beautiful monasters appeared; no segmentation followed, however. This action of trypsin on the interior is probably not direct in nature. As mentioned above, minute quantities of albumin were always added to the jelly-free eggs to prevent their attachment to the glass. Breakdown products of these proteins may be able to diffuse into the interior of the egg and cause an activation of the nuclear apparatus. Addition of isotonic rabbit serum (*cf.* p. 442) effectively delayed the smoothing of the eggs in contact with trypsin and also protected, more or less completely, the membrane-forming mechanism. For example, the following mixtures were compared in their action on eggs:

	Sea-water	0.4% trypsin in sea-water	Isotonic rabbit serum
1.	1.75	0.25	—
2.	1.25	0.25	0.5

In 1, no membranes were formed; in 2, 30–40% of the eggs formed membranes upon fertilization. In a parallel experiment, 1 was rendered hypertonic by addition of 2.5 *N* NaCl (0.6 ml. to 2 ml. of sample). No membrane appeared, whereas in 2, upon addition of the 2.5 *N* NaCl solution, 100% of the eggs formed smooth membranes which possessed a normal birefringence. They were, indeed, similar to the membranes formed in a sample of eggs in sea-water which were subjected to the hypertonic medium. When membranes were uncommonly formed in a 0.05% trypsin solution, they gave the impression of being thinner than the normal membranes and their retardation was lower.

#### *The Formation of the Fertilization Membrane under Various Abnormal Conditions*

In experiments with *Psammechinus* eggs, it was found that a granular membrane also appeared under a number of abnormal conditions other than those considered above. The eggs were kept between slide and coverslip in a drop of sea water, and sperm was added from one side of the coverslip. It often occurred under these conditions that a low granular membrane appeared. The outcome was often the same when the eggs were inseminated in bowls containing sea water of lowered pH, *e.g.*, 6.8.

*Psammechinus* eggs were inseminated in normal sea water and then immediately washed 5 times in Ca-free sea water. Under these conditions, a low and granular membrane appeared. In a control which remained in normal sea water, perfect membranes were found upon insemination.

Unfertilized eggs were immersed in solutions of the organic mercury compound, merthiolate (1), in, for example, the following concentrations: 1 0.01, 2 0.001, and 3 0.0001%. The eggs were inseminated in these solutions and in a parallel control. While this latter showed a normal fertilization membrane, only a very thin wrinkled and granular membrane appeared in 1. The membrane was often thrown off. Paradoxically, in 2, the cytolysis was more complete than in 1, and no membrane appeared. Finally in 3, 25% of the eggs showed a normal membrane upon fertilization, but no cleavage occurred.

In experiments with 0.005% merthiolate, it was observed that the cortical granules were detached, pushed towards the interior of the eggs, and aggregated below the cortex. This is just the opposite to what happens under normal conditions. The thinness of the membrane formed in the presence of merthiolate may be due to the reversed displacement of the cortical granules. The membrane under these circumstances corresponds merely to the thin vitelline membrane.

According to Fr. Lillie (33), copper, even in very great dilutions, exerts an inhibitory effect on the fertilization process. The following solutions of  $\text{CuSO}_4$  were prepared in sea water: 1  $10^{-3}$  M; 2  $10^{-5}$  M; 3  $5 \times 10^{-6}$  M. The eggs in these solutions and a parallel control in sea water were inseminated. In the control, a normal membrane was elevated; a dark cytolysis occurred in 1. No membrane appeared in 2, but in 3, a thin, curled membrane was formed which was granular. Its retardation was low. In some cases the membranes were thrown off. In certain cases it was observed that the granules fell off the membrane into the perivitelline space where they disappeared. In spite of this, the retardation of the membrane remained as low as it was at the first appearance of the membrane. This supports our contention that the merging of the granules with the vitelline membrane, and not their dissolution in the perivitelline space, is the prerequisite for the normal strong increase of the retardation of the fertilization membrane as compared with the vitelline membrane.

Eggs stratified by centrifuging were fertilized. A weakly birefringent granular membrane was formed. Eggs of the same female fertilized without centrifugation lifted off a normal highly birefringent membrane.

#### DISCUSSION

The data submitted above may be combined to give a fairly consistent picture of the mechanism of formation of the fertilization membrane. Above all, our observations elucidate the fate and rôle of the cortical granules, which are undoubtedly included in the membrane. Only when the granules merge with the membrane does this attain its normal degree of birefringence. A transformation of the cortical granules, in accordance

with Moser's assumptions, into vacuoles which later coalesce was never noted in our numerous observations, even when a fairly slow membrane formation occurred, as in *Echinocardium* eggs under the influence of serum or in the experiments with *Strongylocentrotus* eggs described on p. 432. On the other hand, a dissolution of the granules in the perivitelline space was observed (*cf.* p. 446), but the membranes in these cases always proved to be thin and to have a low retardation value. In general, a granular membrane was low but a perivitelline space was formed below it, and it could occasionally be elevated to a height almost reaching that of a normal fertilization membrane, (*cf.* Fig. 14). Evidently, no cortical granules dissolved in this case. Consequently, the colloids of the perivitelline space could not have arisen from dissolving cortical granules.

Our views on the formation of the fertilization membrane are represented in the diagrammatic Fig. 15. In the unfertilized egg, Fig. 15a, the cortical granules (*cg*) are situated below the plasma membrane (*pm*), visible on the dark field as the luminous layer. Outside this, we find the vitelline membrane (*vm*) in which no ordered arrangement of the protein fibrils is found. In 15b, a stage is represented with the granules outside the plasma membrane. The rearrangement of the surface layers takes place in connection with the wave of contraction which spreads over the egg surface from the entrance point of the spermatozoon, *cf.* Peterfi (32), Just (34). The wave in question also involves a change in the color of the surface as viewed in dark field and is rapidly passing in normal eggs. Under abnormal conditions, the contraction is often more pronounced and its regression slow, as was observed for example in *Strongylocentrotus* eggs at the end of their breeding season.

The arrows in Fig. 15a illustrate the movements which are involved in the contraction. The plasma membrane retracts (downward arrow) and the granules are squeezed out along with a matrix substance which also forms the filaments so often observed under abnormal conditions. The filaments are probably also present in a first rapidly passing stage of the membrane formation, *cf.* Fig. 15b and 15c,f. In normal development, the filaments rapidly break up. They may be partly included in the membrane and partly contribute to the osmotically active material of the perivitelline membrane.

The retraction of the plasma membrane may be due to a momentary coagulation of certain components of the cortex. Bernal and Fankuchen (35) observed the separation of preparations of plant virus into two phases, a top and a bottom layer. Furthermore, they noted an extrusion of impurities from the settling bottom layer. Despite the great differences in the systems and in the rate of the processes, the contraction of the egg surface may be comparable with the settling of the bottom layer and

the extrusion of the cortical granules with that of the impurities from the bottom layer.

A fertilization membrane is never formed after removal of the vitelline membrane by trypsin, *cf.* p. 444. The cortical granules are, however, extruded, even in eggs pretreated with trypsin. Under these conditions, no filaments were observed. Evidently, the material of which the threads consist is broken down by trypsin. The cortical granules, on the other hand, seem to be very slowly attacked by trypsin.

Fig. 15c represents a bulge, which has been formed after the merging of the cortical granules with the remainder of the material constituting the membrane, *cf.* p. 433. The corrugated appearance is due, as pointed out above, p. 432, to the presence of numerous small bulges on the surface of the membrane.

In the corrugated stage the membrane has almost attained its final surface area even if the membrane in this stage is only faintly elevated from the egg surface. The area of this latter was found to be about  $30,000 \mu^2$  in the *Psammechinus*, about  $45,000 \mu^2$  in the *Echinocardium*, and about  $50,000 \mu^2$  in the *Strongylocentrotus* egg. The area of the membrane is about twice that of the egg surface. The increase of the area is effected chiefly through the merging of cortical material, granules and their matrix, with the vitelline membrane. The osmotic forces exerted by the colloids present in the vitelline space contribute to the elevation and a smoothing of the membrane, *cf.* Hobson (36).

Fig. 15d represents diagrammatically the conditions in *Psammechinus* eggs with a membrane formed under the action of a hypertonic solution. The cortical granules were found to be aggregated in groups which had not really merged with the membrane. A granular membrane may occasionally be considerably elevated from the egg surface, *cf.* Fig. 14, even in isotonic medium. This circumstance contradicts the view that the cortical granules give rise to the colloids of the perivitelline space.

We are concerned in the case of the fertilization membrane with a negative form-birefringence due to alternation of protein and water layers. Practically no birefringence is shown when the immersing medium is glycerol. The form-birefringence of the membrane was calculated according to Wiener's formula (*cf.* Friedel (37)) on the assumption that  $n_1 = 1.45$  (the refractive index of glycerol) and  $n_2 = 1.33$  (the refractive index of water). Furthermore the relative volume of protein and water was assumed to be equal ( $\vartheta_1 = \vartheta_2 = 0.5$ ).

On these assumptions the value of the birefringence ( $n_a - n_o$ ) was found to be about 0.01. Thus the thickness of the membrane would be of the order  $1 \mu$  according to the well-known formula  $\Gamma = d(n_a - n_o)$  where  $\Gamma$  (amounting to  $12.5 m\mu$ ) means retardation,  $d$  the thickness, and  $n_a - n_o$  the birefringence.

The "corrugated" membrane showed a retardation which was as great as that of the fully developed smooth membrane, although the former appeared thinner than the latter. This proves that the alternating layers are already formed in the corrugated stage. The dispersion of the layers, however, may increase, and a moderate water uptake may render the smooth membrane somewhat thicker than the corrugated. Thereby, a certain decrease of the birefringence should occur which possibly compensates the increase of the retardation due to the increase of thickness. In the smooth stage, new bonds evidently are formed which give a higher degree of mechanical strength to the membrane. It is of significance that cysteine interferes with the change in mechanical properties of the membrane, *cf.* (1).

The structure is evidently less ordered in a granular than in a corrugated or smooth membrane. The merging of the granules with the membrane involves considerable structural changes which reveal themselves in the increase of birefringence. On the other hand, the granular membrane shows a birefringence which certainly is higher than that of the vitelline membrane. As inferred above, p. 424, this is practically non-birefringent. The retardation of a granular membrane may be due to matrix material which, after incorporation, assumes an ordered structure as indicated in Fig. 15b.

A granular membrane appears grayish in the dark field with denser gray spots which may correspond to the cortical granules. A fully developed smooth membrane is not visible in the dark field. A luminous ring apparently represents the membrane. By the use of a Zeiss switch condenser (*Wechselkondensor*) it could be demonstrated that we are concerned with a sort of halo which lies inside the non-luminous membrane (*cf.* (6)). The halo appears only when the membrane is well elevated and smooth. The observations with dark field illumination indicate that the dispersion is greater in the smooth than in the granular membrane.

Some calculations show that the cortical granules probably constitute only a minor part of the membrane. The volume of this latter may be assumed as equal to some value between 30,000 and 60,000  $\mu^3$  (thickness assumed to be 0.5–1  $\mu$ ). The diameter of the cortical granules falls between 0.5–1  $\mu$ . Let us assume 0.8  $\mu$ , which probably is a maximum value. This gives for each granule a volume of 0.27  $\mu^3$ , and the total volume of 30,000 granules amounts to about 8100  $\mu^3$ . This value is much smaller than the total volume of the membrane.

The remainder of the volume corresponds to the vitelline membrane and to the matrix exuded along with the granules. It is, perhaps, of some interest to point out in this connection that granules appear as intermediate stages in the keratinization of mammalian epithelium cells, *cf.* (38) and (39).

The formation of the hyaline rim or layer which appears only about 10 minutes after the fertilization is, to a certain extent, a repetition of what happens in the first stages of the formation of the fertilization membrane. A thin limiting sheath appears outside the plasma membrane and both are connected by a layer which—at least after immersion of the egg in a hypertonic medium—shows a radial striation. Furthermore, free threads were observed to project from the egg surface as the first stage in the dissolution of the hyaline layer in eggs exposed to various agents; concerning further comments on the threads of the hyaline layer, cf. Just (34). T. Gustafson (personal communication) observed that the hyaline layer in *Strongylocentrotus* eggs may separate from the egg surface upon exposure to the detergent Duponal. Under these conditions, the sheath, which normally showed no birefringence, gave a retardation exceeding even that of the fertilization membrane. The change in the sheath was no doubt due to the incorporation of material from underlying parts.

Two agents have been used in experiments described above, viz. *antifertilizin* and *sperm lysin*. The former seems to have a certain precipitating, the latter a dispersing action, on certain constituents of the egg surface. The dissolution of the filaments which extend between membrane and plasma surface is counteracted by antifertilizin but favored by sperm lysin. Under the influence of the former, the initial stage in the membrane formation may occur, cf. p. 437. Clupein could imitate or even surpass antifertilizin in this respect. What happens may be illustrated by comparing Fig. 15a and b. Sperm lysin breaks up the filaments, whereupon a corrugated or curled membrane may elevate. Bee venom proved to be still more active in producing a membrane of normal structure.

Antifertilizin and lysin are present in both eggs and spermatozoa. Our still incomplete experiments may indicate that agents can be extracted from the germ cells which might induce different steps in the formation of the fertilization membrane.

#### ACKNOWLEDGMENTS

We are indebted to Dr. Gunnar Gustafsson, head of the Zoological Station Kristineberg, for his unfailing courtesy, and to Professor Torbjörn Caspersson for help with the photographs of living material.

#### SUMMARY

Studies were carried out on the surface layers and the formation of the fertilization membrane in the eggs of *Psammechinus miliaris*, *Echinocardium cordatum* and *Strongylocentrotus droebachiensis*.

The sign of birefringence and the retardation of the cortical layer were determined. No perceptible change of retardation occurred on fertiliza-

tion. The birefringence of the cortex is due chiefly to ordered lipid layers. The cortical granules have no influence on the birefringence of the cortex. They are formed at the maturation of the egg. By means of a number of different experiments and observations, it was rendered probable that the cortical granules, along with a matrix, merge with the vitelline membrane to form the fertilization membrane. A granular membrane gives a low retardation. Only on incorporation of the cortical granules and their matrix did the retardation of the membrane attain its normal value (about 12.5  $m\mu$ ).

An attempt was made to combine numerous data to a consistent picture of the mechanism of the membrane formation, *cf.* above under "Discussion."

#### REFERENCES

1. RUNNSTRÖM, J., MONNÉ, L., AND BROMAN, L., *Arkiv Zool.* **35A**, No. 3 (1943).
2. HENDÉE, E. C., *Carnegie Inst. Wash. Pub.* **27**, 101 (1931).
3. LINDAHL, P. E., *Protoplasma* **16**, 378 (1932).
4. MOSER, F., *J. Exp. Zool.* **80**, 423 (1939).
5. MOSER, F., *J. Exp. Zool.* **80**, 447 (1939).
6. RUNNSTRÖM, J., *Protoplasma* **4**, 388 (1928).
7. SCHMIDT, W. J., *Ergeb. Physiol., biol. Chem. exptl. Pharmacol.* **44**, 27 (1941).
8. RUNNSTRÖM, J., MONNÉ, L., AND WICKLUND, E., *Nature* **153**, 313 (1944).
9. RUNNSTRÖM, J., AND MONNÉ, L., *Arkiv Zool.* **36A**, No. 18 (1945).
10. JENKINSSON, I. W., *Arch. Entwicklungsmech. Organ.* **32**, 699 (1911).
11. LINDAHL, P. E., *Arch. Entwicklungsmech. Organ.* **126**, 373 (1932).
12. MONRÓY, A., AND MONROY-ODDO, A., *Boll. soc. ital. biol. sper.* **20**, 1 (1945).
13. MONROY, A., *Experientia* **1**, 335 (1945).
14. ERCOLI, A., Nord and Weidenhagen, *Handb. Enzymologie* **1**, 480 (1940).
15. ÖHMAN, L. O., *Arkiv Zool.* **36A**, No. 7 (1944).
16. HERBST, C., *Arch. Entwicklungsmech. Organ.* **9**, 424 (1900).
17. DANIELLI, J. F., in Bourne, Cytology and Cell Physiology. Oxford (1942).
18. RUNNSTRÖM, J., AND MONNÉ, L., *Arkiv Zool.* **36A**, No. 20 (1945).
19. RUNNSTRÖM, J., *Acta Zool.* **25**, 159 (1944).
20. FRANK, J. A., *Biol. Bull.* **76**, 190 (1939).
21. LILLIE, F., Problems of Fertilization. Chicago (1919).
22. TYLER, A., AND O'MELVENY, K., *Biol. Bull.* **81**, 364 (1941).
23. HARTMANN, M., AND SCHARTAU, O., *Biol. Zentr.* **59**, 571 (1939).
24. FLOSDORF, E. W., AND MUDD, S., *J. Immunol.* **34**, 469 (1938).
25. RUNNSTRÖM, J., TISELIUS, A., AND VASSEUR, E., *Arkiv Kemi, Mineral. Geol.* **15A**, No. 16 (1932).
26. RUNNSTRÖM, J., TISELIUS, A., AND LINDVALL, S., *Nature* **153**, 285 (1944).
27. RUNNSTRÖM, J., TISELIUS, A., AND LINDVALL, S., *Arkiv Zool.* **36A**, No. 22 (1945).
28. RUNNSTRÖM, J., AND LINDVALL, S., *Arkiv Zool.* **38A**, No. 10 (1946).
29. GUSTAFSON, T., *Arkiv Zool.* **37B**, No. 1 (1945).
30. MONNÉ, L., *Arkiv Zool.* **35A**, No. 13 (1944).
31. GARREY, W. E., *Biol. Bull.* **37**, 287 (1919).
32. PETERFI, T., *Arch. Entwicklungsmech. Organ.* **112**, 660 (1927).



33. LILLIE, F., *Biol. Bull.* **61**, 125 (1921).
34. JUST, J. E., *Biology of the Cell Surface*. London (1939).
35. BERNAL, J. D., AND FANKUCHEN, J., *J. Gen. Physiol.* **25**, 111 (1941).
36. HOBSON, A. D., *Proc. Roy. Soc. Edinburgh* **47**, 94 (1927).
37. FRIEDEL, J., *Ann. Physik.* **323**, 1031 (1905).
38. UNNA, T. G., *Histochemie d. Haut*. Leipzig-Wien (1928).
39. LORBEERBAUM, L., AND UNNA, T. G., *Dermatol. Wochschr.* **1925**, 1519.

# THE MOLECULAR WEIGHT OF LIGNIN

Nils Gralén\*

*From the Institute of Physical Chemistry, University of Uppsala, Sweden*

*Received Sept. 16, 1946*

## INTRODUCTION

As an almost generally accepted view, lignin belongs to the class of high-molecular compounds. It is very probable that lignin is composed of smaller units of uniform structure linked together to form a chain, straight or branched, just as other natural products, *i.e.*, cellulose, starch and other "polyoses." Many attempts have been made to determine the size of the lignin molecule by various methods, but results do not agree well. In the present work the ultracentrifuge technique has been used for molecular weight determinations. Some of the results have been reported earlier (9).

It is of particular importance to isolate the lignin from wood as mildly as possible to avoid spoiling the lignin molecule. Most of the methods used hitherto include strong alkaline or acid hydrolysis or alcoholysis at high temperature. Holmberg (7) introduced a new technique, using mercapto acids, which seem to be rather mild agents for such isolation. Most of the preparations investigated in this work have been obtained from Holmberg.

In the mercapto acid method of lignin preparation, wood powder is digested with thioglycolic acid and hydrochloric acid at the temperature of boiling water. It is then extracted with a sodium hydroxide solution, which dissolves the compound of lignin and thioglycolic acid. The dissolved material is precipitated with hydrochloric acid. The product thus obtained was analyzed and found to represent almost exactly the formula  $C_9H_9O_3(OCH_3)$  combined with one molecule of thioglycolic acid.

This method has been used with slight variations for the preparation of lignin thioglycolic acid (1, 7, 9) from spruce wood, and also for other species of plants (8). A representative selection of Holmberg's preparations from this study was also subjected to an ultracentrifugal study. It included lycopodium (*Lycopodium annotinum*), rye (*Secale cereale*), beech (*Fagus silvatica*), ash (*Fraxinus excelsior*) and burdock (*Arctium tomentosum*).

Holmberg (10) also introduced the treatment with hypobromite as a method of lignin preparation. A few of these preparations were also examined.

\* Present address: Swedish Institute for Textile Research, Gothenburg, Sweden.

Finally, acetic acid lignin, as introduced by Schütz and Knackstedt (13), also described by Freudenberg (4) and by Brauns and Buchanan (2), and alkali-lignins, prepared by heating wood in alkali under pressure, were used in this investigation. The source for these preparations as well as for the hypobromite lignin was spruce wood.

#### METHOD OF MOLECULAR WEIGHT DETERMINATION

The molecular weights were determined by the Svedberg ultracentrifuge method (14), using the following formula:

$$M = \frac{RTs}{D(1 - V\rho)},$$

where  $R$  is the gas constant,  $T$  the absolute temperature,  $s$  the sedimentation constant,  $D$  the diffusion constant,  $V$  the partial specific volume of the solute and  $\rho$  the density of the solution.

The sedimentation constant was measured in Svedberg's oil turbine ultracentrifuge at a centrifugal force of about 300,000 times gravity and is given in Svedberg units ( $1 S = 10^{-13}$  c.g.s.).

The diffusion constants were measured in the slide cell developed by Lamm (11). The unit for  $D$  is  $10^{-7}$  cm.<sup>2</sup>/sec.

To avoid any electrostatic charge effect on the sedimenting or diffusing particles, all experiments were performed in a solution of electrolytes, namely 0.2  $N$  NaOH + 1.0  $N$  NaCl. The alkali is necessary to dissolve the material.

The partial specific volume was measured pycnometrically in the same solvent. The substance had been dried *in vacuo* over phosphorus pentoxide.

#### MOLECULAR WEIGHTS OF THIOLYCOLIC ACID LIGNIN PREPARATIONS FROM SPRUCE

The sedimentation constants were measured at different concentrations. When the sedimentation constants are as low as those found, it is difficult to make an exact determination. The boundary in the sedimentation column is very diffuse, partly depending on the polydispersity of the material and partly on the rapid diffusion. At a concentration lower than 0.5% it is impossible to determine the sedimentation constant. Fig. 1 shows a sedimentation curve of one of the preparations (Li-Th 1 A<sub>2</sub>) at 1% concentration. The sedimentation constant has always been calculated from the position of the top of the curve. The accuracy for this determination will be about  $\pm 5\%$ . Table I gives a summary of the sedimentation constants of the thioglycolic acid preparations. In most cases  $s_{20}$  varies very little with concentration. An extrapolation to zero concentration has always been made. These values, given in the last column of the table, have been used for the molecular weight calculations.

Due to the polydispersity, the values given will be averages for the different molecular sizes in the mixture. In all cases investigated only one peak has been found on the sedimentation curve and no tendency toward separation into distinct components has been observed. This

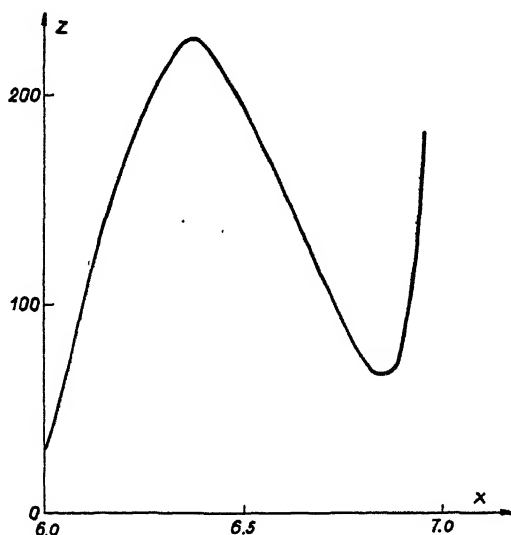


FIG. 1

Sedimentation Curve of Li-Th 1 A<sub>2</sub>

Abscissa: distance from center of rotation. Ordinate: scale line displacement. Centrifugal force 300,000 times gravity. Time: 160 min. after reaching full speed (65,000 r.p.m.).

TABLE I

Preparation	S <sub>20</sub>			
	2%	1%	0.5%	0 ( <i>extrap.</i> )
Li-Th 1 A <sub>2</sub> *	1.24	1.46	1.18	1.3
Li-Th 1 B <sub>2</sub>	1.50	1.53	1.50	1.5
Li-Th 3 B	1.27	1.22	1.32	1.3
Li-Th 5 A <sub>2</sub>	—	1.31	1.30	1.3
Li-Th 5 A <sub>3</sub>	—	1.71	2.40	3.0
Li-Th 5 B <sub>2</sub>	1.41	1.58	1.55	1.6
Li-Th 6 A <sub>2</sub>	1.09	1.41	1.73	1.8
Li-Th 6 B <sub>2</sub>	1.28	1.33	1.42	1.4
Li-Th Ba <sub>2</sub>	—	1.21	1.08	1.0
Li-Th 7 B <sub>1</sub>	1.38	1.38	1.73	1.8
Li-Th 7 B <sub>2</sub>	—	1.21	1.64	1.6

\* The symbols for the preparations are the same as those used by Holmberg in the papers describing the preparations (7, 8, 9, 10).

means that the molecular weight distribution function has one maximum only, and the sedimentation constant given corresponds approximately to the value for that maximum.

The diffusion constants, calculated as weight averages, are given in Table II. In some cases, where the accuracy of the experiment was great

TABLE II

Preparation	$D_m$	$\gamma$
Li-Th 1 A <sub>2</sub>	11.9	0.9
Li-Th 1 B <sub>2</sub>	13.4	0.6
Li-Th 3 B	12.8	0.7
Li-Th 5 A <sub>2</sub>	10.9	0.7
Li-Th 5 A <sub>3</sub>	7.6	1.0
Li-Th 5 B <sub>2</sub>	10.8	0.7
Li-Th 6 A <sub>2</sub>	11.7	1.0
Li-Th 6 B <sub>2</sub>	12.0	0.7
Li-Th AB	19.3	0
Li-Th B <sub>81</sub>	20.8	0.4
Li-Th B <sub>a2</sub>	18.8	0.4
Li-Th 7 B <sub>1</sub>	5.7	—
Li-Th 7 B <sub>2</sub>	5.5	—

enough, a value of the polydispersity coefficient  $\gamma$  is given. It was obtained from the equation  $D_m/D_A = e^{3/8\gamma^2}$  (Gralén, 5), where  $D_m$  is the diffusion constant calculated by the statistical moment method, and  $D_A$  from area and height of the diffusion curve.  $\gamma = 0$  means homogeneity.

The partial specific volumes of the substances were measured at different concentrations. There was, in general, a slight decrease in  $V$  for decreasing concentration. Table III gives the average values of the measurements, which do not differ greatly from the extrapolated values.

TABLE III

Preparation	$V_{\text{aver.}}$
Li-Th 1 A <sub>2</sub>	0.722
Li-Th 1 B <sub>2</sub>	0.716
Li-Th 3 B	0.718
Li-Th 5 A <sub>2</sub>	0.721
Li-Th 5 A <sub>3</sub>	0.718
Li-Th 5 B <sub>2</sub>	0.714
Li-Th 6 A <sub>2</sub>	0.719
Li-Th 6 B <sub>2</sub>	0.715
Li-Th B <sub>a2</sub>	0.735

The B-preparations have been prepared with a higher concentration of thioglycolic acid than the A-preparation and consequently have a higher sulphur content. Their specific volumes are, generally speaking, a little higher than those of the A-preparations.

The molecular weights and other molecular constants of the lignin thioglycolic acids are given in Table IV.

The degree of polymerization, *D.P.*, is calculated from the molecular weight on the assumption that the molecule consists of  $C_9$ -units, the analytical composition considered (*cf.* Holmberg and Gralén, 9). It is seen that the *D.P.* is rather constant around 36, with a few remarkable exceptions. Li-Th 5 A<sub>3</sub> has been prepared from wood treated with hydro-

TABLE IV

Preparation	Mol. wt.	Degree of polymerization	$f/f_0$	Axial ratio
Li-Th 1 A <sub>2</sub>	9,500	38	1.28	5.4
Li-Th 1 B <sub>2</sub>	9,600	36	1.14	3.4
Li-Th 3 B	8,700	33	1.23	4.7
Li-Th 5 A <sub>2</sub>	10,400	45	1.36	6.7
Li-Th 5 A <sub>3</sub>	33,900	146	1.32	6.1
Li-Th 5 B <sub>2</sub>	12,800	50	1.28	5.4
Li-Th 6 A <sub>2</sub>	13,300	56	1.17	3.8
Li-Th 6 B <sub>2</sub>	10,200	39	1.25	4.9
Li-Th AB	ca. 4,000	14	—	—
Li-Th Bs <sub>1</sub>	ca. 4,000	18	—	—
Li-Th Ba <sub>2</sub>	4,400	19	1.04	1.9
Li-Th 7 B <sub>1</sub>	27,300	104	1.88	17
Li-Th 7 B <sub>2</sub>	25,200	100	2.00	20

chloric acid in the boiling water-bath. It has much larger molecules than the ordinary preparations. It is probable that the acid treatment has caused some water to be split off and has given rise to some etherification and condensation of the molecules. The same effect, although to a lesser extent, is true for Li-Th 5 B<sub>2</sub>, from wood treated in the same way, and Li-Th 6 A<sub>2</sub>, prepared from alkali-treated wood. The alkaline treatment of wood thus has an effect comparable to that of the acid treatment. This conclusion has also been drawn from analytical results (*cf.* 9).

Li-Th AB and Li-Th Bs<sub>1</sub> have been boiled with acid after the thioglycolic acid treatment, and Li-Th Ba<sub>2</sub> with alkali. They have a lower molecular weight—around 4,000. Obviously a splitting—approximately to halves—of the original molecule has occurred. The diffusion experiments indicate that at the same time the substance has become more homogeneous. This fact makes it probable that the value 4,000 is a bottom limit where the splitting is slackened or stops. It is of interest to note that almost the same values were found for the molecular weight of lignin on earlier experiments, *viz.*, about 3,900. Loughborough and Stamm (12) studied osmotic pressure, viscosity and diffusion of materials prepared by using sulphuric acid or alcoholysis in acid or alkaline medium. Conner

(3) got the same molecular weight value by measuring high frequency energy losses. His preparation was made by alcoholysis in presence of HCl.

Li-Th 7 B<sub>1</sub> and Li-Th 7 B<sub>2</sub> have been prepared by a very long treatment (3 months) with thioglycolic acid at room temperature. Their molecular weight is about three times that of those prepared at 100°. The splitting action of the acid in the reaction mixture has not gone as far, even though the reaction time was very much longer.

The frictional ratio,  $f/f_0$ , is calculated from the centrifugal data.  $f$  is the observed molecular frictional constant, and  $f_0$  is the calculated frictional constant for an unhydrated compact spherical molecule having the same molecular weight. If the molecules are assumed to be oblong ellipsoids, the axial ratio of these ellipsoids can be calculated from  $f/f_0$  (Herzog, Illig and Kudar, 6; cf. Svedberg and Pedersen, 14). As we do not know whether the molecules are ellipsoids and unhydrated (the last assumption is even improbable), the calculation must give results of approximate character only. It is of interest, however, to make a comparison between the values obtained for the different preparations. For all the preparations with *D.P.* around 36 the axial ratio is about 4–6. Li-Th Ba<sub>2</sub> with only half that *D.P.* has only half that axial ratio, whereas Li-Th 7 B<sub>1</sub> and Li-Th 7 B<sub>2</sub>, with a much higher *D.P.* (about three times), have an axial ratio of 17–20. The axial ratio is thus approximately proportional to the degree of polymerization. This means that the width of the molecules is constant and only their lengths vary. The axial ratios are rather small and one must not consider lignin a chain molecule such as cellulose. If the base units of the molecule are linked in a chain, this must be folded.

The rule of proportionality between molecular weight and axial ratio is not quite without exceptions. It is especially invalid for Li-Th 5 A<sub>3</sub> and Li-Th 6 A<sub>2</sub>. These two preparations differ from the rest in other respects also. They have the highest polydispersity of the materials measured, and they alone show a high dependence of sedimentation constant on concentration.

#### MOLECULAR WEIGHT DETERMINATIONS OF THIOLYCOLIC ACID LIGNIN PREPARATIONS FROM DIFFERENT PLANT SPECIES

These preparations were investigated in the same way as the spruce lignin preparations. The sedimentation and diffusion constants are given in Table V.

The sedimentation constants were measured at a concentration of 0.5%. The thioglycolic acid lignin from *Arctium* did not dissolve quite completely in the alkaline salt solution. Possibly some decomposition had

occurred during the long storage period since the preparation was made (10 years).

The sedimentation curves were quite like those of the spruce lignin and the diffusion curves indicated polydispersity. The partial specific

TABLE V.

Origin	$\eta_{sp}$	$D_{20}$
<i>Lycopodium annotinum</i>	1.31	8.6
<i>Secale cereale</i>	1.36	10.9
<i>Fagus silvatica</i>	1.15	8.4
<i>Fraxinus excelsior</i>	0.98	9.9
<i>Arctium tomentosum</i>	1.19	10.4

volume was assumed to be 0.72. This assumption is very legitimate, because the composition is almost the same as that of the spruce lignin preparations, which all gave about the same specific volume (cf. Table III). The molecular weights and other molecular constants are given in Table VI.

TABLE VI

Origin	Mol. wt.	D.P. ·	$f/f_0$	Axial ratio
<i>Lycopodium annotinum</i>	13,100	53	1.59	11
<i>Secale cereale</i>	10,800	45	1.34	6.4
<i>Fagus silvatica</i>	11,900	46	1.42	8
<i>Fraxinus excelsior</i>	8,600	32	1.60	11
<i>Arctium tomentosum</i>	9,900	37	1.45	8

There is not much difference between these lignins and the spruce lignin (Li-Th 1 A<sub>2</sub>). Maybe there is a tendency to higher molecular weight in the lowest-standing species (*Lycopodium*), but the difference is small and not very significant. This fact makes it very probable that lignin is a universal material which does not differ for different species. In those plants and trees where it occurs, it has about the same analytical composition (the methyl content, is, however, higher for the leaf woods than for the pine woods), and about the same molecular weights. This assumption is also supported by most experience with chemical lignin reactions.

#### MOLECULAR WEIGHTS OF HYPOBROMITE LIGNIN PREPARATIONS

The sedimentation constants at different concentrations, and the diffusion constants of the hypobromite lignin preparations are given in Table VII.



TABLE VII

Preparation	$\bar{S}_{20}$				$D_{20}$
	2%	1%	0.5%	0 ( <i>extrap.</i> )	
Li-Br 1	1.24	1.54	1.31	1.5	14.3
Li-Br-Th A	1.16	1.27	1.34	1.4	12.1
Li-Br-Th B	0.99	1.02	—	1.1	9.4
Li-Br-Me	1.44	1.33	1.56	1.5	12.7
Li-Br 2	1.54	1.40	1.74	1.7	7.7

The partial specific volumes were measured pycnometrically and were found to be;

TABLE VIII

Preparation	$V_{\text{aver.}}$
Li-Br 1	0.649
Li-Br-Th A	0.654
Li-Br-Th B	0.684
Li-Br-Me	0.660

The figures obtained accord well with the analytical composition. Li-Br-Th B has a lower bromine content than the other preparations, and this causes a higher specific volume. Li-Br-Me was methylated after the preparation was made, thus involving an increase in the amount of a lighter group and hence a higher  $V$ . For Li-Br 2 which had almost the same composition as Li-Br 1, a value of 0.649 was assumed.

The molecular weights and degree of polymerization are given in Table IX.

TABLE IX

Preparation	Mol. wt.	$D.P.$	$f/\%$	Axial ratio
Li-Br 1	7,200	32	1.20	4.2
Li-Br-Th A	8,100	32	1.37	6.9
Li-Br-Th B	9,000	34	1.68	13
Li-Br-Me	8,400	37	1.28	5.4
Li-Br 2	15,300	67	1.75	14

The first four preparations were all heated during the preparation to make the precipitate less voluminous and more easily handled. It is seen that all these preparations have the same  $D.P.$  as the thioglycolic acid lignin preparations. Li-Br 2 had not been heated, but was prepared at room temperature. The degradation was less, just as in the case of thioglycolic acid preparations at room temperature. The hypobromite, however, has a stronger effect than the thioglycolic acid at room temperature, probably due to oxidation.

## MOLECULAR WEIGHT OF ACETIC ACID LIGNIN PREPARATIONS

The results of the measurements are given in Table X.

TABLE X

Preparation	$\eta_{sp}$				$D_{90}$
	2%	1%	0.5%	0 (extrap.)	
Li-Ac 1	1.44	1.27	(1.77)	1.5	10.6
Li-Ac 2	—	1.21	1.36	1.4	10.2

The partial specific volumes of these preparations were higher than those of the sulfur- and bromine-containing preparations. For Li-Ac 1  $V_{\text{aver.}} = 0.775$  was found and for Li-Ac 2, 0.745. The molecular weight of Li-Ac 1 from these figures is 15,000 and its degree of polymerization is 75. For Li-Ac 2  $M = 13,000$  and  $D.P. = 74$  is calculated. The frictional ratios for the two preparations is 1.2 and 1.3 respectively.

There is a significant difference in the molecular size between the acetic acid lignins and the thioglycolic acid lignins. Probably the extended acid treatment has caused a condensation of the molecules. The analysis also showed a smaller water content, which favors this belief.

## MOLECULAR WEIGHT OF ALKALI-LIGNINS

Three preparations were examined. Li-Alk 1 was prepared by heating the wood in 1 *N* sodium hydroxide, the temperature being raised to 170°C. during 2 hours, the lignin later being precipitated by sulphuric acid. For Li-Alk 2 the temperature was kept at 170°C. for 2 hours, and for Li-Alk 3 for 5 hours. The yield was increased by extending the time of heating. The analysis showed no noticeable difference between the three preparations.

Only diffusion experiments were performed. The results of these are given in Table XI.

TABLE XI

Preparation	$D_{90}$
Li-Alk 1	13.0
Li-Alk 2	12.0
Li-Alk 3	12.1

The prolonged alkaline treatment at high temperature thus has not changed the molecular size. It is possible, however, that some of the lignin molecules have been demolished so completely that they did not precipitate on acidifying and thus escaped observation.

The diffusion constants without doubt indicate that the molecular weights of the alkali-lignins are of the same order of magnitude as those of the normally prepared thioglycolic acid lignins, about 7,000.

### DISCUSSION AND SUMMARY

The normally prepared thioglycolic acid lignins from spruce have a degree of polymerization of about 36. The analyses have shown that the formula of the base element of lignin is very probably  $C_9H_8O_3 \cdot OCH_3$ , and the molecular weight of pure lignin would thus be  $36 \times 196 = ca. 7,000$ . The hypobromite preparations give the same degree of polymerization. All these preparations show polydispersity and the figures given are averages.

If the wood is pretreated with acid or alkali, it becomes more resistant to thioglycolic acid. The lignin has, at least partly, undergone a condensation accompanied by a water withdrawal. This is seen also in the molecular weight, which is increased. After a second treatment with thioglycolic acid (Li-Th 5 A<sub>3</sub>) a product was obtained with the *D.P.* 146. When a larger amount of thioglycolic acid was used on the acid-pretreated wood (Li-Th 5 B<sub>2</sub>), a normal product was formed. This makes reasonable the assumption that the new bonds formed by the acid-treatment of wood are ether bonds.

When a normal thioglycolic acid lignin was heated with more thioglycolic acid, with hydrochloric acid in acetic acid, or with sodium hydroxide, it was depolymerized to about half its original molecular weight. At the same time there was an indication of homogenization. This makes it probable that the molecular particle of weight 3,500–4,000 is a more stable unit.

Preparations which were made exclusively at room temperature gave higher molecular weights. The thioglycolic acid lignins were about three times the normal size and the hypobromite lignins about twice the normal size. Analytically, they contained a little more water than the heated products.

From sedimentation and diffusion data the shape of the molecules was estimated, and it was found that, in general, the axial ratio of the molecule is proportional to its weight. Hence the width of the lignin molecule is constant and only the length varies in proportion to the weight. The axial ratio of the 7,000-molecule is about 5.

Thioglycolic acid lignin preparations from different plants show about the same molecular weight as spruce lignin. There is possibly a tendency toward larger molecular weights in the lower members of the vegetable kingdom.

Acetic acid lignin preparations had a higher molecular weight than

the thioglycolic acid and hypobromite lignins. This is probably due to some condensation process during the extended acid treatment.

Alkali lignins, prepared by heating wood in 1 *N* sodium hydroxide at 170°C., have molecular weights of the same order as thioglycolic acid lignins, about 7,000.

The author wishes to thank Professor Bror Holmberg for suggesting this investigation and for placing material at his disposal. Thanks are due also to the director of the Institute of Physical Chemistry, Professor The Svedberg, for his kind and helpful interest in the work. Financial assistance was obtained from the Royal Swedish Institute for Engineering Research and from the Rockefeller Foundation.

#### REFERENCES

1. AHLM, C. E., AND BRAUNS, F. E., *J. Am. Chem. Soc.* **61**, 277 (1939).
2. BRAUNS, F. E., AND BUCHANAN, M. A., *J. Am. Chem. Soc.* **67**, 645 (1945).
3. CONNER, W. P., *J. Chem. Phys.* **9**, 591 (1941).
4. FREUDENBERG, K., AND PLANKENHORN, E., *Ber.* **75**, 857 (1942).
5. GRALÉN, N., *Kolloid-Z.* **95**, 188 (1941).
6. HERZOG, R. O., ILLIG, R., AND KUDAR, H., *Z. physik. Chem.* **167A**, 329 (1933).
7. HOLMBERG, B., *I.V.A.: Handlingar* No. 103 (1930).
8. HOLMBERG, B., *Ibid.* No. 131 (1934).
9. HOLMBERG, B., AND GRALÉN, N., *Ibid.* No. 162 (1942).
10. HOLMBERG, B., *Ber.* **75**, 1760 (1942).
11. LAMM, O., *Nova Acta Regiae Soc. Sci. Upsaliensis* **IV**, 10, No. 6 (1937).
12. LOUGHBOROUGH, D. L., AND STAMM, A. J., *J. Phys. Chem.* **40**, 1113 (1936).
13. SCHÜTZ, F., AND KNACKSTEDT, W., *Cellulosechemie* **20**, 15 (1942).
14. SVEDBERG, T., AND PEDERSEN, K. O., *The Ultracentrifuge*. Oxford, 1940.



## LETTERS TO THE EDITOR

Dear Sir:

I have received a letter from Dr. Peter Debye (May, 1946) commenting on the suggestions contained in the article on "The Terminology of Intrinsic Viscosity and Related Functions" that appeared in the May, 1946, issue. In it he expresses general agreement with the proposals, but suggests a further recommendation, one which I should like to endorse and which I believe should be brought to the attention of the readers of your journal.

"Like every physical quantity, the intrinsic viscosity has a dimension and, it happens, the dimension is that of a specific volume. Hence, the sensible thing to do would be to express it in cc./g. Unfortunately, the unit of volume which is used is 100 cc. instead of 1 cc. This has the result that an intrinsic viscosity of 1.5 really means 150 cc./g. Now, if you would induce people to give not only the value (like 1.5) but also the dimensions and units at the same time, everything would be straightened out.

"I do not dare to suggest that the intrinsic viscosity should in the future be expressed in cc./g. because that would mean that all the customary values would have to be multiplied by 100. I suppose that objections due to inertia would be too hard to overcome."

A great deal of confusion would certainly be avoided if the unit of intrinsic viscosity were always given with the number. As there is already so much confusion in the literature it may not be too late to agree on the adoption of cc./g. (or, perhaps better, ml./g.) as the unit; it would be more natural and familiar than dl./g., the obvious but unusual unit corresponding to the Kraemer definition of  $[\eta]$  (in which  $c = \text{g./100 ml. solution}$ ). As Prof. Debye goes on to say, there is a further advantage in expressing the intrinsic viscosity in cc./g. (ml. g.). "Adopting Einstein's picture of spherical particles suspended in the medium, the intrinsic viscosity<sup>1</sup> is exactly 2.50 times the specific volume of the material of the spheres. This means that, in Einstein's picture, the intrinsic viscosity 1.5 for example, as expressed in customary units and meaning 150 cc./g.,

would correspond to  $\frac{150}{2.50} = 60 \text{ cc./g.}$  as a measure of the specific volume

<sup>1</sup> If expressed in the units cc./g. According to Einstein,  $\eta_r = 1 + 2.5\phi$  (where  $\phi = v/V$ , the volume fraction of the suspended material in the suspension). Hence  $\eta_{sp} = 2.5 v/V = 2.5 \frac{c}{100} \bar{v}$  (where  $\bar{v}$  is the partial specific volume of the dispersed phase)

and  $\eta_{sp}/c = \frac{2.5}{100} \bar{v}$ . Therefore when  $c \rightarrow 0$ ,  $100[\eta] = 2.5 \bar{v}$  ( $[\eta]$  expressed in dl./g.).

of the material of such particles. In this sense the calculated value of 60 cc./g. gives a fair indication of how much a polymer of the intrinsic viscosity 1.5 is spread out in the solvent."

On the other hand, aside from the obvious disadvantage of redefining  $[\eta]$ , which Prof. Debye mentions, there is something to be said for a unit (dl./g.) which results in smaller numbers and therefore discourages to some extent the (usually unintentional) claiming of greater precision than the measurements warrant. Moreover, the advantage that Prof. Debye cites can be at least in part secured for dl./g. by using his relation in the form (see footnote (1))  $100 [\eta] = 2.5 \bar{v}$ . Compare, for example, the use, by Lahiri, Karpinski and Mardles (*J. Inst. Petroleum* 31, 271 (1945)), of the shape factor  $\nu = \frac{100[\eta]}{\bar{v}}$ .

Summing up, I should like to associate myself with Prof. Debye in urging most strongly that the units in which  $[\eta]$  is expressed be stated explicitly; but I feel that for practical, if not logical, reasons the unit dl./g. is somewhat preferable to ml./g. (or cc./g.).

L. H. CRAGG

Department of Chemistry,  
McMaster University,  
Hamilton, Ont.

July 12, 1946

## LETTERS TO THE EDITOR

Dear Sir:

In connection with L. H. Cragg's effort to establish a terminology for intrinsic viscosity and related functions (1), the following may be of interest.

Up to the present time, most of the published data gathered with solutions or dispersions of polymers have been at low solids contents. Extrapolation is then carried to zero concentration and the result suitably interpreted.

Apparently, little thought has been given to high solids contents, such as are daily employed in the commercial application of protective coatings and adhesives, *e.g.*, varnishes, lacquers, synthetic resins and rubbery materials, where most solutions were made in, or diluted by, non-polar solvents.

Confining one's attention to non-polar media, and with the additional simplification that, for a given commercial application, only a single solute is considered at a time, it has recently become possible to modify Kraemer's intrinsic viscosity with the solvent molality and calculate viscosities at high concentrations (2). The simple expression,

$$\eta_f = (\log \eta_r \times \text{mols solvent})_{C=K} = \text{constant}$$

appears to hold satisfactorily in the usual coatings and adhesive formulations, where a choice is to be made between "replaceable" solvents or solvent mixtures. It does not hold where the "character of the dispersion" varies widely between two solutions, *e.g.*, between concentrated solutions in toluene and heptane of a high-phthalic alkyd resin which normally requires an aromatic type solvent.

Concentration  $C$  is expressed, as usual, in g. of solute/100 cc. of solution, or in lbs. of solids/gal. of finished paint.

The symbol  $\eta_f$ , tentatively termed "viscosity factor," was naturally chosen with some hesitance, and it is desired to submit the item for Dr. Cragg's treatment.

## REFERENCES

1. *J. Colloid Sci.* **1**, 261 (1946).
2. *Am. Paint J.* **29**, No. 36, p. 27 (1945).

E. H. McARDLE

*Esso Laboratories*  
*Linden, N. J.*  
July 12, 1946





## LETTERS TO THE EDITOR

### CRITICAL CONCENTRATIONS FOR MICELLE FORMATION IN MIXTURES OF ANIONIC SOAPS \*

The nature of the micellar development in solutions of mixed soaps is a problem which has received but little attention. X-ray measurements in concentrated solutions seem to indicate the existence of mixed micelles; *i.e.*, the presence in one colloidal aggregate of the molecules of both soaps (1). The problem can, however, be attacked by the use of dye indicator methods for the determination of critical concentrations (2).

In Fig. 1 are plotted the critical concentrations as determined titrimetrically with pinacyanol chloride for mixtures of potassium caprate and laurate, potassium laurate and sodium dodecyl sulfate, and sodium dodecyl sulfate and potassium myristate. The critical concentrations are expressed in moles l. of total soap. The critical concentration of potassium caprate has not previously been determined by the dye method; the value obtained,  $9.5 \times 10^{-2} M$ , compares favorably with that of  $9.5\text{--}10.0 \times 10^{-2} M$  reported by Ekwall (3). On a total soap basis the greatest change in critical concentration with respect to composition of the mixture occurs when the solution contains a high percentage of the soap possessing the greater critical concentration. It is further apparent that the critical concentration of the mixture is always greater than that of the constituent possessing the lower critical concentration.

It is observed experimentally that, if the critical concentrations of two soaps are considerably different, the soap having the smaller tendency to aggregate exerts an effect similar to that of salts upon the other soap. In mixtures of potassium caprate and laurate, the effect of the caprate upon the critical concentration of the laurate (the total soap concentration  $\times$  the mole fraction of laurate) is similar to that of sodium chloride and other salts (4). This behavior is illustrated in Fig. 2. The dotted curves in Fig. 1 represent the critical concentrations in terms of total soap calculated on the assumption that the soap of higher critical concentration acts as a salt toward the other soap. In mixtures of potassium laurate and sodium dodecyl sulfate, the laurate acts as a salt toward the sulfate from a mole fraction of zero to 0.21 sulfate. These results are not unexpected since it has been demonstrated that, below

\* The work reported in this paper was done in connection with the Government Research Program on Synthetic Rubber under contract with the Office of Rubber Reserve, Reconstruction Finance Corporation.

its critical concentration, a soap exhibits the same behavior as a strong electrolyte (5).

Presumably the micellar structure in solutions containing more than 50 mole-% potassium laurate together with potassium caprate is similar to that of the laurate in salt solutions, while that in solutions containing more than 20 mole-% sodium dodecyl sulfate together with potassium laurate is similar to that in the sulfate-salt systems. Outside of these

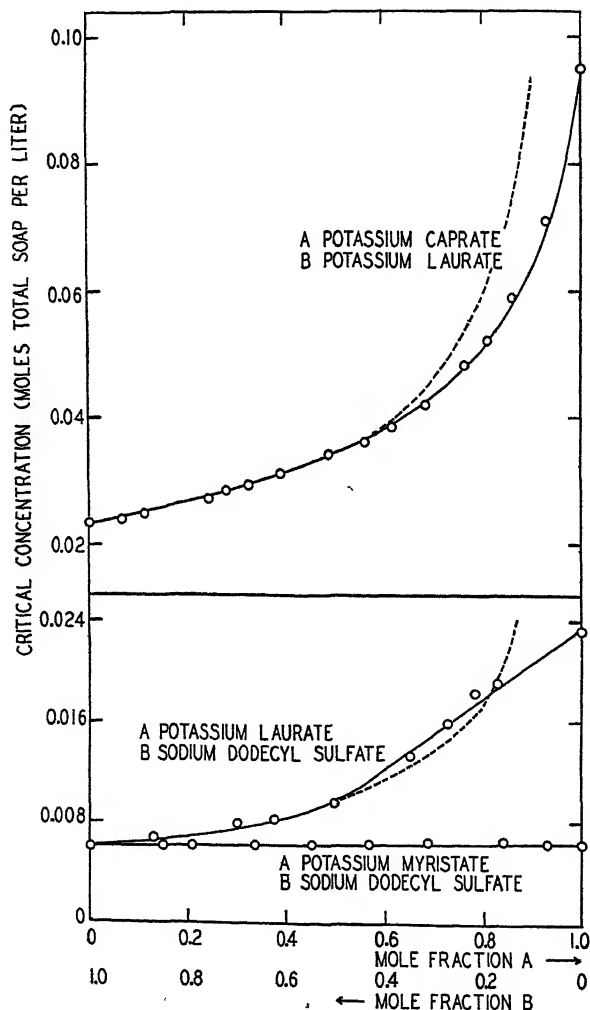


FIG. 1. Critical Concentrations for Micelle Formation in Mixtures of Anionic Soaps. Concentrations are expressed on a total soap basis. The dotted curves are calculated on the basis that the soap of higher critical concentration acts as a salt toward the other soap.

composition ranges the behavior cannot be described in terms of a salt effect; even in potassium laurate solutions containing but little sodium dodecyl sulfate the change in critical concentration of the laurate cannot be ascribed to a salt effect (Fig. 2). This is also true for the laurate-caprate system.

If mixtures of two soaps of approximately the same critical concentration are investigated, no salt effect is observed throughout the whole compositions range. This system is illustrated by a mixture of

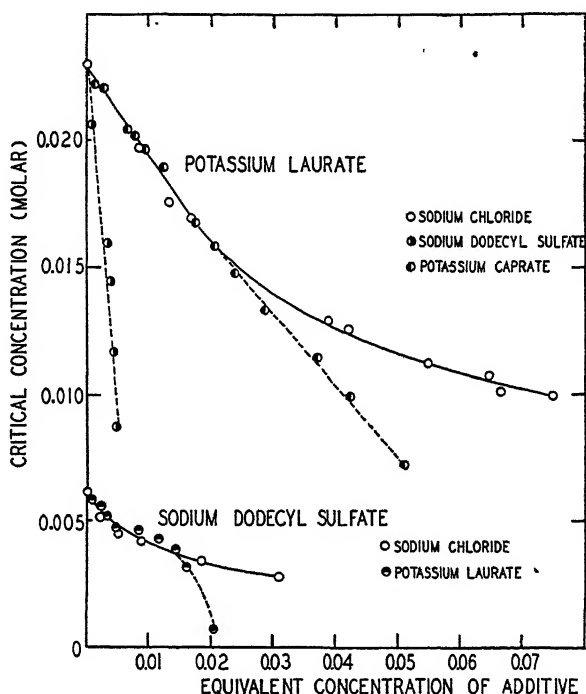


FIG. 2. The Effect of Salts and Other Soaps on the Critical Concentrations of Potassium Laurate and Sodium Dodecyl Sulfate.

potassium myristate and sodium dodecyl sulfate. The critical concentration expressed in terms of total soap remains essentially constant.

It thus appears likely that the micellar structure in solutions containing a mixture of soaps is determined by the relative tendency of the constituents to aggregate. If this tendency is quite dissimilar the soap with lower aggregation value tends to act as a salt toward the other soap. This effect is observed over only a portion of the composition range of the mixture. If the two soaps have approximately the same tendency to aggregate, neither exerts a salt effect upon the other.

## REFERENCES

1. HARKINS, W. D., MATTOON, R. W., AND CORRIN, M. L., *J. Am. Chem. Soc.* **68**, 220 (1946).
2. CORRIN, M. L., KLEVENS, H. B., AND HARKINS, W. D., *J. Chem. Phys.* **14**, 480 (1946); CORRIN, M. L., AND HARKINS, W. D., *J. Chem. Phys.* In Press.
3. EKWALL, P., *Kolloid-Z.* **101**, 135 (1942).
4. CORRIN, M. L., AND HARKINS, W. D., Am. Chem. Soc. Meeting. September, 1946.
5. SCOTT, A. B., AND TARTAR, H. V., *J. Am. Chem. Soc.* **65**, 692 (1943).

*University of Chicago*  
*Chicago, Illinois*

September 25, 1946

M. L. CORRIN  
WILLIAM D. HARKINS

## BOOK REVIEWS

**Optical Instruments.** By EARLE B. BROWN. pp. XII, 567+211 Figs.,  $21\frac{1}{2} \times 13\frac{1}{2}$  cm. Chemical Publishing Co., Inc., Brooklyn, New York. Price \$10.00.

The subject matter of this book is primarily geometric optics and its applications. Part I, entitled "Principles of Geometrical Optics" (174 pages), includes the most important material of this subject in a somewhat condensed form, plus some new material on image inversion and totally reflecting prisms. Part II, entitled "Description, Operation, and Theory of Optical Instruments" (197 pages) deals almost exclusively with their description and operation. Chapter XXII (31 pages) "The Spectroscope" describes the general aspects of this instrument and the ruled diffraction grating. Chapter XXV (21 pages) "Military Instruments," and Chapter XXVI (15 pages) "Range Finders" contain some new material, limited for reasons of security. The author states that, "The instruments and principles which we shall discuss are known to and in use by the armies and navies of all the world at the present time." Part III, entitled "Construction and Maintenance of Optical Instruments" (62 pages) contains a good deal of useful information again in somewhat condensed form. Part IV, entitled "Supplementary Topics" (23 pages), consists chiefly of "Notes on Physical Optics." In addition, there is included an appendix of "Mathematical Proofs" and another entitled "Glossary of Optical Instrument Terms."

In the "Introduction" it is stated that, "The author has attempted to present the broad field of optical instruments as a related whole and to prepare a volume which will be of value and interest to students and teachers in schools and industrial plants, personnel of military and civil establishments, workers and repairmen whose occupation has brought them into contact with various types of optical instruments which it would be to their interest and advantage to understand." It would have been surprising if the author had succeeded in filling so large an order. It appears to this reviewer that the book would serve as a good introduction to geometrical optics for the last four categories enumerated above, but it is not sufficiently comprehensive or detailed in its treatment to serve as a text for students or teachers. In order thoroughly to understand any of the instruments discussed it would be necessary to seek further details in some other source. In this connection it should be mentioned that no references or bibliography are included.

The author also states in the "Introduction" that, "This book has been written in an effort to fulfill the need for a volume which will make a reasonably thorough coverage of the general field of optical instruments. Present volumes are either restricted to a thorough coverage of one instrument or of a small group of similar instruments, or to a theoretical discussion of optical principles." With the exception of the spectroscope and diffraction grating, this book deals almost exclusively with the general field of geometric optics. Comparison with a well known text published in 1932 reveals that the present volume makes no mention of photometers, spectrophotometers, refractometers, densitometers, pyrometers, radiometers and the like. The Michelson interferometer is discussed on one page but no other interferometers are mentioned. Only one form of polariscope, the polarimeter, is described. A few instruments which do not appear in the earlier work are described in the present volume, namely: the Schmidt camera, the sextant, theodolite, opaque projector, cystoscope and some of the prisms.

It seems surprising that a book of 500 pages of text does not contain more necessary details. This is in part due to the large readable type and the somewhat small sized

pages which contain about 320 words each (compared to the above mentioned text of over 600 pages containing about 400 words per page). In addition there is a considerable discussion of useful mechanical details which have, however, crowded out equally necessary optical details. Also, many of the 230 figures, particularly the line drawings, are larger and occupy more space than seems necessary. Some of the drawings leave much to be desired, particularly Figure 19, which illustrates total internal reflection under a condition where it would not occur; Figure 55 "Structure of the Human Eye" which is badly out of proportion; Figure 107 "Photoelectric Exposure Meter" which is so blacked out that its details are indistinguishable; Figure 177 "The Aiming Circle" which is so hastily drawn that its details are unintelligible, and Figure 208 "Interference of Light from Two Sources" which is improperly drawn. It is unfortunate that there are only two photographs, both of which are good.

Most of the principles of geometrical optics are well presented, the derivations of the lens equations being, on the whole, readily understandable. However, it is confusing to have the basic equations for paraxial rays first derived for the case of reflection at a convex spherical mirror when both the object and image are virtual (Figure 22).

Chapter X "Total Reflecting Prisms" presents the subject of image inversion which, as the author says in Chapter II, is "quite confusing, and some attempt to clarify it will be made in Chapter X." The attempt was unsuccessful, at least for this reviewer. The discussion is based on the appearance of one's own reflection in a plane mirror as follows (page 11): "To an observer looking at us from a point behind the mirror, our left would be at his right, and our right at his left. As we see ourselves in the mirror, however, our left appears at our left and our right at our right. In other words, our image in the mirror, as seen by us, is *inverted* from left to right in a horizontal plane, or around a vertical axis." It might seem that the criterion of like opposite like is the criterion of lack of inversion rather than inversion, since as we see ourselves in the mirror, our head is opposite our head and our feet opposite our feet, which condition the author does not consider an inversion. The real image produced by a convex lens is considered to be inverted about two axes, since its top is opposite the bottom of the object and its right opposite the left of the object. The axis of inversion defined by the author is determined by the inversion of the observer behind the mirror who has a subjective preference to turn himself about a vertical axis. If he had stood on his head to observe us, we would then have concluded that the mirror inverted about a horizontal axis. We would have reached the same conclusion if we had observed ourselves in a mirror while lying on our side.

On page 90 the author says, "If the effect of a prism is to deviate the line of sight through  $180^\circ$ , this deviation is exactly the same as an inversion about the axis of deviation. This phenomenon effectively permits the observer to get behind the object and view it from that vantage point. The effect can easily be seen by holding a transparent picture between oneself and a plane mirror. The direct view of the picture and its image in the mirror are identical, the result of the summation of the inversion produced by the mirror and the  $180^\circ$  deviation of the line of sight. This is not the same thing as using a mirror to view something behind oneself, in which case the image is *inverted* as compared with the observer's normal view, which would require that he turn around."

There is not space here to attempt to clarify this problem. It is suggested that a careful distinction should be made between rotation of an image in space and inversion of the aspect of the image. For example: (1) Normal incidence in a mirror produces no rotation in space but does produce  $180^\circ$  deviation in the line of sight. The axis of deviation is indeterminate as far as the mirror is concerned, but depends on the orientation of the object and our subjective preference for viewing it. (2) Grazing incidence produces  $180^\circ$  rotation of the image in the plane of vision, but no deviation of the line of sight. (3) Two mirrors at right angles to each other rotate the image through  $180^\circ$  and also

deviate the line of sight through  $180^\circ$ . The aspect of the image is then the same as that of the object when viewed from behind the mirrors. But in describing the roof prism, the equivalent of two mirrors at right angles, the author says on page 103: "In this case the planes of incidence for the two reflecting surfaces are mutually perpendicular and inversion in two planes results." Observation shows that the image is not inverted according to the author's previous definition of inversion, and when viewing at right angles to the line of intersection of the mirrors, the planes of incidence for the two surfaces are parallel and coincident!

Perhaps the difficulty lies in the definition of inversion. The author's definition is certainly not the same as that applied to the doubly inverted image produced by a convex lens, which is rotated in space through  $180^\circ$  about two mutually perpendicular axes, and is generally considered to be inverted regardless of the direction in which it is viewed.

The subject of resolving power is treated very briefly and lens aberrations are discussed clearly but hardly in sufficient detail.

Several errors were noted in Chapter XXXIII, "Notes on Physical Optics." The following two sentences on page 455 are apparently garbled: "Either wave-length or frequency may be used as a measure in amplitude. When two wave trains of the same wave-length and low frequency being red and low in energy; that of short wave-length and high frequency being violet and of high energy." The two words "and amplitude" should be added after "the same wave-length" in the following sentence (page 455). "When two wave trains of the same wave-length are one-half a wave-length ( $180^\circ$ ) out of phase, the resultant motion of the particle is zero,—"

On page 458 the equation for the spacing of the interference fringes produced by two coherent sources is given incorrectly. On page 470 the resultant according to Huygen's principle of a plane wave at a point is incorrectly derived.

As suggested above this book provides the technician with a useful introduction to geometric optics and the methods of construction and operation of instruments based thereon. However, it does not appear that much has been included that cannot already be found in one volume.

DAVID SINCLAIR, Johns-Manville Research Laboratory

**Chemical Process Principles, Part I: Material and Energy Balances.** OLAF A. HOUGEN AND KENNETH M. WATSON. (Second Printing, 1944) 436 pages. John Wiley and Sons, Inc. Price \$4.50.

This book represents an expansion of the first part of the authors' older text, **INDUSTRIAL CHEMICAL CALCULATIONS**. The aim of the present volume, as indicated by the title, is to introduce the student to the technique involved in setting up material and energy balances for complex chemical processes. In the course of arriving at this objective detailed treatments of stoichiometry, gases and gas mixtures, latent and sensible heat effects and thermochemistry are included. Solution effects and the use of phase diagrams are also covered. A notable feature of this, as of previous editions and printings of this work, is the inclusion of an extensive discussion of methods for estimating missing data. These methods have been brought up to date and represent an extremely useful tool for student and practicing engineer alike.

The material is clearly presented in a logical manner. Every effort has been made to make this volume useful to and usable by the undergraduate engineering student. Occasionally the authors' efforts at simplification have led to inaccuracies of statement, notably in the discussion of adiabatic saturation temperature and wet bulb temperature on page 104. The identity of these values under certain fixed conditions for water-air systems has been carried over to other systems for which the two temperatures can,



and usually do, differ widely. Examples of this sort are infrequent and do not materially detract from the usefulness of the book.

There are numerous well-selected problems available at the end of each chapter. These problems exemplify typical practical problems and offer an excellent chance for the student to test his grasp of the material covered.

Most of the misprints and errors which occurred in the first printing have been corrected and this second printing will be very useful to chemical engineering students.

PHILIP W. SCHUTZ

**Studies in Biophysics: The Critical Temperature of Serum (56°).** By P. LECOMPTE DU NOÛY. 180 pages. Reinhold Publishing Corporation, New York, 1945. Price \$3.50.

The author states at the beginning of his book that the experimental researches he reports constitute a systematic effort to pave the way for a physical chemical attack on the mysterious problems of immunity. To emphasize their labile nature in regard to time he refers to proteins as "fragile, four dimensional bodies," and discards "the classical hypothesis of a colloidal serum" in favor of "the new hypothesis of a serum molecularly dispersed, comprising albumin, globulins, lipoids, etc., in a true solution, either in a state of more or less fragile combination or free."

Dr. du Noüy presents numerous data for the influence of temperature on a variety of sera with usually brief, but often unnecessary details of the techniques and apparatus which were used by him and his collaborators for making the required measurements. He reports that sera which have been heated in sealed vessels for about 10 minutes near 56°, exhibit (a) an increase of viscosity, rotatory power and dispersion, light absorption and scattering, and depolarization factor; (b) a decrease of specific electrical conductance and of "the power of fixation of ether" (emulsifying power); and (c) a modification of the interfacial tension, and of the stability and sedimentation of globulins. Also, the pH appears to drop (a few hundredths pH unit) if the heating is carried out at about 60°, while ultraviolet absorption changes near 65°.

In conclusion he states that the alexinic (complement) power of serum belongs to the "protido-lipoidic complexes, which constitute serum, and not to a separate body"; that "these molecules are made up of elements easily separable, such as globulins, lipoids, etc."; that "these components are cleavable along surfaces which are not necessarily planes but probably undevelopable surfaces"; that the loss of complement activity of serum by heat is "related to the structural and chemical modifications in the serum molecule as a whole" by intramolecular hydration; and, finally, that through a systematic study of the "complete albumin molecule and of the globulin fraction of serum the solution of all immunological problems will be found."

Liberal use of direct quotations has been made in order to be fair to the author's stated meanings. Except for the well known fact that components of serum can be separated and the very dubious assumption that proteins undergo irreversible hydration, the remaining conclusions appear altogether too vague for profitable discussion. The data presented in the book are arranged to show that some sort of irreversible change occurs in serum near 56°. No doubt it does, but one fails to see how it demonstrates irreversible hydration. For example, a decrease of about 1% in the electrical conductivity of serum after heating certainly does not prove that it is "indisputably" due to water fixation by protein with a corresponding increase in salt concentration. Similar interpretations by the author of measurements of viscosity, light scattering, etc., on the basis of hydration appear equally unconvincing.

If the reader is interested in comparing, for purposes of cross correlation, the effect of temperature on the various properties of serum which are discussed in this book he will be disappointed to find the absence of data for the different types of measurements on the same lots of material. It might have been well to present, at least in summary

form, measurements on the several different properties of comparable sera under corresponding conditions, so that one could look for one's own possible correlations between them. The apparatus used in connection with the chosen techniques are, for the most part, well known commercial instruments, some of which, such as the torsion viscosimeter and the interfacial tensiometer, are of Dr. du Noüy's own design. Although it was doubtless adequate for its purpose, the electrical conductivity assembly, which is described in considerable detail, is below modern standards.

This reviewer regrets that he is not able to recommend this monograph as fruitful reading to those interested in problems of immunity. Physical chemists will find little value in the description of the techniques, no great utility in most of the measurements presented, and probably general disagreement with the interpretation.

THEODORE SHEDLOVSKY

**Soap in Industry.** By GEORGIA LEFFINGWELL AND MILTON LESSER. 204 pages. Chemical Publishing Company, Brooklyn, New York, 1946. Price \$4.00.

The authors give a survey of the industrial uses of potash and soda soaps in the following fields: animal husbandry, building and construction, cosmetics, dentistry, inks and inkmaking, insecticides, leather, lubricants, milk production, mining and ore treatment, oil production, paints, paper and packaging, plastics, polishes and cleaners, restaurant sanitation, road building and maintenance, rubber production, textiles, dyeing and printing textiles, wool production and miscellaneous uses.

These chapters give an indication of the manifold uses of soaps and are quite comprehensive in this respect. Much patent literature, not to be found compiled in any other single volume on the soluble soaps, is presented. Formulae are given as such with no attempt at evaluation. For those interested in soaps, this book gives many useful hints as to the utilization of soaps in manufacturing processes.

WILLIAM H. STAHL

**Commercial Waxes, Natural and Synthetic, a Symposium and Compilation.** Edited by H. BENNETT. 583 pp. Chemical Publishing Co., Inc., Brooklyn 2, N. Y., 1944. \$11.00.

New and expanding applications of waxes in protective finishes, packaging, and other fields as well as the increasing commercial availability of new types of waxes, both natural and synthetic, have accentuated the need for a comprehensive volume on the types, sources, properties, and technology of waxes and wax compositions used in industry. The present work represents a commendable effort to fill this need. The editor is the technical director of Glyco Products Co., Inc., and Editor of *The Chemical Formulary*. In addition to substantially all of the pertinent data from various handbooks, a reasonably complete survey of the literature, and considerable previously unpublished data from his own laboratory, the editor has included original contributions and data from more than twenty individuals, as well as information supplied by various manufacturers of waxes and wax compositions.

In the introduction the editor discusses the classification of materials as waxes on the basis of their chemical composition as distinguished from their physical properties, but wisely chooses the latter as the criterion for inclusion of materials in a book on commercial waxes. He also gives a useful listing of the properties which may influence the choice of a wax for a particular application, and classifies waxes, according to their origin, as mineral, vegetable, animal, insect, miscellaneous, synthetic, and compounded. In the first chapter, on Natural Waxes, sixty pages are devoted to paraffin, thirteen pages to other mineral waxes, twelve to vegetable waxes, and five to animal and insect waxes. Sources, properties and uses are discussed, and many useful data are presented in the form of graphs and tables. The second chapter, sixty-two pages, gives similar information

on Manufactured and Synthetic Waxes, while the third chapter of eighty pages is devoted to Physical Properties of Waxes and Wax Compositions, including data on viscosity, surface tension, melting point, solubility, hardness, electrical constants, and other properties, and information on the modification of these properties by additions and combinations. The fourth chapter, thirty-four pages on Wax Technology, deals with determinations of physical and chemical properties, identification of waxes, and general information on preparation of solutions and dispersions of waxes. The fifth chapter consists of one hundred eleven pages of Waxes in Industry, covering some thirty fields of application, ranging from embalming preparations to carbon paper, each section being written by a specialist in that field. Chapter VI, eighteen pages of Tables and Glossary, contains tables of origin, uses, solubility, and other properties of waxes, and definitions of many of the technical terms used in the book. The final chapter, Wax Formulary, one hundred sixty-eight pages, gives more than a thousand formulas for various products containing some wax or other, with brief directions for their preparation. There is a brief Appendix on Substitutes and an adequate subject index, but no author index and no bibliography. Literature references are given as footnotes, and author's names are given under the titles of special sections.

This book will prove very useful to chemists, engineers, and others interested in the application of waxes and wax compositions in many fields of industry because it contains so much data and information not available from any other single source. However, it would be much more useful if the sources of data were more fully given, and the reliability of data indicated or critically evaluated. Other highly desirable features that might have been included are an indication of the present and potential commercial availability of some of the lesser known natural waxes, manufacturers or sources of many of the synthetic waxes mentioned only by trade names, brief statements as to the identity and authority of the various contributors. The arrangement and correlation of data might have been improved considerably, and greater consistency in units, such as use of either °F. or °C., for melting points, rather than whichever the original data was given in, would have simplified comparison of properties.

L. C. CARTWRIGHT

# A STUDY OF THE EFFECT OF VARIOUS FACTORS ON THE SWELLING OF CERTAIN CEREAL STARCHES<sup>1</sup>

R. H. Harris and Ethel Jespersen

*From the North Dakota Agricultural Experiment Station, Fargo, North Dakota*

*Received August 8, 1946*

## INTRODUCTION

The swelling power of starch has long been a matter of interest to starch technologists. This property has been quite generally determined by the use of viscosimetric technique and the hydration of the granules, or the starch swell, deduced from the viscosity results. However, Gortner (1933) has pointed out certain difficulties which are involved in the interpretation of viscosimetric data in terms of hydration and proposed the formula devised by Kunitz (1926) for calculating hydration from data of this nature. While this method is indirect, results obtained by Kunitz with various sols, as well as Gortner's conclusions, tend to justify confidence in hydration values secured by the use of the formula. A certain weakness in the method stems from the use of viscosity data obtained from starch sols owing to the difficulty of getting precise and replicable data.

Because the viscosity depends greatly on the degree of swell of the granules and the extent of granule disintegration, the viscosity of any particular starch will be largely a matter of the pasting temperature, the duration of heating, and the speed, length and character of stirring (*i.e.*, stirring rod versus propeller-type stirrer). There are, no doubt, other as yet unrecognized factors which also play a part. Alsberg (1938) discusses the broad implications of the relationship of the swollen granule to paste viscosity. Other investigators have also commented on the problems involved in viscosity determinations of starch solutions and experiences in the authors' laboratory with the Ostwald and Hoeppler instruments have confirmed these statements (Harris and Mason, 1940; Harris and Jespersen, 1946). These facts have led to a search for other means of assessing starch hydration or swelling power.

Changes in starch paste consistency have also been measured by instruments which detect variations in the resistance of the paste to mixing during gelatinization. Caesar (1932) showed the influence of NaOH

<sup>1</sup> Published with the approval of the Director of the Experiment Station.

upon the consistency of starch as the temperature was increased at a constant rate, employing a "consistometer" to assess hydration changes. Using an improved form of this instrument, Caesar and Moore (1935) followed the entire paste history of tapioca flour, and of heavy- and thin-boiling corn, potato and wheat starches. Each starch was found to yield a characteristic curve type. Anker and Geddes (1944) used the amylograph to detect the effect of a number of variants on pasting properties. Transition temperature, paste temperature at maximum viscosity, maximum paste viscosity, and rate of decrease in viscosity after the maximum, were the pasting properties specifically studied.

An alternative method is to determine directly the swelling power of starch by observing the change in volume of the starch granules following heating. Harrison (1911) correlated swelling power ascertained in this manner with strength of the starch paste. Katz (1928) measured the swelling power of wheat starch from fresh and stale bread, as well as the swell of pure starches in various volumes of water. Ripperton (1931) modified Harrison's method in assessing the swelling power of edible-canna and potato starches, and Tanner and Englis (1940) found little difference among seven samples of corn starch, although a soft starch containing the largest granules of the seven did show slightly higher swelling power. Harris and Jespersen (1946) applied Ripperton's method in modified form to a series of cereal starches and one potato starch and found marked differences among some of the starches examined. These data appeared more useful than viscosity values as secured with the Hoesppler viscosimeter in characterizing changes in starch swelling power.

The present study was initiated to evaluate the influence of a number of factors on the swelling power of starch. Included among these factors were temperature and duration of heating, starch type, starch concentration, method of determination, effect of electrolytes when cooking the starch, and a comparison between heat and chemical gelatinization.

## EXPERIMENTAL

*Materials.* A number of cereals were employed as sources of the starches studied. The wheat starch was prepared from a commercial hard red spring wheat flour while the other flours were experimentally milled in an Allis mill. The barley, a Manchurian variety (N.D. No. 2121), and the rye, a Washington Imperial variety, were grown in the experiment station plots at Fargo in 1945. The Millet, Proso, a yellow variety, was obtained from a local seed company. The corn starch employed was a commercial product purchased from the grocery store.

Wheat starch No. 64 was separated from the gluten by washing from a stiff dough with 0.1% sodium phosphate solution of approximately pH 6.8 (Harris and Jespersen, 1946). Barley starch No. 107 was separated from the whole grain following steeping in distilled water at 40°C. for 48 hours. The steeped grain was ground by passing

several times through a meat grinder, and the starch removed by repeated washings with distilled water on bolting cloths. No treatment with NaOH was found necessary, but recovery of starch was poor and the process was slow and laborious. The remaining starches were prepared by treating with 0.5% NaOH at 5°C. for 18-20 hours with occasional stirring. Some criticism may be offered regarding the use of flours rather than the whole grain, but the removal of the bran and germ was found to facilitate preparation of the starch. Dimler, Davis, Rist and Hilbert (1944) have pointed out that starch may be prepared quite satisfactorily from barley and rye flours through treatment with dilute NaOH. Recoveries of prime-quality starch were 70-80% of the total wheat flour starch. The remainder was a lower-quality fraction, low in protein and suitable for certain uses. This process was thought to be desirable in using any cereal grain as an alternative to corn for starch manufacture.

The experimentally prepared starches were washed a number of times until apparently freed from impurities. They were then fan dried at room temperature and finally passed once through a small coffee grinder. Starches were not treated with solvents to remove fatty material.

The extent of starch granule damage in the starches was determined<sup>2</sup> and it was found that damage was negligible except for the rye and millet starches. The former contained approximately 7% of injured granules, and the latter as much as 30%. Just why these two starches were different from the others in this respect is not clear at this time. Mode of preparation was the same as in the wheat and barley starches prepared by alkali treatment.

*Methods.* Analytical data were secured from the starches by the following methods. The moisture content of the starch was determined by heating 3 g. of starch in an electric oven at 130°C. for 1 hour. The protein content of the starch was determined by the Kjeldahl-Gunning procedure. The ash percentage was found by heating 1 g. of starch in a 30 ml. porcelain capsule for approximately 10 hours at 500°C., while pH was ascertained by the method of Ripperton (1931) in which 5 g. of starch are suspended in 100 ml. redistilled water by means of an electric stirrer. Measurements of the pH values were taken at 5-minute intervals over a period of 15 minutes. Solubility was measured by the method suggested by Meiss, Treadway and Smith (1944) which involves the evaporation of 50 ml. of the filtered centrifugate from an extract of 25 g. in 150 ml. of water. The alkali number was determined by the technique developed by Schoch and Jensen (1945) in which the quantity of 0.2 N NaOH taken up by 500 mg. (dry basis) is measured. Swelling power was found by the method described later.

The starches were heated in 50 ml. centrifuge tubes at the selected temperatures for different time periods. Forty ml. of redistilled water was used in gelatinization, and the starch suspensions were stirred constantly from the commencement of heating by an electric stirrer. The stirring was gentle but sufficient to keep the starch suspended. The stirrer was, of course, carefully rinsed with redistilled water to return adherent particles of starch to the centrifuge tube. A two liter glass beaker containing water served as heating bath. A Precision Scientific Co. electric heater with facilities for controlling the heat intensity was used as source of heat. A thermometer placed in the bath served to indicate the temperature. At first a second thermometer was used in the centrifuge tube to ascertain temperature lag between the bath and content of the tube. This lag was found to be less than 40 seconds and relatively constant. This thermometer was later omitted since it tended to interfere with stirring. As it was found that a difference of 10 minutes in heating time caused little variation in swelling power, any slight discrepancy in heating time at a specified temperature would not noticeably affect swelling power.

<sup>2</sup> Granule damage was determined by Dr. M. M. MacMasters, Chemist, Starch and Dextrose Division, Northern Regional Research Laboratory, Peoria, Illinois.

Swelling power, as employed in this investigation, is the volume or weight of 1 g. of dry starch gelatinized under the specified conditions. The study concerned with methods of determining starch swelling power involved 3 methods which, though essentially much alike, differed significantly in some respects. The first method was as follows. The dry centrifuge tube was weighed before adding the required quantity of starch. After centrifuging the heated sample in an International type S.B. machine for 20 minutes at 1850 r.p.m., the supernatant water was carefully decanted from the residue leaving the firmly packed swollen starch. The tube was drained as thoroughly as possible, and wiped with Kleenex to remove drops of water clinging to the sides. The tube and contents were then weighed, and the weight of the dry tube subtracted to yield the weight of water in the starch. Knowing the amount of dry starch originally present, the water content could be found. A second technique employed measurement of volume following centrifugation; graduated tubes were used, and both methods of determining swelling power employed on one sample. The third method involved removing samples of cooked starch from the central portion of the residue to avoid securing free water in the material, and transferring this to weighed 30 ml. ash capsules. After drying overnight, the capsules were reweighed and the dry starch weight obtained. The difference between the two weights was the amount of water associated with the starch. The same starch sample was employed as before. This method appeared to be less subject to error than the others and was finally adopted for use in further swelling power investigations. It is more tedious than the other methods since 3 weighings are required: (1) the empty capsule, (2) the capsule and starch paste, and (3) the capsule and dried starch. The three methods are all empirical and measure both water in the granules, water adsorbed on them and water mechanically held between them.

Aluminum sulfate at a concentration of 0.001 *N* was employed to evaluate the influence of the trivalent aluminum cation on swelling power when present during heat gelatinization. Ripperton (1931) and Harris and Jespersen (1946) have pointed out the marked effect of cations in changing the swell of cooked starch when present in the cooking water. Others, as Meiss, Treadway and Smith (1944) have also noted the phenomenon. The electrolyte was added by pipette in 0.01 *N* solution to the redistilled water immediately prior to cooking. The volume of the redistilled water used was reduced to compensate for the volume of electrolyte solution added.

## RESULTS AND DISCUSSION

The data secured from the study of the different methods of determining starch swelling power, with closely associated data regarding the

effects of temperature of gelatinization, starch concentration and starch type, on swelling power, are presented as informative averages of the source of variation. A table of statistical analysis is included to show the significance of the variances studied, particularly the interactions. Relations between the methods in terms of starch swelling power will be given. The remainder of the material, dealing with the effect of duration of heating period, and a comparison of starches treated with NaOH and  $\text{Al}_2(\text{SO}_4)_3$  will be shown in the form of diagrams since the data are more readily interpreted in this form.

### *Comparative Properties of the Starches*

The analytical data are shown in Table I. No great disparity in moisture content is evident among the experimentally prepared starches. This indicates uniformity in the drying procedure. Noticeable variation

TABLE I  
*Comparative Data Secured from the Various Starches Arranged in Order of Decreasing Swelling Power at 95°C.*

Lab. No.	Type of starch	Moisture content	Protein content <sup>1</sup>	Ash <sup>1</sup>	pH	Solubility <sup>1</sup>	Alkali number <sup>1</sup>	Swelling power <sup>1</sup>
		<i>per cent</i>	<i>per cent</i>	<i>per cent</i>				<i>per g. starch</i>
580	Millet <sup>2</sup>	14.4	0.93	0.06	9.3	0.0215	11.3	36.3
447	Barley <sup>2</sup>	12.9	0.24	0.25	9.3	0.0207	9.2	35.7
499	Wheat <sup>2</sup>	11.9	0.06	0.31	9.2	0.0180	8.7	32.1
448	Commercial corn starch	9.2	0.33	0.10	6.6	0.0111	10.9	29.4
498	Rye <sup>2</sup>	14.4	0.07	0.10	8.7	0.0191	8.9	27.4
64	Wheat	14.3	0.20	0.09	6.3	0.0182	8.7	20.8
338	Barley	14.4	0.07	0.11	5.6	0.0733	11.1	19.0

<sup>1</sup> Results expressed on moisture free basis.

<sup>2</sup> Prepared by treating with 0.5% NaOH.

in the protein content is evident, the millet starch containing relatively much more than the others. The commercial corn starch is second highest but the difference between No. 447 and No. 64 is very small. No great differences are evident in the ash results. It was found impossible to reduce the pH of the NaOH-treated starches below the values indicated by repeated washings with distilled water. The solubilities are rather constant, with the exception of barley starch prepared by steeping. Both wheat, rye and barley starch No. 447 are quite consistent in alkali number, but barley starch No. 338, which was prepared by steeping with distilled water, and the millet starch No. 580, are significantly higher. Rather extensive variations in swelling power are evident.



*Effect of Duration of Heating Time*

It was found that heating for 15 minutes did not significantly change the slope or position of the swelling curve from 50° to 95°C. (Fig. 1). The difference between the curves at 90°C. and 95°C. is probably due to experimental error, although the starch heated at 95°C. for a 15-minute period showed more tendency to disintegrate. The longer stirring and heating may have induced more swell at 90° before the higher temperature caused disintegration. The data show that a 5-minute immersion in the heating bath with constant stirring was sufficient to fully swell the

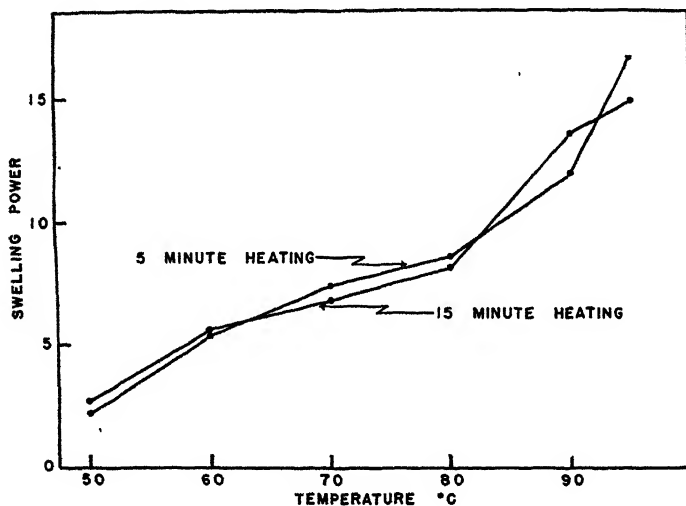


FIG. 1

Comparative Effects of Heating Time on Starch Swelling Power at Different Temperatures

Swelling power measured in g. water/g. starch, dry basis

starch, with less probability of breaking down the swollen granules. This method was more rapid and convenient than methods using longer heating treatments. Several tests made at a heating period of 30 minutes also showed very small and insignificant differences from data obtained from the 5-minute treatments, and all subsequent swelling power determinations were made with the 5-minute period.

*Comparative Effects of Temperature, Starch, Method and Concentration*

This part of the investigation involved a study of methods for ascertaining the swelling power of 3 samples of starch, cooked at 5 temperatures, at 3 concentrations. The 3 starches used were wheat starch

No. 64, barley starch No. 338 and the commercial corn starch No. 447. The temperatures and starch concentrations employed are shown in Table II. Very significant differences are evident between the swelling power at the different temperatures, as would be expected from *a priori* considerations, and the swelling power increased greatly with the gelatinization temperature. The starches also varied among themselves in swelling

TABLE II  
*Effect of Pasting Temperature and Concentration on the Swelling Power of Three Starches*

	Pasting temperature °C.					
	70	80	85	90	95	Mean
<i>Starch no. and type</i>						
338 (Barley)	7.1	7.5	8.2	10.3	17.0	11.3
64 (Wheat)	7.2	8.3	9.1	12.6	20.9	12.9
448 (Corn)	8.4	11.3	14.2	19.4	28.8	18.2
<i>Concentration, dry basis<sup>1</sup></i>						
1%	8.8	10.5	12.0	15.2	21.8	13.6
2%	7.2	8.9	9.7	13.4	20.8	12.0
3%	6.6	7.8	9.8	13.7	24.1	12.4
Mean	7.5	9.1	10.5	14.1	22.2	

<sup>1</sup> Shown as averages for the 3 starches.

power capacity at all temperatures, the barley starch showing the least, and corn starch the highest values. For starch concentration, 1% dry basis gave the highest swelling power and this concentration was used in subsequent work.

The results obtained from the analysis of variance are presented in Table III. In the analysis, the sources of variation have been separated into 4 classifications and evaluated separately. The triple and fourth order interactions have been combined and used as the error term to evaluate the significance of the variances arising between the sources of variation, as well as from the 4 double interactions. This error term is larger than that arising from the error of the laboratory technique as calculated from the replication, and should include the laboratory error since errors between replicate determinations contribute to the high order interactions. It is, therefore, a more rigid test of significance than the laboratory error and increases confidence in conclusions drawn from the analysis.

Comparing the results between the sources of variation, it is evident that all 4 variances are significant at the 1% point. However, there are

very large differences in the relative size of the variances, and these appear to indicate the great importance of differences in cooking temperature and of variations between the 3 starches in respect to swelling power. The variation due to methods was the smallest of the 4 variances.

The second order interactions were all significant at the 1% point with the exception of methods  $\times$  starches, which was significant at the 5% point. These interactions may be interpreted by the statement that the 3 methods did not yield the same relative results for all starches, for all concentrations and temperatures; similarly, the 3 starches did not

TABLE III  
*Analysis of Variance of the Swelling Power Data*

Source of variation	Sums of squares	Degrees of freedom	Variance	F	5% point	1% point
Between methods	10.94	2	5.47	5.14	3.11	4.88
Between starches	1001.81	2	500.91	470.34	3.11	4.88
Between concentrations	63.74	2	31.87	29.93	3.11	4.88
Between temperatures	3718.17	4	929.54	872.81	2.48	3.56
Interactions (first order)						
(Methods $\times$ starches)	13.15	4	3.29	3.09	2.48	3.56
(Methods $\times$ concentrations)	15.96	4	3.99	3.75	2.48	3.56
(Methods $\times$ temperatures)	37.49	8	4.69	4.40	2.05	2.74
(Starches $\times$ concentrations)	40.55	4	10.14	9.52	2.48	3.56
(Starches $\times$ temperatures)	327.87	8	40.98	38.48	2.05	2.74
(Concentrations $\times$ temperatures)	89.40	8	11.18	10.49	2.05	2.74
Higher order interactions (error)	93.76	88	1.07			
Total	5412.84	134				

swell in the same manner as the concentration or temperature varied, and finally, starch concentration had an influence on the swelling power at the different temperatures employed in this study. These conclusions, as regards the interactions of the various sources of variation, would be difficult to assay without recourse to the analysis of variance.

Means, standard deviations and correlation coefficients calculated from the swelling power data are shown in Table IV. Methods A and B which involved determining the increase in weight of the 50 ml. centrifuge tube after gelatinizing the starch in method A, and in ascertaining loss in weight after drying a known quantity of gelatinized starch for B, gave practically the same mean. The other method, in which the volume of swollen starch was found following centrifuging, yielded a higher value, as was anticipated. The results from method B had the largest standard

deviation. Method A values had the lowest variability, and these results would seem to indicate the desirability of the second method in differentiating among the individual starches. The correlation coefficients between pairs of the three methods were all extremely high, and indicate that the swelling power capacity could, for all practical purposes, be

TABLE IV  
*Statistical Constants for the Three Swelling Power Methods (N = 45)*

	Methods		
	A	B	C
Mean	12.4	12.6	13.1
Standard deviations	5.53	6.95	6.41
Correlation coefficient between A and B. . . . . +0.997			
Correlation coefficient between A and C. . . . . +0.981			
Correlation coefficient between B and C. . . . . +0.983			

Note: Method A involved determining the increase in weight of the centrifuge tube after starch gelatinization. Method B, the loss in weight after heating the hydrated starch was found. Method C entailed reading directly the volume of hydrated starch.

determined equally well by each of the methods. Employing the identity  $\sqrt{1 - r_{xy}^2}$  for the error of estimate, we obtain an error of 19.4% in the instance of the lowest correlation coefficient 0.981; the highest coefficient yields 7.7% as the error in predicting method A swell from the results secured by method B.

#### *Comparative Swelling Power*

Comparisons of the swelling power of wheat, barley, rye, corn and millet starch from 60° to 95°C. are shown in Fig. 2. All these starches except the corn were prepared with NaOH. Little differences are to be noted between the wheat and barley starches, except possibly at 60°C. At this temperature the wheat starch appeared to be more swollen than the other starches. The rye starch swelling power paralleled the barley until 80° was reached, then increased at a slower rate, and at 95°C. had the lowest value of any of the starches. The corn starch yielded rather low values until 90° was attained, when it approximated the results for rye starch. The millet starch did not begin to swell appreciably until 65° was reached. The swelling power remained less than that of the other starches until the temperature reached 73° when the swell approximated that of the corn starch. At 75° the millet starch swelling power surpassed that of any of the others, and remained above them to 95°C. The rise in swell

of this starch from 70° to 90° was more rapid than for any of the other starches. As will be pointed out in the following section, treatment with NaOH to separate the starch from flour markedly increases the swelling power. This fact explains the apparent anomaly in the present results as compared with the initial study on methods of ascertaining the swelling power where corn starch yielded higher values than wheat or barley starch prepared without treatment by chemical reagents. The shape of the corn starch curve is somewhat different from the wheat, barley and rye curves and suggests a more rapid increase in swelling power above 85°C.

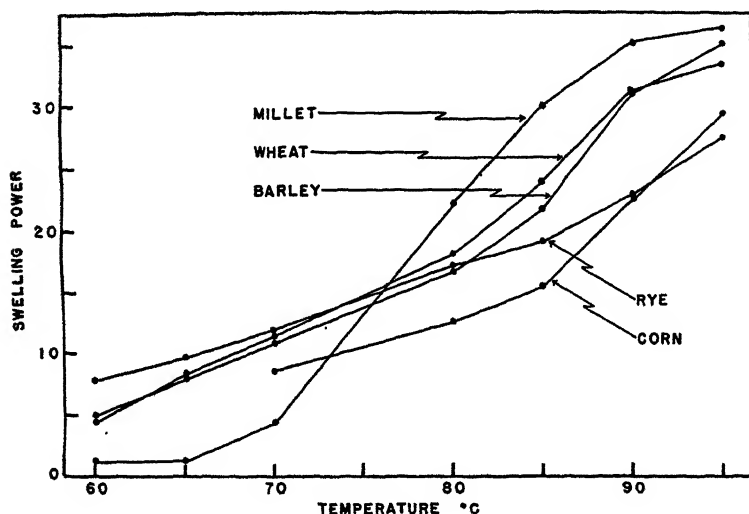


FIG. 2

Swelling Power of Various Starches Prepared with 0.5% NaOH and Commercial Corn Starch over the Temperature Range 60° to 95°C.

The differences between the swelling power of the millet and the other starches in the low initial heating (60°–70°) is probably due to variations in the water content of the granules, since one would expect little variation in interstitial or adsorbed water among the starches. This difference cannot be due to absorption of water owing to granule damage because millet starch contained the largest proportion (30%) of injured granules. It is probably unsafe to speculate on the cause of these differences without more conclusive information.

#### *Effect of Electrolytes*

The effects of changes in methods of wheat starch preparation and the influences of electrolyte treatment at cooking on starch swell are shown

in Fig. 3. First, the effect on swell of pretreatment with NaOH when preparing the starch is very marked, and the course of the swelling curve is greatly altered. There are relatively little differences at 60° between the starches prepared with and without NaOH, but at 65° the curves commence to diverge, and divergence increases with rising temperature, reaching a maximum at 90°C. The increase in swelling power is more uniform and regular in the treated starch, while in the starch separated from flour by washing with water there is comparatively little rise in swelling power until 90° is reached, following which point swelling power

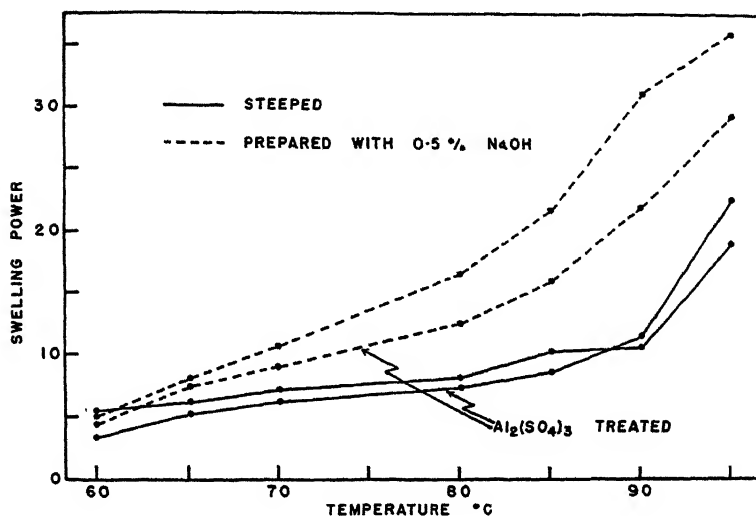


FIG. 3

Effect on Swelling Power of Preparing Wheat Starch by Treatment with 0.5% NaOH, as Compared with the Effect of 0.001 N  $Al_2(SO_4)_3$  at Time of Cooking

increases enormously. The explanation for this difference in swelling behavior of the two starches is difficult to explain; it may be due to differences in degree of hydrogen bonding in the two starches or it may lie in the effect of the pH of the finished starch.

The effect of  $Al_2(SO_4)_3$  in 0.001 N concentration at cooking is also very interesting. There is no effect at all on the starch prepared without NaOH, but with the treated starch significant effects appear, and the swelling power is consistently lowered. Possibly the effect is due to ion antagonism between  $Na^+$  and  $Al^{+++}$  with attendant loss in water bound by electrical charges. There may be a possibility that the starch chains are cross bonded by trivalent aluminum.

Similar comparisons made with barley starch confirmed the results

secured from wheat starch (Fig. 4). The millet starch treated with  $\text{Al}_2(\text{SO}_4)_3$  gave corresponding results to wheat and barley. The decrease in swelling power caused by electrolyte treatment, however, was somewhat less. The effect of the electrolyte on millet starch without NaOH preparation could not be ascertained as only one method of isolation was employed in preparing this starch. It is very apparent that the method of preparation or of gelatinization of starch may entirely mask the effect of inherent differences among individual cereal starches.

Since these results with  $\text{Al}_2(\text{SO}_4)_3$  appeared to contradict those secured by Harris and Jespersen (1946), several determinations of starch swell were made by the method used by the authors in the former study. This

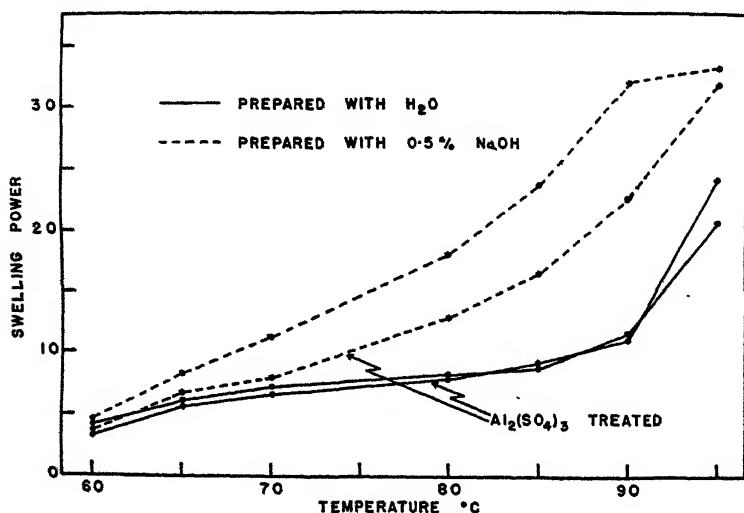


FIG. 4

Effect on Swelling Power of Preparing Barley Starch with 0.5% NaOH as Compared with the Effect of 0.001 *N*  $\text{Al}_2(\text{SO}_4)_3$  at Time of Cooking

method was essentially that described by Ripperton (1931), and consisted in cooking the starch in a boiling water bath for 10 minutes, without appreciable stirring. The 1% solution of cooked starch was then poured into a 25 ml. graduated cylinder, and the cylinder filled to the mark with cold distilled water. The volume of the swollen starch granules was read the following morning. In cereal starches, treatment with  $\text{Al}_2(\text{SO}_4)_3$  at cooking was found to markedly increase swelling power regardless of whether the starches had been prepared with 0.5% NaOH. In the present study, the starch was cooked in 50 ml. centrifuge tubes using 40 ml. of redistilled water and heating for 10 minutes at boiling water temperature (98°C.). The swollen starch was allowed to settle out overnight. The

following morning the volume of the gelatinized starch was observed. It was found that under these conditions the electrolyte did materially increase swelling power. On centrifuging, the difference in volume between the swell induced by cooking in redistilled water and in 0.001  $N$   $Al_2(SO_4)_3$  solution was greatly reduced. The data are shown in Table V.

TABLE V  
*Effect of Method of Determination on Starch Swelling Power*  
Starches not prepared by NaOH treatment

Starch	Cooking treatment	Swelling power per g. dry starch			Per cent increase in swell due to $Al_2(SO_4)_3$	
		Method B	Method D	Method E	Method D	Method E
Wheat	water	20.8	32.8	20.7		
Wheat	0.001 $N$ $Al_2(SO_4)_3$	24.3	48.3	24.1	47.3	16.4
Barley	water	19.0	40.6	20.2		
Barley	0.001 $N$ $Al_2(SO_4)_3$	22.5	55.0	22.5	35.5	10.2
Average for method		21.6	44.2	21.9	41.4	13.3

Note: Method B involved cooking at 95°C. for 5 minutes with stirring; moisture content found by drying. Method D; the starch was cooked in boiling water bath with light stirring in 50 ml. graduated centrifuge tubes, stood 18–20 hours, then volume read off. Method E; same as method D except the volume was read after centrifuging.

These results appear to justify the assumption that treatment with  $Al_2(SO_4)_3$  at boiling temperature increases the swelling volume through causing the granules to form a loosely packed mass when allowed to settle under the gentle influence of gravity. When the pull of gravity is exchanged for the stronger influence of centrifugal force, the granules are more firmly packed and probably much of the extra water is removed; it must accordingly be more loosely held than in the granules swollen in redistilled water alone. There might also be less entrapment of dispersion medium in the latter case.

These data emphasize the familiar fact that starch properties, particularly those of a physico-chemical nature, are closely related to variations in mode of preparation, treatment, technique, *etc.*, connected with starch technology. Details of preparation and cooking treatment must be rigidly followed if inherent differences among native starches are to be properly evaluated, and these results are only valid under the conditions specified. Variations in any of these conditions may easily lead to different results and conclusions.

The method described for measuring swelling power is more tedious than methods which determine viscosity changes occurring in starch



pastes during continuous heating, as the amylograph, or instruments employing similar principles. It does however, attempt to determine starch swelling power directly, without the disturbing effects of resistance to shear, interference of neighboring swollen starch granules to the passage of stirring blades, and other factors. The method is not well-adapted to the measurement of granule breakdown following the peak swell and care must be exercised in interpreting results secured at high temperatures, particularly if there is no perceptible separation of swollen granules after centrifuging.

Experiments with sodium salicylate as a chemical gelatinizing agent have not yielded concordant and satisfying results, but the data obtained do indicate a tendency toward increased swelling power, as compared with swelling power induced by heating in water. This indication is in agreement with the statements which have appeared in the literature (Gortner, 1933; Anker and Geddes, 1944).

The data contained in this report picture the great complexity of factors affecting the swelling power of the starch granule. It is practically useless to report data on starches without also giving details of their history and the technique by which the results were secured. It is important that scrupulous care be taken at all times to maintain the purity of the cooking water, since a very small concentration of electrolyte will greatly affect starch swell. Standardized rates of stirring should be employed and each detail of manipulation be kept constant throughout a series of observations. The data emphasize that the swell, or gelatinization, of starch is a gradual process occurring over a substantial temperature range, and does not take place sharply at a particular temperature. There is apparently some absorption of water at relatively low temperatures, though most of the water taken up at this point may be interstitial and adsorbed water rather than water actually present in the granule. To properly define the individuality of starches it is necessary to procure comparative data over a range of conditions, for example, at different temperatures.

#### ACKNOWLEDGMENTS

The authors are indebted to Dr. T. J. Schoch for valuable comments on the factors affecting viscosity of starch pastes and in connection with the effect of heat on the starch granule. They also wish to acknowledge helpful suggestions from Dr. M. M. MacMasters. The figures were prepared by L. D. Sibbitt.

#### SUMMARY

Three methods of determining the swelling power of cooked starch were studied. The swelling power results by the three methods were very highly correlated. However, the method employing loss in weight of

gelatinized starch by heating in an electric oven appeared to be slightly more convenient than alternative methods of finding the weight of a given quantity of starch after gelatinization or the volume of the swollen starch.

As was expected, an analysis of variance of the data showed significant differences in starch swelling among gelatinization temperatures, among wheat, barley and corn starches and among 1%, 2% and 3% (dry basis) starch concentrations. On the basis of the results it was decided to employ 1% starch concentration with a heating period of 5 minutes.

Significant differences in swelling power were found among starches prepared from wheat, barley, rye, millet and commercial corn starch. The use of 0.5% NaOH in the cold (5°C.) was found to increase markedly the swelling power of cereal starches. A solution of 0.001 *N* Al<sub>2</sub>(SO<sub>4</sub>)<sub>3</sub> when employed in cooking the starch, decreased the swelling power of starch treated with NaOH, but was without effect on starch prepared with water.

The evidence presented shows the great effect on swelling power capacity of mode of starch preparation, variations in cooking technique, etc. Inherent differences in individual starches may be entirely overshadowed by variations in the mode of starch preparation.

#### REFERENCES

- ALSBERG, C. L., *Plant Physiol.* **13**, 295-330 (1938).  
ANKER, C. A., AND GEDDES, W. F., *Cereal Chem.* **21**, 335-360 (1944).  
CAESAR, G. V., *Ind. Eng. Chem.* **24**, 1432-1435 (1932).  
CAESAR, G. V., AND MOORE, E. E., *Ind. Eng. Chem.* **27**, 1447-1451 (1935).  
DIMLER, R. J., DAVIS, H. A., RIST, C. E., AND HILBERT, G. E., *Cereal Chem.* **21**, 430-446 (1944).  
GORTNER, R. A., *Cereal Chem.* **10**, 298-312 (1933).  
HARRIS, R. H., AND JESPERSON, E., *Food Research* **11**, 216-228 (1946).  
HARRIS, R. H., AND MASON, W. F. (unpublished data).  
HARRISON, W., *J. Soc. Dyers Colourists* **27**, 84-88 (1911).  
KATZ, J. R., in Walton, R. P., ed., *A Comprehensive Survey of Starch Chemistry*, Vol. 1, 100-117. Chemical Catalog Co., New York (1928).  
KUNITZ, M., *J. Gen. Physiol.* **9**, 715-725 (1926).  
MEISS, P. E., TREADWAY, R. H., AND SMITH, L. T., *Ind. Eng. Chem.* **36**, 159-163 (1944).  
RIPPERTON, J. C., *Hawaii Agr. Exptl. Sta. Bull.* **63**, 48 p. (1931).  
SCHOCH, T. J., AND JENSEN, C. C., *Ind. Eng. Chem., Anal. Ed.* **12**, 531-532 (1940).  
TANNER, L. P., AND ENGLER, D. T., *Food Research* **5**, 563-581 (1940).



## ON THE TRANSFORMATION OF CELLULOSE II INTO CELLULOSE IV

P. H. Hermans and A. Weidinger

*Communication No. 25 from the Laboratory for Cellulose Research  
of the A.K.U. and Affiliated Companies, Utrecht (Holland)*

*Received July 8, 1946*

### INTRODUCTION

Meyer and Badenhuisen (1) as well as Kubo and Kanamaru (2) believed that they effected a transformation of "hydrate cellulose" (cellulose II) into the native modification (Cellulose I) by heating in glycerol for about one hour at temperatures around 250°C. Later, Hess, Kiessig and Gundermann (3) showed that the product of the transformation represents another lattice modification, which they called "high temperature cellulose" (Cellulose IV), closely resembling Cellulose I.

The relative positions of the equatorial interferences of Cellulose I, II and IV are diagrammatically shown in Fig. 1.

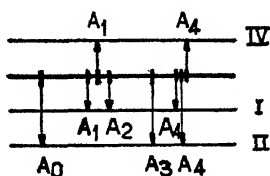


FIG. 1. Diagram of the Positions of the Equatorial Interferences of Cellulose I, II and IV

The completeness of the transformation depends on the kind of fiber and on various other factors which are only partially known. Complete transformation was effected in regenerated fibers, whereas in ramie fibers thus far only partial (about half way) transformation has been effected (3, 4). Kubo (5) later reported that in viscose rayon the transformation can be considerably accelerated by first transforming the fibers into alkali cellulose and heating the latter in glycerol. The time of heating could then be reduced to a few minutes.

In previous work from this laboratory concerning coarse horse-hair-like cellulose model filaments, it was found that the transformation could only be effected satisfactorily if the gel was previously well saturated with glycerol by first allowing it to swell in water, then consecutively treating

it with glycerol-water mixtures of increasing glycerol concentration, and finally with pure glycerol (6). If the air-dry filaments were at once treated with glycerol, they gave poor results or even charred on heating. This led to the presumption that in other cases too the optimal condition for the reaction might be a thorough penetration of the glycerol into the fibers before the heating is commenced, a point left uncontrolled by other authors. The favorable effect of using addition compounds like alkali cellulose as a starting material might then simply be due to the fact that the fibers are in a more or less swollen condition at the moment of their submersion in glycerol, thus facilitating the thorough penetration of the latter.

Following this idea, it has been possible to improve considerably on the transformation of the crystalline portion of mercerized ramie fibers into cellulose IV and to reach almost complete transformation in this case also. The experiments offered here show that the use of alkali cellulose, as such, does not promote the transformation into cellulose IV, but only when the higher degree of swelling which it imposes on the fibers is properly utilized to attain better penetration of the glycerol into the fibers.

It would seem that glycerol acts as a protective plasticizing medium allowing the chain molecules to retain a sufficient mutual mobility in order to arrange themselves according to another more stable lattice modification at 250°C.

### EXPERIMENTAL

Completely mercerized ramie fibers, restretched in the mercerizing liquor to their original length before washing and drying, were used. (See Fig. 3.) The procedure employed in previous work (4) was to allow the fibers to swell in water for  $\frac{1}{2}$  hr., then to boil them in water for 5 min.,<sup>1</sup> to submerge twice for  $\frac{1}{2}$  hr. in alcohol (96%) and finally in glycerol for 1 hr. The fibers were then transferred to small tubes containing vacuum distilled glycerol which were placed in holes drilled in an aluminum block heated at the desired temperature. The result of a series of experiments is listed in Table I. Photometer curves taken along the equator of the X-ray diagrams of the untreated samples (I) and of the treated samples (III) and (VI) are given in Fig. 2. The X-ray diagrams of (I) and (II) are reproduced on Figs. 3 and 4. As an approximate measure of the transformation one may compute the ratio between the intensities of the  $A_1$  and the  $A_0$  interferences as recorded in column 4 of Table I, which may vary from 0

<sup>1</sup> Boiling was carried out to reach a sharper X-ray diffraction picture with well separated 10I and 002 interferences which tend to be less well separated after the mercerization (7).

TABLE I  
Transformation of Ramie Fibers into Cellulose IV

Ref. no.	Heating		$\frac{I(A_1)}{I(A_0)}$	Percentage transformation
	Time	Temp.		
	<i>min.</i>	<i>°C.</i>		
II	90	250	1.0	50
III	120	260	1.0	50
IV	120	260	2.46	70
V	120	270	3.4	77
VI	120	275	3.0	75

before transformation to  $\infty$  at complete transformation. It is seen from this table that the maximum transformation amounts to about 75%.

A second series of experiments were performed using the fibers in the form of alkali cellulose. After mercerizing and restretching the fibers in 18% NaOH solution, they were freed from adhering lye with filter paper

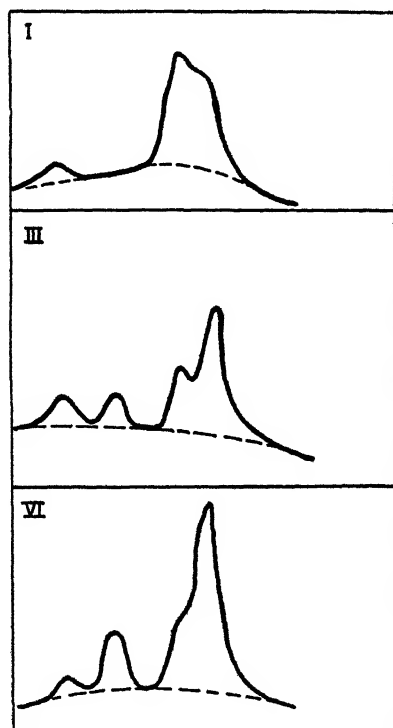


FIG. 2. Photometer Curves along the Equator of Diagrams I, III and VI

and then either at once submerged in glycerol and immediately heated (Series a) or heated after standing in glycerol for  $\frac{1}{2}$  hr. (Series b). The result is recorded in Table II. The temperature was always  $250^{\circ}\text{C}$ . in this case. Shorter times of heating were employed, since a more rapid transformation might be expected. The effect of simply allowing the fibers to

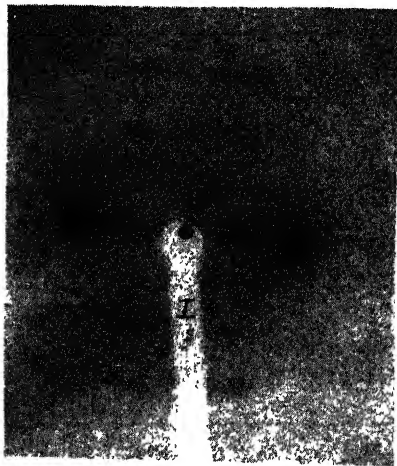


FIG. 3. X-ray Photograph of Mercerized Ramie before Transformation

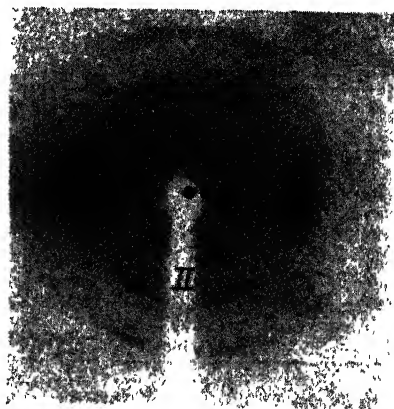


FIG. 4. X-ray Photograph of Ramie 50% Transformed into Cellulose IV

stand in glycerol for  $\frac{1}{2}$  hr. before heating is considerable, indicating that better penetration of the glycerol improves on the result. (The X-ray diagram of X is shown in Fig. 5).

The best result was obtained with a sample which, before heating, remained for 1 hr. in twice renewed glycerol and which was heated for 15

TABLE II

*Transformation Experiments with Alkali Cellulose*

Ref. no.	Heating		$\frac{I(A_1)}{I(A_0)}$	Percentage transformation
	Time	Temp.		
	min.	°C.		
<i>Series a</i>				
VII	3	250	0.6	37
VIII	10	250	1.5	60
<i>Series b</i>				
IX	3	250	0.75	43
X	10	250	6.0	86

(a) Heated immediately; (b) Heated after standing in glycerol for  $\frac{1}{2}$  hr.

min. at 250°C. showing  $I(A_1)/I(A_0) = 7.0$  (88% transformation). See X-ray photograph XI (Fig. 6). Prolonged heating furnishes no further improvement.

Sample XI was examined with X-rays in a comparison camera together with the untreated sample. During exposure, the samples and the films were interchanged every 10 min. to make sure that both samples

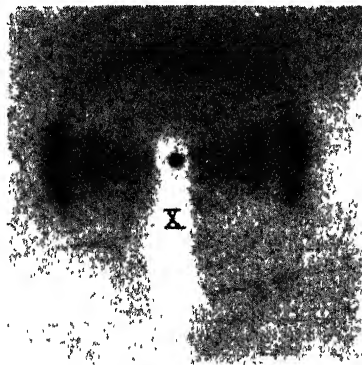


FIG. 5. X-ray Photograph of Ramie 86% Transformed to Cellulose IV

received the same amount of incident radiation. It will be seen from the photograph that these samples were less well orientated than I and II, owing to the fact that the mercerized fibers, still consisting of alkali cellulose when immersed in glycerol previous to the heating operation, show a contraction and partial disorientation. (See also the photograph of Sample X in Fig. 5.)



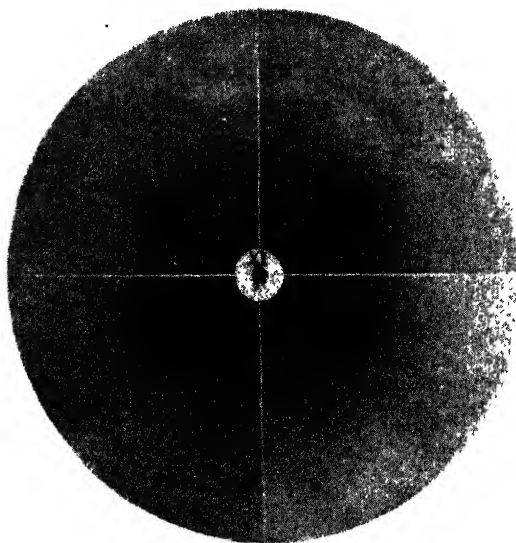


Fig. 6. Comparison Photograph of Ramie before and after Transformation from which Photometer Curves in Fig. 7 Were Taken

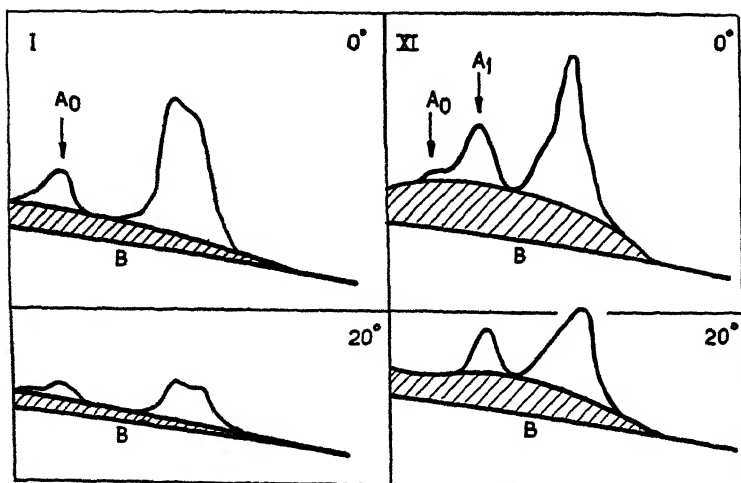


Fig. 7. Photometer Curves of the Diagrams I and XI along the Equator ( $0^\circ$ ) and at an Angular Distance of  $20^\circ$  from the Equator

The photometer curves of XI and that of the untreated sample taken at an angular distance of  $0^\circ$  and at  $20^\circ$  from the equator are reproduced in Fig. 7.

It should be mentioned that similar experiments carried out with regenerated cellulose (isotropic and orientated model filaments and rayon) previously transformed into alkali cellulose were all unsuccessful. The amount of transformation attained never exceeded 66%, whereas complete or almost complete transformation was easily arrived at when applying the ordinary procedure of preparation described at the beginning of this section and a heating time of 15–30 min. Hence, in this respect, we have not been able to reproduce Kubo's results. This author gives no precise data on the preparation of his objects previous to the heating operation, and it follows from our observations that seemingly unimportant details in the mode of operation concerned may have a marked bearing on the outcome of the experiments.

#### OTHER CHANGES IN THE DIFFRACTED RADIATION

Attention should be drawn to the fact that, apart from changes in the position of the "crystalline" interferences due to the coherent diffraction of the crystalline portion of the fibers, other changes in the X-ray diagram occur simultaneously. This can be demonstrated with the aid of the pictures taken in the comparison camera before and after the heating operation. In cellulose diffraction patterns the crystal interferences always appear as peaks superimposed on a more or less intense "base" of more or less diffusely scattered radiation. In a later paper, dealing with a more detailed analysis of the intensity distribution on cellulose diffraction patterns, it will be shown that in orientated fibers, the "base" always consists of a part which is markedly dependent on the angular distance from the equator and another part which is not.

In Fig. 7 the part of the base which is dependent on the angular distance is hatched. It is found by drawing curve B, representing the photometer curves taken at an angular distance of  $40^\circ$  or more from the equator, and which, beyond this angular distance, appear to remain constant within experimental error.

It will be seen from Fig. 7 that the hatched area of the transformed sample (XI) has a considerably larger surface than that of the original one (I). The larger amount of diffusely scattered radiation in the transformed sample can also be visually detected on the comparison photograph (see Fig. 6). The areas below the curves B are practically equal in the two cases. We have integrated the intensity of the radiation represented by the hatched areas over all angular distances from the equator and found that the ratio of the integrated values for XI and I amounts to

1.9.<sup>2</sup> This part of the diffusely scattered radiation is, therefore, almost twice as large in the transformed sample.

This phenomenon seems to be characteristic, since it is always observed in samples transformed into cellulose IV. A part of the hatched base which is dependent on the angular distance and which disappears at almost the same angular distance at which the crystalline interferences disappear is due to the non-monochromatic hard radiation always present in the nickel-filtered Cu-K  $\alpha$ -radiation used and represents "smeared-out" crystalline interferences. This part is, however, confined to the portion between the center of the photograph and the  $A_0$  interference, as was verified by repeating the exposures on two films, one behind the other, and with aluminum foil 0.3 mm. thick inserted between them. This foil absorbs almost all the copper radiation and transmits nearly all the hard radiation. On the second film the equator blackening did not extend beyond the site of the  $A_0$  interference. The considerable increase of the hatched portion observed is, therefore, certainly due to a structural change in the fibers.

It is difficult to indicate the cause of this increase, but we may perhaps suggest the following explanation. The base must in some way be connected with the amorphous portion of the fiber. The *total* amount of the latter decreases rather than increases upon transformation to cellulose IV. Its percentage is considered to run parallel with the sorptive capacity of the fiber for water, and it has been established that ramie fibers show a drop in sorptive capacity of 20–30% after transformation (*cf.* the monograph cited in ref. 4). If, however, the average degree of lateral order of the amorphous substance is enhanced, this may give rise to the formation of a broad band with its intensity maximum somewhere between the crystalline interferences  $A_1$  and  $A_4$ , and this band may show an orientation effect, since the amorphous substance is, partially at least, also orientated. In Fig. 7, it will be seen that the additional area of the hatched surface actually consists of such a band with a maximum intensity between the two crystalline interferences.

#### OPTICAL CONSTANTS OF CELLULOSE IV

In previous work (9) we have studied the change of the optical properties of fibers on transformation into cellulose IV and found that the specific birefringence at ideal orientation in ramie fibers rose from 0.055 to 0.062. These figures referred to a 50–60% transformation. Since we have now reached a higher percentage of transformation with sample XI, it was of interest to measure its optical constants. .

<sup>2</sup> The integration consists in determination of the integral  $\int_0^\alpha O \cos \alpha \, d\alpha$  where  $O$  represents the hatched area and  $\alpha$  the corresponding angular distance from the equator. It can easily be carried out graphically.

The following figures were obtained, according to methods described elsewhere (9):

$n_{11}$	$n_{\perp}$	$n_{11}-n_{\perp}$	$f_z$	$\frac{n_{11}-n_{\perp}}{f_z}$
1.582	1.526 <sup>s</sup>	0.055 <sup>s</sup>	0.86 <sup>s</sup>	0.064

where  $f_z$  represents the orientation factor computed from the X-ray diagram as introduced in the monograph cited in ref. 4. The refractive indices refer to a fiber density of 1.520.

Since the double refraction at ideal orientation (last column of the table) is now increased from 0.062 to 0.064, it is once more confirmed that the intrinsic double refraction rises as the transformation into cellulose IV proceeds. To what extent this is due to an increase in the percentage of crystalline substance or to the different optical constants of the IV modification as compared to the II modification (9), remains undecided.

#### ACKNOWLEDGMENT

The X-ray work was carried out by one of us (W.) as a guest in the Laboratory for Technical Physics of the Technical University in Delft.

#### SUMMARY

Complete transformation of the crystalline portion of mercerized ramie fibers into cellulose IV ("high temperature cellulose") by heating in glycerol has thus far not been effected. According to Kubo the transformation of cellulose II into cellulose IV in rayon is facilitated by first transforming the fiber into alkali cellulose and then heating it in glycerol. In this paper it is shown that, starting from alkali cellulose, the degree of transformation can actually be enhanced in ramie fibers as well, but that the result is due rather to a better previous penetration of the glycerol into the fiber as a result of the high degree of swelling of the alkali cellulose than to the fact that alkali cellulose is used.

The optical constants of the ramie fibers of the highest degree of transformation reached were measured and compared with those of the original product, accounting for the orientation factor as derived from X-ray data. In agreement with earlier work, it was found that the specific birefringence increases as the transformation proceeds.

A quantitative evaluation of X-ray diffraction patterns reveals that, apart from the change in the crystalline interferences which occurs upon transformation into cellulose IV, there is a characteristic change in the base of diffusely scattered radiation. That part of the base, the intensity

of which is dependent on the angular distance from the equator, increases to about twice its original value. A tentative explanation of this phenomenon is offered.

#### REFERENCES

1. MEYER, K. H., AND BADENHUIZEN, L. P., *Nature* **140**, 281 (1937).
2. KUBO, T., AND KANAMARU, K., *J. Soc. Chem. Ind. (Japan)* **41**, 301 (1938).
3. HESS, K., KIESSIG, H., AND GUNDERMANN, J., *Z. Physik. Chem.* **49B**, 64 (1941).
4. HERMANS, P. H., Contribution to the Physics of Cellulose Fibers, p. 176. Elsevier, Amsterdam-New York (1946).
5. KUBO, T., *Kolloid-Z.* **88**, 62 (1939).
6. HERMANS, P. H., ref. (4), p. 30.
7. HERMANS, P. H., ref. (4), p. 102.
8. HERMANS, P. H., ref. (4), pp. 9 and 146.
9. HERMANS, P. H., ref. (4), p. 175.

# A SIMPLE SURFACE PRESSURE BALANCE<sup>1</sup>

I. E. Puddington

*From the Division of Chemistry, National Research Council, Ottawa, Canada*

*Received Sept. 13, 1946*

## INTRODUCTION

Since Langmuir's work (1) on molecular orientation and the measurement of the pressure exerted by mono layers of insoluble fatty acids on the surface of water appeared in 1917, descriptions of many surface balances have been published (2-10). Most of these instruments have been modifications of Langmuir's, wherein the pressure exerted by the film against a movable float, which separates the clean water surface from that containing the film, is suitably measured, and, with two exceptions, (3-8), possess the undesirable feature of depending on some form of barrier such as air jets, gold or platinum foil or silk thread to prevent the film from leaking past the ends of the float. The present communication describes an apparatus in which these "frictionless" barriers are eliminated and which is sufficiently simple to be constructed by the average laboratory worker with a minimum of time and effort. It has a sensitivity which compares favorably with other balances which have been proposed.

## PROPOSED APPARATUS

The device may be described as a two-dimensional Bourdon gauge (11) which is maintained at the surface of the water in such a manner that the area enclosed by the gauge is kept clean, and pressure exerted by any film on the area outside is observed from the distortion of the gauge. In this respect it bears considerable resemblance to the "two-dimensional aneroid" described by Marcelin (3) and may be considered a modification of this instrument.

It was found convenient to make these gauges from 0.02 mm. (0.001 in.) hard brass shim stock, although other materials can be used. Strips, approximately 5 mm. wide, and of various lengths, were cut from a sheet of stock and a bend slightly greater than a right angle made about 2.54 cm. from each end. The ends were then soldered to a heavier brass strip (about 6 × 2 mm. and of appropriate length) which in turn was soldered

<sup>1</sup> Issued as N.R.C No. 1466.

to another brass strip to form a "T," the stem of which contained two dowels, spaced to fit into holes in a projection attached to the end of the trough and flush with its surface. The bottom of the shim stock gauge and the strip to which it is attached should be maintained at, or slightly above, the surface of the trough. The assembled gauge is shown diagrammatically in Fig. 1.

When the trough has been filled with water and swept to ensure a clean surface, the gauge is placed in position. Any pressure exerted by a film external to the gauge will cause a maximum amount of linear movement in the center of the gauge, while the maximum torque will appear at the corners. If either of these movements is suitably magnified and the gauge calibrated with known pressures, a useful surface balance is obtained.

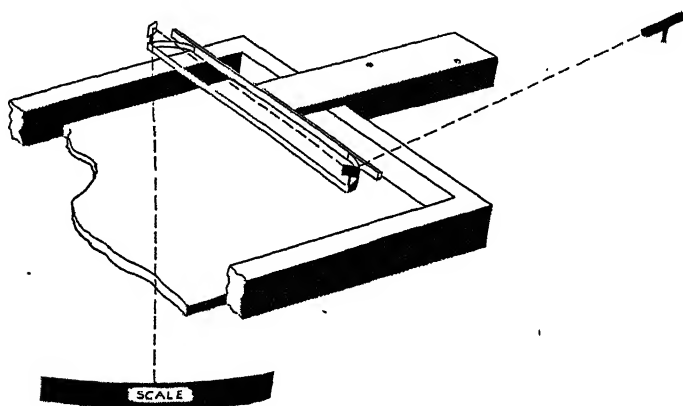


FIG. 1  
Schematic Diagram of Direct-Reading Instrument

A suitable method of obtaining sufficient magnification of the corner torque consists in mounting a light mirror at each corner and adjusting the angles, as shown in Fig. 1, to give a continuous light path from the source to the scale, with the 2 mirrors in series. A direct-reading instrument with a sensitivity depending on the dimensions of the gauge is produced by this procedure. The mirrors used here were portions of silvered microscope cover glasses and may be attached with wax to wire posts soldered to the corners of the gauge, or be held in light wire frames fixed to the posts. The latter method causes less distortion of the mirrors. Considerable care must be observed to select cover glasses with surfaces sufficiently good to produce mirrors which give a minimum of distortion. A single filament bulb and a lens constitute a satisfactory light source although a regular galvanometer lamp is considerably better.

Since the whole balance is held in place with 2 dowels and is quite rugged, it is easily removed from the trough. This provides for easy sweeping of the entire water surface and an uncontaminated area enclosed by the gauge is assured. The gauge may be lightly waxed from a solution of paraffin wax in benzene, followed by baking, to prevent wetting. A piece of shim stock about  $2 \times 0.5$  cm. soldered to the middle of the gauge so as to be completely immersed in the bath prevents excess vibration.

A second method of recording the pressure, which gives somewhat more precision than the procedure just outlined, consists in measuring the distance of linear movement of the center of the shim stock gauge as the pressure is applied. This may be done microscopically, or the motion may be sufficiently magnified by mechanical and optical means to be followed with simple equipment. The following scheme has been found satisfactory for doing this, although the setup is considerably more complicated than in the method just described.

An ordinary micrometer caliper is arranged to control the forward and backward motion of a light metal frame which holds a horizontal torsion wire. This torsion wire, which may be about 12 cm. long and 0.02 mm. in diameter, provides a frictionless bearing for a light mirror mounted with a piece of wax to its center. The bottom of this mirror is attached, by means of a short piece of 0.02 mm. nylon monofilament or metal wire to the middle of the gauge. Any motion of the gauge will cause the mirror to tilt and its motion may then be magnified optically. By adjusting the light spot reflected from the mirror to a chosen zero after each movement of the gauge, the linear travel of the gauge may be read directly from the micrometer, or, if the pressure changes to be measured are small, it is preferable to measure the motion of the gauge in terms of the movement of the reflected light spot on a scale, rather than to attempt setting the micrometer.

Vibrations of the mirror may be damped by suspending a vane attached to it in a cup of viscous oil. It was found more convenient, however, to allow a light aluminum vane attached to the mirror to lie between the pole pieces of an Alnico magnet spaced about 1 mm. apart. This procedure obviates any danger of contamination of the water surface by the oil.

An "exploded" view of the mechanism is shown, in Fig. 2, where the spring at "A" holds the end of the shaft, which carried the frame for the torsion wire "C," firmly against plate "B." The forward and backward motion of "B" is controlled by the micrometer "D." Any torsion in the shaft is prevented by a spring soldered to it and bearing against both arms of a "U" shaped rod "E," firmly attached to the bearing through which the shaft moves. The mirror with its aluminum vane, counter poise and attaching wire are shown at "F" with the gauge and trough at



"G" and "H" respectively. The provision for vertical adjustment of the torsion wire may be omitted if desired.

The trough may be the conventional metal variety but it has been found that "Lucite" or "Plexiglas" troughs, when waxed, are quite satisfactory for ordinary work and are considerably easier to fabricate.

The area of the gauge, which must be known if it is desired to determine the area occupied by the film, is easily found by tracing its outline on a piece of paper and comparing the weight of paper bounded by the tracing with the weight of a known area of paper.

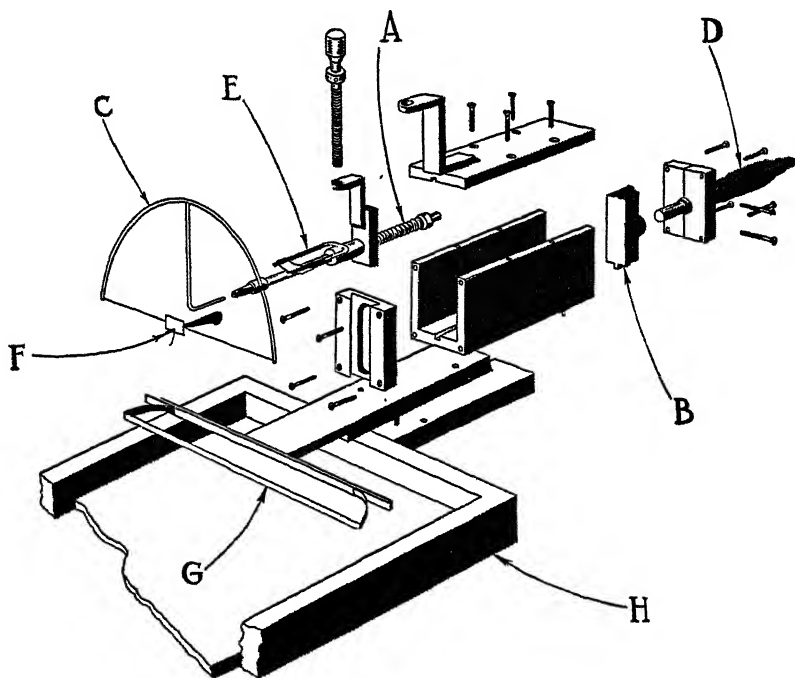


FIG. 2

Exploded View of Null Point Instrument

The gauges may be calibrated with films whose characteristics have been worked out. The "piston" oils (12) were particularly useful in this connection. The film pressures of these oils were obtained by measuring, with an ordinary analytical balance, the vertical pull on two microscope cover glasses dipping into water contained in a waxed petri dish, before and after a small drop of the oils had been applied to the surface of the water. The figures were checked by measuring the lowering of the surface tension of water with a Du Noüy Tensiometer in the presence of these oils. The results obtained are recorded in the table.

TABLE I  
Lowering of Surface Tension of Water  
(Dynes/Cm. at 25°C.)

	Piston Oil		
	Oleic Acid	Ethyl Myristate	Tricresyl Phosphate
Analytical Balance	30.6	17.5	9.62
Du Noüy Tensiometer	30.5	17.4	9.6

The results obtained when the deflection of the gauges is plotted against the pressure applied by the piston oils, are shown in Figs. 3 and 4. Fig. 3 represents the values obtained with the direct-reading instrument using gauges made from strips of shim stock 4.7 mm. wide and 10.0, 12.7, 15.2 and 17.8 cm. long. The longest of these gauges had a range of about 0-15 dynes/cm. and when the scale was read to 0.5 mm., had a sensitivity of 0.01 dyne/cm. The 10 cm. gauge had a probable range of 0-50 dynes/cm. with a sensitivity of 0.1 dyne, while the other gauges had intermediate values.

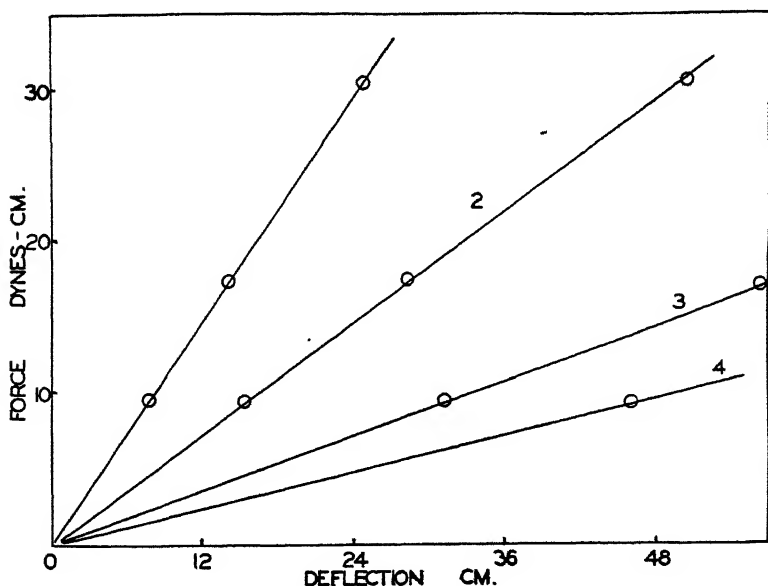


FIG. 3

Calibration Curve for Direct-Reading Instrument

Curves 1, 2, 3, 4 represent results obtained with gauges 4.7 mm. wide and 10.0, 12.7, 15.2 and 17.8 cm. long, respectively.

Fig. 4 shows that the amount of movement of the center of the gauge is also proportional to the force applied. The gauge in this case was prepared from a piece of shim stock 15.2 cm. long and 4.7 mm. wide. This gauge had a range of 0-30 dynes and, by following the movement of the light spot, could be read to  $\pm 0.001$  dyne/cm.

The sensitivity of this type of gauge could be increased considerably by decreasing the width of the shim stock and increasing the mechanical advantage of the mirror lever. The limiting factor in the latter refinement seems to be the difficulty of adjusting the center of gravity of the mirror,

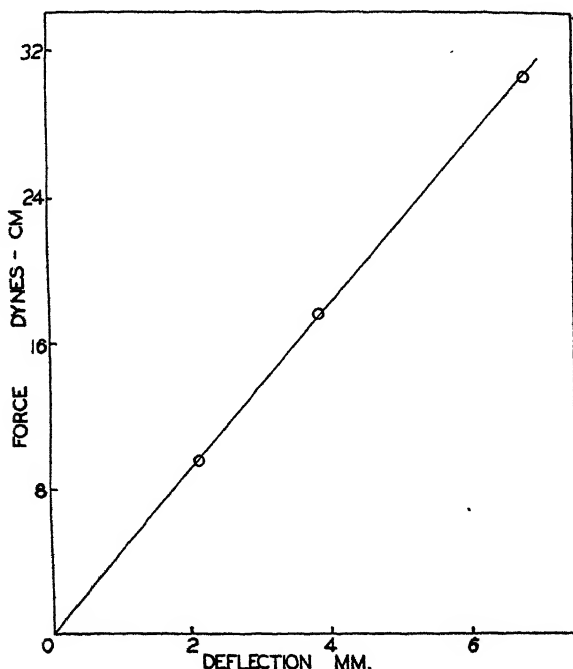


FIG. 4

Calibration Curve for Null Point Instrument

its vane and counter poise sufficiently close to the torsion wire. The difficulty of removing the last traces of accidental contamination from the water surface seriously limits the usefulness of too sensitive instruments and, for general work, the one just described would appear to be the most satisfactory.

For special purposes the parts in contact with the water surface may be of all glass or quartz construction, with virtually any desired sensitivity. One such model, where a suitably shaped quartz fiber 0.1 mm. in diameter provided the deformable part of the gauge, and a 2 mm. rod

formed the base, had a range of 0–10 dynes and a sensitivity of 0.0003 dyne/cm. A coat of General Electric Dri-Film rendered the quartz water-repellent. Calibration in these low ranges is more difficult and is probably best done with a Wilhelmy balance (8).

The zero point in this type of balance is quite sensitive to the level of the water in the trough, and loss from evaporation should be guarded against, or corrected for, during experiments. Mounting the trough on a support as free from vibration as possible is also desirable.

The chief objection to the instrument probably lies in the difficulty of obtaining an absolute calibration for it. The method outlined should be good to a few *per cent*, however, and since absolute values of pressure are not necessary for many problems where film balances are used, this should not detract greatly from its usefulness. A second disadvantage lies in the fact that it is not easily possible to remove surface active contamination which may develop inside the enclosed area during a run, should the substrate contain surface active ingredients. This objection, however, also applies to the conventional horizontal pull type of apparatus. Its sensitivity and ruggedness with its wide pressure range without adjustment, are desirable features. It would appear to be useful for measuring spreading forces at the interface of 2 liquids.

#### SUMMARY

A surface pressure balance, having a sensitivity which compares favorably with other such instruments, has been devised. It is essentially a two-dimensional Bourdon gauge in which the movement is suitably magnified.

#### REFERENCES

1. LANGMUIR, I., *J. Am. Chem. Soc.* **39**, 1848 (1917).
2. MARCELIN, A., *Ann. phys.* **4**, 481 (1925).
3. MARCELIN, A., *Ann. phys.* **4**, 505 (1925).
4. ADAM, N. K., AND JESSOP, G., *Proc. Roy. Soc. (London)* **110A**, 423 (1926).
5. LYONS, C. G., AND RIDEAL, E. K., *Proc. Roy. Soc. (London)* **124A**, 344 (1929).
6. MOSS, S. A., AND RIDEAL, E. K., *J. Chem. Soc.* **1933**, 1525.
7. GORTER, EL., AND SEEDER, W. A., *J. Gen. Physiol.* **18**, 427 (1934).
8. HARKINS, W. D., AND ANDERSON, T. F., *J. Am. Chem. Soc.* **59**, 2189 (1937).
9. LANGMUIR, I., AND SCHAEFER, V. J., *J. Am. Chem. Soc.* **59**, 2404 (1937).
10. PANKHURST, K. G. A., *Trans. Faraday Soc.* **41**, 156 (1945).
11. STRONG, J., *Procedures in Experimental Physics*, 213. Prentice-Hall, Inc., New York (1939).
12. ADAM, N. K., *The Physics and Chemistry of Surfaces*, Third Ed., 414. Oxford University Press (1941).



## OLEOPHOBIC MONOLAYERS.<sup>1</sup>

### I. FILMS ADSORBED FROM SOLUTION IN NON-POLAR LIQUIDS

W. C. Bigelow, D. L. Pickett and W. A. Zisman

*From the Naval Research Laboratory, Washington, D. C.*

*Received September 18, 1946*

#### EXPERIMENTAL

##### *(a). Discovery of the Adsorption of Oleophobic Films from Solution*

While experimenting with dilute solutions of eicosyl alcohol ( $C_{20}H_{41}OH$ ) in *n*-hexadecane, it was found that the solution did not wet the walls of the pyrex, glass-stoppered, Erlenmeyer flask. Since the same result was obtained after the flask had been boiled in chromic acid, washed in steaming distilled water and dried in a clean all-metal oven, it was considered unlikely that the effect observed could have been due to water or an accidental impurity adsorbed on the glass. The solvent was a carefully purified sample which, after several fractional crystallizations from ether solution, had been slowly percolated through a column of silica gel and then a column of alumina. Its melting point was  $18.1^{\circ}C.$ , in good agreement with the best reported value of  $18.14^{\circ}C.$  A drop of this *n*-hexadecane would not spread on water at pH 10 even after long contact, demonstrating its freedom from hydrophilic polar impurities (1, 2). Finally, the eicosyl alcohol used (M.P.  $64-65^{\circ}C.$ ) was exceptionally pure, having been found from much previous research to be free from more adsorbable impurities. The most reasonable conclusion was that the observed phenomenon was due to the adsorption of eicosyl alcohol from solution upon the interior walls of the flask, to form a film possessing the property of being oleophobic to (unwetted by) the oil solution.

A strip of platinum foil 9.5 mm. wide, 25 mm. long and 0.05 mm. thick was spot-welded on the end of a 0.5 mm. platinum wire to form a spade shaped "dipper." This was found convenient for it could be completely degreased by heating it briefly to a dull red heat in a Bunsen flame. As soon as it had cooled to room temperature (in about 15 sec.) it was immersed in the oil solution of eicosyl alcohol. When withdrawn, the dipper emerged dry. A test with a drop of either the solution or the pure hexadecane showed the dipper to be oleophobic, the contact angle at  $25^{\circ}C.$  being

<sup>1</sup> The opinions or assertions contained in this paper are the authors' and are not to be construed as official or reflecting the views of the Navy Department.

$40^\circ \pm 2^\circ$ . The drop of hexadecane moved about freely when the plane of the dipper was properly tilted. This coated surface was also hydrophobic (unwetted by water), for a drop of distilled water made a contact angle of  $90^\circ \pm 2^\circ$  with it. Similar experiments were made with clean dry dippers made of pyrex, soda glass, nickel, iron, steel, 18/8 stainless steel, copper, brass, aluminum, chromium, gold, molybdenum and tantalum and in each case the grease-free surface could be coated by adsorption with a film having the same oleophobic and hydrophobic properties. Clean dippers (including platinum), immersed in pure hexadecane, emerged wetted by the oil. Hence the observed phenomena were due to the adsorption of the solute.

Solutions in hexadecane containing a concentration of 0.1% by weight were prepared of each of the following polar, amphipathic compounds: *n*-eicosyl alcohol, primary *n*-octadecylamine, and *n*-nonadecanoic acid. Films on pyrex and platinum having oleophobic properties similar to those described were formed from these solutions. Concentrations unquestionably below the solubility limits in hexadecane were effective in causing the formation of these films; hence, the oleophobic films were not caused by a precipitation effect nor by picking up an insoluble, floating monolayer from the oil surface. When any one of these 3 dilute solutions was heated to between  $40^\circ$  and  $60^\circ\text{C}$ ., the ability to form an oleophobic film on platinum or glass disappeared, but it returned when the temperature was dropped below  $40^\circ\text{C}$ ., indicating that the effects may be due to reversible adsorption.

The 3 solutions, while maintained at  $25^\circ\text{C}$ ., were diluted 10-fold and poured into clean dry 25 ml. pyrex flasks. The oleophobic property was tested on platinum and glass and the 10-fold dilution process was repeated. Upon testing solutions of weight concentrations of  $10^{-3}$ ,  $10^{-4}$ ,  $10^{-5}$ ,  $10^{-6}$  and  $10^{-7}$ , it was found that oleophobic films adsorbed on platinum down to concentrations of less than  $0.5 \times 10^{-6}$  of the amine, while the acid solutions behaved similarly down to less than  $7 \times 10^{-6}$ . No oleophobic film could be obtained for solutions of eicosyl alcohol whose concentrations were less than  $4.4 \times 10^{-4}$ . At a concentration of  $10^{-3}$  the film was formed in a few seconds. The more dilute the solutions became the more time was found to be required for the polar molecules to diffuse through the oil and completely coat the platinum surface with an oleophobic film. In case of the most dilute solution employed successfully ( $10^{-7}$ ), the time required when no stirring took place was over 8 hours. Of course, the actual concentrations of the more dilute solutions were affected by the loss of the additive which adsorbed on the walls of the containers used, but the necessary corrections were made and were not important until the weight concentrations were below  $10^{-5}$ .

(b). *Theory of the Nature of Oleophobic Films*

Upon analyzing the above data it was noted that the number of polar molecules present in the most dilute solution found to produce an oleophobic film on the platinum dipper (*i.e.*, the octadecylamine solution having a corrected weight conc. of  $10^{-7}$  and a mass of 10 g.) was  $2 \times 10^{15}$  molecules. The total area of both sides of the dipper was about  $5 \text{ cm.}^2$  and the known sectional area of an aliphatic amine molecule is approximately  $25 \times 10^{-16} \text{ cm.}^2$  Thus, it was calculated that a minimum of  $5/25 \times 10^{-16}$  or  $2 \times 10^{15}$  adsorbed molecules would be necessary to coat the dipper surface. Because there were only this many molecules present in the solution, it appeared possible that the oleophobic film was monomolecular in nature, being composed of nearly close packed, oriented molecules.

The fundamental nature of this observation and its theoretical significance made it at once necessary to further the investigation. Therefore the following simple adsorption experiment was carried out. The solvent used was Eastman dicyclohexyl (M.P.  $3.6^\circ\text{C.}$ ; reported value,  $4.0^\circ\text{C.}$ ) purified by percolation through adsorption columns containing silica gel and alumina. A solution having a mass of 4.75 g. and weight concentration of  $2.68 \times 10^{-5}$  of *n*-octadecylamine was prepared in it. This solution was placed in a pyrex glass container having the shape of a rectangular parallelepiped whose internal dimensions were 43. mm. high, 26 mm. wide and 7 mm. thick. The fluid used initially filled the cell to a height of approximately 30 mm. A polished platinum dipper 22 mm.  $\times$  26 mm.  $\times$  0.05 mm. was mounted on the end of a strong platinum wire and arranged so that it could be dipped slowly in and out of the solution. The platinum sheet was allowed to remain immersed in the solution at  $25^\circ\text{C.}$  until oleophobic to the solution and then it was removed slowly to avoid carrying drops of solution with it. Upon removal the dipper was cleaned by a brief heating to dull redness in the non-oxidizing portion of the flame of a Bunsen burner, after which it was allowed 30 seconds to cool to room temperature, then the next dip was made. Observations were made after each dip of the contact angle between the horizontally held oleophobic dipper and a drop of distilled water. Throughout the first 60 dips the C.A. was between  $85^\circ$  and  $90^\circ$ . Between the 60th and 65th dips the C.A. decreased from  $85^\circ$  to  $80^\circ$ , between the 65th and 70th dips it decreased from  $80^\circ$  to  $75^\circ$ , while between the 70th and 75th dips it dropped rapidly below  $75^\circ$ .

A test of the spreading ability on acid water of a drop of the liquid left in the glass cell showed no surface active material to be left after the 75th dip. From this fact, and from the behavior of the solution while withdrawing the dipper from it, it was concluded that all the amine had been removed by from 70 to 75 dips. The observation that the contact angle of water on the film had remained nearly constant throughout the greater



part of the experiment, and that all the amine had been removed from the solution by this dipper technique, was considered to be a further indication that the film was monomolecular in nature over a wide range of solution concentrations. It would also appear that the average lifetime of adsorption for the amine at the oil-platinum interface was practically infinite.

The amount of amine removed from the solution was  $2.85 \times 10^{17}$  molecules. The total area of the dipper was  $1.14 \times 10^{17} \text{ \AA}^2$ , and the internal area of the cell was  $3.02 \times 10^{17} \text{ \AA}^2$ . Therefore the total area covered by the amine in the form of an adsorbed monolayer in 70 dips was  $82.8 \times 10^{17} \text{ \AA}^2$ . This amounts to an average area per adsorbed molecule of about  $82.8 \times 10^{17} / 2.85 \times 10^{17}$  or  $29 \text{ \AA}^2$ . Assuming that 75 dips were necessary to exhaust the amine from the solution the average area per adsorbed molecule would be  $29 \times 75/70$  or  $31 \text{ \AA}^2$ . It is, therefore, concluded that the average area per molecule in the adsorbed film was  $30 \text{ \AA}^2 \pm 1 \text{ \AA}^2$ . Possibly the degree of packing was somewhat greater in the earlier dips, and decreased during the last few dips. However, it does not seem likely that the closest possible packing would occur in a monolayer formed by such an adsorption phenomenon, so that the figure arrived at is probably not far from the actual value.

It is evident from the contrast in the behavior of dilute solutions of the alcohol as compared with the amine or acid that the average lifetime of adsorption of the alcohol must be very much shorter—perhaps by a factor of 1000. This resembles the differences in adsorptivities at the oil-water interface reported previously (1, 2, 3) in connection with studies of the effect of polar compounds and pH on the spreading of drops of oils on water. There a condition of ionization at the interface was found necessary for high adsorptivity of an amine or an acid. Here the high adsorptivity is apparently due to exchange phenomena (or coordination) between the electrons of the metal surface and those of the amine and carboxyl groups respectively.

In relating these results to the molecular structure and packing of the adsorbed polar molecules it is informative to consider the case of *n*-octadecyl amine. A molecule of this amine in its normal or stretched out configuration can be considered as a long rod at the opposite ends of which are located the methyl group and the polar  $-\text{NH}_2$  group. A number of such molecules can adsorb on a flat surface as a close-packed assembly of vertically-oriented rods to form a monolayer adhering to the surface as the result of the attraction of the surface for the  $-\text{NH}_2$  groups. Each methylene group in the aliphatic chains has a highly localized field of force attracting it to the methylene groups in the adjacent chains. Hence, if the molecules are packed sufficiently closely they will cohere due to the force contributions between each pair of horizontally adjacent methylene

groups. The total force will increase with the length of the hydrocarbon chain. Such an adsorbed monolayer exposes to outside approach a surface more or less closely packed with oriented methyl groups. Apparently the hydrocarbon molecules in a drop of hexadecane or dicyclohexyl so weakly adhere to the only accessible portions of this adsorbed monolayer that the surface tension forces of the oil drop are able to draw it up into a drop having a considerable contact angle. If the plane of this surface is tilted, the oil drop adheres so weakly that it rolls about readily or is "oleophobic."

From the above discussion it follows that the greater the chain length of the molecules the more condensed and rigid the film will be. The monolayer will change from the close-packed solid, to the plastic-solid, and even to the liquid state, as the temperature is raised or if the chain length is decreased. Increasing the temperature and decreasing the chain length also increases the solubility of the film in the oil. The net effect will be to decrease the average lifetime of adsorption of the molecules and eventually the film will dissolve or desorb. When the oleophobic film is a plastic-solid or rigid monolayer, very likely it is able to form suspension bridges over each depression in the surface of the solid whose area is not too large compared to the cross sectional area of the molecules. Such an effect should give to the long-chain compounds the ability to form oleophobic films having less roughness than the underlying surfaces and thereby the energy of adhesion between a drop of oil and the film covered surface would be further decreased. Evidence for the correctness of this surmise will be discussed in a later publication.

It was thought that the mechanism of coating the platinum involved the initial presence of a monolayer adsorbed at the oil-air interface, and that it was gathered up when dipping or withdrawing the platinum through such a film. An application of the Gibbs adsorption equation to appropriate surface tension measurements demonstrated that such could not be the case. The surface tension ( $\gamma$ ) of a solution of eicosyl alcohol in *n*-hexadecane was measured accurately. The weight concentration ( $W$ ) was  $3.60 \times 10^{-3}$ , and with the Cenco-Du Noüy interfacial tensiometer the corrected surface tension was found to be 26.15 dynes/cm. at 26°C. At the same temperature the surface tension of the pure *n*-hexadecane ( $\gamma_0$ ) was 26.90 dynes/cm. The number of gram moles adsorbed per unit area is given by:

$$\Gamma = - (W/RT)/d\gamma/dw \text{ where } \Gamma = (1/6.06 \times 10^{23} A) - \delta\rho W/M$$

The second term  $\delta\rho W/M$  is a correction for the amount per unit area of the polar compound normally dissolved in a surface layer of solution of the thickness  $\delta$  of one oriented molecule. Here  $T = 273 + 26 = 299^\circ$ ,  $\delta = 24 \times 10^{-16}$  cm.,  $\rho$  = density of hexadecane = 0.84,  $M$  = gram mole-

cular weight = 300,  $R = 8.314 \times 10^7$ , and  $A$  is the area per molecule adsorbed in the interface. The calculated value of  $\Gamma$  is  $3 \times 10^{-11}$  using the Gibbs relation. As  $\delta p W/M = 0.3 \times 10^{-19}$  it can be neglected in comparison with  $\Gamma$ , and finally the value  $560 \times 10^{-16}$  cm.<sup>2</sup> results for  $A$ . Therefore, the molecules adsorbed in the surface layer were so separated that they occupied an area over 20 times greater than that necessary for closest packing. Obviously the adsorbed film was gaseous and the formation on the platinum of the observed, very condensed film was not due to the collection of a monolayer when passing the dipper through the oil-air interface. Hence, the molecular process responsible for the formation of Langmuir-Blodgett monolayers and multilayers (4, 5, 6, 7) was not involved in the formation of the films described here.

Consistent with the conclusion of the preceding paragraph is the fact that, in using a 0.1% solution of the same alcohol in hexadecane, the film appeared to be deposited instantly, while the rate and method of dipping or withdrawing the platinum through the oil-air interface had no effect on the oleophobic film adsorbed. This is in marked contrast with the phenomena occurring in the Langmuir-Blodgett method. The increasing time necessary for the formation of oleophobic films from increasingly more dilute solution (as was described earlier), is also good evidence for the effect being adsorption from solution.

It is of interest to note here that Langmuir, Blodgett and Schaefer (6) showed some of the films deposited on solids using their techniques were also both oleophobic and hydrophobic. It can be concluded that the films described here are oriented monolayers adsorbed from solution, and that similar films should be formed from a wide variety of aliphatic polar compounds dissolved or dispersed in a variety of organic non-polar or weakly polar liquids. Therefore, a large number of such polar compounds dissolved in *n*-hexadecane were studied, after which typical compounds were examined in solutions in other solvents. The results are described below.

(c). *Some Experimental Methods Developed for Studying  
Oleophobic and Hydrophobic Films on Solids*

Before examining the adsorptive properties of these solutions it will be of interest to describe the techniques used in preparing and inspecting the oleophobic and hydrophobic films, and the precautions required in order to obtain reproducibility and control of the more important variables.

It was found essential to use only grease-free glassware and metal dippers and to work as much as possible in grease-free or uncontaminated air. The metal dippers used were made like those of platinum already described, but in some cases they were much thicker. Some were cleaned and polished with levigated alumina on grease-free "Kittens Ear" polishing

cloth, while the nickel, gold, molybdenum, tantalum and stainless steel were cleaned, after polishing, by immersion in chromic acid solution after which they were washed with warm distilled water. The majority of the experiments were made using mirror-finished platinum foil made as free as possible from the scratches usually formed during rolling operations. This eliminated tedious polishing and permitted effective degreasing by merely heating the foil in a Bunsen flame for a few seconds. It was found that newly cleaned metal surfaces usually were contaminated with adsorbed hydrophobic films after a few minutes of exposure at room temperature to the laboratory atmosphere. This time varied with the room used and the circulation and kind of contamination of the air. It was found best to use thin platinum foil dippers as much as possible because they cooled to room temperature from dull red heat in about 20 seconds and, if dipped immediately thereafter into the oil solution studied, they were usually sufficiently free from adsorbed grease or contamination to permit obtaining repeatable and reliable results. Where badly contaminated air was prevalent, or degreasing with heating and rapid cooling was impracticable, it was necessary to work with a box flushed continuously with clean air slightly above atmospheric pressure, all operations within being done by the use of flexible long rubber gloves built into the box through which the outside operator could manipulate the experiment.

The solvents used had to be free from traces of polar impurities which frequently were present as the inevitable or accidental result of the manufacturing process used or of some previous treatment. The presence of even a slight trace of a more readily adsorbed compound could completely control the nature of the adsorbed film formed. For example, an oleophobic film was adsorbed on platinum from a hexadecane solution of the best grade of commercial oleic acid obtainable, whereas none formed when carefully purified oleic acid was used. Such traces of impurities have given rise to many conflicting statements in the literature.

If sufficiently free of such adsorptive impurities, a drop of the solvent oil should not increase in diameter when floating on alkaline water adjusted to a pH above 10 or on acid water adjusted to a pH below 3 (1, 2). In order to obtain solvents of the desired purity it was often necessary to remove the polar impurities by contacting the solvents with adsorbents such as fuller's earth, alumina, florisil or silica gel. This treatment usually removed impurities to an extent impossible with the standard methods of purification. Care was needed when employing saturated or supersaturated solutions of oleophobic additives for, when precipitates or colloidal dispersions were formed, the dipper, originally coated with an oleophobic monolayer, was often roughened by the deposition on it of an exceeding small quantity of the precipitated material which caused the surface to be wetted by the oil. Under such conditions, though the oleophobic film was

present, the value of the contact angle with oil became variable and uncontrollable. Such effects were never found when working with true solutions.

The contact angle formed by a drop of liquid resting on the adsorbed monolayer was measured by a simple and convenient instrument developed for this work and much used and refined since. This might be called a telescope-goniometer. The first one constructed consisted of a small comparator telescope having a 38 mm. achromatic objective and a Ramsden eyepiece. It was 5" long, having a working distance from objective lens to object of 3" and a linear magnification of approximately 10. Two crosshairs, each mounted as a diameter of the telescope, were so supported that each could be independently rotated in a plane perpendicular to the telescope axis. The plane of rotation of one crosshair was only slightly displaced from that of the other so that the eyepiece could be adjusted to bring both crosshairs quite sharply into focus at the same time. The goniometer was constructed so that, as one crosshair was rotated, a 180° protractor rotated rigidly with it in a plane at right angles to the telescope axis, the protractor being adjusted with the zero degree mark on the scale parallel to the crosshair. As the other crosshair rotated, a pointer, rigidly attached and parallel to it, also rotated about the telescope axis. The drop of oil whose contact angle was to be measured was placed upon the plane surface of the horizontal oleophobic monolayer and the telescope was adjusted until the images of the drop and the two crosshairs were in focus. Then the protractor scale was revolved until its crosshair was parallel to the surface on which the drop rested, and the other crosshair was adjusted until it was tangent to the drop at the point of contact with the oleophobic surface. The angle on the protractor indicated by the pointer was then the contact angle.

The accuracy of this telescope goniometer was tested with a piece of flat, polished stainless steel which had been coated with a smooth layer of clean paraffin wax (melting point 30°–40°C.). The contact angles for a number of drops of distilled water with this surface were measured at 27°C. The average of the readings obtained was  $109^\circ \pm 1^\circ$ , which is in good agreement with the best values reported. All of the results reported here were obtained with this simple instrument. As any roughening of the dipper surface may change the contact angle between a drop of liquid and a surface (8, 9, 10) it was important to use plane polished surfaces to obtain reproducible results characteristic of the nature of film rather than of the polish of the surface. At room temperature and in the ordinary range of relative humidities the contact angle of an oil and a very oleophobic monolayer was found to be reproducible on polished solids to within  $\pm 1^\circ$ . It was found in the case of a monolayer of eicosyl alcohol adsorbed on platinum that, whereas the contact angle with hexadecane

varied from 35° to 40° when the relative humidity varied from 15% to 70%, it was 29° at relative humidities near 100%. Hence, the contact angles of an oil on such a film were considered sufficiently independent of the relative humidity in the range normally encountered to permit their use as an exploratory research tool. For later and more quantitative work better control of both relative humidity and temperature will be necessary.

(d). *The Effect of Varying the Nature of the Polar Molecules Dissolved in Hexadecane*

Various members of the homologous series of the saturated, unbranched, aliphatic, monocarboxylic acids and primary amines were dissolved in hexadecane in increasing concentrations and tested with a platinum dipper for the ability to form oleophobic adsorbed films at 25°C. The effect of the number of carbon atoms per molecule ( $N$ ) was quite simple. Only when  $N$  was 14 or more were the films oleophobic to drops of pure hexadecane. Compounds having  $N$  less than 14 were oleophobic to the solution but not to pure hexadecane. When  $N$  was less than 8 no films oleophobic to the solution were obtained, no matter how high a concentration was used. The aliphatic, unbranched, monohydric alcohols were oleophobic to pure hexadecane only when  $N$  was 16 or more and when it was less than 16 the films were oleophobic to the solution but not to the solvent. When  $N$  was less than 10 no films formed which were oleophobic to the solution, even when the concentration approached 100%. When the film was not oleophobic to pure hexadecane but was to the oil solution, it was found that as  $N$  decreased the minimum concentration ( $W_0$ ) necessary to cause the oleophobic films to form increased.

These variations in film properties with  $N$  are not surprising since the shorter the length of the hydrocarbon chain the less the cohesive forces between aliphatic chains will be able to overcome the effects of thermal agitation, and also the greater will be the solubility of the film in the hexadecane. Hence, a higher concentration of the additive is needed to produce a condensed film. If  $N$  is too low it is not possible to form an oleophobic film at any concentration for a given temperature. This leads one to expect a temperature effect as regards the borderline value of  $N$ , i.e., the minimum value of  $N$  for which films are adsorbed that are oleophobic to pure hexadecane. This was verified by a simple experiment in which it was observed that whereas a monolayer of  $n$ -hexadecyl alcohol on platinum was wetted by pure hexadecane and not by the solution at 25°C., it was unwetted by both at 20°C.

The magnitude of the contact angle exhibited by a drop of hexadecane increased rapidly as  $N$  increased, reaching a maximum of between 40° and 42°. In the case of the primary aliphatic amines, the contact angle

was  $32^\circ$  when  $N$  was 16 and  $42^\circ$  when  $N$  was 18 or higher. The same maximum value of  $42^\circ$  was found for other straight chain compounds studied. This result would be expected from the simple structural theory that the only factor determining the contact angle is the closeness of packing in the outermost methyl-rich plane of the adsorbed monolayer. Accordingly the contact angle should approach a constant maximum value as  $N$  becomes large enough for the film to become rigid.

Although stearamide ( $C_{17}H_{35}CO.NH_2$ ) and myristamide ( $C_{13}H_{27}CO.NH_2$ ) were nearly insoluble in hexadecane at room temperature, they dissolved sufficiently at temperatures of  $50^\circ C.$  or more to permit the adsorption on platinum or pyrex of monolayers which were oleophobic to their solutions. If the adsorbed films so formed were cooled to  $25^\circ C.$ , the stearamide monolayer was found to be oleophobic to pure hexadecane, the contact angle being  $40^\circ$ , while the myristamide monolayer was wetted. These results on the effects of chain length are in agreement with those previously described for the acids, amines and alcohols.

A large number of exceptionally pure aliphatic esters (listed at the end of this report) which were prepared from a long-chain acid (or alcohol) and a short-chain alcohol (or acid) were examined for the ability to form oleophobic films from hexadecane solutions. The maximum concentrations employed were either the solubility limit or were up to 25% by weight, whichever occurred first. In only a few cases were oleophobic films produced. Melissyl acetate ( $C_{31}H_{63}OOCCH_3$ ) and methyl melissate ( $CH_3OOC_{31}H_{61}$ ) formed adsorbed films on platinum or pyrex which were oleophobic to both the solution and to pure hexadecane, the contact angles being somewhere between  $30^\circ$  and  $42^\circ$ . However, no such films were formed by octadecyl acetate ( $C_{18}H_{37}OOCH_3$ ) and methyl stearate ( $CH_3OOC_{17}H_{35}$ ). Because the molecules of each of these esters consisted of one short and one long unbranched, aliphatic chain attached to a single polar group, it would appear that only those esters having the short chain made up of a very few carbon atoms and the long chain of many carbon atoms can attain sufficiently close-packing in the outermost portions of the adsorbed molecules to develop the oleophobic property.

Neither exceptionally pure oleic or elaidic acid, when dissolved in hexadecane, showed the ability to adsorb from solution on platinum or glass to form oleophobic films, even when concentrations as high as 1.5% were used. Furthermore, an oleophobic film did not adsorb on platinum from the pure, liquid oleic acid. Therefore, it appears that high solubility in oil is not the only factor which may be responsible for the inability of a long-chain polar compound to adsorb as an oleophobic monolayer. Now oleic and elaidic acids are the *cis*- and *trans*-isomers respectively of 9,10-octadecenoic acid ( $CH_3(CH_2)_7CH=CH(CH_2)_7COOH$ ). As pointed out by Marsden and Rideal (11) the oleic acid molecule has a normal configura-

tion shaped like the letter V. Such a compound would not be expected to attain the same degree of close packing in a monolayer as would stearic acid and, therefore, it might be expected to form a less oleophobic film than would the saturated acid. However, the normal configuration of elaidic acid is more nearly like that of its saturated homologue, stearic acid, and yet it did not form oleophobic films on platinum or glass. Apparently, the presence of the double bond in this compound either prevented full action of the van der Waals cohesive forces, or it prevented the molecules from adsorbing to form a monolayer with the  $\text{CH}_3$  groups outermost. Pure stearolic acid dissolved in hexadecane was tested up to its solubility limit (approximately 10% by weight) at room temperature and no evidence of the ability to form an adsorbed oleophobic film was found. This acid differs from oleic acid only in that it contains a triple bond in the middle of the chain instead of a double bond. It is possible, but not likely, that the triple bond also distorted the molecule sufficiently so that its normal configuration prevented the close-packing necessary for the formation of an oleophobic monolayer. Similar experiments with various concentrations in hexadecane of pure linoleic and linolenic acids, which possess two and three double bonds, respectively, and with oleyl, linoleyl and linolenyl alcohols, showed that these substances did not form oleophobic adsorbed films. One possibility is that the presence of a double or triple bond in the middle of the chain may result in the adsorption of each molecule with the unsaturated bond as an additional point of attachment to the platinum surface. Still another possibility is that the lack of the oleophobic property found with these unsaturated molecules may be due to the formation of adsorbed acid films more than one molecule thick. Further investigation is needed to decide which of these possible causes is responsible for these observations.

A group of homologous straight-chain compounds having two polar or reactive groups per molecule were studied. The presence of the additional polar group caused the solubility in hexadecane to decrease markedly; however, enough pure compounds of sufficient solubility were available to give results of interest. The hydroxy derivatives of oleic and elaidic acids, ricinoleic and ricinelaidic acids (both of which were reported as exceptionally pure) were examined. These formed adsorbed films which were barely oleophobic to the most concentrated solution obtainable in hexadecane but were wetted by drops of the solvent. The ricinelaidic acid film could be produced on platinum or glass at much lower concentrations than could the film of ricinoleic acid. Highly purified ethyl ricinoleate from the same source was tested in hexadecane solution and as a pure liquid, and in each case it did not adsorb as an oleophobic film. It is probable that these hydroxy, unsaturated, long chain acids do not form oleophobic films when sufficiently pure. Solutions of various concentrations of batyl



alcohol ( $\text{CH}_3(\text{CH}_2)_{17}\text{OCH}_2\text{CH}(\text{OH})\text{CH}_2\text{OH}$ ) in hexadecane were examined at room temperature. At weight concentrations as low as  $10^{-5}$ , films oleophobic to both solution and hexadecane were adsorbed on platinum or glass, the contact angle being around  $42^\circ$ . Since such dilute solutions were so effective, the life-time of adsorption of the batyl alcohol at the oil-metal interface must be much greater than in the case of the monohydric alcohols. A model of this ether-alcohol, made with the Fischer-Hirschfelder atom model kit, revealed that the molecule could easily be arranged in a straight-chain configuration. This compound probably adsorbs like a 20 carbon aliphatic chain attached by a C—C bond to an ethylene glycol group. The ether oxygen in this substance apparently serves merely to increase the length of the aliphatic chain. The presence of the two hydroxy groups (each capable of independent adsorption) at one end of such a polar molecule results in a greater adhesion to the adsorbing surface and therefore an increased average life-time of adsorption from solution. Another conceivable mode of adsorption is that in which the hydroxyl group on the first carbon atom of the chain is attached to the surface while the other, which is attached to the second carbon atom of the chain, is linked to the corresponding hydroxyl of the next molecule in the monolayer by hydrogen bonding. This also would cause an increased lifetime of adsorption of the compound.

Experiments were made with exceptionally pure  $\alpha$ - and  $\beta$ -monopalmitin (12). These two compounds can be considered as consisting of a straight aliphatic chain of 16 carbon atoms attached through an ester group to one end of a glycerol group in the case of the  $\alpha$ -form, or at the middle of a glycerol group in the case of the  $\beta$ -form. When dissolved in hexadecane, both forms deposited films on platinum or pyrex which were oleophobic to the solution and to the pure solvent, the contact angle being between  $35^\circ$  and  $40^\circ$ . An atom model of these molecules showed that both could be close-packed with the molecular axes vertical while both hydroxyl groups of the glycerol touched the adsorbing surface.

Studies made with pure 11-hydroxystearic, 13-hydroxystearic and  $\alpha$ -hydroxypalmitic acid also proved interesting. Although each of these compounds was nearly insoluble in hexadecane at room temperature, by using very dilute solutions at  $25^\circ\text{C}$ . and more concentrated ones at temperatures of  $50^\circ$ – $100^\circ\text{C}$ ., films were adsorbed on platinum or pyrex which were oleophobic to both the solution and the solvent, the contact angle being approximately  $35^\circ$ . Similar results were obtained by the same method with solutions in hexadecane of either 12-ketostearic or 4-ketostearic acid. Apparently one hydroxy or one keto group in the 18 carbon aliphatic chain does not prevent close-packing of the adsorbed molecules. Here it is possible that adjacent oriented molecules are bound together by an electron sharing process between corresponding hydroxyl or keto groups.

Aliphatic polar molecules containing branched hydrocarbon chains usually did not adsorb on platinum or pyrex to form oleophobic films. Such substances as 2-*n*-propylpalmitic acid and 2-methylpalmitic acid were tried, both of which are 16-carbon straight-chain aliphatic acids with a *n*-propyl or a methyl group, respectively, branching off at the  $\beta$ -carbon atom. Solutions in hexadecane in concentrations up to 25% were tried. Cetylmethyl hydrogen *o*-phosphate and the lauryl homologue dissolved in hexadecane gave oleophobic films. In more extreme cases of branching, exemplified by tripalmitin and tristearin, no oleophobic films could be formed.

A number of pure substances were studied, each of which comprised an aliphatic chain attached to one end of a cyclic nucleus but having a symmetry such as to suggest possible adsorption as did the rod-like aliphatic molecules. Solutions of chaulmoogric acid (a 5-carbon unsaturated hydrocarbon ring attached to the end of a 13-carbon aliphatic chain) and stearanilide (an 18-carbon aliphatic chain attached to a polar aromatic ring) in hexadecane were examined but did not produce oleophobic films. Hexadecane solutions of phenylundecylic, phenylstearic and xenylstearic acids, highly branched compounds and aromatic derivatives of undecylenic and oleic acids, behaved similarly, as did solutions of several naphthenic acids prepared and described by Harkness and Bruun (13). It is of interest to note that hexadecane solutions of lecithin (from Eastman) were not oleophobic.

In short, it has been shown that oleophobic films can be obtained from hexadecane solutions of a wide variety of aliphatic polar compounds. It has also been shown that adsorbed films can be formed from certain solutions which are oleophobic to the solution but not to drops of the pure solvent, the effect being due to the solubility of the adsorbed substance. To form such films the geometry of the molecule is all-important. Any aliphatic polar molecule whose normal configuration is like that of a long rod, permitting close-packing when adsorbed, will form oleophobic films over the proper temperature range. Aliphatic molecules having long branches or consisting of both rings and straight chains do not adsorb to form oleophobic films. One or more double or triple bonds in 18-carbon straight chain molecules prevent oleophobic film formation. Molecules with straight hydrocarbon chains and more than one polar group can form oleophobic films if the positions and sizes of the polar groups do not prevent the necessary degree of close-packing when the molecules adsorb.

(e). *Effect of Varying the Solvent*

The oleophobic films previously described were produced by adsorption from solutions in hexadecane. However, it was of interest to observe the behavior of the same polar molecules in solution in various hydro-

carbons and organic fluids. Using as solvents light and heavy grades of white petrolatum, the following compounds were found to adsorb as oleophobic films not wetted by drops of either the solution, the solvent or pure hexadecane: batyl alcohol, primary *n*-octadecyl- and heptadecylamine, the normal saturated fatty acids from eicosanoic down to tetradecanoic, 13-hydroxystearic acid and 11-hydroxystearic acid. The following compounds adsorbed as films which were oleophobic to drops of the petrolatum solution but not to drops of pure hexadecane: tridecanoic, dodecanoic and octanoic acids and hexadecyl, dodecyl and decyl alcohols. No oleophobic films could be obtained from oleic and elaidic acids, ethyl ricinoleate, xenylstearic or tetrahydronaphthylstearic acid. The effect of varying the concentration was studied and the same general behavior was found as with solutions of the same compounds in hexadecane. The only significant difference was in the much longer time necessary for complete adsorption equilibrium. This was to be expected since the much greater viscosity of the petrolatum than the hexadecane required a corresponding increase in time for the polar molecules to diffuse through the oil to the metal-oil interface. It was also found that the compounds not capable of forming oleophobic films from hexadecane solutions behaved similarly in petrolatum solutions.

Each of the following hydrocarbons were also tried as solvents for primary *n*-octadecylamine: *n*-octane, *n*-decane, *n*-dodecane and *n*-tetradecane; benzene, *p*-di-*sec*-amylbenzene, triamylbenzene, dodecylbenzene, *p*-*sec*-dodecyltoluene and *p*-*sec*-octadecyltoluene; *t*-butylnaphthalene, *t*-amyl-naphthalene, amyl-naphthalene and dodecyl-naphthalene; and tetrahydronaphthalene, decahydronaphthalene and dicyclohexyl. Observations were made also on solutions in petroleum ether, diphenyl oxide and bromobenzene. Any of the higher boiling fluids in this list manifesting the ability to spread on alkaline or acid water was contacted with a suitable adsorbent until no spreading was evident. The solvents used were chosen in order to test a variety of organic structures, solubilities and boiling points, and because their use would permit the study of polar compounds found to be insoluble in hexadecane. It was found that oleophobic monolayers of octadecylamine could be adsorbed on platinum or glass from dilute solutions in all of these fluids. This indicated that the phenomena previously described in section (d) could occur from a wide variety of organic liquids and polar compounds.

Many types of polar compounds found oleophobic in hexadecane were next dissolved in the low boiling hydrocarbons petroleum ether and benzene. Here it was found necessary to minimize the tendency for the rapid evaporation of such solvents to leave on the dipper a residue of solid particles of solute since such a deposit often caused wetting by the solution. It was found that eicosyl alcohol in petroleum ether formed

films on platinum which were oleophobic to the solution but not to drops of pure petroleum ether. The contact angles of such a film with respect to drops of hexadecane and water were approximately  $30^\circ$  and  $100^\circ$ , respectively. Solutions of primary octadecylamine in benzene behaved quite similarly. The effect of decreasing the concentration of the amine proportionately increased the time required for completing the close-packed adsorbed monolayer. At a weight concentration of  $1 \times 10^{-4}$  the film was still oleophobic, at  $2 \times 10^{-5}$  it was barely oleophobic, and at greater dilutions the film was wetted by hexadecane. Hence, the average life-time of adsorption in benzene solution was not quite as great as in hexadecane solutions. This difference between the behavior of octadecylamine in hexadecane and in benzene must be due to its much greater solubility in benzene.

*n*-Octadecyl alcohol was dissolved in each of the various oils and solvents listed above and the solutions were examined at different temperatures, using platinum and pyrex dippers. When it was necessary to prepare the solutions by warming the solvent, the film-forming properties of the solutions were observed as the temperature returned to that of the room. Experiments were made up to the solubility limit. With tetradecane and hexadecane, solutions were found having the ability to deposit films on the dippers which were both oleophobic to the solution and to drops of pure hexadecane. From all of the other fluids the films obtained, though oleophobic to the solutions, were not oleophobic to pure hexadecane. These results are in marked contrast to the results with *n*-octadecylamine already described.

Several phenomena are involved here. The solubilities of the polar additives in the lower boiling solvents are often so great that at adsorption equilibrium, even with the large concentrations used, the adsorbed film surface density is not one of close enough packing for the appearance of the oleophobic property. This is merely another statement of one of the few empirical rules of adsorption from solution, *i.e.*, adsorption of the solute is usually more marked the lower the solubility, or the nearer the solution to the solubility limit. As for the higher boiling solvents, the solubility of weakly adsorbing compounds, such as the alcohols, is too low at  $20^\circ$ – $30^\circ\text{C}$ . for a sufficient quantity to be present to adsorb out of solution and form an oleophobic film. In other words, the solubility limit  $W_m$  has been exceeded before a sufficiently close packed monolayer has adsorbed, *i.e.*,  $W_o > W_m$ . An analogous effect was described earlier (2) as the cause of the non-spreading on water of solutions of octadecyl or higher alcohols in white mineral oil. It is concluded that films oleophobic to the solution and to pure hexadecane are not readily obtained with polar solutes having such low energies of adsorption as do the alcohols because of the very careful balancing of solubility and adsorptivity required.

Where the energy of adsorption of the polar solute molecules is high enough (as it appears to be for the primary amines and the acids on platinum) the variety of solvents from which oleophobic films deposit becomes very wide. In such cases  $W_0 < W_m$ . From the results already described (as well as those of earlier work at the oil-water interface 1, 2, 3) it can be concluded that esters, ketones, ethers and similar compounds will adsorb weakly like the alcohols while the acids and amines will adsorb more strongly.

Stearamide in the following hot solvents formed films not wetted by hexadecane; dodecylbenzene, diphenyl oxide,  $\alpha$ -methylnaphthalene. The film was not wetted by hexadecane when adsorbed from hot or cold solutions in decahydronaphthalene, tetrahydronaphthalene, decylnaphthalene or *t*-amyl naphthalene.  $\beta$ -Monopalmitin adsorbed on platinum from either hexadecane or dicyclohexyl solutions at 25°C. to form a monolayer exhibiting a contact angle with pure hexadecane of 40° but solutions in bromobenzene or in dodecylbenzene deposited films unwetted by the solution and wetted by drops of pure hexadecane. Hence the previously described effects, found by varying the solvent used to dissolve octadecyl alcohol, are also found with other polar compounds.

The use of solvents other than hexadecane permitted a much greater variety of polar substances to be examined for the ability to deposit oleophobic films. Solutions of the following compounds in the various solvents already mentioned were examined without any indication of the formation of films oleophobic to the solution or to pure hexadecane; abietic acid,  $\beta$ -(1-naphthyl)-propionic acid,  $\beta$ -naphthoic acid,  $\beta$ -naphthol, triphenylcarbinol, *p*-hydroxydiphenyl, tri-*p*-cyclohexylphenylcarbinol, *p*-aminodiphenyl, acridine, *N*-phenyldiethanolamine and tri-*p*-cresyl phosphate. Even when concentrations up to the solubility limits were tried, no oleophobic films could be formed. A simple explanation is that each of these substances, although adsorbed to some extent, is not able to form a close-packed monolayer the outermost portion or layer of which consists of oriented, densely packed methyl groups. The results observed would then be expected from the structures of all of these compounds with the possible exceptions of the abietic acid and the tri-*p*-cresyl phosphate. From the molecular configuration of the first compound it appears possible that it adsorbs either lying down or as a multilayer due to the presence of the conjugated double bond, while the second compound cannot be described as rod-like or plate-like. Hence, although the molecules of each compound can adsorb and contain methyl groups at the opposite end from the polar group, they apparently are unable to pack closely enough to create a sufficiently high density of methyl groups to permit the development of the oleophobic property.

Using these fluids as solvents a number of additional polar compounds

were found capable of forming oleophobic films on platinum and glass. Thus, cholesterol formed films oleophobic to the solution but not to drops of either the pure solvent or to hexadecane from the following solvents: dicyclohexyl, diphenyl oxide, bromobenzene, triamylbenzene, and *p*-octadecyltoluene. It was unable to form oleophobic films from solutions in amyl-naphthalene, dodecyltoluene,  $\alpha$ -methylnaphthalene, tetrahydronaphthalene and decahydronaphthalene. In case of solutions in dicyclohexyl, oleophobic films were deposited on platinum only when the weight concentration exceeded a value somewhere between  $1 \times 10^{-3}$  and  $5 \times 10^{-3}$ . Hence, cholesterol, like the alcohols, has a low average lifetime of adsorption from such solutions. To be sure that the observed film was not a more surface active impurity than the cholesterol, experiments were repeated using Eastman cholesterol purified by the following procedure. The material was dissolved in benzene and the solution was percolated through an adsorption column of silica gel and of alumina. The percolate was evaporated in a vacuum and the residue dissolved in hot absolute alcohol and allowed to crystallize out at room temperature. This was filtered and dried in a vacuum. Its melting range was 146.1–146.9°C.

To prove that the film deposited on the platinum was actually cholesterol a simple experiment was devised to which was applied each of 3 different color reactions for cholesterol; the Liebermann-Burchard reaction, the Salkowski reaction and the formaldehyde- $\text{H}_2\text{SO}_4$  test (14, 15). The formaldehyde- $\text{H}_2\text{SO}_4$  reaction was reported to be the most sensitive of those listed and it may be of interest to describe the way in which it was employed in this experiment. About 1 ml. of chloroform was placed in a layer over an equal volume of the  $\text{HCHO-H}_2\text{SO}_4$  reagent (1 part 40%  $\text{HCHO}$  to 50 parts conc.  $\text{H}_2\text{SO}_4$ ) in the bottom of a small test tube. A clean platinum dipper .05 mm. thick, 17 mm. long and 7 mm. wide was immersed in the dicyclohexyl solution of purified cholesterol until an oleophobic monolayer had formed on it. The dipper was then withdrawn from the solution, care being taken that no drop of the solution remained on it, and placed in the test tube containing the reagents. The test tube was shaken gently for a minute, after which the dipper was removed (it was no longer oleophobic) and cleaned by washing with a solvent, followed by flaming to dull red heat. The process of coating the dipper with an oleophobic film and transferring it to the reagent test tube was repeated. Upon completing 5 such dips, a definite pink color developed in the chloroform layer in the test tube. The formation of such a color is reported to be a positive test for the presence of cholesterol (14, 15). The other 2 tests were in agreement with this result. Here it will be of interest to note the sensitivity of this color test. From the known area of the dipper, the number of dips, and the approximate cross sectional area

of 50 Å<sup>2</sup>/cholesterol molecule it was calculated that the test had revealed the presence of approximately one part in a million of cholesterol.

The structure of cholesterol may be likened to that of a hydrocarbon plate with an eight-carbon, aliphatic, branched-chain group (or rod) attached to one end and a hydroxyl group at the other end of the plate. Attached to the free end of the aliphatic chain are two methyl groups. Hence, from the above observations it is concluded that cholesterol can adsorb on solids so that the outermost portion of the film forms a plane densely packed with oriented methyl groups. This ability to isolate such a sterol as an oriented monolayer may be of value for the electron diffraction analysis of structure or for the examination of other surface-active properties.

These experiments with a variety of solvents permit the extension to other solvents and oils of the earlier conclusions of section (d). The relation of the effect of the adsorptivity and solubility to the ability to form oleophobic films has been discussed and related to the results with a number of fluids. A more definite conception of the structural types able to form oleophobic films from solution has been obtained and a number of additional oleophobic compounds have been found, cholesterol being especially interesting.

#### (f). *Effect of Varying the Nature of the Test Drop*

The previous tests for the oleophobic nature of the monolayer adsorbed were made by observing the contact angle of a drop of the oil solution or of a drop of hexadecane. It was of interest to observe the tendencies of a variety of pure liquids to wet an oleophobic monolayer. Monolayers on platinum of *n*-octadecylamine, eicosyl alcohol and batyl alcohol deposited from solutions in hexadecane were each tested at 25°C. with a drop of any one of a number of pure hydrocarbon liquids. It was found that the contact angle decreased with the boiling point of the liquid. All of the higher boiling oils such as hexadecane, octadecane, octadecyltoluene, cyclohexyltridecane and petrolatum were oleophobic to the monolayers and exhibited contact angles varying from 45° to 25°. On the other hand, the lower boiling liquids such as hexane, octane, benzene, toluene and cyclohexane, all completely wet the monolayers. Liquids having intermediate boiling points exhibited contact angles varying from 30° to 15°, but in most cases wet the area underneath the drop fairly rapidly. This could be observed by rolling the drop off a given portion of the surface after a definite time of contact. Evidently solution or desorption of the monolayer into the oil drop was principally involved. In some cases this was so pronounced that the contact angle rapidly decreased after the drop was placed on the film-covered surface.

When the wetting of the oleophobic monolayer was tested by each member of a homologous series of pure hydrocarbons, the contact angle decreased with the boiling point and molecular weight. Using the series of normal saturated hydrocarbons, it was found that the contact angles at 25°C. were 38°, 32°, 28°, 20° and 0° for octadecane, tetradecane, dodecane, decane and octane, respectively. The time required for the drop to wet the monolayer beneath decreased with the chain length; therefore it is evident that, instead of *n*-hexadecane, any one of a large number of the higher boiling hydrocarbons or oils could have been used for test solvent drops on oleophobic films. However, it was considered most convenient to use drops of *n*-hexadecane because of its known rod-like structure, and because of the ease with which quantities of the highly purified liquid could be prepared from the available commercial grades of the material.

Although the measurements of the contact angles of drops of pure liquids on previously isolated oleophobic film coatings are of interest in studying the desorption mechanism, they are not as valuable for studying the adsorption equilibria at the solid-liquid interface as are the measurements obtained on drops of the solutions from which the oleophobic films were prepared.

#### *(g). Hydrophobic Property of Oleophobic Films*

A clean metal dipped in a non-polar hydrocarbon liquid remains coated by the oil when withdrawn from the liquid. If a drop of distilled water is then placed on such a surface it sinks through the oil layer and reaches the metal surface displacing the oil (5). In contrast, a drop of distilled water placed on an oleophobic film adsorbed on a metal surface will not wet it but will exhibit a large contact angle. Measurements were made at 25°C. of the contact angles of drops of distilled water with oleophobic monolayers previously isolated on flat polished platinum dippers by adsorption from hexadecane solutions. The contact angles were found to be independent of the concentration of the hexadecane solution as long as the concentration was sufficient for the adsorbed films to be oleophobic to both the solution and pure hexadecane. Table I shows that the contact angle was very nearly 90° for all of the oleophobic films studied. Hence, the contact angle between a drop of water and a surface oleophobic to hexadecane is entirely independent of the nature and location of the polar groups at the other end of the oriented molecules of the monolayer. The hydrophobic property is due, obviously, to the fact that such monolayers present to the water drop a surface consisting of oriented methyl groups, and the approximate constancy and high values give strong evidence for concluding that the degree of packing of the methyl groups is nearly the same in all these films.



The high melting paraffin waxes are solid at 25°C. and smooth solid surfaces coated with them exhibit contact angles with distilled water varying from 100° to 110° at room temperature and ordinary relative humidities, depending on the condition of the paraffin surfaces. If care is used to chill quickly a molten layer of high grade paraffin wax deposited uniformly on a polished solid, the resulting surface will exhibit contact

TABLE I

*Contact Angles Between Water and Oleophobic Monolayer Adsorbed on Platinum*  
Temperature 25°C.

Monolayer Adsorbed on Platinum from Hexadecane Solution

Adsorbed Substances	No. of Carbon Atoms per Molecule	Contact Angle	Per cent Relative Humidity	Remarks
<i>n</i> -Eicosyl alcohol	20	89-92°	50	Platinum foil dipper
<i>n</i> -Eicosyl alcohol	20	91°	42	Plane polished platinum
<i>n</i> -Eicosyl alcohol	20	92°	56	Plane polished platinum
<i>n</i> -Eicosyl alcohol	20	91°	46	Plane polished platinum
<i>n</i> -Eicosyl alcohol	20	91°	59	Plane polished platinum
<i>n</i> -Octadecyl alcohol	18	94°	50	Platinum foil dipper
Ceretyl alcohol	26	81-82°	50	Dipper coated at 45°C.
Batyl alcohol	21	90-91°	50	Platinum foil dipper
Batyl alcohol	21	91°	56	Platinum foil dipper
Primary <i>n</i> -octadecylamine	18	90°	50	Platinum foil dipper
Primary <i>n</i> -octadecylamine	18	91°	56	Platinum foil dipper
Primary <i>n</i> -octadecylamine	18	92°	53	Plane polished platinum
Primary <i>n</i> -octadecylamine	18	91°	59	Plane polished platinum
Primary <i>n</i> -hexadecylamine	16	91°	50	Platinum foil dipper
Primary <i>n</i> -tetradecylamine	14	85-88°	50	Platinum foil dipper
Methyl melissate	32	91°	50	Platinum foil dipper

angles with water ranging from 106° to 109°. The much lower and constant value of 90° found here using oleophobic adsorbed films on polished solids deserves an explanation. The surface of paraffin probably consists of a large number of more or less randomly oriented crystals of the hydrocarbon fractions from which the paraffin was prepared. The roughness of the metal or glass surface coated with paraffin will vary with the purity and the rate of cooling during the coating process. Usually such a paraffin surface is much rougher than is a polished sheet of platinum coated with an adsorbed oleophobic monolayer. The latter will appear even smoother than the solid beneath, for the film covers the surface with a thin carpet which, in effect, disregards the smallest depressions. Such an effect was found by Langmuir, Schaefer and Sobotka (7) and by Bikerman (16) in coating fine wire gauzes with a monolayer by the Langmuir-Blodgett

method. Hence, the lower and more constant value of  $90^\circ$  found here is probably the theoretically most significant hydrophobic contact angle found. It may be of interest to note that the conclusions relative to the effect of roughness are in qualitative agreement with other work on hydrophobic contact angles (8, 9, 10).

*(h). Spreading of Drops of Oils on Flat Horizontal Metal Surfaces*

In addition to observing the adsorption of oils containing oleophobic compounds by the use of small metal dippers immersed in the oils, experiments were made on their behavior when placed upon grease-free, polished, horizontal plates of steel and platinum. Each of the pure organic liquids already discussed was found to spread steadily until the entire metal plate was covered with a layer of liquid. The rate of spreading increased as the boiling point and viscosity decreased. If an oleophobic additive was present in the oil, the drop started to spread, then one or more holes formed in the disc which continued to grow in size until finally the surface was covered by a more or less widely scattered array of droplets separated by apparently clear areas. If the concentration of the additive was sufficiently small, it was possible to create and reproduce a condition in which only one more or less centrally located hole formed. When one hole developed in a drop of oil containing octadecylamine it was found that the maximum area attained by the hole was equal to that which would be occupied by a close-packed monolayer made up through the adsorption of every polar molecule originally present. Also drops of hexadecane and water on the clear area included in the "hole" exhibited contact angles of  $40^\circ$  and  $90^\circ$ , respectively, proving that this portion of the plate was covered by an adsorbed oleophobic monolayer of octadecylamine. If the concentration of the amine additive was much higher it was possible to have the spreading effects occur rapidly, the oil disc spreading and appearing to burst, leaving the surface of the plate covered by a large number of drops each of which exhibited considerable contact angles.

The observed effects can be understood in terms of the adsorption of an oleophobic film at the interface between the drop of oil and the metal. As the energy of adhesion of the oil for the monolayer was less than for the clean metal surface, the oil spread over the metal and quit the area covered by the oleophobic film. The growth of the hole merely accompanied the growth of the area covered by the film. When the total number of oleophobic molecules was less than sufficient to cover the initial area of contact between the drop and the metal, spreading occurred without hole formation, for here the degree of packing of the adsorbed polar molecules was insufficient for the formation of an oleophobic film. It should be

noted that, since the volume of the drop of oil used in this experiment is very small relative to the area of the metal surface on which it is placed, this method is not as sensitive for detecting low concentrations of oleophobic additives as is the dipper technique in which the area of the metal surface can be made very small relative to the amount of solution to which it is exposed.

The following data are of interest in connection with the preceding discussion. Solutions of *n*-octadecylamine in pure hexadecane exhibited normal spreading or wetting on plates of steel and platinum as long as the weight concentration was less than  $5 \times 10^{-4}$ . When the concentration was higher, hole formation and the accompanying accelerated creeping effect were observed on platinum but not on steel. If the concentration exceeded  $1 \times 10^{-3}$ , hole formation and accelerated creeping occurred on steel. Similar effects were found with solutions of stearic and arachidic acids in hexadecane and in white mineral oil.

#### (i). Applications

The new films and their properties described here help the understanding of many observations reported elsewhere in the literature in connection with research on oiliness, wear prevention, emulsification, detergency, wetting and the inhibition of the rusting of steel with polar compounds.

A monolayer of adsorbed polar molecules deposited on a metal by the Langmuir-Blodgett technique has been demonstrated to decrease the coefficient of friction to a very low value (16, 17). However, that technique is limited to substances completely insoluble in water and capable of forming a plastic-solid floating monolayer. The simpler, and more theoretically significant, process of adsorption from oil solutions can now be used for such studies to deposit a much greater variety of substances on any clean metal and the chain length of the polar molecules can be varied from 8 to 26 or more carbon atoms per molecule. There is also the advantage that such films can be studied while in contact with the oil solution from which they adsorbed.

Any substance capable of forming oleophobic films by adsorption from solution can now be deposited on a metal or other solid surface for purposes of physical or chemical examination. This is of particular advantage for the electron diffraction analysis of the structure of monolayers. Since it has been shown that cholesterol can be prepared as an oleophobic monolayer, there appears available a promising method of studying the surface-active properties of this and similar compounds of biological importance.

Because adsorbed films oleophobic to the pure solvent oil as well as the oil solution have been found to have close packing of the outermost

methyl groups, such films will exhibit a low coefficient of friction and close to the maximum wear-preventive property obtainable with a reversibly adsorbed coating one molecule thick. However, the presence of an oleophobic additive in the oil may not always be desirable in practice, since usually the wetting of the lubricated surfaces will be hindered. For example, an oleophobic adsorbed monolayer on the polished cylinder walls and piston rings of an internal combustion engine would prevent the oil from clinging to the entire surface of the rings and cylinder walls. The only lubrication obtained would be that afforded by the monolayer. This condition could be remedied by several means: (1) by having a sufficient number of uniformly distributed fine grooves in the lubricated surface to act as oil retainers during the piston motion, (2) by maintaining the oil at a temperature above the temperature of desorption of the monolayer, or (3) by avoiding the presence of oleophobic compounds.

Another example of the undesirability of the presence of oleophobic compounds is to be found in the development of paints. It was reported by Selden and Pritton (18) that, while the addition of stearic acid to paints greatly decreased their adhesiveness to metals, the use of abietic acid caused an opposite effect. The low adhesiveness due to the first compound might have been caused by the oleophobic film of stearic acid which adsorbed at the metal-paint interface during the drying of the paint, while the greater adhesiveness of the paint when abietic acid was present could be influenced by the non-oleophobic nature of adsorbed abietic acid films.

Another interesting application of oleophobic films involves the prevention of spreading of instrument oils. By choosing the proper solvent and long chain compound it is possible to coat an instrument part with an oleophobic monolayer that will prevent the spreading of a lubricating oil away from the vicinity of the bearings. To prevent the film being dissolved away by the drop of oil, the oleophobic additive should be present in dilute solution in the lubricating oil. If desired the oleophobic coating may be applied to the instrument parts by a dipping process using a solution of an oleophobic compound in a hot or volatile solvent. However, it should be remembered that these monomolecular films can be removed by light scrubbing or abrading.

These oleophobic films have been shown to be very hydrophobic. Many of the results of this investigation can be used, therefore, to interpret experimental data on the wettability of surfaces and the mechanism of inhibition of rusting by the use of the polar type compounds commonly added to turbine oils, hydraulic fluids and other lubricants. The conclusions relative to the mechanism of rust inhibition will be presented separately in the near future. Good use can be made of high molecular weight oleophobic monolayers deposited from solution to protect metal

or other solid surfaces from corrosion due to water and some types of organic vapors.

Much has been written about the contact angles exhibited by drops of water and oils when placed in contact with metals. It has been known for some time that drops of water will always wet a metal completely if the surface is entirely free of adsorbed grease-like films or monolayers. The results presented here lead to like conclusions relative to the wetting of metals by oils; *i.e.*, drops of oils free from oleophobic polar compounds always completely wet clean metal surfaces. It appears that many previously published statements about the spreading of oils on metals are incorrect interpretations of the experimental data, probably as a result of the presence of adsorbed films on the metals or to the presence of organic oleophobic impurities in the oils used for the spreading tests. The penetrating observations of Woog (19) and the valuable study by Bulkley and Snyder (20) relative to the spreading of oils on metals are now fully explained in terms of the oleophobic films phenomena reported here.

#### ACKNOWLEDGMENTS

This investigation has been much expedited by the cooperation of Division B of the National Defense Research Council through whose activities a number of the necessary polar compounds and hydrocarbons were prepared. These compounds were, in general, exceptionally pure. The mode of preparation and the physical and chemical identification constants are given in the following reports of Division B:

Report No. 95 of October 20, 1941;  
Report No. 101 of October 29, 1941;  
Report No. 129 of December 4, 1941; and  
Report No. 752 July 20, 1942.

A brief list of these compounds and their sources is given below. The eicosyl alcohol (M.P. 64–65°C.), ceretyl alcohol (M.P. 79–80°C.), stearolic acid (M.P. 48°C.), *d*-dodecane (B.P. 112–113°C./30 mm.), and dicyclohexyl (B.P. 92–93°C./8 mm.) were prepared under the direction of Prof. Homer Adkins of the Department of Chemistry of the University of Wisconsin. The *n*-amyl laurate (B.P. 125–127°C./1.5 mm.), *n*-decyl stearate (M.P. 37.5–38.0°C.), *n*-decyl laurate (M.P. 21.8°C.), *n*-decyl caproate (B.P. 102–104°C./1.5 mm.), *n*-decyl acetate (B.P. 91.0–92.5°C./1.5 mm.), 11-hydroxystearic acid (M.P. 76.5–77.0°C.), 4-ketostearic acid (M.P. 96°C.), and the 12-ketostearic acid (M.P. 79.5–80.5°C.) were all prepared under the direction of Prof. C. S. Marvel of the Department of Chemistry of the University of Illinois. The following esters were prepared under the direction of Dr. M. L. Wolfrom of the Department of Chemistry of the Ohio State University: *n*-amyl stearate (M.P. 30.0–30.5°C.), *n*-amyl melissate (M.P. 69.5–70.0°C.), *n*-decyl melissate (M.P. 68.8–69.2°C.), *n*-octadecyl caproate (M.P. 23.2–23.6°C.), *n*-octadecyl laurate (M.P. 43.5–44.0°C.), *n*-octadecyl stearate (M.P. 61.5–62.0°C.), methyl melissate (M.P. 74.0–74.2°C.), melissyl acetate (M.P. 72.5–73.0°C.), melissyl caproate (M.P. 67.8–68.0°C.), and melissyl laurate (M.P. 70.0–70.5°C.).

A number of very pure compounds were made available to this laboratory through the cooperation of the persons and organizations indicated below. The methyl, ethyl, and *n*-propyl stearates, the *n*-dodecyl, *n*-tetradecyl, and *n*-octadecyl amides, the docosyl amine, and the hydrochlorides of *n*-octyl, *n*-dodecyl and *n*-hexadecyl amines were ob-

tained from Dr. A. W. Ralston of the Chemical Research Laboratory of Armour and Co. (21). The linoleic and linolenic acids (over 99% pure) were supplied by Dr. J. P. Kass of the Department of Botany of the University of Minnesota. The batyl alcohol (M.P. 70–71°C.) was obtained from Prof. H. N. Holmes of the Department of Chemistry of Oberlin College (22). The ricinoleic acid was obtained from Prof. St. Elmo Brady of Fiske University, Nashville, Tennessee (23). The  $\alpha$ -monopalmitin (M.P. 77°C.) and  $\beta$ -monopalmitin (M.P. 68°C.) were obtained from Dr. B. Daubert of the School of Pharmacy of the University of Pittsburgh (12). The *p*-di-*sec*-amylbenzene (B.P. 110–112°C./4 mm.), *p*-*sec*-dodecyltoluene (B.P. 154–155°C./2 mm), and *p*-*sec*-octadecyltoluene (B.P. 209–211°C./2 mm.) were supplied by Prof. G. H. Hennion of the Department of Chemistry of the University of Notre Dame.

The sources of the remaining pure compounds discussed have been listed in earlier reports of this laboratory (1,2,3).

### SUMMARY

It was found that certain types of polar organic molecules are adsorbed from solutions in non-polar solvents to form well-oriented monolayers on polished solid surfaces. Such monolayers imparted both hydrophobic and oleophobic properties to the polished surfaces of a variety of metallic and non-metallic solids and could be formed from a large variety of solvents, those used ranging from hydrocarbons like hexadecane, mineral oils, benzene, methylnaphthalene and dicyclohexyl to other solvents such as carbon disulfide, carbon tetrachloride, bromobenzene and diphenyl oxide.

It is shown that the mechanism of the formation of these films on platinum was reversible adsorption from solution and that it definitely was not the accumulation of insoluble films floating at the liquid-air interface as in the Langmuir-Blodgett method. It is concluded that the adsorbed films were made up of almost vertically oriented molecules which were nearly close-packed and attached to the surface through a surface active or polar group. Attention is called to the possibility that such films do not conform to the shape of the solid surface but might bridge over those surface depressions whose areas are not too great compared to the cross-sectional area of the molecules.

In order that a compound be able to adsorb as an oleophobic monolayer it appears necessary that its molecular structure be in keeping with the following requirements. First, the molecules of the compound must be capable of approximating close-packed orientation in a monolayer. Second, the surface active or polar group must be located at one extremity of the molecule and one or more methyl groups must be located at the opposite extremity. Finally, the molecules must adsorb to a flat solid surface with sufficient close-packing so that the outermost portion of the film is essentially a plane surface, densely populated with methyl groups.

It was found that compounds whose molecular configurations resemble a long rod or a flat plate, with a polar group attached to one end of the

rod or rim of the plate and one or more methyl groups at the opposite end of the rod or rim of the plate, readily satisfy these requirements. Exceptions were found in the case of aliphatic, unbranched polar molecules containing one or more unsaturated bonds, for these did not form oleophobic films. It is suggested that such molecules adsorb on solids at both the polar end group and the unsaturated bonds so that, instead of orienting with their axes vertical to the surface, they are arranged more nearly horizontally.

Observations were made to determine the smallest concentrations of each of the various types of oleophobic compounds which would permit the formation of oleophobic monolayers on platinum and pyrex. While weight concentrations of only  $10^{-7}$  were required for primary aliphatic amines and monocarboxylic acids, roughly 1000 times more was needed for the aliphatic alcohols, esters and ketones and for cholesterol.

Some of the relations of these findings to past theoretical and applied research are discussed.

#### REFERENCES

1. ZISMAN, W. A., *J. Chem. Phys.* **9**, 534 (1941).
2. ZISMAN, W. A., *J. Chem. Phys.* **9**, 729 (1941).
3. ZISMAN, W. A., *J. Chem. Phys.* **9**, 789 (1941).
4. BLODGETT, K., *J. Am. Chem. Soc.* **57**, 1007 (1935).
5. LANGMUIR, I., *Science* **444** (1938).
6. LANGMUIR, I., BLODGETT, K., AND SCHAEFER, V., *J. Franklin Inst.* **218**, 143 (1943).
7. LANGMUIR, I., SCHAEFER, V., AND SOBOTKA, H., *J. Am. Chem. Soc.* **59**, 1751 (1937).
8. ADAM, N. K., *The Physics and Chemistry of Surfaces*, 3rd Ed., 186. Oxford Press. (1941).
9. DOSS, K. S., AND RAO, B. S., *Proc. Indian Acad. Sci.* **7A**, 113 (1938).
10. CASSIE, A. B., AND BAXTER, S., *Trans. Faraday Soc.* **40**, 546 (1944).
11. MARSDEN, J., AND RIDEAL, E. K., *J. Chem. Soc.* **1938**, 1163.
12. DAUBERT, B., *J. Am. Chem. Soc.* **62**, 1713, 1815 (1940).
13. HARKNESS, R. W., AND BRUUN, J. H., *Ind. Eng. Chem.* **32**, 502 (1940).
14. GORTNER, R. A., *Outlines of Biochemistry*, 2nd Ed., 799. Wiley.
15. WHITBY, G. S., *Biochem. J.* **17**, 5 (1923).
16. BIKERMAN, J. J., *Proc. Roy. Soc. (London)* **170A**, 130 (1939).
17. BOWDEN, F. P., AND LEBEN, L., *Phil. Trans.* **239**, 1 (1940).
18. SELDEN, G., AND PRITTON, C., *Am. Paint J.* Nov. 2, 8-14 (1940).
19. WOOG, P., *Compt. rend.* **181**, 772 (1925) and Contribution à l'étude du graissage onctuosité. Delagrave, Paris (1926).
20. BULKLEY, R., AND SNYDER, G., *J. Am. Chem. Soc.* **55**, 194 (1933).
21. HOERR, C. W., AND RALSTON, A. W., *J. Am. Chem. Soc.* **65**, 976 (1943).
22. HOLMES, H. N., AND CO-WORKERS, *J. Am. Chem. Soc.* **63**, 2607 (1941).
23. BRADY, ST. E., *J. Am. Chem. Soc.* **61**, 3464 (1939).

# THE COAGULATION OF LYOPHILIC COLLOIDS BY ORGANIC SUBSTANCES AND SALTS. IX\*

B. Jirgensons

## INTRODUCTION

The coagulation of hemoglobin, casein, albumin, gelatin and starch sols has been treated in previous publications (1). The concentrations of the organic substances (*e.g.*, of various alcohols, acetone, propane, *etc.*) and of the salts were varied within wide limits. Some fairly general rules were deduced concerning the influence of these concentrations on the stability.

It is known that alcohols, acetone and other surface-active organic substances coagulate lyophilic colloids. The flocculation takes place at some definite high concentration of the organic substance, which is a nonsolvent and precipitates the colloid-dispersed substance. The minimum concentration necessary for flocculation depends above all on the concentration of the colloid and, in the case of proteins, on the pH of the solution. The rules are simple in the case of the isoelectric proteins but were found to be more complicated for positive and negative proteins (*e.g.*, casein at pH = 6.0). If, to a protein solution, alcohol solutions of varying strength are added, turbidity and flocculation are observed not only at 60–90 vol.-%, but also at 20–40 vol.-% of alcohol. At 40–60 vol.-% of alcohol, the mixtures are much clearer and (in the absence of salts) no flocculation takes place.

As a rule, small amounts of salts (no organic matter being present) act as stabilizers, but large concentrations of salts cause coagulation. However, some more complicated cases are also known. It happens that both small and large concentrations of salts cause coagulation while medium concentrations effect peptization. These "irregular series" occur when salts of heavy metals are used as coagulants (2).

The following rules were found by the author (1) when sols of egg albumin, casein and hemoglobin were mixed with both salt and alcohol (or a similar organic substance):

(a) small concentrations of salt (*e.g.*, 0.01 M/l. of NaCl) speed up the coagulation at all concentrations of the organic substance;

\* This paper was submitted for publication through the courtesy of Professor P. Karrer, Chemisches Institut der Universität, Zürich, Switzerland.



(b) large concentrations of salt act either as stabilizers or sensitizers, *i.e.*, they either hinder or assist coagulation. High concentrations of salt (*e.g.*, 0.5 *M*/l. of NaCl or 0.1 *M*/l. of CaCl<sub>2</sub>) assist flocculation when the alcohol concentration is relatively small (5–20 vol.-%) or very high. However, at medium concentrations of organic substances, *e.g.*, at 40–60 vol.-% of propyl alcohol, the alcohol-salt mixture has a strong peptizing action. In this manner protein sols can be obtained which contain alcohol and salts and are permanently stable.

Similar observations were made also on chemically altered proteins, such as desaminated casein, egg albumin and hemoglobin (3).

The small influence of the chemical properties of the particles on the stabilizing or peptizing action of medium concentrations of organic compounds and high salt concentrations is worth noticing. This action is also influenced but little by the pH of the protein. *n-Propyl alcohol*, dioxane, pyridine, allyl alcohol and other organic substances which have relatively high surface activities and relatively small dielectric constants are the strongest stabilizers. Naturally, the organic substance must be well miscible with the protein sol. *Ethyl alcohol* and acetone are less effective stabilizers, but even with these substances and 0.2–0.4 *M* CaCl<sub>2</sub> or MgCl<sub>2</sub>, stable protein sols can be made containing about 50 vol.-% of alcohol or acetone. *Methyl alcohol is not a stabilizer; it causes flocculation also in the presence of salts.* It is the best organic coagulant for albumin, hemoglobin and similar sols containing salts. In other words, *to prevent peptization it is advisable to coagulate a protein sol by methyl alcohol and a salt* (NaCl, KCl, Na<sub>2</sub>SO<sub>4</sub>, CaCl<sub>2</sub> and others, except the salts of heavy metals).

The above rules seem to have a general application. *E.g.*, if 0.2 *M* CaCl<sub>2</sub> solution and varying amounts of propyl alcohol (pH of mixture being 4.5) are added to cheese whey, flocculation is observed at 15–35 vol.-% and at over 70 vol.-% of alcohol; while at 40–60 vol.-% of propyl alcohol, the mixtures remain clear. *Lactalbumin* acts in the same way as egg albumin.

The experiments have now been extended to potato proteins, whose behavior agreed with that of milk and egg albumins and casein. The results follow in the experimental part.

#### EXPERIMENTAL RESULTS

The preparation and chemical properties of the proteins of potato are treated in another paper (in print). For flocculation experiments, 3 different types of potato proteins were used, *viz.*, (a) albumins, (b) globulins, and (c) a protein which was sparingly soluble and, insofar as the solubility is concerned, has some similarity to casein.

Albumin samples were dissolved in water and those of globulins and poorly soluble proteins in caustic soda. The pH of the solutions was measured with a glass electrode. The flocculation experiments were carried out as follows: into a series of test tubes, first equal amounts of protein solution and then identical amounts of alcohol solutions of increasing concentrations were introduced and well mixed. The test tubes were observed for a while, and then equal amounts of a salt solution of known concentration were added to each tube and again well mixed. The combined action of alcohol and salt was then observed.

The results are shown in the tables and figures. The numbers mean:

0—no flocculation, perfectly clear solution;

1–6—turbidity of growing intensity;

6–12—flocculation and increasing precipitation of proteins.

The results on potato albumin are listed first. Table I shows the coagulation of albumen with methyl alcohol and with methyl alcohol and  $\text{CaCl}_2$ . Table II shows the action of ethyl alcohol.

TABLE I

*Precipitation of 0.05% Potato Albumin by Methyl Alcohol and Methyl Alcohol and Calcium Chloride. pH = 4.2*

Vol.-% of alcohol	0	11	22	33	44	55	66	77	88	
State after 60 min.	0	0	0	0	0	3	9	12	12	Without salt
after 2.5 hrs.	0	0	0	0	0	4	6	8	10	{ With 0.2 M of $\text{CaCl}_2$ /l. of mixt.
after 24 hrs.	0	0	0	0	0	8	9	10	12	
	0	10	20	30	40	50	60	70	80	Vol.-% of $\text{CH}_3\text{OH}$ after addition of $\text{CaCl}_2$

TABLE II

*Precipitation of 0.05% Potato Albumin by Ethyl Alcohol and Ethyl Alcohol and Calcium Chloride. pH = 4.2*

Vol.-% of alcohol	0	11	22	33	44	55	66	77	88	
State after 60 min.	0	0	0	0	3	5	10	12	12	Without $\text{CaCl}_2$
after 2.5 hrs.	0	0	0	0	2	4	3	4	8	{ With 0.2 M of $\text{CaCl}_2$ /l. of mixt.
after 24 hrs.	0	0	0	0	8	10	8	8	8	
	0	10	20	30	40	50	60	70	80	Vol.-% of alcohol after addition of $\text{CaCl}_2$

Table I shows that no irregular coagulation takes place when methyl alcohol and  $\text{CaCl}_2$  are used, *i.e.*, the more methyl alcohol added, the more complete is the coagulation.

Ethyl alcohol (Table II), on the contrary, shows the peptizing action at about 60 vol.-%. Identical results are obtained when sodium chloride or any other neutral salt is taken instead of  $\text{CaCl}_2$ .

The maximum and minimum of flocculation are especially well seen when potato albumin is coagulated by *n*-propyl alcohol and  $\text{CaCl}_2$  (Tables III–VI). They were observed also at relatively small concentrations of  $\text{CaCl}_2$  (Table IV) and are independent of, or very little dependent on, the pH of the albumin. It is seen that 20–40 vol.-% propyl alcohol (together with  $\text{CaCl}_2$ ) acts as a coagulant while 40–70 vol.-% alcohol has a peptizing action.

When the concentration of the alcohol is plotted along the abscissa and the degree of coagulation along the ordinate, a typical curve with a maximum and a minimum is obtained (see Fig. 1).

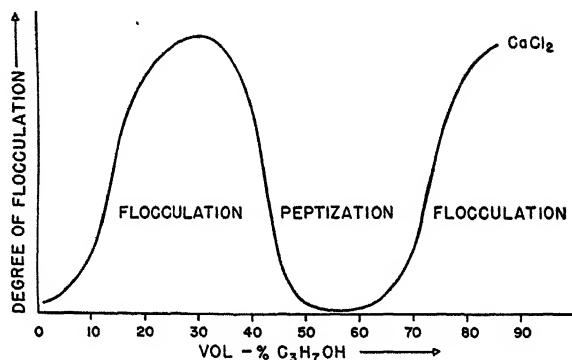


FIG. 1

TABLE III

*Precipitation of 0.1% Potato Albumin by n-Propyl Alcohol and Calcium Chloride. pH = 4.6*

Vol.-% of $\text{C}_3\text{H}_7\text{OH}$	0	11	22	33	44	55	66	77	88	
State after 30 min.	0	0	0	0	0	2	6	7	8	Without $\text{CaCl}_2$
after 3 hrs.	0	0	3	10	0	0	1	2	10	{ With 0.38 M of $\text{CaCl}_2$ /l. of mixt.
after 20 hrs.	0	0	8	12 max.	8	0 min.	1	2	12	
	0	10	20	30	40	50	60	70	80	Vol.-% of alcohol after addition of $\text{CaCl}_2$

TABLE IV

*Precipitation of 0.1% Potato Albumin by n-Propyl Alcohol  
and Calcium Chloride. pH = 4.6*

Vol.-% of C <sub>3</sub> H <sub>7</sub> OH	0	11	22	33	44	55	66	77	88	
State after 5 min.	0	0	0	0	0	0	5	7	8	Without CaCl <sub>2</sub>
after 15 min.	0	0	0	0	9	0	0	0	2	{ With 0.02 M of CaCl <sub>2</sub> /l. of mixt.
after 16 hrs.	0	1	3	5 max.	0 min.	1	2	3	12	
	0	10	20	30	40	50	60	70	80	Vol.-% of alcohol after addition of CaCl <sub>2</sub>

TABLE V

*Precipitation of 0.1% Potato Albumin by n-Propyl Alcohol  
and Calcium Chloride. pH = 2.6*

Vol.-% of C <sub>3</sub> H <sub>7</sub> OH	0	11	22	33	44	55	66	77	88	
State after 30 min.	0	0	0	0	0	0	6	7	8	Without CaCl <sub>2</sub>
after 60 min.	0	0	2	6	1	0	0	1	3	{ With 0.38 M of CaCl <sub>2</sub> /l. of mixt.
after 18 hrs.	0	2	10	12 max.	12 min.	0	0	1	5	
	0	10	20	30	40	50	60	70	80	Vol.-% of alcohol after addition of CaCl <sub>2</sub>

TABLE VI

*Precipitation of 0.1% Potato Albumin by n-Propyl Alcohol  
and Calcium Chloride. pH = 9.0*

Vol.-% of C <sub>3</sub> H <sub>7</sub> OH	0	11	22	33	44	55	66	77	88	
State after 5 min.	0	1	2	5	5	5	8	8	8	Without CaCl <sub>2</sub>
after 4 hrs.	0	0	1	11	4	1	1	1	8	{ With 0.38 M/l. of CaCl <sub>2</sub>
after 24 hrs.	0	0	2	12 max.	6	1	1 min.	1	12	
	0	10	20	30	40	50	60	70	80	Vol.-% of alcohol after addition of CaCl <sub>2</sub>

The flocculation minimum is much less pronounced or disappears completely when  $C_3H_7OH$  is used in conjunction with  $NaCl$ ,  $Na_2SO_4$  or an alkali phosphate instead of  $CaCl_2$ . When an acid albumin is coagulated, polyvalent anions cause strong flocculation and cannot peptize a protein even in the presence of 50–60 vol.-% of propyl alcohol (Fig. 2). On the

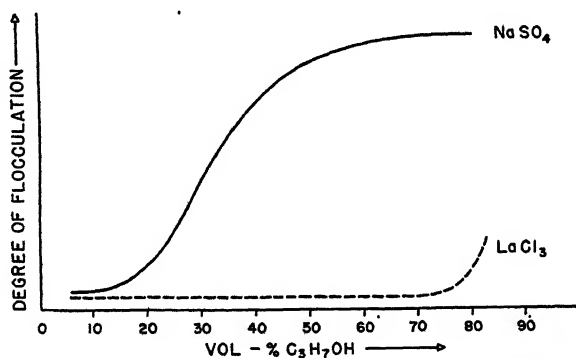


FIG. 2

contrary, no coagulation is observed at all when, to an acid protein sol, lanthanum chloride and propyl alcohol are added. The lanthanum ions (0.01 *M/l.*) peptize so strongly that no flocculation occurs at any concentration of propyl alcohol.

In the experiments on *potato globulins*, 0.2 g. of globulin were dissolved in 4 cc. of 0.1 *N*  $NaOH$  + 16 cc. of  $H_2O$ . The pH of this solution was 9.7. Hardly any flocculation of the globulin took place from this solution when alcohols were added, and no flocculation was achieved by 0.1–1 *M/l.* of  $CaCl_2$ . However, a mixture of salt and alcohol readily caused flocculation. Table VII shows that 40–50 vol.-%  $C_3H_7OH$  had only a transitory stabilizing effect.

TABLE VII  
*Precipitation of 0.1% Globulin by n-Propyl Alcohol  
and Calcium Chloride, 0.2 M/l.*

Vol.-% of $C_3H_7OH$	0	10	20	30	40	50	60	70	80
State after 5 min.	0	1	5	6	1	2	4	6	10
after 60 min.	0	2	12	12	6	5	12	12	12
after 3 hrs.	0	3	12	12	10	10	12	12	12

The poorly soluble *potato protein* was obtained by treating potato juice with an acid. A 0.4% solution of this protein in  $NaOH$  was used, the pH being 9.5. Hardly any flocculation was achieved by alcohol, but 0.002–

0.004 *M*/l. of  $\text{CaCl}_2$  caused coagulation. In this respect, the protein behaves like an alkali caseinate.

Irregular series which the author observed on casein years ago appeared also when this protein was coagulated by propyl alcohol and  $\text{CaCl}_2$  (see Table VIII).

TABLE VIII

*Precipitation of 0.04% Poorly-Soluble Potato Protein by n-Propyl Alcohol and Calcium Chloride, 0.2 M/l.*

Vol.-% of $\text{C}_3\text{H}_7\text{OH}$	0	10	20	30	40	50	60	70	80
State after 5 min.	4	6	6	3	1	1	1	2	4
after 90 min.	11	11	11	8	1	1	4	10	11
after 22 hrs.	12	12	12	12	2	2	6	12	12
					min.				

A *desaminated albumin* was prepared, dissolved and coagulated. Potato albumin (2.5 g.) was desaminated with 5 g. of  $\text{NaNO}_2$  in 2 *N*  $\text{CH}_3\text{COOH}$ . The yellowish deposit of the desaminated albumin was filtered and washed. 0.5 g. of the dry substance was dissolved in 25 cc. of 0.01 *N*  $\text{NaOH}$ . A solution of desaminated albumin having  $\text{pH} = 8.4$  could not be coagulated by propyl alcohol alone.  $\text{CaCl}_2$  also promoted little flocculation, *i.e.*, its minimum concentration was very high; about 0.05–0.1 *M*/l. But a mixture of alcohol and salt produced a coagulation readily, and only a transitory stabilization was observed at 40–60 vol.-% of propyl alcohol.

#### DISCUSSION OF RESULTS

A great similarity is observed between the behavior of potato albumin and that of egg albumin studied earlier (1). However, a difference is present in the case of potato albumin, *i.e.*, the stabilization is also observed when the salt concentration is relatively small (Table IV). The peptization regions are wider for potato than for egg albumin. Both albumins are easily peptized by 50–60 vol.-% of propyl alcohol and  $\text{CaCl}_2$ , while the corresponding desaminated products are both difficult to peptize. In this respect, a perfect agreement is observed.

The comparison of various potato proteins shows that coagulation of the albumin is relatively difficult; whereas, the globulin and the poorly soluble protein are easily precipitated. The peptization of these two proteins with 50 vol.-% of propyl alcohol and  $\text{CaCl}_2$  is less marked than that of the albumin. What might be the explanation for this behavior?

First, the cause of coagulation and peptization will be discussed. Alcohols are commonly considered to be dehydrating agents. If alcohol is slowly added to a gelatin sol, for example, the solution becomes opalescent at some definite concentration of the alcohol and flocculates on addition of a small amount of salt (O. Scarpa, H. R. Kruyt and others). It is believed that alcohol reduces the degree of hydration and that salts discharge and "salt out." Thus it could be expected that alcohol and salt ( $\text{NaCl}$ ,  $\text{NaNO}_3$ ,  $\text{CaCl}_2$ ,  $\text{MgCl}_2$ , and other salts, except those of heavy metals) acting together would be a more efficient coagulant than either alcohol or salt alone. But 40–60 vol.-% of propyl alcohol +  $\text{CaCl}_2$  have a strong peptizing action.

Potato albumin, casein or hemoglobin can be directly dissolved in a solution of 50 vol.-% of propyl alcohol +  $\text{CaCl}_2$ . Protein solutions in mixtures of 50 vol.-% propyl alcohol, allyl alcohol, pyridine, acetic acid, *etc.*, and  $\text{CaCl}_2$  (0.2–0.4 M/l.) have an unlimited stability.

Therefore, we are forced to admit that some organic substances can have a strong peptizing action (4). Some substances, such as formic acid, acetic acid, urea, *etc.*, exert this action also in the absence of salts, some others (50 vol.-% propyl alcohol or acetone) only in the presence of salts. Earlier (1) it was assumed that protein particles can, under definite conditions, be solvated by the organic substance and salt or that soluble complexes form between the atom groups of the protein, the salt and the organic substance.

Thus far, it was impossible to prove that particles of stabilized mixtures really were more solvated than those of sensitized mixtures. Fig. 2 shows that charging by salt ions determines the flocculation. When acid potato albumin is being coagulated by propyl alcohol,  $\text{LaCl}_3$  has a strong peptizing and  $\text{Na}_2\text{SO}_4$  a strong sensitizing action. Lanthanum chloride peptizes even at 15–40 vol.-%  $\text{C}_3\text{H}_7\text{OH}$ , and sodium sulfate coagulates also at 40–60 vol.-% of  $\text{C}_3\text{H}_7\text{OH}$ . In this case only the salt, not the organic substance, is important. Lanthanum ions have a strong charging and  $\text{SO}_4^{--}$  has a strong discharging effect, and they determine the behavior. It may be that, under certain conditions, 50 vol.-% propyl alcohol enhances the charging effect of  $\text{Ca}^{++}$  on protein particles (5).

The chemical structure and the particle size seem to determine the ease (or otherwise) of peptizing by alcohol and salts. Only the size of the particles can be discussed now. In a study of the coagulation of degradation products of gelatin (6) it was found that these proteins are more resistant to coagulation with  $\text{NaCl}$  and propyl alcohol the smaller their molecular weight. This observation can be considered an instance of the general rule which states that the ease of flocculation is a function of the particle size. The smaller the particle, the greater the amount of the coagulant or non-solvent required for flocculation (7). Furthermore, the

less the solubility of a protein, the greater its particles and the more easily it flocculates. Albumins have smaller molecular weights than globulins or caseins. The albumins are easily soluble in water while the globulins and caseins are insoluble. The degradation products of casein (8) produced by heating it with glycerol have an average molecular weight of 1500–2000 and are soluble in water. Casein itself has a molecular weight ( $M$ ) of about 100,000. Legumin (the globulin of the seeds of common vetch) has a molecular weight of about 300,000 and is insoluble in water (9). On the contrary, legumelin, the albumin of the vetch, has  $M = 15,000$  and is soluble in water. These two proteins of the vetch, as well as the degradation products of casein, compared to casein itself (and to lactalbumin and lactoglobulin) are chemically so closely related that the difference in their solubilities can only be explained by the particle size. This rule, applied to potato proteins, indicates that potato albumin is easily peptized because of its small particles and that potato globulins and the poorly-soluble protein have larger particles. The molecular weights of the proteins of potato have not yet been determined.

It is possible that the particles of desaminated albumen are greater than those of albumin, although the chemical properties, and also very probably the shape of the particles, play a part in this instance. When  $-OH$  groups are substituted for  $-NH_2$ , the  $NH_3^+$  ionization centers disappear. Simultaneously, the condensed protein particles seem to acquire an elongated shape (10).

#### SUMMARY

Albumin, globulin and a poorly-soluble protein were prepared from potato juice, and their coagulation by alcohol and salts was investigated. The following results were obtained:

(a) Diluted solutions of potato albumin flocculate on addition of 50 vol.-% or more of methyl alcohol and salt. The greater the amount of alcohol the greater the flocculation.

(b) Ethyl alcohol acts like  $CH_3OH$ , except that between 40 and 80 vol.-% of  $C_2H_5OH$  the flocculation is nearly constant and incomplete.

(c) Propyl alcohol and  $CaCl_2$  give a flocculation maximum and minimum (peptization). Flocculation takes place at 15–35 vol.-% and at over 70 vol.-% of propyl alcohol, and the peptization at 40–60 vol.-% of  $C_3H_7OH$ . The peptization is independent of the pH of the albumin.

(d) Lanthanum chloride has a peptizing action at alcohol concentrations up to 80 vol.-%. Sodium sulfate promotes the coagulation of an acid albumin sol.

(e) Fifty vol.-% of propyl alcohol and  $CaCl_2$  have a weak peptizing action on potato globulin and the poorly-soluble potato protein. These proteins flocculate readily in the presence of an alcohol-salt solution.



(f) Fifty vol.-% of propyl alcohol and  $\text{CaCl}_2$  peptize desaminated potato albumin less than the native albumin.

## REFERENCES

1. JIRGENSONS, B., *Kolloid-Z.* **41**, 331 (1927); **42**, 59 (1927); **47**, 236 (1929); **63**, 78 (1933); *Kolloid-Beih.* **44**, 285 (1936); *Kolloid-Z.* **99**, 89 (1942); **99**, 314 (1942), etc.
2. See, e.g., A. W. THOMAS AND E. R. NORRIS, *J. Am. Chem. Soc.* **47**, 501 (1925); WO. PAULI AND E. VALKO, *Kolloidchemie der Eiweisskörper*. Steinkopff, Dresden and Leipzig (1933).
3. JIRGENSONS, B., *Kolloid-Z.* **99**, 89 (1942); *J. prakt. Chem.* **161**, 293 (1943).
4. See, e.g., F. LOISELEUR, *Bull. soc. chim. biol.* **14**, 1088 (1932); *Chem. Zentralbl.* **1933**, II, 2540; WO. PAULI AND L. HOFMANN, *Kolloid-Beih.* **42**, 34 (1935); A. E. SANDELIN, *Molkereiwissenschaftl. Z.* (Helsinki) **1943**, No. 1-2.
5. Cf. E. GRAF, *Kolloid-Beih.* **46**, 229 (1937); B. JIRGENSONS, *Kolloid-Z.* **47**, 236 (1929).
6. JIRGENSONS, B., *Kolloid-Z.* **99**, 89 (1942).
7. SCHULZ, G. V., AND JIRGENSONS, B., *Z. physik. Chem.* **46B**, 105 (1940); JIRGENSONS, B., *J. prakt. Chem.* **161**, 30 (1942); COHN, E. J., *Naturwissenschaften* **20**, 663 (1932); *Physiol. Rev.* **5**, 410 (1925).
8. JIRGENSONS, B., *Biochem. Z.* **246**, 219 (1932); *J. prakt. Chem.* **159**, 303 (1942).
9. SVEDBERG, T., AND PEDERSEN, K. O., *Die Ultrazentrifuge*. Steinkopff, Dresden and Leipzig (1940).
10. JIRGENSONS, B., *J. prakt. Chem.* **161**, 181 (1943); **161**, 293 (1943).

## AUTHOR INDEX

- B**
- BARNES, M. D., AND LAMER, V. K. Monodispersed hydrophobic colloidal dispersions and light scattering properties. II. Total scattering from transmittance as a basis for the calculation of particle size and concentration, 79
- BARNES, M. D. See LaMer, 71
- BEYER, G. L. See Sheppard, 213
- BIGELOW, W. C., PICKETT, D. L., AND ZISMAN, W. A. Oleophobic monolayers. I. Films adsorbed from solution in non-polar liquids, 513
- BOBALEK, E. G. See Hartman, 271
- C**
- CORRIN, M. L., AND HARKINS, W. D. Critical concentration for micelle formation in mixtures of anionic soaps, 469
- CORRIN, M. L. See Harkins, 105
- CRAGG, L. H. The terminology of intrinsic viscosity and related functions, 261
- Letter to the editor, 465
- CRISP, D. J. Surface films of polymers. Part I. Films of the fluid type, 49
- Part II. Films of the coherent and semi-crystalline type, 161
- D**
- DOSCHER, T. M., AND VOLD, R. D. Phase relations in the system: sodium stearate-cetane, 299
- F**
- FRUMKIN, A. New electrocapillary phenomena, 277
- G**
- GONICK, E., AND MCBAIN, J. W. Physical-chemical properties of solutions of the colloidal electrolyte hexanolamine oleate, 127
- GONICK, E. Micellar association of ionic and non-ionic detergents in non-ionizing solvents, 393
- GRALÉN, N. The molecular weight of lignin, 453
- GUSTAVSON, K. H. Investigation of the formation of chromium salt complexes by means of organolites, 397
- H**
- HARKINS, W. D., MATTOON, R. W., AND CORRIN, M. L. Structure of soap micelles as indicated by X-rays and interpreted by the theory of molecular orientation. II. The solubilization of hydrocarbons and other oils in aqueous soap solutions, 105
- HARKINS, W. D. See Jura, 137
- HARKINS, W. D. See Corrin, 469
- HARRIS, R. H., AND JESPERSON, E. A study of the effect of various factors on the swelling of certain cereal starches, 479
- HARTMAN, R. J., KERN, R. A., AND BOBALEK, E. G. Adsorption isotherms of some substituted benzoic acids, 271
- HERMANS, J. J. The behavior of rubber-like materials when stretched, 235
- HERMANS, J. J. See Hermans, P. H., 251
- HERMANS, P. H., AND WEIDINGER, A. The hydrates of cellulose, 185
- On the transformation of cellulose II into cellulose IV, 495
- HERMANS, P. H., HERMANS, J. J., AND VERMAAS, D. Optical properties of the system cellulose-water, 251
- HIEBERT, E. N. See Walton, 385
- J**
- JENNY, H. Adsorbed nitrate ions in relation to plant growth, 33
- JESPERSON, E. See Harris, 479
- JIRGENSONS, B. The coagulation of lyophilic colloids by organic substances and salts. IX, 539
- JURA, G., AND HARKINS, W. D. The contact angle between water and a monolayer of egg albumin on glass as a function of film pressure, 137

## K

KERN, R. A. See Hartman, 271

## L

LAMER, V. K., AND BARNES, M. D. Monodispersed hydrophobic colloidal dispersions and light scattering properties. I. Preparation and light scattering properties of monodispersed colloidal sulfur, 71

LAMER, V. K. See Barnes, 79

## M

MACLAY, W. D. See Owens, 313

MARION, S. P., AND THOMAS, A. W. Effect of diverse anions on the pH of maximum precipitation of "aluminum hydroxide," 221

MATTOON, R. W. See Harkins, 105

MCARDLE, E. H. Letter to the editor, 467

MCBAIN, J. W. See Gonick, 127

MITRA, R. P. See Mukherjee, 141

MONNÉ, L. See Runnström, 421

MOONEY, M. A. viscometer for measurements during thixotropic recovery; results with a compounded latex, 195

MUKHERJEE, J. N., AND MITRA, R. P. Some aspects of the electrochemistry of clays, 141

## N

NEALE, S. M. Fundamentals of dye absorption, 371

## O

O'BRIEN, A. S. See Sheppard, 213

OWENS, H. S., AND MACLAY, W. D. Effect of methoxyl content of pectin on the properties of high-solids gels, 313

## P

PICKETT, D. L. See Bigelow, 513

PUDDINGTON, I. E. A simple surface pressure balance, 505

## R

RUNNSTRÖM, J., MONNÉ, L., AND WICKLUND, E. Studies on the surface layers and the formation of the fertilization membrane in sea urchin eggs, 421

## S

SEIFRIZ, W. Torsion in protoplasm, 27

SHEPPARD, S. E., O'BRIEN, A. S., AND BEYER, G. L. Studies in amphipathic adsorption. I. The adsorption of polyvinyl alcohol on silver bromide, 213

SHOLTES, E. H. See Walton 385

SPIEGEL, E. A. See Spiegel-Adolf, 21

SPIEGEL-ADOLF, M., AND SPIEGEL, E. A. Polarization and permeability (quantitative measurements), 21

STAMBERGER, P. The method of purifying and concentrating colloidal dispersions by electrodecentration, 93

SZENT-GYÖRGYI, A. Contraction and the chemical structure of the muscle fibril, 1

## T

THOMAS, A. W. See Marion, 221

TREITEL, O. Elasticity, plasticity and fine structure of plant cell walls, 327

## V

VERMAAS, D. See Hermans, P. H., 251

VOLD, R. D. See Doscher, 299

## W

WALTON, H. F., HIEBERT, E. N., AND SHOLTES, E. H. Quaternary ammonium salts as colloidal electrolytes, 385

WEIDINGER, A. See Hermans, P. H., 185, 495

WICKLUND, E. See Runnström, 421

WOODS, H. J. The contribution of entropy to the elastic properties of keratin, myosin and some other high polymers, 407

## Z

ZISMAN, W. A. See Bigelow, 513

## SUBJECT INDEX

- Absorption, fundamentals of dye —, NEALE, 371
- Adsorption, adsorbed nitrate, ions in relation to plant growth, JENNY, 33
- amphipathic, — of polyvinyl alcohol on silver bromide, SHEPPARD, O'BRIEN AND BEYER, 213
- Albumin, egg, contact angle between water and a monolayer of — on glass as a function of film pressure, JURA AND HARKINS, 137
- Aluminum hydroxide, effect of diverse anions on the pH of maximum precipitation of —, MARION AND THOMAS, 221
- Anions, effect of diverse — on the pH of maximum precipitation of "aluminum hydroxide," MARION AND THOMAS, 221
- Balance, simple surface pressure —, PUDINGTON, 505
- Cellulose, hydrates of —, HERMANS AND WEIDINGER, 185
- optical properties of the system — -water, HERMANS, HERMANS AND VERMAAS, 251
- transformation of — II into — IV, HERMANS AND WEIDINGER, 495
- Cetane, phase relations in the system: sodium stearate —, DOSCHER AND VOLD, 299
- Clays, some aspects of the electrochemistry of —, MUKHERJEE AND MITRA, 141
- Coagulation, — of lyophilic colloids by organic substances and salts, JIRGENSONS, 539
- Complexes, formation of chromium salt — by means of organolites, GUSTAVSON, 397
- Contact angle, — between water and a monolayer of egg albumin on glass as a function of film pressure, JURA AND HARKINS, 137
- Contraction, — and the chemical structure of the muscle fibril, SZENT-GYÖRGYI, 1
- Detergents, micellar association of ionic and non-ionic — in non-ionizing solvents, GONICK, 393
- Eggs, sea urchin, studies on the surface layers and the formation of the fertilization membrane in —, RUNNSTRÖM, MONNÉ AND WICKLUND, 421
- Elasticity, —, plasticity and fine structure of plant cell walls, TREITEL, 327
- Electrocapillary phenomena, new, FRUMKIN, 277
- Electrochemistry, some aspects of the — of clays, MUKHERJEE AND MITRA, 141
- Electrodecantation, the method of purifying and concentrating colloidal dispersions by —, STAMBERGER, 93
- Electrolytes, Quarternary ammonium salts as colloidal —, WALTON, HIEBERT AND SHOLTES, 385
- Entropy, contribution of — to the elastic properties of keratin, myosin and some other high polymers, WOODS, 407
- Films, fluid, — type, CRISP, 49
- oleophobic monolayer adsorbed from solution in non-polar liquids, BIGELOW, PICKETT AND ZISMAN, 513
- surface, films of the fluid type, CRISP, 49
- of the coherent and semi-crystalline type, CRISP, 161
- Gels, effect of methoxyl content of pectin on the properties of high-solids gels, OWENS AND MACLAY, 313
- Growth, plant, adsorbed nitrate ions in relation to —, JENNY, 33
- Hexanolamine oleate, physical-chemical properties of solutions of the colloidal electrolyte —, GONICK AND MCBAIN, 127

- Isotherms, adsorption, — of some substituted benzoic acids, HARTMAN, KERN AND BOBALEK, 271
- Keratin, contribution of entropy to the elastic properties of —, myosin and some other high polymers, Woods, 407
- Latex, a viscometer for measurements during thixotropic recovery; results with a compounded —, MOONEY, 195
- Light scattering, preparation and — properties of monodispersed colloidal sulfur, LA MER AND BARNES, 71  
total scattering from transmittance as a basis for the calculation of particle size and concentration, BARNES AND LA MER, 79
- Lignin, the molecular weight of —, GRALÉN, 453
- Liquids, non-polar, films adsorbed from solution in —, BIGELOW, PICKETT AND ZISMAN, 513
- Lyophiles, coagulation of lyophilic colloids by organic substances and salts, JIRGENSONS, 539
- Micelle, critical concentration for — formation in mixtures of anionic soaps, CORBIN AND HARKINS, 469
- Micelles, micellar association of ionic and non-ionic detergents in non-ionizing solvents, GONICK, 393  
soap, solubilization of hydrocarbons and other oils in aqueous soap solutions, HARKINS, MATTOON AND CORBIN, 105
- Monolayers, oleophobic films adsorbed from solution in non-polar liquids, BIGELOW, PICKETT AND ZISMAN, 513
- Muscle, contraction and the chemical structure of the — fibril, SZENT-GYÖRGYI, 1
- Myosin, contribution to the elastic properties of keratin, — and some other high polymers, Woods, 407
- Nitrate ions, adsorbed — in relation to plant growth, JENNY, 33
- Optical properties, — of the system cellulose-water, HERMANS, HERMANS AND VERMAAS, 251
- Organic substances, coagulation of lyophilic colloids by — and salts, JIRGENSONS, 539
- Organolites, formation of chromium salt complexes by means of —, GUSTAVSON, 397
- Pectin, effect of methoxyl content of — on the properties of high-solids gels, OWENS AND MACLAY, 313
- Permeability, polarization and —, SPIEGEL-ADOLF AND SPIEGEL, 21
- Phase relations, — in the system: sodium stearate-cetane, DOSCHER AND VOLD, 299
- Plant cell walls, elasticity, plasticity and fine structures of —, TREITEL, 327
- Plasticity, elasticity, — and fine structure of plant cell walls, TREITEL, 327
- Polarization, — and permeability, SPIEGEL-ADOLF AND SPIEGEL, 21
- Polymers, surface films of —, CRISP, 49
- Polyvinyl alcohol, absorption of — on silver bromide, SHEPPARD, O'BRIEN AND BEYER, 213
- Precipitation, effect of diverse anions on the pH of maximum — of "aluminum hydroxide," MARION AND THOMAS, 221
- Pressure, film, contact angle between water and a monolayer of egg albumin on glass as a function of —, JURA AND HARKINS, 137
- Protoplasm, torsion in —, SEIFEIZ, 27
- Rubberlike materials, behavior of — when stretched, HERMANS, 235
- Salts, coagulation of lyophilic colloids by organic substances and —, JIRGENSONS, 539  
formation of chromium salt complexes by means of organolites, GUSTAVSON, 397  
quarternary ammonium — as colloidal electrolytes, WALTON, HIEBERT AND SHOLTES, 385
- Silver bromide, adsorption of polyvinyl alcohol on —, SHEPPARD, O'BRIEN AND BEYER, 213
- Soaps, critical concentrations for micelle formation in mixtures of anionic —, CORBIN AND HARKINS, 469

- Sodium stearate, phase relations in the system: — -cetane, DOSCHER AND VOLD, 299
- Solubilization, — of hydrocarbons and other oils in aqueous soap solutions, HARKINS, MATTOON AND CORRIN, 105
- Starches, cereal, a study of the effect of certain factors on the swelling of —, HARRIS AND JESPERSON, 479
- Structure, chemical, contraction and the — of the muscle fibril, SZENT-GYÖRGYI, 1
- Sulfur, preparation and light scattering properties of monodispersed colloidal —, LA MER AND BARNES, 71
- Surface pressure, simple — balance, PUDINGTON, 505
- Swelling, a study of the effect of various factors on the — of certain cereal starches, HARRIS AND JESPERSON, 479
- Terminology, — of intrinsic viscosity and related functions, CRAGG, 261; 465  
MCARDLE, 467
- Torsion, — in protoplasm, SEIFRIZ, 27
- Transmittance, total scattering from — as a basis for the calculation of particle size and concentration, BARNES AND LA MER, 79
- Viscometer, — for measurements during thixotropic recovery; results with a compounded latex, MOONEY, 195

## INDEX OF BOOK REVIEWS

- ANSON, M. L., AND EDSALL, J. T. *Advances in Protein Chemistry*, Vol. II (*J. Steinhardt*), 382
- BENNETT, H. (editor), *Commercial Waxes, Natural and Synthetic, a Symposium and Compilation* (*L. C. Cartwright*), 477
- BROWN, E. B. *Optical Instruments* (*D. Sinclair*), 473
- DEARLE, D. A. *Plastic Molding and Plant Management* (*D. M. Buchanan and R. J. Moore*), 381
- DUNOÛY, P. L. *Studies in Biophysics: The Critical Temperature of Serum (56°)*, (*T. Shedlovsky*), 476
- FLECK, H. R. *Plastics, Scientific and Technological* (*R. M. Fuoss*), 293
- HAWLEY, G. G., AND LEIFSON, S. W. *Atomic Energy in War and Peace* (*F. Brescia*), 211
- HOUGEN, O. A., AND WATSON, K. M. *Chemical Process Principles, Part I. Material and Energy Balances* (*P. W. Schutz*), 475
- LEFFINGWELL, G., AND LESSER, M. *Soap in Industry* (*W. H. Stahl*), 477
- LOHSE, H. W. *Catalytic Chemistry* (*S. H. Maron*), 210
- MUNOZ, F. J., AND CHARIPPER, H. A. *The Microscope and Its Use* (*H. Ris*), 383
- PIGMAN, W. W., AND WOLFROM, M. L. *Advances in Carbohydrate Chemistry* (*C. S. Hurd*), 381
- RABINOWITCH, E. I. *Photosynthesis and Related Processes, Vol. I* (*J. Franck*), 209
- SUTERMEISTER, E., AND BROWNE, F. L. *Casein and Its Industrial Applications* (*H. K. Salzberg*), 296
- TWISS, S. B. (editor), *Advancing Fronts in Chemistry, Vol. I. High Polymers* (*R. M. Fuoss*), 293
- WALKER, F. *Formaldehyde* (*R. J. Moore*), 296
- WINTON, A. L., AND WINTON, K. B. *Analysis of Foods* (*M. I. Bailey*), 383
- WISE, L. E. (editor), *Wood Chemistry* (*A. J. Panshin*), 294
- YOUNG, C. B. F., AND COONS, K. N. *Surface Active Agents* (*M. D. Hassialis*), 297



**Indian Agricultural Research Institute (Pusa)**

**LIBRARY, NEW DELHI-110012**

This book can be issued on or before ..... \*

Return Date	Return Date